Ultra High Voltage Transmission in Alternating Current

Applied Research in the Brazilian Electrical System

交流特高压输电技术在巴西的应用研究

Transmissão em Ultra Alta Tensão em Corrente Alternada

Pesquisa Aplicada no Sistema Elétrico Brasileiro

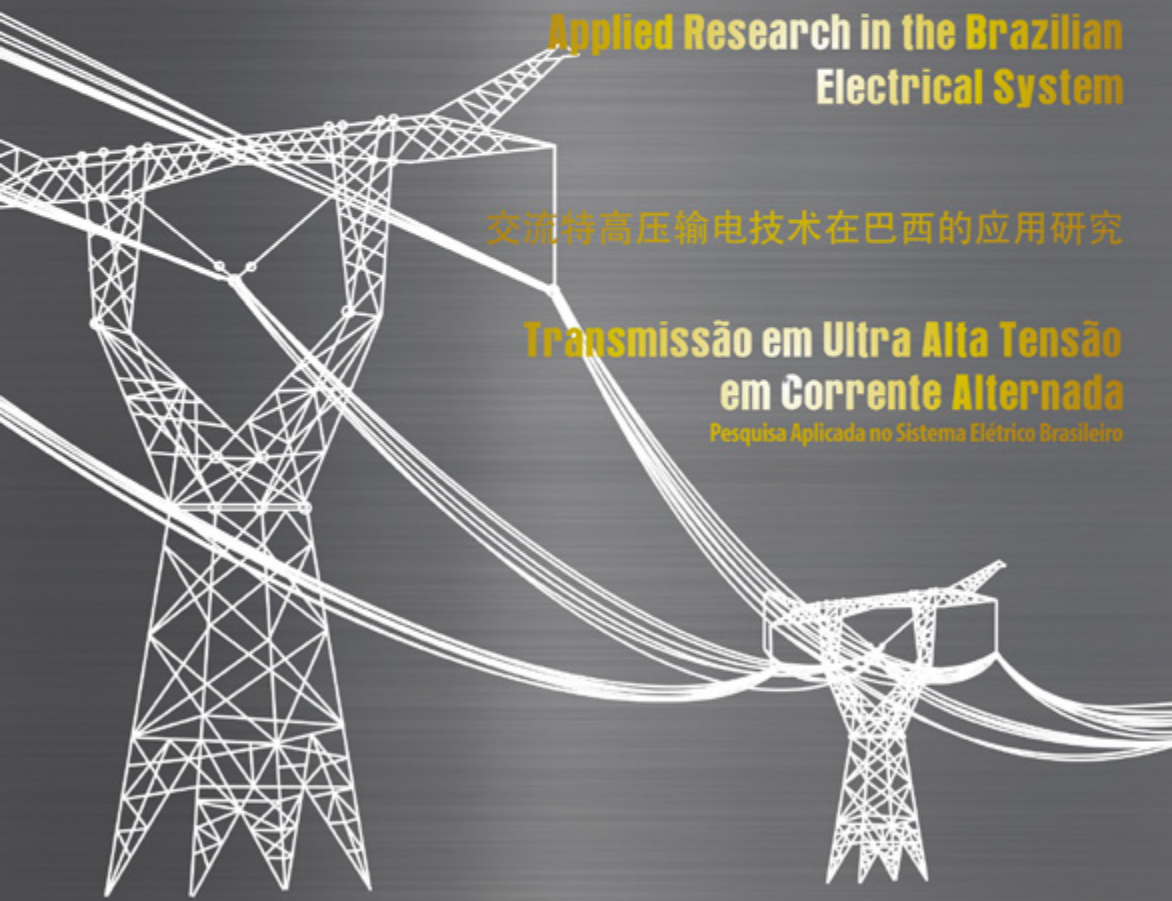

PROJECT COORDINATOR

José Antonio Jardini
ITAEE

PROJECT MANAGERS

Geraldo Luiz Costa Nicola
Eletrobras Eletronorte

John Francis Graham
State Grid Brazil Holding

Liu Guijun
State Grid Brazil Holding

AUTHORS IN ALPHABETICAL ORDER

Adriano Aparecido Dellallibera
Balestro

Alex da Silva Sousa
Geoambiente

Carlos Alberto Rayol
Eletrobras Eletronorte

Eber Havila Rose
Eletrobras Eletronorte

Felipe Rocha Velloso de Almeida Pedroso
FDTE

Geraldo Luiz Costa Nicola
Eletrobras Eletronorte

Gerson Yukio Saiki
ITAEE

Huederson Aparecido Botura da Silva
Balestro

John Francis Graham
State Grid Brazil Holding

José Antonio Jardini
ITAEE

José William de Medeiros
Eletrobras Eletronorte

Liu Guijun
State Grid Brazil Holding

Maira Dzedzej
Geoambiente

Marcos Tiago Bassini
FDTE

Mauricio George Miguel Jardini
ITAEE

Patrícia Oliveira da Silveira
ITAEE

Renato Grigoletto de Biase
ITAEE

Ricardo Leon Vasquez Arnez
ITAEE

Sergio de Oliveira Frontin
FDTE

Thales Sousa
FDTE

Valdomiro Vega García
FDTE

Ultra High Voltage Transmission in Alternating Current

Applied Research in the Brazilian Electrical System

State Grid Brazil Holding S.A.

Cai Hongxian
President & CEO

Qu Yang
Vice President

Eletrobras Eletronorte

Vilmos da Silva Grunvald
President

Roberto Parucker
Engineering Director

Organizers

José Antonio Jardini
Sergio de Oliveira Frontin
Geraldo Luiz Costa Nicola
John Francis Graham
Wang Yuanhang
Liu Guijun

1st Edition

Brasília
2017

Teixeira Gráfica e Editora LTDA.
Edition: 1,000 books

AGÊNCIA NACIONAL DE ENERGIA ELÉTRICA – Aneel
SGAN Quadra 603, Módulos I e J, Asa Norte, Brasília (DF) – CEP: 70830-030
Romeu Donizete Rufino
General Director

CENTRAIS ELÉTRICAS DO NORTE DO BRASIL S.A. – Eletronorte
SCN Quadra 06, Conjunto A, Blocos B e C, Entrada Norte 2, Asa Norte, Brasília (DF) – CEP: 70716-901
Vilmos da Silva Grunvald
President

STATE GRID BRAZIL HOLDING – SGBH
Avenida Presidente Vargas, 955, SGCC Rio Tower, Centro, Rio de Janeiro (RJ) – CEP: 20071-004
Cai Hongxian
President & CEO

INSTITUTO TÉCNICO DE AUTOMAÇÃO E ESTUDOS ELÉTRICOS – ITAEE
Rua Capitao Otávio Machado, 525, São Paulo (SP) – CEP: 04718-000
José Antonio Jardini
President

INDÚSTRIA ELETROMECÂNICA BALESTRO LTDA. – Balestro
Rua Santa Cruz, 1550, Jardim Santa Cruz, Mogi Mirim (SP) – CEP: 13800-440
Carlos Eduardo Balestro
General Director

FUNDAÇÃO PARA O DESENVOLVIMENTO TECNOLÓGICO DA ENGENHARIA – FDTE
Rua Padre Eugênio Lopes 361, Morumbi. CEP: 05615-010. São Paulo – SP
Anapaula Haipek Campos
Director Superintendent

Cover, graphic design and layout
Casa 73 Editora

Revision
Carolina Lopes e Vanessa Aquino

Translation
Claudia Muller

Cataloging in Publication - CIP
CEDOC / ANEEL

Ultra High Voltage Transmission in Alternating Current : Applied Research in the Brazilian Electrical System / José Antonio Jardini, Sergio de Oliveira Frontin, Geraldo Luiz Costa Nicola, John Francis Graham, Wang Yuanhang, Liu Guijun (orgs.). – Brasília, Brazil : Casa 73, 2018.

652 p. : il.

ISBN: 978-85-88041-15-8

1. Electrical energy. 2. Ultra High Voltage Transmission. 3. Electrical energy Transmission – Research and Development – Brazil. I. Title.

UDC: 621.315(81)

This publication is part of the activities carried out under the ANEEL's R&D program referred to the project called *Ultra High Voltage Transmission within the Brazilian National Interconnected System*.

The views and opinions expressed in this book belong solely to the authors and are based on the reports produced by the entities that developed the project. Likewise, the conclusions presented do not necessarily reflect the position of ANEEL or any of the sponsoring companies of this research project.

The material contained in this publication may be reproduced, stored or transmitted, provided the source is acknowledged

The above-cited companies reserve all rights.

SUMMARY

Preface 15
Executive Summary 19

CHAPTER 1
Perspectives for the Application of 1,000 kV AC Transmission Systems in Brazil

1. Introduction 24
2. Brazilian System Year 2015 25
   2.1 Generation and Load 25
   2.2 Generation Expansion 26
   2.3 Transmission 27
3. Economic Transmission System 28
4. Insertion of the 1,000 kV System 31
5. Reliability 32
6. Economic Feasibility 32
7. Conclusions 33
8. References 33

CHAPTER 2
History of Ultra-High Voltage Alternating Current, Experience and Applications

1. Introduction 36
2. Evolution of Power Transmission System Voltage Levels in Brazil 37
3. Evolution of Power Transmission System Voltage Levels at a Global Level 39
   3.1 United States of America 40
   3.2 Italy 40
   3.3 Russia 41
   3.4 Japan 41
   3.5 India 42
   3.6 China 43
4. Detailing of China's UHV AC System 44
   4.1 Planning Aspects 45
   4.2 Operation Aspects 45
5. Conclusions 46
6. References 46

CHAPTER 3

Analysis of Scenarios for the Application of the 1,000 kV system in the Brazilian Interconnected Power System

1. Introduction 48
2. Strategies Used 48
3. Analysis of the Lines Foreseen in the 2023 Ten Year Expansion Plan without Generation Expansion Plans 48
   3.1 Evaluated Alternatives 48
   3.2 Performance Evaluation 52
4. Flexibility for the Region with Wind/Photovoltaic Generation 52
5. Conclusions 53
6. References 53

CHAPTER 4

Technical, Economic, and Socio-Environmental Feasibility Studies of the Alternatives (R1)

1. Objective 56
2. Introduction 56
3. Assumptions and General Criteria 57
   3.1 Studies Conducted by EPE 57
   3.2 Bases and General Criteria 58
4. Performance of the Transmission System Alternatives 61
   4.1 Power Flow Studies (2024 Ten-Year Expansion Plan) 61
      4.1.1 Dispatch features 61
      4.1.2 Contingencies analyzed 63
      4.1.3 Reactive support in the local system 64
      4.1.4 Results of power flow studies 65
      4.1.5 Considerations about power export 82
   4.2 Electromechanical Transient Studies 82
      4.2.1 Case I 84
      4.2.2 Case II 85
      4.2.3 Case III 86
      4.2.4 Case IV 87
      4.2.5 Case V 88
      4.2.6 Case VI 89
      4.2.7 Case VII 90
      4.2.8 Case VIII 91
      4.2.9 Case IX 92
   4.3 Short-Circuit Studies 92
5. Socio-environmental Evaluation of the Transmission System Corridor Alternatives 96
   5.1 Alternative 1 – Shortest Corridor 97
   5.2 Alternative 2 – Corridor that Avoids Some Environmental Impediments 98

5.3 Analysis of the Alternatives 100
5.4 Selected Alternative 105
5.5 Socio-environmental Analysis 106
5.6 Description of the Selected Alternative 106
5.6.1 Macro-characterization of the Milagres (Ceará) to Ourolândia (Bahia) section 108
5.6.2 Macro-characterization of the Ourolândia (Bahia) to Igaporã (Bahia) section 117
5.6.3 Macro-characterization of the Igaporã (Bahia) to Pirapora (Minas Gerais) section 124
5.6.4 Recommendations for the line routing and elaboration of the R3 Report 132
6. Economic Evaluation 135
6.1 Alternative 1 136
6.1.1 Rating of the transformers of Alternative 1 137
6.2 Alternative 2 138
6.3 Alternative 3 138
6.4 Alternative 4 139
6.5 Economic Parameters 140
6.6 Cost of Transmission Lines 140
6.7 Cost of Substations, Equipment and Converters 143
6.7.1 General module 143
6.7.2 Switching module 143
6.7.3 Transformers 144
6.7.4 Shunt reactors 145
6.7.5 Series capacitor 147
6.7.6 Direct current converters 148
6.8 Joule Losses 149
6.8.1 Joule losses in the AC lines 149
6.8.2 Joule losses in the DC lines 150
6.8.3 Joule losses in the converters 150
6.8.4 Joule losses in the transformers 150
6.9 Investments Evaluation 151
6.9.1 Transmission lines 151
6.9.2 1,000 kV transformers for Alternative 1 151
6.9.3 Substations 152
6.9.4 Cost of the converters 157
6.9.5 Losses in the transmission lines 157
6.9.6 Transformers losses for Alternative 1 159
6.9.7 Losses in the converters 160
6.10 Comparison of the Alternatives 160
6.11 Sensitivities 161
6.11.1 Sensitivity 1 161
6.11.2 Sensitivity 2 162
6.11.3 Sensitivity 3 162

7. Description of the 1,000 kV Reference Alternative 163
7.1 Transmission Line 163
7.1.1 Initial and final loading in normal state and emergency 166
7.1.2 Shunt reactive compensation 168
7.1.3 Series reactive compensation 168
7.2 Substations 168
7.2.1 Busbar arrangement 168
7.2.2 Area necessary for new substations 169
7.2.3 Macro-location of the Milagres substation 169
7.2.4 Macro-location of the Ourolândia substation 169
7.2.5 Macro-location of the Igaporã substation 170
7.2.6 Macro-location of the Pirapora substation 171
7.2.7 Macro-location of the Ribeirão das Neves substation 171
7.2.8 Transformer units 172
8. Future Expansion of the 1,000 kV Reference Alternative 172
8.1 Performance Evaluation for Expansion 174
8.1.1 Power Flow Studies 174
8.1.2 Study of electromechanical transients, expansion of the 1,000 kV system with 4 sections and 3 of them with 2 circuits 189
8.1.3 Short-circuit studies, expansion of the 1,000 kV system 193
8.2 Cost Evaluation 196
8.2.1 Alternative 1 Expansion (1,000 kV) 197
8.2.2 Alternative 2 Expansion (500 kV) 198
8.2.3 DC Alternative 199
8.3 Results of the Cost Evaluation 200
9. Conclusions and Recommendations 200
10. References 203
ATTACHMENT – Detailing of the Costing of the Transmission Lines 206

CHAPTER 5

Detailed Studies of the Reference Alternative (R2)

1. Introduction 220
2. Description of the 1,000 kV Transmission Alternative 221
2.1 Milagres III Substation 221
2.2 Ourolândia III Substation 222
2.3 Igaporã IV Substation 223
2.4 Pirapora III Substation 224
3. Geometry of the 1,000 kV Transmission Line Towers 225
4. Switching Overvoltage Studies 227
4.1 Configuration of the Network Analyzed 227
4.2 Data Used 227
4.2.1 Line reactor and neutral reactor 228
4.2.2 Series capacitor 228

4.2.3 Surge arresters in the substations and equipment 228
4.2.4 Metal Oxide Varistors (MOV) of the series capacitors 229
4.2.5 General scheme of the grid studied 230
4.3 Line energization 231
4.4 Single-pole Reclosing 232
4.5 Three-pole Reclosing 234
4.6 Fault Application, Fault Clearing, and Load Rejection 235
4.6.1 Fault application 235
4.6.2 Fault clearing 236
4.6.3 Load rejection 238
5. Secondary Arc Extinction (Residual Load) 239
5.1 Residual Charge – Single-Pole Opening 239
5.2 Residual Charge – Three-Pole Opening 240
5.3 Line Reactor Position 241
6. Transient Recovery Voltage (TRV) 241
6.1 Short-Line Fault 242
6.2 Terminal Fault 244
7. Transformer Energization 246
7.1 Findings 246
8. Resonance Analysis – Line and its Reactor 247
8.1 Results with only one 1,000 kV Line 248
8.2 Resonance in the System with Two Lines per Section 248
9. Transmission Line 248
9.1 Economic Conductor 248
9.2 Overvoltage at Operating and Switching Frequency 251
9.2.1 Overvoltage at power frequency 251
9.2.2 Switching overvoltages 251
9.3 Insulation Coordination 256
9.3.1 Power frequency insulation 256
9.3.2 Switching insulation 259
9.3.3 Towers 263
9.3.4 Overvoltage due to lightning 265
9.3.5 Positioning of ground wires 265
9.3.6 Outages due to indirect strokes (backflashover) 266
9.3.7 Simulations with IEEE Flash 266
9.4 Corona effect 266
9.4.1 Gradient on the surface of the conductors 266
9.4.2 Radio interference 268
9.4.3 Audible noise 269
9.5 Electric and Magnetic Fields 270
9.5.1 Electric field 270
9.5.2 Magnetic field 271
9.6 Determining the Right-of-Way 272
9.7 Determining the Height of the Conductors 272
9.8 Current Capacity 272

9.9 Mechanical Design 273
9.9.1 Wind pressures 273
9.9.2 Tensions and sags 274
10. Equipment Requirements 277
10.1 Substations 277
10.2 Overvoltage, Insulation, and Surge Arrester Requirements 278
10.2.1 Overvoltages 278
10.2.2 Surge arrester requirements 279
10.2.3 Insulation coordination 280
10.3 Busbar Arrangement 280
10.4 Size of the AIS Substation 281
10.5 Equipment 281
10.5.1 Transformer 282
10.5.2 Line reactor (neutral reactor) 282
10.5.3 Series capacitor 282
10.5.4 Circuit breakers 283
10.5.5 Switching and other devices (insulator pole, air switches, and instrument transformer) 283
10.5.6 Surge arresters 283
10.6 Costs 284
10.6.1 Transformers and line reactors 284
10.6.2 Circuit breakers 285
10.6.3 Substation cost 285
10.7 GIS 1,000 kV 285
11. Expansion of the Reference Alternative 286
11.1 Load Rejection and Surge Arrester 287
11.2 Line Energization 288
11.3 Fault Application 290
11.4 Single-phase Residual Load 290
11.5 Single-pole Reclosing 291
11.6 Three-pole Reclosing 292
11.7 Transient Recovery Voltage (TRV) 293
11.8 Series Capacitor 294
12. References 295

Attachments – Chapter 5

ATTACHMENT 1 – Line Energization 297
1.1 Objective 297
1.2 General Description of the Calculation 297
1.3 Systematic Energization 298
1.4 Statistic Energization 299
1.5 Determining the Worst Case 302
1.6 Sensitivities 303
1.6.1 Position of the line reactor and series capacitor inserted 303
1.6.2 Synchronized energization 304

ATTACHMENT 2 – Single-pole Reclosing 307
2.1 Objective 307
2.2 Methodology 307
2.3 Results of the Milagres-Ourolândia line 309
2.3.1 Reclosing via Milagres 309
2.3.2 Reclosing via Ourolândia 311
2.4 Results of the Ourolândia – Igaporã line 312
2.4.1 Reclosing via Ourolândia 312
2.4.2 Reclosing via Igaporã 314
2.5 Results of the Igaporã – Pirapora Line 314
2.5.1 Reclosing via Igaporã 314
2.5.2 Reclosing via Pirapora 316
2.6 Findings 316
ATTACHMENT 3 – Three-pole Reclosing 317
3.1 Objective 317
3.2 With and Without Bypass of the Series Capacitor – Reclosing 318
3.3 Sensitivity Regarding the Length of the Sections 320
3.4 Use of Fast Grounding Switch 322
3.5 Statistic Distributions 322
3.5.1 Milagres – Ourolândia 322
3.5.2 Ourolândia – Igaporã 324
3.5.3 Igaporã – Pirapora 326
3.5.4 Transient oscillograms 328
3.5.5 Milagres – Ourolândia (via Milagres) 328
ATTACHMENT 4 – Fault Application and Clearing, and Load Rejection 329
4.1 Objective 329
4.2 Fault application 329
4.3 Fault Clearing 333
4.3.1 Results obtained 333
4.3.2 Sensitivity analysis 335
4.3.3 Overvoltages in the healthy system 336
4.4 Load Rejection 338
4.4.1 Opening without short 338
4.4.2 Short followed by opening 339
4.4.3 Opening followed by short 341
ATTACHMENT 5 – Residual Load and Arc Extinction 343
5.1 Objective 343
5.2 Single-phase Residual Load 343
5.2.1 General conditions 343
5.2.2 Arc extinction 345
5.2.3 Arc extinction phenomenon 345
5.2.4 Arc extinction 348
5.2.5 Bypass of the series capacitor on the instant of the fault 349
5.2.6 Extinction of the arc "on-load", case of tower with another geometry 349
5.2.7 Influence of system frequency variation in the arc extinction 349

5.3 Three-Phase Residual Load 351
5.3.1 Results 351
5.3.2 Position of the reactor 352
ATTACHMENT 6 – Transient Recovery Voltage (TRV) 353
6.1 General Procedure 353
6.2 Results Ourolândia – Igaporã Section 354
6.2.1 Short-Line Fault 354
6.2.2 Terminal fault (Ourolândia side) 368
6.2.3 Terminal fault (Igaporã side) 372
6.3 Other sections 375
ATTACHMENT 7 – Transformer Energization 376
7.1 Transformer Characteristics 376
7.2 Energization Sequence 376
7.3 Energization of the Ourolândia Transformer – Results 376
7.3.1 Energization via the 500 kV side 376
7.3.2 Controlled energization of the transformer via the 500 kV side 378
7.3.3 Energization via the 1,000 kV side 393
7.4 Displacement of ±1 ms at the Closing 400
7.5 Transformers Connected in Parallel (Ourolândia) 401
7.5.1 Assumptions for analysis of sympathetic energization 401
7.5.2 Best connection instant of the transformer in parallel, 500 kV side (with synchronizer) 402
7.5.3 Worst connection instant of the transformer in parallel (with synchronizer) 402
7.6 3,000 MVA Transformer 403
7.6.1 Energization via the 500 kV side 403
7.6.2 Energization via the 1,000 kV side 403
ATTACHMENT 8 – Resonance Analysis - Line and Parallel Reactor 405
8.1 Objective 405
8.2 Results of the System with 1,000 kV Line 407
8.3 Resonance of the system in two circuits per 1,000 kV section 408
ATTACHMENT 9 – Load Rejection and Surge Arrester Effect (Expanded System) 411
9.1. Objective 411
9.1.1 Load rejection (Case a) 411
9.1.2 Load rejection followed by short circuit(Case b) 414
9.1.3 Short followed by rejection (Case c) 417
9.1.4 Unsuccessful single-pole reclosing (Case d) 419
9.1.5 Unsuccessful three-pole reclosing (Case e) 421
9.1.6 Line and busbar surge arrester simulations 423
9.1.7 Analysis with different types of surge arresters 423
ATTACHMENT 10 – Line Energization (Expanded System) 426
10.1 Objective 426
10.2 Findings 426
10.3 Transmission Line Energization 426

10.3.1 Systematic energization 427
10.3.2 Statistic energization 427
10.3.3 Deterministic of the worst case 429
ATTACHMENT 11 – Fault Application (Expanded System) 430
11.1 Objective 430
11.2 Results 430
ATTACHMENT 12 – Single-Phase Residual Load (Expanded System) 432
12.1 Objective 432
12.2 Results 432
12.3 Extinction of the secondary arc 432
12.3.1 Influence of system frequency variation in the line arc extinction, worst case 436
ATTACHMENT 13 – Single-Pole Reclosing (Expanded System) 438
13.1 Objective 438
ATTACHMENT 14 – Three-pole Reclosing (Expanded System) 440
14.1 Objective 440
14.2 Systematic Analysis: 440
ATTACHMENT 15 – Transient Recovery Voltage (Expanded System) 443
15.1 Objective 443
15.2 Main Results 443
15.2.1 Ourolândia – Igaporã Section 443
15.2.2 Results for the Igaporã – Pirapora section 445
ATTACHMENT 16 – Analysis of the Series Capacitor (Expanded System) 448
16.1 Objective 448
16.2 1,000 kV System 448
16.3 Determining series compensation characteristics 449
16.3.1 Fluxes during emergency 449
16.3.2 Calculation of state currents and transients. 450
16.3.3 Voltages and power 451
16.3.4 MOV Requirements 452
ATTACHMENT 17 – Studies and Development of Polymeric Surge Arrester and Insulator Prototypes for the UHV Transmission System 454
17.1 Objective 454
17.2 Surge arrester for the 1,000 kV System 454
17.3 Manufacturing 458
17.4 Laboratory Tests 459
17.5 Polymeric Insulators for the 1,000 kV System 462
17.6 Control of the Electric Field 463
17.7 Electrical Behavior under Rain 464
ATTACHMENT 18 – Mechanical Design of the UHV Line 468
18.1 Objective 468
18.2 General Data 468
18.2.1 Cables 468
18.2.2 Tower 468

18.3 Reference Wind 469
18.4 Conditions Studied 469
18.5 Loadings Due to Extreme Wind 470
18.5.1 Dynamic reference pressure 470
18.5.2 Extreme wind pressure on the cables 470
18.5.3 Extreme wind pressure on the insulator strings 471
18.6 High Intensity Winds 472
18.6.1 Pressure of the high intensity wind on the cables and strings 472
18.6.2 Pressure of the high intensity wind on the structures and strings 473
18.7 Tension on Cables and Sags 473
18.8 Calculation of the Stress on the Towers 475
18.8.1 Vertical loads 475
18.8.2 Transverse loads 475
18.8.3 Longitudinal loads 476
18.9 Loading Trees 476

CHAPTER 6

Socio-environmental Characterization and Analysis of the Project (R3)

1. Introduction 482
2. Justification 483
3. General Characterization of the Project Area 484
4. Procedures and Research Source 486
5. Socio-environmental Characterization 488
5.1 Physical Environment 488
5.1.1 Climatology 488
5.1.2 Geomorphology/Geology/Mining Resources/Geotechnics 496
5.1.3 Soils 502
5.1.4 Water resources and water uses 509
5.2 Biotic Environment 513
5.2.1 Land use and vegetation 513
5.2.2 Ecosystem and fauna 517
5.2.3 Protected areas 518
5.3 Socioeconomic Environment 523
5.3.1 Demographics aspects 523
5.3.2 Territorial organization and regional structure 528
5.3.3 Land property structure, settlements and conflict areas 528
5.3.3 Cultural and natural eeritage 533
5.3.4 Indigenous and quilombolic lands 535
5.4 Ecolgical Economic Zoning (EEZ) 539
6. Integrated Analysis and Definition of Areas of Greater and Lesser Socio-environmental Sensitivity 542
6.1 Milagres (Ceará) to Ourolândia (Bahia) Section 546
6.2 Ourolândia (Bahia) to Igaporã (Bahia) Section 548
6.3 Igaporã (Bahia) to Pirapora (Minas Gerais) Section 550

7. Recommendations and Preferred Route for the Line Path 552
7.1 Adjustments to the Preliminary Path and Final Route 562
8. Socio-environmental Characterization of the Corridor of the Main Route of the Line 572
8.1 Variables Considered in the Socio-environmental Characterization 572
8.2 Description of the Path and 30 km Wide Corridor 574
8.3 Macro-characterization of the Section Milagres (Ceará) to Ourolândia (Bahia) 577
8.4 Macro-characterization of the Section Ourolândia (Bahia) to Igaporã (Bahia) 585
8.5 Macro-characterization of the Section Igaporã (Bahia) to Pirapora (Minas Gerais) 592
9. General Recommendations for Future Actions 601
10. References 602

CHAPTER 7

Characterization of the Existing Grid for Integration of the 1,000 kV AC System

1. Introduction 606
2. R4 Elaboration Process 606
3. General Conditions for the Sectioning of Transmission Lines 607
4. Connection of the 1,000 kV System to the Existing System 609
4.1 Sectioning at the Milagres III – 1,000/500 kV Substation 609
4.2 Sectioning at the Ourolândia III – 1,000/500 kV Substation 610
4.3 Sectioning at the Igaporã IV – 1,000/500 kV Substation 610
4.4 Sectioning at the Pirapora III – 1,000/500 kV Substation 611
5. Substations of the 1,000 kV System 611
5.1 Milagres III – 1,000/500 kV Substation 611
5.2 Ourolândia III – 1,000/500 kV Substation 612
5.3 Sectioning at the Igaporã IV – 1,000/500 kV Substation 613
5.4 Pirapora III – 1,000/500 kV Substation 614
6. Conclusions 614
7. References 615

CHAPTER 8

Transmission Project Auction Process

1. Introduction 618
2. The Ten-Year Energy Expansion Plan and the National Energy Plan 618
3. Technical Reports R1, R2, R3, and R4 621
4. The Transmission Auction Process 621
5. The Transmission Auction Notice 623
6. The Concession Agreement 624

7. Agreements Related to Transmission Services 626
7.1 Transmission Service Provision Contract (CPST) 627
7.2 Transmission System Use Contract (CUST) 627
7.3 Transmission System Connection Contract (CCT) 628
7.4 Facility Sharing Contract (CCI) 629
8. Transmission System Rates – RAP – TUST 629
8.1 Permitted Annual Revenues (RAP) 629
8.2 Transmission System Usage Fee (TUST) 630
8.3 Technical Calculation of Transmission Services and Charges 630
9. Auction Notice Technical Attachment 631
10. Relevant Points for the Ultra-High Voltage System Auction 632
10.1 Reimbursement of Expenses (items 4.6 and 4.7 of the Auction Notice) 632
10.2 Deadline for the Presentation of the Basic Design (item 4.8 of the Auction Notice) 633
10.3 Entry into Commercial Operations (item 4.13 of the Auction Notice) 633
10.4 Calculation of Maximum Permitted Annual Revenue (item 5.5 of the Auction Notice) 633
10.5 RAP Discount - Variable Portion – PV (item 5.8 of the Notice) 634
10.6 Auction Schedule (item 17 of the Auction Notice) 634
10.7 Project Monitoring and Training (item 15.1 of Attachment 6 of the Auction Notice) 634
11. Conclusions 635
12. References 635

CHAPTER 9

Complementary Investigations

1. Objective 638
2. Prospect of the Study 639
3. Reactive Compensation 639
4. Arrangement and Type of Substations 640
5. Technological Innovations Applied to Equipment 642
6. Technological Innovations Applied to Transmission Lines 642
7. Monitoring Systems 643
8. Integration of Renewable Sources to the Interconnected System 646
9. Technological Observatory 647
10. Conclusions 648
11. References 650

The Opportunity to Implement an Ultra High Voltage Alternating Current System in Brazil

Cai Hongxian
President & CEO - State Grid Brazil Holding S.A.

Roberto Parucker
Engineering Director - Eletrobras Eletronorte

This book presents the results of an R&D project that describes the implementation of the first stage of an alternating current UHV system in Brazil as part of the integrated grid expansion. This complements the present use of UHV DC for long distance transmission and the resulting hybrid grid, with an UHV AC/DC overlay, gives secure and stable operation of the power system, especially in the presence of renewable generation with intermittent and distributed characteristics.

In the last three decades of the twentieth century, understanding of the use of UHV in alternating current (UHV AC) was present in transmission studies worldwide. Brazil also initiated the attempt to study this transmission alternative, which was implemented by the Amazon Transmission Group (GTA) under the coordination of Eletrobras, but inhibited by the economic crisis occurring in the 1980s.

When time came to the twenty-first century, due to the explosive development of the economy in China, the need to transmit power over long distances from power base to load center prompted the research and application of UHV transmission technology, including UHV DC (± 800 and, later, at ± 1,100 kV) and UHV AC (1,000kV). In the 2009-2017 period, China implemented more than ten thousand kilometers of circuits with hundreds

of reactors and transformers in this voltage class. These numbers provide an irrefutable demonstration of technological maturity for Western and Asian industry, especially Chinese.

This R&D project was born from the perception that interregional interconnections in Brazil could not fulfill their functions properly, larger flows not being possible under normal conditions and during contingencies. In the Decennial Plan 2026 published by Energy Research Company (EPE), it is indicated that the Northeast region will in a short time change its condition as net energy importer to exporter with the availability of 12.5 GW to be exported to the Midwest and Southeast regions. In this context, the opportunity arises to implement a high capacity transmission connection by the use of Ultra High Voltage (UHV) technology (above 800 kV).

In 2012, through a research project studying the transmission of large blocks of energy between the Amazon, Northeast and Southeast regions, the research team led by Eletronorte reached several conclusions related to UHV transmission technologies. In the point-to-point interconnections, around 1,300 km, the transmission in UHV 1,000 kV AC had better performance than the alternatives in direct current, ± 800 kV, for example. In situations where the intermediate connections are relevant, in terms of generation or load, the economic distance can be longer and make viable alternating current interconnections close to 2,000 km.

From 2014, Eletronorte and State Grid Brazil Holding (hereinafter referred to 'SGBH') made a joint effort to carry out the application research of UHV AC in Brazil. The research project involved technical exchange with the State Grid Corporation of China, which allowed the sharing of the experience gained in the implementation of the 1,000 kV AC system in China. In May 2017, at the office of SGBH in Rio de Janeiro and in September 2017 at the Ministry of Mines and Energy in Brasilia, seminars were held to disseminate the results of the research that gave rise to this book.

It is concluded that the UHV AC power transmission at 1,000 kV is an available alternative technology for long-distance transmission, especially for multi-point scenarios. It is observed that losses in 1,000 kV AC are considerably smaller than the losses in the 500 kV systems. Another intrinsic feature, which contributes favorably to large interconnections in this voltage class, is the almost immunity to outages due to lightning strikes, which results in a stronger interregional interconnection.

Besides, it is pointed out that the challenges in building the 1,000 kV AC transmission projects are not very different from those of the ± 800 kV projects of the transmission system for the Belo Monte power plant. In 2017 the

first UHV DC project developed jointly by SGBH and Eletrobras went into operation. Exploration of the synergies between UHV AC and UHV DC is becoming a reality for the expansion of the integrated network.

Another essential aspect is the technological maturity of the industrial capability based in Brazil of four major manufacturers that supplied equipment for the implementation of the 1,000 kV AC system in China, as well as the design and construction companies of lines and substations with recent experiences in ± 800 kV transmission projects.

The potential renewable generation capacity in the north of Minas Gerais and the interior of Bahia, suggests that a second 1.000 kV circuit from Ourolândia to Pirapora should be studied, including an extension with two circuits to Belo Horizonte. These studies should include optimization of the location close to Belo Horizonte, and possibly the use of a double circuit tower in this section.

Therefore, the necessary conditions for the implementation of UHV AC in the Brazilian Electric System are fully available for the planning of the transmission expansion in the face of surplus energy availability in the Northeast and demand, load or storage, in the Southeast. Further, State Grid is even more willing to share with Brazil the mature experience that China has accumulated in the field of UHV and its related practices.

Cai Hongxian

Roberto Parucker

Executive Summary

José Antonio Jardini
Sergio de Oliveira Frontin

This book presents details of the research project "Ultra-High-Voltage Transmission in the Brazilian Interconnected Power System." The project was financed with resources from the ANEEL's R&D program, commissioned jointly by Eletrobras Eletronorte and *State Grid Brazil Holding*, with a duration of three years. It has been developed by Fundação para o Desenvolvimento Tecnológico da Engenharia (FDTE), Instituto Técnico de Automação e Estudos Elétricos (ITAEE), and by Indústria Eletromecânica Balestro (Balestro).

The assessment was focused on the technical and economic performance of a system with a voltage higher than 800 kV, in alternating current, to be used in the expansion of the Brazilian electric system and to facilitate the integration of renewable power generation (wind and solar) into the Brazilian electric system.

The 1,000 kV system was conceived in its first stage to serve the regions of Milagres (Ceará - CE), Ourolândia (Bahia - BA), Igaporã (Bahia - BA), and Pirapora (Minas Gerais - MG), with four 1,000/500 kV substations, and three transmission lines with about 440 km each. The Ultra High Voltage (UHV) system should have flexibility to export an excess power of about 5,000 MW from renewable generation located in the states of Ceará, Bahia, and Minas Gerais. This excess power is foreseen in the 500 kV grid as part of the 2024 Ten-Year Expansion Plan of the Empresa de Pesquisa Energética (EPE).

The UHV system can be upgraded by adding a second circuit from Ourolândia to Ribeirão das Neves (Minas Gerais - MG) and export another 5.000 MW of wind and solar power generation available in the interior of Bahia and Minas Gerais.

The assessment for its insertion is based on the methodology used by EPE and is documented in the reports termed as R1, R2, R3, and R4.

In Chapter 1, *Perspectives of Application of 1,000 kV AC Transmission Systems in Brazil*, an overview of the power demand expansion in Brazil, and the need to consider transmission voltages higher than 800 kV is presented.

The solution studied was a transmission corridor from the South of the state of Ceará to Minas Gerais, passing through Bahia. The project is consistent and adherent with the planning methodology practiced in Brazil.

Chapter 2, *History of Alternating Current Ultra-High Voltage Power Transmission Current Applications and Experiences*, shows the evolution of the transmission voltages in the Brazilian electric system, whose base voltage is now 500 kV, including a 765 kV system to transmit part of the power generated in the Itaipu hydroelectric power plant. It also presents the global evolution of the application of high and extra high voltages, addressing also pilot projects with voltages higher than 800 kV developed in the 1990s, later referred to as Ultra-High Voltage. In particular, it discusses practical applications of 1,000 kV voltages (1,100 kV maximum) concluding with the recent application of the 1,000 kV system in China. By the end of 2017, more than 10 thousand kilometers of 1,000 kV circuits will be in operation in China with 141 thousand MVA of transformation capacity and a clear standardization of SF_6 gas insulated switchgears (GIS).

Chapter 3, *Analysis of Scenarios for the Application of 1,000 kV in the Brazilian Interconnected Power System*, presents a research on a suitable route for the implementation of the 1,000 kV system within the Ten-Year Expansion Plan of the Brazilian system. This route might be considered for the implementation of a pilot line, or even a definitive one, regarding the current technology, especially that from China, India, and Japan.

The possibility to replace 500 kV lines with a 1,000 kV system required for the hydraulic generation expansion of the Amazon region and in the North-South interconnection, was in this chapter addressed. It was also examined the option to provide a ring, which could distribute energy along the main Northeastern capitals, or to connect the HVDC terminals of the Southeastern region. Last, it was identified the economic potential of the 1,000 kV system in the Northeastern region which has a big expansion potential for renewable sources of power.

Chapter 4, Technical, Economic and Socio-Environmental Feasibility Studies *(R1)*, presents the studies usually required by EPE for the preparation of the R1 report, including power flow, electromechanical stability; short-circuit analysis, and economic comparisons with alternatives in 500 kV or in direct current with multiterminal arrangement. It also presents a preliminary analysis of the socio-environmental impact of the project.

Chapter 5, *Detailed Studies of the Reference Alternative (R2)*, presents the details of the studies for the elaboration of the R2 report, which addresses electromagnetic transients and stability analysis. These studies were used for the detailed design of the 1,000 kV towers, their foundations, and for the specifications of the line conductors and equipment at the substations.

Chapter 6, *Socio-environmental Characterization and Analysis of the Project Alternative (R3)*, presents details of the socio-environmental impact assessment of the UHV system. A 30 km wide corridor was then defined, in which a possible route for the lines was located, avoiding areas of greater socio-environmental impact, or which presented implementation difficulties.

Chapter 7, *Characterization of the Existing Grid. Interface with the 1.000 kV System (R4)*, identifies the characteristics of the existing substations that may connect the 1,000/500 kV substations. The existing installations mentioned refer to the current stage of the substations and lines, which require timely upgrades in the event of an actual auction process.

Chapter 8, *Transmission Project Auction Process*, presents a description of issues like the businesses structure in the electric power area, auctions, contracts, and regulatory responsibilities in Brazil. The introduction of a 1,000 kV system is a technological innovation in the country, and there are expectations as to the adequacy of some requirements and procedures, such as deadlines, warranties, and penalties, compatible with the innovation characteristic, so as not to discourage the interest in the auctions of projects for the implementation of the system.

In Chapter 9, the Complementary Investigations deemed necessary for this R&D project are presented. The studies required in the R1, R2, R3 and R4 planning stages were presented in previous chapters and demonstrated the technical and economic viability of the project compared to other transmission alternatives.

It is estimated that the start-up of the initial stage would be 2025/2026. Assuming about four years for the implementation of the system, the project should be put into auction, as a transmission project, in 2021/2022. Therefore, it is foreseen that the complimentary research and in-depth related studies for this transmission alternative should be carried out in 2018 and 2019.

In this context, the main objective of this chapter is to present the complementary investigations considered necessary due to probable changes in the assumptions initially adopted, changes in scenarios and, mainly, due to new information to be received from equipment manufacturers and from State Grid related to the experience of its UHV systems currently in operation. In this way, the UHV system proposed would be inserted in the National Interconnected System in a safe, reliable and economical manner.

Finally, some further economic feasibility analyses are expected to be carried out considering updated costs from manufactures. There are expectations of the inclusion of this alternative in the next Ten-Year Expansion Plan, thus, sanctioning this new technology for transmission concession auctions. We understand that this is a fair conclusion for this R&D project developed with public resources.

Thanks are due to the Agência Nacional de Energia Elétrica (ANEEL), for the timely public call to develop a research on the Ultra-High Voltage technology, to Eletrobras Eletronorte and *State Grid Brazil Holding* for the continuous technical and managerial support, and to EPE and ONS, for the reviews and contributions throughout the development of the project.

CHAPTER 1

Perspectives for the Application of 1,000 kV AC Transmission Systems in Brazil

José Antonio Jardini
Patrícia Oliveira da Silveira

Aneel Research and Development Program.
Executors: FDTE, ITAEE, Balestro. proponents: Eletrobras Eletronorte, State Grid Brazil Holding.

1. Introduction

The Brazilian electric system is supplied mainly by hydroelectric plants, and some thermal generation. There is great potential for wind and solar power generation in the Northeastern region of Brazil, mainly on the coast of Rio Grande do Norte and Ceará, and in the central area of Bahia, locations that are distant from the main load centers, which are located mostly in the Southeastern region where reservoir level recovery is a relevant strategy. On certain occasions, the power generated by the wind power plants should be used at its maximum capacity, and allow for the reduction of hydroelectric power generation and recovery of the southeast region's reservoirs. Therefore, it will be necessary to transfer large blocks of the generated power to the Southeastern region of the country.

A R&D project, financed by Aneel's program, has been developed to evaluate the technical and economic feasibility of a transmission system between the Northeast and the Southeast at 1,000 kV, alternating current. The 1,000 kV interconnection studied transmits over 3,000 MW at the peak demand, under normal conditions. An economic comparison was made among several transmission alternatives and various transmission levels, including Direct Current transmission (HVDC). From this analysis, i.e. investment costs plus Joule losses, the alternative at 1,000 kV presented the lowest global cost. The 1,000 kV transmission system is a very attractive alternative for the interconnection, in addition to the fact that the existing 500 kV system may come to be surpassed in its capacity with the expansion of the wind and solar power generation.

Currently, there are some projects installed in China at this voltage level whose total length account for more than 10,000 km of circuits (single and double), demonstrating the feasibility of the 1,000 kV alternative, in addition to some other advanced studies in Japan and India. With regards to equipment, at least four large Brazilian transformer and reactor manufacturers have access to the technology to meet this need. The 1,000 kV alternative in Brazil was studied in terms of power flow and stability, both under normal operation conditions and under emergency conditions of the 500 kV trunk system, meeting the system expansion planning criteria. Considering the 2024 expansion horizon, some emergencies near the 1,000 kV line were also simulated. The referred criteria for such a conditions were duly met. The project also advanced with regards to the transient overvoltage and insulation coordination studies for the specification of substation equipment and transmission line design.

2. Brazilian System Year 2015

2.1 Generation and Load

The power generated, average load and maximum load per region in Brazil for the year 2015 are presented in Table 2.1. The referred year was an unusually dry year. The installed capacity for the same year is presented in Table 2.2.

Table 2.1: Generation (average MW), Load (average MW) and Peak Load (MW)

Generation	N	NE	SE	S	Total
Hydraulic	5,000	3,000	16,300	19,500	43,800
Thermal (fossil)	2,300	3,500	7,000	1,600	14,400
Nuclear			1,700		1,700
Wind		300	500		800
Total	7,300	6,800	25,500	21,100	60,700
Load (including losses)	5,000	9,700	36,000	10,000	60,700
Peak Load	6,500	12,300	51,500	16,600	~85,000

Source: ONS

Table 2.2: Installed generation capacity (2015)

Type	GW
Hydro	95
Thermal (Fossil)	20
Nuclear	2
Biomass	11
Wind	5
Total	133

Source: ONS

Notes:
1. The hydroelectric power generation includes small plants.
2. Thermal (fossil): 1/3 conventional, 2/3 in emergency with high operational cost, activated only at very dry times, when the level of the reservoirs is low.
3. Biomass: sugar cane and wood, has a seasonal characteristic, operated 60% of the time.

As can be observed in Table 2.1, the load is mostly concentrated in the Southeastern part of the country – Rio de Janeiro, São Paulo and Belo Horizonte. In 2015, the South and North had a net power export, while the Southeast and Northeast regions imported power. Some large hydroelectric power plants are concentrated in the hydrographic basins: Grande, Paranaíba, Paraná, São Francisco River and also on the right margin of the Amazon River. The latter having a high potential for power expansion.

2.2 Generation Expansion

The generation expansion (2024) considers the following blocks of power:

Table 2.3: Generation Expansion (2024)

Type	GW
Hydro	30
Thermal (Fossil)	10
Biomass	8
Wind	20
Photovoltaic	7
Total	75

Source: EPE, PDE 2024

The future hydroelectric power plants are located on the tributaries of the Amazon River, far from the load centers. Thus, direct current transmission systems become a more attractive means of power transmission. Other types of power generation are spread throughout the country and a large portion of the wind and solar power generation is located on the coast and in the central area of the Northeastern region.

It is known that wind power and other intermittent generation sources will play an important role in the future of the Brazilian electric system, the expansion of which is in conformity with the international environmental protection agreements. Therefore, one must understand that the generation potential is in regions where this potential is larger than the load. This means that the excess power must be transmitted to a neighboring region. The load forecast for the Northeast region indicates that there will be a power increase of approximately 5 GW, while the generation expansion for this region may exceed 20 GW, which allows the export of about 15 GW excess power to the Southeast, the largest consuming center in the country.

The areas with large wind power potential are shown in Figure 2.1 (red ellipses). The solar power potential covers almost the same areas. In Figure 2.1, the location of the proposed 1,000 kV system (green line) can be seen. In the 1,000 kV alternative, there are two intermediate substations, the function of which is collecting the exceeding wind and photovoltaic power from the Northeastern region and transmitting it the Southeastern region.

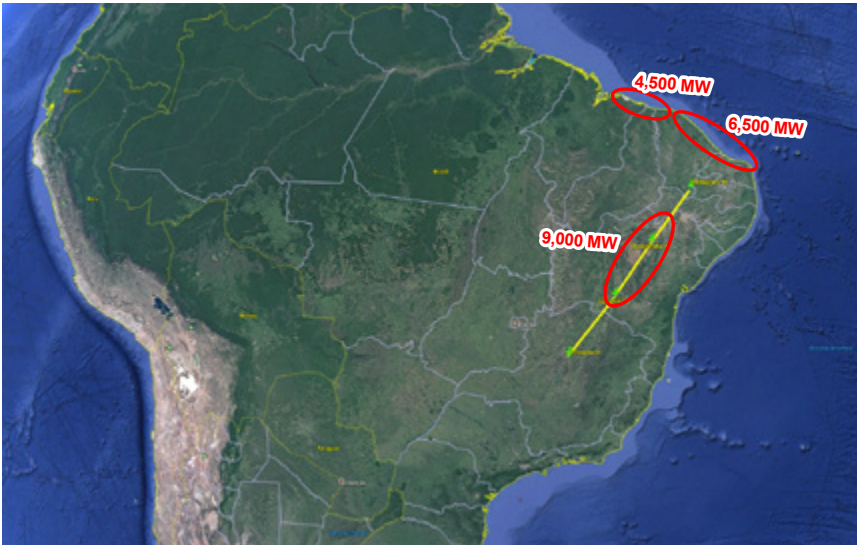

Figure 2.1: Wind potential (Northeastern Region)

2.3 Transmission

The grid of the Brazilian transmission system, where the 1,000 kV interconnection is being studied, is indicated in Figure 2.2, for the year 2015, as an example. The system is composed, mainly, of 500 kV lines, in addition to 230 kV, 345 kV, 440 kV, 765 kV lines, and also includes direct current systems at ±600 and ±800 kV. In the space of 10 years, a significant expansion in the system is foreseen, limited, however, to the same existing voltage levels. The implementation of a 1,000 kV Alternating Current Ultra-High-Voltage line for long distance transmission would constitute a pioneering mode of transmission in Brazil and the western countries.

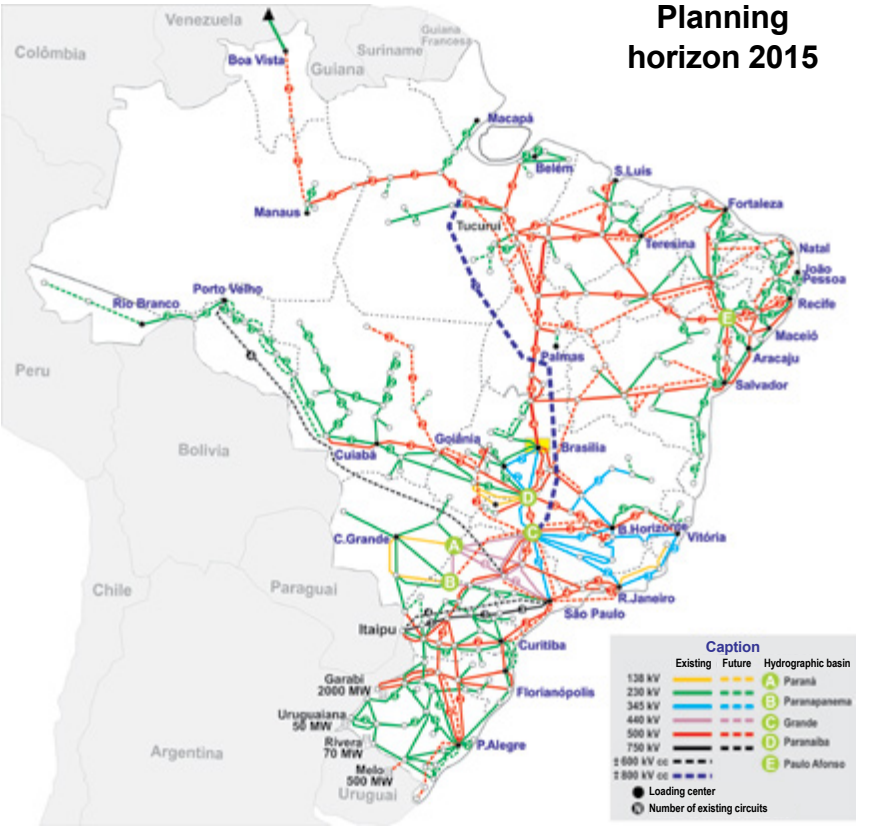

Figure 2.2: Brazilian Transmission System (source ONS)

3. Economic Transmission System

In a recent research, an economic evaluation study was conducted on AC and DC systems [1], [2] which included ten direct current lines at different voltages, from ±300 kV up to ±800 kV, from 2 to 6 conductors, with line length of up to 3,000 km, and ten alternating current lines with voltages equal to 500 kV, 765 kV, and 1,000 kV, from 4 to 8 conductors.

These configurations were used to estimate the unit cost of the lines, *Cl*, and adjust it in a regression equation, as follows:

$$Cl = a + b\,V + N\,S\,(c\,N + d) \qquad (\$/km)$$

Where:
a, *b*, *c*, *d* are regression parameters (different for AC and DC).
V is the maximum voltage.
N is the number of conductors per bundle.
S corresponds to the aluminum cross section (ACSR) of a conductor.

The cost of equipment, series and shunt compensation were updated based on Aneel's Price Database. By adopting some assumptions, such as angle of voltage across the line and percentage of parallel reactive compensation, we obtain the investment costs in reactive compensation. With the investment values and the costs of the losses in a period of time, we obtain the cost of the system. This was done for several voltage combinations, line lengths, and voltages. The values for Alternating Current (AC) and Direct Current (DC), and the break-even point between AC/DC are presented in Figure 3.1.

According to the assumptions adopted in this study, it was verified that a point-to-point AC transmission was more economical for distances close to 1,200 km; and that, in the case of transmission blocks equal to, or higher than 3,000 MW, the 1,000 kV AC system was better than the 500 kV (limited to transmission levels of about 1,500 MW). The expansion of the system in 765 kV, in terms of power flow increase, would not be enough and, therefore, the 1,000 kV was very promising to transmit, for example, wind and solar power from the Northeastern to the Southeastern region.

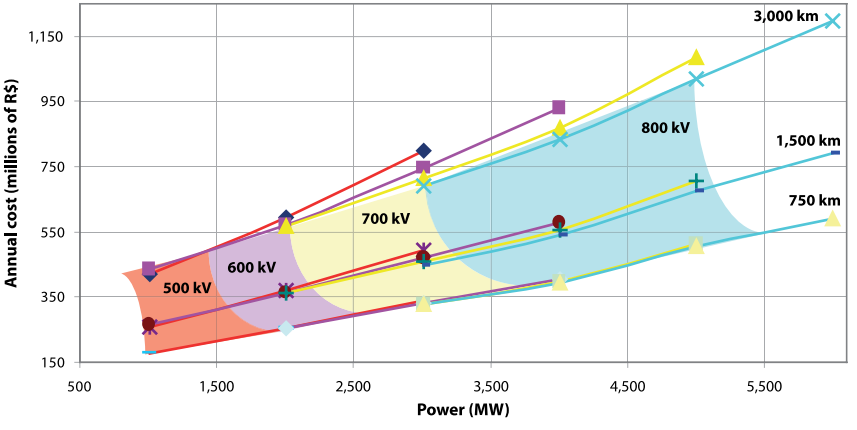

(a)

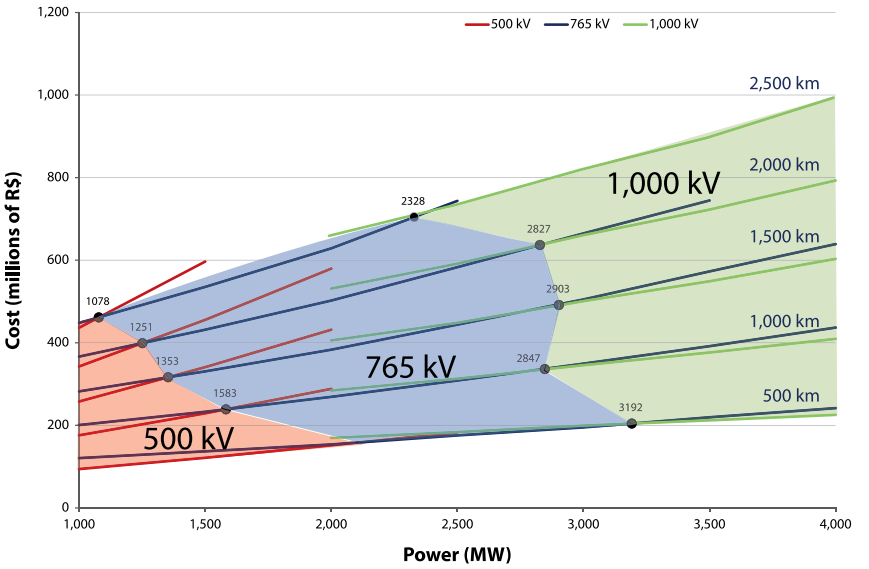

(b)

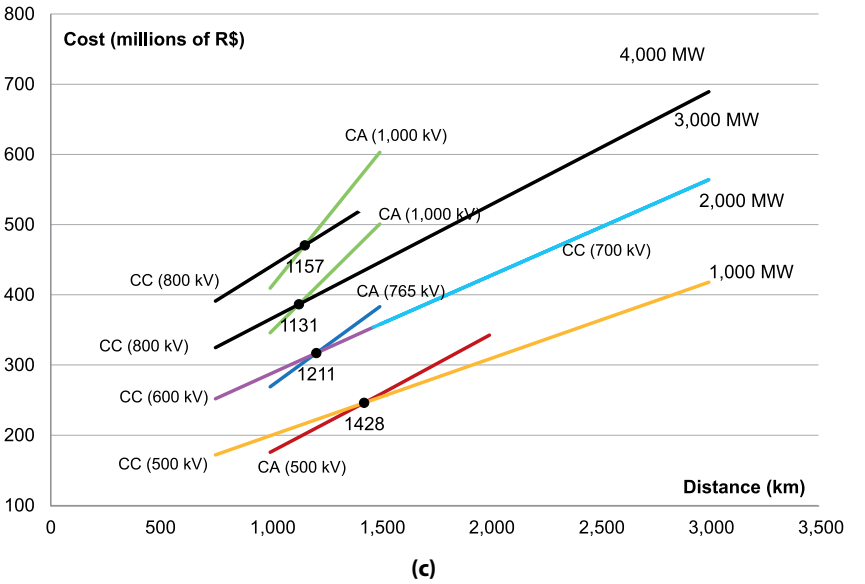

(c)

Figure 3.1: Economic transmission system: (a) DC; (b) AC; (c) break-even length

4. Insertion of the 1,000 kV System

The new hydroelectric power plants in the Amazon Region, without reservoirs to prevent the flooding of large areas, can be dispatched directly from the water flow in the rivers (run-of-river hydroelectric plant). The wind and solar power are intermittent generation systems and, therefore, voltage regulation must be done using one of the hydraulic power sources out of the Amazon region, which in turn depend on the precipitation rate (rain).

The transmission restriction and the delays in the start of operation of the hydroelectric power plants under construction, together with a period of very low rainfall in the Northeastern and Southeastern regions, lead the existing reservoir storage to very low levels (critical operations). In this situation, the emergency thermal generation had to be dispatched to save the water in the reservoirs, at a high power cost. In the next few years, this power generation scenario will depend both on wind and solar power generation, as well as on rain.

Thus, these restrictions are indications of scenarios with reduced hydroelectrical generation, and large expansion of wind/solar generation. In a probable dispatch of generation for the year 2024, a large transfer of energy from the Northeastern region to the Southeastern region is foreseen and, under these conditions, the 1,000 kV system will be essential for the operation of the grid.

The 1,000 kV system studied is composed by three sections of 440 km each. The lines have 50% series compensation and 85% shunt compensation, divided equally between each end terminal of each line section. The line is designed for about 4,000 MW and has 8x795 MCM *Tern* ACSR conductors, ~ 400 mm^2, with 45.7 cm spacing among conductors. Two types of towers are being considered in the design, a self-supported tower and a guyed mast tower. The study was done based on the EPE 2024 expansion planning which showed that it would be an additional expansion of 5 GW of renewable generation coming from the Northeastern region.

The 1,000 kV system, in addition to being technically feasible, proved to be very flexible with the intermediate substations collecting the excess generation along its route. This flexibility also includes the ease of expansion to meet a generation expansion scenario much higher than the initial one.

On the other hand, the line conductors can still be economical even for a 5 GW line flow, with a lower loss factor [11] than the one adopted in the project, and, during emergency or temporary conditions, it can transmit a little more power with reinforcement of the local 500 kV system (plus a possible adjustment of the series compensation).

The proposal for the insertion of the 1,000 kV AC transmission refers to a line interconnecting the Milagres substation, in Ceará, to the Pirapora substation, in Minas Gerais, with two intermediate substations: Ourolândia, and Igaporã, both in the state of Bahia. The expansion of this system all the way to the region of Belo Horizonte, with the addition of a second circuit from Ourolândia to Pirapora and a fourth double circuit section down to P. Neves, allows the transmission of an additional 5 GW during the peak hours in the Southeastern region. This additional power comes from renewable generation in the interior of the state of Ceará, in the central area of Bahia, and in the north of Minas Gerais.

5. Reliability

The 1,000 kV alternative was studied for the year 2024 in terms of power flow and stability, and met the system expansion criteria, with potential to export an additional 5 GW of renewable generation. The interconnection at 1,000 kV in four substations in a single circuit has proven to be robust, meeting the n-1 transmission planning criterion even for the section with the heaviest load. The 500 kV emergency lines close to the 1,000 kV system and the sections of the 1,000 kV line were evaluated for the 2024 expansion planning configuration. The emergency criteria imposed, voltage range and load of the system components were properly met.

6. Economic Feasibility

For the economic feasibility evaluation of the 1,000 kV system with three sections of 440 km each, and one circuit per section, comparisons were made to the following alternatives:

- 500 kV system with three sections of 440 km each, two lines per section, and 40% series compensation (capacitor).
- Multiterminal DC system with VCS converters, ±600 kV, with three sections of 440 km each.
- Point-to-point DC system of ±800 kV.

The results and analyses done as a result of this comparisons will be presented in detail in Chapter 4.

7. Conclusions

Wind power and other types of intermittent generation will play an important role in the future expansion of the Brazilian electric system. These power plants will be located in regions with excess generation and, therefore, a system capable to transmit large blocks of power to regions with higher demand is needed. In this context, the 1,000 kV system is an alternative with technical and economic advantages, in addition to having the flexibility for future expansion.

8. References

[1] SANTOS, M. L.; JARDINI, J. A.; CASOLARI, R. P.; VASQUEZ-ARNEZ, R. L.; SAIKI, G. Y.; SOUSA, T.; NICOLA, G. L. *Power Transmission Over Long Distances: Economic Comparison between HVDC and Half-Wavelength Line*. IEEE, PWRD, 2013.

[2] NOLASCO, J. F.; JARDINI, J. A.; GRAHAM, J. F., et all. *Impacts of HVDC Transmission Lines in the Economics of HVDC Systems*. CIGRE TB-388, 2009.

[3] SANTOS, M. L.; JARDINI, J. A.; MASUDA, M.; and NICOLA, G. L. C. *A Study and Design of Half-Wavelength Lines as an Option for Long Distance Power Transmission*. In: IEEE Power Energy Soc. Trondheim PowerTech, Trondheim, Norway, 2011.

[4] SANTOS, M. L.; JARDINI, J. A.; MASUDA, M.; and NICOLA, G. L. C. *Electrical Requirements for Half-Wavelength Power Transmission Line Design*. In: Proc. IEEE/Power Energy Soc. Transm. Distrib. Conf. Expo. LatinAmerica, 2010, pp. 486–490.

[5] JARDINI, J. A., et all. *Projeto Transmitir, Alternativas não Convencionais para Transmissão de Energia Elétrica*. Estudos Técnicos e Econômicos, Ed. Teixeira, pp: 368, 2012

[6] JARDINI, J. A.; SILVEIRA, P. O.; PEDROSO, F. R. V. A.; NICOLA, G. L. C.; GRAHAM, J. F. Electromagnetic Transients in a 1.000 kV system. Part I - Modeling and arc extension. In: *2016 IEEE PES Transmission & Distribution Conference and Exposition Latin America* (T&D LA), Morelia, Sept. 21-23, 2016. Available at: <http://ieee-tdla16.org/>.

[7] JARDINI, J. A.; SAIKI, G. Y.; BASSINI, M. T.; NICOLA, G. L. C.; GRAHAM, J. F. Electromagnetic Transients in a 1,000 kV System: Part II – Line Energization, Reclosing and Insulation Coordination. In: *2016 IEEE PES Transmission & Distribution Conference and Exposition Latin America* (T&D LA), Morelia, 21-23 sept. 2016. Available at: <http://ieee-tdla16.org/>.

[8] JARDINI, J. A.; BASSINI, M. T.; VASQUEZ-ARNEZ, R. L.; FRONTIN, S. O.; NICOLA, G. L. C.; GRAHAM, J. F. Electromagnetic Transients in a 1,000 kV System: Part III - Fault Inception, Cleaning and Load Rejection. In: *2016 IEEE PES Transmission & Distribution Conference and Exposition Latin America* (T&D LA), Morelia, Sept. 21-23, 2016. Available at: <http://ieee-tdla16.org/>.

[9] VASQUEZ-ARNEZ, R. L.; JARDINI, J. A.; NICOLA, G. L. C.; ROSE, E. H.; GRAHAM, J. F.; GUIJUN, L. Energization Study of an Ultra High Voltage Power Transformer Aimed at Connecting a 1.000 kV Line into the Brazilian Power Grid. In: *XVII Encuentro Regional Iberoamericano de CIGRÉ* (XVII ERIAC), Ciudad del Este, May 21-25, 2017.

[10] JARDINI, J. A.; VASQUEZ-ARNEZ, R. L.; FRONTIN, S. O.; NICOLA, G. L. C.; ARAUJO, M. C. de; GRAHAM, J. F.; GUIJUN, L. Basic Design of a 1.000 kV AC Line to Transmit Power from the Northeast to the Southeast Region of Brazil. In: *XVII Encuentro Regional Iberoamericano de CIGRÉ* (XVII ERIAC), Ciudad del Este, 21-25 de mayo, 2017.

[11] SILVEIRA, P. O.; JARDINI, J. A.; SAIKI, G. Y.; NICOLA, G. L. C.; MACHADO, V. G.; JESUS, J. F. de; PICCIRILI, R. L. M.; GRAHAM, J. F.; GUIJUN, L. Viability of Insertion of a 1.000 kV System into the Brazilian Network. In: *XVII Encuentro Regional Iberoamericano de CIGRÉ* (XVII ERIAC), Ciudad del Este, 21-25 de mayo, 2017.

[12] L. Zhenya. *Ultra-High Voltage AC/DC Grid*. Elsevier Academic Press, 2014.

[13] XIAN, Zutao; LIN, Jiming; BAN, Liangeng; ZHENG, Bin. Investigation of TRV across Circuit-Breaker of Series Compensated Double-Circuit UHV Transmission Lines. *2010 International Conference on Power System Technology*, Hangzhou, 2010.

[14] YUAN, Jun; YU, Zhanqing. Lightning Shielding Protection Design and Actualization of 1000 kV UHV AC Overhead Transmission Line in China. *2010 Asia-Pacific Symposium on Electromagnetic Compatibility* (APEMC), 2010. pp. 1578 - 1581. DOI: 10.1109/APEMC.2010.5475687.

CHAPTER 2

History of Ultra-High Voltage Alternating Current, Experience and Applications

José Antônio Jardini
Sergio de Oliveira Frontin
John Francis Graham
Liu Guijun

1. Introduction

This chapter presents the evolution of power-transmission voltage levels nationally and internationally with a historical summary of the Ultra-High Voltage Alternating Current (UHV AC) applications. It also presents the current aspects of the *State Grid Corporation of China* (SGCC), its experience in the planning and operation of transmission systems at this voltage level.

The transmission systems to carry power from the generation sources to the consumption centers have evolved technologically through time. The aim is to increase the power transmission ratio per right-of-way while observing the system's global economic optimization, design and planning criteria as well as the environmental impacts. Among the possible alternatives to comply with these assumptions it can be mentioned the upgrading and uprating the existing lines, using special conductors, converting alternating current to direct current lines, or simply by increasing the current or voltage levels. In this context, a summary of the voltage evolution at the planning stage of the Brazilian electric system, comparing the levels used in Brazil with the evolution of voltage levels at a global level and, especially in China, is presented.

It is important to mention that in 2016, the *International Electrotechnical Commission* (IEC) established the IEC TC 122 – UHV AC Transmission System Committee, which presented the following scope:

> *Standardization in the field of AC transmission technology for highest voltage of the system exceeding 800 kV, particularly the preparation of systems-oriented specifications such as those for planning, design, technical requirements, construction, commissioning, reliability, availability, operation and maintenance. Development of processes for specifying requirements and demonstrating where the required performance of UHV systems is assured.*

Thus, the Ultra-High Voltage is defined as the maximum system voltage level exceeding 800 kV and, upon this premise; IEC recommends the levels of 1,100 and 1,200 kV as the maximum voltage for specification and standardization of equipment in this modality of transmission.

2. Evolution of Power Transmission System Voltage Levels in Brazil

In Brazil, until the 50s, there were systems that could be classified as isolated. Examples of these systems are those related to the power plants of the Paranapanema River, Tietê River, Henry Borden, and Paraíba River; the latter supplying power to cities like São Paulo and Rio de Janeiro.

The first systems exceeding 230 kV (maximum voltage 245 kV) were Três Marias, Belo Horizonte, and Furnas, connected to São Paulo, Rio de Janeiro, and Belo Horizonte, at the 300, 345, and 362 kV levels. Another isolated system that can be include is the Jupiá power plant 440 kV (460 kV) which supplied power to São Paulo.

During the 60s, the electric sector opted for an integrated planning and for the interconnection of the Brazilian electric system. It was then when the Comitê de Estudos Energéticos da Região Centro-Sul (Committee for Power Studies of the Central-Southern Region) was created, aiming to plan power supply systems for the states of Minas Gerais, Rio de Janeiro and São Paulo. Through an international consulting company called Canambra (Canada-America-Brazil), the study was organized into three groups: power and hydrology, in Belo Horizonte; basic power plant project, in São Paulo; and transmission project, in Rio de Janeiro, coordinated respectively by Cemig, Cesp, and Furnas.

The first joint planning for the power system (elaborated in 1964) defined the power generations and lines for the upcoming years 1970, 1975, and 1980. The transmission study was coordinated by specialists from the *Tennessee Valley Authority* (TVA), an American company.

This group proposed the elimination of some voltages, such as 300 kV, 180 kV, 88 kV, and an evolution with two transmission alternatives, 500 kV (550 kV) and 440 kV (460 kV), were studied.

Although the transmission at 440 kV presented a marginal economic advantage, the expansion at 500 kV was chosen because it differed from the European Standard Standardization, 400 kV (420 kV). However, the 440 kV (460 kV) voltage was maintained for the expansion of Cesp's grid.

Following this planning, they proceeded with the construction of the lines associated to the plants on the Grande, Paranaíba, and Paraná Rivers.

The Itaipu and Ilha Grande plants were at the limit of the planning horizon, and their transmission system design was elaborated in the 1970s.

Itaipu's power volume and distance justified the use of higher voltages, 765 kV (800 kV) in AC (Alternating Current), initially with five lines up to São Paulo. The final design included three AC lines and two DC bipoles (±600 kV each). The 500 kV (550) kV alternative, although studied, did not show to be economically viable.

As soon as the planning for the Central-Southern region was completed, the planning for the Southern region was elaborated (Paraná, Santa Catarina, and Rio Grande do Sul).

In the 1980s, the transmission planning was conducted by Eletrobras, through the Grupo Coordenador de Planejamento do Sistema (GCPS - System Planning Coordinating Group), which evaluated the evolution of the Brazilian electric system up to the year 2000. During this period, when the hydropower potential of the Southeastern region was exhausted, some studies began on the development of power plants on the tributaries of the Amazon River, starting with the Tucuruí Plant, via the Comitê de Planejamento da Transmissão da Amazônia (CPTA - Amazon region Transmission Planning Committee). Simultaneously, and as a complementary action, Chesf/Eletronorte created the H2000 group to evaluate the expansion of their systems for the inclusion of power generated in the Amazon region.

These groups studied the transmission systems for the plants located in the Araguaia-Tocantins, Tucuruí, Xingu, Belo Monte, Tapajós, and Itaituba Rivers, among others. During this period, the 500 kV N-NE and N-S interconnections were designed. Voltages exceeding 500 kV (550) kV AC and higher than ±600 kV DC were considered, following the expansion trend in other parts of the world.

Such a committee observed that the transmission at 765 kV (800 kV) would not bring any significant benefit when compared to, say, a 500 kV transmission system, and that the transmission at ±800 kV DC would be more interesting in terms carrying bulk power and long-distance flexibility, for distances over 1,200 km.

On the other hand, the evolution of researches related to 1,000 kV voltages conducted around the world were also monitored. Subsequently, EPE (Empresa de Pesquisa Energética) considered this voltage level as one of the alternatives for the power transmission from the Madeira, Santo Antônio, Jirau and Belo Monte power plants.

In summary, the following timeline related to the evolution of voltage levels in Brazil was elaborated:

- 230 kV – 1954
- 345 kV – 1960 – 6 years later
- 440 kV – 1971 – 11 years later
- 500 kV – 1975 – 4 years later
- 765 kV – 1982 – 7 years later
- ±600 kV DC – 1984 – 2 years later
- ±800 kV DC – 2018 – 34 years later

It is interesting to observe that the highest voltage level currently in operation in Brazil refers to 765 kV AC (Itaipu power plant AC system), and ±800 kV (Belo Monte power plant DC system) which started its operation 34 years after the ±600 kV DC voltage at Itaipu began.

3. Evolution of Power Transmission System Voltage Levels at a Global Level

Various AC voltages for transmission are used around the world, and some examples are shown below.

In the United States of America, 345 kV (362 kV) is largely used. During the 60s, there were already several 500 kV (550 kV) lines, and some 765 kV were built in the 70s by AEP (*American Electric Power*) and the *Commonwealth Edison*. In Canada, Hydro Quebec uses voltages at the 330 kV (345 kV) and 735 kV levels, the latter since the 60s.

In Europe, the basic voltage for transmission is 400 kV (420 kV). In Japan, the 500 kV (550 kV) voltage is used since the 60s, and in China there are projects at 500 kV (550 kV) and 765 kV voltages. In India, there are voltages at 400 kV (420 kV) and 765 kV (800 kV).

During the 80s, many researches have been conducted regarding the 1,000 kV (1,100 kV) voltage level, and some even to 1,500 kV. Large research centers, such as CESI (Italy), *Les Renardieres* (France), IREQ (Canada), KEMA (Holland), GE Pittsfield (USA), among others including the USSR and Japan, and manufacturers such as ABB, Siemens, GE, Alstom, Toshiba, Mitsubishi and Hitachi were used to this aim. Some of these initiatives were:

3.1 United States of America

The American Electric Power (AEP), in partnership with ABB, developed several studies and tests on transmissions up to 1,500 kV. In a station located in South Bend (Indiana), a test line with one phase and three sections of 305 m each was built.

The Bonneville Power Administration (BPA) effectively built a pilot station at 1,200 kV (2.1 km), in Lyons (Oregon), to investigate the technical and economic feasibility and possible environmental impacts at this voltage level.

The *General Electric* (GE) company, in partnership with the *Electric Power Research Institute* (EPRI), implemented a short experimental line, a corona testing cage, and a testing chamber for insulation under pollution.

These projects produced an enormous amount of information, leading to the conclusion that there would be no obstruction to the evolution of this voltage level [5, 7].

Although the scientific contribution to the current subject has been exceptional, we must highlight that in the United States there is no immediate intention of using this voltage level (exceeding 800 kV), with a preference for expanding their grid by reinforcing the current 765 kV system, and implementing direct current interconnections.

3.2 Italy

The 1,050 kV AC alternative for planning the expansion of the transmission system was envisioned by Italy in 1970. The objective was to connect 3 or 4 high-capacity power plants to load centers distant 200-250 km. The studies conducted suggested that two 1,050 kV lines would be a reliable and economically acceptable solution. Bearing this in mind, Italy initiated a series of studies and researches implementing laboratories and test lines to obtain some inputs, aiming at the specification and manufacturing of lines, equipment, and substations [5]. This project, though, was interrupted due to the lower load demand than the threshold expected, and new generation technologies indicated that the most adequate solution would be the use of distributed medium sized sources, instead of high-capacity sources located in a single place.

It is also worth mentioning that the researchers involved in this project published useful information on the investigations conducted which constitute important contributions to the implementation of this modality of transmission.

In 1993, the Italian company *Ente Nazionale per La Energia Elletrica* (Enel) completed its 1,050 kV pilot-test station in Suvereto. This pilot

project comprised a 2.8-km, 1,050 kV line, single-phase transformers (420/1,050 kV of 400 MVA each), and SF_6 based switchgears. Also, a test line was implemented in the Passo de Pradarena, which was used for aeolian vibration, wind and snow load, galloping, and spacer performance tests.

CESI's (*Centro Elletrotecnico Sperimetale Italiano*) laboratories, in Milan, conducted studies and tests related to phase-to-phase and phase-to-ground insulation support, insulator pollution, selection of conductor bundles, unconventional towers, foundations, etc. [7].

3.3 Russia

With the aim of transmitting power from Siberia to the central region of the country, Russia (then USSR), designed a 1,150 kV transmission system. This system, composed by two lines, linking Ekibastuz – Kokchetav (500 km) and Kokchetav – Kustanay (400 km) in Kazakhstan, was commissioned during 1982-1988. These lines operated for about two years at 1,150 kV; subsequently, started operating at 525 kV. This change was caused by the dissolution of the Soviet Union, in 1991, which partially interrupted the operation of some regional interconnections. It was also affected by the economic crisis that resulted in a significant reduction of energy demand. In this scenario, the UHV transmission became inefficient and the system started operating at 525 kV. Later, based on such an experience acquired, over 1,000 km of 1,150 kV lines were built which are still in operation at also 525 kV [5].

3.4 Japan

In the mid-70s, the Japanese company *Tokyo Electric Power Company* (TEPCO) studied the expansion of its 550 kV transmission network. Keeping on mind right-of-way restrictions, Tepco decided to invest in transmission alternatives such as double-circuit 1,100 kV lines. The attractiveness of this alternative resides in the fact that this voltage level can transmit 3 to 4 times more power than a 550 kV line.

To develop the equipment, Tepco built a test station at the ShinHaruna 550 kV substation. The facilities have a single-phase transformer bank, with each phase composed by two separate units, in a SF_6 span, a full-scale test line, test cage, etc. The tests began in 1996, focusing mainly on corona studies, insulator pollution, etc.

Considering that the 1,100 kV line runs through mountain regions and are exposed to severe wind and ice conditions, a full-scale test line was built at the Takaishiyama Mountain in 1978 to study the mechanical loads on the conductor bundle. In this area, altitudes reach 1,951 meters, temperatures vary between -30/20 °C, and the winds move at up to 57 m/s.

In 1999, TEPCO had already built the double-circuit, 1,100 kV line (240 km section) from the East to the West route, and another 190 km section from North to South. This system, which started operating at 550 kV, went into operation at 1,100 kV only in 2010 [5].

3.5 India

The Indian company *Power Grid Corporation of India Limited* (Powergrid) suggested that, by 2012, the country's demand would exceed 157 GW, and would reach 600 GW in 2025. India largely depends on 400 kV and 765 kV AC transmission systems, and a ±800 kV (6,000 MW) DC system. To meet the future demand, it would be necessary to implement generation sources available at few locations distant from the load centers. The transmission system reinforcement was planned considering the construction of numerous 400 kV lines and their substations, and about 9,000 km of 765 kV lines, along with 15 substations at the same voltage level.

To develop the 1,200 kV AC technology, India has been operating a test station since 2012 at the city of Bina (Madhya Pradesh, central region of the country). This project was developed in association with 25 manufacturers that use the platform and infrastructure set up by Powergrid to install and test their equipment.

Several studies and tests were also conducted to determine the equipment specifications and transmission line configurations. Among the activities performed it can be mentioned the studies and tests related to corona phenomenon, insulation supportability for gaps in air, voltage distribution along insulators, measurements of audible noise, radio interference, electrostatic effects at ground level, etc. [1].

Following these researches, in December 2013, India implemented a single-circuit line designed for a maximum voltage of 1,200 kV (350 km) between Wardha – Aurangabad. Presently, this line operates at 400 kV. The equipment vendors for this project were all from India, including some subsidiaries of international companies.

3.6 China

In China, the available power resources are far away from the load centers. About 76% of the coal reserves and most of the wind and solar power potentials are in the North and Northwest of China, and 80% of the hydro power resources are located in the Southwest. However, over 70% of the load is concentrated in the East and Central China. To meet these demands, China found necessary to develop a UHV transmission system to transfer large amounts of power over long distances varying from 800 km to 3,000 km.

At the end of 2014, the State Grid Corporation of China launched a strategic plan to develop UHV systems both AC and DC. The final objective is to build a nationwide 1,000 kV AC power grid overlaid on the existing 500 kV AC system, incorporating point-to-point bulk power transmission over very long distances with ±800kV DC transmission technology [14].

Researches and studies have demonstrated that this is the best alternative from a technical and economic perspective. This AC/DC system presents many advantages regarding safety and stability, since, during emergency conditions, the DC system control functions work effectively.

In 2007, a 1,100 kV 1 km test line was powered at the *Wuhan High Voltage Research Institute*. In the same testing framework, they analyzed a single-circuit line with horizontal configuration, and a double circuit line with vertical configuration.

In 2006, the implementation of a 1,100 kV pilot project connecting the Northern and Central regions was approved. This system is composed by two single-circuit sections between Jindongnan – Nanyang, and Nanyang – Jingmen. This system started operating in 2009 with a total length of 640 km.

Later, other UHV AC systems went into operation whereas some others are under the planning or construction stage. Thus, China's performance is significant in the planning, design, construction, and operation of UltraHigh Voltage systems. Therefore, it should be highlighted the experience gained by China so as to extract inputs for the implementation of systems at this voltage level in Brazil. See the item bellow:

4. Detailing of China's UHV AC System

The evolution of the voltage levels in China occurred as follows:

- 1954 – 220 kV
- 1972 – 330 kV
- 1981 – 500 kV
- 1989 - ± 500 kV DC
- 2005 – 765 kV
- 2009 – 1,000 kV
- 2009 – ± 660 kV DC
- 2010 – ± 800 kV DC

When compared to the evolution of the voltage levels in Brazil, the following are relevant factors:

Both in Brazil and in China, the 230 kV level was implemented in 1954.

To meet the demand growth during the 1960s, 1971, 1975, 1982, and 1984 and for power transmission over long distances, the following voltage levels were successively used in Brazil: 345 kV, 440 kV, 500 kV, 765 kV and ±600 kV DC. On the other hand, the evolution of these voltage levels in China occurred during 1972, 1981, and 2005 for the voltage levels of 330 kV, 500 kV and 765 kV. It can be observed that Brazil was technologically more advanced than China up to 2005.

As of 1982 and 1984, with the implementation of 765 kV and ±600 kV DC levels of the transmission system for the Itaipu power plant, Brazil did not evolve much, with the exception of the ±800 kV DC level foreseen for the year 2018, when it can be tested the transmission system for the Belo Monte power plant.

In contrast, in the last ten years (2007-2017), China has implemented several systems with voltage levels in DC (±500, ±660, ±800 kV DC), and AC Ultra-High Voltage levels (1,000 kV) at an impressive rhythm. Thus, the SGCC (*State Grid Corporation of China*) is the only one in the world operating ultra-high voltage systems at both AC and DC systems.

For the purpose of this project, we present below some facts related to the experience of SGCC in the planning, implementation, and operation stage of the UHV AC systems.

4.1 Planning Aspects

As already mentioned, China's first UHV AC system started operating in 2009, followed by other five systems, successively, in 2013, 2014, and 2016, as presented in the figure bellow. It can be observed that the first system used single-circuit lines, while the rest were built with double circuit lines, with some sections having a hybrid construction (single and doble circuit). Two additional UHVAC systems are scheduled to start operating in 2017: Yuheng – Weifang (2 x 1,059 km), and Ximeng – Shengli (2 x 240 km).

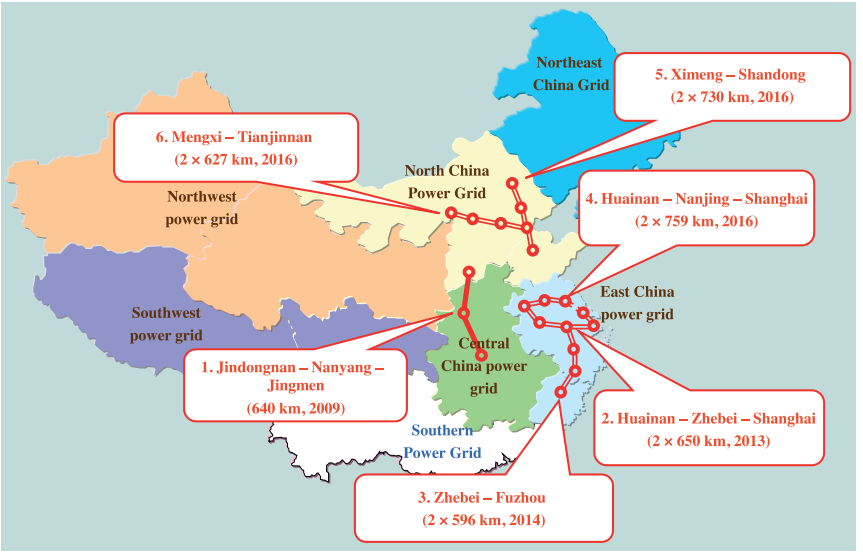

Figure 4.1: Existing UHV AC systems in China

4.2 Operation Aspects

Currently, there are proximity 10,000 km (circuits) of 1,000 kV lines operating in China, and more than 141,000 MVA of transformer capacity.

Some minor equipment problems were identified and resolved with no major consequences, such as: failure in SF_6 connection insulators, failures in some polymer insulators caused by bird pecks, partial discharges in a shunt reactor resulting from assembly problems, etc.

Comparing the 500 kV and 765 kV systems for the same state in time of their development, it can be seen that the UHV AC systems are as good or possibly better from the technical readiness point of view.

5. Conclusions

The UHV AC transmission may be considered a technically feasible and economically competitive alternative for the transmission of large blocks of power over long distances. This statement may be proven by means of several researches conducted, technical reports published and, mainly, the experience of China with the planning, implementation, and operation of several 1,000 kV lines.

Based on the experiences reported by SGCC, it can be inferred that the difficulties in constructing a 1,000 kV system should not be greater than building an equivalent 765 kV AC system, or even a ±800 kV DC line.

Regarding the equipment vendors for this voltage level, China, India, and Japan have already this technology with some European manufacturers similarly offering related equipment and components.

6. References

[1] BHATNAGAR, M. C.; DE BHOWMICK, B. N.; NAYAK, R. N; et al. 1,200 kV Transmission System and Status of Development of Substation Equipment Transmission Line Material. In: *India. IEC/CIGRE Second International Symposium on Standards for Ultra High Voltage Transmission,* New Deli, 2009.

[2] JARDINI J. et al. *Alternativas não Convencionais para a Transmissão de Energia Elétrica - Estado da Arte*. Brasília: Editora Goya, 2011.

[3] JARDINI J. et al. *Alternativas não Convencionais para a Transmissão de Energia Elétrica – Estudos Técnicos e Econômicos*. Brasília: Editora Goya, 2012.

[4] FRONTIN, S. O. et al. *Ultra-High Voltage Technology.* (CIGRE Brochure 85). Working Group 04 (UHV Testing Facilities and Research) of the Study Committee 38 (Power System Analysis and Techniques), Jun/1994.

[5] *Technical Requirements for Substation Equipment Exceeding 800 kV.* (CIGRE Brochure 362). Work coordinated by the Working Group CIGRE A3.22. Paris. Dec/2008.

[6] *Technical Requirements for Substation Exceeding 800 kV* (CIGRE Brochure 400). Work elaborated by the Working Group CIGRE B3. 22. Paris. Dec/2009.

[7] LINGS, R.; CHARTIER, V.; MARUVADA, P. S. *Overview of Transmission Lines Above 700 kV.* Inaugural IEEE PES 2005 Conference and Exposition. Durban, South Africa. 2005.

[8] HUANG, D.; RUAN, J. *Construction of UHC AC and DC Test Bases in China.* IEEE, 2008.

[9] SIEMENS.*1.200 kV AC Substations. Full Scale Products and Integrated Solutions.* 2nd International Symposium on International Standards for Ultra High Voltage. New Delhi, Jan. 29 -30, 2009.

[10] ABB. *Development and Testing of 1,100 kV GIS.* 2nd International Symposium on International Standards for Ultra High Voltage. New Delhi, Jan. 29 -30, 2009.

[11] *Background of Technical Specifications for Substation Equipment Exceeding 800 kV*. CIGRE Working Group A3.22. Paris. 2009.

[12] GOSWAMI, M. M.; LAKHIANI, V. K. *Transformers for 1,200 kV Testing Station at Bina.* Fifteenth National Power Systems Conference. Bombay, India. 2008.

[13] GOMES, R. et al. *A Gestão do Sistema de Transmissão no Brasil*. Fundação Getúlio Vargas. Rio de Janeiro, 2012.

[14] SHU Y. B. *Operation Experience of 1.000 kV High Voltage AC Transmission Technology*. B2-111, Cigre. Paris, 2016.

CHAPTER 3

Analysis of Scenarios for the Application of the 1,000 kV system in the Brazilian Interconnected Power System

José Antonio Jardini
Renato Grigoletto de Biase
Gerson Yukio Saiki
Ricardo Leon Vasquez Arnez
Geraldo Luiz Costa Nicola

1. Introduction

This chapter presents an analysis on the research conducted aiming at identifying the most suitable location where the 1,000 kV UHV AC transmission line would be placed within the Brazilian Interconnected Power System (SIN).

As a start-up point, the following basic characteristics were considered:

- - Power to be transmitted: 3,000 to 4,000 MW.
- - Voltage level: 1,000 kV (rated), 1,100 kV maximum rated.

2. Strategies Used

The research was conducted considering three stages:

- In the first stage, the Ten-Year Expansion Plan released by EPE to find a future 500 kV system that might be replaced with a 1,000 kV line, with no major impact in its costs, was considered. On the other hand, this line should be in the construction plan for the period of 2020-2025. This way, the experience acquired can be applied to other future projects of this kind.
- In the second stage, it was investigated some possible generation expansions unforeseen in the Ten Year Plan for which the new line might be useful.
- Finally, it was analyzed the flexibility that a 1,000 kV system might bring to a location with high potential for renewable wind and photovoltaic power which, due to their nature, are difficult to schedule for a long term period.

3. Analysis of the Lines Foreseen in the 2023 Ten Year Expansion Plan without Generation Expansion Plans

3.1 Evaluated Alternatives

To choose the pilot line, the 2023 Ten Year Expansion Plan [1] along with the Anarede carga pesada, Norte Exportador file [2], was used.

With both references, a research was conducted on the power transmission projects existing in the Ten Year Expansion Plan, scheduled for implementation after 2018, at 500 kV AC.

The first possibilities for the initial study of the 1,000 kV AC system being:

- 1,000 kV loop (Figure 3.1) connecting the region of Fortaleza (CE), Recife (PE), Luiz Gonzaga (PE/BA), and Camaçari (BA).
- 1,000 kV line connecting the Tapajós Complex to Xingú, and Xingú to Tucuruí, all in the state of Pará.
- 1,000 kV line connecting the Tapajós Complex to the Rurópolis substation where the 1,000 kV line (Figure 3.2) would replace one of the circuits at 500 kV.
- Reinforcements to the North-South interconnection. Initially, these efforts studied the insertion of a 1,000 kV AC line as a replacement to the 500 kV lines in five sections of the following interconnection:
  - ▹ One 1,000 kV line connecting the Tucuruí UPP substation (PA) to the Itacaiúnas substation (PA);
  - ▹ One 1,000 kV line connecting the Itacaiúnas substation (PA) to the Colinas substation (TO);
  - ▹ One 1,000 kV line connecting the Miracema substation (TO) to the Gurupi substation (TO);
  - ▹ One 1,000 kV line connecting the Gurupi substation (TO) to the Serra da Mesa substation (GO);
  - ▹ One 1,000 kV line connecting the Serra da Mesa substation (GO) to the Samambaia substation (DF).
  - ▹ Line from Tucuruí (PA) to Samambaia (DF) with branches at Itacaiúnas (PA), Miracema (TO), Gurupi (TO), and Serra da Mesa (GO).
- Reinforcements to the North-Northeast interconnection.
  - ▹ 1,000 kV line (Figure 3.3) connecting Tucuruí (PA) to Presidente Dutra (MA); Presidente Dutra (MA) to Milagres (CE); and Milagres (CE) to Campina Grande (PB).
  - ▹ 1,000 kV line connecting Tucuruí (PA) directly to Campina Grande (PB).
- Reinforcements to the North-South interconnection, with generation increase of 3,000 MW in the Northeast.
  - ▹ 1,000 kV line connecting Tucuruí (PA) directly to Emborcação (MG).
  - ▹ 1,000 kV loop (Figure 3.4) interconnecting the inverter terminals of the direct current transmission systems of Itaipu at Tijuco Preto (SP), of Rio Madeira at Araraquara (SP), Xingu at Estreito (MG) and Adrianópolis (RJ), and Tapajós, at Vespasiano (MG).

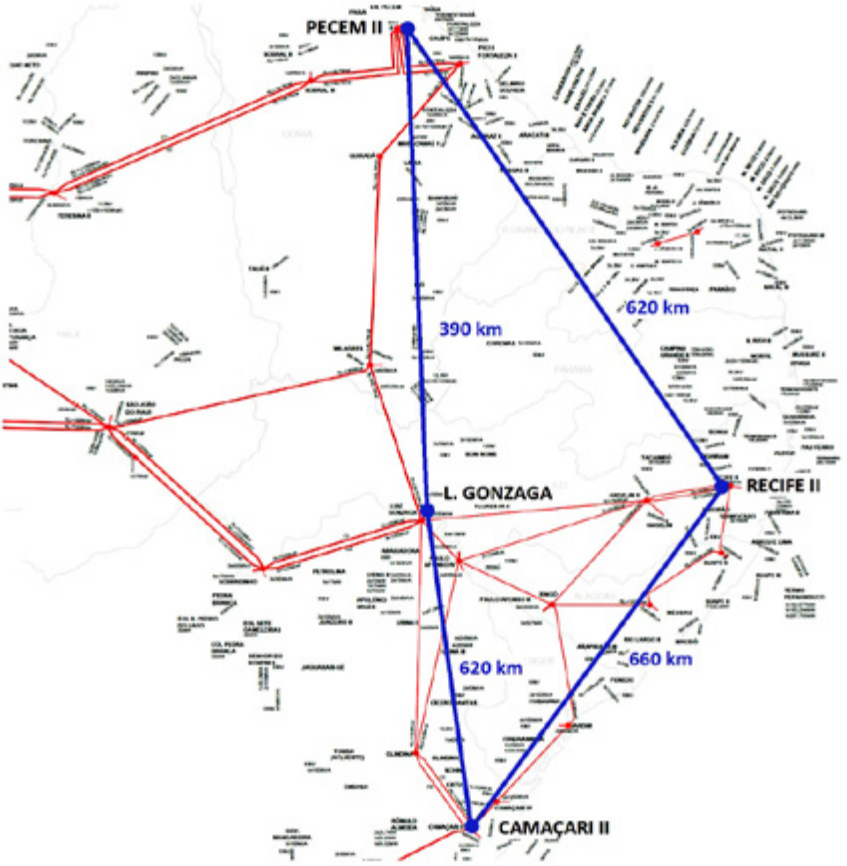

Figure 3.1: 1,000 kV loop in the Northeastern region.

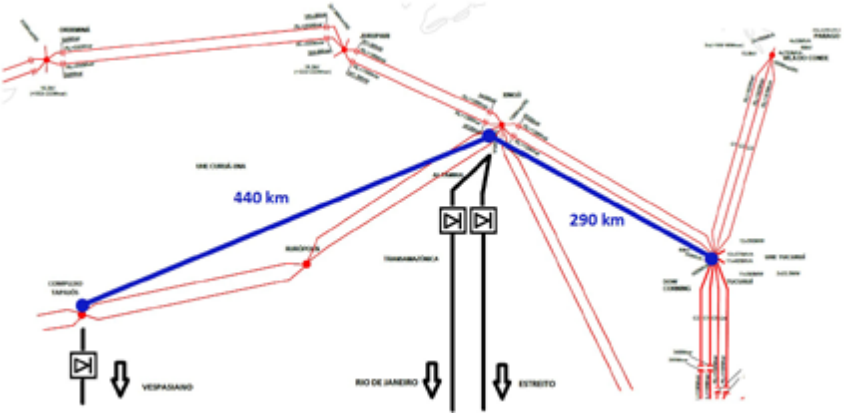

Figure 3.2: 1,000 kV line in the Northern region.

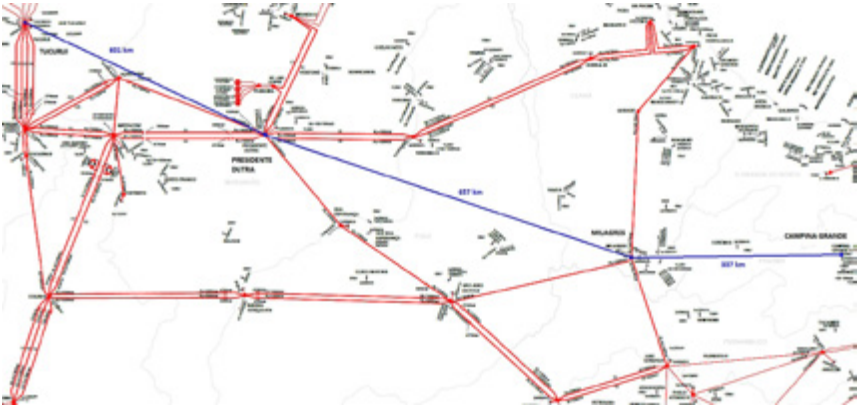

Figure 3.3: 1,000 kV lines evaluated as a reinforcement to the North-Northeast interconnection.

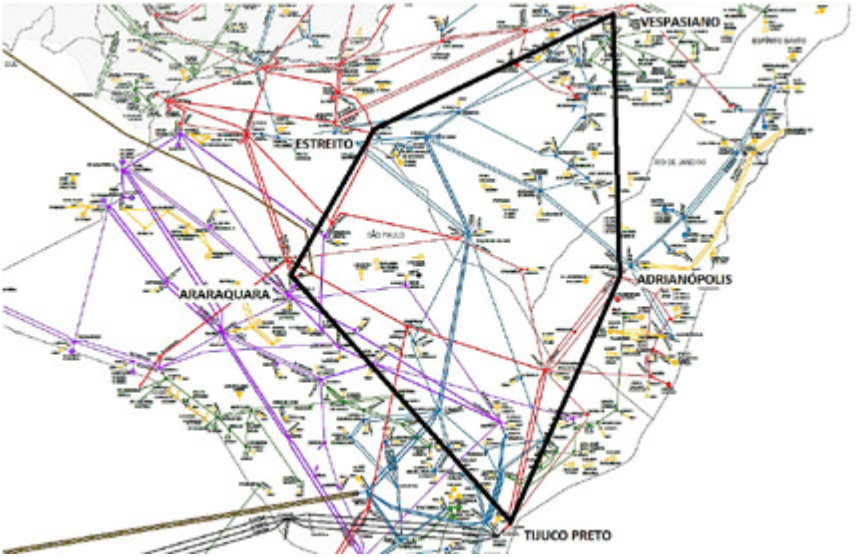

Figure 3.4: 1,000 kV loop in the Southeastern region.

3.2 Performance Evaluation

All the alternatives were evaluated considering load flow requirements.

To evaluate the various possibilities of line sections where the 1,000 kV transmission system may be applied, the proposed alternatives mentioned had to be modeled and simulated. The 1,000 kV lines were connected using 500/1,000 kV transformers with 3,000 MVA rated power equipped with on-load tap changers to control the voltage at ±10% of the rated voltage. In all the cases, reactors banks for parallel compensation of 100% (50% in each line terminal) were modeled. Unless otherwise mentioned, series compensation was not used.

The cases were analyzed with the full system state and with some contingencies (regarding at all times the n-1 criterion).

The conclusion was that an interesting and attractive alternative would be:

Tapajós – Rurópolis line, with a 1,000 kV line connecting the Tapajós Complex (PA) to the Rurópolis substation (PA).

4. Flexibility for the Region with Wind/ Photovoltaic Generation

During the studies, EPE issued an evaluation report on the North and Northeast Generation scenario during humid or dry weather, which corroborated the need to reinforce the N–SE, NE–N, and NE–SE interconnections.

Part of the NE generation resulted from a large expansion of the wind power in the NE region. Thus, one of the recommendations was the reinforcement of the NE-SE interconnection through the South of Bahia, Minas Gerais, and Espírito Santo corridor.

Reinforcement by means of higher capacity 500 kV lines (6 conductors per phase) in the region of Bom Jesus da Lapa and Gilbués, Rio das Éguas, in addition to Igaporã, Janaúba, Pirapora, Presidente Juscelino, and Itabira were also proposed. This indicated the suitability of providing a flexible corridor with greater transmission capacity in existing corridors, which showed the feasibility for inserting a 1,000 kV system in the region.

This system was then conceived, in its initial phase, with three sections of 440 km each, and four substations close to: Milagres, Ourolândia, Igaporã, and Pirapora. The system was studied in detail in the molds of the EPE studies, which resulted in the so-called R1, R2, R3, and R4 reports.

Further, the impact of an expanded 1,000 kV system was also studied. This expansion includes the addition of a new section from Pirapora to Neves station, and a second reinforcing circuit from Ourolândia to Neves.

5. Conclusions

With the objective of identifying the possibility of inserting an AC 1,000 kV transmission system, several alternatives with their respective power flow analyses were conducted.

The chosen alternative was the insertion of a 1,000 kV system from Milagres (CE) to the Pirapora (MG) region.

This alternative will be analyzed in detail in chapters 4 and 5, in which several other aspects of this alternative are also analyzed, namely: electromechanical performance; technical-economic and socio-environmental feasibility; transient overvoltage and insulation coordination studies; busbar arrangement study; equipment specifications, etc.

Despite those studies are necessary to confirm the chosen alternative, it appeared as a fact the following points:

The system has the capacity to export the excess power from wind and solar power generation in the Northeastern region to meet the demands of the Southeastern region; thus, helping in the recuperation of the hydroelectric plant reservoirs.

The UHV transmission system has reached its technological maturity at a global level in all phases of its implementation. This achievement is largely due to the experience acquired by China, Japan and India. From that, it can be inferred that the Brazilian industrial park is also well capable to manufacture equipment for this voltage level.

6. References

[1] EMPRESA DE PESQUISA ENERGÉTICA – EPE. *Plano Decenal de Expansão de Energia 2023 de 01/26/2016*. Available at: <http://www.epe.gov.br/PDEE/Relat%C3%B3rio%20Final%20do%20PDE%202023.pdf>. Accessed on: 03/28/2016.

[2] EMPRESA DE PESQUISA ENERGÉTICA – EPE. Dados para Estudos de Planejamento da Transmissão - PDE 2023 (Reference 07/11/2014). Available at: *<http://www.epe.gov.br/Transmissao/Paginas/Dados paraestudosdeplanejamentodatransmiss%C3%A3o-DE2023(arquivosdisponibilizadosem11072014).aspx>.* Accessed on: January 26, 2015,

CHAPTER 4

Technical, Economic, and Socio-Environmental Feasibility Studies of the Alternatives (R1)

José Antonio Jardini
Patrícia Oliveira da Silveira
Marcos Tiago Bassini
Gerson Yukio Saiki
Thales Sousa
Geraldo Luiz Costa Nicola

1. Objective

The objective of this chapter is to present the technical, economic and socio-environmental studies for a single circuit 1,000 kV transmission line (initial phase) connecting the Milagres (Ceará), Ourolândia (Bahia), Igaporã (Bahia), Pirapora (Minas Gerais) substations, with a total length of about 1,320 km. This alternative was analyzed using the data from the Ten-year Expansion Plan - PDE 2024, with the addition of 5,500 MW of generation aiming at representing the potential wind and photovoltaic power increase in the Northeast region. The EPE studies show that there will be a bottleneck in the transmission of this potential to the Southeast region as of 2019.

The feasibility to expand the 1,000 kV AC system (additional future phase) was also studied. For such a study, 11,000 MW (additional 5,500 MW) were added to the generation in the Northeast region. The main studies conducted were power flow (steady state and during contingencies), electromechanical stability, and a comparison of investments between the 1,000 kV AC system, a system at 500 kV AC, and HVDC bipoles. In this expansion, the Ribeirão das Neves (Minas Gerais) substation was included, connecting to the Pirapora substation. An additional single circuit was also included in the sections from Ourolândia to Ribeirão das Neves.

2. Introduction

At the end of 2012, a strategic R&D project called "*Non-Conventional Alternatives for Long Distance Power Transmission*" was completed. Among the products of this project were the edition of three books and two seminars where the state-of-the-art of several technologies for power transmission together with the technical and economic studies for the most promising alternatives, were presented. Among the alternatives analyzed, the one that stood out was the ultra-high voltage (UHV) transmission. Regarding the direct current transmission, bidding processes for ±800 kV projects have already been conducted, which will consolidate the Brazilian experience for this type of transmission along with the already existing ±600 kV DC projects (Itaipu and Madeira). As for the UHV transmission in alternating current, the implementation of a pilot project is deemed necessary, so that the existing knowledge and experiences may be equally expanded.

The definition of the location for the implementation of this pilot project required the analysis of the 2024 Ten Year Energy Expansion Plan (PDE 2024). The 500 kV transmission projects that should start operating after 2018, in various regions of Brazil, were also analyzed for their possible substitution with 1,000 kV AC transmission systems.

3. Assumptions and General Criteria

3.1 Studies Conducted by EPE

At the end of 2014, EPE issued the EPE-DE-RE-140/2014-r0 report, called: "Expansion of the Interconnection Capacity for the Excess Power Outflow from the North and Northeast Regions." In this document, EPE proposed a power offer scenario in the North and Northeast regions with an average 45 GW. In these conditions, the excess power from the North and Northeast regions after subtracting the internal demand was about 30 GW. Considering the capacity of the transmission lines from these regions to the Southeast region, there would be a restriction to export the excess power in 2019 of approximately 8,700 MW (average).

Based on this document, EPE conducted additional studies for the expansion of the transmission system between the North-Northeast regions to the Southeast. Such studies are contained in the documents listed next:

- **EPE-DEE-RE-146/2014-rev0**, (October 31, 2014), "*Transmission Expansion Studies – N-SE and NE-SE Interconnection Expansions to Meet the Needs of Extreme Export Scenarios of the North and Northeast Regions – Initial Alternative Conception*" [1].
- **EPE-DEE-NT-049/2015-rev0**, (March 16, 2015), "*Transmission System Expansion Planning Studies – Excess Power Outflow from the North and Northeast Regions – Interconnection capacity increase requirements*" [2].
- **EPE-DEE-RE-147/2014-rev2**, (December 08, 2014), "*Studies for Transmission Expansion Bidding, Technical & Economical Analysis of Alternatives: R1 Report, Study to Redirect the Wind Power Potential from the East Area of the Northeast Region*" [3].

- **EPE-DEE-RE-148/2014-rev1,** (December 08, 2014), "*Studies for Transmission Expansion Bidding, Technical & Economical Analysis of Alternatives: R1 Report, Northeast-Southeast Interconnection Capacity Increase*" [4].
- **EPE-DEE-DEA-RE-001/2014-ver0**, "*Studies for Transmission Expansion Bidding, Study to Redirect the Wind Power Potential from the Central Region of Bahia*" [5].
- **EPE-DEE-RE-065/2016-rev0,** (November 18, 2016), "*Studies for Transmission Expansion Bidding, Technical & Economical Analysis of Alternatives: R1 Report Study to Redirect the Wind Power Potential from the Seridó Region*" [6].

These documents analyze the power export from the North and Northeast regions to the Southeast region, mainly due to wind power generation projects. Based on them, some alternatives were studied for the insertion of the 1,000 kV transmission system to reinforce the export capability.

In this context, the 1,000 kV AC transmission alternative was chosen to connect the south of the state of Ceará to the state of Minas Gerais, passing through the central region of the state of Bahia. This line will connect the Milagres and Pirapora substations, and will work as a corridor for the export of wind and photovoltaic power from the Northeast to the Southeast region; and two intermediate substations will also be the collectors of these sources. The system may be expanded later, connecting Pirapora to Ribeirão das Neves.

3.2 Bases and General Criteria

The power flow studies were done for heavy load and light load conditions (both during the rainy season of the North) considering the 2024 ten-year expansion plan. In the study, the files made available by EPE were used, namely:

- EPE 2024 TEN YEAR 2024 HEAVY LOAD YEAR 2024 WET NORTH, for the heavy load studies (01/26/2016). This file was accessed on: 03/28/2016.
- EPE 2024 TEN YEAR 2024 LIGHT LOAD YEAR 2024 WET NORTH, for the light load studies (01/26/2016). This file was accessed on: 03/28/2016.

The following substation was added to the above files: Santa Luzia substation (Paraíba), a 238 km long transmission line (500 kV) between Santa Luzia and Milagres, and another 500 kV line, 126 km long line, between Santa Luzia and Campina Grande.

The loads of the SIN (Brazilian Interconnected Power System) were maintained and added 5,500 MW of power coming from Northeast region with the corresponding generation reduction in the Southeast region. The increases were made as shown in Table 3.1.

Table 3.1: Increase in generation (MW) in the Northeast region

Location	Increase (MW)
Santa Luzia	2,000
Campo Novo	200
João Câmara	1,600
Ourolândia	900
Gentio do Ouro	100
Sobradinho	100
Juazeiro	600
Total	**5.500**

The Grid Procedures of the National System Operator - submodule 23.3 were followed to evaluate the power flow and voltage levels during contingency conditions regarding also the *n*-1 criterion.

As for the electromechanical stability and dynamic analyses, it was used the database of the Anatem program (2016-2024 horizon) and published by EPE (2024 Ten-Year Expansion Plan) on 04/01/2016.

The simulations were performed considering the following aspects:

- The base file for power flow is the heavy load (Humid North) condition of the 2024 ten year expansion plan horizon, considering the same generation increase included during the power flow study.
- The machine controls of the new generation plants included to the base file were obtained from the EPE database corresponding to machines with similar capacity.

To evaluate the performance, all the models followed the Grid Procedures – Submodule 23.3.

For the short-circuit analysis, it was used the database available in the Anafas program (2016-2024 horizon), regarding the PDE 2024 (Ten Year Expansion Plan), published by EPE on 02/23/2016. It was considered the same generation increases included in the power flow analysis.

The comparison of investments was performed using the ANEEL's 2015 price bank, issued according to the Homologation Resolution # 758 in Jan. 6, 2009 (http://www.aneel.gov.br/cedoc/areh2009758.zip).

The cost of the 1,000 kV line was obtained considering the unit costs of all the components foreseen in it. The weight of the towers and foundations were obtained from specific projects elaborated. The cost of the lines and converters of the DC system were calculated using expressions found at the CIGRÉ's Brochure 388, properly adjusted for the reference date.

The cost of the switching modules, general modules, and equipment were also obtained from the ANEEL's price bank, extrapolated for the 1,000 kV AC and ±800 kV DC cases, since these systems were not yet available in the ANEEL's database.

The costs of land (General Infrastructure Module, and Switching Infrastructure Module) of the 1,000 kV and 500 kV substations were calculated considering the need for future expansion with new substations.

The Dollar exchange rate, used to update some unit prices impact significantly the DC converters and, as there was large variation in the exchange rate for that currency, the DC alternatives were affected in the economic comparison. The exchange rate used was R$ 3.05 per Dollar, which was the reference value used in the auction of the Belo Monte converters. The converter cost equation were used for that purpose.

It was also analyzed a DC alternative using VSC converters in a multi-terminal configuration. The cost of the VSC converters was considered to be 20% higher than the cost of the LCC converters. This 20% increase was based on information from a seminar held by CIGRÉ in Brazil in 2015, with the participation of manufacturers and specialists from the electric sector.

4. Performance of the Transmission System Alternatives

4.1 Power Flow Studies (2024 Ten-Year Expansion Plan)

In this item, the performance of the 1,000 kV alternative for the transmission of the generation potential of the North and Northeast regions as well as its capability to cater the various heavy load and light load scenarios (both during the Humid North scenario), is presented.

The 1,000 kV system analyzed comprises new substations (to avoid the difficulty of expanding the existing substations, and allow the connection of future systems), namely: Milagres III (500/1,000 kV), with the sectioning of the two Milagres – Luís Gonzaga lines (500 kV); Ourolândia III (500/1,000 kV), sectioning the Ourolândia – Juazeiro line (500 kV); Igaporã IV (500/1,000 kV), sectioning the two Igaporã – Janaúba lines (500 kV); and Pirapora III (500/1.000 kV), sectioning the two Pirapora – Ribeirão das Neves lines (500 kV). Also, the 1,000 kV line that comprises the substations of Milagres, Ourolândia, Igaporã, and Pirapora substations will have three sections each with a length of about 440 km.

As a comparative evaluation of the performance, the same scenarios and emergency conditions were also analyzed in relation to the PDE 2024 base case.

4.1.1 Dispatch features

To identify the load and generation scenarios used in this chapter, Table 4.1 shows the dispatches of the hydroelectric power plants at Tucuruí, Belo Monte, and the Tapajós Complex located in the North region; Xingó and Paulo Afonso in the Northeast region; Furnas, Marimbondo, Água Vermelha, Itumbiara, Emborcação, Porto Primavera, Ilha Solteira, and Itaipu in the Southeast and Central-West regions, which are presented by EPE at the PDE 2024 file. It is also presented the combined total power dispatched by the wind power plants located in the Northeast region. Despite Table 4.1 shows the heavy and light load scenarios during the wet and dry North conditions, the simulations presented in this study were done only for the Humid North scenario, since it presents heavier line loadings, thus, being more critical.

Table 4.1: **Power d**ispatch (MW) of some power plants characterizing the various scenarios studied

	Heavy load Humid North	Heavy load Dry North	Light load Humid North	Light load Dry North
Belo Monte	10,780	1,100	10,780	1,100
Tucuruí	7,855	4,134	7,775	2,027
Tapajós	3,961	425	3,914	626
Total	**22,596**	**5,659**	**22,469**	**3,753**
Furnas	1,049	1,259	223	292
Marimbondo	1,190	1,428	250	327
Água Vermelha	1,117	1,340	254	325
Itumbiara	1,824	2,188	411	528
Emborcação	954	1,144	290	347
Porto Primavera	1,232	1,478	185	269
Ilha Solteira	2,709	3,169	563	160
Itaipu 60 Hz	6,300	6,300	4,200	4,200
Itaipu 50 Hz	6,751	6,952	5,064	6,126
Total	**23,126**	**25,258**	**11,440**	**12,574**
Xingó	3,003	1,581	2,981	2,213
Paulo Afonso	2,337	1,230	2,319	1,722
Total	5,340	2,811	5,300	3,935
Northeast Wind Plants	14,200	14,200	8,500	14,200

It can be seen that the power plants located In the North region have a full dispatch during the humid period. The heavy load scenario differs from the light load scenario in the dispatch variation of the plants located in the Southeast and Central-West regions. The wind generation dispatch in the Northeast remains constant at 14,200 MW, except for the case of light load (Humid North scenario). The generation difference between the Humid North and the Dry North scenarios is supplied mainly by thermal generation.

In the PDE 2024, there were already added 5,500 MW which represents the wind generation increase in the Northeast. Figure 4.1 shows the locations where the generation increase was considered.

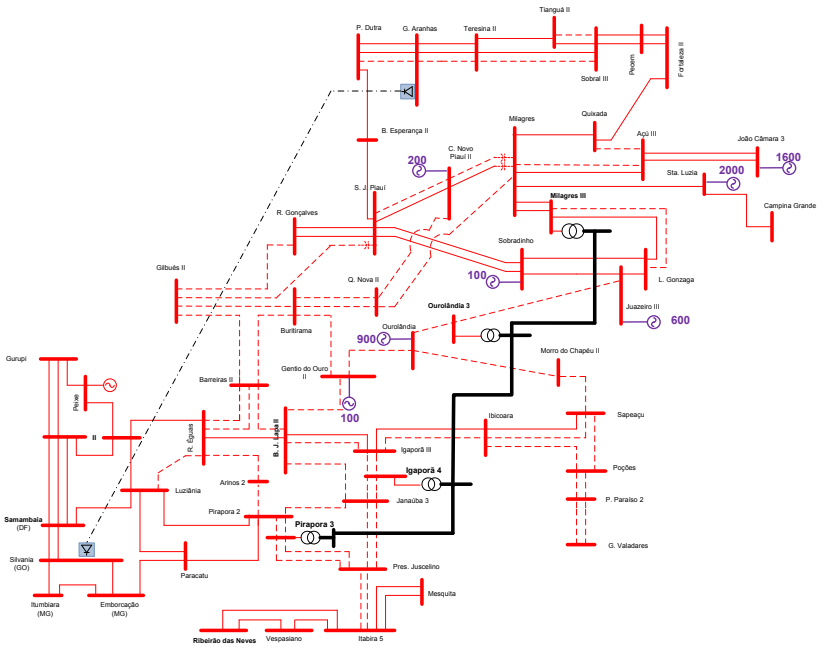

Figure 4.1: Location of the 5,500 MW increase in the Northeast generation

It was also added to the PDE 2024 the 500 kV Santa Luzia Substation, where it is expected the connection of some wind power plants, a line between Santa Luzia and Milagres, and another line between Santa Luzia and Campina Grande.

4.1.2 Contingencies analyzed

Several contingencies were simulated over the loading scenarios above referred. The aim is to evaluate the effect of the contingencies over the existing system and also evaluate the 1,000 kV system reinforcement on the central region of Bahia and the north of Minas Gerais. The main conditions evaluated for both heavy and light load, were:

- Opening of the 500 kV line between Gentio do Ouro and Bom Jesus da Lapa;
- Opening of the 500 kV line between Bom Jesus da Lapa and Janaúba;
- Opening of the 500 kV line between Juazeiro and Ourolândia 3;
- Opening of the 500 kV line between Morro do Chapéu and Sapeaçu;
- Opening of the 500 kV line between Igaporã and Janaúba;

- Opening of the 500 kV line between Janaúba and Ribeirão das Neves;
- Opening of the 500 kV line between Ribeirão das Neves and Itabira;
- Opening of the 500 kV line between Silvânia and Emborcação;
- Opening of the 500 kV line between Silvânia and Itumbiara;
- Opening of the 500 kV line between Silvânia and Trindade;
- Disconnection of 500/1,000 kV Transformers;
- Loss of one pole in the so termed Bipole B and the overload in the sound pole;
- Opening of any section within the 1,000 kV line;
- Opening of one of the 1,000 kV-line terminals to evaluate sustained overvoltages during energization and load rejection.

4.1.3 Reactive support in the local system

4.1.3.1 Heavy load

For the heavy load case, an additional reactive capacitive support in some of the SIN busbars, is necessary. This ensures that the voltage in those buses, during the occurrence of some contingencies, are kept within thresholds limits. The following shunt capacitor banks were allocated.

- 500 Mvar at the Ribeirão das Neves substation (MG, 500 kV side).
- 300 Mvar at the Governador Valadares substation (MG, 230 kV side).

For contingencies in the 1st and 2nd sections of the 1,000 kV line, it was observed the need of 200 Mvar inductive reactive compensation near the Ribeirão das Neves region, which can be resolved with the connection of the reactor banks already foreseen for that region.

4.1.3.2 Light load

Capacitive reactive support was found to be necessary in the Governador Valadares (230 kV) region, to keep the voltages (during some contingencies) within the admissible threshold values. A 130 Mvar capacitor bank was allocated to fulfil this need.

Also, during some contingencies as well as for the base case, it was seen the need of inductive reactive compensation near the Ribeirão das Neves region

(up to 600 Mvar). Similarly, this need can be resolved with the connection of the reactor banks already foreseen in the system for this region.

4.1.4 Results of power flow studies

4.1.4.1 Heavy Load – Humid North (2024)

A summary of the power flow through the 1,000 kV line for the Heavy Load condition – Humid North (PDE 2024), with an increase of 5,500 MW in the Northeast region, is presented in Table 4.2.

Table 4.2: Power flow (MW) inside the sections of the 1,000 kV line (heavy load)

FROM Busbar	TO Busbar	Flow (MW)
Milagres	Ourolândia	1,829
Ourolândia	Igaporã	3,217
Igaporã	Pirapora	2,178

Figure 4.2 shows the power flow results (steady state condition) on the 1,000 kV line and the neighboring 500 kV grid.

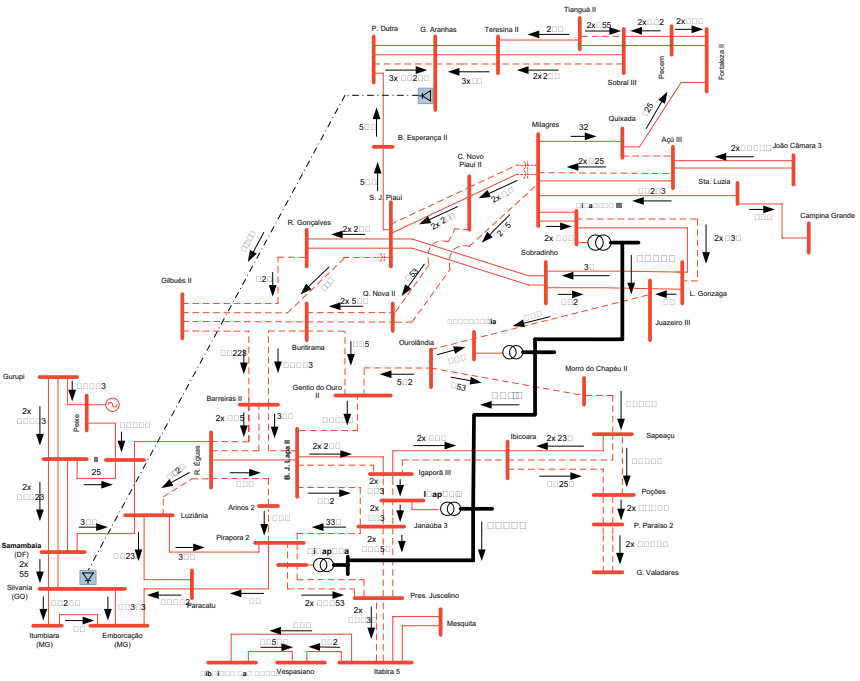

Figure 4.2: Power flow (MW) during steady state, heavy load

In all simulated contingencies, the system voltages and loading were within the emergency thresholds.

For contingencies occurring inside the 1,000 kV line, the power flow is redistributed throughout the 500 kV system.

As for the simulations regarding "energization and load rejection" of the three 1,000 kV sections, both the voltages and loadings of each section remained within the defined emergency thresholds (below 1.15 pu). Table 4.3, summarizes the voltages and power flow in the 1,000 kV system.

Table 4.3: Voltages after energization and load rejection (heavy load)

FROM Busbar	TO Busbar	Terminal	Voltage (pu)
Milagres	Ourolândia	Milagres	1.087
Milagres	Ourolândia	Ourolândia	1.080
Ourolândia	Igaporã	Ourolândia	1.103
Ourolândia	Igaporã	Igaporã	1.087
Igaporã	Pirapora	Igaporã	1.092
Igaporã	Pirapora	Pirapora	1.103

Next, the results of the simulations performed, focusing on the loading of the 1,000 kV system during emergencies, are presented.

a) Disconnection of 500/1,000 kV transformers

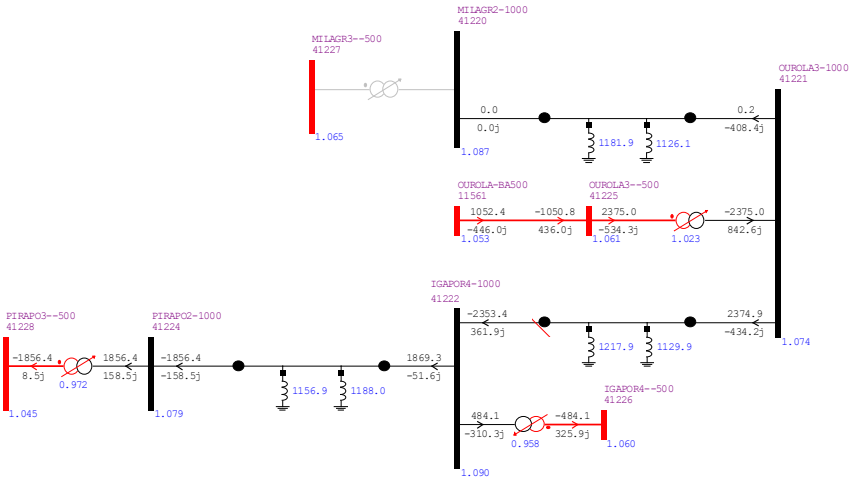

Figure 4.3: Power flow for the loss of the transformers at Milagres

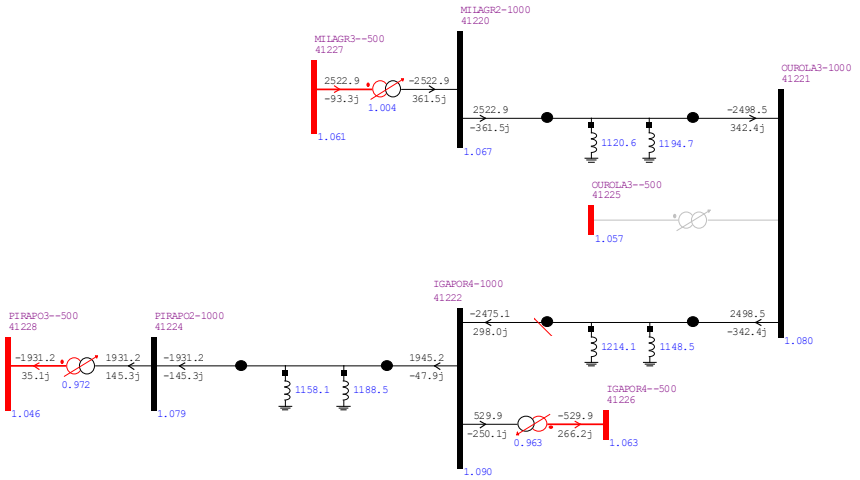

Figure 4.4: Power flow for the loss of the transformers at Ourolândia

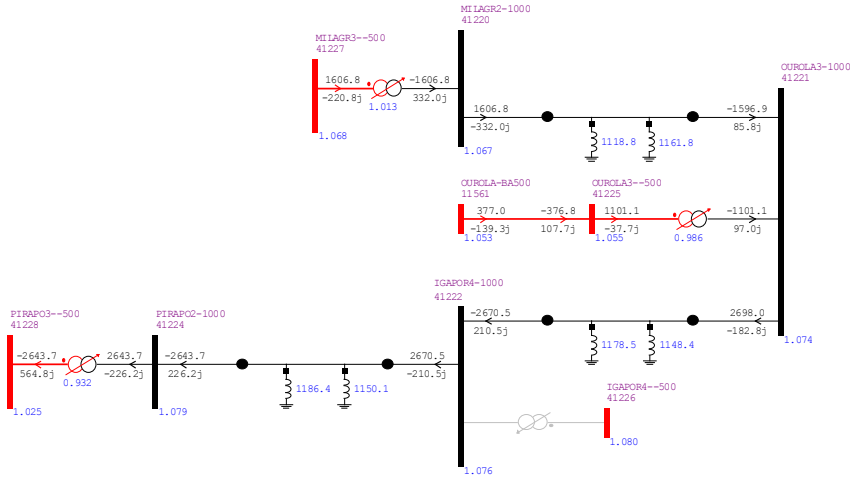

Figure 4.5: Power flow for the loss of the transformers at Igaporã

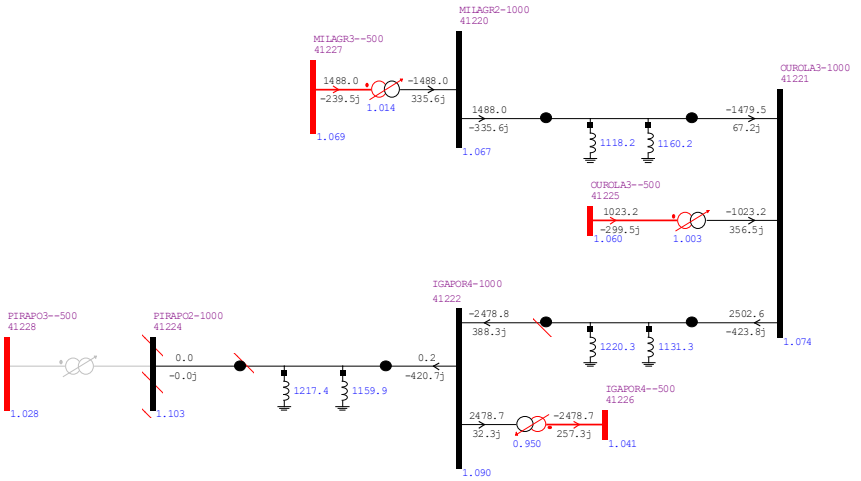

Figure 4.6: Power flow for the loss of the transformers at Pirapora

b) Disconnection of any line section of the 1,000 kV system

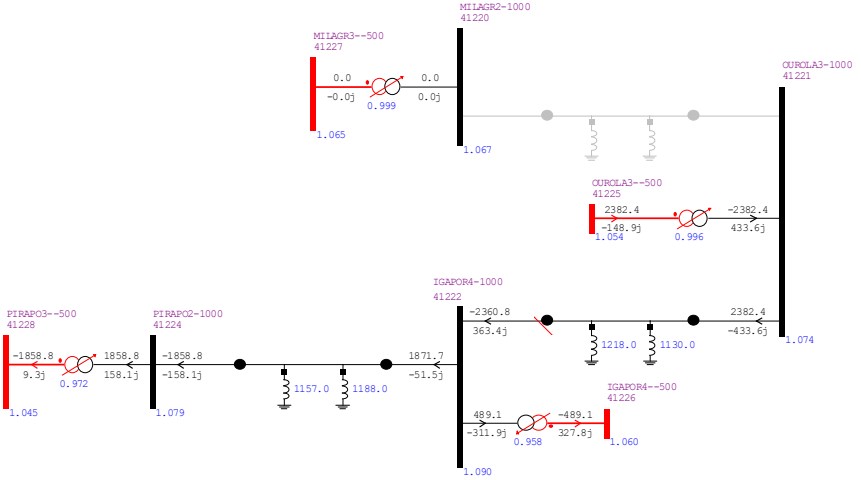

Figure 4.7: Power flow during the loss of the Milagres – Ourolândia section

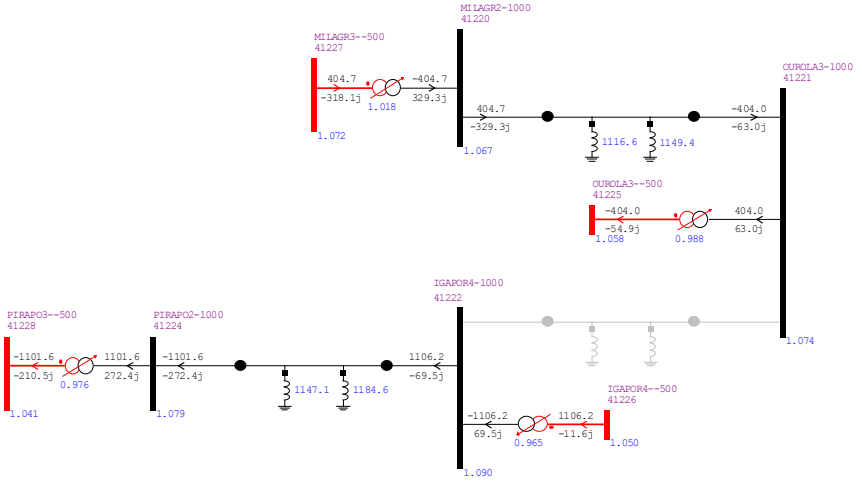

Figure 4.8: Power flow during the loss of the Ourolândia – Igaporã section

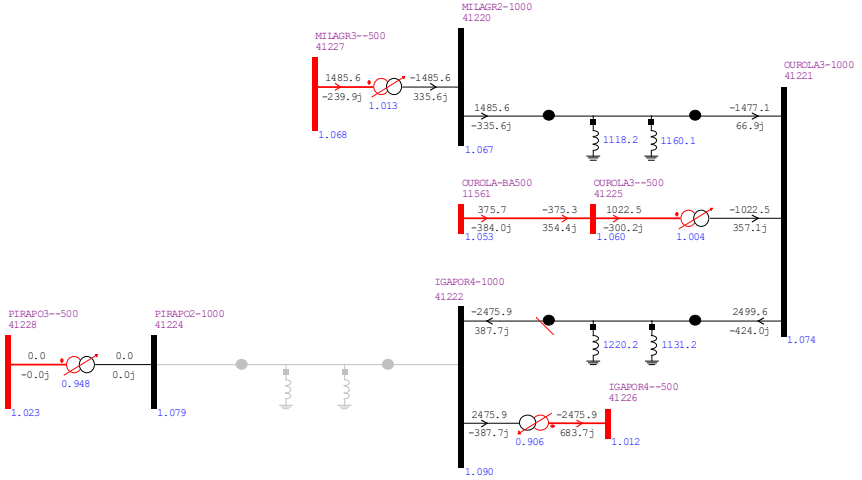

Figure 4.9: Power flow during the loss of the Igaporã – Pirapora section

c) Disconnection of one pole at the Graça Aranha – Silvânia HVDC and overload of the other

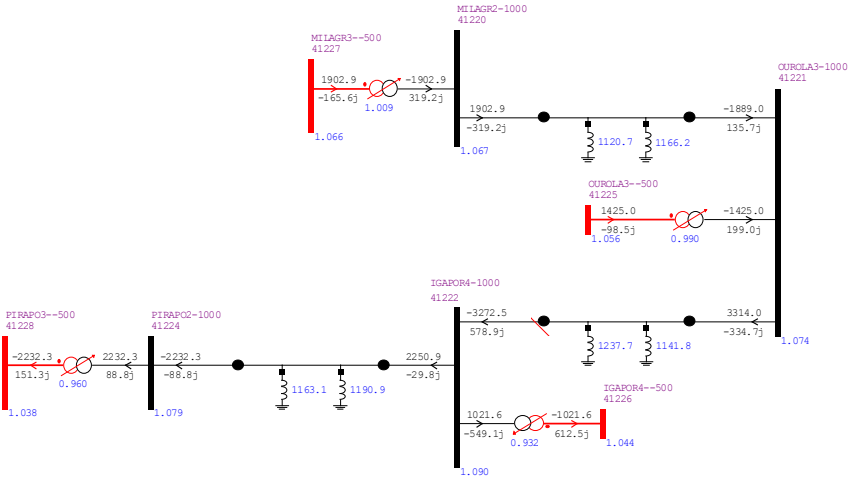

Figure 4.10: Power flow in the 1,000 kV system after the disconnection of one pole of the bipole B (Graça Aranha - Silvânia)

d) Energization and load rejection of the 1,000 kV line

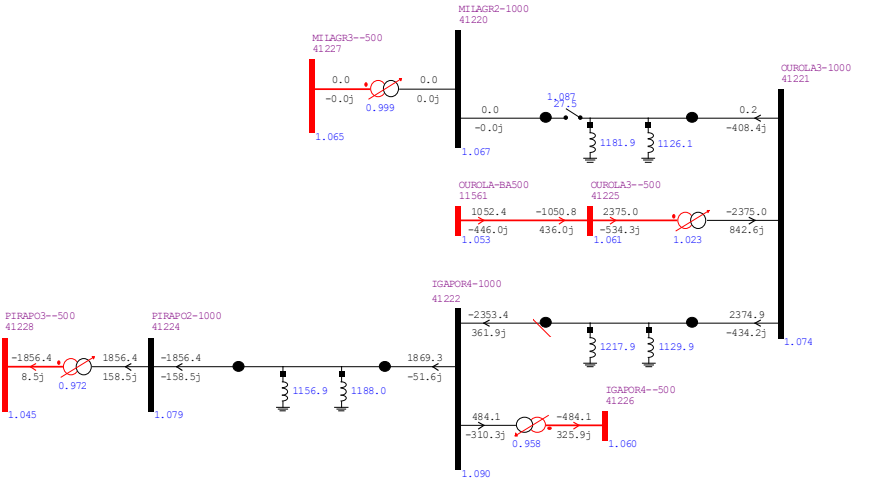

Figure 4.11: Sustained overvoltage after opening the 1,000 kV line at Milagres or energization through Ourolândia

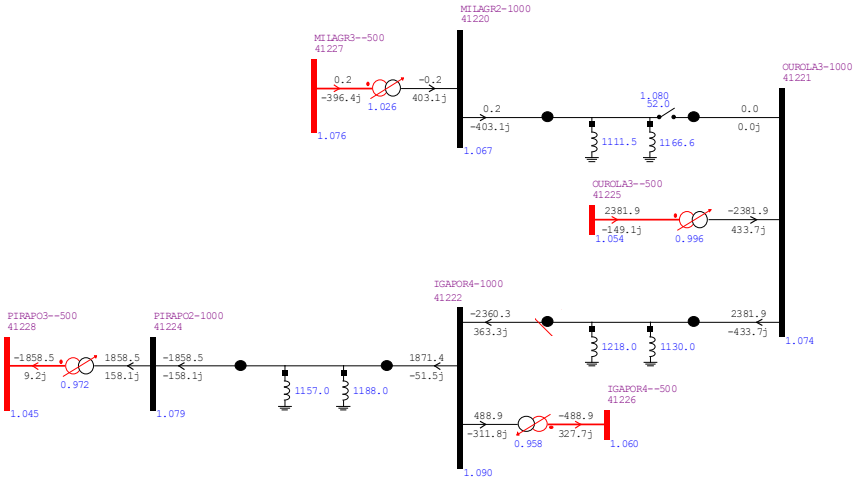

Figure 4.12: Sustained overvoltage after opening the 1,000 kV line at Ourolândia or energization through Milagres

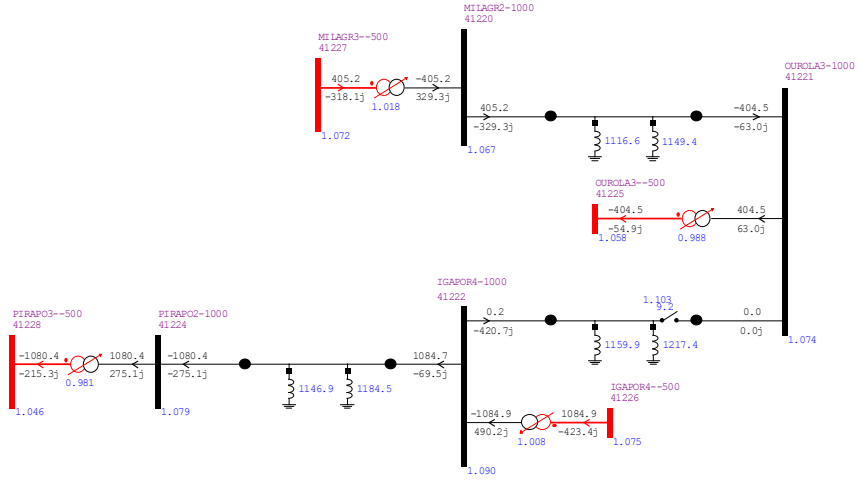

Figure 4.13: Sustained overvoltage after opening the 1,000 kV TL at Ourolândia or energization through Igaporã

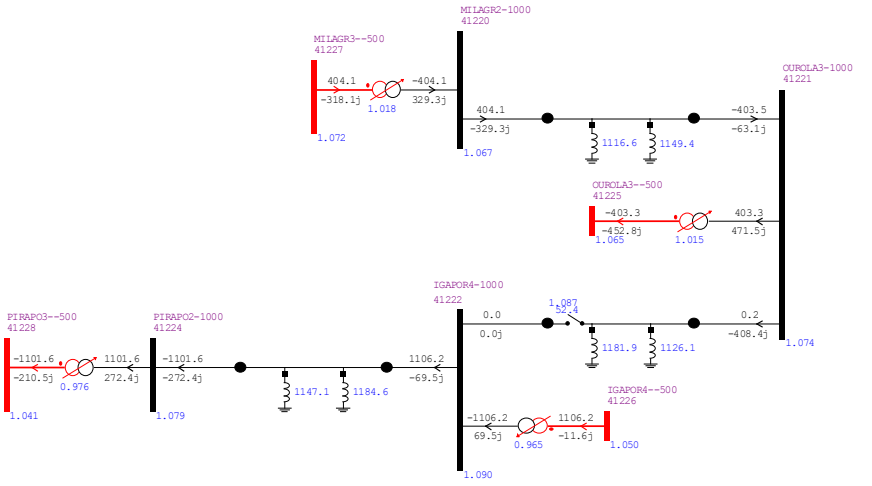

Figure 4.14: Sustained overvoltage after opening the 1,000 kV line at Igaporã or energization through Ourolândia

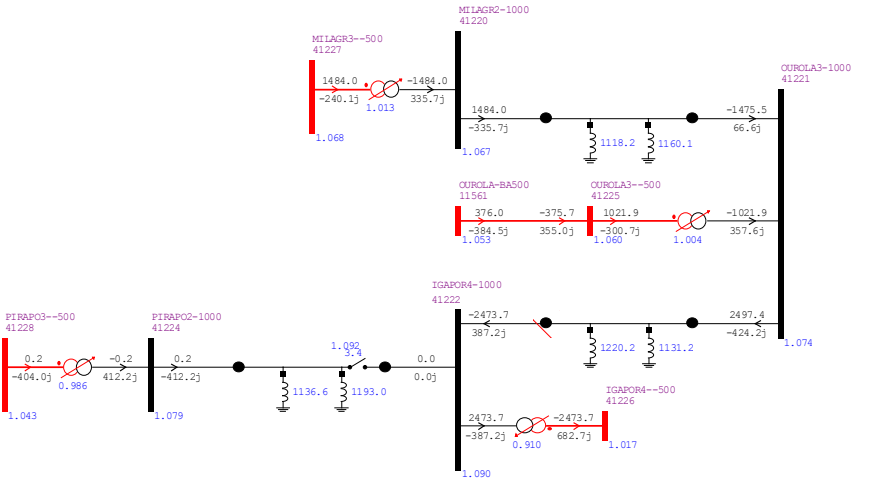

Figure 4.15: Sustained overvoltage after opening the 1,000 kV line at Igaporã or energization through Pirapora

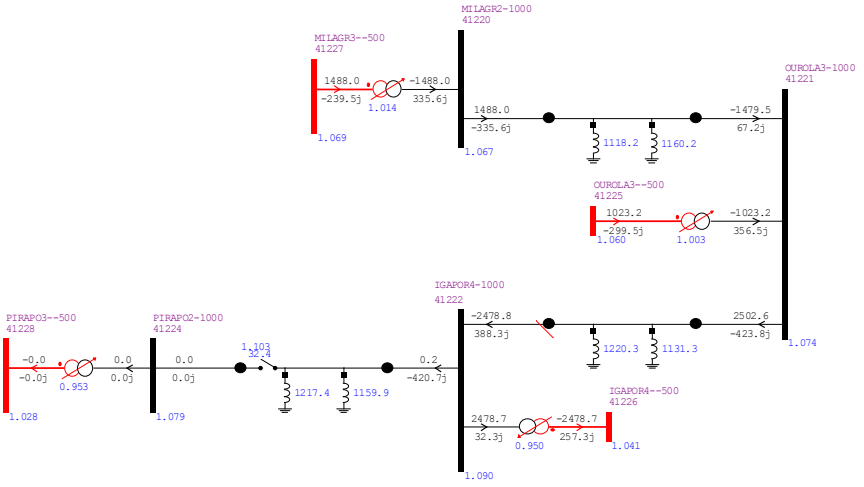

Figure 4.16: Sustained overvoltage after opening the 1,000 kV TL at Pirapora or energization through Igaporã

4.1.4.2 Light Load – Humid North (2024)

Table 4.4 shows the power flow results (at steady-state) in the 1,000 kV system for the light load condition considering an increase of 5,500 MW in the Northeast region.

Table 4.4: Power flow (MW) inside the 1,000 kV system (light load)

FROM Busbar	TO Busbar	Flow (MW)
Milagres	Ourolândia	1,430
Ourolândia	Igaporã	2,579
Igaporã	Pirapora	1,687

In Figure 4.17 the power flow in the 1,000 kV system and in the 500 kV grid nearby (light load at steady state), is presented.

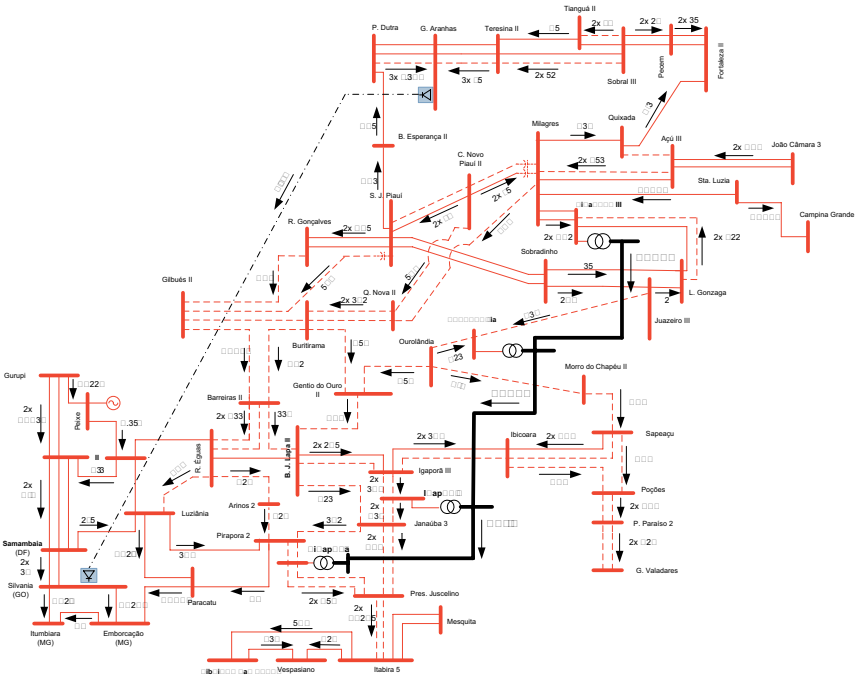

Figure 4.17: Power flow (MW) during light load (steady state), reference alternative

In all the simulated contingencies for the light load case, the voltages and loading levels of the network were within the emergency thresholds. During the contingencies inside the 1,000 kV system, the load flows are redistributed throughout the system via the 500 kV lines.

As for the simulations regarding "energization and load rejection" all three sections of the 1,000 kV system presented voltages and loadings levels within the defined emergency thresholds (below 1.15 pu). Table 4.5 summarizes the pu voltages inside the 1,000 kV system.

Table 4.5: Voltages after rejection and energization (light load)

FROM Busbar	TO Busbar	Terminal	Voltage (pu)
Milagres	Ourolândia	Milagres	1.078
Milagres	Ourolândia	Ourolândia	1.080
Ourolândia	Igaporã	Ourolândia	1.060
Ourolândia	Igaporã	Igaporã	1.078
Igaporã	Pirapora	Igaporã	1.030
Igaporã	Pirapora	Pirapora	1.060

Next, the results of the simulations regarding the loading condition of the 1,000 kV system (during emergency conditions), are presented.

a) Disconnection of 500/1,000 kV transformers

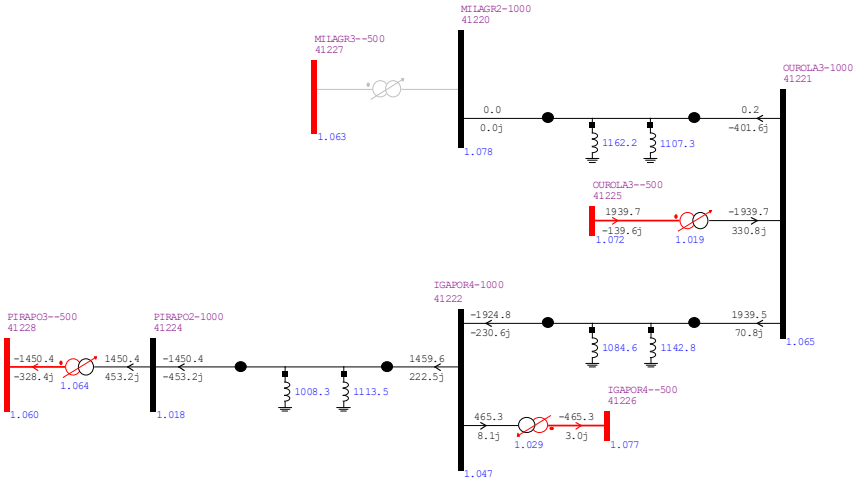

Figure 4.18: Power flow during the loss of the transformer at Milagres

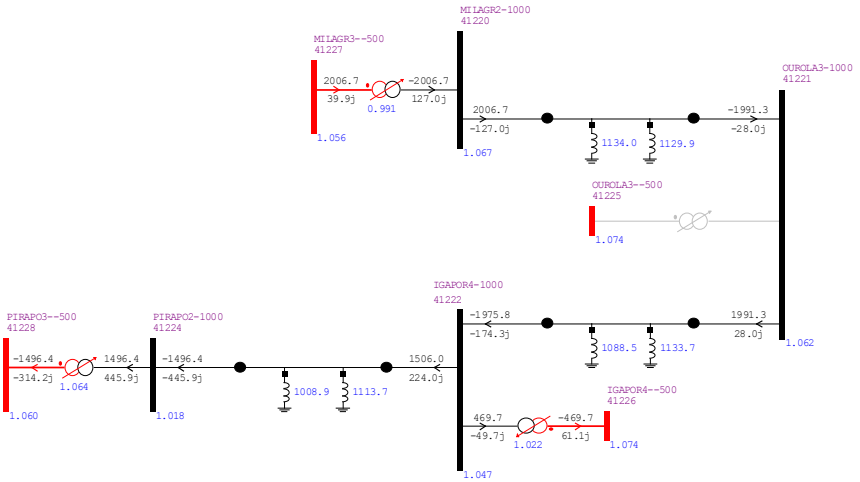

Figure 4.19: Power flow during the loss of the transformer at Ourolândia.

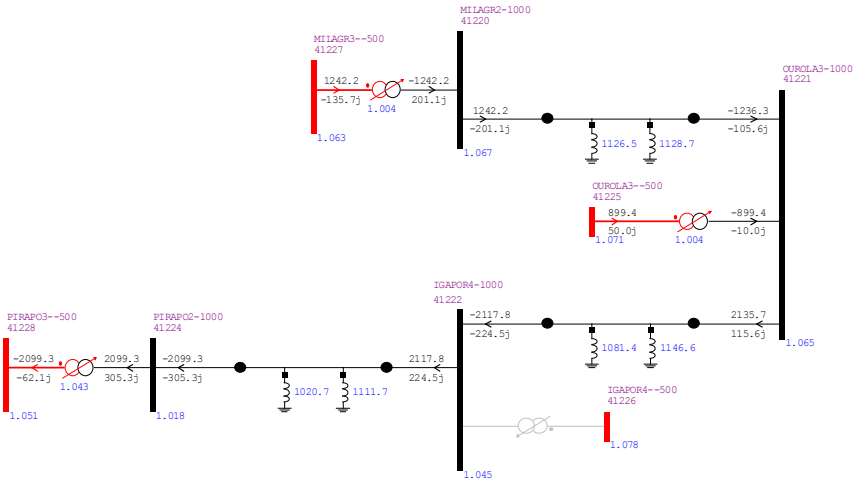

Figure 4.20: Power flow during the loss of the transformer at Igaporã.

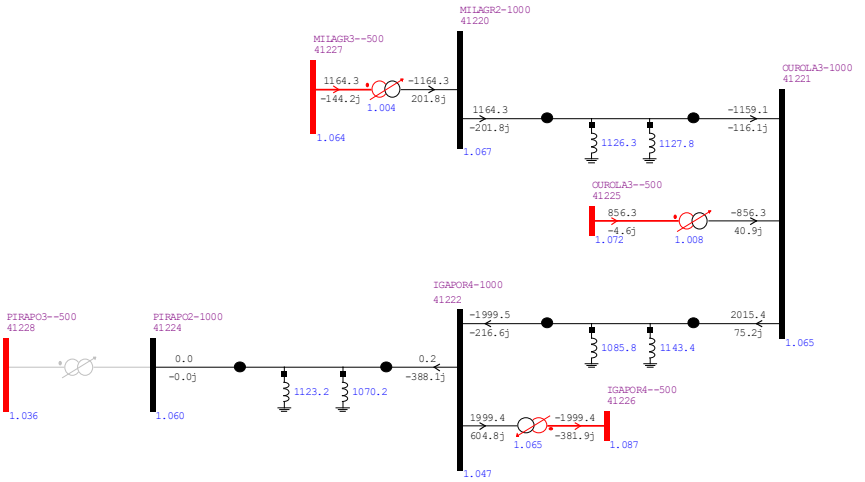

Figure 4.21: Power flow during the loss of the transformer at Pirapora.

b) Disconnection of any section within the 1,000 kV system

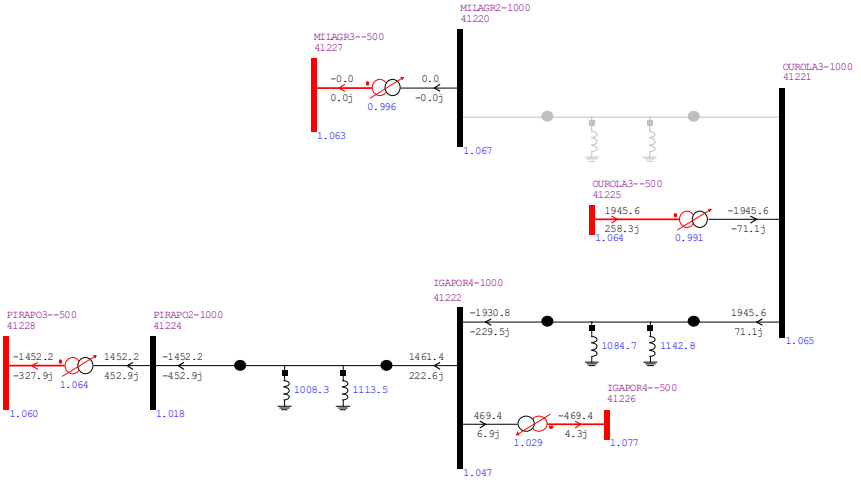

Figure 4.22: Power flow for the loss of the Milagres – Ourolândia section.

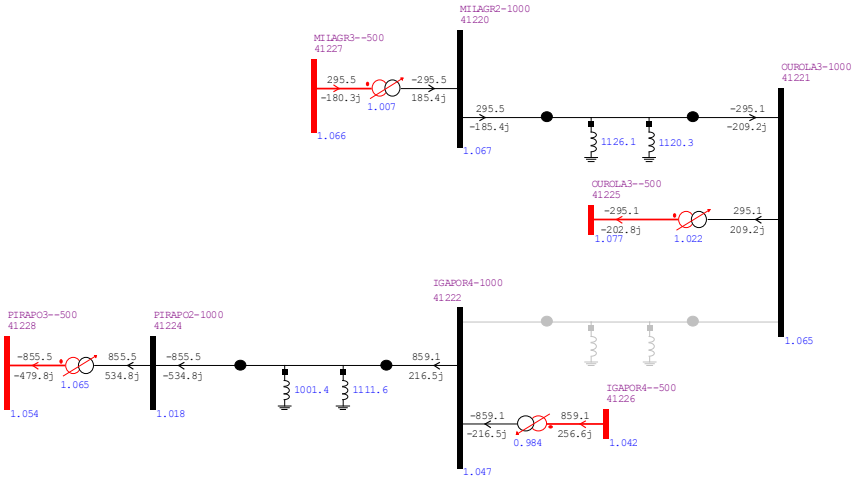

Figure 4.23: Power flow for the loss of the Ourolândia – Igaporã section.

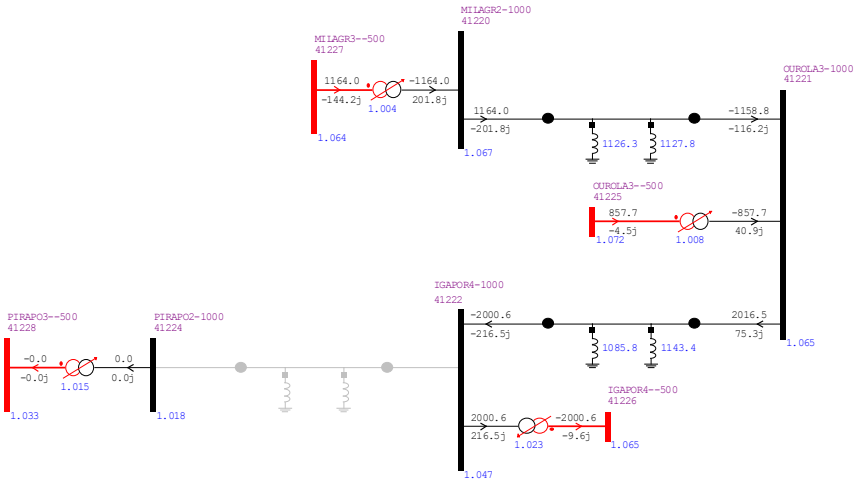

Figure 4.24: Power flow for the loss of the Igaporã – Pirapora section.

c) Disconnection of one pole of the Graça Aranha – Silvânia HVDC line and overload of the other pole

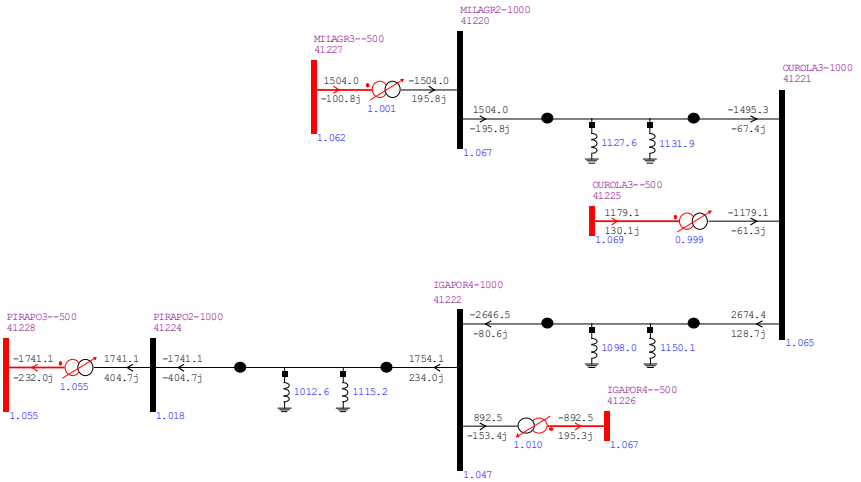

Figure 4.25: Power flow in the 1,000 kV after the loss of one pole at the Graça Aranha - Silvânia HVDC line (bipole B)

d) Energization and load rejection of the 1,000 kV line

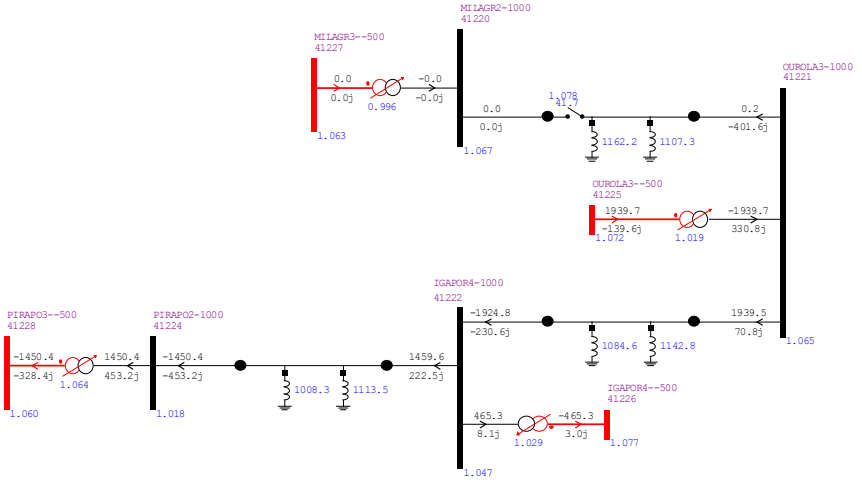

Figure 4.26: Sustained overvoltages after the opening of the 1,000 kV line at Milagres or energization through Ourolândia

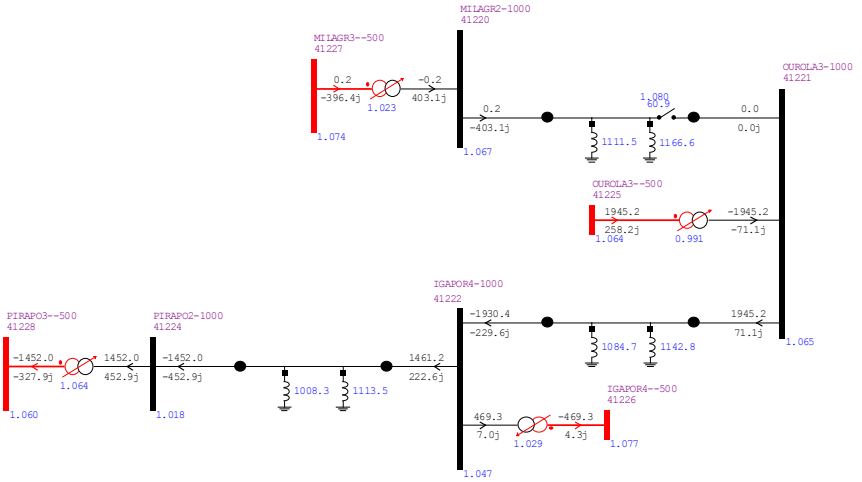

Figure 4.27: Sustained overvoltages after the opening of the 1,000 kV TL at Ourolândia or energization through Milagres.

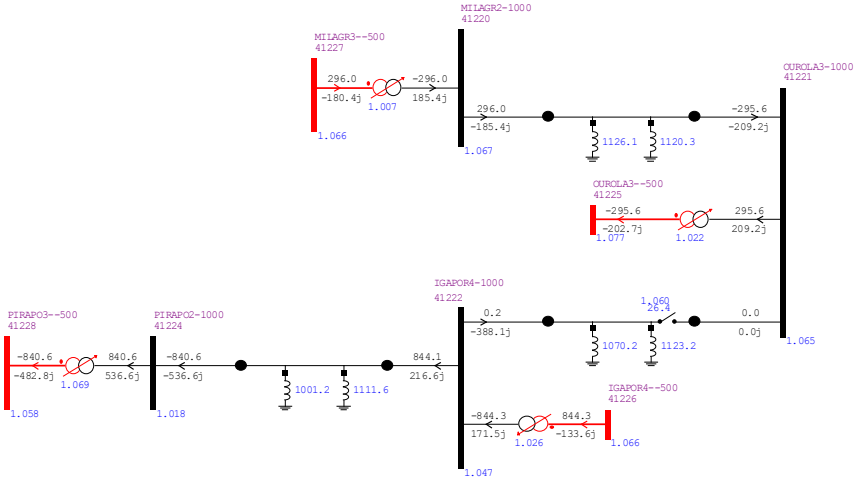

Figure 4.28: Sustained overvoltages after the opening of the 1,000 kV TL at Ourolândia or energization through Igaporã

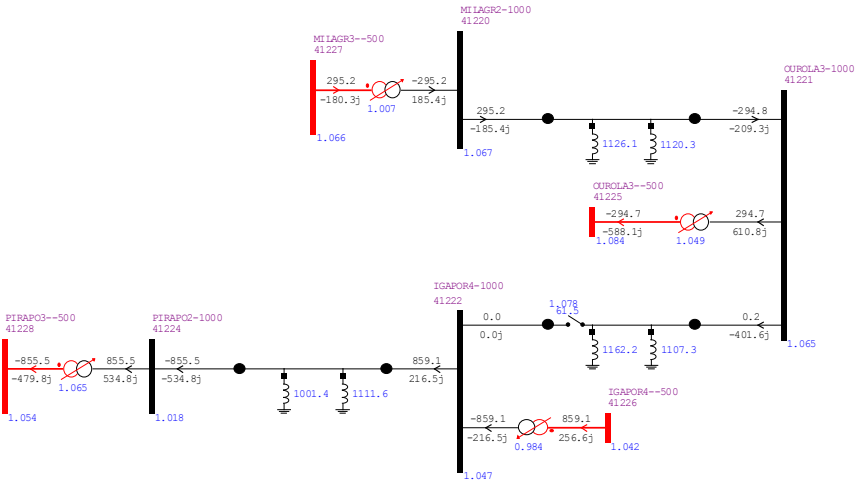

Figure 4.29: Sustained overvoltages after the opening of the 1,000 kV line at Igaporã or energization through Ourolândia

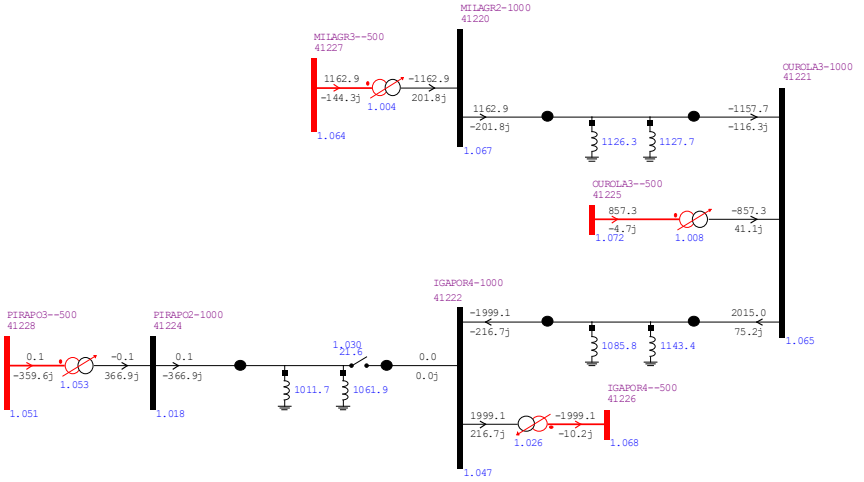

Figure 4.30: Sustained overvoltages after the opening of the 1,000 kV line at Igaporã or energization through Pirapora

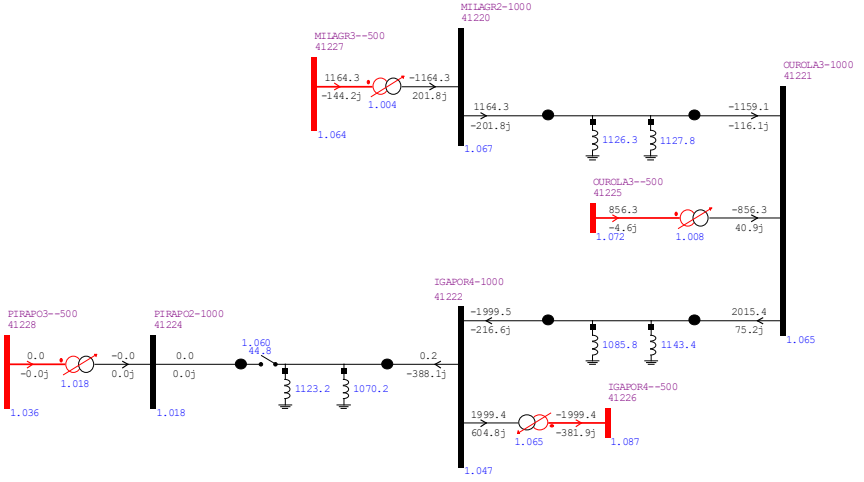

Figure 4.31: Sustained overvoltages after the opening of the 1,000 kV TL at Pirapora or energization through Igaporã

4.1.5 Considerations about power export

The energy export from the power plants in the North region have direct impact on the loading of the north-south interconnection, with the Bipole B, due to its relative proximity to the north-south Interconnection, contributing to alleviate its loading during the Wet North scenarios. It was observed that the 1,000 kV system, due to its distance from the North-south central line, does not contribute to alleviate such loading, acting primarily over the export of the wind and photovoltaic power concentrated in the central region of the Northeast, East side of the Northeast, and North side of the Southeast region.

The 1,000 kV system positions itself as a backbone with several intermediate power collecting points, facilitating the export of the renewable and intermittent energy from the region, and adding flexibility to the 500 kV system and to the SIN.

In the 2024 horizon, for the most critical scenario (Heavy Load - Wet North), the use of the 1,000 kV system, jointly with Bipole A and Bipole B, complements the operation of the SIN and offers a good flexibility to cater all the loading scenarios.

4.2 Electromechanical Transient Studies

This item presents the results of the power frequency overvoltage studies conducted considering the 1,000 kV system in its initial phase. The objective is to check whether temporary or sustained voltage values affect the specifications of the equipment connected to the system. Such voltages may result from scheduled and/or unscheduled switchings at some points nearby the UHV line.

Recall that from a previous power flow study under normal and emergency conditions it was observed the need of reactive power support in some points of the grid. Thus, it was added 600 Mvar to the Ribeirão das Neves busbar (500 kV), 300 Mvar to the Governador Valadares busbar (230 kV).

The electromechanical transient conditions were analyzed regarding the PDE 2024 base case.

Next, the results corresponding to the application of a solid phase-to-ground fault in the 1,000 kV busbars, with the subsequent opening of the 1,000 kV line, and a three-phase fault with the consequent opening of the UHV line, are presented. All the situations were evaluated without the reclosing of the 1,000 kV line. The following were the analyzed cases:

I. Single-phase fault at Milagres (1,000 kV) followed by the opening of the Milagres – Ourolândia line;
II. Single-phase fault at Ourolândia (1,000 kV) followed by the opening of the Milagres – Ourolândia line;
III. Single-phase fault at Ourolândia (1,000 kV) followed by the opening of the Ourolândia – Igaporã line;
IV. Single-phase fault at Igaporã (1,000 kV) followed by the opening of the Ourolândia – Igaporã line;
V. Single-phase fault at Igaporã (1,000 kV) followed by the opening of the Igaporã – Pirapora line;
VI. Single-phase fault at Pirapora (1,000 kV) followed by the opening of the Igaporã – Pirapora line;
VII. Opening of the Milagres – Ourolândia line;
VIII. Opening of the Ourolândia – Igaporã line;
IX. Opening of the Igaporã – Pirapora line.

4.2.1 Case 1

In Figure 4.32, the voltage on the busbars of the 1,000 kV system are shown.

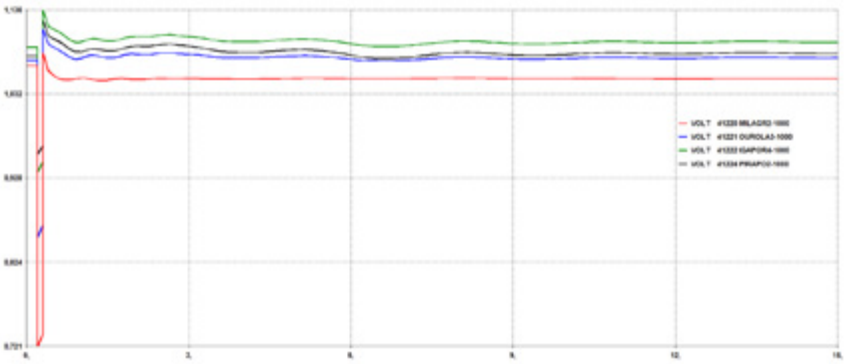

Figure 4.32: Voltage on the 1,000 kV busbars – single-phase short-circuit at Milagres with subsequent opening of the Milagres – Ourolândia line, without reclosing (s x pu)

In Figure 4.33, the active power at Paulo Afonso, Tucuruí 1, Três Marias, and Itumbiara hydropower plants, as well as the wind power from the Ourolândia and João Câmara region is shown. This study was conducted regarding the generation increase (previously described) of 900 and 1,600 MW, respectively.

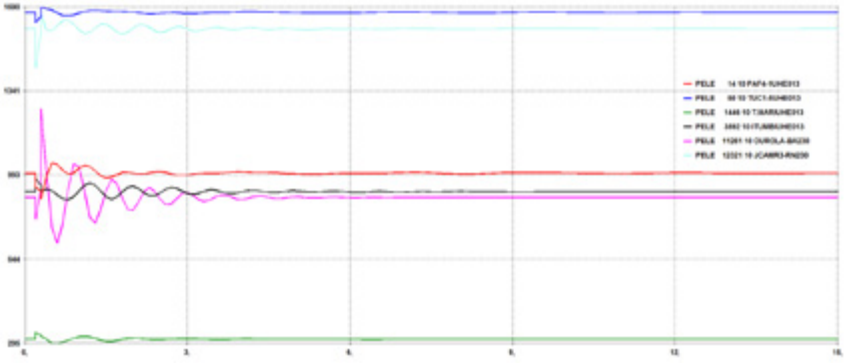

Figure 4.33: Power in system: single-phase short-circuit at Milagres with subsequent opening of the Milagres – Ourolândia line, without reclosing (s x pu)

Similar graphs are presented next for the remaining cases.

4.2.2 Case II

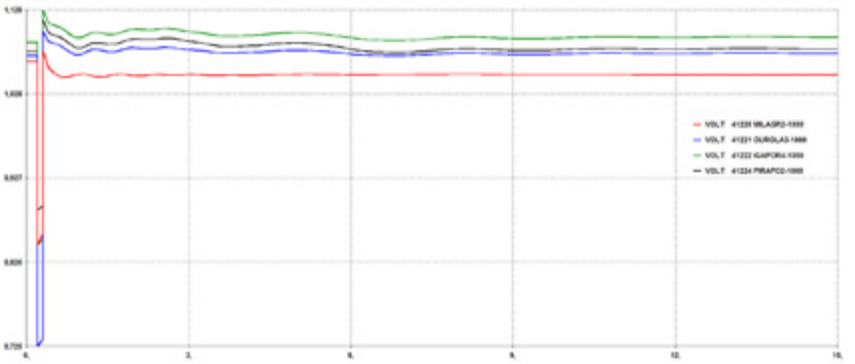

Figure 4.34: Voltage on the 1,000 kV busbars – single-phase short-circuit at Ourolândia with subsequent opening of the Milagres – Ourolândia line, without reclosing (s x pu)

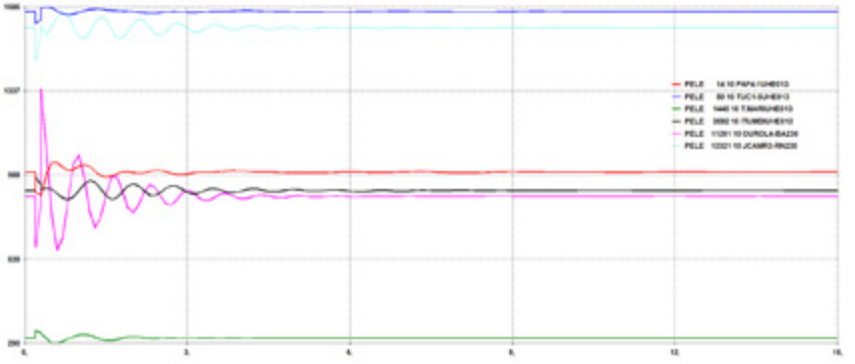

Figure 4.35: Power in the system: single-phase short-circuit at Ourolândia with subsequent opening of the Milagres – Ourolândia line, without reclosing (s x pu)

4.2.3 Case III

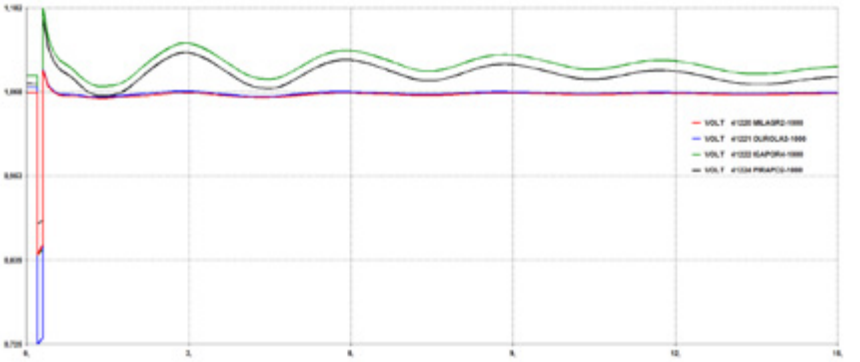

Figure 4.36: Voltage on the 1,000 kV busbars – single-phase short-circuit at Ourolândia with subsequent opening of the Ourolândia – Igaporã line, without reclosing (s x pu)

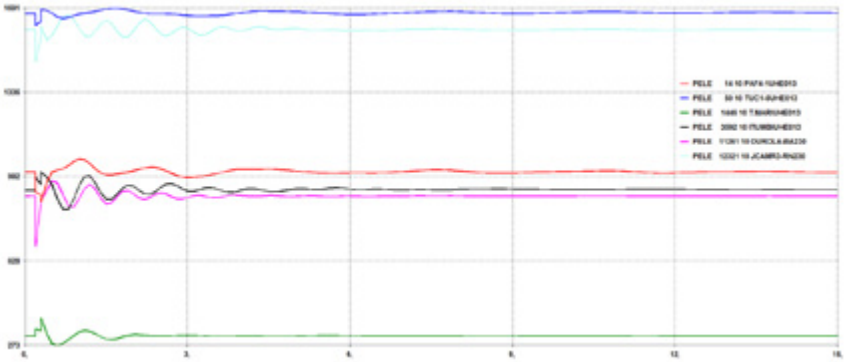

Figure 4.37: Power in the system: single-phase short-circuit at Ourolândia with subsequent opening of the Ourolândia – Igaporã line, without reclosing (s x pu)

4.2.4 Case IV

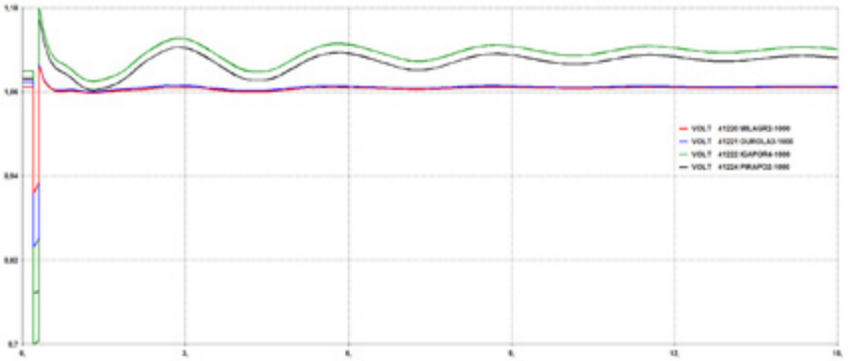

Figure 4.38: Voltage on the 1,000 kV busbars – single-phase short-circuit at Igaporã with subsequent opening of the Ourolândia – Igaporã line, without reclosing (s x pu)

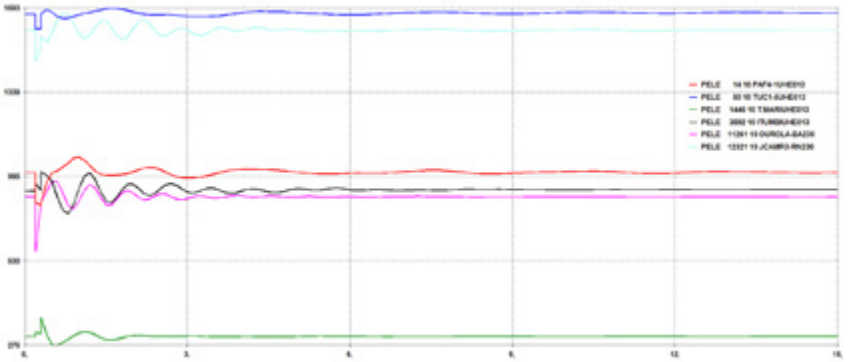

Figure 4.39: Power in the system: single-phase short-circuit at Igaporã with subsequent opening of the Ourolândia – Igaporã line, without reclosing (s x pu)

4.2.5 Case V

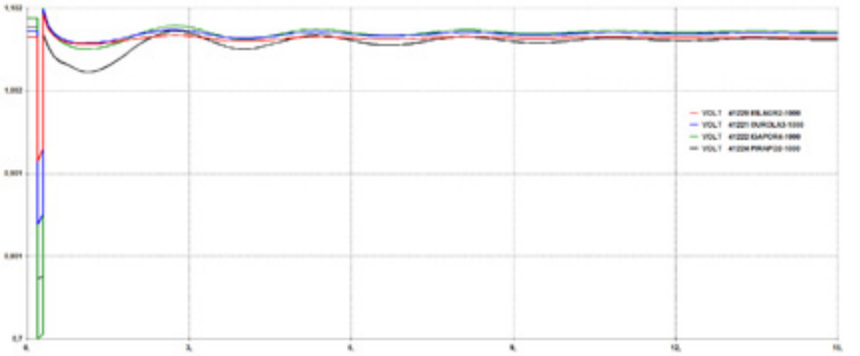

Figure 4.40: Voltage on the 1,000 kV busbars – single-phase short-circuit at Igaporã with subsequent opening of the Igaporã – Pirapora line, without reclosing (s x pu)

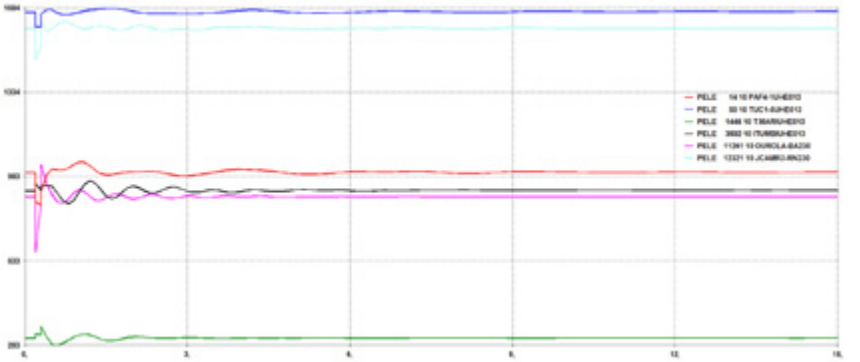

Figure 4.41: Power in the system: single-phase short-circuit at Igaporã with subsequent opening of the Igaporã – Pirapora line, without reclosing (s x pu)

4.2.6 Case VI

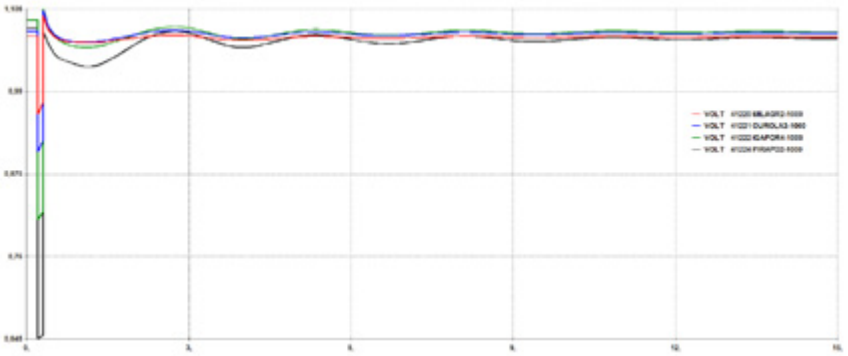

Figure 4.42: Voltage on the 1,000 kV busbars – single-phase short-circuit at Pirapora with subsequent opening of the Igaporã – Pirapora line, without reclosing (s x pu).

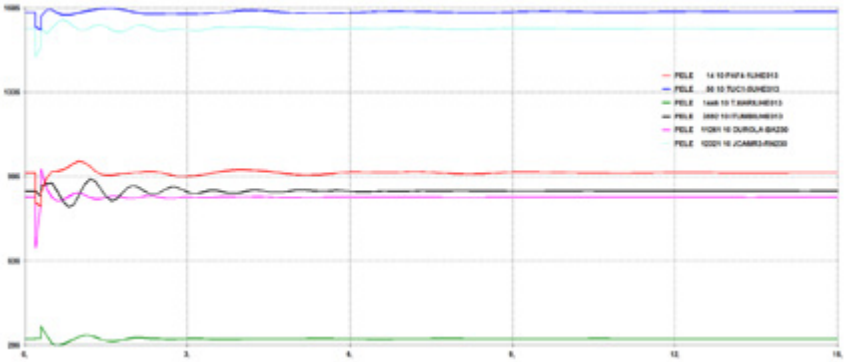

Figure 4.43: Power in the system: single-phase short-circuit at Pirapora with subsequent opening of the Igaporã – Pirapora line, without reclosing (s x pu)

4.2.7 Case VII

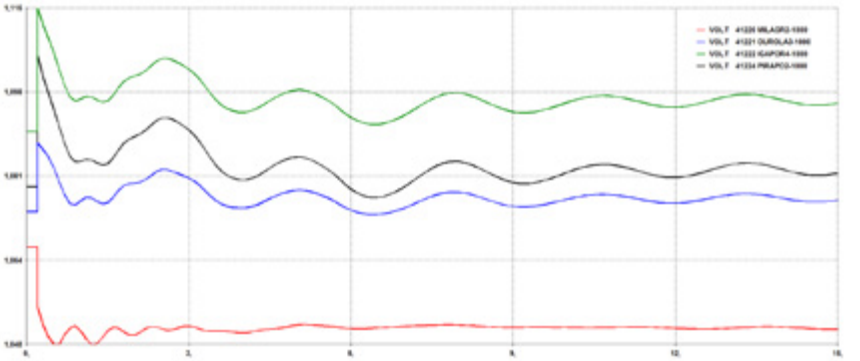

Figure 4.44: Voltage on the 1,000 kV busbars – opening of the Milagres – Ourolândia line, without reclosing (s x pu)

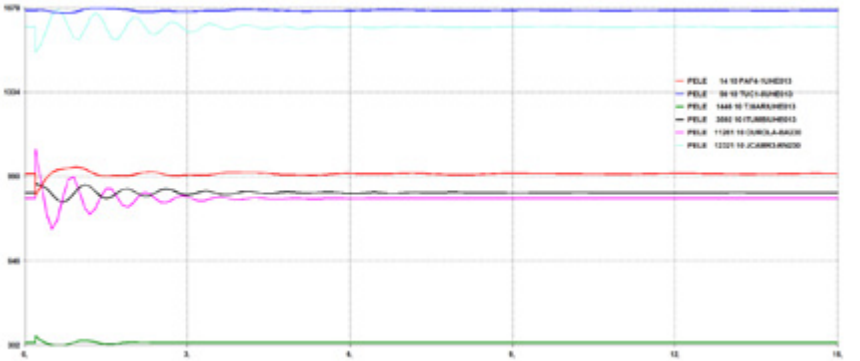

Figure 4.45: Power in the system: opening of the Milagres – Ourolândia line, without reclosing (s x pu)

4.2.8 Case VIII

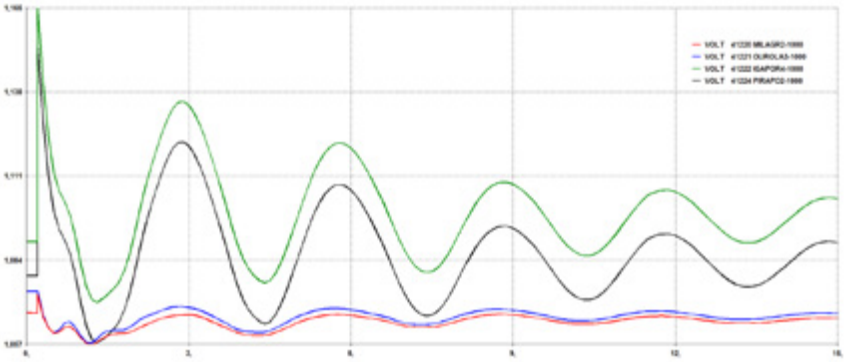

Figure 4.46: Voltage on the 1,000 kV busbars – opening of the Ourolândia – Igaporã line, without reclosing (s x pu)

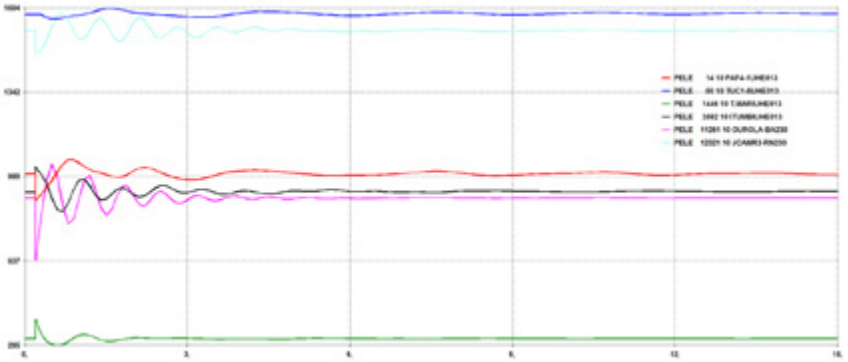

Figure 4.47: Power in the system: opening of the Ourolândia – Igaporã line, without reclosing (s x pu)

4.2.9 Case IX

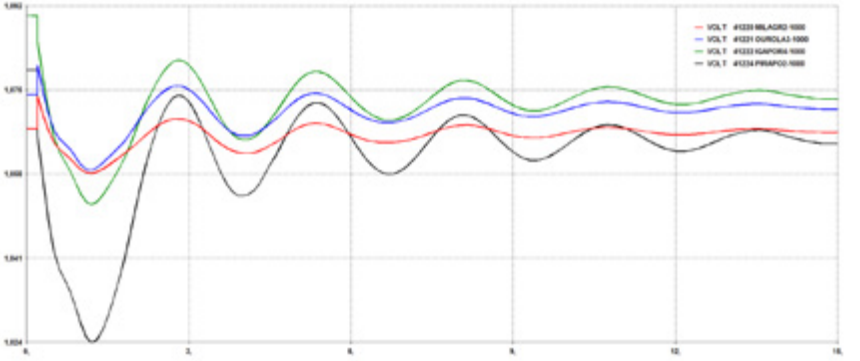

Figure 4.48: Voltage on the 1,000 kV busbars – opening of the Igaporã – Pirapora line, without reclosing (s x pu)

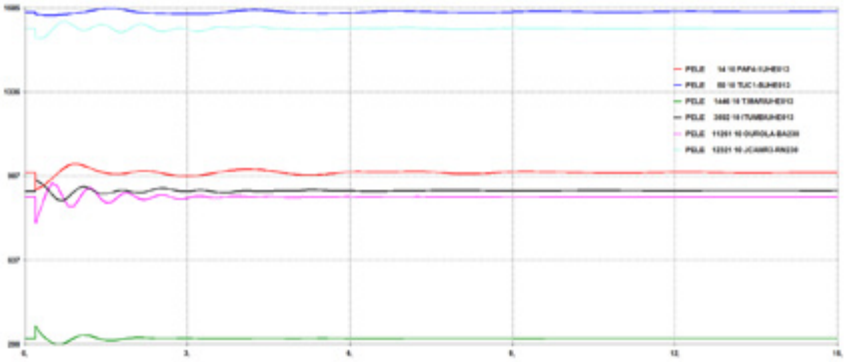

Figure 4.49: Power in the system: opening of the Igaporã – Pirapora line, without reclosing (s x pu)

4.3 Short-Circuit Studies

The short-circuit levels in the UHV system were performed considering the sub-transient regime with all the sources represented as synchronous machines. It was also used the database of the EPE's short-circuit studies (maximum short-circuit file of the PDE 2016-2024).

The short-circuit currents of the main substations within the Basic Grid are shown in Table 4.6 (expected for the year 2024). Simulations were conducted for the case with the 1,000 kV alternative inserted and another without it. None of the existing circuit-breakers had its current capacity exceeded after the

insertion of the 1,000 kV system, except for the Ipatinga 230 kV busbar, which presented a value slightly higher than the circuit breaker capacity during a single-phase short-circuit. This capacity surpass occurs even in absence of the 1,000 kV system. The influence of the 1,000 kV system over the short-circuit level was small. The above conclusion refers only to symmetrical short-circuit currents. Other restrictions such as TRV, X/R relation, etc. were not evaluated.

Table 4.6: Short-circuit levels

Identification			2024 without the UHV system				2024 with the UHV system				Circuit breaker (kA)
Number	Bus	Voltage	3Φ (kA)	X/R	1Φ (kA)	X/R	3Φ (kA)	X/R	1Φ (kA)	X/R	
206	SOBRAD-BA230	230	18.37	16.22	16.45	16.41	19.31	16.08	18.24	16.86	40
209	POCOE2-BA230	230	12.93	16.95	10.44	11.36	13.03	17.06	10.49	11.35	NA
213	ITAGIB-BA230	230	6.00	6.35	4.45	5.58	6.01	6.34	4.46	5.57	NA
276	FUNIL--BA230	230	8.94	7.13	8.85	8.51	8.96	7.12	8.86	8.5	40
288	IBICOA-BA230	230	8.37	32.14	7.61	17.23	8.47	33.09	7.68	17.25	NA
376	BRUMAD-BA230	230	3.46	7.08	3.86	8.42	3.47	7.07	3.88	8.42	40
394	IGAPO2-BA230	230	32.95	20.68	31.96	16.86	36.65	22.96	35.04	17.01	NA
505	L.GONZ-PE500	500	37.96	20.24	37.55	16.39	38.99	20.38	38.32	16.28	50
506	SOBRAD-BA500	500	21.52	6.30	21.33	11.86	22.57	6.51	22.53	12.03	40
516	QUIXAD-CE500	500	10.75	13.22	7.37	7.53	10.98	13.36	7.5	7.46	50
521	MILAGR-CE500	500	24.07	11.25	18.22	8.55	29.53	12.1	26.05	8.59	50
523	JCAMR3-RN500	500	18.51	17.47	19.19	16.37	20.57	18.07	22.62	19.05	NA
544	C.GRAN-PB500	500	16.58	16.29	13.37	10.03	19.99	10.03	24.25	10.46	NA
555	M.CHAP-BA500	500	9.04	15.23	8.15	13.23	10.35	16.01	9.04	12.98	NA
574	CAMACA-BA500	500	19.58	17.51	19.48	12.81	19.71	17.52	19.57	12.8	40
585	BJLAPA-BA500	500	17.95	14.69	15.25	11.89	19.14	15	15.88	11.73	40
587	R.EGUA-BA500	500	20.45	9.76	11.74	6.46	20.77	9.79	11.82	6.44	40
588	IBICOA-BA500	500	14.12	15.24	10.01	7.42	14.82	15.54	10.3	7.29	40
589	SAPEAC-BA500	500	17.21	14.96	15.17	9.8	17.51	15.08	15.34	9.78	40
846	BARRER-BA500	500	20.09	10.31	12.41	6.96	20.36	10.33	12.49	6.94	NA
1482	BARREI-MG345	345	17.23	11.24	14.92	7.77	17.36	11.24	14.99	7.76	25
1483	ITABI2-MG500	500	16.28	13.92	15.45	10.23	16.39	13.94	15.52	10.23	NA
1484	ITABI2-MG345	345	19.36	13.38	19.88	10.1	19.45	13.39	19.94	10.1	NA
1485	BDESPA-MG500	500	18.43	14.64	15.89	9.02	18.56	14.66	15.95	9.01	40
1488	JAGUAR-MG500	500	25.91	18.03	20.78	11.83	25.96	18.03	20.8	11.83	38
1489	JFORA1-MG345	345	6.82	9.72	6.84	10.47	6.83	9.72	6.84	10.46	40
1493	MCLARO-MG345	345	6.49	11.47	6.26	10.13	6.64	11.49	6.35	10.09	40
1494	MESQUI-MG500	500	14.66	15.07	13.54	12.24	14.82	15.13	13.63	12.24	38
1496	NEVES1-MG345	345	19.26	14.35	19.17	12.25	19.47	14.4	19.31	12.25	25
1497	NEVES1-MG500	500	17.32	15.11	16.37	11.33	17.54	15.18	16.5	11.33	38
1498	OPRET2-MG345	345	19.56	13.52	20.58	11.4	19.66	13.53	20.66	11.41	40
1499	OPRET2-MG500	500	15.39	13.85	14.75	10.37	15.48	13.86	14.81	10.37	40
1500	PIMENT-MG345	345	18.90	11.77	12.89	6.02	18.93	11.76	12.9	6.01	25
1501	SJBICA-MG345	345	9.31	11.30	5.45	5.38	9.33	11.3	5.45	5.38	NA

Identification			2024 without the UHV system				2024 with the UHV system				Circuit breaker (kA)
Number	Bus	Voltage	3Φ (kA)	X/R	1Φ (kA)	X/R	3Φ (kA)	X/R	1Φ (kA)	X/R	
1502	SGOTAR-MG345	345	11.16	18.96	11.08	14.53	11.21	18.97	11.11	14.53	40
1503	SGOTAR-MG500	500	14.50	14.49	10.98	8.68	14.57	14.51	11.01	8.67	50
1504	SGPARA-MG500	500	11.48	12.97	10.17	8.11	11.53	12.97	10.19	8.1	50
1505	SLAGO4-MG345	345	16.21	11.31	12.35	6.03	16.45	11.35	12.44	6.01	NA
1508	TAQUAR-MG345	345	19.19	11.47	17.53	8.93	19.34	11.48	17.62	8.92	24
1509	EMBORC-MG500	500	25.15	16.95	23.63	15.56	25.24	16.98	23.69	15.56	38
1510	IRAPE--MG345	345	4.55	18.28	5.50	20.05	4.58	18.17	5.53	19.95	25
1512	NPONTE-MG500	500	24.03	17.48	19.35	10.76	24.09	17.49	19.38	10.75	31.5
1515	TMARIA-MG345	345	10.17	12.32	9.82	12.58	10.31	12.29	9.91	12.56	50
1518	VESPA2-MG500	500	15.92	14.68	13.65	9.11	16.11	14.75	13.75	9.1	50
1519	VPALMA-MG345	345	11.15	12.91	10.22	10.47	11.68	13.19	10.55	10.45	50
1521	IRAPE--MG230	230	5.19	18.63	6.38	20.12	5.21	18.53	6.41	20.03	25
1523	PARACA-MG500	500	12.62	12.79	8.70	9.14	12.80	12.87	8.77	9.11	NA
1524	PIRAP2-MG345	345	15.84	18.90	16.51	15.39	17.39	21.45	18.08	16.19	NA
1525	PIRAP2-MG500	500	16.53	14.37	13.87	11.01	19.92	15.62	16.4	10.58	NA
1600	BRAUN2-MG230	230	8.78	6.87	8.06	7.6	8.80	6.86	8.07	7.59	NA
1609	JMONL4-MG230	230	8.36	6.39	5.63	4.73	8.38	6.39	5.63	4.73	NA
1610	SABAR3-MG230	230	10.90	7.72	8.10	5.42	10.94	7.71	8.12	5.42	NA
1612	BCOCA3-MG230	230	7.02	6.13	4.51	4.35	7.04	6.12	4.52	4.34	50
1613	JMOBLG-MG230	230	7.88	6.28	5.23	4.63	7.90	6.27	5.23	4.62	25
1616	CPENA--MG230	230	6.15	7.21	4.73	6.26	6.15	7.21	4.73	6.25	40
1619	GVALA2-MG230	230	13.58	10.14	12.92	9.47	13.62	10.14	12.94	9.47	NA
1620	ITABI4-MG230	230	21.09	12.81	19.68	8.75	21.29	12.86	19.8	8.75	NA
1623	**IPATI1-MG230**	**230**	**22.79**	**12.95**	**24.39**	**11.56**	**22.92**	**12.96**	**24.5**	**11.57**	**23.9**
1626	ITABI2-MG230	230	20.50	11.64	18.40	7.73	20.68	11.67	18.5	7.72	23.9
1630	MESQUI-MG230	230	24.39	15.47	26.90	14.68	24.55	15.52	27.03	14.71	40
1635	TAQUAR-MG230	230	19.20	13.68	18.77	11.85	19.31	13.69	18.84	11.84	NA
1637	AIMORE-MG230	230	7.14	11.76	8.39	13.71	7.14	11.75	8.39	13.7	31.5
1638	GUI.AM-MG230	230	9.37	7.03	8.49	6.72	9.39	7.02	8.51	6.72	NA
1640	PESTRE-MG230	230	9.05	6.97	8.19	7.57	9.07	6.96	8.2	7.56	NA
1645	BAGUAR-MG230	230	8.36	7.58	7.93	10.25	8.38	7.58	7.94	10.24	NA
1646	TIMOTE-MG230	230	12.33	7.40	10.46	6.93	12.37	7.39	10.48	6.93	NA
1650	JECEAB-MG345	345	14.77	10.67	12.24	5.78	14.81	10.66	12.26	5.78	NA
2154	P.FIAL-MG345	345	5.74	10.73	4.61	9.18	5.74	10.73	4.61	9.18	NA
3562	MASCAR-ES230	230	6.83	10.81	7.43	10.78	6.83	10.81	7.43	10.77	31.5
3580	VERONA-ES230	230	2.49	5.97	2.20	6.15	2.49	5.97	2.2	6.15	NA
3605	B.BRAN-MG345	345	11.20	11.26	8.82	6.54	11.23	11.26	8.83	6.54	NA
3795	VIANA--ES345	345	12.98	13.17	12.83	11.94	13.01	13.17	12.85	11.94	40
3807	ITUTIN-MG345	345	14.43	10.26	11.58	8.39	14.44	10.25	11.59	8.39	25
3848	VIANA2-ES345	345	12.81	13.39	12.09	10.41	12.83	13.4	12.1	10.41	NA
3849	VIANA--ES500	500	7.36	16.68	6.38	12.68	7.37	16.69	6.39	12.68	NA
3860	ITUMBI-MG500	500	30.62	20.57	29.77	19.21	30.65	20.57	29.79	19.21	31.5
4300	LUZIAN-DF500	500	23.05	9.86	17.51	8.65	23.39	9.92	17.65	8.65	NA
4302	ESTREI-MG500	500	33.44	18.09	23.10	8.3	33.49	18.09	23.12	8.3	NA
4303	TRINDA-GO500	500	12.68	14.77	9.72	8.62	12.69	14.78	9.73	8.62	NA

Identification			2024 without the UHV system				2024 with the UHV system				Circuit breaker (kA)
Number	Bus	Voltage	3Φ (kA)	X/R	1Φ (kA)	X/R	3Φ (kA)	X/R	1Φ (kA)	X/R	
11260	G.OURO-BA230	230	16.92	21.90	14.24	13.82	17.69	22.91	16.05	16.28	NA
11261	OUROLA-BA230	230	17.52	17.85	13.16	7.94	23.38	25.34	26.12	22.43	NA
11282	JUAZE3-PE230	230	18.11	13.98	18.91	12.28	20.24	15.46	23.71	15.6	NA
11394	IGAPO3-BA230	230	34.61	21.95	33.75	17.14	38.88	25.2	37.55	17.58	NA
11546	CMIRIM-RN500	500	16.46	17.33	14.69	10.96	18.07	16.18	16.19	10.17	NA
11560	G.OURO-BA500	500	13.04	14.57	9.93	9.67	13.87	14.97	11.09	10.67	NA
11561	OUROLA-BA500	500	12.07	14.79	7.93	6.29	18.18	19.2	15.71	12.46	NA
11565	AÇUIII-RN500	500	17.64	14.60	12.99	7.73	18.64	15.16	13.52	7.6	NA
11567	MILAG2-CE500	500	24.41	11.26	18.38	8.43	30.10	12.11	26.88	8.64	NA
11582	JUAZE3-BA500	500	17.04	12.51	13.63	9.66	18.60	13.46	15.53	11.16	NA
11594	IGAPO3-BA500	500	19.11	16.86	16.73	13.07	23.30	18.42	19.85	12.43	NA
11595	PINDA2-BA230	230	31.39	19.98	30.14	16.38	34.73	21.86	32.82	16.39	NA
12201	CNOVO2-PI230	230	23.36	21.22	18.45	11.07	24.60	21.93	22.06	14.5	NA
12321	JCAMR3-RN230	230	27.28	21.68	28.56	19.22	32.22	24.06	39.44	25.41	NA
26454	BETIM6-MG345	345	17.92	12.14	15.69	8.44	18.09	12.16	15.78	8.43	NA
26460	TIMOT2-MG230	230	12.90	7.57	10.94	6.87	12.94	7.56	10.96	6.87	NA
26461	SARZED-MG345	345	15.30	11.14	11.34	5.93	15.40	11.14	11.38	5.92	NA
26465	JUSCEL-MG500	500	16.31	15.17	12.13	8.46	17.47	15.64	12.75	8.34	NA
26470	JUSCEL-MG345	345	13.61	17.14	12.92	12.36	13.96	17.69	13.21	12.51	NA
26510	ITABI5-MG500	500	17.95	14.97	16.01	10.09	18.32	15.12	16.22	10.07	NA
26513	ITABI5-MG230	230	24.38	16.18	25.92	13.99	24.64	16.33	26.12	14.04	NA
38888	LINHAR-ES230	230	3.48	7.20	2.75	6.2	3.48	7.2	2.75	6.2	NA
38900	JANAU3-MG500	500	15.96	14.96	11.06	8.31	17.38	15.29	11.62	8.1	NA
38921	GVALA6-MG500	500	10.68	13.56	9.79	12.58	10.73	13.57	9.83	12.58	NA
38974	MUTUM--MG500	500	11.41	14.89	9.02	8.94	11.46	14.91	9.04	8.93	NA
38986	GVALA6-MG230	230	16.92	13.16	18.41	13.61	16.97	13.17	18.45	13.62	NA
39311	JNEIV2-ES345	345	9.42	11.60	8.27	9.5	9.44	11.61	8.28	9.5	NA
39313	R.N.S.-ES345	345	13.41	12.59	12.13	9.77	13.43	12.59	12.14	9.77	NA
39511	JNEIV2-ES500	500	6.06	14.49	5.01	10.58	6.08	14.51	5.02	10.58	NA
40700	VIGA---MG345	345	13.99	10.53	11.15	5.52	14.02	10.53	11.16	5.51	NA
41120	MIL-JUA--CAP	1,000	0	0	0	0	12.27	16.2	12.98	16.32	new
41121	OUR-MIL-CAP	1,000	0	0	0	0	14.43	14.38	9.14	6.41	new
41220	MILAGR2-1000	1,000	0	0	0	0	9.62	21.35	9.24	20.64	new
41221	OUROLA3-1000	1,000	0	0	0	0	10.23	21.41	7.18	8.09	new
41222	IGAPOR4-1000	1,000	0	0	0	0	9.94	22.03	7.21	9.18	new
41224	PIRAPO2-1000	1,000	0	0	0	0	7.74	21.22	6.14	12.87	new
41225	OUROLA3--500	500	0	0	0	0	19.13	20.58	14.62	8.33	new
41226	IGAPOR4--500	500	0	0	0	0	22.42	18.57	16.66	8.5	new
41227	MILAGR3--500	500	0	0	0	0	29.41	12.76	32.73	12.75	new
41228	PIRAPO3--500	500	0	0	0	0	19.51	16.33	16.21	10.79	new
41321	OUR-IGA-CAP	1,000	0	0	0	0	14.29	14.47	9.19	6.34	new
41322	IGA-OUR-CAP	1,000	0	0	0	0	13.24	16.23	9.13	7.45	new
41523	IGA-PIR-CAP	1,000	0	0	0	0	16.25	12.97	10.01	6.63	new
41524	PIR-IGA-CAP	1,000	0	0	0	0	8.43	19.88	6.98	12.32	new
60000	S.LUZIA-500	500	0	0	0	0	11.33	4.51	15	4.89	new

5. Socio-environmental Evaluation of the Transmission System Corridor Alternatives

The content of this item considers only socio-environmental aspects, thus, the UHV line will be divided as follows:

- **Section 1** – Milagres to Ourolândia;
- **Section 2** – Ourolândia to Igaporã;
- **Section 3** – Igaporã to Pirapora.

The UHV line crosses the states of Ceará, Pernambuco, Bahia, and Minas Gerais, with the largest part located in the state of Bahia and within the caatinga biome. Figure 5.1 illustrates the sections/corridors being studied considering the shortest lengths between substations, which means that it is not yet considered specific studies for the definition of the best corridor.

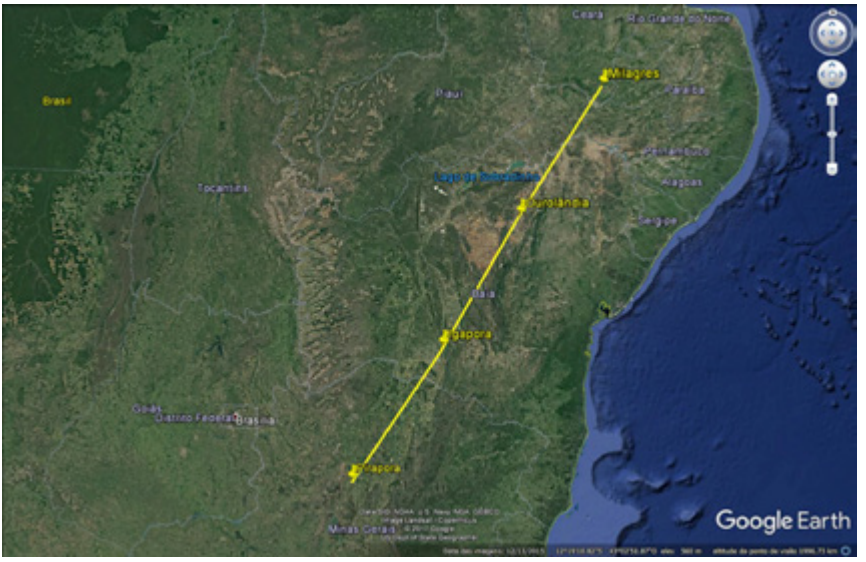

Figure 5.1: Location of the shortest sections between the substations

The socio-environmental analysis considers two corridor alternatives: a first alternative with the shortest path and another alternative that considers deviating the main socio-environmental impediments.

5.1 Alternative 1 – Shortest Corridor

This alternative was defined by drawing straight lines between Milagres and Ourolândia (Section 1); Ourolândia and Igaporã (Section 2); and Igaporã and Pirapora (Section 3). The total length of the path is approximately 1,282.477 km running through 48 municipalities, 13 of which are in the state of Minas Gerais, 7 in the state of Pernambuco, 5 in the state of Ceará, and 23 in the state of Bahia. The 30 km wide corridor in this alternative has an area of 39,193.95 km^2, 81% of which is within the Caatinga Biome and 19% within the Cerrado Biome.

Along the path, there is a river crossing (Rio das Velhas) located at South of Section 3. There are 24 crossings points of federal, state and municipal paved roads, and 1 railway crossing point.

In this corridor, the natural vegetation, anthropic areas, and water resources correspond to 37.56%, 61.79%, and 0.65% of the total area, respectively. Also, there are significant areas of agriculture and silviculture, which together represent 1.36% of the total length of the corridor. The main areas are located in the municipalities of Brejo Santo (Ceará), Porteiras (Ceará), and Cedro (Ceará), in the northern portion of Section 1; Santa Maria da Boa Vista (Pernambuco), and Orocó (Pernambuco), in the central region of Section 1; Juazeiro (Bahia), in the southern part of Section 1; Jaíba (Bahia) and Verdelândia (Minas Gerais), to the center of Section 3; and Mirabela (Minas Gerais), and Coração de Jesus (Minas Gerais), in the southern portion of Section 3.

The cities, towns and villages correspond to 0.22% of the corridor area. Among the areas with buildings within the corridor it can be mentioned the main offices of the municipalities of Brejo Santo (Ceará), in the northern part of Section 1; Seabra (Bahia), in the central region of Section 2; Guanambi (Bahia), in the extreme northern part of Section 3; Mirabela (Minas Gerais), in the central portion of Section 3; and Coração de Jesus (Minas Gerais), Pirapora (Minas Gerais), and Buritizeiro (Minas Gerais), in the southern part of Section 3.

Regarding special and/or protected areas there are eight Conservation Units (CUs), and seven *quilombolic* communities. Table 5.1 presents a summary of the main socio-environmental interferences for the shortest path having a 30-km wide corridor.

Table 5.1: Main socio-environmental interferences along the line route

Description	Quantitative	
Length of the line (km)	1,282.477	
Conservation Units	**Corridor Axis**	**Corridor (30 km)**
	5	8
Native vegetation (km^2) in the 30 wide corridor	14,722.165	
Agriculture (km^2)	478.854	
Indigenous land areas	**Corridor Axis**	**Corridor (30 km)**
	0	0
Quilombolic	**Corridor Axis**	**Corridor (30 km)**
	4	7
Incra Settlements	**Corridor Axis**	**Corridor (30 km)**
	14	68
Caverns (#) in the 30 km wide corridor	147	
Municipalities crossed	**Corridor Axis**	**Corridor (30 km)**
	48	78
Urban areas (km^2)	86.46	

5.2 Alternative 2 – Corridor that Avoids Some Environmental Impediments

This alternative considers socio-environmental interferences that prevent or greatly hinder the installation of the UHV line. To design the line route between each substation, the previous shortest path alternative was diverted (to a lesser extent possible) from Integral Protection Conservation Units, indigenous lands, and other interferences. Thus, a new path with approximately 1,336.09 km crossing 52 municipalities (15 of which are in the state of Minas Gerais, 5 in Pernambuco, 6 in Ceará, and 26 in Bahia) was setup. The 30 km wide corridor has an area of approximately 40,767.73 km^2, 75.89% of which are within the *caatinga* biome, 23.12% within the *cerrado* biome, and 0.98% in the *mata atlântica* (*subtropical forest*) biome.

Along the route alternative defined, there is a crossing of the São Francisco River, in the central portion of Section 1, and a crossing point over the Rio das Velhas, close to the Pirapora substation. Also, it was spotted the existence of 40 crossing points of federal, state and municipal paved roads and 5 railway crossings points.

Natural vegetation, anthropic areas, and water resources account for 37.90%, 61.49%, and 0.61% of the total area of the corridor, respectively. There are significant areas of agriculture and silviculture, which together represent 1.43% of the total length of the corridor. The main areas of agriculture and silviculture are located in the following municipalities: Brejo Santo (Ceará),

Porteiras (Ceará), Cedro (Ceará), and Penaforte (Ceará), in the northern portion of Section 1; Santa Maria da Boa Vista (Pernambuco), Cabrobó (Pernambuco), and Orocó (Pernambuco), in the central region of Section 1; Juazeiro (Bahia), Abaré (Bahia), and Curaçá (Bahia), in the southern part of Section 1; Várzea Nova (Bahia), and Jacobina (Bahia), in the northern part of Section 2; Urandi (Bahia), and Sebastião Laranjeiras (Bahia), in the northern part of Section 3, Nova Porteirinha (Minas Gerais), and Janaúba (Minas Gerais), in the center region of Section 3; and finally Mirabela (Minas Gerais), and Coração de Jesus (Minas Gerais), in the southern portion of Section 3.

Cities, towns and villages correspond to about 0.21% of the corridor with the shortest route. Among the areas with buildings within the corridor, it was spotted the main offices of the municipalities of Brejo Santo (Ceará), in the northern of Section 1; Seabra (Bahia), in the central region of Section 2; Guanambi (Bahia), in the extreme northern part of Section 3; Mirabela (Minas Gerais), in the central portion of Section 3; and Coração de Jesus (Minas Gerais), Pirapora (Minas Gerais), and Buritizeiro (Minas Gerais), in the southern region of Section 3.

Regarding special and/or protected areas there are eight Conservation Units and six *quilombolic* communities. In Table 5.2, a summary of the main socio-environmental interferences of this alternative, is presented.

Table 5.2: Main socio-environmental interferences in the alternative that avoids environmental impediments

Description	Quantitative	
Length of the line (km)	1,336.09	
Conservation Units	**Corridor Axis**	**Corridor (30 km)**
	2	8
Native vegetation (km^2) in the 30 wide corridor	15,202.88	
Agriculture (km^2)	506.61	
Indigenous Land areas	**Corridor Axis**	**Corridor (30 km)**
	0	2
Quilombolic	**Corridor Axis**	**Corridor (30 km)**
	0	6
Incra Settlements	**Corridor Axis**	**Corridor (30 km)**
	0	53
Caverns in the 30 km wide corridor	253	
Municipalities crossed	**Corridor Axis**	**Corridor (30 km)**
	52	89
Urban Areas (km^2)	87.58	

5.3 Analysis of the Alternatives

To choose the best corridor and axis alternative for the proposed transmission line, each previously described section was analyzed for both options indicated above. These evaluations aimed at identifying the alternative with the best socio-environmental performance for the implementation of the main route by means of socio-environmental indicators and variables.

The indicators were elaborated based on the variables chosen, taking into account their interference on legally protected areas and regions of great social and environmental significance. Also, the impact of the path corridor in several types of land uses and covers was considered. Secondary databases of Probio (2007) and IBGE (2012) were used. Additionally, satellite images of the Landsat 8 satellite were used.

During these evaluations, the following socio-environmental variables were observed:

- Integral Protection Conservation Units (IPCU);
- Sustainable Use Conservation Units (SUCU);
- Caves;
- Archaeological sites;
- Quilombolic communities;
- Indigenous lands (IL);
- Settlements;
- Priority Areas for Biodiversity Conservation (PABC);
- Land use and cover;
- Railways;
- Roads.

The Conservation Units (CU) are defined by the National System of Conservation Units (NSCU) as legally protected areas with relevant natural characteristics. Its purpose is to promote conservation, biodiversity preservation, and sustainable development. Each CU is subdivided into Integral Protection Conservation Units (IPCU), and Sustainable Use Conservation Units (SUCU).

In the IPCU, only the indirect use of natural resources is allowed, that is, without consuming, collecting, damaging or destroying them. Among the IPCUs are Ecological Stations (ECS), Biological Reserves (Rebio), National Parks (Parna), Natural Monuments (NM), and Wildlife Sanctuaries (WS) (ICMBio 2015).

The objective of the SUCUs is to make nature conservation compatible with the sustainable use of its natural resources, reconciling the use of the environment and guaranteeing the conservation of renewable natural resources. Among the SUCUs there are Environmental Protection Areas (EPA), Areas of Relevant Ecological Interest (AREI), National Forests (Flona), Extractive Reserves (Resex), Fauna Reserves (Refau), Sustainable Development Reserves (SDR), and Private Reserve of Natural Heritage (PRNH) (ICMBio, 2015).

The CU data used to compose the indicators was extracted from the National Register of Conservation Units (2015), from the Ministry of the Environment (ME).

The data of caves and geological sites were obtained from the National Center for Research and Conservation of Caves (Cecav, 2015) and the Ministry of the Environment (2006), respectively. The information about the caves refers to locations identified and validated by a technical staff or a similar organization that meets the reliability levels required by ICMBio. The geological sites were compiled by the ME from the Geodiversity Map of Brazil.

In delimiting the path corridor, it was tried to avoid areas with indigenous lands, settlements, and *quilombolic* communities. The information referred to these areas was obtained from Funai (2015), and Incra (2015), respectively.

Data related to the land use and its cover was obtained from various sources, namely:

- Deforestation data from the Satellite Deforestation Monitoring of the Brazilian Biomes Project (PMDBBS), from the ME (2008 to 2010);
- Areas containing buildings, IBGE (2015);
- Hydrography, IBGE (2015),
- Land Use and Coverage Map, IBGE (2012).

To determine Priority Areas, data from the Ministry of the Environment (2007) was used. These areas represent locations of considerable importance for conservation, sustainable use, and distribution of biodiversity benefits.

Data corresponding to roads were obtained from the IBGE database (2015). State, federal, and municipal roads were evaluated, regardless of the type of pavement, due to their relevance to the choosing of the line route. Similarly, the data about Railways was obtained from the National Plan of Logistics and Transportation (PNLT) of the Ministry of Transportation (2010).

The socio-environmental relevance and measurability of the variables were essential in choosing the composition of the indicators. This measurement and weighting is done by a multi-disciplinary team.

To choose the best location alternative, evaluations were conducted in each section described above. The variables were defined based on reviews of other reports elaborated by EPE, and the experience of a multi-disciplinary study team.

The indicators were established based on the variables defined, and related studies conducted by the team, by EPE, by ANEEL, technical notes on the subject, and specific features of the project.

While choosing the corridor that may be crossed by the main route, the objective was to establish the area that would be subject to less socio-environmental impact with the allocation of the future line. For this analysis, the *Analytical Hierarchy Process* (AHP) method was used.

The AHP method, largely used in multi-criteria decisions, was proposed by Saaty (1987), and is based on a hierarchical structure of the problem, where comparisons of the variables are made pairwise in a preference matrix (LUZ et al., 2006). Through this pairwise analysis, the relative importance of the variables appears. according to some degrees of importance as described in Table 5.3:

Table 5.3: Preference options for pairwise comparison

Definition and explanation	Degree of importance
Equal Importance	1
Slightly more important	3
Much more important	5
Heavily more important	7
Absolutely more important	9

The AHP was used to choose the corridor, because it allows weighting different variables involved in the diagnostic and decision-making process, allowing for the objective integration of the chosen indicators.

Thus, to calculate the indicators, the previously mentioned variables were divided into classes, as described below:

Table 5.4: Classification of variables for indicators calculation

Variable	Classes
IPCU	Presence or absence
SUCU	
Caves	
Quilombos	
Indigenous lands	
Geological sites	
Settlements	
Railway	
Road	
Land use	Natural vegetation
	Other uses
	Agricultural area
	Water bodies
	Silviculture
	Built area
Priority areas	Extremely high
	Very High
	High

To obtain the final score for the indicators, in addition to the weights of the variables obtained using the AHP, the grades for the classes, and the area (for the IPCU, SUCU, TI, settlements, quilombolic areas, priority areas and land use) or density (for caves, geological sites, railways, and roads) of the variable in the path corridor were considered. Therefore, the values in the table represent the socio-environmental impacts in each alternative, weighted according to their weights, areas and densities described above.

The weighting was a result of the understanding of various representatives of the multi-disciplinary team, according to their areas of education and work: biologists, forestry and environmental engineers, geographers, agronomists, etc.

Thus, location alternative 2 presented a corridor more favorable to the implementation of the main route from a socio-environmental perspective (lower socio-environmental impact), according to the indicators presented in Table 5.5. That is, the lower score indicated the lowest impact for location alternative 2.

Table 5.5: Socio-environmental indicators for the two alternatives

Variable	Classes	Location alternative 1 (shorter path)	Location alternative 2 (considers environmental impediments)
IPCU	Presence	0.687	0.444
Caves	Presence	0.009	0.015
Quilombos	Presence	0.113	0.045
Indigenous lands	Presence	–	0.029
	Absence	0	–
Geological sites	Absence	0	0
Settlements	Presence	0.121	0.066
Land use	Natural vegetation	0.599	0.594
	Other uses	0.192	0.193
	Agricultural area	0.012	0.012
	Water bodies	0.002	0.002
	Silviculture	0.002	0.003
	Built area	0.006	0.006
Priority areas	Extremely high	0.309	0.384
	Very High	0.35	0.291
	High	0.14	0.159
Railway	Absence	0	0
Road	Presence	–	0.001
	Absence	0	–
SUCU	Presence	0.149	0.173
Final grade		2.691	2.417

5.4 Selected Alternative

In quantitative terms, this item considers the spatial analysis of secondary data from Geographic Information Systems (GIS), made available by official sources, and processing based on this data.

The socio-environmental indicators that supported the evaluation of the path alternatives, and the adoption of the lower impact one, were built based on the secondary data, and on the knowledge of the project team.

The following main activities were performed:

- **Acquisition of images**: – Images were acquired from the Landsat-8 satellite, with spatial resolution of 30 meters, and imaging date of 2015. The images were acquired in 12 scenes, and cut to the area of study, meeting the presented scope.
- **Treatment of the images acquired**: – The images were mosaicked and highlighted for visual display only. The orthorectification was done by the image supply service.
- **Study of the location alternatives**: – two path options are presented considering: Shortest path between the substations, and path based on the analysis of the above-mentioned secondary data. Which means, deviating from environmental impediments such as Integral Protection Conservation Units, indigenous lands, settlement concentrations, and large urban areas.
- **Environmental indicators**: – Based on the chosen variables, simple indicators were generated for comparison of the alternatives identified. The data used for the location alternative study was identified and made available by public, private, and mixed institutions specific in their respective work and research areas.
- **Characterization of the 30 km right-of-way**: – Based on all the geo-referenced information, we proceeded to the detailing and characterization of the right-of-way/corridor defined for the chosen path, and for each of the sections.

5.5 Socio-environmental Analysis

The purpose of the socio-environmental analysis is to assist on the decision making regarding the routing alternatives that cause the least socio-environmental impact to their areas of influence, based on the diagnosis and evaluation of several aspects. For this, elements that reflect the impacts on the physical, biotic, and socioeconomic environments considering aspects related to terrestrial ecosystems, indigenous and traditional populations, population density, and urban concentrations are taken into account. This diagnosis supports the evaluation and decision making in the projects through the identification of sustainability indicators for the corridor, delimiting areas of high social and environmental fragility linked to the alternatives presented.

5.6 Description of the Selected Alternative

Next, the macro-environmental characteristics of the right-of-way chosen as the most socio-environmentally feasible, which may be crossed by the main route, is presented.

This right-of-way corresponds to a 30 km wide corridor within which the best location for the route of the transmission line will be chosen.

Table 5.6 describes the municipalities, the state, and the geographic coordinates of each power substation that interconnects the sections.

Table 5.6: Location of the substations

Substation name	Municipality	State	Coordinates	
			Latitude	Longitude
Milagres	Milagres	Ceará	7° 18′ 25,159″ S	38° 56′ 18,368″ S
Ourolândia	Mirangaba	Bahia	10° 41′ 35,809″ S	40° 55′ 3,556″ S
Igaporã	Caetité	Bahia	14° 4′ 17,485″ S	42° 44′ 27,484″ S
Pirapora	Pirapora	Minas Gerais	17° 20′ 17,257″ S	44° 52′ 12,367″ S

The analyses are presented for each section between the substations, as can be seen in Figure 5.2.

- **Section 1** – Milagres to Ourolândia;
- **Section 2** – Ourolândia to Igaporã;
- **Section 3** – Igaporã to Pirapora.

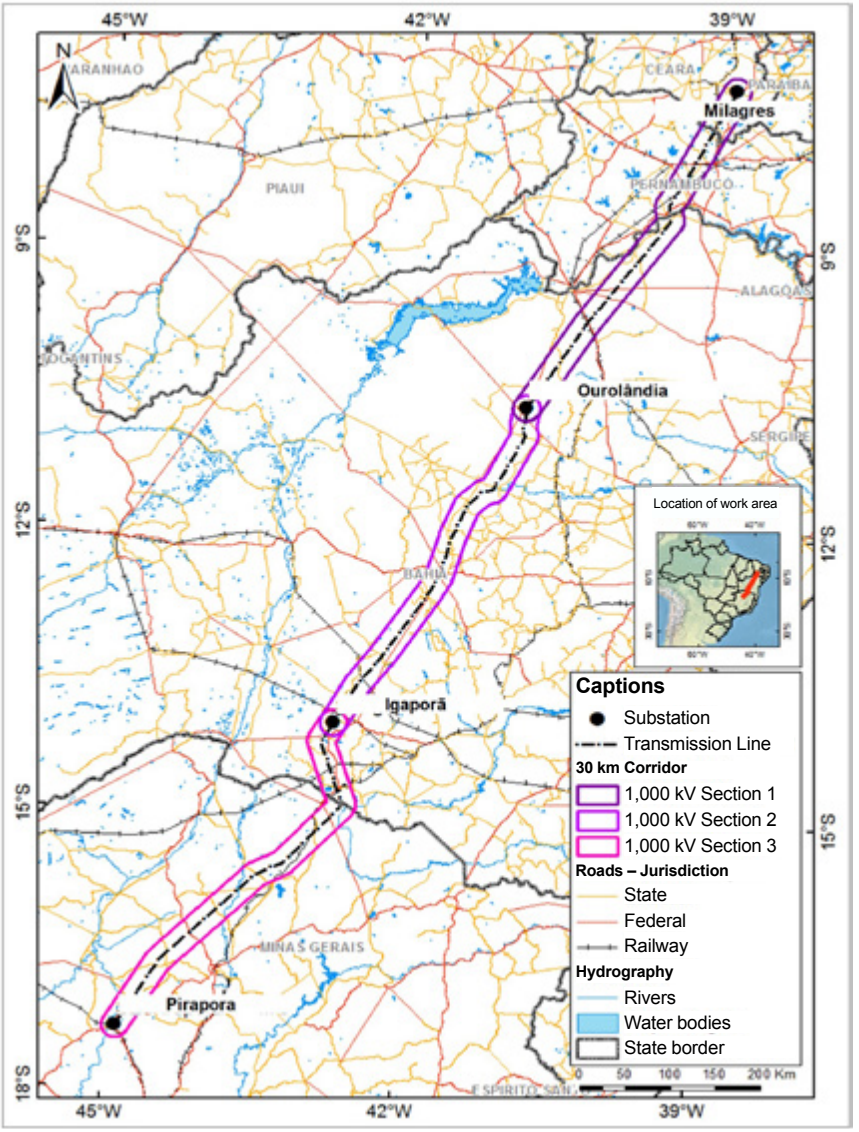

Figure 5.2: Location of the corridors divided per sections

5.6.1 Macro-characterization of the Milagres (Ceará) to Ourolândia (Bahia) section

Section 1 (T1) comprises the corridor area that starts at Milagres, located in the municipality of Milagres, in the southeast region of the state of Ceará. This is a 13,799.57 km² area. The São Francisco River crosses the south part of the T1 corridor, which should be carefully evaluated for the location of the main route of the line, so as to choose the best crossing point. The municipalities crossed by T1 and their respective population densities are described in Table 5.7, and shown in Figure 5.3.

Table 5.7: List of municipalities crossed by the T1 corridor – Milagres to Ourolândia

State	Mesoregion	Microregion	Municipality	Population	Population density (people/km²)
CE	South of Ceará	Barro	Barro	21,479	20 to 50
			Mauriti	44,167	20 to 50
		Brejo Santo	Jati	7,632	20 to 50
			Penaforte	8,196	50 to 100
			Abaiara	10,474	50 to 100
			Brejo Santo	45,162	50 to 100
			Milagres	28,262	20 to 50
			Jardim	26,646	20 to 50
			Missão Velha	34,206	50 to 100
			Porteiras	15,052	50 to 100
PE	São Francisco in Pernambuco	Petrolina	Terra Nova	9,257	20 to 50
			Cabrobó	30,775	10 to 20
			Orocó	13,129	20 to 50
			Santa Maria da Boa Vista	39,393	10 to 20
			Cedro	10,774	50 to 100
	Semi-arid area of Pernambuco	Salgueiro	Parnamirim	20,167	5 to 10
			Salgueiro	56,050	20 to 50
			Serrita	18,323	10 to 20
BA	Vale São-Franciscano da Bahia	Juazeiro	Juazeiro	197,397	20 to 50
			Curaçá	32134	up to 5
		Paulo Afonso	Abaré	16,991	5 to 10
	Central/North of Bahia	Jacobina	Jacobina	79,112	20 to 50
			Mirangaba	16,270	5 to 10
			Ourolândia	16,389	10 to 20
		Senhor do Bonfim	Campo Formoso	66,441	5 to 10
			Jaguarari	30,281	10 to 20
			Umburanas	16,908	5 to 10

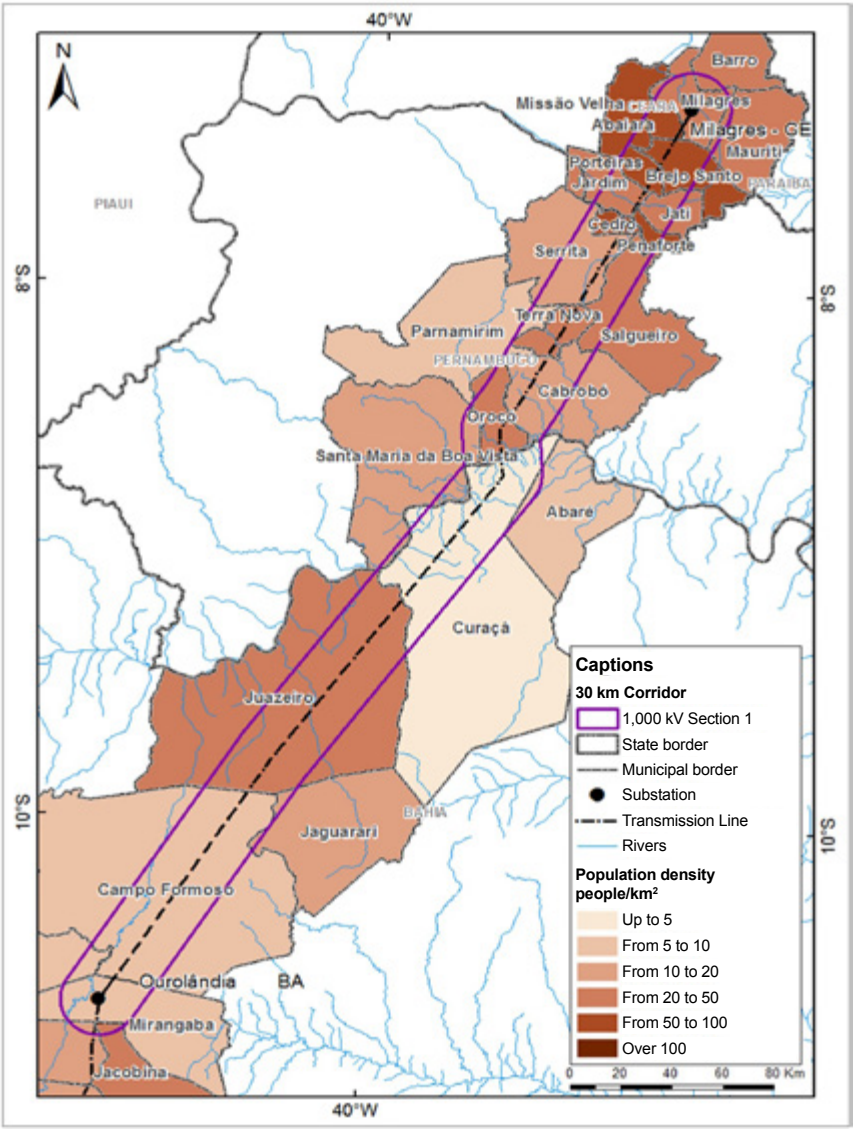

Figure 5.3: Location of the T1 corridor – Milagres to Ourolândia

According to the Land Use and Coverage Map published by IBGE (2012), T1 presents significant agricultural areas located mainly in the municipalities of: Brejo Santo (Ceará), Porteiras (Ceará), Cedro (Ceará), and Penaforte (Ceará), in the northern portion of the corridor; and Orocó (Pernambuco), Cabrobó (Pernambuco), and Santa Maria da Boa Vista (Pernambuco), Juazeiro (Bahia), and Curaçá (Bahia), in the central region.

The T1 corridor lies entirely in the *caatinga* biome. The vegetation cover and land use classes of this section are listed in Table 5.8. Figure 5.4 shows the distribution of the vegetation cover and the occupation within the T1 corridor.

Table 5.8: Vegetation cover and land use in the T1 corridor - Milagres to Ourolândia

Dominant classes	Area in the corridor (km²)	%
Agricultural area	298.65	2.164
Other uses (such as pasture)	7,123.70	51.623
Built area	14.34	0.104
Water bodies	167.21	1.212
Natural vegetation	6,195.67	44.898
Total	**13,799.57**	**100**

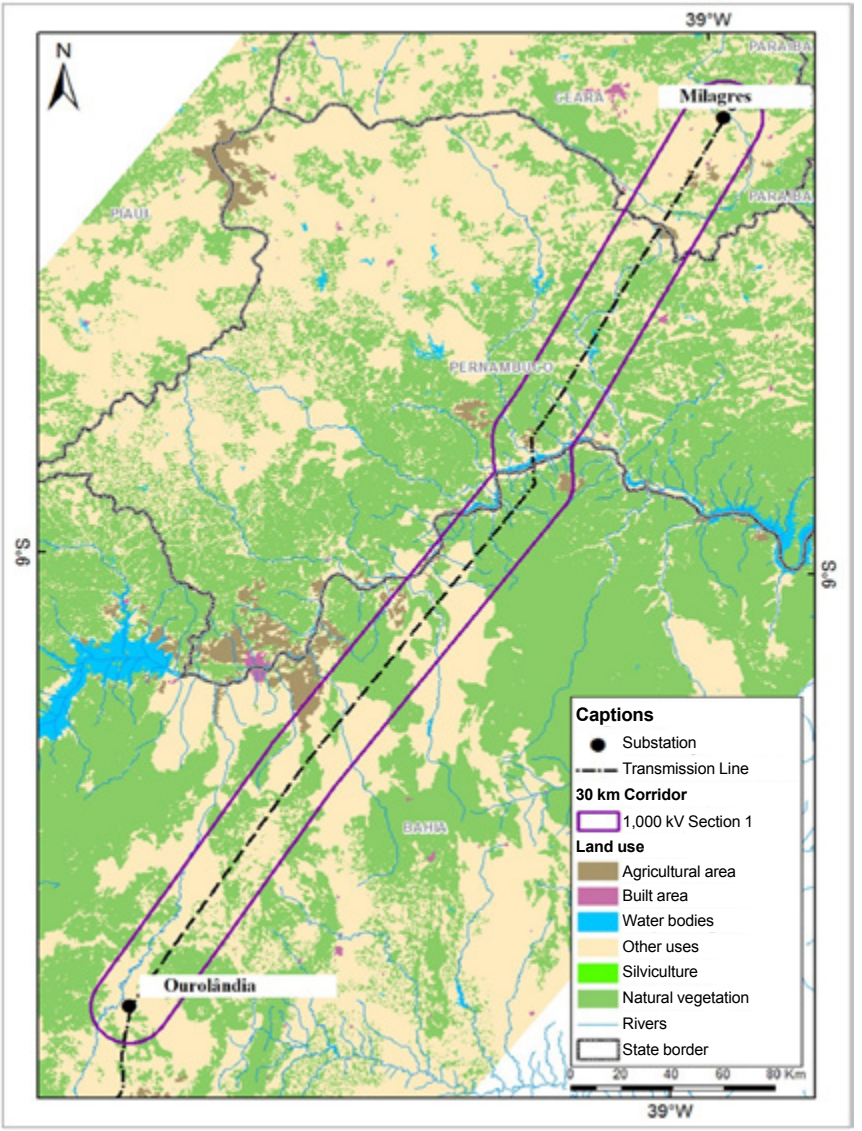

Figure 5.4: Vegetation cover and land use in the T1 corridor - Milagres to Ourolândia

Within the region comprised by the T1 corridor, there are only sustainable use CUs (see Table 5.9). One of these CUs is a public sustainable use forest managed by ICMBio. Even with the existing sustainable CUs, the axis of the chosen corridor was designed avoiding these areas as much as possible. Within the corridor of Section 1 there are two indigenous lands, TI Truká and TI Tumbalal, which are shown in Table 5.10 and presented in Figure 5.5.

Table 5.9: Conservation Units in the T1 corridor – Milagres (CE) to Ourolândia (BA)

CU name	Group	Category	Sphere
Environmental Protection Area Chapada do Araripe	SU	Environmental Protection Area	Federal
Floresta Nacional de Negreiros	SU	Forest	Federal

Table 5.10: Indigenous lands (TI) in the T1 corridor – Milagres (CE) to Ourolândia (BA)

TI Name	Situation
Truká	Regular
Tumbalal	Delimited and approved by Funai

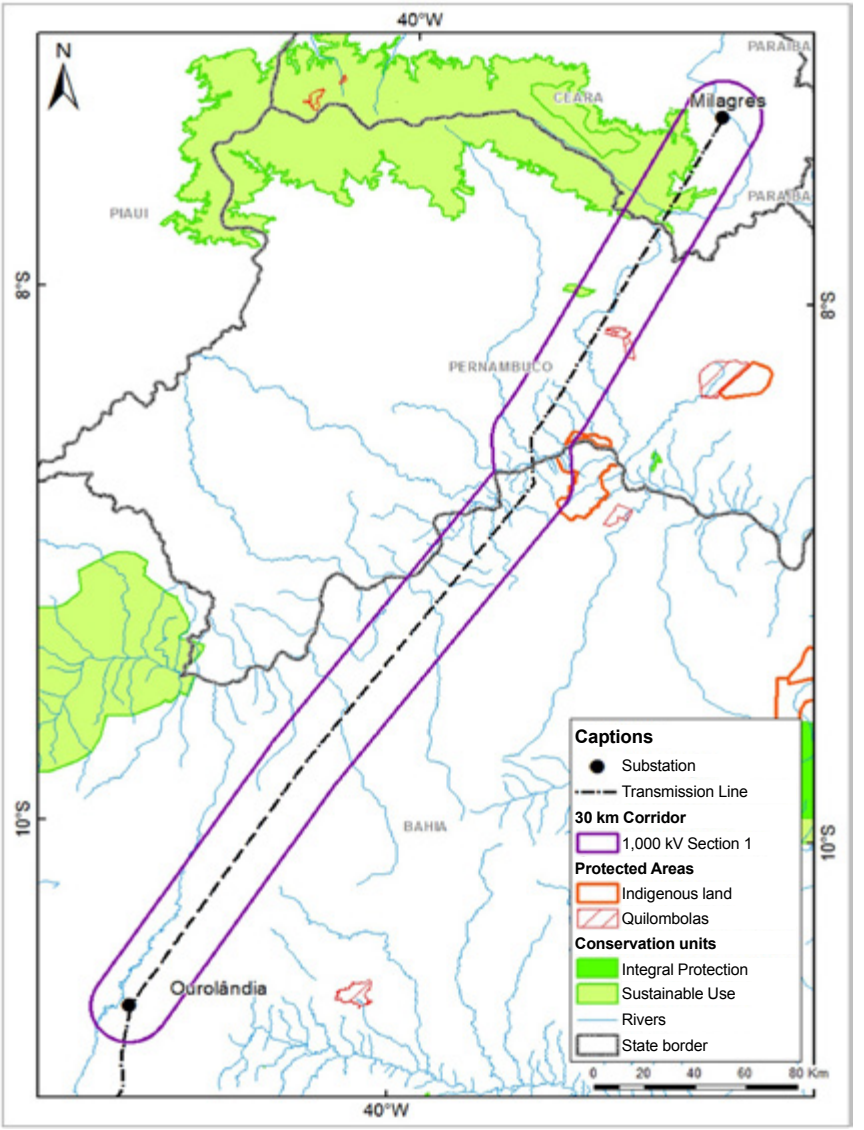

Figure 5.5: Conservation units, indigenous lands and *quilombolic* communities within the T1 corridor – Milagres (Ceará) to Ourolândia (Ceará)

There are several Priority Areas for Biodiversity Conservation (PABC) comprised in the T1 corridor. Table 5.11 describes these priority areas, their degree of importance, and priority action, according to the Ministry of the Environment (ME) criteria. The priority areas comprised in the T1 corridor or even located close to it are shown in Figure 5.6.

Table 5.11: Priority Areas for Biodiversity Conservation within the T1 corridor – Milagres (Ceará) to Ourolândia (Bahia)

Name of PABC	Code	Importance	Priority action
Rio Curaçá and Ridge areas	Ca053	Extremely high	Create CU – Undefined
Region of Carrancas	Ca047	Very High	Recovery
Channel of the São Francisco River	Ca054	Extremely high	Create CU – PI
Petrolina	Ca064	Very High	Create CU – PI
TI Truka	Ca254	Extremely high	Protected Area
Cabrobó	Ca079	Very High	Recovery
Chapada do Araripe (East)	Ca093	Extremely high	Create CU – PI
Kariris	Ca100	Extremely high	Create CU – Undefined
Baixo da Melância	Ca062	Extremely high	Create CU – SU
APA Chapada do Araripe – Catolé	Ca258	Extremely high	Protected Area
APA Chapada do Araripe – Catolé	Ca259	Extremely high	Protected Area

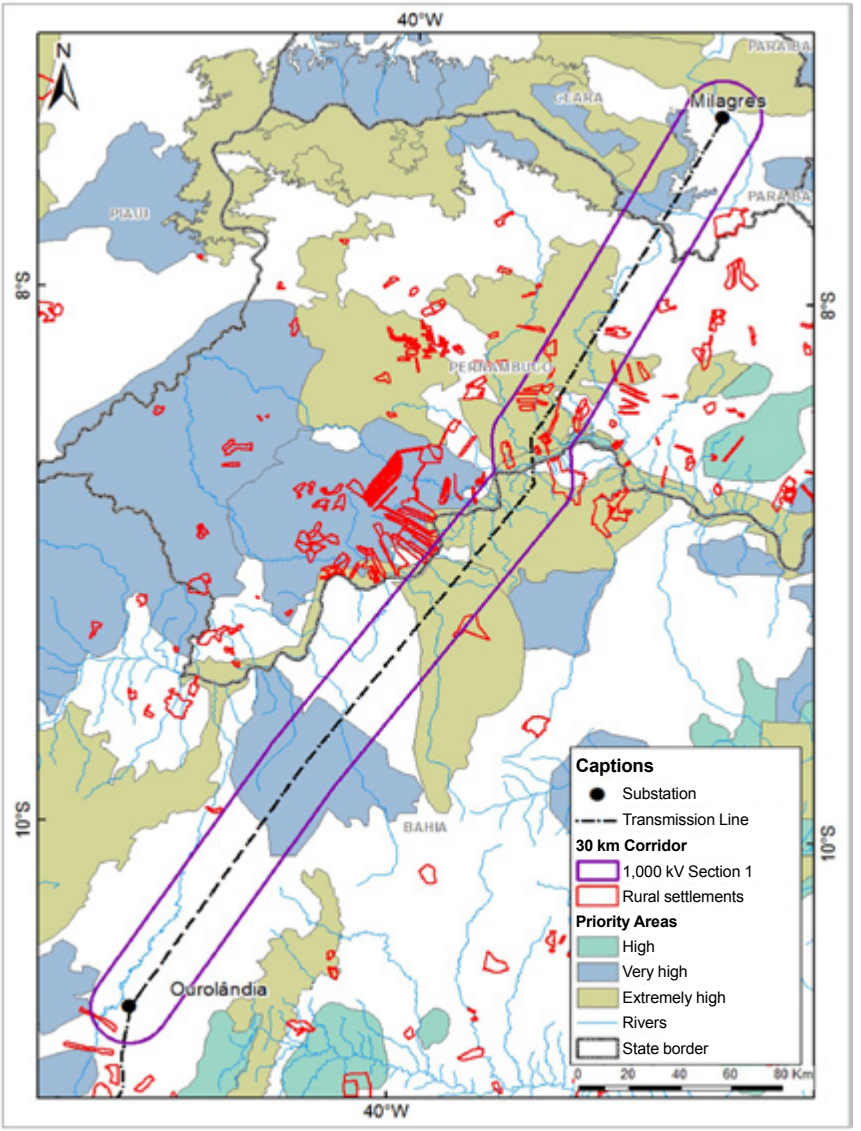

Figure 5.6: Priority Areas for Biodiversity Conservation and rural settlements inside the T1 corridor – Milagres (Ceará) to Ourolândia (Bahia)

The area of the T1 corridor comprises 31 rural settlement projects, most of them in the state of Pernambuco, and two in the state of Bahia. The settlement projects (SP) are concentrated mainly in the municipalities of Cabrobó, Orocó, Santa Maria da Boa Vista, and Terra Nova. The path chosen was able to divert from all the settlements. Among the rural SPs considered inside the T1 corridor is the *Contendas quilombolic* community, located in the municipality of Terra Nova - Pernambuco. Table 5.12 lists the number of PAs per municipality.

Table 5.12: Rural settlement projects present in the T1 corridor - Milagres to Ourolândia

Municipality	Settlement projects (SP)
Cabrobó - Pernambuco	10
Coribe - Pernambuco	1
Curaçá - Bahia	1
Mirangaba - Bahia	1
Orocó - Pernambuco	10
Salgueiro - Pernambuco	1
Santa Maria da Boa Vista - Pernambuco	5
Terra Nova - Pernambuco	2

In Table 5.13, a summary of the main socio-environmental information found inside the T1 corridor - Milagres to Ourolândia, is presented.

Table 5.13: Summary of the main socio-environmental information found inside the T1 corridor - Milagres to Ourolândia

Description	Quantitative
Length of the line (km)	436.63
Conservation Units (#)	2
Native vegetation (km^2)	6,195.67
Agriculture (km^2)	298.65
Indigenous lands (#)	2
Quilombos (#)	2
Incra settlements (#)	31
Caves (#)	7
Municipalities crossed	27
Urban Areas (km^2)	14.34

5.6.2 Macro-characterization of the Ourolândia (Bahia) to Igaporã (Bahia) section

Section 2 (T2) comprises the area of the corridor that starts at Ourolândia (located in the municipality of Mirangaba) in the northern part of the state of Bahia, and goes to Igaporã (located in the municipality of Caetité) in the central-south region of Bahia. This section has approximately 13,703.92 km^2. The municipalities crossed by T2 and their respective population densities are described in Table 5.14, and shown in Figure 5.7.

Table 5.14: List of municipalities crossed by the T2 corridor (Ourolândia to Igaporã)

State	Mesoregion	Microregion	Municipality	Population	Population density (people/km^2)
BA	Central/North of Bahia	Irecê	Barro Alto	13,571	20 to 50
			Cafarnaum	17,169	20 to 50
			Canarana	23,950	20 to 50
			Iraquara	22,569	20 to 50
			Mulungu do Morro	12,212	20 to 50
			Souto Soares	15,855	10 to 20
		Jacobina	Jacobina	79,112	20 to 50
			Miguel Calmon	26,440	10 to 20
			Mirangaba	16,270	5 to 10
			Morro do Chapéu	35,065	5 to 10
			Ourolândia	16,389	10 to 20
			Várzea Nova	13,049	10 to 20
		Senhor do Bonfim	Campo Formoso	66,441	5 to 10
			Umburanas	16,908	5 to 10
	Central/South of Bahia	Guanambi	Caetité	47,368	10 to 20
			Guanambi	78,644	50 to 100
			Igaporã	15,183	10 to 20
			Matina	11,135	10 to 20
		Livramento do Brumado	Érico Cardoso	10,840	10 to 20
			Livramento de Nossa Senhora	42,655	10 to 20
			Paramirim	20,967	10 to 20
			Rio do Pires	11,909	10 to 20
		Seabra	Boninal	13,683	10 to 20
			Bonito	14,816	10 to 20
			Palmeiras	8,351	10 to 20
			Piatã	17,973	5 to 10
			Seabra	41,714	10 to 20
		Boquira	Botuporã	11,143	10 to 20
			Caturama	8,838	10 to 20
			Ibitiara	15,490	5 to 10
			Novo Horizonte	10,500	10 to 20
			Tanque Novo	16,108	20 to 50

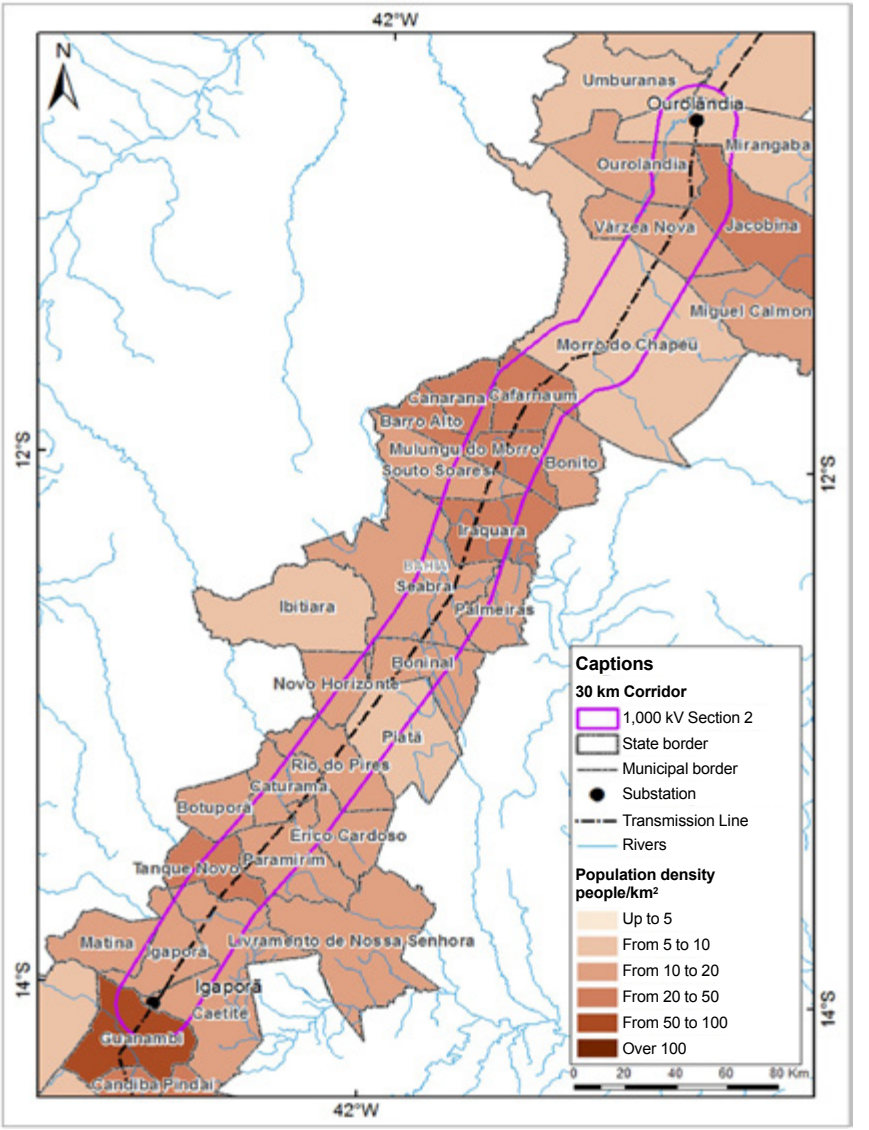

Figure 5.7: Location of the T2 corridor (Ourolândia to Igaporã)

According to data from the Satellite Deforestation Monitoring of the Brazilian Biomes Project (PMDBBS), Section 2 (T2) has predominantly pasturing areas (66.247% of the area). In the municipalities of Várzea Nova (Bahia) and Jacobina (Bahia), located in the north of T2, it is concentrate the most expressive agricultural areas. The main urban/built areas are located in the extreme northern region (municipalities of Várzea Nova in Bahia, and Morro do Chapéu) as well as in the center of T2 (municipalities of Seabra, Boninal, Souto Soares, Iraquara and Mulungu do Morro, all in the state of Bahia), and in the southern region of the corridor (municipalities of Igaporã, Paramirim, Tanque Nova and Guanambi, all also in the state of Bahia). The T2 corridor is fully inserted in the *caatinga* biome. The vegetation cover and land use classes of this section are listed in Table 5.15. In Figure 5.8, the distribution of the vegetation cover and the occupation within the T2 corridor are shown.

Table 5.15: Vegetation cover and land use inside the T2 corridor – Ourolândia to Igaporã

Dominant classes	Area in the corridor (km²)	%
Agricultural area	79.76	0.582
Other uses (such as pasture)	9,078.46	66.247
Built area	17.38	0.127
Water bodies	9.34	0.068
Natural vegetation	4,518.98	32.976
Total	13,703.92	100

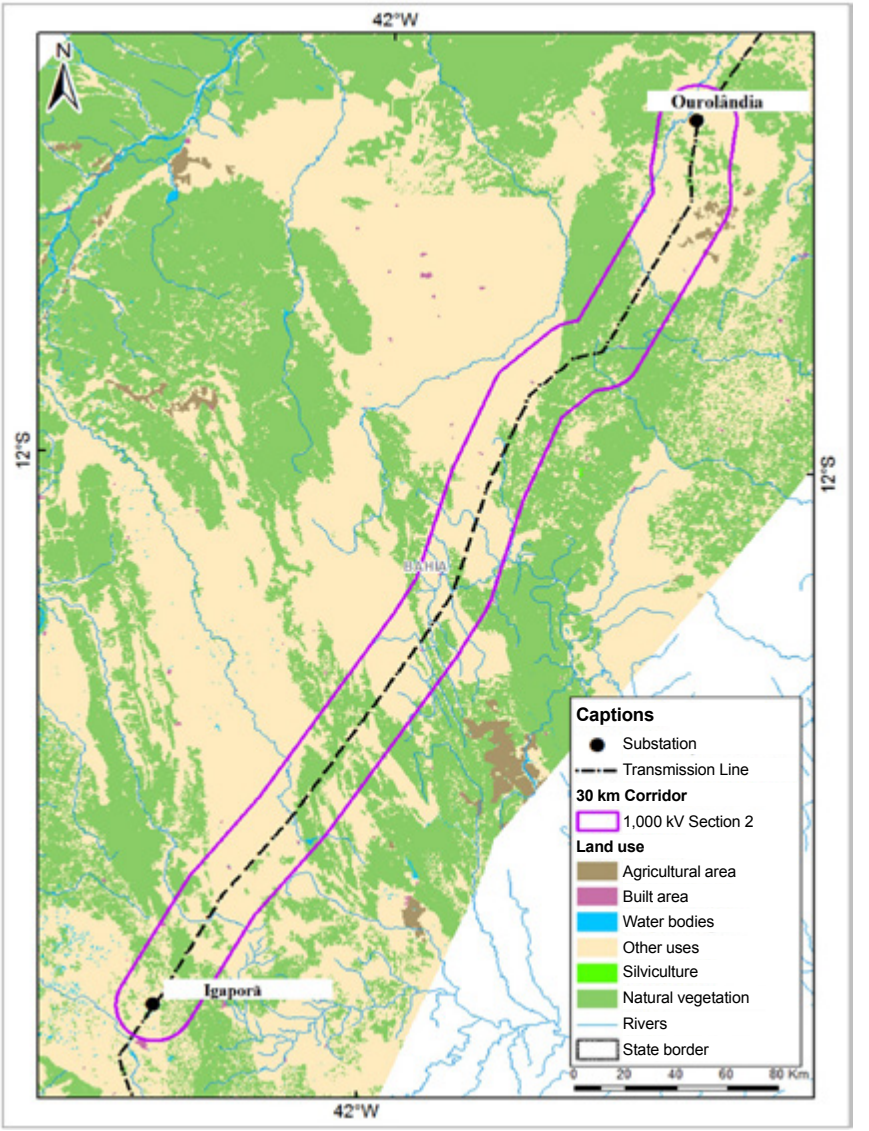

Figure 5.8: Vegetation cover and land use within the T2 corridor (Ourolândia to Igaporã)

Within the region comprised by the T2 corridor there are only two sustainable use CUs and one integral protection CU as listed in Table 5.16. Further, there are no indigenous lands within T2. (see Figure 5.9).

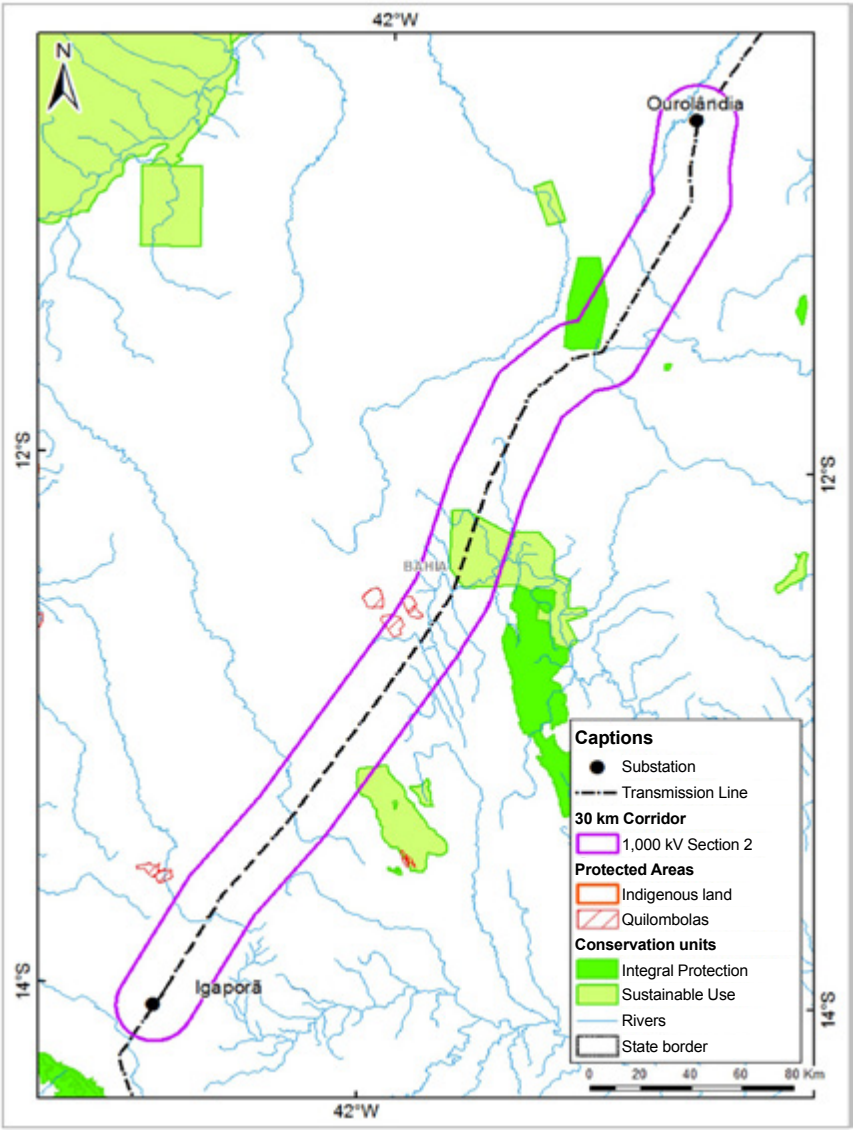

Figure 5.9: Conservation units, indigenous lands and *quilombolic* communities inside the T2 corridor (Ourolândia to Igaporã)

Table 5.16: Conservation Units in the T2 corridor, Ourolândia (Bahia) to Igaporã (Bahia)

CU name	Group	Category	State
Environmental Protection Area Marimbus/Iraquara	SU	Environmental Protection Area	Bahia
Environmental Protection Area Serra do Barbado	SU	Environmental Protection Area	Bahia
Morro do Chapéu State Park	PI	State Park	Bahia

There are several Priority Areas for Biodiversity Conservation comprised in this corridor (T2). Table 5.17 describes these priority areas, their degree of importance and the immediate priority action according to the Ministry of the Environment criteria. The priority areas comprised within the T2 corridor, or even those located close to it, are shown in Figure 5.10.

Table 5.17: Priority Areas for Biodiversity Conservation in the T2 corridor (Ourolândia to Igaporã)

Name of PABC	Code	Importance	Priority action
Guanambi	Ca004	Insufficiently known	Promote Sustainable Use
Igaporá	Ca008	Insufficiently known	Recovery
Paramirim	Ca015	High	Recovery
Corredor dos Brejões	Ca033	Extremely high	Create CU – Undefined
Marimbus/Iraquara	Ca020	Extremely high	Create CU – PI
Serra do Barbado	Ca009	Extremely high	Create CU – PI
Oliveira dos Brejinhos	Ca019	Insufficiently known	Create CU – Undefined
Morro do Chapéu Region	Ca023	Extremely high	Mosaic/corridor
Serra do Tombador	Ca030	High	Recovery
Morro do Chapéu State Park	Ca233	Extremely high	Protected area
Umburanas	Ca037	High	Recovery

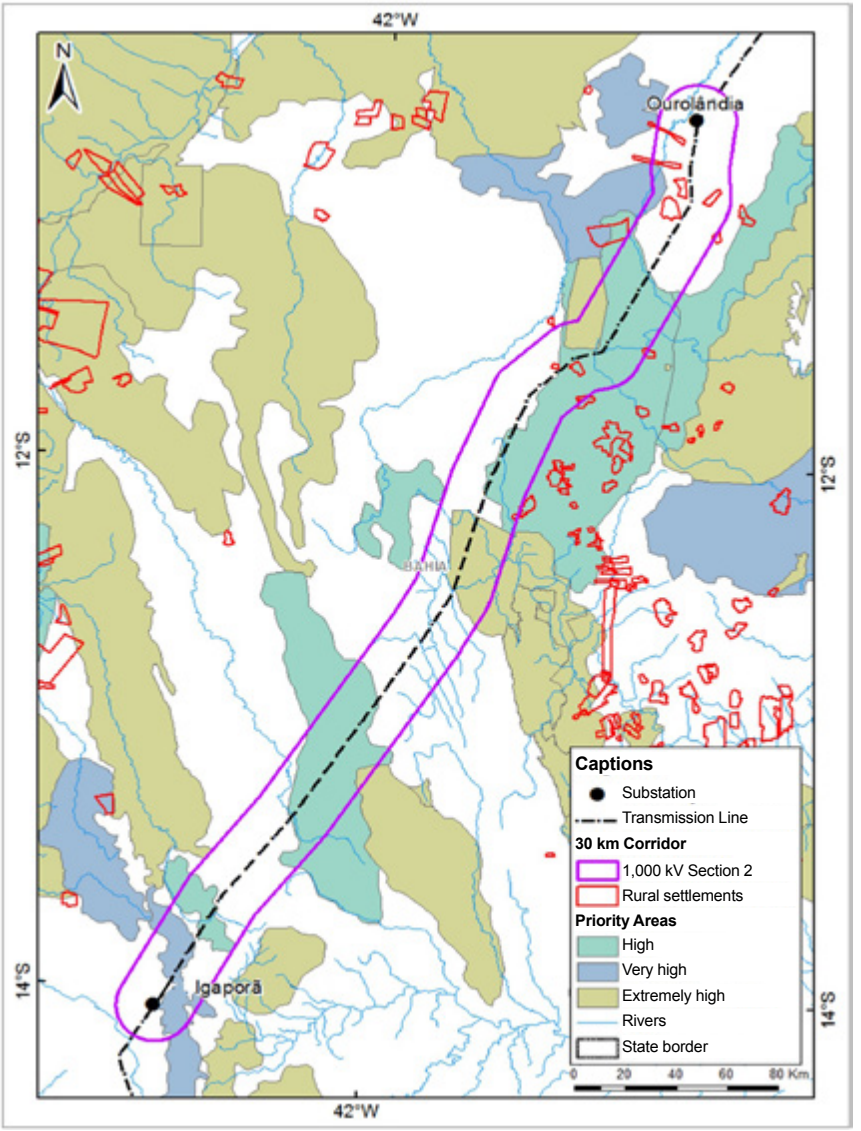

Figure 5.10: Priority Areas for Biodiversity Conservation and rural settlements within the T2 corridor (Ourolândia to Igaporã)

The T2 corridor also comprises 12 rural settlement projects. This section presents less concentration of settlement projects (SPs), which allowed a greater flexibility to divert them during the definition of the path. In Table 5.18, the total number of SPs per municipality, is listed.

Table 5.18: Rural settlement projects present inside the T2 corridor (Ourolândia to Igaporã)

Municipality	Settlement projects
Iraquara - Bahia	1
Jacobina - Bahia	2
Morro do Chapéu - Bahia	5
Ourolândia - Bahia	3
Mirangaba - Bahia	1

In Table 5.19, a summary of the main socio-environmental information found inside the T2 corridor (Ourolândia to Igaporã), is presented.

Table 5.19: Summary of the main socio-environmental information found inside the T2 corridor (Ourolândia to Igaporã)

Description	Amount
Length of the line (km)	433.57
Conservation Units	3
Native vegetation (km^2)	4,518.98
Agriculture (km^2)	79.76
Indigenous lands	0
Quilombos	3
Incra settlements	12
Caves	178
Municipalities crossed	32
Urban areas (km^2)	17.38

5.6.3 Macro-characterization of the Igaporã (Bahia) to Pirapora (Minas Gerais) section

Section 3 (T3) comprises the area of the corridor that begins at the Igaporã substation located in the municipality of Caetité (central-southern area of the state of Bahia), and runs to the Pirapora substation, located in the municipality of Pirapora (state of Minas Gerais). This is a 14,663.61 km^2 area. The São Francisco and Rio das Velhas rivers cut the southern part of the T3 corridor. In this section, a crossing point of the Rio das Velhas, will be unavoidable. The municipalities crossed by the T3 corridor and their respective population densities are listed in Table 5.20, and shown in Figure 5.11.

Table 5.20: List of municipalities crossed by T3 corridor – Igaporã to Pirapora

State	Mesoregion	Microregion	Municipality	Population	Population density (people/km²)
BA	Central/South of Bahia	Guanambi	Caetité	47,368	10 to 20
			Candiba	13,201	20 to 50
			Guanambi	78,644	50 to 100
			Igaporã	15,183	10 to 20
			Jacaraci	13,631	10 to 20
			Licínio de Almeida	12,309	10 to 20
			Matina	11,135	10 to 20
			Mortugaba	12,476	20 to 50
			Palmas de Monte Alto	20,757	5 to 10
			Pindaí	15,616	20 to 50
			Sebastião Laranjeiras	10,340	5 to 10
			Urandi	16,447	10 to 20
MG	North of Minas	Montes Claros	Brasília de Minas	31,094	20 to 50
			Capitão Enéas	14,151	10 to 20
			Coração de Jesus	25,918	10 to 20
			Mirabela	13,003	10 to 20
			Montes Claros	360,405	50 to 100
			Patis	5,565	10 to 20
			São João da Lagoa	4,651	up to 5
			São João da Ponte	25,293	10 to 20
			São João do Pacuí	4,056	5 to 10
			Verdelândia	8,281	5 to 10
		Janaúba	Catuti	5,094	10 to 20
			Espinosa	31,028	10 to 20
			Janaúba	66,495	20 to 50
			Mamomas	6,311	20 to 50
			Mato Verde	12,657	20 to 50
			Monte Azul	21,936	20 to 50
			Nova Porteirinha	7,371	50 to 100
			Pai Pedro	5,917	5 to 10
			Porteirinha	37,492	20 to 50
		Pirapora	Buritizeiro	26,774	up to 5
			Ibiaí	7,803	5 to 10
			Jequitaí	7,917	5 to 10
			Lagoa dos Patos	4,218	5 to 10
			Pirapora	52,929	50 to 100
			Várzea da Palma	35,699	10 to 20
		Salinas	Montezuma	7,455	5 to 10
			Santo Antônio do Retiro	6,955	5 to 10

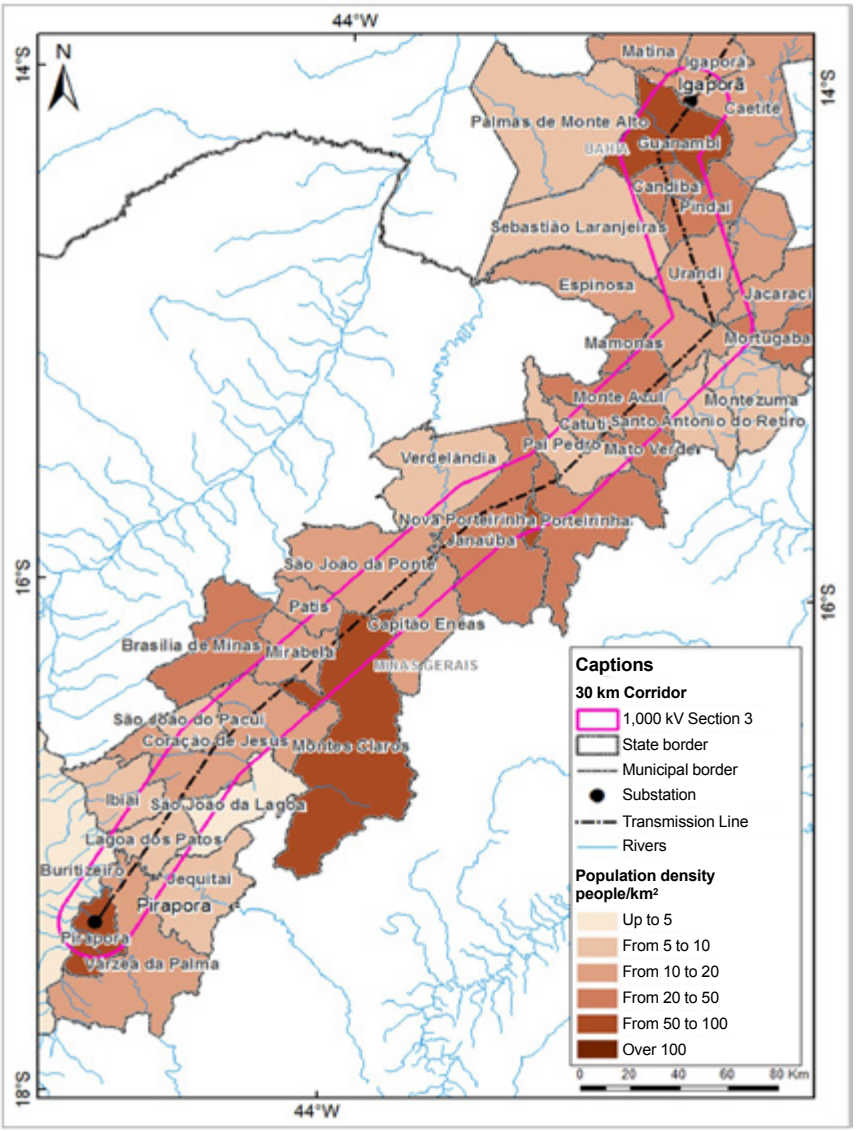

Figure 5.11: Location of the T3 corridor (Igaporã to Pirapora)

According to data from the Satellite Deforestation Monitoring of the Brazilian Biomes Project (PMDBBS), corridor T3 has also a predominantly pasturing area (approximately 64.347% of the area). The more expressive agricultural areas are concentrated in the municipalities of Porteirinha, Nova Porteirinha, Janaúba, Capitão Enéas and Verdelândia (all in the state of Minas Gerais) located in the central portion of T3, and in the municipality of Ibiaí (Minas Gerais), located in the southern region of the corridor. Inside the T3 corridor there are also important silviculture areas that spread through the municipalities of Sebastião Laranjeiras (Bahia), and Urandi (Bahia), located in the northern part of the corridor, and Janaúba, Verdelândia, Mirabela and Coração de Jesus (all in the state of Minas Gerais), located in its central portion. About 64.29% of the T3 corridor is within the *cerrado* biome and only 2.73% in the *mata atlântica* (subtropical forest) biome. The vegetation cover and land use classes of this section are listed in Table 5.21. In Figure 5.12, the distribution of the vegetation cover, and the occupation within the T3 corridor, is shown.

Table 5.21: Vegetation cover and land use in the T3 corridor (Igaporã to Pirapora)

Dominant classes	Area in the corridor (km2)	%
Agricultural area	128.20	0.874
Other uses (such as pasture)	9,489.95	64.347
Built area	56.41	0.385
Water bodies	70.09	0.478
Silviculture	77.95	0.532
Natural vegetation	4,841.01	33.014
Total	14,663.61	100

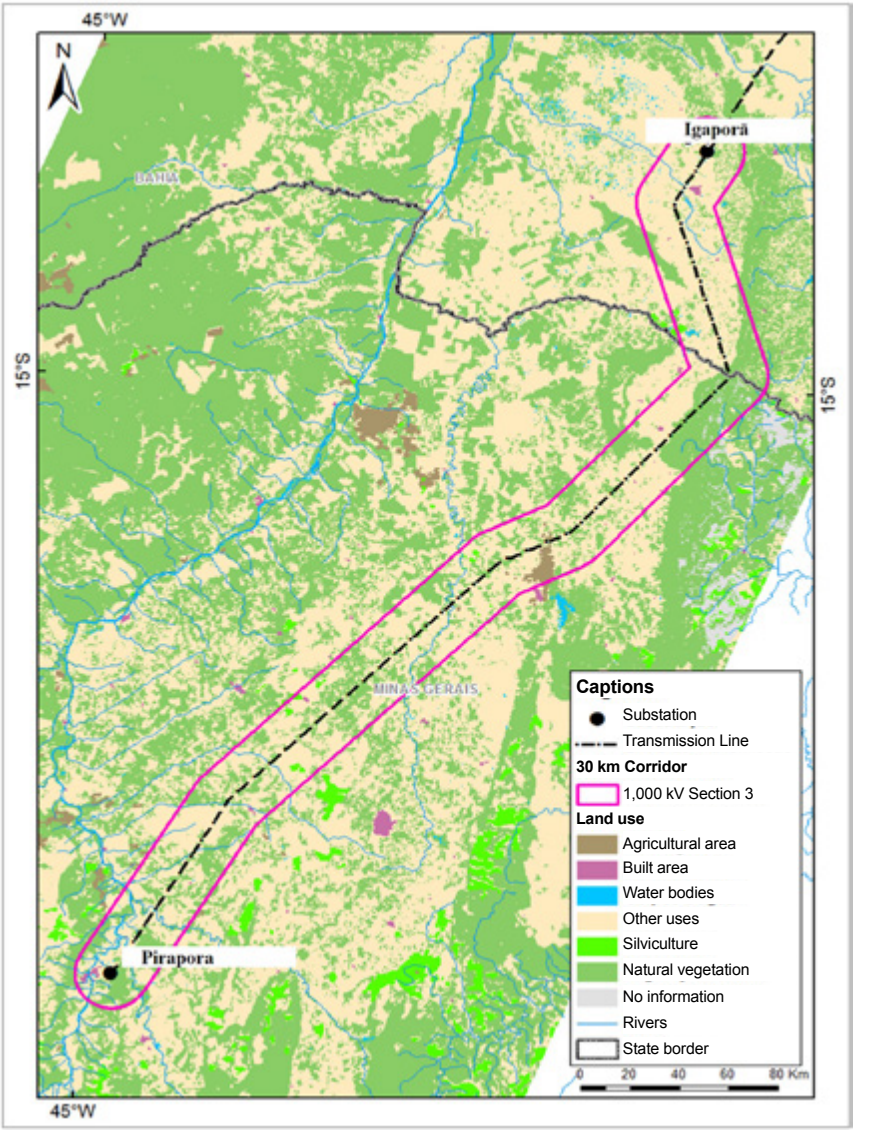

Figure 5.12: Vegetation cover and land use inside the T3 corridor (Igaporã to Pirapora)

Within the T3 corridor, there are only integral protection CUs (see Table 5.22). The path alternative was designed to avoid these areas. On the other hand, there are no indigenous lands, the closest one (Xacriabe indigenous land) being located at about 100 km far from the corridor (Figure 5.13).

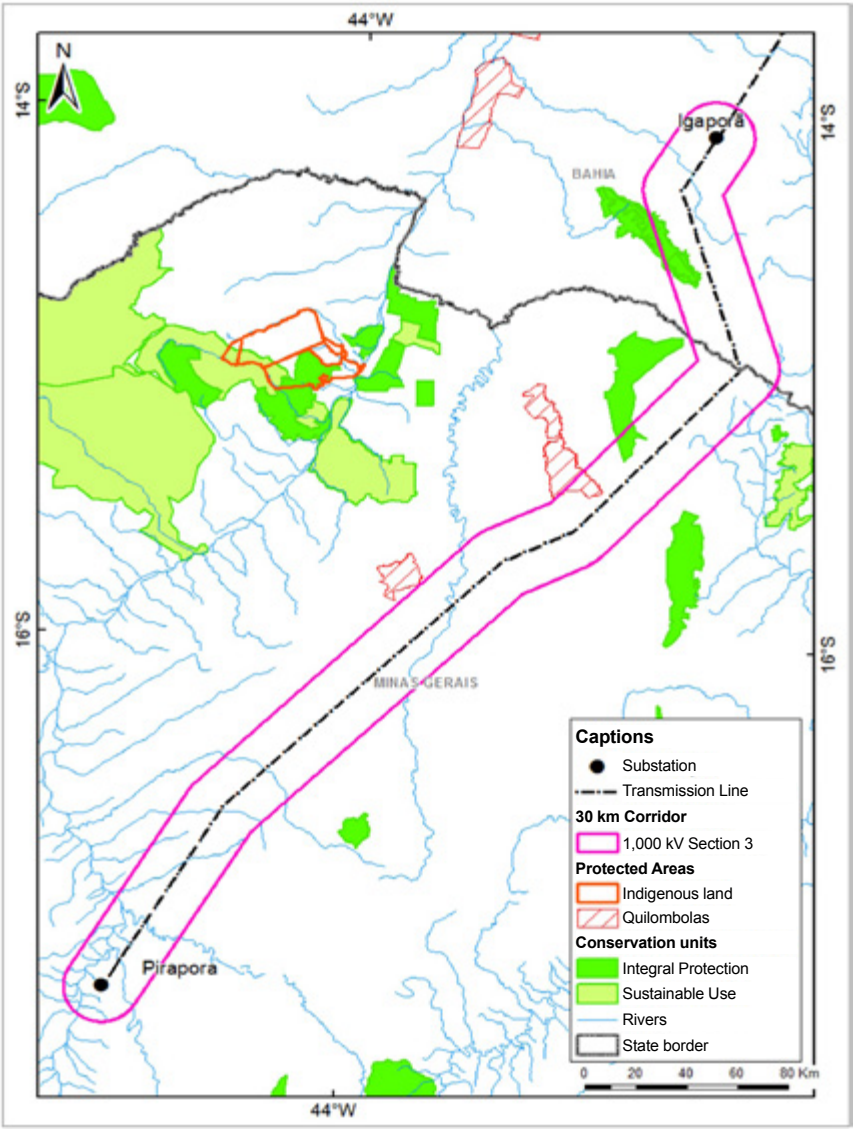

Figure 5.13: Conservation Units, indigenous lands, and quilombolic communities in the T3 corridor – Igaporã to Pirapora

Table 5.22: Conservation Units in the T3 corridor (Igaporã to Pirapora)

CU name	Group	Category	State
Caminho dos Gerais State Park	PI	State Park	Minas Gerais
Serra dos Montes Altos State Park	PI	State Park	Bahia
Serra dos Montes Altos Wildlife Refuge	PI	Wildlife Refuge	Bahia

There are several Priority Areas for Biodiversity Conservation inside the T3 corridor. In Table 5.23, a list of such priority areas showing their degree of importance, and priority action, is presented. The priority areas comprised in the T3 corridor, or those located close to it, are shown in Figure 5.14.

Table 5.23: Priority Areas for Biodiversity Conservation within the T3 corridor (Igaporã to Pirapora)

Name of PABC	Code	Importance	Priority action
Alto – Médio São Francisco	Ce106	Extremely high	Recovery
Areião	Ce139	Extremely high	Create CU – SU
Buritizeiro	Ce098	High	Recovery
Northern Ridge	Ce123	Extremely high	Recovery
Guanambi	Ca004	Insufficiently known	Promote Sustainable Use
Jaíba	Ca001	Extremely high	Inventory
Jacaraci	Ca002	Insufficiently known	Recovery
Rio Pardo – Santo Antônio do Retiro	Ce130	Extremely high	Inventory
São João da Ponte	Ce124	Very High	Promote Sustainable Use
Verdelândia	Ce134	Extremely high	Recovery
Verdelândia – Varzelândia	Ce126	Very High	Recovery

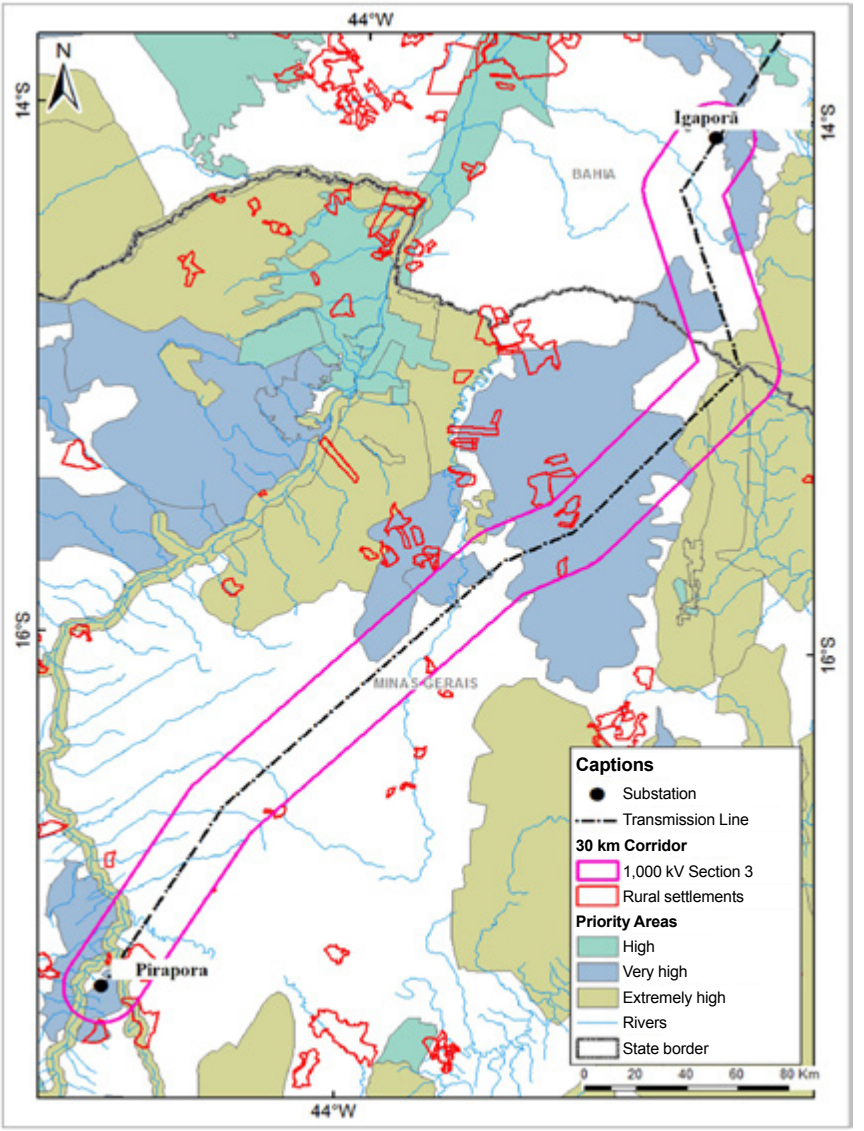

Figure 5.14: Priority Areas for Biodiversity Conservation and rural settlements inside the T3 corridor (Igaporã to Pirapora)

The area of the T3 corridor comprises 11 rural settlement projects (SP). The path was modeled to divert those settlements. Table 5.24 presents the number of SPs per municipality.

Table 5.24: Rural settlement projects found within the T3 corridor (Igaporã to Pirapora)

Municipality	Settlement projects (SP)
Capitão Enéas – Minas Gerais	1
Coração de Jesus – Minas Gerais	1
Janaúba – Minas Gerais	1
Nova Porteirinha – Minas Gerais	1
Pirapora – Minas Gerais	2
Porteirinha – Minas Gerais	2
Várzea da Palma – Minas Gerais	3

In Table 5.25, a summary of the main socio-environmental information found inside the T3 corridor (Igaporã to Pirapora), is presented.

Table 5.25: Summary of the main socio-environmental information found inside the T3 corridor (Igaporã to Pirapora)

Description	amounte
Length of the line (km)	465.89
Conservation Units	3
Native vegetation (km^2)	4,841.01
Agriculture (km^2)	128.20
Indigenous lands	0
Quilombos	1
Incra settlements	11
Caves	76
Municipalities crossed	39
Urban areas (km^2)	56.41

5.6.4 Recommendations for the line routing and elaboration of the R3 Report

The corridor overlapping areas of the three above mentioned sections present socio-environmental sensitivity. Such a sensitivity is the result of the presence of conservation units, indigenous lands, conservation priority areas, existence of caves, remnants of vegetation, proximity to urban areas, settlements, and the crossing points of large rivers, mainly the São Francisco River.

It is recommended to conduct a more detailed study for a more advanced report. Such study should consider details of the socio environmental interventions and impacts, especially those related to archaeological sites, settlements, Conservation Units and their respective management plans.

Additionally, an assessment of the physical and biotic environmental characteristics, including the presence of endemism and specific geomorphological formations, should be conducted.

The study should be conducted on the corridor area to be modeled by the multi-disciplinary team of the consulting company, continuing and complementing the socio-environmental study herein presented. Also, such a study should be presented in the R3 Report, including additional details of the variables presented here. Additionally, some weighting complementary variables such as mining rights, soil types, geological sites, etc., must be considered.

Thus, the main recommendations and suggestions for a better definition of the routes are as follow:

5.6.4.1 Section 1: Milagres to Ourolândia

- The corridor of Section 1 comprises a Flona (National Forest) and, although it is a sustainable use CU, it is recommended to avoid crossing it, since the proposed corridor allows its diversion.
- The T1 corridor area overlaps some agricultural areas, which must be analyzed *in situ* to identify the cultures that would be crossed, evaluate the value of the land associated to these cultures, or elaborate a feasibility study considering changing the route.
- This corridor crosses several Priority Areas for Biodiversity Conservation – PABCs. It will be necessary a further detailing for choosing the main route within the corridor to cause a lower impact on it, mainly due to the existence of extremely high priority PABCs, and some integral protection CUs to be created in the area. Therefore, a more detailed analysis is recommended for choosing the path for the main route, so as to reduce the impact of the project, for example, by reducing the number of crossings points of the PABC Channel of the São Francisco River, Ca054.

This section crosses a considerably large area of native vegetation. It is recommended that these areas, or at least the larger lengths of these areas, be avoided when defining the main route of the line. Thus, there will be less suppression areas and a lower impact on the land.

5.6.4.2 Section 2: Ourolândia to Igaporã

- Inside the corridor of Section 2 there is a considerable number of caves. Therefore, it is suggested the realization of complementary studies while choosing the main route to avoid crossing such areas.
- The northern part of the T2 corridor area is overlapped to some agricultural areas, which must be analyzed *in situ,* so as to identify the cultures that would be crossed, evaluate the value of the land associated to these cultures, or elaborate a feasibility study considering changing the route.
- This corridor crosses several PABCs, but further detailing will be necessary to choose the main route within the corridor, thus, causing a lower impact on it, mainly due to the existing extremely high priority PABCs, and integral protection CUs to be created in the area. Therefore, a more detailed analysis to choose the path for the main route, so as to reduce the impact of the project, is recommended.
- The T2 corridor crosses a considerably large area of native vegetation. It is recommended that these areas, or at least the larger lengths of these areas, be avoided when defining the main route of the line. This way, there will be less suppression areas with a lower impact on the land.

5.6.4.3 Section 3: Igaporã to Pirapora

- This section comprises a state park and a wildlife refuge, which are Integral Protection CUs, so the crossing of these areas should be avoided, since the proposed corridor allows diverting these areas.
- In the corridor of Section, 3 there is a considerable number of caves. It is recommended that the main rout diverts from these areas.
- The central portion of the T3 corridor overlaps some agricultural areas, which must be analyzed *in situ,* so as to identify the cultures that would be crossed, evaluate the value of the land associated to these cultures, which means, elaborate a feasibility study to choose the best route.
- This corridor crosses several PABCs, but further detailing will be necessary to choose the main route within the corridor. Consequently, a lower impact, mainly due to the existence of extremely high priority PABCs, will be caused to the land.

- The T3 corridor crosses a considerable area of native vegetation. It is recommended that these areas, or at least the larger lengths of these areas, be avoided when defining the main route of the line. This way, the project will cause less suppression areas and lower impact to the region.
- At about 8 km from Pirapora, the corridor crosses the São Francisco River and the Rio das Velhas. This crossing point must be carefully studied, not only to find the best position for crossing the river, but also because of the presence of many agricultural areas and due to the type of soil existing in the region.

6. Economic Evaluation

An economic comparison was conducted between three alternatives, and another only illustrative configuration (non-competing):

- Alternative 1: 1,000 kV Transmission system in alternating current.
- Alternative 2: 500 kV Transmission system in alternating current.
- Alternative 3: ±600 kV Transmission system in direct current.
- Alternative 4: 1 bipole at ±800 kV, 4,000 MW UHV DC (illustrative configuration).

The first alternative consists of a single-circuit 1,000 kV AC transmission system between Milagres and Pirapora. The second alternative consists of a 500 kV AC transmission system, with two single circuits, between Milagres and Pirapora. The third alternative considers an HVDC multi-terminal system (±600 kV) based on VSC (*Voltage Source Converter*) converters. The last configuration is composed of a ±800 kV transmission system based on LCC (*Line Commutated Converters*) converters.

Recently, EPE released the studies of a ±800 kV bipole, with 4,000 MW rating, referred to as Bipole B. This bipole connects the substations of Graça Aranha (Maranhão) and Silvânia (Goiás), which would alleviate the north-south lines during the power injection from new generation projects in the north and northeast regions. This bipole does not compete with the alternatives analyzed, thus, it is used only as an illustrative alternative (Alternative 4) due to its innovative character and dimensions.

To set the overall cost of the UHV transmission line, it was considered that each line section (Milagres – Ourolândia, Ourolândia – Igaporã, and Igaporã – Pirapora), has a length equal to 440 km.

6.1 Alternative 1

This alternative is composed of four 500/1,000 kV substations linking the three line sections. All the substations are based on the one and a half circuit-breaker configuration. The Milagres Substation has a 3,000 MVA (1,000/500 kV) transformer bank. In its 500 kV sector, there are four line inputs for the sectioning of the two lines that connect Milagres II to Luiz Gonzaga. The Ourolândia Substation has a 2,500 MVA (1,000/500 kV) transformer bank. In its 500 kV sector, there are two line inputs due to the sectioning of the line from Ourolândia to Juazeiro. The Igaporã Substation has a 2,500 MVA (1,000/500 kV) transformer bank. In its 500 kV sector there are four line inputs due to the sectioning of two lines from Igaporã to Janaúba. The Pirapora Substation has a 2,500 MVA (1,000/500 kV) transformer bank. In its 500 kV sector there are four line inputs due to the sectioning of the two lines from Pirapora to Ribeirão das Neves. The areas of the substations were estimated taking into account a future expansion.

Figure 6.1, below, presents the single line diagram of Alternative 1.

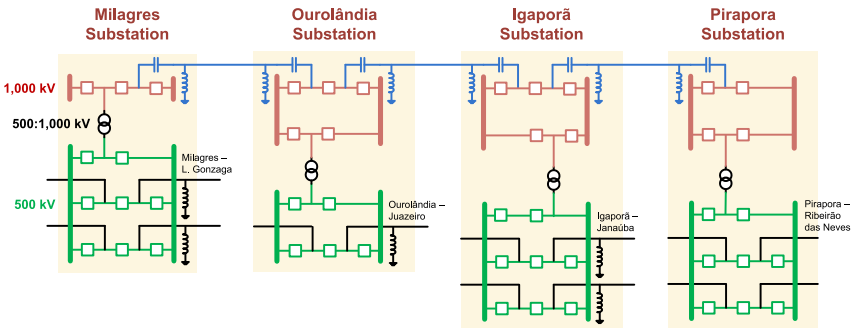

Figure 6.1: Single line diagram of Alternative 1

6.1.1 Rating of the transformers of Alternative 1

From the meetings held with the main Brazilian manufacturers of power transformers, it was learned that typical power values for this voltage level would be 2,000 MVA, 2,500 MVA, and 3,000 MVA (banks composed of three single-phase transformers).

To rate the transformers of Alternative 1, it was necessary to evaluate the future expansion of this system, the detailed study of which is not within the scope of this chapter. Briefly, it was first set a single circuit line up to Ribeirão das Neves (Minas Gerais), distant 300 km from the Pirapora substation. Next, an additional single-circuit line was inserted between Ourolândia and Ribeirão das Neves. Having the steady state power flow and contingency conditions, it was rated the 1,000/500 kV transformers. For the contingency situations, an overload of 20% in the transformers was considered acceptable.

Table 6.1: **Rating** of the power transformers (MVA) – Alternative 1

Substation	Initial alternative		First expansion		Second expansion	
	Steady state	Worst contingency	Steady state	Worst contingency	Steady state	Worst contingency
Milagres	1,858	2,549	2,133	2,943	2,614	2,871
Ourolândia	1,419	2,520	1,700	2,906	3 x 1,473	3 x 2,111
Igaporã	1,156	2,569	878	2,626	1,181	1,410
Pirapora	2,164	2,703	944	2,617	1,178	1,346
Ribeirão das Neves	0	0	3 x 1,342	3 x 1,924	3 x 2,112	3 x 3,006

It can be seen (Table 6.1) that for the second expansion, the Milagres substation would additionally require 2,500 MVA (steady state). For this reason, a 3,000 MVA transformer was chosen for this substation. For the rest of the substations, 2,500 MVA transformers were chosen.

6.2 Alternative 2

This alternative is also composed of four new substations. All the substations are based on the one and a half circuit breaker configuration. The line sectioning of the existing 500 kV lines are the same as in Alternative 1.

The areas of the substations were considered taking into account a future expansion. In Figure 6.2, the single line diagram of Alternative 2, is presented.

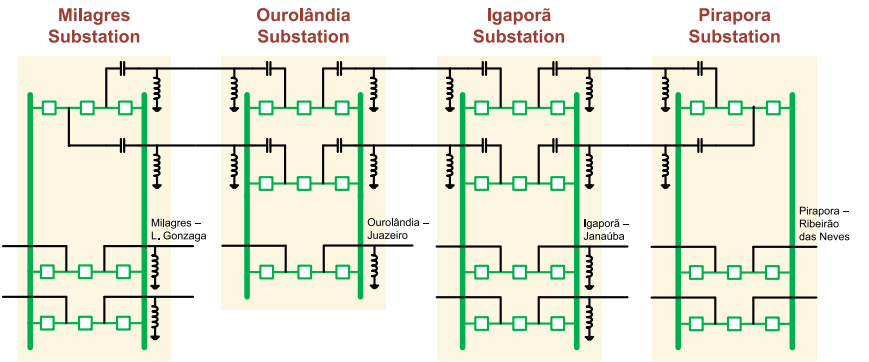

Figure 6.2: Single line diagram of Alternative 2

6.3 Alternative 3

Similarly, alternative 3 is composed of four new substations. All the substations are based on the one and a half circuit-breaker configuration. The line sectioning of the existing 500 kV lines are the same as in Alternative 1. The type of converters considered are VSC (*Voltage Source Converter*).

In Figure 6.2, the layout of Alternative 3 is presented.

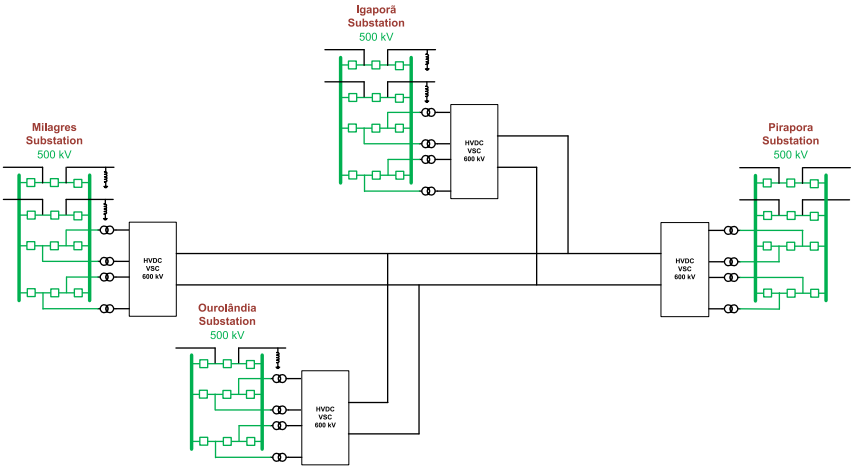

Figure 6.3: Single line diagram of Alternative 3

6.4 Alternative 4

Alternative 4 Is an illustrative alternative is composed of two new substations. All the substations present a one and a half circuit breaker (DJM) configuration, and a 500 kV sector. The sectioning of the 500 kV lines existing at Milagres and Pirapora is the same as in Alternative 1. The converters are LCC (*Line Commutated Converter*). In this case, the length of the line is of 1,400 km.

In Figure 6.4, the single line diagram of Alternative 4, is shown.

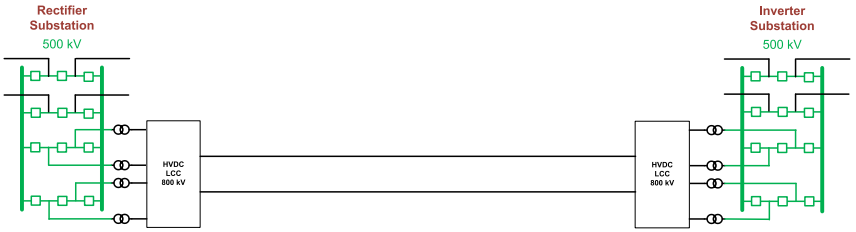

Figure 6.4: Single line diagram of Alternative 4

6.5 Economic Parameters

The comparison of investments was performed using the ANEEL's 2015 price bank, accessed on Jan. 6, 2009 (http://www.aneel.gov.br/cedoc/areh2009758.zip).

The weights of the towers for Alternative 1, were calculated based on the detailed basic electromechanical design. The cost of the lines and converters of the DC system were calculated using expressions from the CIGRÉ's Brochure 388 (properly adjusted).

The costs of the switching modules, general modules and equipment of Alternative 1 were obtained from the ANEEL's price bank (extrapolated for the 1,000 kV AC line, since costs for this voltage level are not in the ANEEL's database). As for the 500 kV equipment (towers and VSC converters), the Aneel's price bank was used.

For the economic evaluation of the alternatives, the following values were adopted (Table 6.2):

Table 6.2: Adopted values

Description	Value	Unit
Marginal expansion cost (Ce)	154.00	R$/MWh
Interest rate	8	% p.y.
Line and equipment life period	30	Years
Operation and maintenance	2	% p.y.
Loss Factor (lf)	0.5	
Demand cost (Cp)	0	R$/MWh
Dollar exchange rate	3.05	R$/US$

6.6 Cost of Transmission Lines

The costs of the transmission lines were obtained from the ANEEL's price bank based on the calculated tower and foundations weight values. The weight of the towers for the 1,000 kV system were calculated considering a detailed design. For the 800 kV DC line, the tower weights are those used in the first Belo Monte bipole.

The transmission towers (weights) for Alternative 1 (1,000 kV) were calculated specifically for this project [32] and [33]. In Figures 6.5 and 6.6, the layouts of the designed towers is presented.

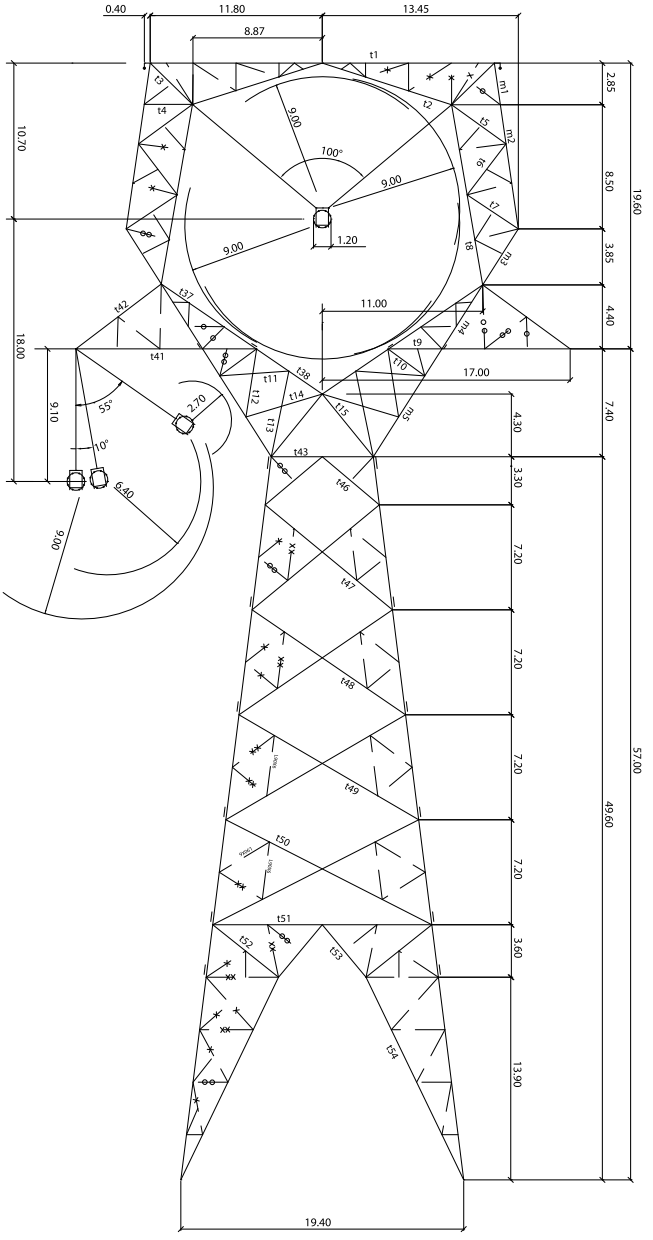

Figure 6.5: Self-supporting tower (1,000 kV)

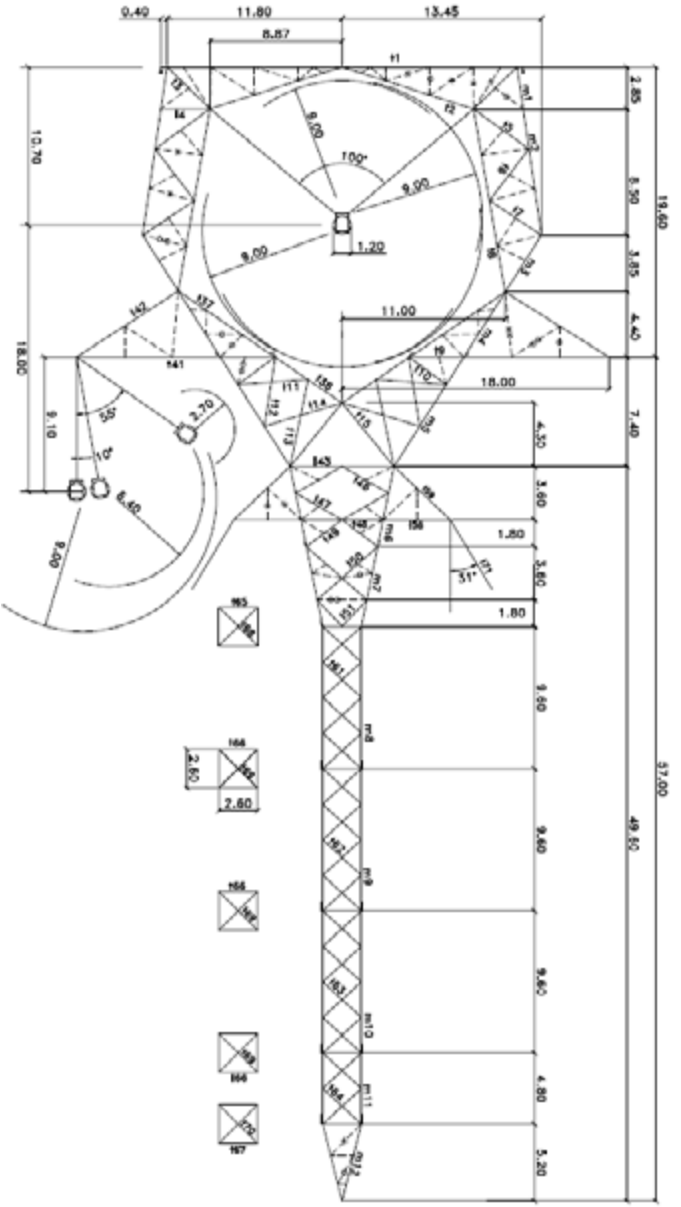

Figure 6.6: Guyed single mast tower (1,000 kV)

For the other alternatives, the tower prices were obtained from ANEEL's price bank.

6.7 Cost of Substations, Equipment and Converters

As stated above, prices of equipment to operate at 1,000 kV AC are not available, so, extrapolations for equipment at this voltage level were carried out based on 500 kV and 750 kV equipment. These procedures are presented next.

The following items present the cost determination for substations and equipment for Alternative 1.

6.7.1 General module

To calculate the general module, the ANEEL price bank (2015) was used. As an input data a value equal to R$ 0.43/m^2, which corresponds to the average value for rural locations in Brazil, was used.

For the 500 kV yard, it was used the one and a half circuit-breaker configuration. The same adaptations to the ANEEL price bank were done to obtain the cost of the 1,000 kV sectors [34].

6.7.2 Switching module

The costs of the switching modules were also obtained from the ANEEL's price bank (2015). The values for the 1,000 kV switching modules were analogously obtained through linear extrapolation considering the prices of the 500 kV and 750 kV modules.

A discrepancy in costs for the line input module (LI) and bus interconnection (BI) was found. For the 750 kV and 1,000 kV the minimum value of the BI module was higher than LI, so the same value of LI for BI (in the 1,000 kV) was adopted.

The costs for the switching modules are presented below. In the ANEEL's spreadsheet, the costs are presented for the five regions of Brazil. To calculate the switching modules, average value of these regions was used.

Table 6.3 shows the values of the switching modules, all for the one and a half circuit-breaker configuration.

Table 6.3: Cost of the switching modules

Module	Voltage (kV)	Cost (R$)
Series Capacitor Connection (CCS)	500	2,698,482.00
	750	3,480,214.00
	1,000	4,261,945.00
Compensator Connection (CC)	500	8,567,287.00
	750	13,535,927.00
	1,000	18,504,567.00
Bus Reactor Connection (CRB)	500	7,637,748.00
	750	12,541,006.00
	1,000	17,444,263.00
Line Reactor Connection (CRL)	500	4,959,224.00
	750	7,656,564.00
	1,000	10,353,903.00
Transformer Connection (CT)	500	8,183,424.00
	750	12,769,286.00
	1,000	17,355,147.00
Line Input (EL)	500	9,301,589.00
	750	14,519,342.00
	1,000	19,737,095.00
Bus Interconnection (IB)	500	8,564,022.00
	750	14,519,342.00
	1,000	19,737,095.00

6.7.3 Transformers

Table 6.4, shows the costs of single-phase auto-transformers with on-load tap changers (OLTC) for 500 kV and 750 kV. These costs were obtained from the ANEEL's price bank (2015).

Table 6.4: Costs for the single-phase auto-transformer with on-load tap changers (R$).

MVA	Aneel			Calculated	
	500/345	750/345	750/500	1,000/345	1,000/500
100	9,822,896.00	11,931,986.00	12,508,323.00	14,041,077.00	14,719,286.00
150	11,441,010.00	13,405,703.00	14,059,604.00	15,370,397.00	16,120,131.00
200	12,589,080.00	14,451,323.00	15,160,256.00	16,313,565.00	17,113,854.00
250	13,479,592.00	15,262,368.00	16,013,988.00	17,045,143.00	17,884,559.00
300	14,207,194.00	15,925,040.00	16,711,537.00	17,642,886.00	18,514,224.00
350	14,822,373.00	16,485,321.00	17,301,307.00	18,148,270.00	19,046,568.00
400	15,355,264.00	16,970,659.00	17,812,189.00	18,586,054.00	19,507,687.00
450	15,825,308.00	17,398,758.00	18,262,819.00	18,972,207.00	19,914,409.00
500	16,245,777.00	17,781,704.00	18,665,921.00	19,317,632.00	20,278,225.00

To obtain the cost of the 1,000/345 kV auto-transformers, it was used linear extrapolation between the costs corresponding to 500/345 and 750/345 kV auto-transformers for each rated power (Table 6.4). It was seen that the 750/500 kV auto-transformers are 5% more expensive, when compared to the 750/345 kV auto-transformers. This relation was used when calculating the 1,000/500 kV auto-transformers.

The cost equations for the auto-transformer with OLTC are:

$$C_{1,000/345} = 3{,}278{,}505.24 \cdot \ln(S) - 1{,}056{,}994.093 \quad \text{(R\$)}$$
$$C_{1,000/500} = 3{,}453{,}902.03 \cdot \ln(S) - 1{,}186{,}212.01 \quad \text{(R\$)}$$

Where, S is the single-phase auto-transformer apparent power in MVA.

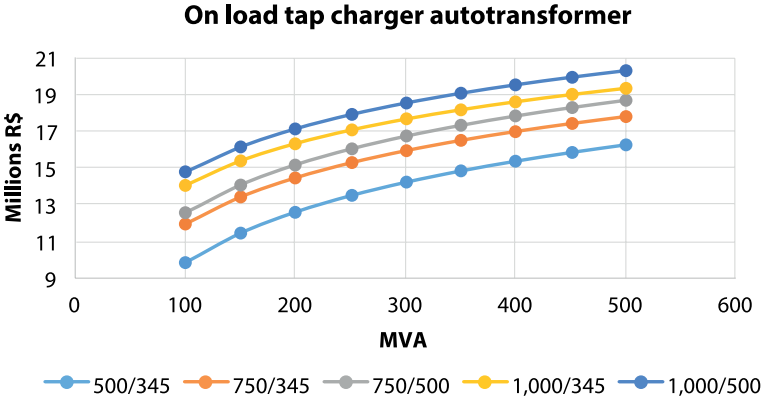

Figure 6.7: Costs of single-phase auto-transformers with OLTC

6.7.4 Shunt reactors

Table 6.5 presents the cost values of 500 and 750 kV single-phase shunt reactors. Based on these values, a linear extrapolation was applied to obtain the 1,000 kV shunt reactors.

Table 6.5: Costs of the 500, 750, and 1,000 kV shunt reactors

Mvar	Aneel		Calculated
	500 kV	750 kV	1,000 kV
25	3,926,964.00	4,224,201.00	4,521,438.00
50	5,011,741.00	5,395,759.00	5,779,778.00
75	5,646,294.00	6,081,077.00	6,515,860.00
100	6,096,517.00	6,567,318.00	7,038,119.00
125	6,445,737.00	6,944,475.00	7,443,214.00
150	6,731,070.00	7,252,636.00	7,774,201.00
175	6,972,316.00	7,513,181.00	8,054,046.00
200	7,181,293.00	7,738,876.00	8,296,459.00
225	7,365,624.00	7,937,953.00	8,510,283.00
250	7,530,513.00	8,116,034.00	8,701,555.00
275	7,679,674.00	8,277,127.00	8,874,581.00
300	7,815,847.00	8,424,194.00	9,032,541.00
325	7,941,114.00	8,559,482.00	9,177,851.00
350	8,057,093.00	8,684,740.00	9,312,387.00

From Table 6.5, the following 1,000 kV shunt reactor cost equation can be obtained:

$$C_{\text{shunt reac}} = 0.18154 \cdot 10^7 \cdot \ln(Q) - 0.13221 \cdot 10^7 \qquad \text{(R\$)}$$

Where,
Q is the single-phase reactive power (Mvar) of the reactor.

Figure 6.8 presents the cost of the shunt reactor for voltage equal to 500 kV, 750 kV and 1,000 kV..

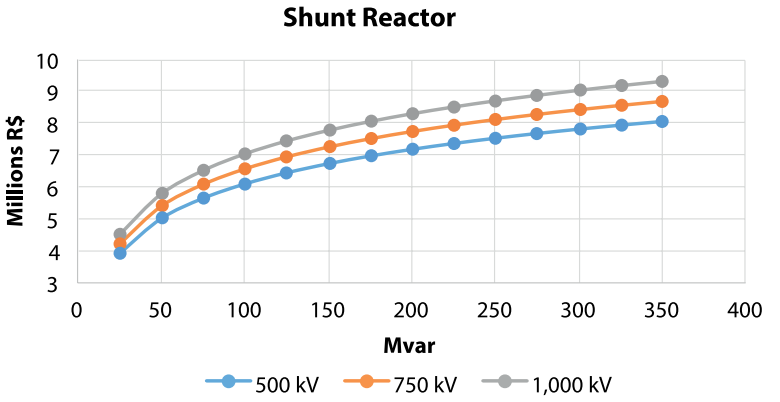

Figure 6.8: Costs of single-phase shunt reactors

6.7.5 Series capacitor

Table 6.6 presents the cost of series capacitors for voltages equal to 500 kV and 750 k. These values were obtained from the ANEEL's price bank (2015). The last column shows the calculated value for the 1,000 kV system.

Table 6.6: Costs of the 500, 750, and 1,000 kV series capacitor (single-phase)

Mvar/phase	Aneel		Calculated
	500 kV	750 kV	1,000 kV
100	16,712,703.00	17,529,494.00	18,346,286.00
110	18,337,489.00	19,235,521.00	20,133,552.00
120	19,962,276.00	20,941,547.00	21,920,817.00
130	21,587,063.00	22,647,573.00	23,708,083.00
140	23,211,850.00	24,353,599.00	25,495,348.00

From Table 6.6, it can be seen that the cost of the series capacitor bank has a linear relation with the reactive power for both voltages.

Similarly, for the 1,000 kV system, it was performed a linear extrapolation for each power. The cost function for the series capacitor (single-phase) is:

$$C_{\text{series cap}} = 178{,}727 \cdot Q + 473{,}631 \qquad \text{(R\$)}$$

Where,
Q is the reactive power (Mvar), per phase.

Figure 6.9, presents the cost of the series capacitor for the 500 kV, 750 kV, and 1,000 kV system In relation to the reactive power.

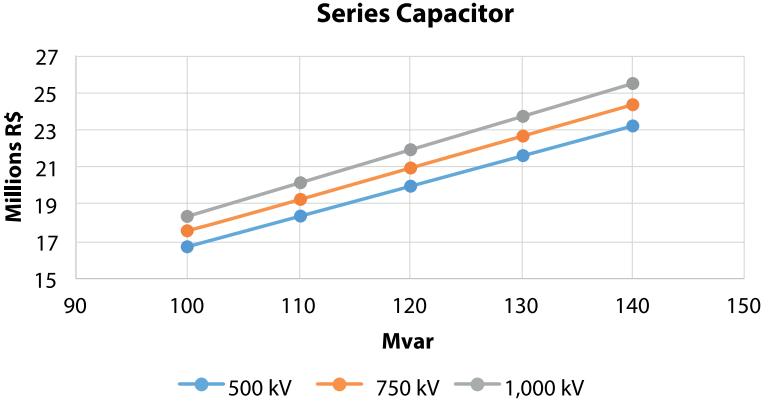

Figure 6.9: Cost of the series capacitor (single-phase)

6.7.6 Direct current converters

For the DC transmission systems, the cost of the converters (rectifiers and inverters for the VSC - *Voltage Sourced Converter* and LCC - *Line Commutated Converter*) was calculated.

The cost of the (LCC) converters in R$ is given by [35]:

$$Cost_{\text{Conv}} = Dollar \cdot 1.5 \cdot 0.698 \cdot V^{0.317} \cdot P^{0.557} \cdot 10^{6}$$

Where,
V is the pole-to-ground (neutral) voltage in kV.
P is the bipole power (MW).
Dollar is the dollar exchange rate for Reais.

In an event sponsored by Cigré, in November 2015 (Rio de Janeiro), it was informed that the cost of a VSC is approximately 20% more than a LCC converter. This value was used in the cost. As for the dollar exchange rate, it was used a value equal to R$. 3.05 per dollar, which is the value that matched with the cost of the Belo Monte converters using the converter cost equation. Therefore, the cost equation for the VSC converter (R$) can be updated through:

$$Cost_{\text{VSC Conv}} = 1.2 \cdot 3.05 \cdot 1.5 \cdot 0.698 \cdot V^{0.317} \cdot P^{0.557} \cdot 10^{6} \quad \text{(R\$)}$$

While, the cost of the LCC converter (R$) is given by:

$$Custo_{\text{LCC Conv}} = 3.05 \cdot 1.5 \cdot 0.698 \cdot V^{0.317} \cdot P^{0.557} \cdot 10^{6} \quad \text{(R\$)}$$

6.8 Joule Losses

The cost of the Joule losses were obtained for the transmission lines, transformers and converters.

6.8.1 Joule losses in the AC lines

The Joule losses (JL) in the transmission lines (MW/km) are calculated through:

$$JL_{CA} = 3 \cdot r \cdot I^2 = r \cdot \left(\frac{P}{V_{ff}} \right)^2$$

$$JL_{CA} = \frac{r_0}{S} = \left(\frac{P}{V_{ff}} \right)^2$$

Where,
r_0 is the conductor resistivity = 58 Ω MCM/km.
S is the section of the conductor of one phase in MCM.
V_{ff} is the phase-to-phase voltage in kV.
P is the three-phase power in MW.

Note: The cost of corona losses in the lines were not calculated.

The cost of the Joule Losses (R$/year) is given by:

$$C_{JL} = (C_P + 8{,}760 \cdot C_e \cdot l_f) \cdot J_L \qquad \text{(R\$/year)}$$

In Table 6.2, above, the values adopted for C_p, C_e, and l_f and their definitions are presented.

6.8.2 Joule losses in the DC lines

The Joule losses (JL) in the transmission lines (MW/km) are calculated through:

$$JL_{CC} = \frac{1}{2} \cdot \frac{r}{N \cdot S_1} \cdot \left(\frac{P_{\max}}{V} \right)$$

Where,
P_{max} is the maximum power in the bipole (MW).
r is the resistivity of the aluminum conductor (58 Ω.MCM/km).
N is the number of subconductors.
S_1 is the section of a conductor (MCM) of one pole.

The cost of the Joule Losses (R$/year) is given by:

$$C_{JL} = (C_P + 8{,}760 \cdot C_e \cdot l_f) \cdot JL_{CC}$$

Similarly, in Table 6.2, above, the values adopted for C_p, C_e, and l_f were presented.

6.8.3 Joule losses in the converters

The value of the maximum losses in the converter (one terminal) will be considered as 0.75% of the total maximum power. Thus, the cost (R$/year) becomes:

$$Custo_{JouleConv} = \frac{0{,}75}{100} \cdot P_{\max} \cdot 10^3 \cdot \left(C_p + C_e \cdot 8760 \cdot l_f \right)$$

In Table 6.2, above, the values adopted for C_p, C_e, and l_f was presented.

6.8.4 Joule losses in the transformers

For the transformers, it was considered 0.3% of the power flowing through each of them in the substation. The power flow of each transformer correspond to steady-state conditions.

6.9 Investments Evaluation

For the investment evaluation, it was used the present value of the annual costs for a life cycle equal to 25 years.

6.9.1 Transmission lines

Table 6.7: Cost of the transmission lines

Alternative	Description	TL Length (km)	TL costs (R$)
1	1,000 kV (8x795 MCM)	1,320	2,508,213,882.00
2	500 kV (6x795 MCM)	2,640	3,403,535,898.00
3	600 kV (4x2,300 MCM)	1,320	1,792,084,493.00
4	LCC 800 kV (6x1,590 MCM)	1,400	2,130,113,725.00

The details of the transmission line costs are presented in Annex 1.

6.9.2 1,000 kV transformers for Alternative 1

The Milagres substation will require a 3,000 MVA transformer composed of four (3+1) single-phase 1,000 MVA units, one of them being a spare unit. The remaining substations will use 2,500 MVA transformers, and a single-phase spare unit per substation. The cost of the transformers is presented in Table 6.8, below.

Table 6.8: Cost of the transformers in the substations, Alternative 1

Substation	Transformer (MVA)	Value of the single-phase unit (R$)	Number of single-phase units	Total (R$)
Milagres	3,000	22,672,498	4	90,689,991.00
Ourolândia	2,500	22,042,777	4	88,171,108.00
Igaporã	2,500	22,042,777	4	88,171,108.00
Pirapora	2,500	22,042,777	4	88,171,108.00

The total value of the transformers in the four substations being R$ 355,203,316.00.

6.9.3 Substations

6.9.3.1 Substations for Alternative 1

For this alternative, the costs are presented for each of the substations (Table 6.9 to Table 6.10).

Table 6.9: 1,000 kV area (Milagres)

	Number	Unit value (R$)	Total (R$)
MIG + MIM*	1	28,053,793.36	28,053,793.36
Shunt reactor (333 Mvar single-phase units)	4	9,221,992.94	36,887,971.75
Series capacitor (250 Mvar/phase)	3	45,155,381.00	135,466,143.00
CT	1	17,355,147.43	17,355,147.43
EL	1	19,737,095.12	19,737,095.12
IB	1	19,737,095.12	19,737,095.12
CRL	1	10,353,903.49	10,353,903.49
CCS	1	4,261,945.11	4,261,945.11
Total			**271,854,094.38**

* MIG = General Infrastructure Module; MIM = Switching Infrastructure Modules

Table 6.10: 500 kV area (Milagres)

	Number	Unit value (R$)	Total (R$)
CT	1	8,183,423.61	8,183,423.61
IB	3	8,564,021.85	25,692,065.55
EL	4	9,301,589.15	37,206,356.60
CRL	2	4,959,223.65	9,918,447.30
Total			**81,000,293.06**

Table 6.11: 1,000 kV area (Ourolândia)

	Number	Unit value (R$)	Total (R$)
MIG + MIM*	1	34,379,593.48	34,379,593.48
Shunt reactor (333 Mvar single-phase units)	7	9,221,992.94	64,553,950.57
Series capacitor (250 Mvar/phase)	6	45,155,381.00	270,932,286.00
CT	1	17,355,147.43	17,355,147.43
EL	2	19,737,095.12	39,474,190.24
IB	2	19,737,095.12	39,474,190.24
CRL	2	10,353,903.49	20,707,806.98
CCS	2	4,261,945.11	8,523,890.22
Total			**495,401,055.16**

* MIG = General Infrastructure Module; MIM = Switching Infrastructure Modules

Table 6.12: 500 kV area (Ourolândia)

500 kV	Number	Unit value (R$)	Total (R$)
CT	1	8,183,423.61	8,183,423.61
IB	2	8,564,021.85	17,128,043.70
EL	2	9,301,589.15	18,603,178.30
CRL	1	4,959,223.65	4,959,223.65
Total			**48,873,869.26**

Table 6.13: 1,000 kV area (Igaporã)

	Number	Unit value (R$)	Total (R$)
MIG + MIM*	1	38,251,367.46	38,251,367.46
Shunt reactor (333 Mvar single-phase units)	7	9,221,992.94	64,553,950.57
Series capacitor (250 Mvar/phase)	6	45,155,381.00	270,932,286.00
CT	1	17,355,147.43	17,355,147.43
EL	2	19,737,095.12	39,474,190.24
IB	2	19,737,095.12	39,474,190.24
CRL	2	10,353,903.49	20,707,806.98
CCS	2	4,261,945.11	8,523,890.22
Total			**499,272,829.14**

* MIG = General Infrastructure Module; MIM = Switching Infrastructure Modules

Table 6.14: 500 kV area (Ourolândia)

500 kV	Number	Unit value (R$)	Total (R$)
CT	1	8,183,423.61	8,183,423.61
IB	3	8,564,021.85	25,692,065.55
EL	4	9,301,589.15	37,206,356.60
CRL	2	4,959,223.65	9,918,447.30
Total			**81,000,293.06**

Table 6.15: 1,000 kV area (Pirapora)

1,000 kV	Number	Unit value (R$)	Total (R$)
MIG + MIM*	1	36,430,969.14	36,430,969.14
Shunt reactor (333 Mvar single-phase units)	4	9,221,992.94	36,887,971.75
Series capacitor (250 Mvar/phase)	3	45,155,381.00	135,466,143.00
CT	1	17,355,147.43	17,355,147.43
EL	1	19,737,095.12	19,737,095.12
IB	1	19,737,095.12	19,737,095.12
CRL	1	10,353,903.49	10,353,903.49
CCS	1	4,261,945.11	4,261,945.11
Total			**280,230,270.16**

* MIG = General Infrastructure Module; MIM = Switching Infrastructure Modules

Table 6.16: 500 kV area (Pirapora)

500 kV	Number	Unit value (R$)	Total (R$)
CT	1	8,183,423.61	8,183,423.61
IB	3	8,564,021.85	25,692,065.55
EL	4	9,301,589.15	37,206,356.60
Total			**71,081,845.76**

6.9.3.2 500 kV Substations for Alternative 2

Table 6.17: Milagres 500 kV

	Number	Unit value (R$)	Total (R$)
MIG + MIM*	1	23,002,731.40	23,002,731.40
Shunt reactor (113 Mvar single-phase units)	7	6,287,787.68	44,014,513.75
Series capacitor (63 Mvar/phase)	6	10,700,991.31	64,205,947.89
IB	3	8,564,021.85	25,692,065.55
EL	6	9,301,589.15	55,809,534.90
CRL	4	4,959,223.65	19,836,894.60
CCS	2	2,698,482.16	5,396,964.32
Total			**237,958,652.41**

* MIG = General Infrastructure Module; MIM = Switching Infrastructure Modules

Table 6.18: Ourolândia 500 kV

	Number	Unit value (R$)	Total (R$)
MIG + MIM*	1	37,925,865.88	37,925,865.88
Shunt reactor (113 Mvar single-phase units)	13	6,287,787.68	81,741,239.82
Series capacitor (63 Mvar/phase)	12	10,700,991.31	128,411,895.77
IB	3	8,564,021.85	25,692,065.55
EL	6	9,301,589.15	55,809,534.90
CRL	5	4,959,223.65	24,796,118.25
CCS	4	2,698,482.16	10,793,928.64
Total			**365,170,648.82**

* MIG = General Infrastructure Module; MIM = Switching Infrastructure Modules

Table 6.19: Igaporã 500 kV

	Number	Unit value (R$)	Total (R$)
MIG + MIM*	1	49,118,216.74	49,118,216.74
Shunt reactor (113 Mvar single-phase units)	13	6,287,787.68	81,741,239.82
Series capacitor (63 Mvar/phase)	12	10,700,991.31	128,411,895.77
IB	4	8,564,021.85	34,256,087.40
EL	8	9,301,589.15	74,412,713.20
CRL	6	4,959,223.65	29,755,341.90
CCS	4	2,698,482.16	10,793,928.64
Total			**408,489,423.48**

* MIG = General Infrastructure Module; MIM = Switching Infrastructure Modules

Table 6.20: Pirapora 500 kV

	Number	Unit value (R$)	Total (R$)
MIG + MIM*	1	49,118,216.74	49,118,216.74
Shunt reactor (113 Mvar single-phase units)	7	6,287,787.68	44,014,513.75
Series capacitor (63 Mvar/phase)	6	10,700,991.31	64,205,947.89
IB	3	8,564,021.85	25,692,065.55
EL	6	9,301,589.15	55,809,534.90
CRL	2	4,959,223.65	9,918,447.30
CCS	2	2,698,482.16	5,396,964.32
Total			**254,155,690.45**

* MIG = General Infrastructure Module; MIM = Switching Infrastructure Modules

6.9.3.3 500 kV Substations for Alternative 3

Table 6.21: Milagres (Rectifier)

	Number	Unit value (R$)	Total (R$)
MIG + MIM*	1	19,271,948.00	19,271,948.00
CT	4	8,183,424.00	32,733,694.00
IB	4	8,564,022.00	34,256,087.00
EL	4	9,301,589.00	37,206,357.00
CRL	2	4,959,224.00	9,918,447.00
Total			**133,386,534.00**

* MIG = General Infrastructure Module; MIM = Switching Infrastructure Modules

Table 6.22: Ourolândia (Rectifier)

	Number	Unit value (R$)	Total (R$)
MIG + MIM*	1	17,406,556.00	17,406,556.00
CT	4	8,183,424.00	32,733,694.00
IB	3	8,564,022.00	25,692,066.00
EL	2	9,301,589.00	18,603,178.00
CRL	1	4,959,224.00	4,959,224.00
Total			**99,394,718.00**

* MIG = General Infrastructure Module; MIM = Switching Infrastructure Modules

Table 6.23: Igaporã (Inverter)

	Number	Unit value (R$)	Total (R$)
MIG + MIM*	1	19,271,948.00	19,271,948.00
CT	4	8,183,424.00	32,733,694.00
IB	4	8,564,022.00	34,256,087.00
EL	4	9,301,589.00	37,206,357.00
CRL	2	4,959,224.00	9,918,447.00
Total			**133,386,534.00**

* MIG = General Infrastructure Module; MIM = Switching Infrastructure Modules

Table 6.24: Pirapora (Inverter)

	Number	Unit value (R$)	Total (R$)
MIG + MIM*	1	17,406,556.00	17,406,556.00
CT	4	8,183,424.00	32,733,694.00
IB	4	8,564,022.00	34,256,087.00
EL	4	9,301,589.00	37,206,357.00
Total			121,602,694

* MIG = General Infrastructure Module; MIM = Switching Infrastructure Modules

6.9.3.4 500 kV Substations for Alternative 4

Table 6.25: Rectifier

	Number	Unit value (R$)	Total (R$)
MIG + MIM*	1	19,271,948.00	19,271,948.00
CT	4	8,183,424.00	32,733,694.00
IB	4	8,564,022.00	34,256,087.00
EL	4	9,301,589.00	37,206,357.00
Total			123,468,086

* MIG = General Infrastructure Module; MIM = Switching Infrastructure Modules.

Table 6.26: Inverter

	Number	Unit value (R$)	Total (R$)
MIG + MIM*	1	21,137,340.00	21,137,340.00
CT	4	8,183,424.00	32,733,694.00
IB	4	8,564,022.00	34,256,087.00
EL	4	9,301,589.00	37,206,357.00
Total			125,333,478

* MIG = General Infrastructure Module; MIM = Switching Infrastructure Modules

6.9.4 Cost of the converters

The cost equation of the CC converter was presented in item 6.7.6.

6.9.4.1 Cost of the converters for Alternative 3

To determine the cost of the converters (Alternative 3), it was used the equations presented in item 6.7.6, for which it was added 20% (VSC converters) as stated in the assumptions.

Table 6.27: Alternative 3 converters

	Milagres	Ourolândia	Igaporã	Pirapora
Type	R VSC*	R VSC	I VSC*	I VSC
Voltage (kV)	600	600	600	600
Power (MW)	2,000	1,200	1,000	2,200
Number of bipoles	1	1	1	1
Total cost of the converters (R$)	1,005,161,226.06	756,251,020.77	683,222,279.19	1,059,964,824.07

* R = Rectifier; I = Inverter

6.9.4.2 Cost of the converters for Alternative 4

Table 6.28: Alternative 4 converters

	Milagres and Pirapora
Type	LCC
Voltage (kV)	800
Power (MW)	4,000
Number of bipoles	1
Total cost of the converters (R$)	2,699,999,999.67

6.9.5 Losses in the transmission lines

The expressions to calculate losses in transmission lines (DC and AC) were presented in items 6.8.1 and 6.8.2.

Tables 6.29 to 6.32 present the annual losses for the four alternatives.

Table 6.29: Annual losses in the lines of Alternative 1

Section	N	V (kV)	S (MCM)	Number circuits	Length of section (km)	Power per section and circuit (MW)	Losses per section (MW/km)	Losses (MW)	Cost of TL Losses (R$/year)
Milagres – Ourolândia	8	1,000	795	1	440	1,829	0.0305	13.42	9,054,111.00
Ourolândia – Igaporã	8	1,000	795	1	440	3,217	0.0944	41.52	28,010,477.00
Igaporã – Pirapora	8	1,000	795	1	440	2,178	0.0433	19.03	12,839,087.00
Total annual losses in the line									**49,903,675.00**

Table 6.30: Annual losses in the lines of Alternative 2

Section	N	V (kV)	S (MCM)	Number circuits	Length of section (km)	Power per section and circuit (MW)	Losses per section (MW/km)	Losses (MW)	Cost of TL Losses (R$/year)
Milagres – Ourolândia	6	500	795	2	440	820	0.0327	28.78	19,412,203.00
Ourolândia – Igaporã	6	500	795	2	440	1,609	0.1258	110.74	74,694,606.00
Igaporã – Pirapora	6	500	795	2	440	1,041	0.0527	46.38	31,285,894.00
Total annual losses in the line									**125,392,702.00**

Table 6.31: Annual losses in the lines of Alternative 3

Section	N	V (kV)	S (MCM)	Number circuits	Length of section (km)	Power per section and circuit (MW)	Losses per section (MW/km)	Losses (MW)	Cost of TL Losses (R$/year)
Milagres – Ourolândia	4	600	2,300	1	440	2,000	0.0350	15.41	10,394,777.00
Ourolândia – Igaporã	4	600	2,300	1	440	3,200	0.0897	39.45	26,610,629.00
Igaporã – Pirapora	4	600	2,300	1	440	2,200	0.0424	18.65	12,577,680.00
Total annual losses in the line									**49,583,085.00**

Table 6.32: Annual losses in the lines of Alternative 4

Section	N	V (kV)	S (MCM)	Number circuits	Length of section (km)	Power per section and circuit (MW)	Losses per section (MW/km)	Losses (MW)	Cost of TL Losses (R$/year)
Rectifier – Inverter	6	800	1,590	1	1,400	4,000	0.0760	106.39	**71,764,969.00**

In Table 6.33, the total losses on the line for a 30-year period (present value) is presented. For this purpose the values presented in Table 6.2 was used.

Table 6.33: Total losses for a 30year period

Alternative	Total cost (R$)
1	561,804,757.00
2	1,411,643,875.00
3	558,195,633.00
4	807,914,468.00

6.9.6 Transformers losses for Alternative 1

As stated above, these losses were estimated as being 0.3% of the power flowing through the transformer. Table 6.34 presents the power flow through the transformers.

Table 6.34: Power (MW) through the transformers

Substation	Power (MW)
Milagres	1,829
Ourolândia	1,400
Igaporã	1,000
Pirapora	2,161
Total	6,390

The total power through all the transformers is 6,390 MW, which gives an approximate loss of 19.17 MW. Using the value of R$ 154.00/MWh and a loss factor of 0.5, the annual cost of the losses becomes R$ 12,930,548.00, resulting in a total loss for a 30-year period equal to R$ 145,569,312.00 (interest of 8% p.y., Table 6.2).

6.9.7 Losses in the converters

The cost of the Joule losses in the converters was presented in item 6.8.3. The values for the costs of energy, loss factor, and interest rates are those presented in Table 6.2.

6.9.7.1 Losses in the converters for Alternative 3

The cost of the annual losses of the converters is of R$ 32,376,960.00. For 30 years, the total cost is of R$ 364,492,801.00.

6.9.7.2 Losses in the converters for Alternative 4

The cost of the annual losses of the converters is R$ 40,471,200.00. For the 30 years of life, the total cost will be R$ 455,616,001.00.

6.10 Comparison of the Alternatives

Table 6.35 presents the evaluation of the investments for the three alternatives along with the illustrative alternative (Alternative 4).

Table 6.35: Evaluation of the costs of the alternatives

	R$			
Alternative	**1**	**2**	**3**	**4**
Transmission lines	2,508,213,882.00	3,304,093,874.00	1,792,084,493.00	2,130,113,725.00
Transformers	355,203,316.00	0	0	0
Substations	1,828,713,550.00	1,265,774,415.00	407,976,468.00	258,720,012.00
Converters	0	0	3,504,599,350.00	2,700,000,000.00
Equipment subtotal	**4,692,130,748.00**	**4,569,868,290.00**	**5,704,660,311.00**	**5,088,833,737.00**
Losses in the lines	561,804,757.00	1,411,643,875.00	558,195,633.00	807,914,468.00
Losses in the transformers	145,569,312.00	0	0	0
Losses in the converters	0	0	364,492,801.00	455,616,001.00
Total	**5,399,504,818.00**	**5,981,512,165.00**	**6,627,348,744.00**	**6,352,364,205.00**
Comparison	1.00	1.11	1.23	1.18

Based on the values presented in Table 6.35, it can be stated that Alternative 1 (1,000 kV) has the lowest value. The second best alternative (500 kV) presents a value 11% higher than the first alternative. Alternative 3 has a value 23% higher than the first alternative, whereas Alternative 4 is 18% higher than Alternative 1. Therefore, the best alternative for the 1,000 kV system would be Alternative 1.

6.11 Sensitivities

Some sensitivity analyses were performed for the alternatives studied. They were:

- Modify the loss factor from 0.5 to 0.35.
- Modify the loss calculation considering the bipole carrying 3,000 MW instead of 4,000 MW and reduce the loss factor to 0.35.
- Calculation of the bipole losses for 3,000 MW and a loss factor equal to 0.5.

6.11.1 Sensitivity 1

In this sensitivity analysis, the loss factor was altered to 0.35. Table 6.36, below, presents the results of this analysis.

Table 6.36: Investment evaluation – Loss factor of 0.35

	R$			
Alternative	**1**	**2**	**3**	**4**
Transmission lines	2,508,213,882.00	3,304,093,874.00	1,792,084,496.00	2,130,113,725.00
Transformers	355,203,316.00	0	0	0
Substations	1,828,713,550.00	1,265,774,415.00	407,976,468.00	258,720,012.00
Converters	0	0	3,504,599,350.00	2,700,000,000.00
Equipment subtotal	**4,692,130,748.00**	**4,569,868,290.00**	**5,704,660,314.00**	**5,088,833,737.00**
Losses in the lines	393,263,330.00	988,150,713.00	390,736,943.00	565,540,127.00
Losses in the transformers	101,898,519.00	0	0	0
Losses in the converters	0	0	255,144,961.00	318,931,201.00
Total	**5,187,292,597.00**	**5,558,019,002.00**	**6,350,542,218.00**	**5,973,305,065.00**
Comparison	1.00	1.07	1.22	1.15

With the loss factor altered to 0.35, the difference between alternatives 2, 3, and 4 compared to Alternative 1 decreased.

6.11.2 Sensitivity 2

In this sensitivity analysis, Alternative 4 presents power of 3,000 MW, and loss factor 0.35. Table 6.37, below, presents the results of this analysis.

Table 6.37: Investment evaluation – 3,000 MW Bipole and Loss factor of 0.35

	R$			
Alternative	**1**	**2**	**3**	**4**
Transmission lines	2,508,213,882.00	3,304,093,874.00	1,792,084,496.00	2,130,113,725.00
Transformers	355,203,316.00	0	0	0
Substations	1,828,713,550.00	1,265,774,415.00	407,976,468.00	258,720,012.00
Converters	0	0	3,504,599,350.00	2,300,238,604.00
Equipment subtotal	**4,692,130,748.00**	**4,569,868,290.00**	**5,704,660,314.00**	**4,689,072,341.00**
Losses in the lines	393,263,330.00	988,150,713.00	390,736,943.00	318,116,322.00
Losses in the transformers	101,898,519.00	0	0	0
Losses in the converters	0	0	255,144,961.00	239,198,401.00
Total	**5,187,292,597.00**	**5,558,019,002.00**	**6,350,542,218.00**	**5,246,387,063.00**
Comparison	1.00	1.07	1.22	1.01

In this analysis, the difference between the Alternative 4 and Alternative 1 decreased even more, although the value for Alternative 1 is still the lowest.

6.11.3 Sensitivity 3

In this sensitivity analysis, the Alternative 4 presents power of 3,000 MW, and loss factor 0.5. Table 6.38, below, presents the results of this analysis.

Table 6.38: Investment evaluation – 3,000 MW Bipole and Loss factor of 0.5

	R$			
Alternative	**1**	**2**	**3**	**4**
Transmission lines	2,508,213,882.00	3,304,093,874.00	1,792,084,496.00	2,130,113,725.00
Transformers	355,203,316.00	0	0	0
Substations	1,828,713,550.00	1,265,774,415.00	407,976,468.00	258,720,012.00
Converters	0	0	3,504,599,350.00	2,300,238,604.00
Equipment subtotal	**4,692,130,748.00**	**4,569,868,290.00**	**5,704,660,314.00**	**4,689,072,341.00**
Losses in the lines	561,804,757.00	1,411,643,875.00	558,195,633.00	454,451,888.00
Losses in the transformers	145,569,312.00	0	0	0
Losses in the converters	0	0	364,492,801.00	341,712,001.00
Total	**5,399,504,818.00**	**5,981,512,165.00**	**6,627,348,748.00**	**5,485,236,230.00**
Comparison	1.00	1.13	1.25	1.02

In this analysis, the difference between the illustrative alternative (Alternative 4) and Alternative 1 increased a little when compared to the previous sensitivity analysis.

Based on the investment values calculated, we verify that the reference alternative (1,000 kV) presents lower value even considering the sensitivity studies. Based on these results, the reference alternative (Alternative 1) is justified.

7. Description of the 1,000 kV Reference Alternative

This item presents a description of the reference alternative in 1,000 kV, denominated Alternative 1 in the economic evaluation above.

7.1 Transmission Line

The transmission line of the reference alternative presents length of 1,320 km, divided into three sections of 440 km.

Figure 7.1 presents the typical geometry considered in the calculations of the electrical parameters.

This is a self-supporting tower, and alternatives such as guyed single must, guyed, and trapezoid towers were also studied.

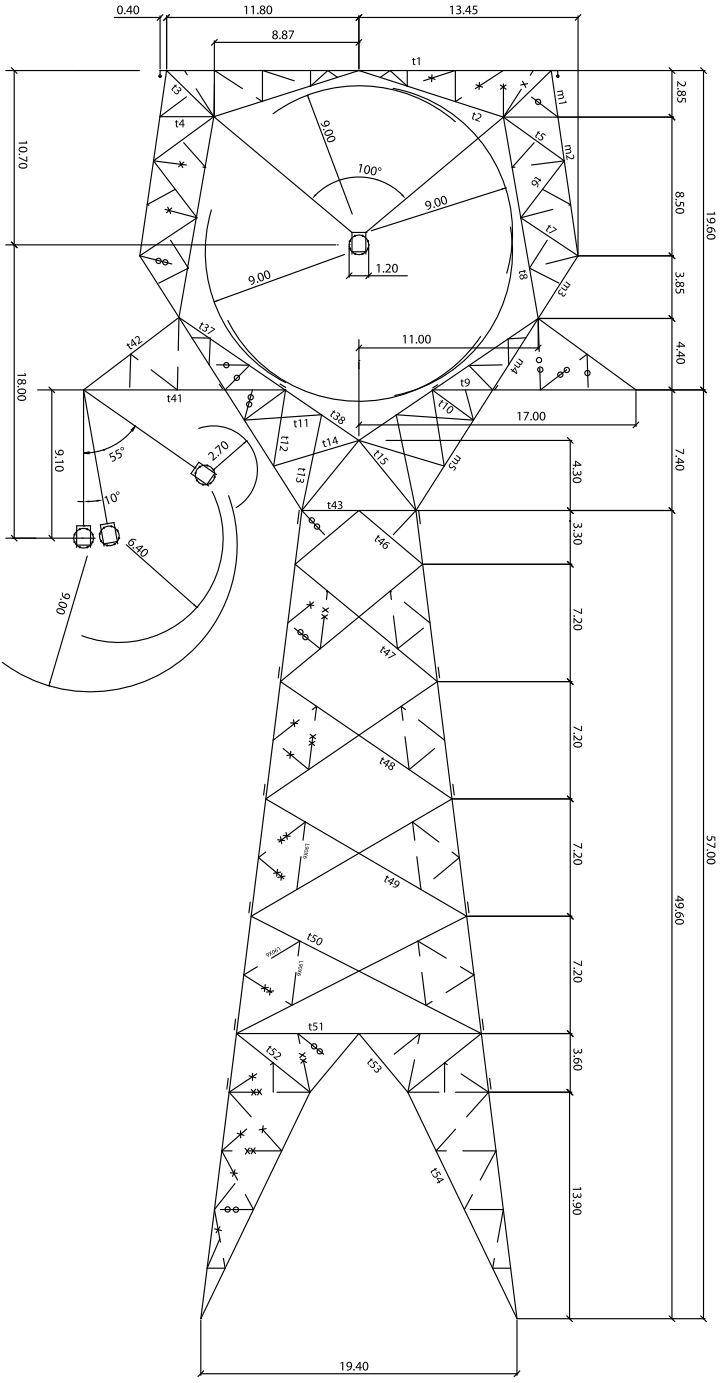

Figure 7.1: Typical geometry of a 1,000 kV line

In Figure 7.2, the distribution of the subconductors per phase is presented.

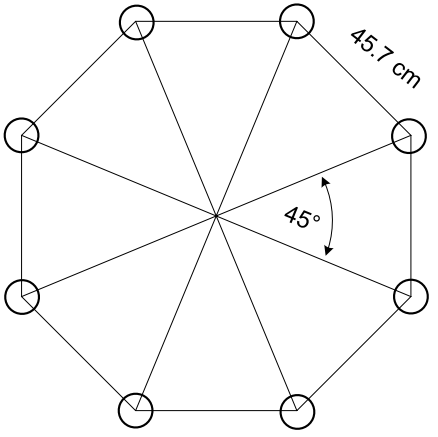

Figure 7.2: 795 MCM subconductor bundle

This conductor indicated in the ACSR (steel core aluminum cable) 795 MCM (Tern), in a bundle of 8 subconductors per phase.

- Rated diameter of complete conductor: 27.03 mm.
- Diameter with steel core: 6.75 mm.
- DC resistance at 20°C: 0.07192 Ω/km/cond.

Table 7.1, below, presents the spatial distribution of the conductors and ground wires.

Table 7.1: Spatial distribution of conductors and ground wires

	Height (m)	Horizontal spacing (m)	Height mid-span (m)
Phases A and C	47.9	17	25.9
Phase B	65.9	0	43.9
Ground wires	76.6	11.8	59

With the data presented above, and using the ATP (*Alternative Transient Program*) program, the line parameters that are presented in Table 7.2, are obtained.

Table 7.2: Parameters of the reference alternative line

r_1 (Ohm/km)	x_1 (Ohm/km)	c_1 (nF/km)	r_0 (Ohm/km)	x_0 (Ohm/km)	c_0 (nF/km)
0.00969	0.30679	14.193	0.30270	1.16895	8.65

7.1.1 Initial and final loading in normal state and emergency

Table 7.3 shows the loadings of the 1,000 kV sections, in steady state and emergency, in the heavy load, Wet North scenario, considering an increase of 5,500 MW in the Northeast region generation over the PDE 2024.

Table 7.3: Loading (MW) of the 1,000 kV lines. Reference alternative. Heavy load

PDE 2024 Heavy load – Humid North	Milagres III – Ourolândia III section	Ourolândia III – Igaporã IV section	Igaporã IV – Pirapora III section
Steady state	1,829	3,217	2,178
Contingencies			
Opening of the 500kV line between Gentio do Ouro II and Bom Jesus da Lapa II	1,863	3,561	2,221
Opening of the 500kV line between Bom Jesus da Lapa II and Janaúba 3	1,864	3,322	2,294
Opening of the 500kV line between Juazeiro III and Ourolândia III	2,142	3,048	2,103
Opening of the 500kV line between Morro do Chapéu II and Sapeaçu	1,636	3,533	2,239
Opening of the 500kV line between Igaporã IV and Janaúba 3	1,808	3,175	2,370
Opening of the 500kV line between Janaúba III and Ribeirão das Neves	1,816	3,203	2,373
Opening of the 500kV line between Ribeirão das Neves and Itabira 5	1,788	3,136	2,091
Opening of the 500kV line between Silvânia and Emborcação	1,880	3,300	2,255
Opening of the 500kV line between Silvânia and Itumbiara	1,876	3,293	2,243
Opening of the 500kV line between Silvânia and Trindade	1,866	3,277	2,227
Disconnection of the 1,000/500 kV transformer of Milagres III	0	2,375	1,869
Disconnection of the 1,000/500 kV transformer of Ourolândia III	2,523	2,499	1,945
Disconnection of the 1,000/500 kV transformer of Igaporã IV	1,607	2,698	2,671
Disconnection of the 1,000/500 kV transformer of Pirapora III	1,488	2,502	0
Loss of one pole of Bipole B, with overload in the other pole	1,903	3,314	2,251
Opening of the 1,000 kV line between Milagres III and Ourolândia III	0	2,382	1,872
Opening of the 1,000 kV line between Ourolândia III and Igaporã IV	405	0	1,106
Opening of the 1000 kV line between Igaporã IV and Pirapora III	1,486	2,500	0

Table 7.4 shows the loadings of the 1,000 kV sections, in steady state and emergency, in the light load, Wet North scenario, considering the same generation increase used in the heavy load case.

Table 7.4: Loading (MW) of the 1,000 kV lines. Reference alternative. Light load

PDE 2024 Light load – Humid North	Milagres III – Ourolândia III section	Ourolândia III – Igaporã IV section	Igaporã IV – Pirapora III section
Steady state	1,430	2,579	1,687
Contingencies			
Opening of the 500 kV line between Gentio do Ouro and Bom Jesus da Lapa	1,453	2,860	1,723
Opening of the 500 kV line between Bom Jesus da Lapa and Janaúba	1,457	2,661	1,771
Simple opening of the 500 kV line between Juazeiro and Ourolândia 3	1,719	2,429	1,623
Opening of the 500 kV line between Morro do Chapéu and Sapeaçu	1,273	2,831	1,737
Opening of the 500 kV line between Igaporã 4 and Janaúba 3	1,413	2,546	1,828
Opening of the 500 kV line between Janaúba 3 and Ribeirão das Neves	1,418	2,566	1,824
Opening of the 500 kV line between Ribeirão das Neves and Itabira 5	1,399	2,517	1,621
Opening of the 500 kV line between Silvânia and Emborcação	1,474	2,651	1,748
Opening of the 500 kV line between Silvânia and Itumbiara	1,469	2,642	1,735
Opening of the 500 kV line between Silvânia and Trindade	1,461	2,629	1,724
Disconnection of the 1,000/500 kV transformer of Milagres	0	1,940	1,460
Disconnection of the 1,000/500 kV transformer of Ourolândia 3	2,007	1,991	1,506
Disconnection of the 1,000/500 kV transformer of Igaporã 4	1,242	2,136	2,118
Disconnection of the 1,000/500 kV transformer of Pirapora 3	1,164	2,015	0
Loss of one pole of Bipole B, with overload in the other pole	1,504	2,674	1,754
Opening of the 1,000 kV line between Milagres and Ourolândia 3	0	1,946	1,461
Opening of the 1,000 kV line between Ourolândia 3 and Igaporã 4	296	0	859
Opening of the 1,000 kV line between Igaporã 4 and Pirapora 3	1,164	2,017	0

On the other hand, aiming at a future use expansion, the line must be considered to operate with the following maximum loads:

- 4,600 MVA in steady state
- 6,300 MVA in emergency for 30 minutes

7.1.2 Shunt reactive compensation

The reactive compensation used is of 85%, fixed, therefore, with power of 333 Mvar/phase and per 1,000 kV terminal.

7.1.3 Series reactive compensation

The series compensation used in the reference alternative is of 50%, with 25% per terminal. The power is of 250 Mvar/phase and per terminal.

7.2 Substations

7.2.1 Busbar arrangement

According to the Grid Procedures, Sub-module 23.3, for a voltage equal to or higher than 345 kV, the arrangement should be of double bar, with one and a half circuit breaker. Figure 7.3, below, presents the simplified single line diagram of the reference alternative, with current configuration and future expansion.

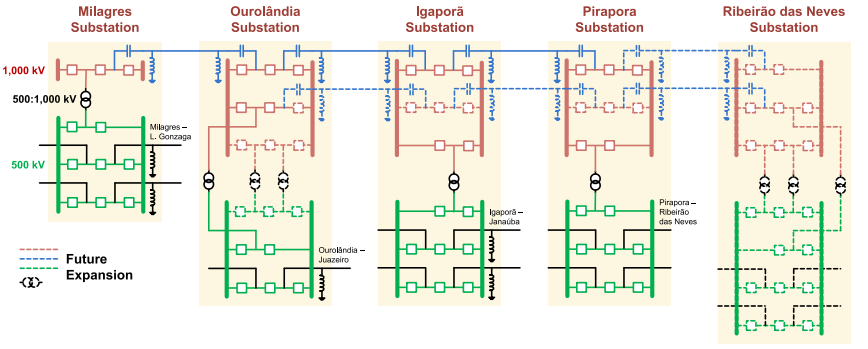

Figure 7.3: Single line diagram of the reference alternative

7.2.2 Area necessary for new substations

The area necessary for new substations was obtained from Technical Brochure 32 from Cigré. The area is of 165,000 m² for an air insulated substation, with space for two lines (future expansion), and three transformers.

The project also contemplates a SF6 insulated substation (1,000 and 500 kV) and, in this case, the arrangement may be different, provided it does not hinder the reliability index.

7.2.3 Macro-location of the Milagres substation

New substation, located in the south of the state of Ceará. It is located at about 400 km from Fortaleza/Ceará, and 430 km from Natal/Rio Grande do Norte, favoring the future expansion of the 1,000 kV system, and the connection to the wind potential of the east of the Northeast region of Brazil.

Figure 7.4: Macro-location of the Milagres substation

7.2.4 Macro-location of the Ourolândia substation

New substation, located in the center of the state of Bahia, favoring the connection to the wind potential of the central area of Bahia, and the outflow of the potential of the east of the Northeast region.

Figure 7.5: Macro-location of the Ourolândia substation

7.2.5 Macro-location of the Igaporã substation

New substation, located in the south of Bahia, and in a wind power potential center, favoring the connection to it, and the outflow to the southeast.

Figure 7.6: Macro-location of the Igaporã substation

7.2.6 Macro-location of the Pirapora substation

New substation, located in the center of the state of Minas Gerais, close to Belo Horizonte.

Figure 7.7: Macro-location of the Pirapora substation

7.2.7 Macro-location of the Ribeirão das Neves substation

New substation, located to the north of Belo Horizonte. This substation may come to be part of the expansion of the reference alternative.

Figure 7.8: Macro-location of the Ribeirão das Neves substation

7.2.8 Transformer units

In Table 7.5, the data for the transformers is presented.

Table 7.5: Transformer units (single-phase units)

Substation	Bank power (MVA)	Voltages in the P, S windings (kV)	Shunt (%)	PS Impedance (%)
Milagres	3,000	1,000/500	± 15x0.5%	14
Ourolândia	2,550	1,000/500	± 15x0.5%	14
Igaporã	2,550	1,000/500	± 15x0.5%	14
Pirapora	2,550	1,000/500	± 15x0.5%	14
Ribeirão das Neves*	2,550	1,000/500	± 15x0.5%	14

* The Ribeirão das Neves substation may come to be part of a future expansion of the reference alternative.
** A spare unit should be included in each substation.

The voltage of the transformer tertiary (probably 138 kV) has not been defined yet, and awaits meetings with the equipment manufacturers. The greatest limitation for choosing these values is the maximum transport weight estimated at 270 ton for 850 MVA.

The impedance (1,000 – 500 kV) of the transformers is 14% in their base rating.

8. Future Expansion of the 1,000 kV Reference Alternative

The initial alternative is composed of a 1,000 kV AC line connecting the substations of Milagres, Ourolândia, Igaporã, and Pirapora, with length of 1,320 km. This alternative was conceived considering the conclusions of EPE's studies regarding the transmission bottleneck resulting of the increase in the wind and photovoltaic power potential in the Northeast region. For the insertion of this system, the study used the data of the PDE 2024, with a generation increase of 5,500 MW at locations of high wind and photovoltaic power potential.

The analysis of the possible expansion of the initial alternative was done in two stages:

1. Insertion of an additional single-circuit 300 km section connecting the substations of Pirapora to Ribeirão das Neves, with the same scenario of the previous generation, that is, with a generation increase of 5,500 MW over the PDE 2024.

2. Additional insertion of the above-mentioned case of an additional single circuit connecting the substations of Ourolândia, Igaporã, Pirapora, and Ribeirão das Neves. This expansion was studied with an increase of 5,500 MW over the previous scenario, which means this expansion includes a generation increase of 11,000 MW over the PDE 2024. Figure 8.1 shows the locations where the generation increases were made.

Because of the overload observed in the 500 kV lines of some sections, in the case presented in Figure 8.1, a reinforcement was made in the 500 kV (shown in yellow), by means of an additional circuit in the following sections:

- Ourolândia – Ourolândia III 500 kV
- Ourolândia III – Juazeiro 500 kV
- Milagres II – Santa Luzia
- Santa Luzia – Campina Grande

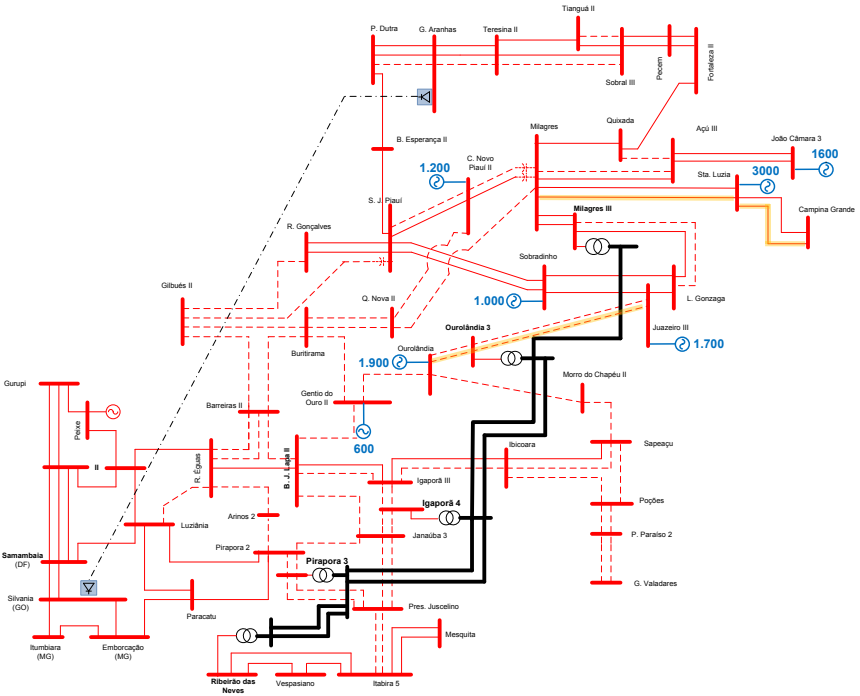

Figure 8.1: Location of the 11,000 MW increase in the Northeast generation

8.1 Performance Evaluation for Expansion

8.1.1 Power Flow Studies

This item presents the power flow results for steady state and contingency, in a heavy load, Humid North scenario, in the following cases:

- 1,000 kV system, with four sections, and one circuit per section, considering a generation increase in the Northeast region of 5,500 MW over the PDE 2024
- 1,000 kV system, with four sections, and one and two circuits per section, considering a generation increase in the Northeast region of 11,000 MW over the PDE 2024

Aiming at evaluating the performance of the alternatives, several contingencies were applied, observing their impacts on the existing grid, and also the effects of the 1,000 kV system reinforcement on the central region of Bahia e the north of Minas Gerais. The main conditions evaluated were:

- Opening of the 500 kV line between Gentio do Ouro and Bom Jesus da Lapa;
- Opening of the 500 kV line between Bom Jesus da Lapa and Janaúba;
- Opening of the 500 kV line between Juazeiro and Ourolândia;
- Opening of the 500 kV line between Morro do Chapéu and Sapeaçu;
- Opening of the 500 kV line between Igaporã and Janaúba;
- Opening of the 500 kV line between Janaúba and Ribeirão das Neves;
- Opening of the 500 kV line between Ribeirão das Neves and Itabira;
- Opening of the 500 kV line between Silvânia and Emborcação;
- Opening of the 500 kV line between Silvânia and Itumbiara;
- Opening of the 500 kV line between Silvânia and Trindade;
- Disconnection of 1,000/500 kV transformers;
- Loss of one pole of Bipole B, with overload in the other pole;
- Opening of the 1,000 kV sections.

8.1.1.1 1,000 kV system with 4 sections and 1 circuit per section

The 1,000 kV system analyzed in this item is composed of the initial alternative, and an additional fourth 300 km section, connecting Pirapora to Ribeirão das Neves. The interconnection of the 1,000 kV line to the 500 kV of Ribeirão das Neves is done by means of three 1,000/500 kV transformers, with 2,500 MVA.

a) Reactive support

The additional reactive capacitive support is necessary in other busbars of the SIN, to ensure the voltages are maintained within the thresholds admissible in these regions during some contingencies. The following the shunt capacitor banks were allocated.

- 400 Mvar at 500 kV Ribeirão das Neves
- 40 Mvar at 230 kV Governador Valadares

During some contingencies, mainly in the 1st and 2nd sections of the 1,000 kV line, we observed the need for inductive reactive in the region of Ribeirão das Neves and Governador Valadares, about 900 Mvar and 400 Mvar, respectively, which can be resolved with the connection of the already foreseen reactor banks.

b) Results of the simulations

For the case of Heavy Load – Wet North (PDE 2024), Table 8.1, below, summarizes the active power flows in steady state, through the 1,000 kV line.

Table 8.1: Flows (MW) in the sections of the 1,000 kV line (heavy load)

FROM Busbar	TO Busbar	Flow (MW)
Milagres	Ourolândia	2,110
Ourolândia	Igaporã	3,791
Igaporã	Pirapora	3,719
Pirapora	Ribeirão das Neves	4.062

Figure 8.2 presents the flows in the 1,000 kV lines, and in the 500 kV grid nearby, for the steady state condition.

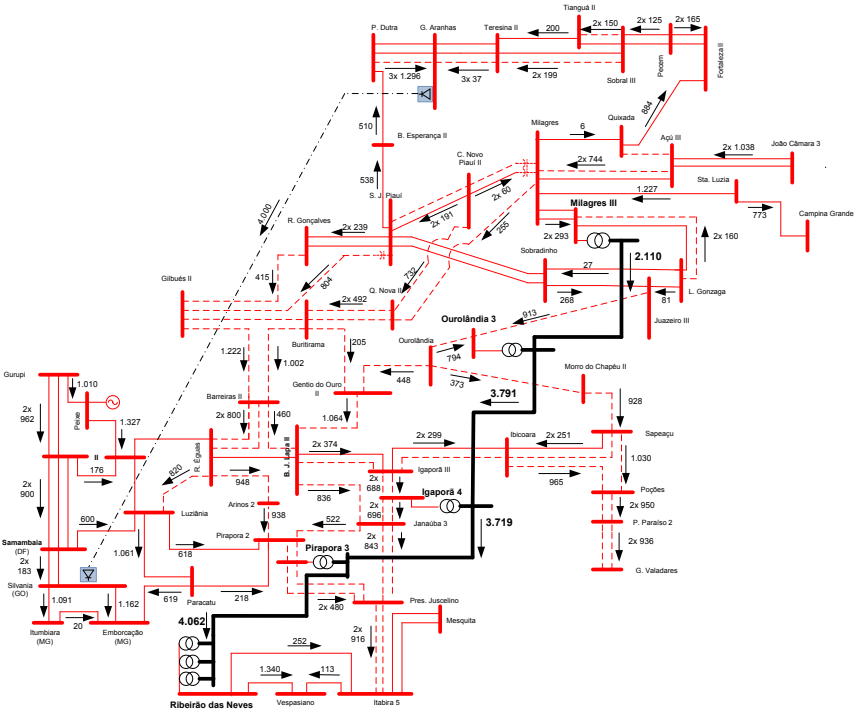

Figure 8.2: Power flow (MW) in steady state

It is possible to observe that the insertion of the fourth section contributes to an increase of the loading of the 1,000 kV system. The load in the second section, which previously was the heaviest at 3,217 MW, went to 3,791 MW with the inclusion of the fourth section, which in turn, presents loading of 4,062 MW. The section between Pirapora and Ribeirão das Neves also contributes to alleviate the loading of the 500 kV system in the region.

In all simulated contingencies, the lines voltages and loads stayed within the emergency thresholds. In the 1,000 kV line contingencies, the flows are redistributed through the system through the 500 kV lines.

Following, are presented some results of the contingencies performed, focusing on the 1,000 kV system.

b1) Disconnection of 500/1,000 kV transformers

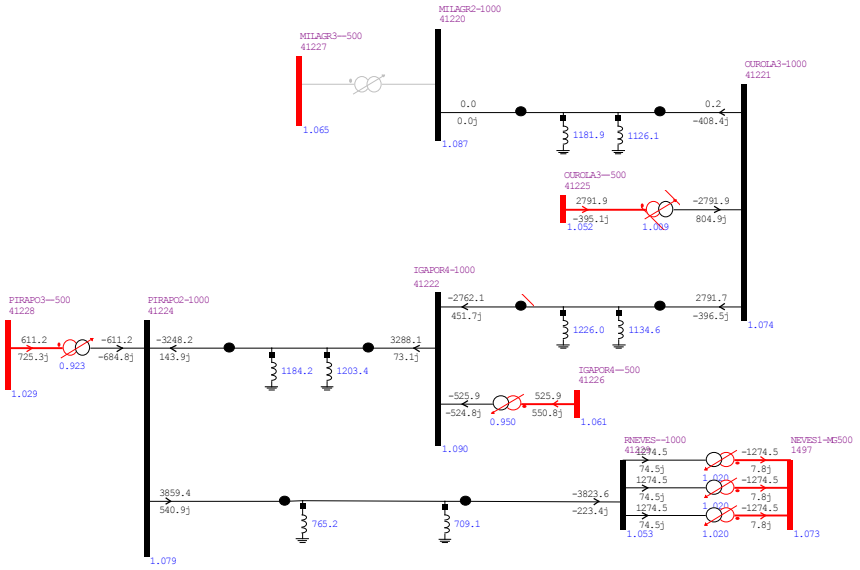

Figure 8.3: Power flow in the loss of the transformers at Milagres

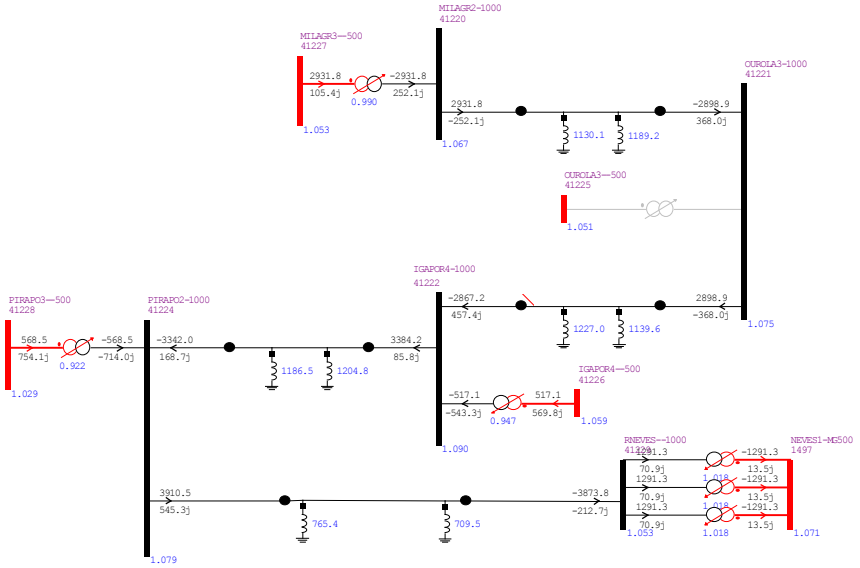

Figure 8.4: Power flow during the loss of the transformers at Ourolândia

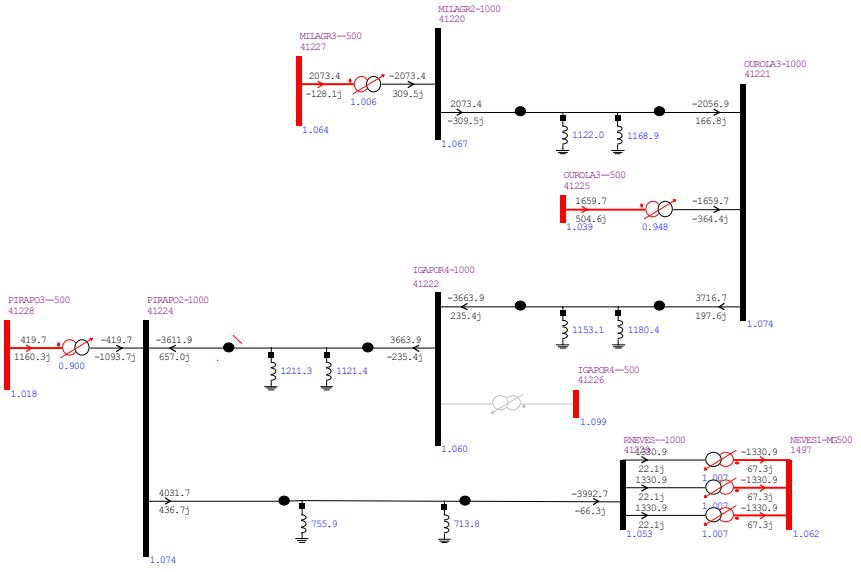

Figure 8.5: Power flow during the loss of the transformers at Igaporã

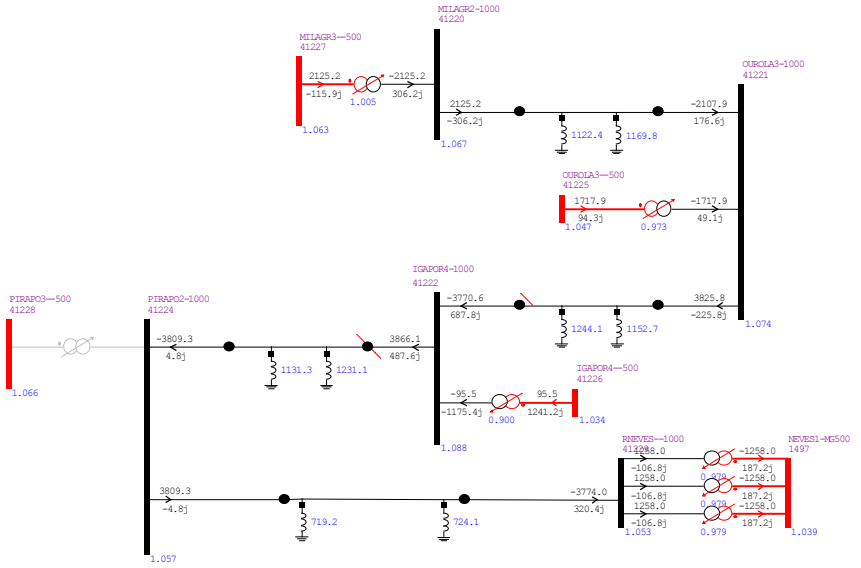

Figure 8.6: Power flow during the loss of the transformers at Pirapora

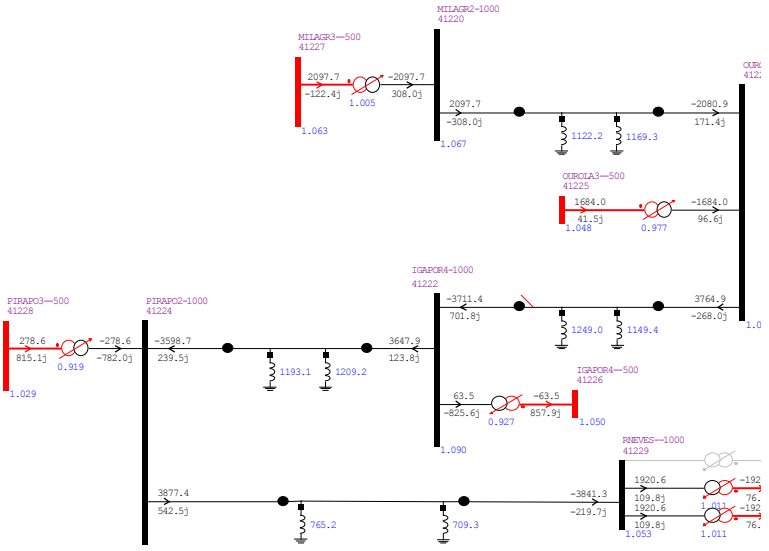

Figure 8.7: Power flow during the loss of one of the transformers at Ribeirão das Neves

b2) Disconnection of the 1,000 kV lines

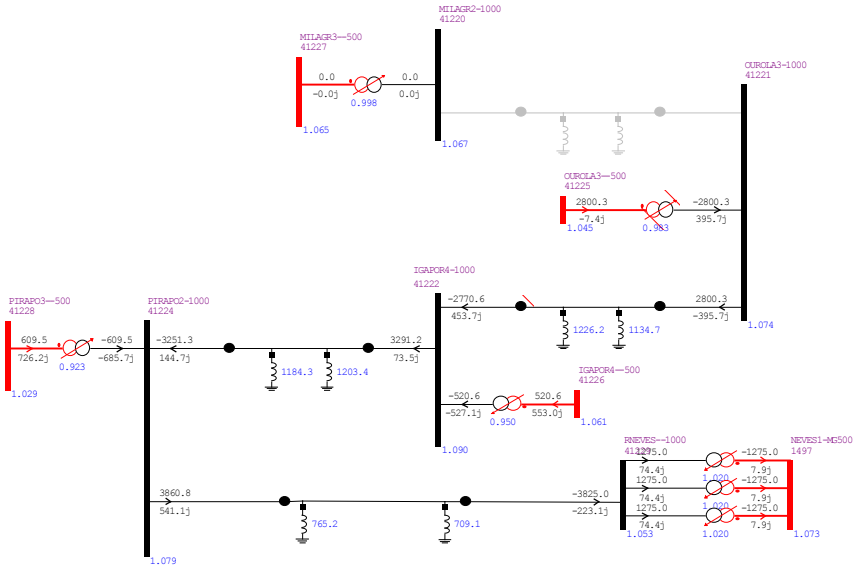

Figure 8.8: Power flow during the disconnection of the Milagres – Ourolândia section

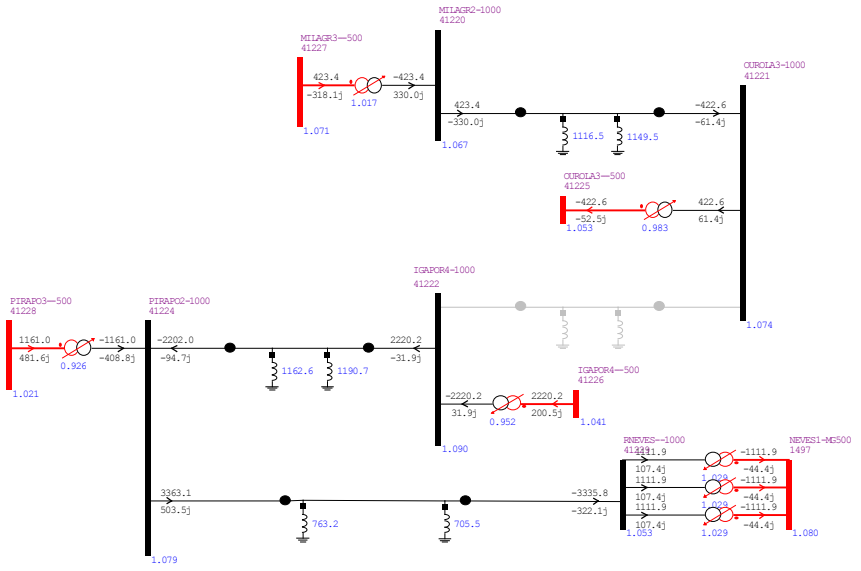

Figure 8.9: Power flow during the disconnection of the Ourolândia – Igaporã section

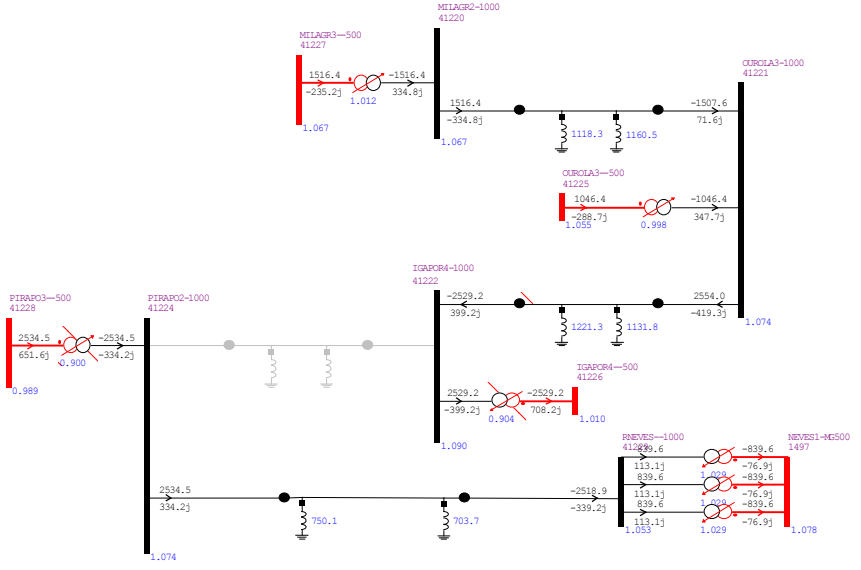

Figure 8.10: Power flow during the disconnection of the Igaporã – Pirapora section

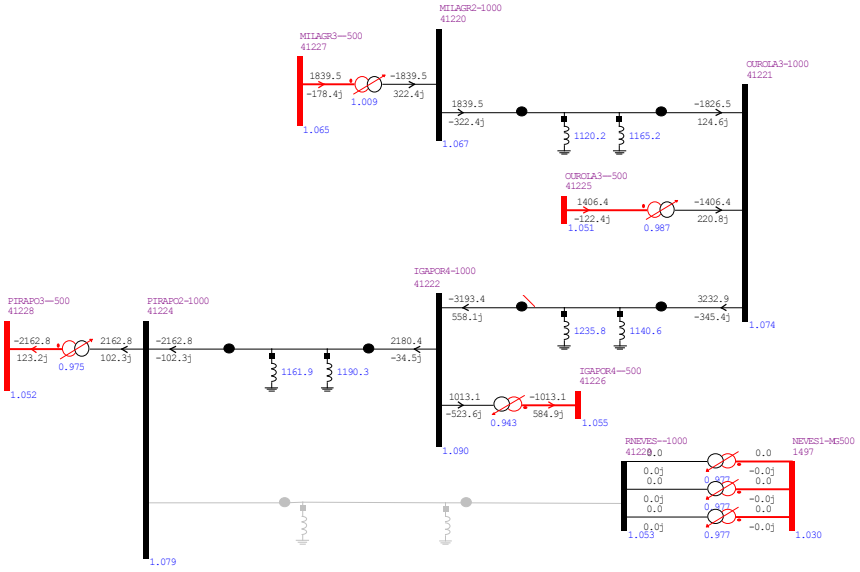

Figure 8.11: Power flow during the disconnection of the Pirapora – Ribeirão das Neves section

c) Disconnection of one pole in Graça Aranha – Silvânia and overload of the other pole

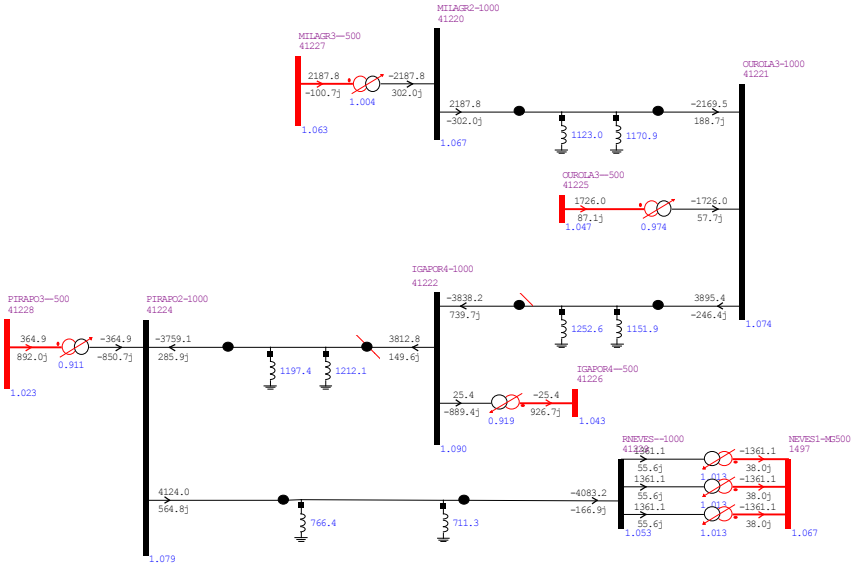

Figure 8.12: Power flow at 1,000 kV after the disconnection of one pole of bipole B

8.1.1.2 1,000 kV system with 4 sections and 3 of them with 2 circuits

In this item, the generation in the Northeast region was increased to 11,000 MW over the PDE 2024, twice the amount of the previous items, to represent a future generation scenario in the Northeast region, but in a more distant scenario than in the previous cases. For this scenario, we considered the expansion of the 1,000 kV system, with four sections, with the sections between Ourolândia – Igaporã, Igaporã – Pirapora, and Pirapora – Ribeirão das Neves, presenting two 1,000 kV circuits. As in the previous item, the interconnection of the 1,000 kV line with the 500 kV of Ribeirão das Neves is done by means of three 1,000/500 kV transformers, with 2,500 MVA each. This case required the addition of two transformers at the Ourolândia substation, with the same configurations of the transformers of Ribeirão das Neves.

Because of the overload observed in the 500 kV lines of some sections, in this case, a reinforcement was made in the 500 kV, by means of the addition of one circuit to the following existing sections:

- Ourolândia – Ourolândia III 500 kV
- Ourolândia III – Juazeiro 500 kV
- Milagres II – Santa Luzia
- Santa Luzia – Campina Grande

a) Reactive support

The additional reactive capacitive support is necessary in other busbars of the SIN, to ensure the voltages are maintained within the thresholds admissible in these regions during some contingencies. The following shunt capacitor banks were allocated:

- 660 Mvar at 500 kV Ribeirão das Neves
- 200 Mvar at 230 kV Governador Valadares

We also observed the need for 730 Mvar in the region of Silvânia (Goiás) during contingency, and of 240 Mvar in the base case.

b) Results of the simulations

For the case of Heavy Load – Wet North (PDE 2024), considering an increase of 11,000 MW in the Northeast region generation, Table 8.2, below, summarizes the active power flows through the 1,000 kV lines, considering four sections, and one and two circuits per section.

Table 8.2: Flows (MW) in the sections of the 1,000 kV line (heavy load)

FROM Busbar	TO Busbar	Flow (MW)
Milagres	Ourolândia	2,605
Ourolândia	Igaporã	6,960
Igaporã	Pirapora	6,672
Pirapora	Ribeirão das Neves	6,352

Figure 8.13 presents the flows in the 1,000 kV lines, and in the 500 kV grid nearby, for the case in steady state (heavy load).

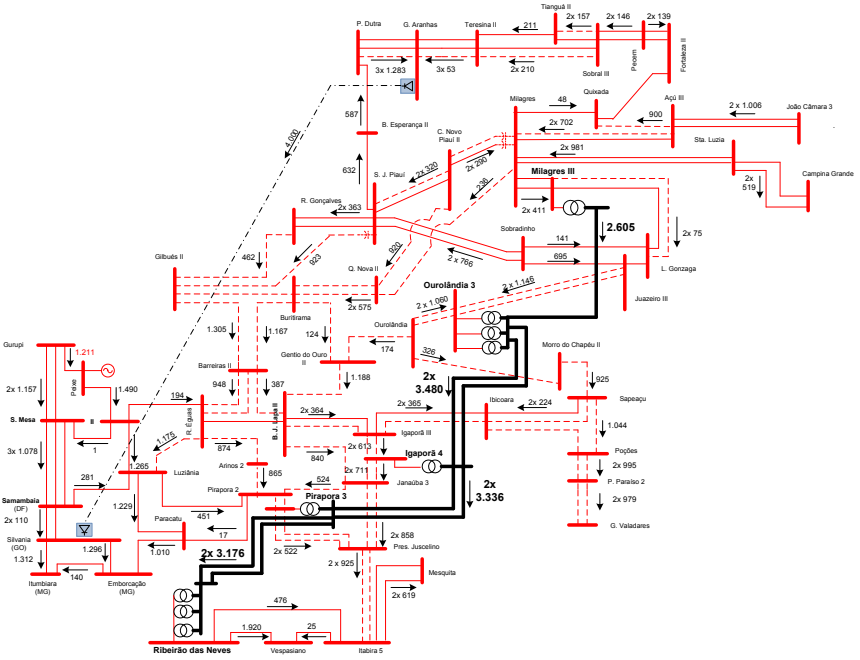

Figure 8.13: Power flow (MW) in steady state

As shown in Figure 8.13, the loading of the 1,000 kV line is significant in all the sections, but mainly in the second, (6,960 MW), and the third, (6,672 MW).

In all simulated contingencies, the lines voltages and loads stayed within the emergency thresholds. In the 1,000 kV line contingencies, part of the flows is redistributed through the system via the 500 kV lines. The highest loading found in a 1,000 kV line during contingency was of 5,929 MW, in the section between Ourolândia and Igaporã, in the contingency of the second 1,000 kV line of this section.

Next, some results of the contingencies performed, focusing on the 1,000 kV system, are presented.

b1) Disconnection of 500/1,000 kV transformers

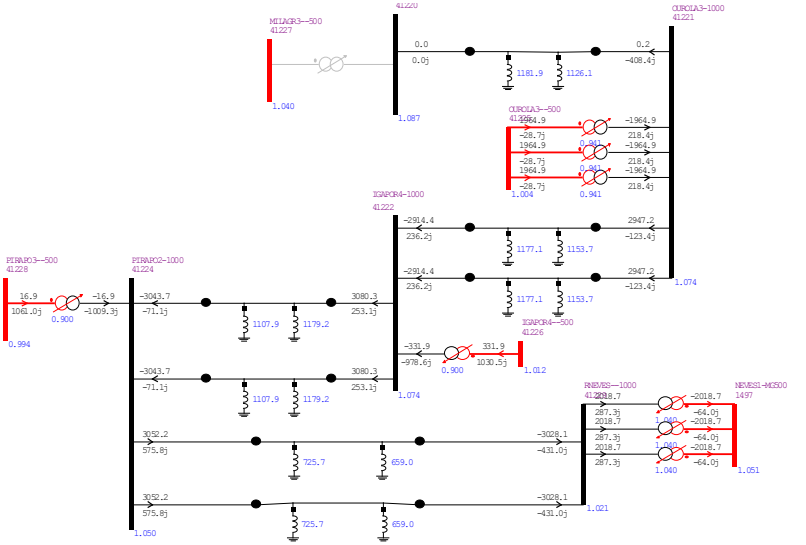

Figure 8.14: Power flow during the loss of the transformers at Milagres

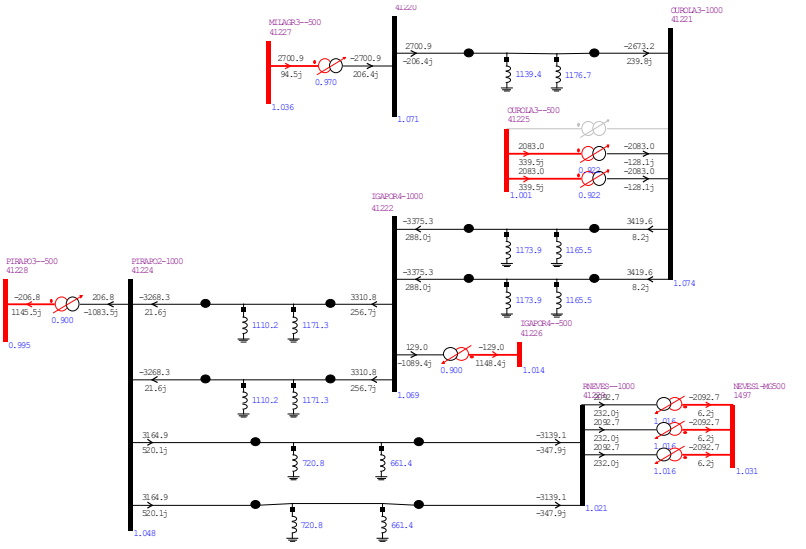

Figure 8.15: Power flow during the loss of one of the transformers at Ourolândia

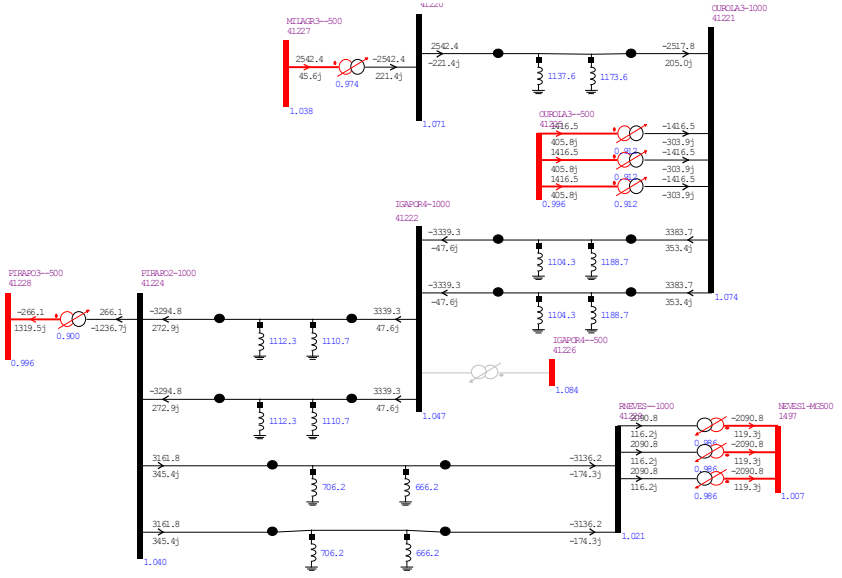

Figure 8.16: Power flow during the loss of the transformers at Igaporã

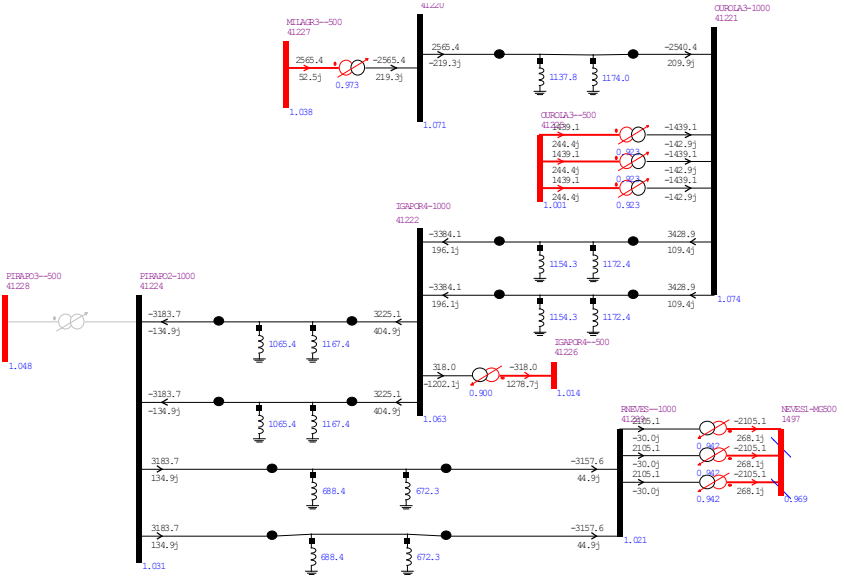

Figure 8.17: Power flow during the loss of the transformers at Pirapora

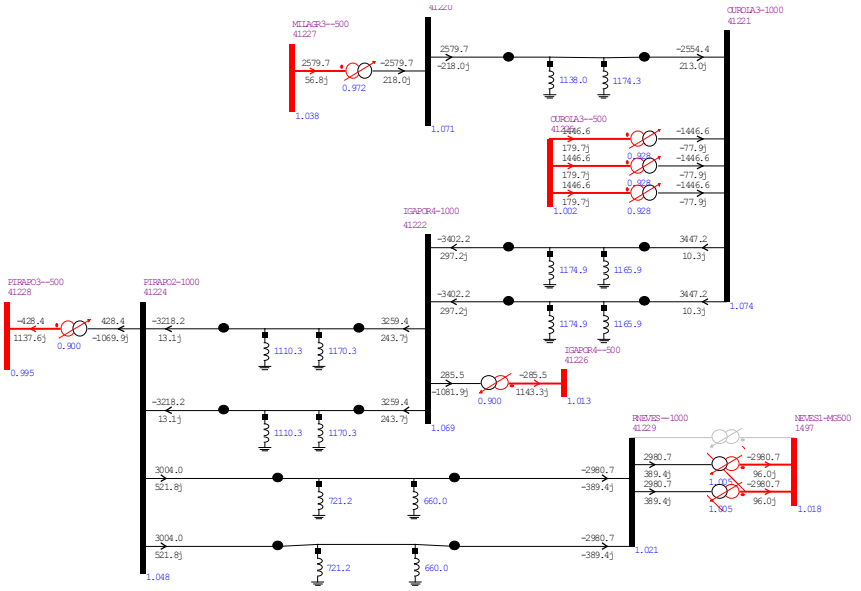

Figure 8.18: Power flow during the loss of one of the transformers at Ribeirão das Neves

b2) Disconnection of the 1,000 kV lines

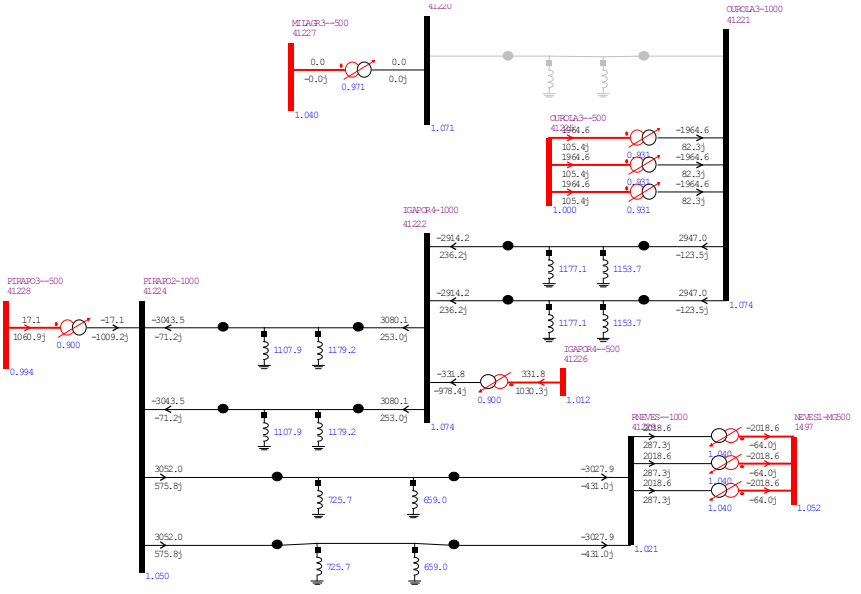

Figure 8.19: Power flow during the disconnection of the Milagres – Ourolândia section

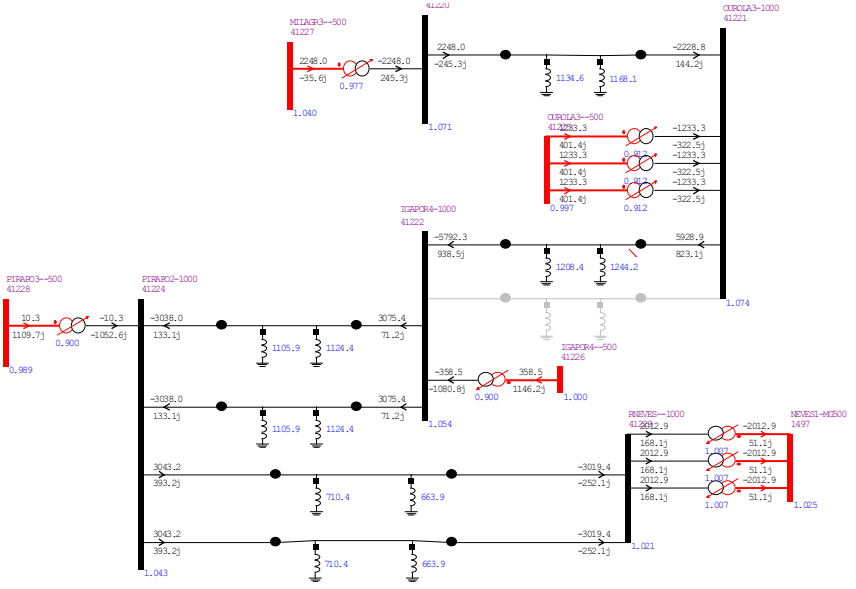

Figure 8.20: Power flow during the disconnection of the Ourolândia – Igaporã section

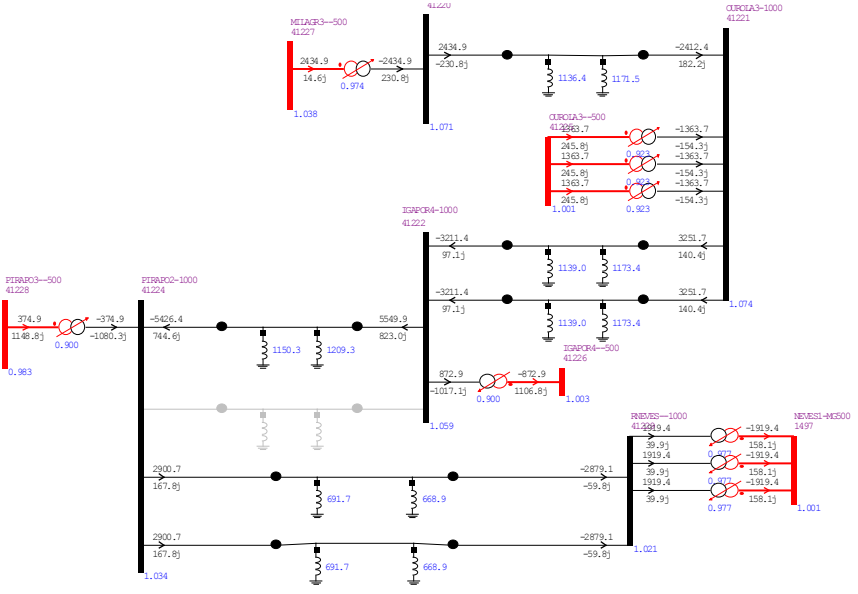

Figure 8.21: Power flow during the disconnection of the Igaporã – Pirapora section

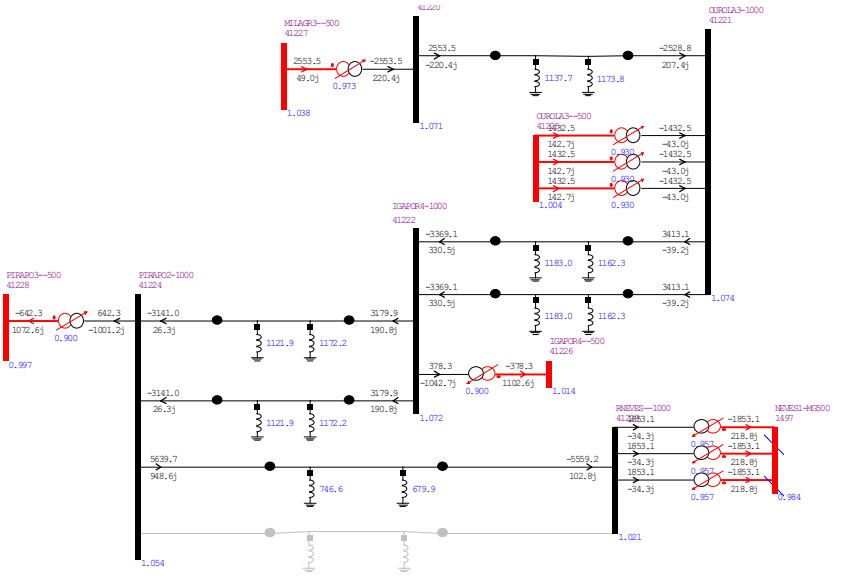

Figure 8.22: Power flow during the disconnection of the Pirapora – Ribeirão das Neves section

c) Disconnection of one pole in Graça Aranha – Silvânia and overload of the other

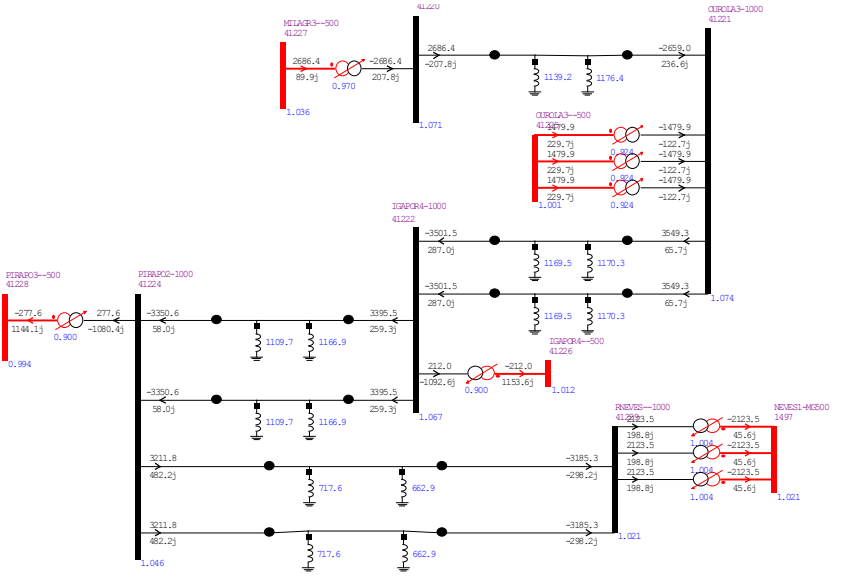

Figure 8.23: Power flow at 1,000 kV after the disconnection of one pole of bipole B

8.1.2 Study of electromechanical transients, expansion of the 1,000 kV system with 4 sections and 3 of them with 2 circuits

Sustained overvoltage studies were conducted for the case of expansion of the 1,000 kV system, where the line has 1 and 2 circuits per section, aiming at verifying the possibility of occurrence of prohibitive temporary or sustained voltage values, and system frequency values.

For these analyses, we used the databases of Anatem program, with 2016-2024 horizons, in the scope of the PDE 2024 (Ten Year Expansion Plan), published by EPE, at EPE's site on 04/01/2016. The power flow basis file used is the heavy load (Humid North), considering the same generation increases inserted in the power flow studies, as shown previously.

In the disconnection of the line in the base case in steady state, we verified the need of reactive support in the region of Ribeirão das Neves, in Minas Gerais. To meet this need, 500 MVA were added by means of synchronous compensation in this region.

Single-phase fault was applied to the 1,000 kV busbars, with the subsequent opening of the 1,000 kV line, and three-phase fault, represented by means of the opening of the 1,000 kV line. In the scenarios analyzed, even with the significant increase of wind generation (11,000 MW) in the northeast region, the studies did not verify, in any of the cases, any violation of the transient or sustained voltage levels.

Following, are presented the results for the second section (Igaporã – Ourolândia), which presented the highest load.

Figure 8.24 shows the voltages in the 1,000 kV line during single-phase fault at the Ourolândia busbar, followed by the opening of one line in the Ourolândia – Igaporã section.

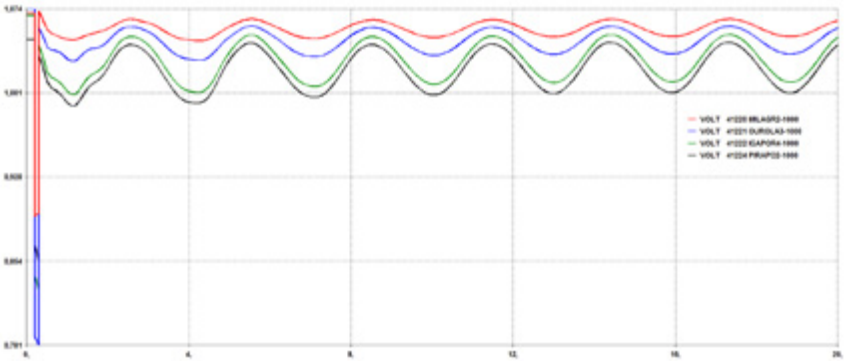

Figure 8.24: Voltages in the 1,000 kV busbars – single-phase short-circuit at Ourolândia, with the opening of one circuit of the 1,000 kV Ourolândia – Igaporã line

Figure 8.25 shows the active power of the hydroelectric power plants of Paulo Afonso, Tucuruí 1, Três Marias, and Itumbiara, and of the wind power plants in the region of Ourolândia and João Câmara.

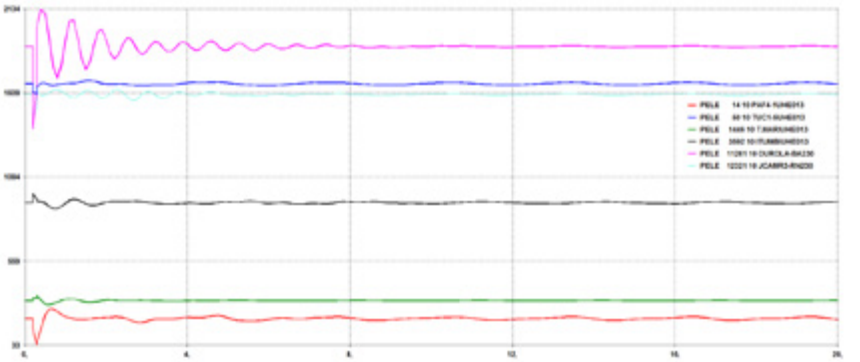

Figure 8.25: Power in the system: single-phase short-circuit at Ourolândia, with the opening of one circuit of the 1,000 kV Ourolândia – Igaporã line

Figures 8.26 and 8.27 show the results during single-phase fault at the Igaporã busbar, followed by the opening of one line in the Ourolândia – Igaporã section.

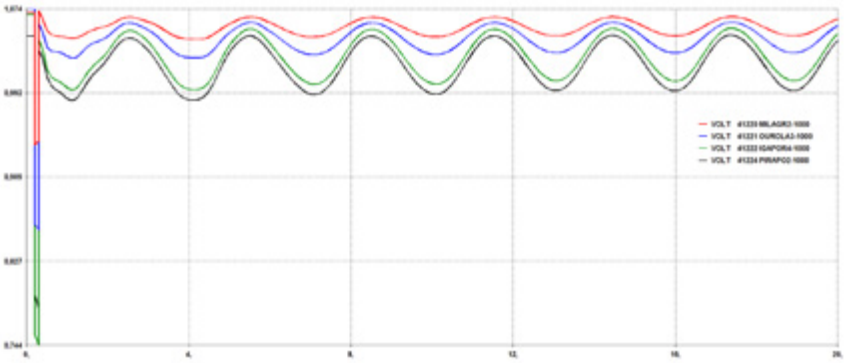

Figure 8.26: Voltages in the 1,000 kV busbars – single-phase short-circuit at Igaporã, with the opening of one circuit of the 1,000 kV Ourolândia – Igaporã line

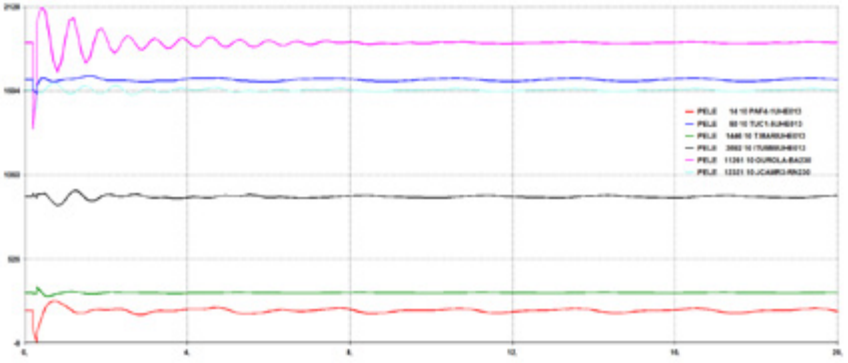

Figure 8.27: Power in the system: single-phase short-circuit at Igaporã, with the opening of one circuit of the 1,000 kV Ourolândia – Igaporã line

Figures 8.28 and 8.29 show the results during the opening of one of the lines of the second 1,000 kV section (Ourolândia – Igaporã).

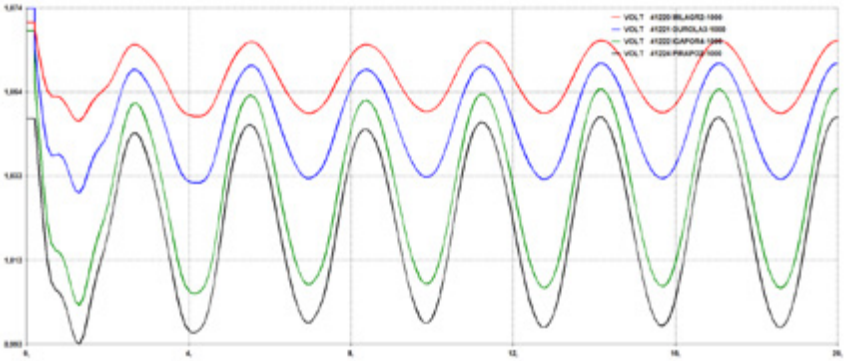

Figure 8.28: Voltages in the 1,000 kV busbars – single-phase short-circuit of the 1,000 kV Ourolândia – Igaporã line

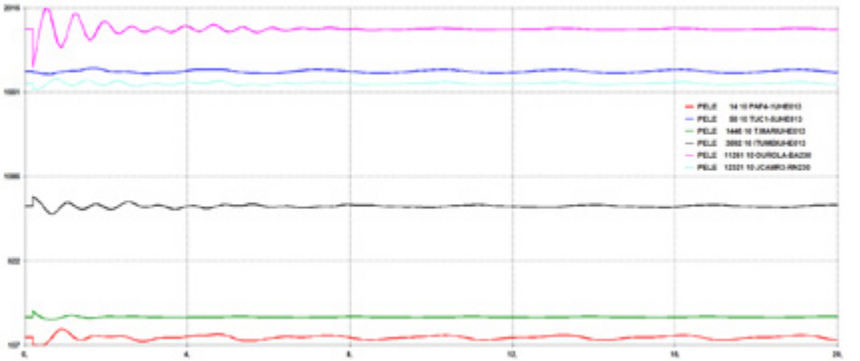

Figure 8.29: Power in the system: opening of one circuit of the 1,000 kV Ourolândia – Igaporã line

8.1.3 Short-circuit studies, expansion of the 1,000 kV system

The calculation of the short-circuit levels was done considering them for the case of the expansion of the 1,000 kV system, where the line has 1 and 2 circuits per section, in subtransient state, with all the machines operating. The database used was EPE's short-circuit studies database, referring to the PDE 2016-2024 (maximum short-circuit file).

The values referring to the short-circuit currents for the main substations of the basic grid are presented in Table 8.3, for the year 2024, which shows the case with the initial alternative, and the case considering the expansion of the 1,000 kV line (4 sections, from Milagres to Ribeirão das Neves, and 1 and 2 circuits per section). None of the circuit breakers were surpassed after the entry in operation of the 1,000 kV system. We can say that the expansion had little influence on the short-circuit levels.

Table 8.3: Short-circuit levels, expansion of the 1,000 kV system

Identification			2024 with works (1,000 kV TL, 3 sections, 1 circuit, reference alternative)				2024 with works (1,000 kV TL, 4 sections, 1 and 2 circuits)				Circuit breaker (kA)
Number	Bus	Voltage	3Φ (kA)	X/R	1Φ (kA)	X/R	3Φ (kA)	X/R	1Φ (kA)	X/R	
206	SOBRAD-BA230	230	19.31	16.08	18.24	16.86	22.61	17.24	26.32	19.83	40
209	POCOE2-BA230	230	13.03	17.06	10.49	11.35	13.06	17.09	10.51	11.35	NA
213	ITAGIB-BA230	230	6.01	6.34	4.46	5.57	6.02	6.34	4.46	5.57	NA
276	FUNIL--BA230	230	8.96	7.12	8.86	8.5	8.97	7.11	8.87	8.5	40
288	IBICOA-BA230	230	8.47	33.09	7.68	17.25	8.50	33.47	7.7	17.26	NA
376	BRUMAD-BA230	230	3.47	7.07	3.88	8.42	3.48	7.07	3.88	8.42	40
394	IGAPO2-BA230	230	36.65	22.96	35.04	17.01	38.12	24.17	36.31	17.19	NA
505	L.GONZ-PE500	500	38.99	20.38	38.32	16.28	39.49	20.32	38.62	16.25	50
506	SOBRAD-BA500	500	22.57	6.51	22.53	12.03	23.99	6.82	24.51	12.13	40
516	QUIXAD-CE500	500	10.98	13.36	7.5	7.46	11.03	13.36	7.51	7.47	50
521	MILAGR-CE500	500	29.53	12.1	26.05	8.59	30.97	12.45	25.56	8.54	50
523	JCAMR3-RN500	500	20.57	18.07	22.62	19.05	20.70	17.71	22.71	18.83	NA
544	C.GRAN-PB500	500	19.99	10.03	24.25	10.46	20.39	9.26	21.43	8.42	NA
555	M.CHAP-BA500	500	10.35	16.01	9.04	12.98	10.96	15.83	9.38	12.71	NA
574	CAMACA-BA500	500	19.71	17.52	19.57	12.8	19.80	17.48	19.62	12.77	40
585	BJLAPA-BA500	500	19.14	15	15.88	11.73	19.89	15.32	16.29	11.64	40
587	R.EGUA-BA500	500	20.77	9.79	11.82	6.44	21.17	9.84	11.94	6.42	40
588	IBICOA-BA500	500	14.82	15.54	10.3	7.29	15.08	15.68	10.4	7.24	40
589	SAPEAC-BA500	500	17.51	15.08	15.34	9.78	17.66	15.1	15.41	9.76	40
846	BARRER-BA500	500	20.36	10.33	12.49	6.94	20.75	10.39	12.62	6.91	NA
1482	BARREI-MG345	345	17.36	11.24	14.99	7.76	18.38	11.41	15.51	7.7	25
1483	ITABI2-MG500	500	16.39	13.94	15.52	10.23	17.88	14.26	16.4	10.12	NA
1484	ITABI2-MG345	345	19.45	13.39	19.94	10.1	20.57	13.73	20.72	10.1	NA

Identification			2024 with works (1,000 kV TL, 3 sections, 1 circuit, reference alternative)				2024 with works (1,000 kV TL, 4 sections, 1 and 2 circuits)				Circuit breaker (kA)
Number	Bus	Voltage	3Φ (kA)	X/R	1Φ (kA)	X/R	3Φ (kA)	X/R	1Φ (kA)	X/R	
1485	BDESPA-MG500	500	18.56	14.66	15.95	9.01	20.67	15.06	17	8.77	40
1488	JAGUAR-MG500	500	25.96	18.03	20.8	11.83	26.42	18.04	20.99	11.79	38
1489	JFORA1-MG345	345	6.83	9.72	6.84	10.46	6.86	9.69	6.87	10.44	40
1493	MCLARO-MG345	345	6.64	11.49	6.35	10.09	6.71	11.53	6.4	10.08	40
1494	MESQUI-MG500	500	14.82	15.13	13.63	12.24	15.43	15.16	13.97	12.17	38
1496	NEVES1-MG345	345	19.47	14.4	19.31	12.25	21.52	15.79	21.1	13.14	25
1497	NEVES1-MG500	500	17.54	15.18	16.5	11.33	25.73	17.16	22.84	10.93	38
1498	OPRET2-MG345	345	19.66	13.53	20.66	11.41	20.88	13.93	21.55	11.48	40
1499	OPRET2-MG500	500	15.48	13.86	14.81	10.37	16.78	14.17	15.59	10.28	40
1500	PIMENT-MG345	345	18.93	11.76	12.9	6.01	19.15	11.73	12.97	5.99	25
1501	SJBICA-MG345	345	9.33	11.3	5.45	5.38	9.56	11.36	5.51	5.35	NA
1502	SGOTAR-MG345	345	11.21	18.97	11.11	14.53	11.38	19.35	11.23	14.62	40
1503	SGOTAR-MG500	500	14.57	14.51	11.01	8.67	15.18	14.65	11.25	8.61	50
1504	SGPARA-MG500	500	11.53	12.97	10.19	8.1	12.26	13.12	10.57	8	50
1505	SLAGO4-MG345	345	16.45	11.35	12.44	6.01	17.21	11.36	12.76	5.93	NA
1508	TAQUAR-MG345	345	19.34	11.48	17.62	8.92	20.65	11.71	18.36	8.88	24
1509	EMBORC-MG500	500	25.24	16.98	23.69	15.56	25.35	16.96	23.75	15.56	38
1510	IRAPE--MG345	345	4.58	18.17	5.53	19.95	4.59	18.15	5.54	19.93	25
1512	NPONTE-MG500	500	24.09	17.49	19.38	10.75	24.28	17.48	19.46	10.73	31.5
1515	TMARIA-MG345	345	10.31	12.29	9.91	12.56	10.36	12.29	9.94	12.55	50
1518	VESPA2-MG500	500	16.11	14.75	13.75	9.1	20.07	15.53	15.94	8.53	50
1519	VPALMA-MG345	345	11.68	13.19	10.55	10.45	11.93	13.43	10.74	10.45	50
1521	IRAPE--MG230	230	5.21	18.53	6.41	20.03	5.22	18.5	6.42	20.01	25
1523	PARACA-MG500	500	12.80	12.87	8.77	9.11	12.89	12.93	8.82	9.09	NA
1524	PIRAP2-MG345	345	17.39	21.45	18.08	16.19	18.30	23.96	19.59	18.46	NA
1525	PIRAP2-MG500	500	19.92	15.62	16.4	10.58	22.41	17.2	19.75	11.39	NA
1600	BRAUN2-MG230	230	8.80	6.86	8.07	7.59	8.87	6.81	8.11	7.56	NA
1609	JMONL4-MG230	230	8.38	6.39	5.63	4.73	8.52	6.35	5.67	4.71	NA
1610	SABAR3-MG230	230	10.94	7.71	8.12	5.42	11.19	7.68	8.21	5.39	NA
1612	BCOCA3-MG230	230	7.04	6.12	4.52	4.34	7.14	6.09	4.55	4.33	50
1613	JMOBLG-MG230	230	7.90	6.27	5.23	4.62	8.02	6.23	5.27	4.6	25
1616	CPENA--MG230	230	6.15	7.21	4.73	6.25	6.16	7.2	4.74	6.25	40
1619	GVALA2-MG230	230	13.62	10.14	12.94	9.47	13.66	10.11	12.97	9.45	NA
1620	ITABI4-MG230	230	21.29	12.86	19.8	8.75	22.20	12.96	20.34	8.68	NA
1623	IPATI1-MG230	230	22.92	12.96	24.5	11.57	23.43	12.97	24.88	11.54	23.9
1626	ITABI2-MG230	230	20.68	11.67	18.5	7.72	21.48	11.69	18.93	7.65	23.9
1630	MESQUI-MG230	230	24.55	15.52	27.03	14.71	25.14	15.61	27.51	14.74	40
1635	TAQUAR-MG230	230	19.31	13.69	18.84	11.84	20.13	14.01	19.37	11.92	NA
1637	AIMORE-MG230	230	7.14	11.75	8.39	13.7	7.14	11.73	8.39	13.68	31.5
1638	GUI.AM-MG230	230	9.39	7.02	8.51	6.72	9.49	6.97	8.56	6.68	NA
1640	PESTRE-MG230	230	9.07	6.96	8.2	7.56	9.14	6.91	8.24	7.53	NA
1645	BAGUAR-MG230	230	8.38	7.58	7.94	10.24	8.41	7.55	7.95	10.22	NA
1646	TIMOTE-MG230	230	12.37	7.39	10.48	6.93	12.51	7.35	10.54	6.9	NA
1650	JECEAB-MG345	345	14.81	10.66	12.26	5.78	15.27	10.69	12.46	5.73	NA

Identification			2024 with works (1,000 kV TL, 3 sections, 1 circuit, reference alternative)				2024 with works (1,000 kV TL, 4 sections, 1 and 2 circuits)				Circuit breaker (kA)
Number	Bus	Voltage	3Φ (kA)	X/R	1Φ (kA)	X/R	3Φ (kA)	X/R	1Φ (kA)	X/R	
2154	P.FIAL-MG345	345	5.74	10.73	4.61	9.18	5.79	10.75	4.63	9.18	NA
3562	MASCAR-ES230	230	6.83	10.81	7.43	10.77	6.83	10.79	7.43	10.76	31.5
3580	VERONA-ES230	230	2.49	5.97	2.2	6.15	2.49	5.96	2.2	6.14	NA
3605	B.BRAN-MG345	345	11.23	11.26	8.83	6.54	11.56	11.33	8.97	6.5	NA
3795	VIANA--ES345	345	13.01	13.17	12.85	11.94	13.08	13.18	12.89	11.94	40
3807	ITUTIN-MG345	345	14.44	10.25	11.59	8.39	14.55	10.22	11.63	8.37	25
3848	VIANA2-ES345	345	12.83	13.4	12.1	10.41	12.91	13.4	12.15	10.4	NA
3849	VIANA--ES500	500	7.37	16.69	6.39	12.68	7.41	16.71	6.41	12.68	NA
3860	ITUMBI-MG500	500	30.65	20.57	29.79	19.21	30.68	20.56	29.81	19.2	31.5
4300	LUZIAN-DF500	500	23.39	9.92	17.65	8.65	23.66	9.95	17.77	8.63	NA
4302	ESTREI-MG500	500	33.49	18.09	23.12	8.3	33.87	18.07	23.24	8.27	NA
4303	TRINDA-GO500	500	12.69	14.78	9.73	8.62	12.69	14.78	9.73	8.62	NA
11260	G.OURO-BA230	230	17.69	22.91	16.05	16.28	19.37	24.93	21.18	23.92	NA
11261	OUROLA-BA230	230	23.38	25.34	26.12	22.43	27.82	29.65	33.83	29.23	NA
11282	JUAZE3-PE230	230	20.24	15.46	23.71	15.6	24.12	17.04	30.45	18.07	NA
11394	IGAPO3-BA230	230	38.88	25.2	37.55	17.58	40.60	27.01	39.15	17.97	NA
11546	CMIRIM-RN500	500	18.07	16.18	16.19	10.17	18.20	15.71	16.19	10.07	NA
11560	G.OURO-BA500	500	13.87	14.97	11.09	10.67	14.81	15.64	13.43	13.9	NA
11561	OUROLA-BA500	500	18.18	19.2	15.71	12.46	22.43	20.07	19.6	13.6	NA
11565	AÇUIII-RN500	500	18.64	15.16	13.52	7.6	18.80	15.1	13.55	7.6	NA
11567	MILAG2-CE500	500	30.10	12.11	26.88	8.64	31.62	12.47	26.29	8.55	NA
11582	JUAZE3-BA500	500	18.60	13.46	15.53	11.16	20.14	14.45	17.09	12.23	NA
11594	IGAPO3-BA500	500	23.30	18.42	19.85	12.43	25.16	19.46	21.3	12.33	NA
11595	PINDA2-BA230	230	34.73	21.86	32.82	16.39	36.05	22.83	33.91	16.5	NA
12201	CNOVO2-PI230	230	24.60	21.93	22.06	14.5	27.56	24.67	31.37	24.3	NA
12321	JCAMR3-RN230	230	32.22	24.06	39.44	25.41	32.33	23.73	39.54	25.14	NA
26454	BETIM6-MG345	345	18.09	12.16	15.78	8.43	19.32	12.48	16.46	8.38	NA
26460	TIMOT2-MG230	230	12.94	7.56	10.96	6.87	13.09	7.52	11.03	6.84	NA
26461	SARZED-MG345	345	15.40	11.14	11.38	5.92	16.19	11.28	11.68	5.85	NA
26465	JUSCEL-MG500	500	17.47	15.64	12.75	8.34	17.91	15.91	12.99	8.28	NA
26470	JUSCEL-MG345	345	13.96	17.69	13.21	12.51	14.17	17.7	13.36	12.48	NA
26510	ITABI5-MG500	500	18.32	15.12	16.22	10.07	20.01	15.33	17.13	9.84	NA
26513	ITABI5-MG230	230	24.64	16.33	26.12	14.04	25.87	16.73	27.06	14.12	NA
38888	LINHAR-ES230	230	3.48	7.2	2.75	6.2	3.48	7.19	2.75	6.2	NA
38900	JANAU3-MG500	500	17.38	15.29	11.62	8.1	18.18	15.67	12.03	7.98	NA
38921	GVALA6-MG500	500	10.73	13.57	9.83	12.58	10.79	13.55	9.86	12.57	NA
38974	MUTUM--MG500	500	11.46	14.91	9.04	8.93	11.56	14.89	9.08	8.91	NA
38986	GVALA6-MG230	230	16.97	13.17	18.45	13.62	17.05	13.13	18.51	13.59	NA
39311	JNEIV2-ES345	345	9.44	11.61	8.28	9.5	9.50	11.63	8.31	9.5	NA
39313	R.N.S.-ES345	345	13.43	12.59	12.14	9.77	13.48	12.59	12.17	9.76	NA
39511	JNEIV2-ES500	500	6.08	14.51	5.02	10.58	6.13	14.52	5.04	10.57	NA
40700	VIGA---MG345	345	14.02	10.53	11.16	5.51	14.43	10.55	11.34	5.47	NA
41120	MIL-OUR-CAP	1,000	12.27	16.2	12.98	16.32	13.04	16.84	11.71	11.85	new
41121	OUR-MIL-CAP	1,000	14.43	14.38	9.14	6.41	29.30	8.29	15.20	4.61	new

Identification			2024 with works (1,000 kV TL, 3 sections, 1 circuit, reference alternative)				2024 with works (1,000 kV TL, 4 sections, 1 and 2 circuits)				Circuit breaker (kA)
Number	Bus	Voltage	3Φ (kA)	X/R	1Φ (kA)	X/R	3Φ (kA)	X/R	1Φ (kA)	X/R	
41220	MILAGR2-1000	1,000	9.62	21.35	9.24	20.64	10.56	21.02	8.92	14.21	new
41221	OUROLA3-1000	1,000	10.23	21.41	7.18	8.09	13.64	20.38	9.52	7.59	new
41222	IGAPOR4-1000	1,000	9.94	22.03	7.21	9.18	13.92	20.49	9.77	8.14	new
41224	PIRAPO2-1000	1,000	7.74	21.22	6.14	12.87	13.29	19.42	10.4	10.02	new
41225	OUROLA3--500	500	19.13	20.58	14.62	8.33	25.31	21.34	18.67	7.89	new
41226	IGAPOR4--500	500	22.42	18.57	16.66	8.5	24.88	20.23	19.01	8.94	new
41227	MILAGR3--500	500	29.41	12.76	32.73	12.75	31.06	13.28	28.24	9.78	new
41228	PIRAPO3--500	500	19.51	16.33	16.21	10.79	22.69	18.58	19.89	11.7	new
41321	OUR-IGA-CAP	1,000	14.29	14.47	9.19	6.34	47.16	4.5	17.9	3.74	new
41322	IGA-OUR-CAP	1,000	13.24	16.23	9.13	7.45	54.36	3.95	19.26	3.83	new
41330	OUR-IGA-CAP2	1,000	0.00	0	0	0	47.16	4.5	17.9	3.74	new
41331	IGA-OUR-CAP2	1,000	0.00	0	0	0	54.36	3.95	19.26	3.83	new
41523	IGA-PIR-CAP	1,000	16.25	12.97	10.01	6.63	60.43	3.62	19.61	3.77	new
41524	PIR-IGA-CAP	1,000	8.43	19.88	6.98	12.32	43.08	4.6	22.02	4.36	new
41530	IGA-PIR-CAP2	1,000	0.00	0	0	0	60.43	3.62	19.61	3.77	new
41531	PIR-IGA-CAP2	1,000	0.00	0	0	0	43.08	4.6	22.02	4.36	new
60000	S.LUZIA-500	500	11.33	4.51	15	4.89	12.63	5.04	14.98	5.35	new

8.2 Cost Evaluation

The cost evaluation was done for three alternatives. The first alternative consists of a 1,000 kV AC transmission system, with one circuit between Milagres and Ourolândia, and two circuits between Ourolândia and Ribeirão das Neves. The second alternative consists of a 500 kV AC transmission system, with two circuits between Milagres and Ourolândia, and five circuits between Ourolândia and Ribeirão das Neves. The fourth alternative is composed of two 4,000 MW at 800 kV DC, with the first being between Milagres and Ribeirão das Neves, and the second between Ourolândia and Ribeirão das Neves.

For the cost of the transmission lines, the following distances were adopted: 440 km between Milagres – Ourolândia, Ourolândia – Igaporã, Igaporã – Pirapora, and 300 km between Pirapora and Ribeirão das Neves.

The comparison of investments was performed using ANEEL's 2015 price bank, made available by Homologation Resolution # 758, of January 6, 2009, via the link: http://www.aneel.gov.br/cedoc/areh2009758.zip.

The weight values used as the same from the initial alternative.

8.2.1 Alternative 1 Expansion (1,000 kV)

The expansion of Alternative 1 is composed of:

- Construction of a new Ribeirão das Neves substation, distant 300 km from the Pirapora substation.
- Expansion of the reference alternative up to Ribeirão das Neves.
- An additional single circuit between Ourolândia and Ribeirão das Neves.
- Two additional transformers at Ourolândia.
- Three additional transformers at Ribeirão das Neves.

Figure 8.30, below, presents the single line diagram of the expansion of the reference alternative.

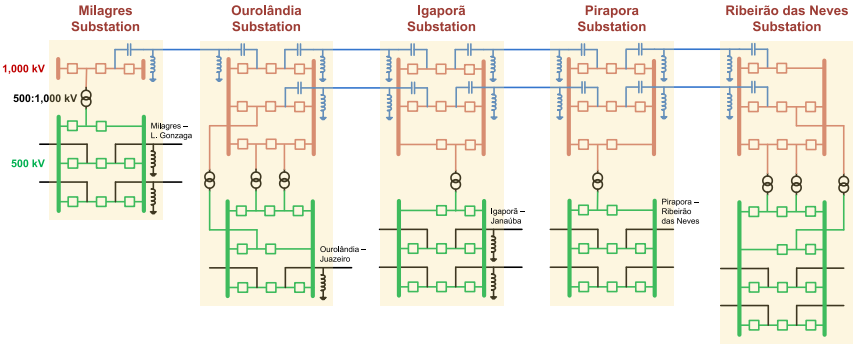

Figure 8.30: Expansion of the alternative at 1,000 kV AC

The system presented in Figure 8.30 is composed of new substations, one and a half circuit breaker, lines with 50% series compensation, 85% shunt compensation, with 8 x 795 MCM, 2,500 MVA transformers, with only the first substation with a 3,000 MVA transformer.

In all the substations, there is sectioning of the 500 kV lines existing (or already auctioned) in the region. At the Milagres substation, there is sectioning of two 500 kV lines between Milagres – Luiz Gonzaga; at Ourolândia, there is sectioning of one line between Ourolândia – Juazeiro; at Igaporã, there is sectioning of two lines between Igaporã – Janaúba; at Pirapora, there is sectioning of two lines between Pirapora – Ribeirão das Neves; and at Ribeirão das Neves, there is sectioning of two lines.

The costs include a single-phase line reactor and auto-transformer spare unit in each substation.

8.2.2 Alternative 2 Expansion (500 kV)

The expansion of Alternative 2 is composed of:

- Construction of a new Ribeirão das Neves substation, 300 km from the Pirapora substation.
- Expansion of the reference alternative up to Ribeirão das Neves.
- Three additional single circuits between Ourolândia and Ribeirão das Neves.

Figure 8.31, below, presents the single line diagram of the expansion of Alternative 2.

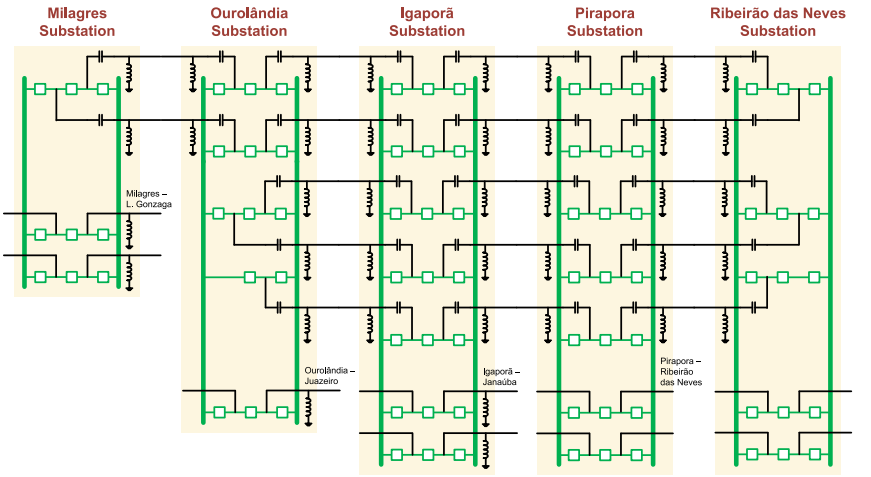

Figure 8.31: Expansion of the alternative at 500 kV AC

The system presented in Figure 8.31 is composed of new substations, one and a half circuit breaker, lines with 40% series compensation, 70% shunt compensation, with 6 x 795 MCM.

The costs include a single-phase line reactor spare unit in each substation.

8.2.3 DC Alternative

This alternative is composed of two 4,000 MW, ± 800 kV bipoles. The transmission lines are ± 800 kV (6 x 1,590 MCM). One of the lines is 1,620 km long, connecting Milagres to Ribeirão das Neves, and the other is 1.180 km long, connecting Ourolândia to Ribeirão das Neves.

The direct current transmission system at ±800 kV with two 4,000 MW bipoles is shown below.

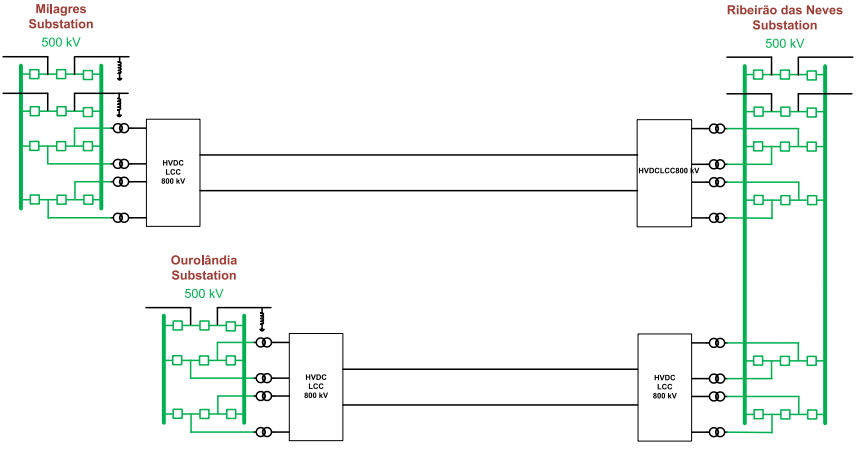

Figure 8.32: Alternative at ±800 kV DC.

The system presented in Figure 8.32 is composed of new substations, one and a half circuit breaker, lines with 6 x 1,590 MCM.

8.3 Results of the Cost Evaluation

The results of the cost evaluation for the three alternatives is presented in Table 8.4, below. The evaluation used the same values and assumptions of the evaluation of the investments.

Table 8.4: Comparison of investments

	R$		
Alternative	**1,000 kV CA**	**500 kV CA**	**2 800 kV bipoles**
Transmission lines	5,320,453,689.00	8,485,513,814.00	4,260,227,451.00
Transformers	707,887,749.00	0	0
Substations	3,797,843,670.00	2,955,858,458.00	407,976,468.00
Converters	0	0	5,399,999,999.00
Equipment subtotal	**9,826,185,108.00**	**11,441,372,272.00**	**10,068,203,918.00**
Losses in the lines	2,041,976,070.00	4,355,922,094.00	1,615,828,935.00
Losses in the transformers	312,507,015.00	0	0
Losses in the converters	0	0	911,232,002.00
Total	**12,180,668,193.00**	**15,797,294,366.00**	**12,595,264,855.00**
Relative comparison	1.00	1.30	1.03

We verify that the alternative at 1,000 kV AC presents the lowest cost. The alternative at DC presents the second lowest cost, and the 500 kV alternative presents the highest cost. The difference of investments between the 1,000 kV AC, and ±800 kV DC alternatives is lower in the expansion. However, we must highlight that the 1,000 kV AC alternative is the most adequate, considering the greater flexibility of implementation in different stages, considering the wind and photovoltaic generation increase. We must also mention that the expansion in stages was not used, since for this a transition date would have to be defined.

9. Conclusions and Recommendations

The main conclusions of this study are as follow:

1. The evaluations of power flow in steady state, during line energizations and forced load rejections, show that a level of 85% parallel compensation in the line is enough to maintain the voltages within the defined thresholds of 1.00 – 1.15 pu of the 1,000 kV system.
   The studies of load flow in emergency for lines and transformers for the year 2024 indicate that, for heavy loads, there was a need to add reactive support in the 500 kV grid, in the region of Minas Gerais. It

is worth highlighting that this ruling case contemplates the system with a requested generation increase of 5,500 MW (referring to the wind and solar potentials in the Northeast region), in addition to the scenario published by EPE.

The analyzed cases show that there is a power export potential of over 3,000 MW through a single circuit at 1,000 kV, from the Northeast to the Southeast, collecting the renewable power generation potential in the region. The connection at 1,000 kV in 4 substations in a single circuit has proven to be robust, meeting the n-1 criterion even for the section with the heaviest load.

2. In the scenarios analyzed, even with the significant increase of wind generation in the northeast region, the studies did not, in any of the cases, find any violation of the transient or sustained voltage levels in the electromechanical stability evaluations.

3. The short-circuit currents were evaluated for the main substations of the Basic Grid, for the year 2024, with the simulation of a case without the works proposed in the 1,000 kV alternative, and another one with the works proposed. No circuit breaker in the existing grid was surpassed after the entry in operation of the 1,000 kV, except for the Ipatinga 230 kV busbar (Minas Gerais), which presented a value slightly higher than that of the circuit breaker during single-phase short, a fact that also occurs without the presence of the 1,000 kV line.

4. For the economic evaluation, ANEEL's 2015 price bank was used, along with cost spreadsheets for transmission lines used in the *Transmitir* project, the unit costs of which were updated using ANEEL's price bank and other factors. The price bank does not contemplate 1,000 kV equipment, so the values for these devices were obtained by extrapolation of the values for the 500 kV and 750 kV equipment.

   Aiming at evaluating the reference alternative, comparisons were made to the following alternatives: 500 kV AC system with two circuits, DC system using VSC (*Voltage Sourced Converter*) in the multi-terminal configuration, and, finally, a conventional 4,000 MW DC system, as an illustrative cost reference. Table 9.1, below, presents a summary of the economic evaluation conducted in this study. We verify that the reference alternative (1,000 kV AC system) is the one that presents the lowest global cost, when compared to the other alternatives.

5. With regards to the socio-environmental studies, two studies were conducted, with the first being the corridor connecting, in a straight line, the substations of Milagres to Ourolândia, Ourolândia to Igaporã, and Igaporã to Pirapora. The second corridor was the one causing lower socio-environmental impact between the referred substations. The main conclusion with regards to the lower impact corridor (avoiding obstacles) is that the socio-environmental sensitivity is a result of the presence of indigenous lands, priority areas for conservation, existence of caves, remnants of vegetation, proximity to urban areas, settlements, and the crossing of large rivers (mainly the São Francisco River). Chapter 6 will complement and detail the socio-environmental studies initiated in this report to verify the socio-environmental sensitivity presented in this chapter.

6. Studies of the expansion of the reference alternative were conducted for two situations. The first includes an additional single circuit between Ourolândia e Ribeirão das Neves (Minas Gerais), where the increase inserted in the generation in the Northeast region was of 5,500 MW, and the second (expanded alternative) includes the addition of a second circuit in the sections from Ourolândia to Ribeirão das Neves, where the increase inserted in the generation in the Northeast region was of 11,000 MW (additional increase of 5,500 MW). The Ribeirão das Neves 1,000 kV substation does not exist in the reference alternative. Power flow studies were conducted for steady state and contingencies. The cases analyzed show that there is a power export potential of over 4,000 MW through the 1,000 kV, for the case with one circuit, and of up to 6,000 MW with the expanded alternative collecting the renewable power generation potential in the region. The 1,000 kV alternative proved to be robust in both cases, complying with the n-1 criterion. The studies did not verify, in any of the cases, any violation of the transient or sustained voltage levels in the electromechanical stability evaluations. The short-circuit currents were evaluated for the main substations of the Basic Grid, for the year 2024, and for the case of the expansion of the 1,000 kV line. None of the existing circuit breakers was surpassed after the entry in operation of the 1,000 kV system.

7. Regarding the comparison of investments, the initial system at 1,000 kV presented the lowest value when compared to the 500 kV and DC systems.

Table 9.1, below, presents the evaluation of the investments for the alternatives studied.

Table 9.1: Evaluation of the investments for the alternatives

	R$			
Alternative	**1,000 kV CA**	**500 kV CA**	**600 kV DC (VSC multi-terminal)**	**(800 kV DC LCC)**
Transmission lines	2,508,213,882.00	3,304,093,874.00	1,792,084,493.00	2,130,113,725.00
Transformers	355,203,316.00	0	0	0
Substations	1,828,713,550.00	1,265,774,415.00	407,976,468.00	258,720,012.00
Converters	0	0	3,504,599,350.00	2,700,000,000.00
Equipment subtotal	**4,692,130,748.00**	**4,569,868,290.00**	**5,704,660,311.00**	**5,088,833,737.00**
Losses in the lines	561,804,757.00	1,411,643,875.00	558,195,633.00	807,914,468.00
Losses in the transformers	145,569,312.00	0	0	0
Losses in the converters	0	0	364,492,801.00	455,616,001.00
Total	**5,399,504,818.00**	**5,981,512,165.00**	**6,627,348,744.00**	**6,352,364,205.00**
Relative comparison	1.00	1.11	1.23	1.18

The 1,000 kV AC transmission alternative contains the substations of Milagres, Ourolândia, Igaporã, and Pirapora. The line has a length of 1,320 km, divided in equal sections of 440 km each.

10. References

[1] EMPRESA DE PESQUISA ENERGÉTICA (EPE). *"Transmission Expansion Studies – N-SE and NE-SE Interconnection Expansions to Meet the Needs of Extreme Export Scenarios of the North and Northeast Regions – Initial Alternative Conception."* 2014.

[2] EMPRESA DE PESQUISA ENERGÉTICA (EPE). "*Transmission System Expansion Planning Studies – Excess Power Outflow from the North and Northeast Regions – Interconnection capacity increase requirements.*" 2015.

[3] EMPRESA DE PESQUISA ENERGÉTICA (EPE). "*Studies for Transmission Expansion Bidding, Technical & Economical Analysis of Alternatives: R1 Report, Study to Redirect the Wind Power Potential from the East Area of the Northeast Region.*" 2014.

[4] EMPRESA DE PESQUISA ENERGÉTICA (EPE). "*Studies for Transmission Expansion Bidding, Technical & Economical Analysis of Alternatives: R1 Report, Northeast-Southeast Interconnection Capacity Increase.*" 2014.

[5] EMPRESA DE PESQUISA ENERGÉTICA (EPE). "*Studies for Transmission Expansion Bidding, Study to Redirect the Wind Power Potential from the Central Region of Bahia*. 2014.

[6] EMPRESA DE PESQUISA ENERGÉTICA (EPE). "*Studies for Transmission Expansion Bidding, Technical & Economical Analysis of Alternatives: R1 Report, Study to Redirect the Wind and Photovoltaic Power Potential from the Seridó Region*," 2016.

[7] AGÊNCIA NACIONAL DE ÁGUAS (ANA), 2006. *Atlas Nordeste de Abastecimento Urbano de Água.* Available at: <http://www.ana.gov.br/bibliotecavirtual/arquivos/20061213161802_atlas.pdf> Accessed on: 7/11/2016.

[8] AHP. Available at: <http://ppegeo.igc.usp.br/scielo.php?pid=S010190822009000400006&script=sci_arttext&tlng=es>. Accessed on: 04/01/2015.

[9] AGÊNCIA NACIONAL DE ENERGIA ELÉTRICA (ANEEL). 2013. *Technical Note n. 0203/2013-SCT-SRT/ANEEL*. Available at: <http://www.aneel.gov.br/aplicacoes/audiencia/arquivo/2013/081/documento/nt_n%C2%BA_203_sct_e_srt.pdf> Accessed on: 12/18/2015n%C2%BA_203_sct_e_srt.pdf>Accessed on: 12/18/2015

[10] BRAZIL. Ministry of Mines and Energy. Secretaria Geral. Projeto RADAMBRASIL: *Sheet SD. 24 Salvador*. Rio de Janeiro, 1981. 620 p. (Levantamento de Recursos Naturais, v. 24).

[11] BRAZIL. Ministry of Mines and Energy. Secretaria Geral. Projeto RADAMBRASIL: *Sheet SA. 23 São Luis and part of Folha SA. 24 Fortaleza*. Rio de Janeiro, 1973. 331 p. (Levantamento de Recursos Naturais, v. 3).

[12] CASTRO, A.S.; CAVALCANTE, A. *Flores da caatinga*. Campina Grande: Instituto Nacional do Semiárido, 2010. 116p.

[13] COFINS. *Desenvolvimento rural do semiárido brasileiro: Transformações recentes, desafios e perspectivas*. 2013. Available at: <https://confins.revues.org/8633>. Accessed on: 07/11/2016.

[14] FUNDAÇÃO NACIONAL DO ÍNDIO (FUNAI). *Dados de Terras indígenas*. Available at: <www.funai.gov.br/index.php/shape>. Accessed on: 12/14/2015.

[15] INSTITUTO BRASILEIRO DE GEOGRAFIA E ESTATÍSTICA (IBGE). 2012. *Dados de uso do solo e cobertura vegetal*. Available at: <www.ibge.gov.br/home/geociencias/recursosnaturais>. Accessed on: 12/15/2015.

[16] INSTITUTO BRASILEIRO DE GEOGRAFIA E ESTATÍSTICA (IBGE). *Hidrografia*. Available at: <www.ibge.gov.br/home/geociencias/recursosnaturais>. Accessed on: 12/15/2015.

[17] INSTITUTO BRASILEIRO DE GEOGRAFIA E ESTATÍSTICA (IBGE). *Rodovias*. Available at: <www.ibge.gov.br/home/geociencias/recursosnaturais>. Accessed on: 12/15/2015.

[18] INSTITUTO BRASILEIRO DE GEOGRAFIA E ESTATÍSTICA (IBGE). *Manual técnico da vegetação brasileira*. 2nd. ed. (rev. and enhanced). Rio de Janeiro: Manuais Técnicos em Geociências, number 1, 2012. 275p.

[19] INSTITUTO CHICO MENDES DE BIODIVERSIDADE (ICMBio). *Unidades de conservação*. Available at: <http://www.icmbio.gov.br/portal/biodiversidade/unidades-deconservacao/grupos.html and http://www.florestal.gov.br/snif/recursos-florestais/sistema-nacional-de-unidadesdeconservacao?print=1&tmpl=component>. Accessed on: 12/14/2015.

[20] INSTITUTO CHICO MENDES DE BIODIVERSIDADE (ICMBio). *Unidades de conservação*. Available at: <http://www.icmbio.gov.br/portal/biodiversidade/unidades-de-conservacao/grupos.html> and <http://www.florestal.gov.br/snif/recursos-florestais/sistema-nacional-de-unidades-de-conservacao?print=1&tmpl=component>. Accessed on: 12/12/2015.

[21] INSTITUTO CHICO MENDES DE BIODIVERSIDADE (ICMBio); CENTRO NACIONAL DE PESQUISA E CONSERVAÇÃO DE CAVERNAS (CECAV). *Dados de cavernas*. Available at: <www.icmbio.gov.br/cecav/downloads/mapas.html>. Accessed on: 12/14/2015.

[22] INSTITUTO NACIONAL DE COLONIZAÇÃO E REFORMA AGRÁRIA (INCRA). *Dados de assentamentos*. Available at: <acervofundiario.incra.gov.br>. Accessed on: 12/14/2015.

[23] INSTITUTO NACIONAL DE METEREOLOGIA (INMET). *Normas Climatológicas do Brasil 1961-1990*. Available at: <http://www.inmet.gov.br/portal/index.php?r=clima/normaisClimatologicas>. Accessed on: 12/11/2016.

[24] INSTITUTO NACIONAL DE PESQUISAS ESPACIAIS (INPE). *Infográfico – Densidade de raios no Brasil*. Available at: <http://www.inpe.br/webelat/homepage/menu/infor/infografico.-.densidade.de.raios.no.brasil.php>. Accessed on: 07/11/2016.

[25] LUZ, S.; SELLITTO, M. ; GOMES, L. *Medição de desempenho ambiental baseada em método multicriterial de apoio à decisão: estudo de caso na indústria automotiva*. Gestão & Produção, v.13, n.3, p.557-570, 2006.

[26] MINISTÉRIO DO MEIO AMBIENTE (MMA). *Dados de desmatamento do Projeto de Monitoramento do Desmatamento dos Biomas Brasileiros por Satélite (PMDBBS), 2008*. Available at: <mapas.mma.gov.br/i3geo/datadownload.htm>. Accessed on: 12/18/2015.

[27] MINISTÉRIO DO MEIO AMBIENTE (MMA). *Mapas de Cobertura Vegetal dos Biomas Brasileiros*. Probio, 2007. Available at: <mapas.mma.gov.br/mapas/aplic/probio/datadownload.htm>. Accessed on: 12/14/2015.

[28] MINISTÉRIO DO MEIO AMBIENTE (MMA). *Sítios arqueológicos*. Available at: <mapas.mma.gov.br/i3geo/datadownload.htm>. Accessed on: 12/15/2015.

[29] MINISTÉRIO DOS TRANSPORTES (MT). *Dados de Ferrovias do Plano Nacional de Logística e Transportes (PNLT), 2010*. Available at: <http://www.transportes.gov.br/conteudo/61-relatorios/2822-base-de-dadosgeorreferenciados-pnlt-2010.html>. Accessed on: 12/14/2015.

[30] SAATY, T.L. *Axiomatic foundation of the analytic hierarchy process*. Management Science, v. 32, n.7, p. 841-855, July 1987.

[31] SUDENE. *Semiárido*. Available at: <http://www.sudene.gov.br/acessoainforma%C3%A7%C3%A3o/instituconal/area-de-atuacao-dasudene/semiarido>. Accessed on: 12/11/2016.

[32] 4500083056 – NT 15-R0 – *Torre Monomastro*. São Paulo, 2016.

[33] 4500083056 – NT 13-R0 – *Torre Autoportante*. São Paulo, 2016.

[34] JARDINI, J.A; e *et.al.*, *Alternativas não Convencionais para a Transmissão de Energia Elétrica* – Estudos Técnicos e Econômicos, Brasília, DF: Ed. Goya, 2012.

[35] TECHNICAL BROCHURE 388, Joint Working Group B2/B4/C1.17, TB 388 - *Impacts of HVDC Line on the Economics of HVDC Projects*, CIGRÉ, 2009.

ATTACHMENT – Detailing of the Costing of the Transmission Lines

This attachment presents the tables with the costing of the lines for the alternatives studied.

a) 1,000 kV AC Line

- Span: 500 m
- 80% of guyed towers (28,641 kg) and 20% self-supporting towers (46,145 kg)

				Value	Unit	Quantity	Unit	Total (R$)
Direct costs								
3.1,1	Basic direct costs							
	3.1.1.1		Land and rights-of-way	53,857.40	R$/km	1,320.00	km	71,091,768.00
	3.1.1.2		Materials Procurement					
		A)	Frameworks					
			• Steel frameworks	5.90	R$/kg	84,853,824.00	kg	500,637,561.60
		B)	Cables and hardware for framework purposes					
		C)	Guying	17.70	R$/kg	494,208.00	kg	8,747,481.60
		D)	Foundations					
			• Anchor rods/Guys	35.38	R$/km	1,320.00	km	46,701.60
		E)	Conductor cable (8 x 795 MCM)	15.24	R$/kg	42,324,480.00	kg	645,025,075.20
		F)	Conventional ground wire	7.61	R$/kg	567,600.00	kg	4,319,436.00
		G)	Optical ground wire	13,160.00	R$/km	1,320.00	km	17,371,200.00
		H)	Insulators	260.39	R$/unit	607,200.00	unit	158,108,808.00
		I)	Hardware and accessories					
			• Conductor cable Suspension set	4,309.06	R$/unit	8,976.00	unit	38,678,122.56
			• Conductor cable Anchoring set	8,768.06	R$/unit	1,306.80	unit	11,458,100.81
			• Conductor cable Jumper set	2,763.98	R$/unit	646.80	unit	1,787,742.26

				Value	Unit	Quantity	Unit	Total (R$)
		• Ground wire Suspension set		63.65	R$/unit	2,996.40	unit	190,720.86
		• Ground wire Anchoring set		24.86	R$/unit	514.80	unit	12,797.93
		• Conductor cable Dampers		144.21	R$/unit	118,351.20	unit	17,067,426.55
		• Ground wire Dampers		21.24	R$/unit	6,600.00	unit	140,184.00
		• Conductor Spacers		615.87	R$/unit	118,351.20	unit	72,888,953.54
	J)	Grounding		2,982.69	R$/km	1,320.00	km	3,937,150.80
	K)	Other accessories	**0.3%** over Materials Procurement (A-J)					4,441,252.39
3.1.1.3		Inspection of Materials	**1%** over Materials Procurement (3.1.1.2)					14,804,174.63
3.1.1.4		Construction Site	**1%** over Materials Procurement (3.1.1.2)					14,804,174.63
3.1.1.5		Construction						
	A)	Clearing of the right-of-way		0.33	R$/m²	125,400,000.00	m²	41,382,000.00
	B)	Building of Foundations						
		• Excavation		64.29	R$/m³	182,307.84	m³	11,720,571.03
		• Concreting		2,637.72	R$/m³	117,216.00	m³	309,182,987.52
	C)	Framework Assembly						
		• Concrete	**40%** over the acquisition of concrete frameworks					
		• Self-supporting Steel	**20%** over the acquisition of Steel frameworks					136,173,416.76
	D)	Conductor cable Installation	**15%** over the acquisition of the Conductor cable					96,753,761.28
	E)	Installation of Conventional ground wire	**50%** over the acquisition of the Conventional ground wire					2,159,718.00
	F)	Installation of Optical ground wire	**25%** over the acquisition of the Optical ground wire					4,342,800.00

					Value	Unit	Quantity	Unit	Total (R$)
		G)	Grounding Installation	**100%** over the acquisition of the materials used in the Grounding					3,937,150.80
		H)	Building of accesses		6,249.21	R$/km	1,320.00	km	8,248,957.20
	3.1.1.6		Technical Services						
		A)	Topography Services		4,242.00	R$/km	1,320.00	km	5,599,440.00
		B)	Geology/Survey Services		5,128.17	R$/km	1,320.00	km	6,769,184.40
3.1.2	Engineering Studies								
	3.1.2.1		Basic Project	**1%** over the Basic direct costs (3.1.1)					22,118,288.20
	3.1.2.2		Executive Design	**2%** over the Basic direct costs (3.1.1)					44,236,576.40
3.1.3	Environmental Costs			**3%** over the Basic direct costs (3.1.1)					66,354,864.60
3.1.4	Local Management			**2%** over the Basic direct costs (3.1.1)					44,236,576.40
Indirect costs									
3.2.1	Central Management			**2%** over the Direct costs (3.1)					47,775,502.51
Occasional				**3%** over the Direct costs (3.1)					71,663,253.77
							Total		**2,508,213,882**

Cost per km of the 1,000 kV line: R$ 1,900,162.03/km

b) 500 kV AC Line

- Span: 500 m
- 80% of guyed towers (11,500 kg) and 20% self-supporting towers (15,900 kg)

				Value	Unit	Quantity	Unit	Total (R$)
Direct costs								
3.1.1	Basic direct costs							
	3.1.1.1		Land and rights-of-way	34,015.20	R$/km	1,320.00	km	44,900,064
	3.1.1.2		Materials Procurement					
		A)	Frameworks					
			• Steel frameworks	5.90	R$/kg	32,683,200.00	kg	192,830,880
		D)	Foundations					
			• Grid Foundation	R$		Quantity		
			• Anchor rods/Guys	35.38	R$/km	1,320.00	km	46,702
		E)	Conductor cable (6 x 795 MCM)	15.24	R$/kg	31,743,360.00	kg	483,768,806
		F)	Conventional ground wire	7.61	R$/kg	567,600.00	kg	4,319,436
		G)	Optical ground wire	13,160.00	R$/km	1,320.00	km	17,371,200
		H)	Insulators	260.39	R$/unit	196,270.80	unit	51,106,954
		I)	Hardware and accessories					
			• Conductor cable Suspension set	5,164.33	R$/unit	8,672.40	unit	44,787,135
			• Conductor cable Anchoring set	8,951.30	R$/unit	653.40	unit	5,848,779
			• Conductor cable Jumper set	1,525.47	R$/unit	277.20	unit	422,861
			• Ground wire Suspension set	63.65	R$/unit	2,996.40	unit	190,721
			• Ground wire Anchoring set	24.86	R$/unit	514.80	unit	12,798
			• Conductor cable Dampers	144.21	R$/unit	118,351.20	unit	17,067,427
			• Ground wire Dampers	21.24	R$/unit	6,600.00	unit	140,184
			• Conductor Spacers	629.06	R$/unit	81,180.00	unit	51,066,685

				Value	Unit	Quantity	Unit	Total (R$)
	J)	Grounding		2,982.69	R$/km	1,320.00	km	3,937,151
	K)	Other accessories	**0.3%** over Materials Procurement (A-J)					2,618,753
3.1.1.3		Inspection of Materials	**1%** over Materials Procurement (3.1.1.2)					8,729,177
3.1.1.4		Construction Site	**1%** over Materials Procurement (3.1.1.2)					8,729,177
3.1.1.5		Construction						
	A)	Clearing of the right-of-way		0.33	R$/m²	125,400,000.00	m²	41,382,000
	B)	Building of Foundations						
		• Excavation		64.29	R$/m³	182,307.84	m³	11,720,571
		• Concreting		2,637.72	R$/m³	117,216.00	m³	309,182,988
	C)	Framework Assembly						
		• Concrete	**40%** over the acquisition of concrete frameworks					
		• Self-supporting Steel	**20%** over the acquisition of Steel frameworks					
		• Guyed Steel	**27.5%** over the acquisition of Steel frameworks					53,028,492
	D)	Conductor cable Installation	**15%** over the acquisition of the Conductor cable					72,565,321
	E)	Installation of Conventional ground wire	**50%** over the acquisition of the Conventional ground wire					2,159,718
	F)	Installation of Optical ground wire	**25%** over the acquisition of the Optical ground wire					4,342,800
	G)	Grounding Installation	**100%** over the acquisition of the materials used in the Grounding					3,937,151
	H)	Building of accesses		6,249.21	R$/km	1,320.00	km	8,248,957

				Value	Unit	Quantity	Unit	Total (R$)
	3.1.1.6	Technical Services						
		A) Topography Services		4,242.00	R$/km	1,320.00	km	5,599,440
		B) Geology/Survey Services		5,128.17	R$/km	1,320.00	km	6,769,184
3.1.2	Engineering Studies							
	3.1.2.1	Basic Project	**1%** over the Basic direct costs (3.1.1)					14,568,315
	3.1.2.2	Executive Design	**2%** over the Basic direct costs (3.1.1)					29,136,630
3.1.3	Environmental Costs		**3%** over the Basic direct costs (3.1.1)					43,704,945
3.1.4	Local Management		**2%** over the Basic direct costs (3.1.1)					29,136,630
Indirect costs								
3.2.1	Central Management		**2%** over the Direct costs (3.1)					31,467,561
Occasional			**3%** over the Direct costs (3.1)					47,201,341
						Total		**1,652,046,935**

Cost per km of the 500 kV AC line: R$ 1,251,550.71/km

c) 600 kV DC Line

- Span: 500 m
- 80% of guyed towers (18,500 kg) and 20% self-supporting towers (32,325 kg)

				Value	Unit	Quantity	Unit	Total (R$)
Direct costs								
3.1.1	Basic direct costs							
	3.1.1.1		Land and rights-of-way	40,818.24	R$/km	1,320.00	km	53,880,076.80
	3.1.1.2		Materials Procurement					
		A)	Frameworks	R$		Quantity		
			• Steel frameworks	5.90	R$/kg	56,139,600.00	kg	331,223,640.00
		B)	Cables and hardware for framework purposes					
		C)	Guying	17.70	R$/kg	3,459,456.00	kg	61,232,371.20
		D)	Foundations					
			• Anchor rods/Guys	35.38	R$/km	1,320.00	km	46,701.60
		E)	Conductor cable (4 x 2300 MCM)	15.24	R$/kg	39,716,160.00	kg	605,274,278.40
		F)	Conventional ground wire	7.61	R$/kg	567,600.00	kg	4,319,436.00
		G)	Optical ground wire	18,500.00	R$/km	1,320.00	km	24,420,000.00
		H)	Insulators	229.24	R$/unit	551,760.00	unit	126,484,910.64
		I)	Hardware and accessories					
			• Conductor cable Suspension set	3,442.89	R$/unit	6,164.40	unit	21,223,351.12
			• Conductor cable Anchoring set	5,330.87	R$/unit	105.60	unit	562,939.87
			• Conductor cable Jumper set	1,905.15	R$/unit	52.80	unit	100,591.92
			• Ground wire Suspension set	63.65	R$/unit	2,996.40	unit	190,720.86
			• Ground wire Anchoring set	24.86	R$/unit	514.80	unit	12,797.93
			• Conductor cable Dampers	255.40	R$/unit	33,752.40	unit	8,620,362.96
			• Ground wire Dampers	21.24	R$/unit	6,600.00	unit	140,184.00
			• Conductor Spacers	25.57	R$/unit	457,248.00	unit	11,691,831.36

				Value	Unit	Quantity	Unit	Total (R$)
	J)	Grounding		2,982.69	R$/km	1,320.00	km	3,937,150.80
	K)	Other accessories	**0.3%** over Materials Procurement (A-J)					3,598,443.81
3.1.1.3		Inspection of Materials	**1%** over Materials Procurement (3.1.1.2)					11,994,812.69
3.1.1.4		Construction Site	**1%** over Materials Procurement (3.1.1.2)					11,994,812.69
3.1.1.5		Construction						
	A)	Clearing of the right-of-way		0.33	R$/m²	95,040,000.00	m²	31,363,200.00
	B)	Building of Foundations						
		Excavation		64.29	R$/m³	41,124.60	m³	2,643,900.28
		Concreting		2,637.72	R$/m³	21,092.52	m³	55,636,169.03
	C)	Framework Assembly						
		• Concrete	**40%** over the acquisition of concrete frameworks					
		• Self-supporting Steel	**20%** over the acquisition of Steel frameworks					86,118,146.40
		• Guyed Steel	**27.5%** over the acquisition of Steel frameworks					
	D)	Conductor cable Installation	**15%** over the acquisition of the Conductor cable					90,791,141.76
	E)	Installation of Conventional ground wire	**50%** over the acquisition of the Conventional ground wire					2,159,718.00
	F)	Installation of Optical ground wire	**25%** over the acquisition of the Optical ground wire					6,105,000.00
	G)	Grounding Installation	**100%** over the acquisition of the materials used in the Grounding					3,937,150.80
	H)	Building of accesses		6,249.21	R$/km	1,320.00	km	8,248,957.20

				Value	Unit	Quantity	Unit	Total (R$)
	3.1.1.6	Technical Services						
		A) Topography Services		4,242.00	R$/km	1,320.00	km	5,599,440.00
		B) Geology/Survey Services		5,128.17	R$/km	1,320.00	km	6,769,184.40
3.1.2	Engineering Studies							
	3.1.2.1	Basic Project	**1%** over the Basic direct costs (3.1.1)					15,803,214.23
	3.1.2.2	Executive Design	**2%** over the Basic direct costs (3.1.1)					31,606,428.45
3.1.3	Environmental Costs		**3%** over the Basic direct costs (3.1.1)					47,409,642.68
3.1.4	Local Management		**2%** over the Basic direct costs (3.1.1)					31,606,428.45
Indirect costs								
3.2.1	Central Management		**2%** over the Direct costs (3.1)					34,134,942.73
Occasional			**3%** over the Direct costs (3.1)					51,202,414.09
						Total		**1,792,084,493**

Cost per km of the 600 kV DC line: R$ 1,357,639.77/km

d) 800 kV DC Line

- Span: 500 m
- 80% of guyed towers (18,500 kg) and 20% self-supporting towers (32,325 kg)

				Value	Unit	Quantity	Unit	Total (R$)
Direct costs								
3.1.1	Basic direct costs							
	3.1.1.1		Land and rights-of-way	49,888.96	R$/km	1,400.00	km	69,844,544.00
	3.1.1.2		Materials Procurement					
		A)	Frameworks					
			• Steel frameworks	5.90	R$/kg	59,542,000.00	kg	351,297,800.00
			• Concrete frameworks					
		B)	Cables and hardware for framework purposes					
		C)	Guying	17.70	R$/kg	524,160.00	kg	9,277,632.00
		D)	Foundations					
			Grid Foundation					
			Anchor rods/Guys	35.38	R$/km	1,400.00	km	49,532.00
		E)	Conductor cable (6 x 1590 MCM)	15.24	R$/kg	44,872,800.00	kg	683,861,472.00
		F)	Conventional ground wire	7.61	R$/kg	602,000.00	kg	4,581,220.00
		G)	Optical ground wire	18,500.00	R$/km	1,400.00	km	25,900,000.00
		H)	Insulators	229.24	R$/unit	585,200.00	unit	134,150,662.80
		I)	Hardware and accessories					
			• Conductor cable Suspension set	4,687.67	R$/unit	9,800.00	unit	45,939,166.00
			• Conductor cable Anchoring set	7,258.20	R$/unit	154.00	unit	1,117,762.80
			• Conductor cable Jumper set	2,594.00	R$/unit	70.00	unit	181,580.00
			• Ground wire Suspension set	63.65	R$/unit	3,178.00	unit	202,279.70
			• Ground wire Anchoring set	24.86	R$/unit	546.00	unit	13,573.56

				Value	Unit	Quantity	Unit	Total (R$)
	• Conductor cable Dampers			618.74	R$/unit	49,000.00	unit	30,318,260.00
	• Ground wire Dampers			21.24	R$/unit	7,000.00	unit	148,680.00
	• Conductor Spacers			35.00	R$/unit	866,236.00	unit	30,318,260.00
	J) Grounding			2,982.69	R$/km	1,400.00	km	4,175,766.00
	K) Other accessories		**0.3%** over Materials Procurement (A-J)					3,964,600.94
3.1.1.3	Inspection of Materials		**1%** over Materials Procurement (3.1.1.2)					13,215,336.47
3.1.1.4	Construction Site		**1%** over Materials Procurement (3.1.1.2)					13,215,336.47
3.1.1.5	Construction							
	A) Clearing of the right-of-way			0.33	R$/m²	123,200,000.00	m²	40,656,000.00
	B) Building of Foundations							
	• Excavation			64.29	R$/m³	99,342.62	m3	6,386,737.20
	• Assembly of grids							
	• Installation of Rods/Guys							
	• Concreting			2,637.72	R$/m³	68,568.99	m³	180,865,806.48
	C) Framework Assembly							
	• Concrete		**40%** over the acquisition of concrete frameworks					
	• Self-supporting Steel		**20%** over the acquisition of Steel frameworks					91,337,428.00
	• Guyed Steel		**27.5%** over the acquisition of Steel frameworks					
	D) Conductor cable Installation		**15%** over the acquisition of the Conductor cable					102,579,220.80
	E) Installation of Conventional ground wire		**50%** over the acquisition of the Conventional ground wire					2,290,610.00
	F) Installation of Optical ground wire		**25%** over the acquisition of the Optical ground wire					6,475,000.00

					Value	Unit	Quantity	Unit	Total (R$)
		G)	Grounding Installation	**100%** over the acquisition of the materials used in the Grounding					4,175,766.00
		H)	Building of accesses		6,249.21	R$/km	1,400.00	km	8,748,894.00
	3.1.1.6		Technical Services						
		A)	Topography Services		4,242.00	R$/km	1,400.00	km	5,938,800.00
		B)	Geology/Survey Services		5,128.17	R$/km	1,400.00	km	7,179,438.00
3.1.2	Engineering Studies								
	3.1.2.1		Basic Project	**1%** over the Basic direct costs (3.1.1)					18,784,071.65
	3.1.2.2		Executive Design	**2%** over the Basic direct costs (3.1.1)					37,568,143.30
3.1.3	Environmental Costs			**3%** over the Basic direct costs (3.1.1)					56,352,214.96
3.1.4	Local Management			**2%** over the Basic direct costs (3.1.1)					37,568,143.30
Indirect costs									
3.2.1	Central Management			**2%** over the Direct costs (3.1)					40,573,594.77
Occasional				**3%** over the Direct costs (3.1)					60,860,392.15
							Total		**2,130,113,725**

Cost per km of the 800 kV DC line: R$ 1,521,509.80/km

CHAPTER 5

Detailed Studies of the Reference Alternative (R2)

José Antonio Jardini
Gerson Yukio Saiki
Ricardo Leon Vasquez Arnez
Marcos Thiago Bassini
Valdomiro Vega García
Felipe Rocha Velloso de Almeida Pedroso
Adriano Dellallibera
Huedesson Botura
Eber Havila Rose

1. Introduction

This project was dedicated to the technical, economic and socio-environmental feasibility studies of alternatives for the transmission of wind and photovoltaic power from the Northeastern to the Southeastern region of Brazil. The alternative selected (reference) is a 1,000 kV AC transmission system.

The reference alternative is composed of four new substations: Milagres III (Ceará), Ourolândia III (Bahia), Igaporã IV (Bahia), and Pirapora III (Minas Gerais). The transmission line is composed of three sections of 440 km, totaling 1,320 km. Figure 1.1 presents the location of the reference alternative.

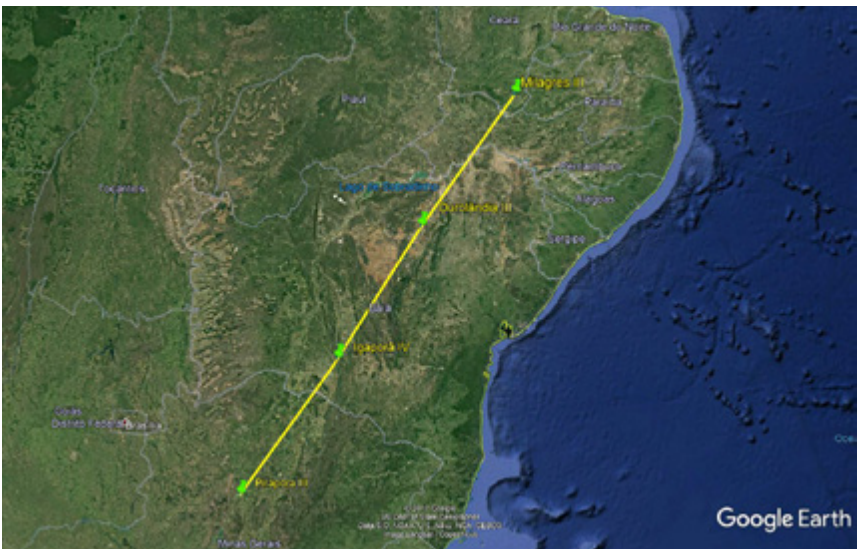

Figure 1.1: Path of the reference alternative – 1,000 kV AC

In this chapter, the objective is to present details of the studies (i.e. steady-state, electromechanical and electromagnetic transients) of the reference alternative. It also presents the studies for the line design, and the definition of equipment requirements. An analysis was also made of a "possible expansion" of the reference alternative, which consists of adding one more section from the Pirapora substation up to the Ribeirão das Neves substation, plus the addition of another single circuit to the last two previous sections (reference alternative) including the added section.

2. Description of the 1,000 kV Transmission Alternative

For the insertion of the 1,000 kV transmission alternative into the Brazilian Interconnected Power System (SIN), it was necessary to choose the region for the location of each of the substations, and define the sectioning of the existing and/or future 500 kV lines in the region.

The 1,000/500 kV substations are all new, so they are not expansions of existing substations. Their locations were chosen so as to maintain equal extensions in each section of the line (440 km).

Sections with equal lengths were chosen aiming at a similarity in terms of equipment requirements. Next, the location of the substations and the lines that need to be sectioned, are presented.

2.1 Milagres III Substation

At the region of the Milagres substation location, there are eight 500 kV lines:

- 2 to Luiz Gonzaga;
- 1 to Queimada Nova;
- 2 to Curral Novo do Piauí;
- 1 to Quixadá; and
- 2 to Açú.

The location was chosen to the southeast of the already existing Milagres substation (Figure 2.1). Thus, the two lines from Milagres to Luiz Gonzaga will be sectioned. In each line, there is a reactor that needs to be moved because of the construction of the new substation.

Figure 2.1: Region of the location of the Milagres III substation

2.2 Ourolândia III Substation

At the region of the Ourolândia substation, there are three 500 kV lines:

- 1 to Morro do Chapéu;
- 1 to Juazeiro; and
- 1 to Gentio do Ouro.

The location was chosen to the Northeast of the already existing Ourolândia substation (Figure 2.2). Thus, the line from Ourolândia to Juazeiro will be sectioned. There is a line reactor that needs to be moved because of the construction of the new substation.

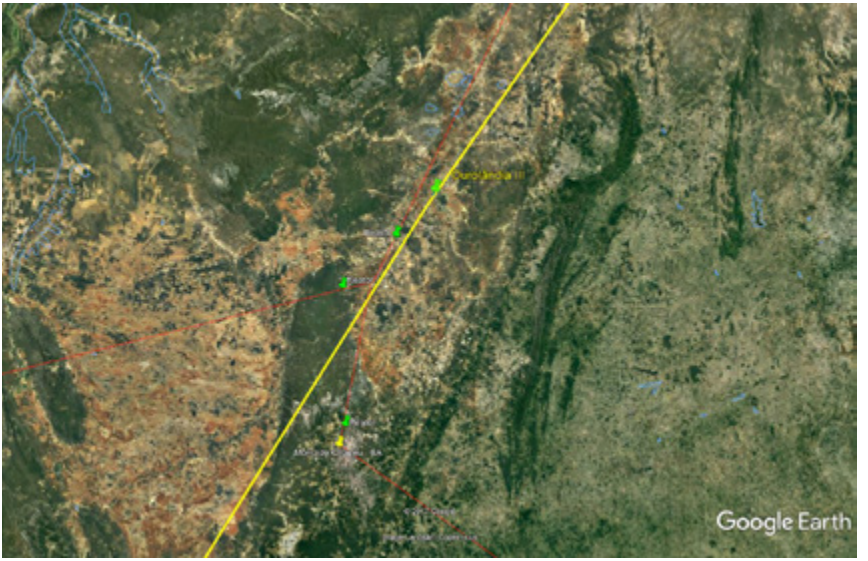

Figure 2.2: Region of the location of the Ourolândia III substation

2.3 Igaporã IV Substation

At the region of the Igaporã substation, there are six 500 kV lines:

- 2 to Bom Jesus da Lapa;
- 2 to Ibicoara; and
- 2 to Janaúba.

The location was chosen to south of the already existing Igaporã substation (Figure 2.3). Thus, the two lines from Igaporã to Janaúba will be sectioned. There is one reactor in each line that needs to be moved because of the construction of the new substation.

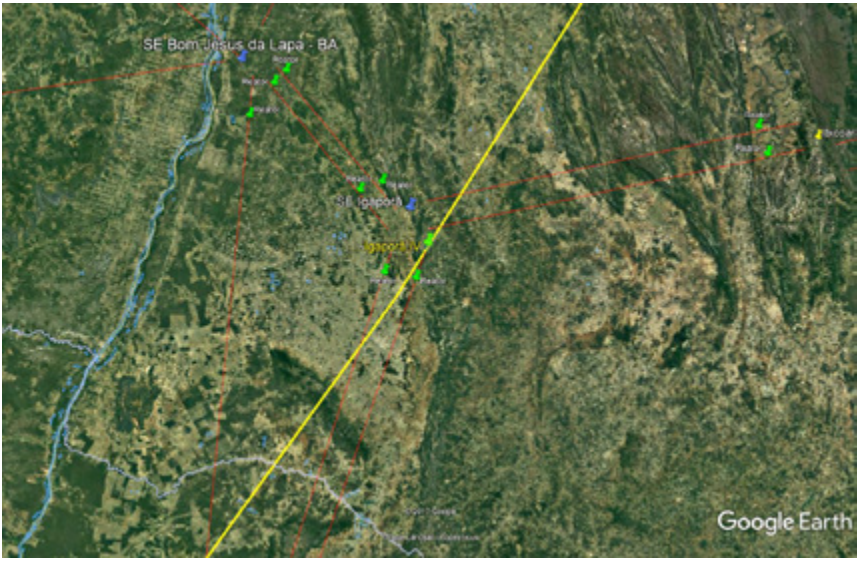

Figure 2.3: Region of the location of the Igaporã IV substation

2.4 Pirapora III Substation

At the region of the Pirapora substation, there are six 500 kV lines:

- 1 to Janaúba;
- 1 to Arinos;
- 1 to Luziânia;
- 1 to Paracatu; and
- 2 to Ribeirão das Neves.

The location was chosen to South of the already existing Pirapora substation (Figure 2.4). Thus, the two lines to Ribeirão das Neves will be sectioned. In this case, there are no line reactors that need to be moved.

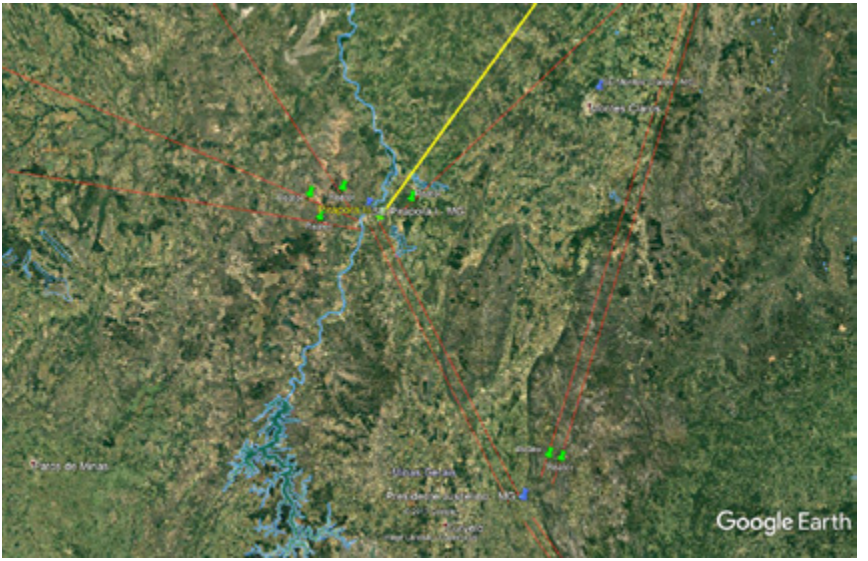

Figure 2.4: Region of the location of the Pirapora III substation

3. Geometry of the 1,000 kV Transmission Line Towers

The transmission system is composed of lines with 8 conductors per phase, ACSR 795 MCM (*Tern*), 50% series compensation, and 85% shunt compensation, 1 3/8" EHS ground wire, and one OPGW ground wire.

The height of the conductors and ground wires used for the studies are:

- external phases: 47.9 m (sag of 22 m);
- internal phases: 65.9 m (sag of 22 m);
- Ground wires: 76.6 m (sag of 17.6 m).

These values were confirmed by means of the electrical design of the line, presented later in this document.

Figure 3.1 presents the distances of the cables used for calculation of the transmission line parameters.

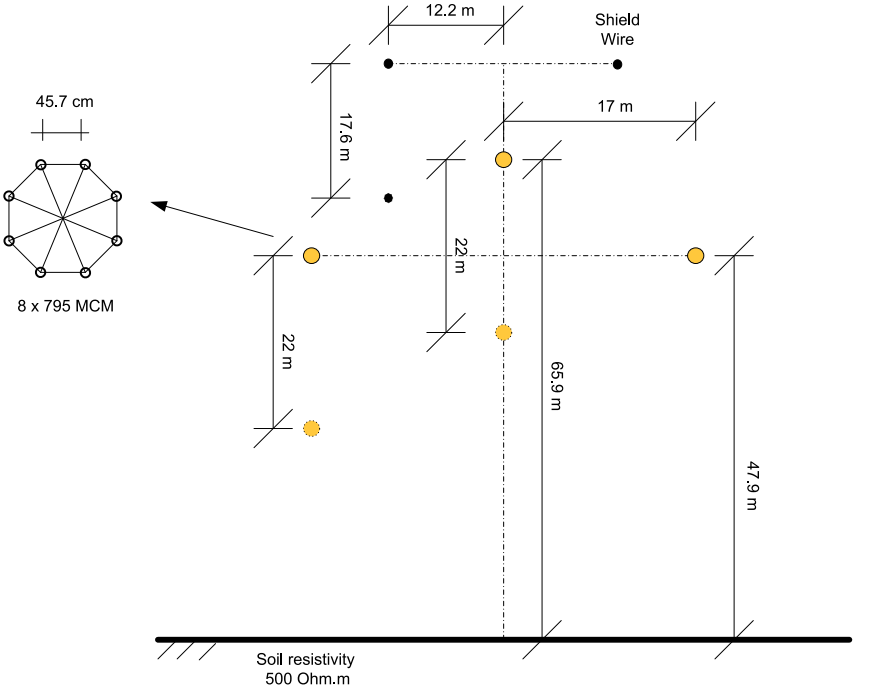

Figure 3.1: Distances for calculation of the 1,000 kV line parameters (without scale)

The positive sequence and zero sequence parameters obtained of the line are:

- $R_1 = 0.0097\Omega/km$
- $R_0 = 0.3027\Omega/km$
- $X_1 = 0.3068\Omega/km$
- $X_0 = 1.1689\Omega/km$
- $B_1 = 5.351E\text{-}6$ Mho/km
- $B_0 = 3.259$ E-6 Mho/km
- $Q_1 = 5.35$ Mvar/km
- $Q_0 = 3.26$ Mvar/km

The parameters above were calculated using the ATP (*Alternative Transient Program*) program.

4. Switching Overvoltage Studies

4.1 Configuration of the Network Analyzed

The transient control equipment to be considered can be: pre-insertion resistor, opening resistor (possible), neutral reactors, ZnO surge arresters, synchronized closing, and fast switches to discharge trapped charge. The studies were done replacing the SIN grid with an equivalent, in which the 500 kV lines are explicit up to the busbars near the 1,000 kV system substations.

4.2 Data Used

The lines of the 1,000 kV system are composed of three equal sections with the length of 440 km each. The 1,000 kV transmission system is connected to the 500 kV network by means of 500/1,000 kV transformers, with rated power of 2,500/3,000 MVA, and leakage reactance of 14% (some simulations were also done with 1,500 MVA and reactance of 18%), with on-load taps for voltage control of ±7.5% of the rated voltage.

The sectioning of the line into three sections implies the need for four substations with transformation capacity for connections with the 500 kV system.

The parallel and series compensations were allocated to the line terminals, with half of the total compensation per terminal. The line capacitive reactive power was compensated to approximately 85%, while the series reactance was compensated to approximately 50%.

To allow for the monitoring of the voltage profiles along the sections, each section was divided into four equal sub-sections. The 1,000 kV line was modeled using distributed parameters, represented by the component LCC (*Line/Cable Constants*), in which the geometry of the tower and of the conductors used is specified.

The equivalent sources modeled in the ATP were adjusted based on the steady state condition of the Anarede program, for the operating conditions of the 2024 Ten Year Expansion Plan (PDE 2024).

The impedances of the equivalent sources used on the 500 kV side were calculated based on the three-phase and single-phase short-circuit powers, obtained for the same horizon in the Anafas, based on which the positive and zero sequence impedances of the equivalent voltage supply are determined.

4.2.1 Line reactor and neutral reactor

Line reactors were connected to both ends of each section of the 1,000 kV line. The values of the reactors are:

- X_1 = 1.000 Ω (positive seq.)
- Q_1 = 1,000 Mvar (three-phase, with 1,000 kV voltage)

The value of Q_1 (in each terminal of the 440 km section) considers ~85% of shunt compensation. The capacitive Mvar of the line for the 440 km section is equal to 2,350 Mvar. This value divided by 2, considering compensation of 85% (*shunt*) results in one reactor of 1,000 Mvar; that is, 1,000 Ω/phase.

The neutral reactor was calculated and included in the system aiming to reduce secondary arc currents and possible overvoltages stemming from the possibility of resonance in the 1000 kV system. A neutral reactor with 250 Ω (60 Hz) was determined for such a purpose.

4.2.2 Series capacitor

Regarding the series compensation, a series compensation of 50% in all the sections, with half of this value in each of the terminals of each section, was considered. The 50% values of the series compensation (per phase) result in 32 ~ 33.7 Ω (if considered the π model, equivalent or rated), thus, selecting the value

$X_1 = 35\ \Omega$ or $C_1 \cong 76\ \mu F$

Note: two configurations were examined in the study: line reactor between the busbar and the series capacitor or on the line side, after the series capacitor.

4.2.3 Surge arresters in the substations and equipment

The model of the 1,000 kV system also considers substation surge arresters at the extremities of each section. In the simulations, these surge arresters were modeled using the component Type 92 (ZnO), for which the characteristic I-V curve is shown in Figure 4.1.

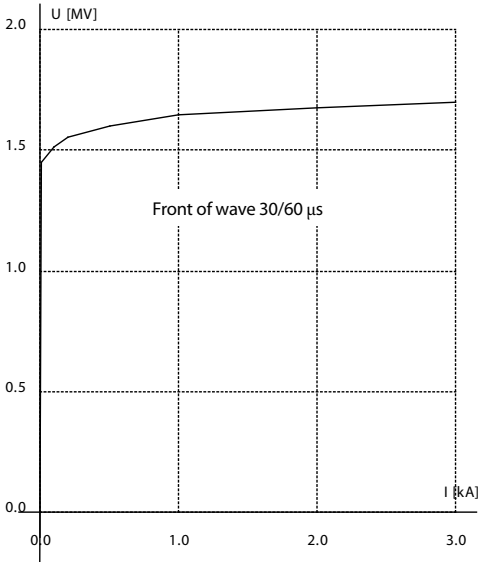

Figure 4.1: Characteristic V-I curve of the surge arresters used (1 column)

The curve used in the simulations was extrapolated from the curve of a commercial surge arrester manufactured by ABB (Ur = 624 kVrms). Initial analyses determined that the rated voltage for the surge arresters for this project would be of Ur = 828 kV. Having the rated voltage relations for both surge arresters (828/624), the curve corresponding to the surge arresters for the 1,000 kV, was obtained.

4.2.4 Metal Oxide Varistors (MOV) of the series capacitors

In the program, these non-linear resistors were also modeled using Type 92 (ZnO), for which the characteristic V-I curve, for a wavefront of 30/60 ms (current), is shown in Table 4.1. The MOV rated voltage is equivalent to the Ur =162 kV surge arresters.

Table 4.1: Characteristic V-I curve for the series capacitor MOV

I (A)	V (kV)
500	316
1,000	328
2,000	336

4.2.5 General scheme of the grid studied

Figure 4.2 indicates the grid model used in the studies.

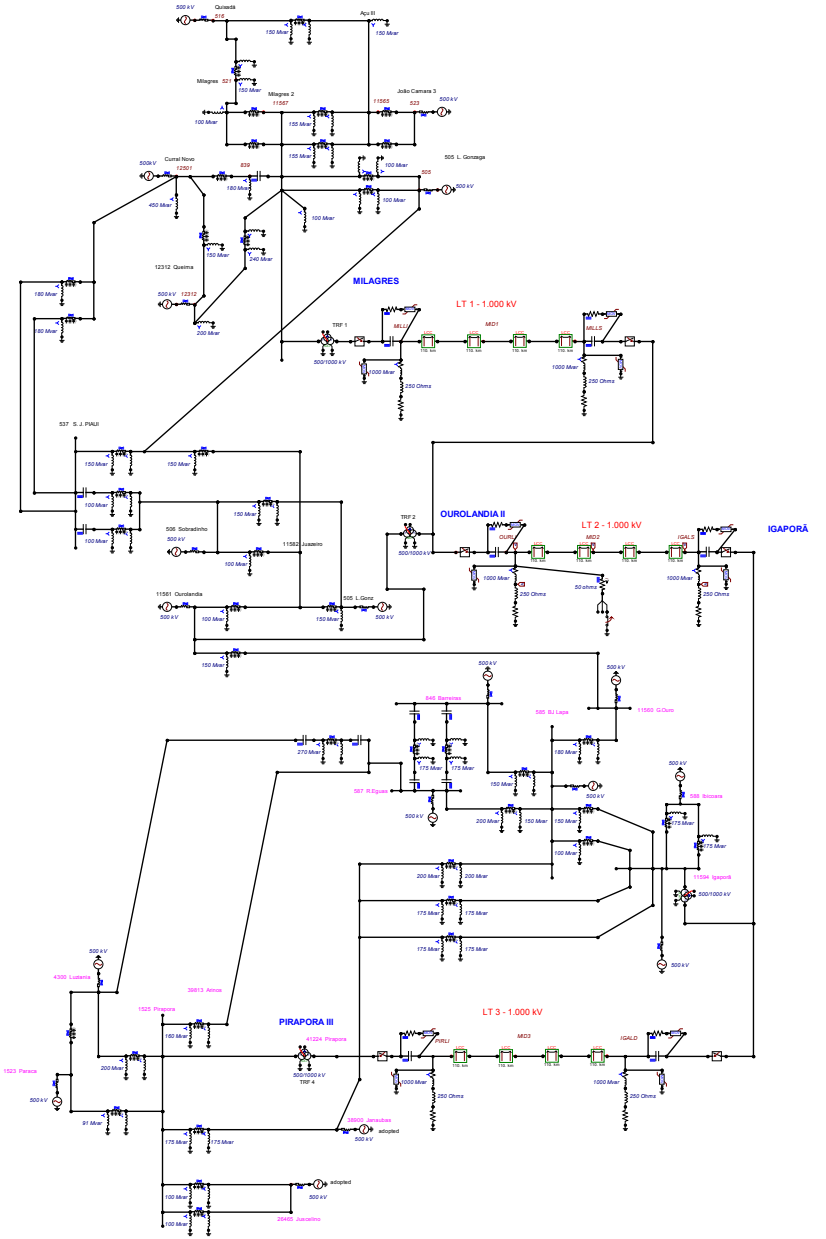

Figure 4.2: Scheme of the grid used in the study

4.3 Line energization

Energizations were simulated in the three sections of the 1,000 kV lines. The highest overvoltage occurred in the Ourolândia – Igaporã section, when energized from Ourolândia. Statistic energizations and sensitivity cases were also performed.

The reference case considers the use of 400 Ω pre-insertion resistor and average insertion time of 8 ms.

For the case of the energization of the Ourolândia – Igaporã line, energized via Ourolândia, it was obtained phase-to-ground and phase-to-phase overvoltage value distributions for five points of the line. Table 4.2 presents the values for this case.

Table 4.2: Result of the statistic energization

Overvoltage location	Phase-to-ground and Phase-to-phase	Average overvoltage (pu)	Standard deviation (pu)	Maximum overvoltage (pu)
Start of the TL	Phase A	1.3786	0.0393	1.4533
	Phase B	1.2857	0.0489	1.4273
	Phase C	1.2805	0.0415	1.3957
	Phase A – Phase B	2.3240	0.0744	2.5750
	Phase B – Phase C	2.1741	0.0850	2.4195
	Phase A – Phase C	2.3064	0.0827	2.5339
25% of the TL	Phase A	1.5001	0.0596	1.6550
	Phase B	1.4197	0.0794	1.6351
	Phase C	1.3813	0.0419	1.5358
	Phase A – Phase B	2.5850	0.0932	2.8542
	Phase B – Phase C	2.3433	0.1175	2.7067
	Phase A – Phase C	2.4858	0.0810	2.6875
Middle of TL	Phase A	1.5920	0.0808	1.7551
	Phase B	1.4947	0.1105	1.7891
	Phase C	1.4531	0.0452	1.6064
	Phase A – Phase B	2.7522	0.1244	2.9948
	Phase B – Phase C	2.4539	0.1409	2.9151
	Phase A – Phase C	2.6057	0.0732	2.8700
75 % of the TL	Phase A	1.6316	0.0970	1.8305
	Phase B	1.5167	0.1276	1.8416
	Phase C	1.4872	0.0555	1.7042
	Phase A – Phase B	2.8334	0.1526	3.1747
	Phase B – Phase C	2.4782	0.1581	3.0326
	Phase A – Phase C	2.6579	0.0817	2.9276
End of TL	Phase A	1.6231	0.1069	1.8456
	Phase B	1.5070	0.1421	**1.8579**
	Phase C	1.4759	0.0581	1.7100
	Phase A – Phase B	2.8260	0.1667	**3.2780**
	Phase B – Phase C	2.4634	0.1719	3.1131
	Phase A – Phase C	2.6435	0.0976	2.9956

Note: $1\text{pu} = 1.000 \cdot \frac{\sqrt{2}}{\sqrt{3}} = 816{,}5 \text{ kV}$

Other details are presented in Annex 1.

Figure 4.3 presents the phase-to-ground overvoltages for the worst case.

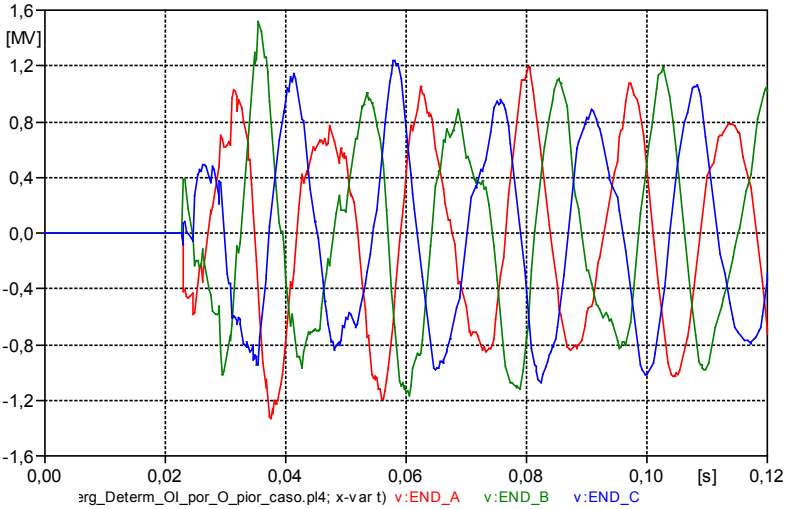

Figure 4.3: Voltage at the end of the line (Igaporã)

Overvoltage sensitivity calculations were made regarding the time for insertion, synchronized closing, position of the line reactor and series capacitor inserted.

4.4 Single-pole Reclosing

After completing the single-pole reclosing simulations for the three sections of the 1,000 kV line, we were able to verify that the overvoltages originated during this procedure are not high enough to affect the definition of the insulation level of the line.

The average value (Vμ) and maximum voltage (V_{max}) obtained for each of these sections (reclosing with statistic switch) were of:

- Milagres – Ourolândia: V_{μ}= 1.576 pu, V_{max} = 1.700 pu
- Ourolândia – Igaporã: V_{μ}= 1.745 pu, V_{max} = 1.853 pu
- Igaporã – Pirapora: V_{μ}= 1.486 pu, V_{max} = 1.694 pu

Table 4.3: Reclosing with statistic switch from the Ourolândia side, for short-circuit in the middle of the line

Overvoltage location	Phase	Average (pu)	Standard deviation (pu)	Maximum overvoltage (pu)
0% of the TL (Ourolândia)	A	1.341	0.040	1.474
	B	1.166	0.022	1.205
	C	1.122	0.039	1.169
25% of the TL	A	1.517	0.043	1.644
	B	1.188	0.022	1.241
	C	1.151	0.026	1.206
50% of the TL	A	1.662	0.056	1.764
	B	1.182	0.017	1.223
	C	1.160	0.026	1.206
75% of the TL	A	1.741	0.056	1.840
	B	1.134	0.019	1.182
	C	1.160	0.029	1.202
100% of the TL (Igaporã)	A	1.745	0.064	**1.853**
	B	1.075	0.004	1.101
		1.133	0.018	1.164

Figure 4.3 presents the voltages in the Igaporã busbar (100% of the line).

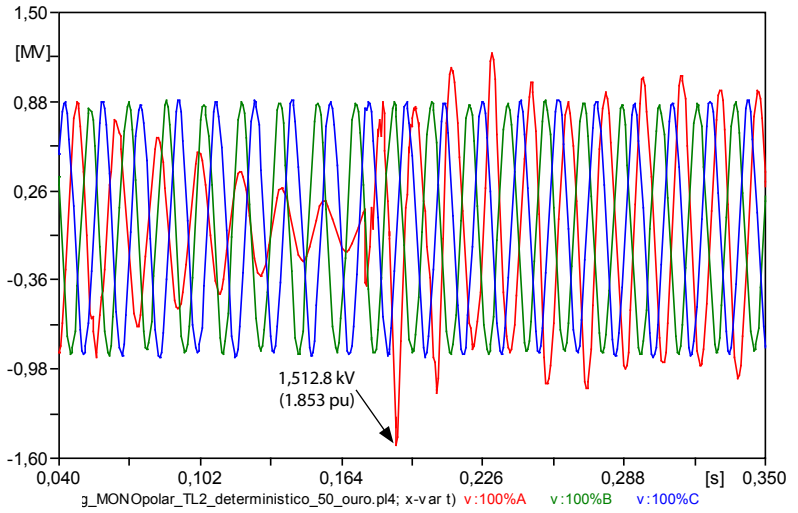

Figure 4.3: Voltages in the open extremity of section 2 (Ourolândia – Igaporã) with the reclosing being performed from the Ourolândia side

Other details are presented in Annex 2.

4.5 Three-pole Reclosing

The highest overvoltages occur in the Milagres – Ourolândia section, reconnected via Milagres, as presented in Table 4.4.

Table 4.4: Overvoltages in the Milagres – Ourolândia section, via Milagres. Capacitor

Milagres – Ourolândia	Phase-to-ground and Phase-to-phase	Average (pu)	Standard deviation (pu)	μ + 3σ (pu)
Start of the TL	Phase A	1.239	0.065	1.435
	Phase B	1.295	0.040	1.414
	Phase C	1.291	0.056	1.459
	Phase A – Phase B	2.168	0.093	2.448
	Phase B – Phase C	2.249	0.069	2.457
	Phase A – Phase C	2.198	0.104	2.509
25 % of the TL	Phase A	1.304	0.082	1.551
	Phase B	1.388	0.048	1.531
	Phase C	1.396	0.073	1.616
	Phase A – Phase B	2.287	0.089	2.554
	Phase B – Phase C	2.423	0.095	2.710
	Phase A – Phase C	2.358	0.147	2.798
Middle of TL	Phase A	1.357	0.093	1.635
	Phase B	1.445	0.054	1.606
	Phase C	1.469	0.089	1.737
	Phase A – Phase B	2.361	0.088	2.627
	Phase B – Phase C	2.527	0.114	2.870
	Phase A – Phase C	2.469	0.179	3.005
75 % of the TL	Phase A	1.378	0.099	1.674
	Phase B	1.464	0.061	1.646
	Phase C	**1.497**	0.097	1.788
	Phase A – Phase B	2.383	0.097	2.674
	Phase B – Phase C	2.561	0.128	2.945
	Phase A – Phase C	2.509	0.194	**3.092**
End of TL	Phase A	1.362	0.099	1.660
	Phase B	1.452	0.063	1.640
	Phase C	1.491	0.106	**1.809**
	Phase A – Phase B	2.355	0.100	2.656
	Phase B – Phase C	2.542	0.137	2.952
	Phase A – Phase C	2.480	0.200	3.081

Other details are presented in Annex 3.

4.6 Fault Application, Fault Clearing, and Load Rejection

Regarding the study involving single-phase faults (fault application) and consequent occurrence of overvoltages along the lines, we observed that these faults are not critical for choosing the insulation level of the line. These overvoltages proved to be lower than the values obtained when of the study of other types of phenomena, for example, line energization.

The fault application study was conducted in all the sections of the 1,000 kV transmission line. A single-phase fault was applied to several points of the line sections, with subsequent opening of the circuit breakers in this line. Simulations were made with single-pole and three-pole opening of the feeder circuit breaker, with or without line surge arresters, with various sequences of circuit breaker openings, and verification of the overvoltages in the healthy system and in the defective line. The overvoltages will be considered in the insulation coordination.

With regards to load rejection, with or without fault, the surge arresters in the 1,000 kV system (one column) do not absorb power beyond their capacity, although, in some cases, they conduct current.

Note: it is important to highlight, however, that for the dimensioning of the surge arrester more serious contingencies are necessary, as shown in the equipment section.

More details about the study are presented in Annex 4.

4.6.1 Fault application

The worst case was a single-phase fault in the middle of the Ourolândia – Igaporã section, the results for which are presented in Table 4.5.

Table 4.5: Overvoltages on the healthy phases (B and C) of the Ourolândia – Igaporã section for the single-phase fault in the middle of the Ourolândia – Igaporã section

		Peak values (pu) in section Ourolândia – Igaporã				
Position in the voltage wave, fault application	**Fault application instant (s)**	**BC_0**	**BC_{25}**	**BC_{50}**	**BC_{75}**	**BC_{100}**
Cycle peak (+)	0.0974	1.115	1.328	1.517	1.344	1.129
Crossing by zero	0.0933	1.110	1.199	1.378	1.237	1.106
Cycle peak (-)	0.0892	1.133	1.323	**1.522**	1.346	1.143

4.6.2 Fault clearing

In the fault clearing, we analyze the overvoltages resulting of the opening of the transmission line after the occurrence of a single-phase fault in some points of the line. Simulations were performed in the three sections of the line. The results of the simulations performed with the three-pole opening of the feeder circuit breaker are presented in Table 4.6.

Table 4.6: Overvoltages for the three-pole opening of the line

TL Section	Fault location	Overvoltages (pu)		
		TL_0	TL_{50}	TL_{100}
Milagres – Ourolândia (MO)	MO_{100}	1.43	1.77	1.87
	MO_{75}	1.48	1.69	1.79
	MO_{50}	1.41	1.67	1.76
	MO_{25}	1.58	1.51	1.27
	MO_0	1.58	1.43	1.24
Ourolândia – Igaporã (OI)	OI_{100}	1.48	1.77	1.87
	OI_{75}	1.49	1.74	1.83
	OI_{50}	1.42	1.73	1.81
	OI_{25}	1.59	1.49	1.30
	O_{I0}	1.58	1.46	1.38
Igaporã – Pirapora (IP)	IP_{100}	1.39	1.83	**1.92**
	IP_{75}	1.35	1.76	1.84
	IP_{50}	1.35	1.80	1.82
	IP_{25}	1.68	1.64	1.25
	IP_0	1.85	1.68	1.44

The highest overvoltage occurred in the Igaporã – Pirapora section, with the short-circuit applied at Pirapora. Figure 4.4 presents the voltage at the Pirapora terminal for this case.

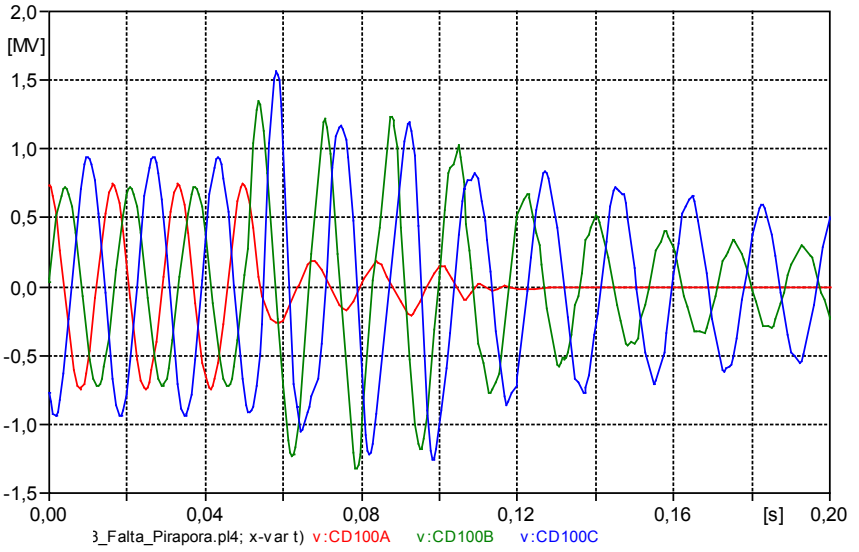

Figure 4.4: Voltage at Pirapora

The same procedure was adopted for the single-pole opening of the feeder circuit breakers. Table 4.7 presents the values of this study.

Table 4.7: Overvoltages for the single-pole opening of the LT

TL Section	Fault location	Overvoltages (pu)		
		TL_0	TL_{50}	TL_{100}
Milagres – Ourolândia (MO)	MO_{100}	1.17	1.31	1.32
	MO_{75}	1.15	1.23	1.18
	MO_{50}	1.20	1.32	1.15
	MO_{25}	1.22	1.29	1.23
	MO_0	**1.35**	1.34	1.28
Ourolândia – Igaporã (OI)	OI_{100}	1.24	1.30	1.23
	OI_{75}	1.19	1.24	1.16
	OI_{50}	1.21	**1.35**	1.15
	OI_{25}	1.24	1.28	1.15
	O_{I0}	1.31	1.34	1.17
Igaporã – Pirapora (IP)	IP_{100}	1.18	1.24	1.15
	IP_{75}	1.15	1.23	1.15
	IP_{50}	1.14	1.34	1.15
	IP_{25}	1.15	1.25	1.14
	IP_0	1.23	1.19	1.21

The overvoltages in the system out of the defective line were lower than 1.35 pu.

4.6.3 Load rejection

The load rejection study was conducted according to the sequence presented as follows:

- Open one of the sides of the line sections at 50 ms.
- Analyze which line section presents higher overvoltage, in which point of the line the overvoltage occurs, and if this will result in surge arrester to operate.
- Analyze the load rejection overvoltages with the occurrence of short-circuit before the opening of one of the sides of the line and, after opening, analyze the voltages and power in the surge arresters.
- Repeat, if that is the case, but applying the short after the load rejection.

The most critical case was the opening at Igaporã, followed by the short-circuit. The values are presented in Table 4.8.

Table 4.8: Phase-ground voltage (pu) in the Ourolândia – Igaporã line (without surge arrester)

Phase	Ourolândia	Igaporã
A	1.33	1.61
B	1.32	2.27
C	1.24	1.92

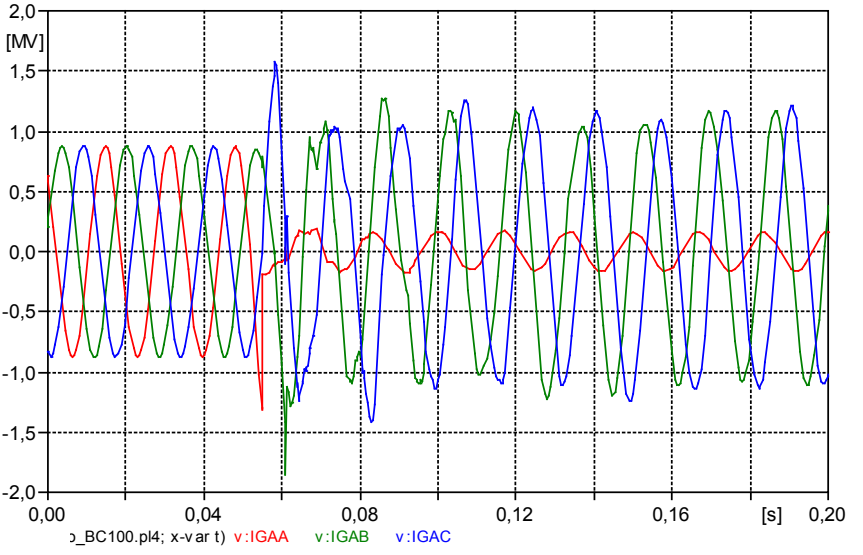

Figure 4.5: Oscillograms of the voltages in Igaporã

It was observed that the surge arresters absorbed energy lower than 120 kJ. Some other details are presented in Annex 4.

5. Secondary Arc Extinction (Residual Load)

5.1 Residual Charge – Single-Pole Opening

Regarding the secondary arc extinction phenomenon, it can be concluded that, with the 1,000 kV line, the secondary arc current (I_{ARC}) values and recovery voltage (V_{REC}) are lower than the critical values in all the points where the fault was applied, and in all the sections. The critical values being 50 A_{rms} or 70 A_p current, and first voltage peak on the recovery voltage of 100 kV.

Regarding the neutral reactor, the analysis of the Igaporã – Pirapora line showed that the maximum voltage (peak value) over it is equal to 135 kV.

Tables 5.1 to 5.3 present the values of arc extinction obtained.

Table 5.1: Results for Section 1 (Milagres – Ourolândia)

	Fault point (TL = 440 km)	Peak values			
		I_{ARC} (A)	V_{REC} (kV)	$V_{REACTOR}$ neutral (kV)	
				Milagres	Ourolândia
Section 1 Milagres to Ourolândia Xn1 = Xn2 = 250 Ω	Milagres (0%)	68.0	33.3	125.3	126.8
	25%	52.5	27.4	125.5	124.5
	50%	41.9	22.3	126.5	123.6
	75%	35.5	18.5	128.4	123.7
	Ourolândia (100%)	34.2	16.7	131.2	125.1

Table 5.2: Results for Section 2 (Ourolândia – Igaporã)

	Fault point (TL = 440 km)	Peak values			
		I_{ARC} (A)	V_{REC} (kV)	$V_{REACTOR}$ neutral (kV)	
				Ourolândia	Igaporã
Section 2 Ourolândia to Igaporã Xn1 = Xn2 = 250 Ω	Ourolândia (0%)	70.1	34.1	127.0	126.2
	25%	53.4	27.9	127.6	123.9
	50%	41.9	22.4	129.1	122.9
	75%	34.9	18.2	131.5	123.1
	Igaporã (100%)	33.7	16.4	134.7	124.5

Table 5.3: Results for Section 3 (Igaporã – Pirapora)

	Fault point (TL = 440 km)	Peak values			
		I_{ARC} (A)	V_{REC} (kV)	$V_{REACTOR}$ neutral (kV)	
				Igaporã	Pirapora
Section 3 Igaporã to Pirapora Xn1 = Xn2 = 250 Ω	Igaporã (0%)	70.8	34.4	125.0	125.2
	25%	53.3	27.8	122.5	126.1
	50%	41.1	21.9	121.4	127.8
	75%	33.4	17.4	121.4	130.4
	Pirapora (100%)	31.9	15.5	122.6	133.8

In the above tables, we can observe that both the arc currents and the recovery voltages for the short-circuits simulated in the five points of the line comply with the specified values (50 A_{rms} and 100 kVp) in all the sections.

5.2 Residual Charge – Three-Pole Opening

For these studies, the single-pole faults were introduced along the line, starting at 50 ms of the simulation, followed by a three-pole opening of the circuit breakers at 100 ms, and then the fault clearing at 400 ms.

The residual load obtained for each case, and for the most critical case is described in Table 5.4, where all the values represent the voltage and peak current in fault. The voltage and current limiting values are respected in all the situations. The situation where there is higher overvoltage and arc current is in the Igaporã – Pirapora line, with fault at 75% of Igaporã. It is relevant to mention that the current and voltage values are extremely low.

Table 5.4: Igaporã – Pirapora

Fault location	I_{FAULT} (Ap)	V_{FAULT} (kVp)
0%	0.89	0.29
25%	1.19	0.03
50%	0.77	0.41
75%	**1.21**	0.15
100%	1.1	0.43

5.3 Line Reactor Position

The line reactor can be connected to the other side of the line or on the busbar side of the series capacitor. The simulations mentioned refer to the first case. In the second, if the line reactor is connected to the busbar, when the line is opened, a residual load may remain in the series capacitor that discharges via reactor and fault. This last case was simulated increasing the secondary arc current, but, even so, it still remained very low.

Other details are presented in Annex 5.

6. Transient Recovery Voltage (TRV)

The circuit breakers TRV is defined as the difference of potentials across the terminals of the circuit breaker after it is opened, as a result of a fault in the system. The nature and value of the TRV depend on factors like the type of circuit interrupted (resistive, capacitive, or inductive), the system's impedance seen from the circuit breaker terminals, the system's rated voltage, the current in the circuit breaker, the type, magnitude, and location of the fault, among other factors. As a result of the elimination of the fault current, the recovery voltage that appears across the poles of the circuit breaker will present transient oscillations until the steady state is reached. Care should be taken so that, during the TRV analysis, the circuit breaker does not surpass the envelope curve magnitude, or the front of the envelope curve referred to as *Rate of Rise of Recovery Voltage* (RRRV).

For specification of the circuit breaker, it is necessary to determine the values of the TRV by means of transient studies, taking into consideration the following more critical opening conditions, which, depending on the circuit breaker application point, must be considered partially or in full.

- Terminal fault: should be applied in the busbar and on the line output, representing the condition of highest TRV after fault interruption.
- Short-line fault: condition with characteristics of higher request on the circuit breaker at the start of the TRV,

Thus, the value of the TRV should be evaluated, verifying if the voltage magnitude at the circuit breaker terminal does not surpass the value of the envelope curve provided by the manufacturer, or that specified in the study or standards.

It should also be verified that the rate of rise of recovery voltage (RRRV) does not exceed the inclination of the circuit breaker envelope curve.

The results of the following simulations will be presented:

- Short-line fault for both circuit breakers in each section: applied to 2 km, 10 km, 50% of the length of the section (220 km), and 90% of the length of the section (396 km).
- Three-phase "grounded" and "ungrounded" terminal faults at both sides of the circuit breaker (line side and transformer side).

6.1 Short-Line Fault

None of the cases analyzed (Short-Line Fault - SLF) presented TRV problems, neither in magnitude, nor in wavefront, since they were lower than the values of the envelope curve adopted, except for the case described next.

For the case of the SLF at a distance of 2 km from the Igaporã terminal, opening of the Igaporã – Ourolândia line via Igaporã, without bypassing the series capacitor, the envelope curve was surpassed. The surpassing values in this case are presented in Figure 6.1.

However, when simulated this case considering the series capacitor already bypassed – which would be a more realistic case – this surpassing of the front of the envelope curve did not occur.

We highlight that the T-100 *Short Line Fault* (SLF) envelope, in the case of the short-line fault (single-phase), was adopted for this analysis. When simulated this surpassed case and used the T-10 envelope curve, there was no such overrun neither in magnitude nor in their wavefront.

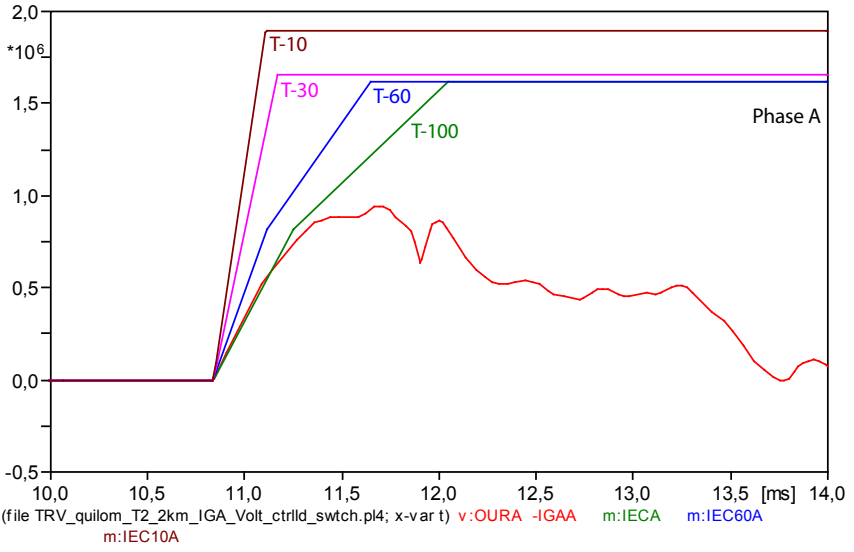
2,0
*10^6
1,5
1,0
0,5
0,0
-0,5
T-10
T-30
T-60
T-100
Phase A
10,0
10,5
11,0
11,5
12,0
12,5
13,0
13,5
[ms]
14,0
(file TRV_quilom_T2_2km_IGA_Volt_ctrlld_swtch.pl4; x-var t) v:OURA -IGAA m:IECA m:IEC60A
m:IEC10A

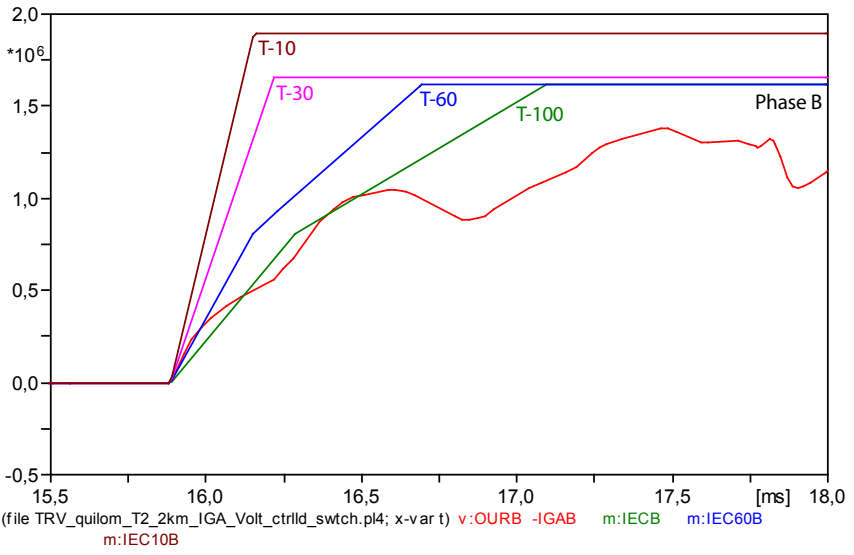
2,0
*10^6
1,5
1,0
0,5
0,0
-0,5
T-10
T-30
T-60
T-100
Phase B
15,5
16,0
16,5
17,0
17,5
[ms]
18,0
(file TRV_quilom_T2_2km_IGA_Volt_ctrlld_swtch.pl4; x-var t) v:OURB -IGAB m:IECB m:IEC60B
m:IEC10B

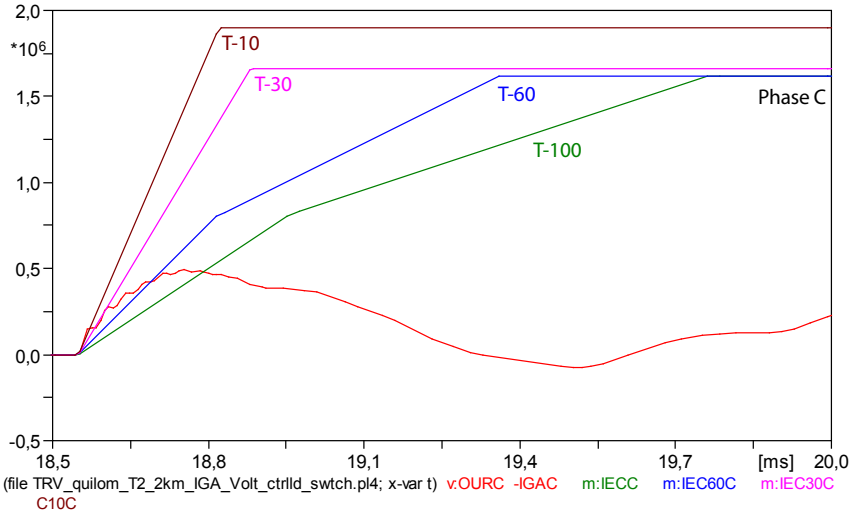

Phase	Icc via DJ (kAp)	T (%)	Surpassed	Type of surpassing
A	3.1	3.48	No	–
B	3.8	4.27	Yes	R_B
C	33.0	37.04	Yes	R_C

Figure 6.1: Short-line fault 2 km from Igaporã (with inserted series capacitor)

Letters R and M in the column type of surpassing indicate whether the surpass was in RRRV (wavefront) or in magnitude.

6.2 Terminal Fault

Of all the cases analyzed, the envelope curve was surpassed in its magnitude only in the case of a three-phase terminal fault (grounded and ungrounded) in the Igaporã – Pirapora section, when the fault occurs at the Pirapora terminal.

Figure 6.2 presents the case of the insulated three-phase terminal fault on the Pirapora side.

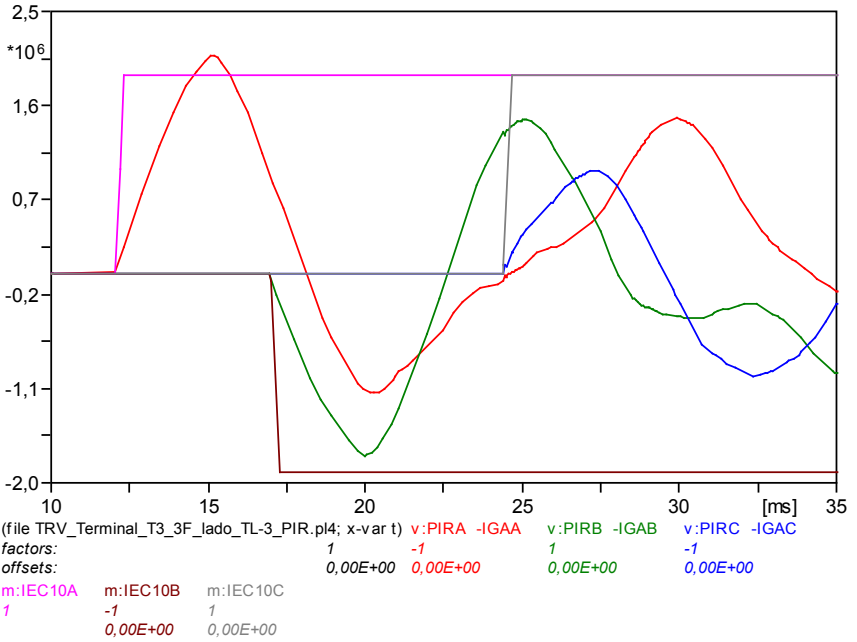

Phase	Icc via DJ (kAp)	T (%)	Surpassed T-10	Type of surpassing
A (red)	7.30	8.19	Yes	M_A
B (green)	7.30	8.19	No	–
C (blue)	7.30	8.19	No	–

Figure 6.2: Three-phase insulated terminal fault (TRF-4 side, Pirapora)

For the three-phase grounded terminal fault, the magnitude of phase A was surpassed. The surpassing value was approximately 193.2 kV above the T-10 envelope curve. There was no surpassing of the RRRV in any of the phases, including the T-100 curve (fault current peak value = 7.30 kA).

Other details are presented in Annex 6.

7. Transformer Energization

The transformer energization procedure may imply its saturation. Since this is a non-linear phenomenon, the presence of inrush currents and their implications appear, such as the generation of harmonic and DC components, in addition to the fundamental component.

During the energization of the transformer, its core may become saturated due to the sudden application of voltage, establishing a transient magnetizing current (inrush), the magnitude of which, in the initial instants, may become 10 or 25 times greater than the rated current of the transformer (including a DC component). The effect of said current is a voltage drop and a probable activation of instantaneous and/or differential relays. The current value reached in the transient state depends on two factors: i) point in the voltage cycle where the energization switch is closed; ii) magnetic conditions of the core, including the intensity and polarity of the residual flow. High inrush currents may even impose a high level of electromechanical stress onto the windings of the transformer.

This item presents the results of the electromagnetic transient studies resulting of the energization of the 500/1,000 kV auto-transformers via the primary side (500 kV), and the secondary side (1,000 kV); an evaluation of the inrush currents during the energization of the auto-transformers will also be performed.

Two options of transformer energization will be analyzed: use of pre-insertion resistors, and/or use of controlled switching devices.

7.1 Findings

The study performed on the energization of transformers found that:

- The inrush currents depend on the residual flux existing in the transformer core and on the closing instants of the circuit breaker poles.
- Due to the saturation of the transformer, these currents are not purely sinusoidal, but have a relatively high harmonic content, especially those of inferior order;
- In most cases, the inrush current presented a progressive decline that depends on the damping of the system;

- In the case of the energization of parallel transformers, it was observed that the energization of the second transformer imposed a distortion effect, and an increase of the inrush current also in the transformer already energized. This effect is even more pronounced if the second transformer is energized in an instant different from the best closing instant of the second transformer.

Thus, we were able to reach the following conclusions:

- Although the energization via the 500 kV side presents more inrush currents, this option proved more favorable in terms of simplicity, and absence of components originated, possibly, from interactions with the rest of the system.
- In the option of the energization via the 1,000 kV side, the possibility of occurrence of electromagnetic interaction between the transformer and the elements in its proximity require further analyses, as are the cases of the series compensation, shunt compensation, electrical parameters of the 1,000 kV, and others. In the specific case of the transformer analyzed, it was even necessary to perform the bypass of one of the series capacitors close to the transformer, under conjecture of electromagnetic interaction with the transformer.

It is recommend the use of closing synchronizers in the circuit breakers, considering the prospective and residual flux, the function of which was decisive in reducing the inrush currents.

Pre-insertion resistors in the order of 1,000 Ω have a very positive effect in the reduction of the *inrush* currents and overvoltages.

Other details are presented in Annex 7.

8. Resonance Analysis – Line and its Reactor

The possibility of resonance due to the parallel compensation of the 1,000 kV line, and the influence of the neutral reactor for its mitigation, was analyzed.

The study consisted of evaluating the response in transmission line frequency with parallel compensation when opening of one phase or two phases of the line. The coupling of the capacitances between the phases may present resonance frequencies when one or two phases are open.

To simplify the analysis, the internal impedance of the equivalent sources and the series impedance of the line were neglected. Thus, the equivalent circuit is formed only by the impedances of the parallel reactor, neutral reactor and the capacitive coupling of the phases.

8.1 Results with only one 1,000 kV Line

It was verified that there could be resonance frequencies both for one and for two open phases, within the frequency ranges of 56 Hz to 66 Hz, in this case without the neutral reactor in the line reactors.

The insertion of the 250 Ω neutral reactor proved to be adequate also for mitigating resonances in the specified range.

8.2 Resonance in the System with Two Lines per Section

To verify if there would be resonance in the range of 56 Hz to 66 Hz, when a second 1,000 kV circuit is connected, a second modeling in the PSCAD program was conducted.

In this case, there might also be resonance in the frequency range mentioned between the positive and zero sequence during the opening of the lines, either one or two phases; however, the presence of the neutral reactor proved to be adequate for mitigation of this phenomenon.

Other details are presented in Annex 8.

9. Transmission Line

9.1 Economic Conductor

The economic conductor is the one that minimizes the annual cost per kilometer of the line plus losses.

The cost of the line per kilometer is given by:

$$C_{lt} = 235208 + 484{,}8762\ V_m + N{\cdot}S_1\ (3.3475\ N + 89.7166)$$

Where:

V_m is the maximum voltage = 1,100 kV;

S_1 é is the conductor section in MCM (1 MCM ~ 2 mm^2) of a sub-conductor; and

N is the number of sub-conductors per bundle.

To calculate the annual cost of the line, we considered:

- Interest rate = 8%.
- Years for amortization = 30.
- Maintenance = 0.02% of the cost of the line per year.

Based in these values, the annual factor calculated over the investments is:

$$fr = 0.1175$$

Thus, the total cost of the line, per kilometer, for N = 8, will be:

$$C_{lt} = 768572 + 932 \cdot S_1$$

and the annual cost is:

$$C_{lty} = 90307 + 109.5 \cdot S_1$$

The annual cost of the Joule losses will be:

$$C_{py} = (C_1 + C_2 \cdot fp \cdot 8760)\left(\frac{57}{S_1 \cdot N}\right) \cdot \left(\frac{P}{V}\right)^2$$

Where:

C_2 is the cost of energy = 154 R$/MWh;

C_1 is the fixed cost of power = 0;

fp is the loss factor (= 0.5 or 0.35);

P is the peak capacity (3,000 or 4,000 MW); and

V is the average voltage = 1,000 kV.

Thus, resulting in:

$$C_{py} = \frac{K}{S_1}$$

With K being the values of Table 9.1.

Table 9.1: Values of K (Joule losses)

MW	fp	K
4,000	0.5	78,244,320
4,000	0.35	54,771,024
3,000	0.5	44,012,430
3,000	0.35	30,808,701

The economic conductor will be:

$$S_{1econ} = \sqrt{\frac{K}{109,5}}$$

Resulting in:

Table 9.2: Economic conductor S1 econ in MCM

MW	fp = 0.35	fp = 0.50
3,000	530	634
4,000	707	845

Figure 9.1 shows the values of Table 9.2.

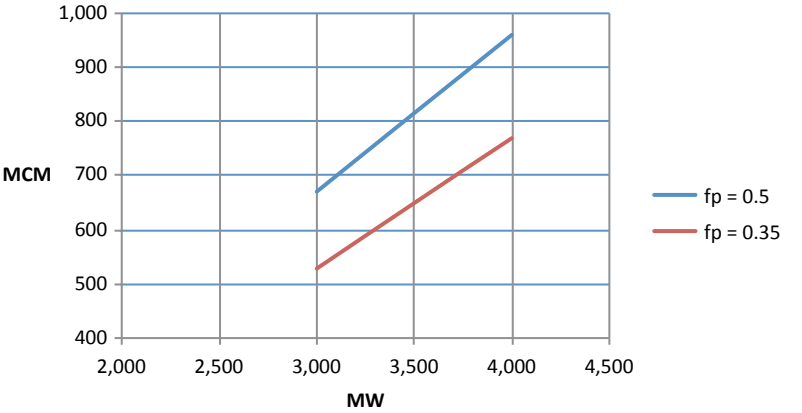

Figure 9.1: Economic section

Considering that the line will be implemented in a wind and photovoltaic generation region, the fp value should be low.

On the other hand, there is a minimum section to prevent excessive corona effect. Thus, to proceed with the calculations, the section ACSR 8 x 795 (*Tern*) will be used.

Note: in the case of the use of 6 conductors per phase, the economic sections would be 1,192.5 and 954 MCM for 4,000 MW and fp 0.5 and 0.35 respectively.

Naturally, in this case, it will be necessary to verify the voltage gradient in the conductor.

9.2 Overvoltage at Operating and Switching Frequency

The line must have insulation (insulator string and distances in air) to support steady-state (power frequency) and switching overvoltages.

9.2.1 Overvoltage at power frequency

From the perspective of voltage at power frequency, the line must withstand the maximum voltage of the system (1,100 kV), and the energization and load rejection overvoltages, altered in the transient period by the operation of the voltage and speed governors in the plants (eventually the action of controllable shunt compensation).

As a design criterion, the objective established here is that, in the new state, after the transient, the parallel compensation in the lines must be such that the overvoltage at power frequency is lower than 1.2 pu (1,200 kV).

9.2.2 Switching overvoltages

It will be considered overvoltages stemming from:

- Line energization;
- Single-pole and three-pole reclosing;
- Load rejection;
- Occurrence of short circuit; and
- Elimination of short circuit.

The control equipment to be considered can be: pre-insertion resistor, opening resistor (possibly), neutral reactors, ZnO surge arresters, synchronized closing, and fast switches to discharge trapped charge.

The studies were done replacing the SIN grid with an equivalent, in which the 500 kV lines are explicit up to the busbars near the 1,000 kV substations.

9.2.2.1 Line energization

Energizations of the three sections of the line were processed, via both terminals. The results of the worst case (energization of the Ourolândia – Igaporã line via Ourolândia) are in Table 9.3.

Table 9.3: Energization of the Ourolândia – Igaporã line via Ourolândia

Overvoltage location	Phase	Average overvoltage (pu)	Standard deviation (pu)	Maximum overvoltage (pu)
Start of the TL	Phase A	1.3786	0.0393	1.4533
	Phase B	1.2857	0.0489	1.4273
	Phase C	1.2805	0.0415	1.3957
	Phase A–B	2.324	0.0744	2.575
	Phase B-C	2.1741	0.085	2.4195
	Phase A-C	2.3064	0.0827	2.5339
25% of the TL	Phase A	1.5001	0.0596	1.655
	Phase B	1.4197	0.0794	1.6351
	Phase C	1.3813	0.0419	1.5358
	Phase A–B	2.585	0.0932	2.8542
	Phase B-C	2.3433	0.1175	2.7067
	Phase A-C	2.4858	0.081	2.6875
Middle of TL	Phase A	1.592	0.0808	1.7551
	Phase B	1.4947	0.1105	1.7891
	Phase C	1.4531	0.0452	1.6064
	Phase A–B	2.7522	0.1244	2.9948
	Phase B-C	2.4539	0.1409	2.9151
	Phase A-C	2.6057	0.0732	2.87
75 % of the TL	Phase A	1.6316	0.097	1.8305
	Phase B	1.5167	0.1276	1.8416
	Phase C	1.4872	0.0555	1.7042
	Phase A–B	2.8334	0.1526	3.1747
	Phase B-C	2.4782	0.1581	3.0326
	Phase A-C	2.6579	0.0817	2.9276
End of TL	Phase A	1.6231	0.1069	1.8456
	Phase B	1.507	0.1421	**1.8579**
	Phase C	1.4759	0.0581	1.71
	Phase A–B	2.826	0.1667	**3.278**
	Phase B-C	2.4634	0.1719	3.1131
	Phase A-C	2.6435	0.0976	2.9956

9.2.2.2 Three-pole reclosing

The highest overvoltages occur in the Milagres – Ourolândia section, reconnected via Ourolândia (Table 9.4).

Table 9.4: Three-pole reclosing of the Milagres – Ourolândia line

With series capacitor inserted				
Milagres – Ourolândia	**Phase**	**Varage voltage (pu)**	**Standard deviation (pu)**	**μ + 3σ (pu)**
Start of the TL	Phase A	1.239	0.065	1.435
	Phase B	1.295	0.040	1.414
	Phase C	1.291	0.056	1.459
	Phase A–B	2.168	0.093	2.448
	Phase B-C	2.249	0.069	2.457
	Phase A-C	2.198	0.104	2.509
25% of the TL	Phase A	1.304	0.082	1.551
	Phase B	1.388	0.048	1.531
	Phase C	1.396	0.073	1.616
	Phase A–B	2.287	0.089	2.554
	Phase B-C	2.423	0.095	2.710
	Phase A-C	2.358	0.147	2.798
Middle of TL	Phase A	1.357	0.093	1.635
	Phase B	1.445	0.054	1.606
	Phase C	1.469	0.089	1.737
	Phase A–B	2.361	0.088	2.627
	Phase B-C	2.527	0.114	2.870
	Phase A-C	2.469	0.179	3.005
75 % of the TL	Phase A	1.378	0.099	1.674
	Phase B	1.464	0.061	1.646
	Phase C	**1.497**	0.097	1.788
	Phase A–B	2.383	0.097	2.674
	Phase B-C	2.561	0.128	2.945
	Phase A-C	2.509	0.194	**3.092**
End of TL	Phase A	1.362	0.099	1.660
	Phase B	1.452	0.063	1.640
	Phase C	1.491	0.106	**1.809**
	Phase A–B	2.355	0.100	2.656
	Phase B-C	2.542	0.137	2.952
	Phase A-C	2.480	0.200	3.081

9.2.2.3 Single-pole reclosing

The highest overvoltages occur in the Ourolândia – Igaporã section, reconnected via Ourolândia (Table 9.5).

Table 9.5: Single-pole reclosing of the Ourolândia – Igaporã line, reconnected via Ourolândia

	0% L (start)			25% L			50% L			75% L			100% L (end)		
	A	B	C	A	B	C	A	B	C	A	B	C	A	B	C
Average value (pu)	1.34	1.17	1.12	1.52	1.19	1.15	1.66	1.18	1.16	1.74	1.13	1.16	1.75	1.08	1.13
Standard deviation (pu)	0.04	0.02	0.04	0.04	0.02	0.03	0.06	0.02	0.03	0.06	0.02	0.03	0.06	0	0.02
Higher value (pu)	1.47	1.21	1.17	1.64	1.24	1.21	1.76	1.22	1.21	1.84	1.18	1.2	1.85	1.1	1.16

9.2.2.4 Occurrence of fault

Once a fault is applied, traveling waves appear on the lines, generating transients, which can elevate the voltages in the line. In addition to the waves, other phenomena that can influence the transients in a line are the number of lines in the substation, reactive compensation and, mainly, the operation of the surge arresters.

The worst case for the application of faults is when the voltages are at their peak (positive or negative), which occurs in the middle of the Ourolândia – Igaporã section, and coincides with the middle of the line (Milagres and Pirapora).

9.2.2.5 Fault clearing

For the circuit breakers' opening after a single-phase fault, the overvoltages occur at the end of the line sections.

The results of the worst case are described in Table 9.6.

Table 9.6: Overvoltage after clearing the fault

Line	Failure location	Overvoltages (pu)*		
		0%	50%	100%
Ourolândia – Igaporã	Ourolândia – Igaporã$_{100}$	1.48	1.77	1.87
	Ourolândia – Igaporã$_{75}$	1.49	1.74	1.83
	Ourolândia – Igaporã$_{50}$	1.42	1.73	1.81
	Ourolândia – Igaporã$_{25}$	1.59	1.49	1.3
	Ourolândia – Igaporã$_{0}$	1.58	1.46	1.38

9.2.2.6 Load rejection

In this case, only one side of the line is opened (at 50 ms), simulating a Load rejection that can be followed or preceded by a short-circuit.

First, the lines were opened at 50 ms (in all the sections – only one circuit breaker at a time), without the fault, and an analysis was made of the situations and points of the line in which the highest voltages occur (Table 9.7).

Table 9.7: Highest load rejection overvoltages, with no fault

Line	Circuit breaker at the busbar	Phase with highest voltage measured	Overvoltages (pu)
Milagres – Ourolândia	Ourolândia	C	1.58
Ourolândia – Igaporã	Igaporã	C	1.64
Igaporã – Pirapora	Pirapora	A	1.68

Next, it was analyzed the opening the lines with the fault applied both before the opening and after the opening.

The worst case occurred when there is a fault application after the opening of the circuit breaker; see the results in Table 9.8.

Table 9.8: Highest load rejection overvoltages, with fault

Line	Circuit breaker at the busbar	Phase with highest voltage measured	Overvoltages (pu)
Milagres – Ourolândia	Ourolândia	C	2.03
Ourolândia – Igaporã	Igaporã	B	2.27
Igaporã – Pirapora	Pirapora	C	2.10

In these cases, the shunt surge arresters, that would mitigate the overvoltages, were not included in the circuit.

9.3 Insulation Coordination

The line insulation must withstand the power frequency overvoltages and those from lightning. Thus, it must be determined the insulator string configuration, and the minimum distances between the live parts and grounded parts (*gaps*).

9.3.1 Power frequency insulation

9.3.1.1 Insulator string

The line will mostly pass through "light" pollution zones (no industries, low density of industries and homes, agriculture, mountains, more than 10-20 km from the sea).

IEC 71-2 recommends the distances for leakage through the insulators (*creepage distance*) described in Table 9.9.

Table 9.9: Creepage distance

Pollution	*Creepage* mm per kVrms phase-to-phase
Light	16.0
Medium	20.0

Therefore, for "light" pollution, the necessary leakage distance is of

$$1.2 \cdot 1{,}000 \cdot 16 = 19{,}200 \text{ mm}$$

From a manufacturers' catalog, the options can be obtained (Table 9.10):

Table 9.10: Insulator characteristics

	IEC	ANSI	Seves AC Catalog		
Type	**F24 170**	**N21/156**	**CS11**	**F400 205**	**F530 240**
Diameter (mm)	280	280	280	360	360
Step (mm)	170	156	170 156	205	240
Creepage (mm)	380	380	380	550	620
kN	240	222	222	400	530

Under the maximum transverse wind and cable weight, the tension of the insulators will be of 180 kN. Therefore, the F400 insulator can be chosen, presenting a safety coefficient of 2.2. The bundle being considered is of 8 ACSR 795 MCM *Tern* conductors.

According to the IEC standard, we have:

Number of insulators = 19,200/550 = 35
Length of string = 35 · 205 = 7,175 mm

It must be observed, however, that in the case of the string in V, 90°, the horizontal and vertical projection will be:

7,175 · 0.707 = 5,072 mm (add hardware 0.25 m and bundle radius 0.6 m)

Note: there is a project of polymeric insulators being developed that could be used in this line (Annex 17).

9.3.1.2 Distance from the live part to ground

Considering the standard deviation of 2%, then the 50% value for the project will be:

$$V_s = \frac{1200\sqrt{\frac{2}{3}}}{1-0,006} = 1042 \qquad kV\ (fase\text{-}terra)$$

Considering a correction of 0.92 due to atmospheric conditions, the value would be 1,133 kV, and the insulation distance would be of 2.50 (conductor-to-tower).

For a phase-to-phase distance, we would need 6 to 7 m (overvoltage of 1.73 · 1,133 = 1,960 kV).

9.3.1.3 Swing of the conductors

Under the effect of the wind, the "I" string will present swing at the tower and in the cable at the middle of the span. These swings are important for insulation to be maintained in the line, and without objects at the limit of the right-of-way.

Based on NBR 5422/1985, in the Northeastern region where the line will cross, the following wind distribution values were adopted:

$\alpha \leq 0.3$
$\beta \leq 11$

For return in 50 years, we would have the wind (average of 10 min):

$$V_{50} = \beta - \frac{In\left(-In\left(1-\left(\frac{1}{T}\right)\right)\right)}{\alpha}$$

$$V_{50} = 11 - \frac{In\left(-In\left(1-\left(\frac{1}{50}\right)\right)\right)}{0,56} = 24,0 \quad \frac{m}{s} \quad => V_{10}$$

The correction of the wind for the average height of 30 m:

$$V_{30} = V_{10} \cdot \left(\frac{30}{10}\right)^{\frac{1}{11}} = 26,5 \quad \frac{m}{s}$$

The correction of the integration interval of 30 s:

$k_d = 1.21$ (Type B terrain)

And, therefore, the design speed for swing:

$$V_p = 26,5 \cdot 1,21 = 32,1 \quad \frac{m}{s}$$

The conductor swing angle (NBR 5422):

$$tan\ \beta_r = \frac{q_0 d}{P\left(\frac{V}{H}\right)}$$

$$q_0 = \frac{1}{2}\rho\ V_p^2 = \frac{1}{2}1,293\left(32,1\right)^2 \quad \text{e} \quad \text{d} = 0,0296 \text{ m}$$

and the relation of weight/wind in a span:

$$\frac{V}{H} = 0,7$$

The value of wind effectiveness in the span is K = 0.32 and the swing angle:

$\beta = tan^{-1}(K \cdot tan(\beta_r))$
β = 32,2 (for the *Tern* conductor)

The calculation of the swing can also be done according to the TB 048. It recommends the use of wind speed (average of 10 min), and span factor equal to 0.73; or by IEC 826, same wind and span factor 0.87. In these cases, the angles would be 49º for the Rail conductor, and 54º, for the *Tern* conductor.

So, a swing of 54º with minimum conductor mass distance of 2.5 m was adopted.

To determine the width of the right-of-way, it is needed the swing at mid-span, which is calculated under the same conditions mentioned above, but with wind span over weight span relation equal to 1.0. In this case, the swing angle is ~44º for the *Tern*. Additionally, the horizontal projection of the sag plus string to be added to the 2.5 m distance must be considered.

9.3.2 Switching insulation

According to the ANEEL's Auction Notices, the insulation (*gaps*) must be verified so as not to incur risk of disconnection due to switching overvoltage (Table 9.11).

Table 9.11: Maximum risk of fault per circuit (energization and reclosing)

Switching	Risk of fault (dimensionless)	
	Phase-to-ground	Phase-to-phase
Energization	0.001	0.0001
Reclosing	0.01	0.001

9.3.2.1 Energization

The calculation was done for the most critical case and is summarized as follows. Table 9.12 presents the overvoltages in various points of the grid (average and deviation); risk gaussian (m_{risk} = m-CFO; s_{equiv}); and risk in each phase.

Table 9.12: Calculation of risk per points of the grid (CFO=> F-T 2025 kV, and F-F 3575 kV)

		Average (m)	Deviation (s)	(m-CFO)	s_{equiv}	Risk
Start	Phase A	1,125.6	32.1	-899.4	125.7	4.13E-13
	Phase B	1,049.8	39.9	-975.2	127.9	1.22E-14
	Phase C	1,045.5	33.9	-979.5	126.1	4.11E-15
	Phase A – B	1,897.5	60.7	-1,677.5	222.9	2.65E-14
	Phase B – C	1,775.1	69.4	-1,799.9	225.4	0.00E+00
	Phase A – C	1,883.2	67.5	-1,691.8	224.9	2.66E-14
25%	Phase A	1,224.8	48.7	-800.2	130.9	4.87E-10
	Phase B	1,159.2	64.8	-865.8	137.7	1.62E-10
	Phase C	1,127.8	34.2	-897.2	126.2	5.90E-13
	Phase A – B	2,110.6	76.1	-1,464.4	227.6	6.22E-11
	Phase B – C	1,913.3	95.9	-1,661.7	235	7.65E-13
	Phase A – C	2,029.6	66.1	-1,545.4	224.5	2.90E-12
50%	Phase A	1,299.9	66	-725.1	138.3	7.82E-08
	Phase B	1,220.4	90.2	-804.6	151.3	5.29E-08
	Phase C	1,186.5	36.9	-838.5	127	2.00E-11
	Phase A – B	2,247.2	101.6	-1,327.8	237.3	1.10E-08
	Phase B – C	2,003.6	115	-1,571.4	243.4	5.38E-11
	Phase A – C	2,127.5	59.8	-1,447.5	222.7	4.00E-11
75%	Phase A	1,332.2	79.2	-692.8	145	8.90E-07
	Phase B	1,238.4	104.2	-786.6	160.1	4.44E-07
	Phase C	1,214.3	45.3	-810.7	129.7	2.03E-10
	Phase A – B	2,313.5	124.6	-1,261.5	248.1	1.83E-07
	Phase B – C	2,023.4	129.1	-1,551.6	250.3	2.87E-10
	Phase A – C	2,170.2	66.7	-1,404.8	224.6	2.00E-10
End	Phase A	1,325.3	87.3	-699.7	149.6	1.45E-06
	Phase B	1,230.5	116	-794.5	168	1.13E-06
	Phase C	1,205.1	47.4	-819.9	130.4	1.63E-10
	Phase A – B	2,307.4	136.1	-1,267.6	254	3.02E-07
	Phase B – C	2,011.4	140.4	-1,563.6	256.3	5.31E-10
		2,158.4	79.7	-1,416.6	228.8	2.99E-10

The total risks per point are allocated in Figure 9.2.

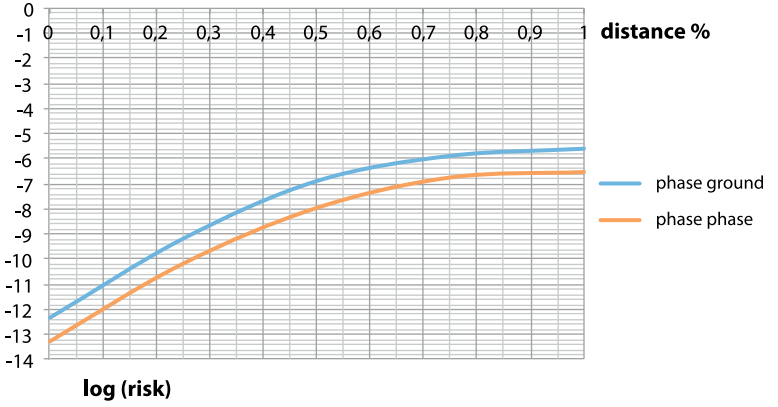

Figure 9.2: Risk logarithm per tower

By composing the risk, now for all the towers (900), it can be obtained (Table 9.13).

Table 9.13: Risk per section

Number of towers	Distance pu	Risk per tower F-T	Risk log	Risk per tower F-F	Risk log
90	1	2.58E-06	-5.59	3.03E-07	-6.51
90	0.9	2.00E-06	-5.7	2.51E-07	-6.6
45	0.8	1.59E-06	-5.8	2.51E-07	-6.6
45	0.75	1.34E-06	-5.87	1.84E-07	6.73
90	0.7	1.00E-06	-6	1.26E-07	-6.9
90	0.6	3.98E-07	-6.4	3,98E-08	-7.4
90	0.5	1.31E-07	-6.88	1.11E-08	-7.95
90	0.4	2.00E-08	-7.7	2.00E-09	-8.7
45	0.3	2.00E-09	-8.7	2.00E-10	-9.7
45	0.25	6.49E-10	-8.7	6,58E-11	-10.18
90	0.2	2.51E-10	-9.6	1.59E-11	-10.8
90	0.1	6.31E-12	-11.2	1.00E-12	-12
0	0	4.29E-13	-12.36	5.32E-14	-13.27
Total 900	–	6.83E-04	–	8.56E-05	–

Resulting in:

- phase-to-ground: $0,7 \cdot 10^{-3}$ for 2,025 kV.
- phase-to-phase: $0,9 \cdot 10^{-4}$ for 3,575 kV.

The corresponding gaps can be calculated by:

$$CFO = k\left(\frac{3400}{1+\frac{8}{d}}\right)$$

With d being the *gap* in (m) and *k* the *gap* factor, for:

- k = 1.15 conductor-to-tower window.
- k = 1.35 conductor-to-tower.
- k = 1.4 conductor-to-guy wire.
- k = 1.3 conductor-to-any object (agricultural machinery – add 4m; then obtain the conductor-to-ground distance).
- k = 1.52 between conductors in the span (α = 0.33 IEC).

The *gaps* would be (Table 9.14):

Table 9.14: *Gaps* for switching overvoltages

CFO (kV)	2,025	3,575
Conductor-to-tower window	8.6	–
Conductor-to-tower	6.4	–
Conductor-to-guy wire	6	–
Conductor-ground (with object)	10.9	–
Between conductors in the span	–	18

Note: the correction due to atmospheric conditions is 1.0 for the region.

For strings in "I", some international practices admit angle of about 10° simultaneously with surge for the phase-to-ground distances.

9.3.2.2 Reclosing

Using the same CFO values, the following risks for the reclosing overvoltages can be obtained:

- Three-pole reclosing ≧ 4.4 E-06 phase-to-ground and 2.2 E-06 phase-to-phase.
- Single-pole reclosing ≧ 7.9 E-04 phase-to-ground.

Therefore, meeting the defined criteria.

9.3.3 Towers

Three types of towers will be considered: self-supporting (Figure 9.3); single mast guyed (Figure 9.4); and trapezoid (Figure 9.5).

The following conditions must be respected:

9.3.3.1 Power frequency

- Number of insulators 400 kN, 205/360 mm, *creepage* 550 mm: F-T => 35 insulators, length > 7.2 m.
- *Gap* in air 2.5 m
- Swing angle (I string) 54º.

9.3.3.2 Switching surge

- *Gap* in air:
  - Window 8.6 m.
  - Tower 6.4.
  - Stay 6.0.
  - To ground 10.9 m (with object of 4.5 m).
- Swing angle (I string) 10º.
- *Gap* F-F 18.0 m (without swing).

Note: The distance from the conductor to the ground is governed by the electric field.

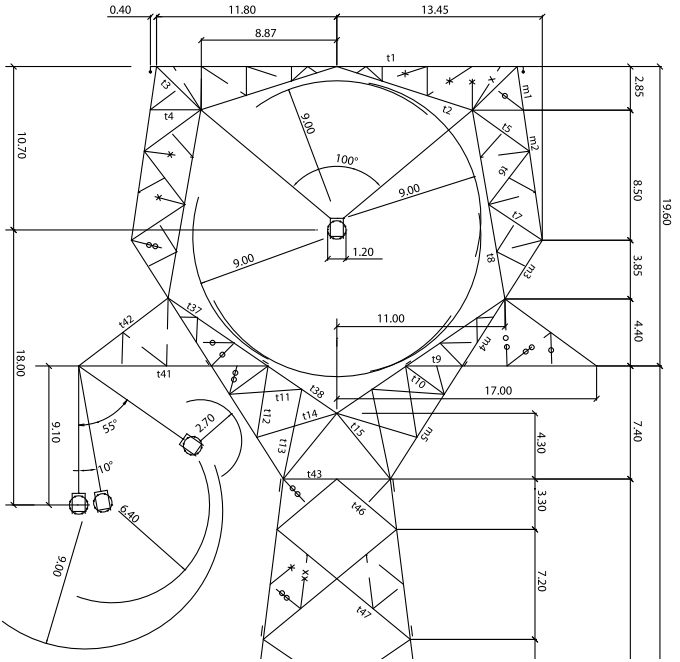

Figure 9.3: Self-supporting tower (weight 46.1 tons)

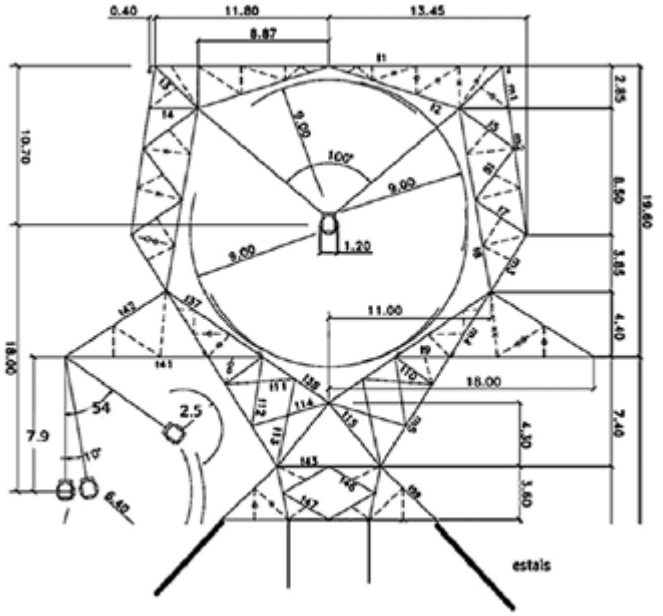

Figure 9.4: Guyed single mast tower (weight 33.7 tons)

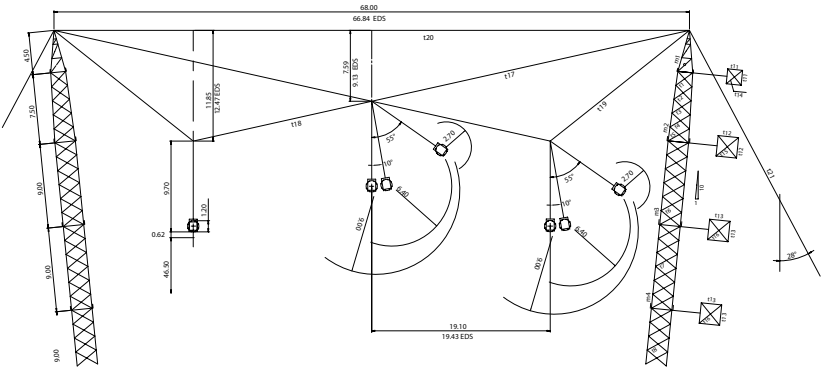

Figure 9.5: Trapezoid tower (weight 17.6 tons)

9.3.4 Overvoltage due to lightning

Atmospheric discharges influence the sizing of the shielding angle of ground wires over the conductors, as well as in line insulation and tower grounding.

9.3.5 Positioning of ground wires

The positioning of ground wires is done so that lightning of intensity higher than the critical does not directly hit into the phase conductors. The critical value for lightning intensity is:

$$I_C = 2 \cdot \frac{CFO}{Z_C}$$

Being that, in this present case:

$CFO > 4{,}350$ kV (for the *gaps* determined by switching overvoltage)

$Z_C \sim 300\ \Omega$

$I_C = 29$ kA

According to the equations in [1], the shielding angle (for conductor lightning) could be of up to 27º (flat terrain).

This angle can be smaller from a perspective of outage due to indirect stroke (*backflashover*), using a smaller angle due to the phase-ground wire coupling, which is the case for the types of towers being discussed.

9.3.6 Outages due to indirect strokes (backflashover)

Regarding the outages caused by lightning hitting the tower or the shield wires, the requirement is 1 outage per 100 km of line per year. Considering the insulation for impulse level (higher than 3,000 kV), the number of faults become very small (if not null).

9.3.7 Simulations with IEEE Flash

By using the Flash software, it was determined the discharge rate (*flashovers*), the minimum critical current, and the shielding angles. For the tower in Figure 9.3, the results are presented in Table 9.15.

Table 9.15: Performance for atmospheric discharges

Flashover Rates		
Backflash	0.36	/100 km/year
Shielding fault	0.00	/100 km/year
Total	0.36	/100 km/year

9.4 Corona effect

The consequences of the corona effect are the noises that affect radio reception (radio interference) and cause audible sounds (audible noise), in addition to TV interference, and losses in the lines other than the resistive losses.

The indication of this phenomenon is the maximum electric gradient on the surface of the conductors.

9.4.1 Gradient on the surface of the conductors

The calculation is done for the maximum operating voltage and uses the following expression.

$$V = HQ$$

With V being the phase-ground voltage; Q the load per phase; and H the Maxwell potential coefficients, line geometry functions (bundle configuration, heights, and conductor abscissas).

To represent the conductor to ground height, the calculation can be done considering the equivalent height (mid-span plus 1/3 of sag), or the mid-span configuration, the latter resulting in higher results.

Once the load per phase is determined, it can be admitted (by approximation) that it is distributed equally per sub-conductor, which allows for calculating the average maximum gradient on the surface, considering the diameter of the sub-conductor. The maximum gradient is the average maximum gradient multiplied by the distortion factor (function of conductor radius, number of conductors per phase, and bundle radius).

These gradients must be lower than the Peek's critical gradient, which, in turn, is a function of diameter, relative air density, and surface factor. A security margin of 5 to 10% is usually considered.

The calculations were done here for the towers considered.

Regarding the configuration of the conductors, the following alternatives were analyzed: 8 x 954; 8 x 795; 6 x 954; 6 x 1192, 5 MCM.

The results are presented in Table 9.16.

Table 9.16: Maximum power gradients on the surface of the conductors (kV/cm)

Tower	kV/cm		Configuration	Note
	Central	External	N x MCM	
Self-supporting	15.99	16.06	8 x 954	Equivalent height
Single mast guyed	17.16	17.13	8 x 795	Equivalent height
Trapezoid	19.05	17.53	8 x 795	Equivalent height
Self-supporting	17.24	17.31	8 x 795	Equivalent height
Single mast guyed	17.04	17.51	8 x 795	Mid-span
Trapezoid	19.02	17.79	8 x 795	Mid-span
Self-supporting	17.15	17.64	8 x 795	Mid-span
Single mast guyed	19.10	19.10	6 x 954	Equivalent height
Single mast guyed	17.43	17.43	6 x 1,192.5	Equivalent height
Single mast guyed	18.99	19.53	6 x 954	Mid-span

Table 9.17: Peek's gradient (kV/cm)

Safety factor	1	0.9	MCM
Peek's gradient	19.75	17.78	954
Peek's gradient	20.09	18.08	795
Peek's gradient	19.39	17.45	1,192.5

It was seen that the configurations with eight sub-conductors meets the criteria (in the case of the trapezoid tower, increase the space between the phases), and so does the configuration in six conductors.

9.4.2 Radio interference

The noise values in the AM band were calculated for the three types of towers, and considering the minimum conductor to ground heights determined in the electric field item. The results are presented in Figure 9.6 for atmospheric conditions corresponding to 50% of the time (fair weather). The signal level was considered 66 dBμ and the signal-noise relation 24 dBμ (noise 42 dBμ).

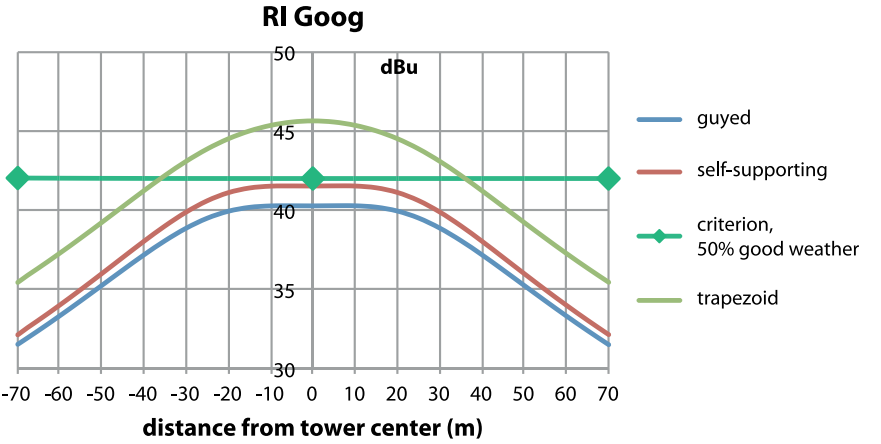

Figure 9.6: Noise (radio interference)

This phenomenon does not govern the definition of the right-of-way.

9.4.3 Audible noise

Audible noise was calculated for the three tower alternatives (Figure 9.7), and compared to the project criterion of 58 dBA, for the humid conductor condition (average value).

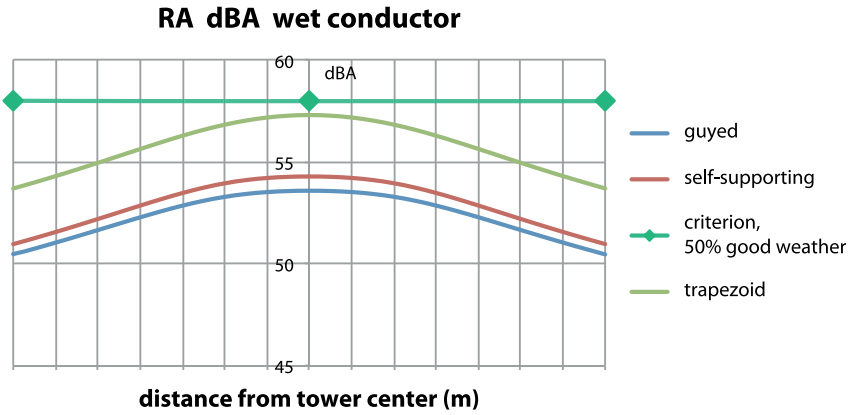

Figure 9.7: Audible noise

This phenomenon also does not govern the definition of the right-of-way.

9.5 Electric and Magnetic Fields

9.5.1 Electric field

The electric field on the ground was calculated for the alternative 8 x 795 MCM, considering the conductor at the minimum height from the ground. The effect of the loads on the phases and on their images on the ground were considered. The results are presented in Figure 9.8.

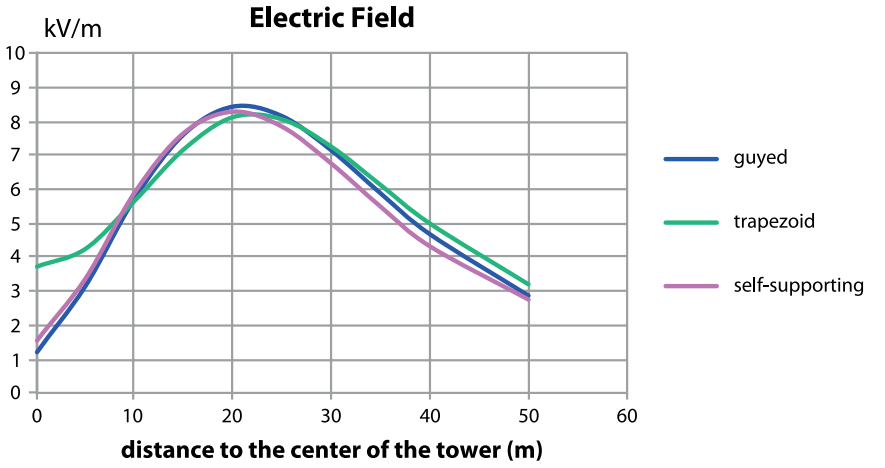

Figure 9.8: Electric field on the ground (8x795 MCM)

As a reference criterion, it was adopted 8.33 kV/m within the right-of-way, and 4.17 kV at the limit of the right-of-way (ANEEL Resolution 616), which resulted in the following values for minimum height from the conductor to the ground and width of the right-of-way (Table 9.18).

Table 9.18: Minimum conductor height and right-of-way

	Minimum height (m) phases a/b/c	Right-of-way
Single mast guyed	24.5/42.5/24.5	85
Trapezoid	25.0/29.2/25.0	90
Self-supporting	24.5/42.5/24.5	85

9.5.2 Magnetic field

The magnetic field calculations were made for the three types of towers, and considering the minimum conductor heights. The results are presented in Figure 9.9.

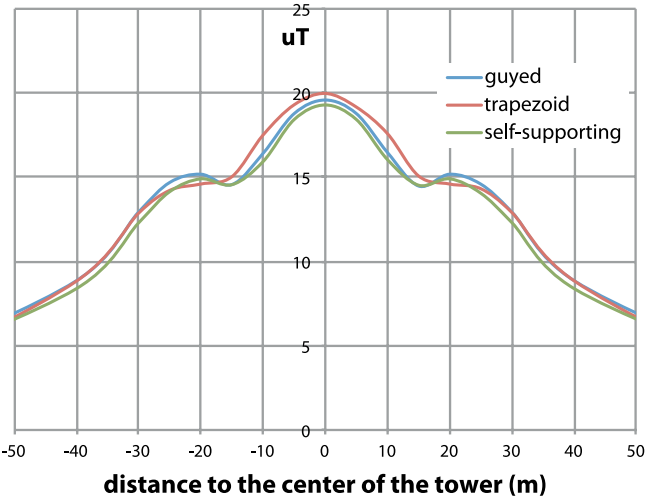

Figure 9.9: Magnetic field

The criterion established (ICNIRP- for the general public) was of 83.3 μT, which has been increased recently. Thus, all the alternatives meet the established criteria.

9.6 Determining the Right-of-Way

The right-of-way must meet the electric and magnetic fields, corona effect, and insulation coordination criteria (safety).

Regarding the insulation coordination, the criteria to be considered is preserving the distance of 2.5 m with wind, a return period of 50 years (swing of 44º).

Therefore, it is necessary to determine the temperature expected for the conductor, and then determine the conductor sag. Assuming 50° C as maximum conductor temperature, for a span of 500 m the sag of the conductor (795 MCM) would be of 22 m. Considering the swing of the conductor and string (I), the limit of the right-of-way would be of 24 m from the center of the external conductor.

Table 9.19 shows the various requirements.

Table 9.19: Right-of-way (m)

	RI RA	Electric field	Insulation	Final
Single mast guyed	NA	85	84	85
Trapezoid	NA	95	86	95
Chinese	NA	85	82	85

9.7 Determining the Height of the Conductors

The minimum height of the conductor to the ground is determined through the electric field criteria (Table 9.18).

To determine the height of the conductors in the tower for a span of 500 m, we must add the sag and the height of the string in I, that is, ~ 30 m.

9.8 Current Capacity

The line will have a minimum transmitting capacity of 5,000 MVA. Therefore, 2.9 kA per phase, which means approximately 360 A per conductor (bundle of 8 conductors). Assuming wind speed of 0.6 m/s, and environment temperature of 40ºC, the conductor temperature would go to < 50ºC. This should be, initially, the maximum temperature of the line design.

During emergency conditions, it should transmit the equivalent to 35% more (admissible series capacitor overload), which means 3.6 kA. This current would cause an elevation of 15°C in the conductor that, being at the ambient temperature of 40°C, would amount to 55° C, and to additional sag lower than 0.5 m.

9.9 Mechanical Design

The mechanical design of the transmission line aims to define the stress conditions on the tower and foundations for their sizing, efforts resulting from the weight of the cables, winds, and assembly conditions.

The towers and foundations were calculated for a wind span of 500 m, weight span of 750 m, and angle zero.

9.9.1 Wind pressures

Regarding the wind, the design requirement established by ANEEL is the intensity corresponding to the return period of 250 years. Based on the same distribution defined in item 9.3, it can be obtained for the basic speed according to NBR 5422 (10 meters from the ground, interval period of 10 minutes):

$$V0 = 29.4 m/s \text{ or } 105.8 km/h$$

For the Colinas-Miracema-Gurupi-Peixe-Serra da Mesa line, the local speed indicated was 85 km/h. For the lines of the Teles Pires plant, the wind speed adopted was of 120 km/h, but on the conductor (10 m above the ground). Other lines from Eletronorte were designed for winds higher than 110 km/h. Thus, it was concluded that the adoption of the above-proposed value, would be adequate.

9.9.1.1 Maximum design wind on the cables

The forecasts for pressure on the conductor, considering the average height and IEC 60826 methodology, are:

- external cable 107.3 kgf/m^2;
- internal cable (higher) 114.8 kgf/m^2;
- Ground wires 118.3 kgf/m^2.

9.9.1.2 High intensity wind

There is no internationally accepted and standardized criterion for defining the wind velocity resulting of Electric Storms (high intensity wind). In the absence of specific data about wind speeds during this type of storms, it has been customary to increase the extreme gust wind (t = 3 s) for the return period of the design by a factor close to 20%, with a narrow acting front. Thus, next, we will determine only the high intensity wind for the return period of 250 years, to be adopted in the design.

The value of the high intensity wind will be determined by the criterion above. Considering the extreme wind speed for the return period of T = 250 years, we obtain the following value for the high intensity wind (V_{ai}):

$$V_{ai} = 29.4 \cdot 1.39 \cdot 1.2 = 49.04 \text{ m/s}$$

The factor 1.39 is applied to the 10-minute wind to obtain the gust at 3 seconds. We consider that this wind acts only on part of the span, thus, the adopted pressure on the cables was of 37.5 kgf/m^2.

9.9.1.3 Other pressures

- For the insulator strings, we determined 167.7 and 161.1 kgf/m^2 for the external and internal phases, respectively.
- For the structure, the pressures were determined according to NBR 5422 (see Annex 18).

9.9.2 Tensions and sags

9.9.2.1 Cable data

The conductor to be used is Aluminum Conductor Steel Reinforced (ACSR) type, with a single gauge in the entire length of the line is the ACSR *Tern*, with the characteristics of Table 9.19.

The ground wire to be used in the calculation is the galvanized steel, 3/8" EAR, and its data is indicated in Table 9.19.

Table 9.19: Characteristics of the cables used

Description	Unit	795 MCM	∅ 3/8"
Type of cable	Stranded cable	ACSR	EAR
Rated diameter of the wire	mm	3.38-Al 2.25-steel	3.05
Number of wires	37 wires	45x7	7
Rated diameter of the cable	mm (")	27.03	9.52 (3/8)
Minimum failure load	kgf	10,025	6,990
Approximate weight	kgf/m	1.366	0.406

9.9.2.2 Combinations of temperature and wind pressures for calculation of tensions and sags

The combinations of wind speeds and temperature for the purpose of determining tensions and sags are shown in Tables 9.20 and 9.21. For the ground wires, the wind pressures are slightly higher, due to their higher height related to the ground (Table 9.22).

Table 9.20: Tensions and sags for the external conductor

Cond.	θ (°C)	Wind pressure (kgf/m^2)	Tf (kgf)	Tf (%)	Ti (kgf)	Sag final (m)
EDS predominant tension	24	0	2,005	20.0	2,145	20.83
Vmax	20	107.3	4,434	44.2	4,542	22.54
V45	20	53.65	2,889	28.8	3,049	21.35
V_{ai90}	20	37.5	2,493	24.9	2,649	21.03
V_{ai45}	20	18.75	2,152	21.5	2,299	20.76
θmin	7	0	2,080	20.7	2,233	20.06
θmax	75	0	1,819	18.1	1,927	22.97

Tf – final tension; **Ti** – initial tension

Table 9.21: Tensions and sags for the internal conductor

Cond	θ (°C)	Wind pressure (kgf/m^2)	Tf (kgf)	Tf (%)	Ti (kgf)	Sag final (m)
EDS	24	0	2,005	20.0	2,145	20.83
Vmax	20	114.8	4,656	46.4	4,747	22.69
V45	20	57.4	2,989	29.8	3,149	21.42
V_{ai90}	20	37.5	2,493	24.9	2,649	21.02
V_{ai45}	20	18.75	2,152	21.5	2,299	20.75
θmin	7	0	2,080	20.7	2,233	20.06
θmax	75	0	1,818	18.1	1,927	22.96

Tf – final tension; **Ti** – initial tension

Table 9.22: Tensions and sags for the ground wire 3/8" EAR

SW	θ (ºC)	Wind pressure (kgf/m²)	Tf (kgf)	Tf (%)	Ground wire sag (m)	Fcond(m)
EDS	24	0	680	9.7	18.68	20.83
Vmax	20	107.3	1,700	24.3	21.28	22.54
V45	20	53.65	1,076	15.4	19.66	21.35
V_{ai90}	20	37.5	871	12.5	19.10	21.03
V_{ai45}	20	18.75	737	10.5	18.73	20.76
θmin	7	0	697	10.0	18.23	20.06
θmax	40	0	666	9.5	19.10	22.97

Tf – final tension; **Ti** – initial tension

9.9.2.3 Calculation criteria

The cables should be sized to withstand tension states – basic, and normal tension –, defined based on the combination of climate and cable aging conditions as follows.

a) Basic state

- For minimum temperature conditions, the maximum axial tension must be limited to 33% of the cable failure tension.
- For wind conditions with the return period of 50 years, the maximum axial tension must be limited to 50% of the cable failure tension.
- For extreme wind conditions, as defined in item 5, the maximum axial tension must be limited to 70% of the cable failure tension.

b) Normal tension state (EDS - *everyday stress*)

- In the final settlement, at average temperature, no wind, the average tension level of the cables must comply with the definitions in the NBR 5422 standard. Which means, EDS equal to 30% of the failure load. Additionally, the average tension of the cables must be compatible with the mechanical performance with regards to the stress along the life period of the transmission line.

More calculation details and the loading tree are presented in Annex 18.

10. Equipment Requirements

The feasibility studies for the expansion of the SIN to lodge the expansion of wind and photovoltaic power were performed considering a 1,000 kV rated system, with four 500/1,000 kV substations, dividing the line into three sections with approximately the same length, 440 km each. The series compensation is approximately 50%, whereas the parallel compensation 85%.

This item presents the evaluation of the equipment requirements.

10.1 Substations

The study considered that the four substations will be new ones (i.e. they are not expansions of the existing substations), connected through sectioning of the existing 500 kV lines, so as to allow for future expansion of the 1,000 kV system, and the connection of the generation system.

For the 1,000 kV yard, technology alternatives are considered:

- *Open Air Insulation Substation* (AIS).
- *Gas Insulated Substation* (GIS).
- *Hybrid Substation* (HGIS) (gas insulated equipment, and air insulated busbars.

For the final decision about which technology will be used, the following information was requested from the manufacturers:

- Feasibility of the equipment with the desired specifications.
- Weights (total and for transportation).
- Dimensions.
- Estimated costs (basic specifications, and sensitivity to the parameters).

10.2 Overvoltage, Insulation, and Surge Arrester Requirements

10.2.1 Overvoltages

Detailed overvoltage studies were conducted in the system, and the highest values obtained (in the substations) in values per unit of $1.000 \cdot \sqrt{2}/\sqrt{3}$ kVp are:

- Line energization
  - ▷ Phase-to-ground
    V_m (maximum measured) = 1.86 pu
    V2 (2% probability of being exceeded) = 1.84 pu

  - ▷ Phase-to-phase
    V_m = 3.28 pu
    V_2= 3.16 pu

Note: the circuit breaker has a 400 Ω pre-insertion resistor (inserted for 8 ms) – values without the action of line or reactor surge arrester.

- Line reclosing
  - ▷ Phase-to-ground
    Vm = 1.81 pu
    V2 = 1.70 pu

  - ▷ Phase-to-phase
    Vm = 2.95 pu
    V2 = 2.82 pu

Note: Three-phase reclosing after about 0.3 s. Without the action of the surge arrester.

For single-phase reclosing, the overvoltage values were approximately the same.

- Extinction of the secondary arc

The shunt reactors must be provided with a 250 Ω neutral reactor (60≈Hz).

The secondary arc sustained due to the single-phase fault with single-phase opening is 70 Ap lower, and the first recovery voltage peak is of 34 kVp. The maximum voltage sustained in the neutral reactor is of 130 kV.

For the three-phase opening, the arc current is small, and the neutral reactor voltage is of 180 kVp.

- Fault application (due to the single-phase fault)

The highest overvoltage Vm values are in the healthy phases, in the middle of the intermediary section (Vm = 1.52 pu). However, in the substations, the highest value measured was lower than 1.15 pu.

- Removal of single-phase fault

For three-phase opening V_m = 1.92 pu
For single-phase opening V_m = 1.35 pu

- Load rejection (or feeder circuit-breaker opening the load)

The voltage sustained was lower than 1.15 pu.

If a fault occurs after the opening of the circuit breaker in one extremity, the overvoltage in the healthy phase is of 2.27 pu. In this case, the surge arrester conducts current.

10.2.2 Surge arrester requirements

The surge arrester modeled had 828 kV rating, one column, with the V-I characteristics presented in tables 10.1 and 10.2.

Table 10.1: V-I Curve (30/60 us)

I (kA)	V (kV)	V (pu)
0.5	1,596	1.95
1	1,643	2.01
2	1,673	2.04
3	1,692	2.07

Table 10.2: V-I Curve (impulse)

I (kA)	V (kV)
10	1,827
20	1,973
40	2,143

Alternatives with 780 kV and 828 kV ratings, with 4 columns in parallel, and one special with 6 columns with smaller varistors, were also examined.

Details of the prototype of the 6 columns surge arrester is presented in Annex 17,

10.2.3 Insulation coordination

Assuming coordination currents of 2 kA for switching surge, and 20 kA for atmospheric surge, with safety margins of 1.15 and 1.25, respectively, the following results were obtained:

- Withstanding ($V_{10\%}$) for switching surges equal to 1950 kV – surge arresters with one column. In the case of the other two above-mentioned alternatives, the withstanding value for switching surges would be 1,800 kV.
- Withstanding ($V_{10\%}$) for lightning surges would be 2,400 kV.

Due to the above-mentioned levels, the air distance from the conductor to tower is 7.0 m and between phases 18 m (CFO = 3,575 kV). To meet the electric field criteria, the minimum distance to the ground should be 26 m.

Although the pollution level in most of the system may be classified as "light", for the substation insulation the adoption of a "medium" pollution level or 25 mm per kVrms phase-to-phase is recommended. This would lead to an "I" string with 55 insulators (205/360 mm, height/diameter of an insulator unit) and a length of 11.3 m.

10.3 Busbar Arrangement

As an initial rule, the substations will have a one and a half circuit breaker arrangement (Figure 10.1). However, when using GIS double busbar arrangement, the single circuit breaker (four switches) should also be considered.

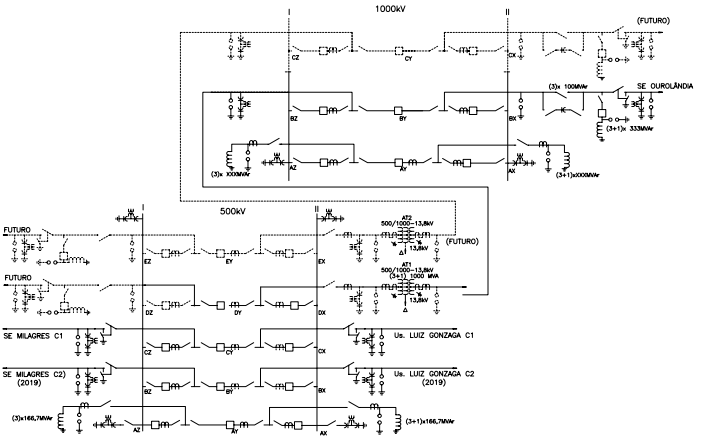

Figure 10.1: Example of busbar arrangement

10.4 Size of the AIS Substation

An air insulated substation (AIS), with one and a half 500 kV circuit breaker arrangement has the following dimensions:

- Span width: W = 45 m.
- Length of section switch up to the middle circuit breaker SG = 125 m.
- Length of series capacitor and line reactor SC + SR = 141 m.
- Height of busbar HB = 16 m; and HE = 24 m for line input.

Based on this, the estimated length of the 1,000 kV span should be of about SC + SG + SR = 500 m, and the width W = 55 m. Consequently, an area of A = 27.500 m^2 per span.

Note: reference [2] indicates the following values for the 1,000 kV substation:

- W = 48 m
- HB = 15 m
- A = 11,900 m^2 (without series capacitor)
- SG + SR = 248 m

Consequently, the size of the AIS Substation, with space for two lines plus three transformers would be of 165,000 m^2.

10.5 Equipment

For the final design, it is necessary to consider also the dimensions and costs of the equipment:

- Transformers.
- Line Reactor (plus neutral reactor).
- Series Capacitor.
- Circuit Breaker.
- Switching Devices (in general).
- Surge arresters.

10.5.1 Transformer

In this phase, the substation needs a voltage ratio of 500/1,000 kV with transformer capacities equal to 2,500 to 3,000 MVA (three-phase). Therefore, each single-phase auto-transformer will have a rated power in the range of 850 to 1,000 MVA (limited, very likely, by the transportation requirements).

Additional studies indicated a rated relation of 500/1,000 kV, grounded Y auto-transformer, with tertiary winding in delta, with 69 to 138 kV voltage, depending on the use. The surge arresters should be placed on each side of the transformer, as close as possible to the bushings.

According to the ONS rules, the transformers should have on-load tap changers (±10%), and primary-secondary reactance (X_{PS}) ≤ 12%. After debates with manufacturers in Brazil, an on-load tap changer with range of ±7.5% (33 positions) and reactance of X_{PS} = 14% was chosen, as a cost and weight compromise. The 850 MVA unit will weight 270 ton. For transportation, and have a total weight of 450 ton.

10.5.2 Line reactor (neutral reactor)

The line reactor banks will be composed of three single-phase units of 333 Mvar in 1,000 /√3 kV, which means rating of 403 Mvar at 1,100 /√3 kV.

The neutral reactor reactance should be 250 Ω at 60 Hz.

10.5.3 Series capacitor

The impedance of the series capacitor is 35 Ω/phase on each end of the line (section). Considering a rated current equal to 2.7 kA, it was obtained a capacitor with 250 Mvar/phase. The capacitor will have to withstand an overload of 35% for 30 minutes (3.6 kA). The continuous rated voltage of the series capacitor is of 93.4 kV.

The series capacitors must be equipped with MOV, gap and bypass circuit breaker for protection.

As there are many possibilities of generation dispatches, and the 500 kV lines in parallel restrict the flow of the 1,000 kV system, the series compensation can be bypassed in certain conditions.

The MOV should have characteristics similar to a ZnO 162 kV surge arrester.

More details will be provided in Annex 18.

10.5.4 Circuit breakers

The circuit breakers must have rated current of 4.0 kA, rated short-circuit current of 63 kA, and TRV according to the requirements of Table 10.3 [3]. The X/R relation is of 20 or 7.6 for three-phase or single-phase short.

Table 10.3: TRV according to [3]

Test duty	k_{pp}	k_{af}	u_c kV	t_2 or t_3 µs	U_1 kV	T_1 ms	RRRV kV/µs
T_{10}	1.2	1.76	1,897	271	–	–	7
T_{30}	1.2	1.54	1,660	332	–	–	5
T_{60}	1.2	1.5	1,617	808	808	269	3
T_{100}	1.2	1.5	1,617	1,212	808	404	2
T_{LF}	1.3	1.7 x 0.9	1,786				*

* See reference [3]

The feeder circuit breakers should contain closing resistor of 400 Ω with insertion time of 8 ms.

The transformer circuit breakers will be provided of synchronized closing and, eventually, closing resistor of 1,000 Ω.

10.5.5 Switching and other devices (insulator pole, air switches, and instrument transformer)

This equipment must have the previously mentioned insulation characteristics.

10.5.6 Surge arresters

One column, 828 kV surge arresters were simulated during overvoltages and, in general, did not conduct significant currents.

Other rated voltage values (for example, 5% lower) to provide a reduction in the equipment insulation level or increase in the insulation margin were also verified. The energy absorbed by these surge arresters was close to the one obtained for the 828 kV surge arrester in the general cases of overvoltage and N-1 contingency. However, the surge arrester must comply with the most critical criteria, for example, opening of two 1,000 kV lines on one extremity, followed by the occurrence of single-phase short, single-pole opening, unsuccessful single-pole reclosing, followed by three-pole line opening.

In this case, the surge arresters must have four columns, the overvoltage would fall to 1.95 pu, and the energy they must absorb would be 51 MJoule.

As an alternative, a 6 column 828 kV surge arrester was studied (Annex 9), under development in Brazil, that meets this demand. In both cases, the surge arrester guarantees adequate switching surge insulation margin for the equipment.

10.6 Costs

This section presents the procedures used in the studies to estimate the costs of the substations.

10.6.1 Transformers and line reactors

Reference [2] presents the following procedure for estimating the transformer and reactor costs.

$$\frac{C1}{C0} = \left(\frac{p}{P0}\right)^{0,75}$$ related to rated power P.

$$\frac{C2}{C0} \approx \left(\frac{U}{U0}\right)^{0,8}$$ related to voltage U.

In Brazil, Aneel's spreadsheets present the following estimated costs (FOB):

- Single-phase auto-transformer 750/√3: 345/√3kV, 500 MVA R$ 17.8 x 10^6.
- Single-phase line reactor 750/√3, 333 Mvar R$ 8.6 x 10^6.

Considering 1 US$ = 3.7 R$, Table 10.4 presents the results of the values.

Table 10.4: Costs of transformer and line reactor (10^6 US$)

Equipment	Desired classification	Reference price	Corrected for C1 and C2
Auto-transformer	500 MVA 1,000/√3 : 500/√3	4.9	6.07
Line reactor	333 Mvar 1,000/√3	2.26	2.80

10.6.2 Circuit breakers

Reference [2] indicates the following relation: 1.7 to 2.5 of 765 for 1,100 kV:

The estimated ANEEL cost for a 765 kV circuit breaker is equal to R$ 4.7×10^6 = US$ 1.27×10^6. Therefore, the 1,100 kV circuit breaker should cost $1.7 \times$ US$ 1.27×10^6 = US$ 2,16 x 10^6.

10.6.3 Substation cost

Reference [2] indicates the following relation:

$$\frac{C}{C0} = \left(\frac{U}{U0}\right)^{1,5}$$

The ANEEL cost for a bay of one and a half 765 kV circuit breaker is US$ 7.6×10^6. Therefore, the estimated cost of a bay of 1,100 kV results in US$ 13.1×10^6.

10.7 GIS 1,000 kV

GIS at 1,100 kV has been used in Japan and China and demonstrated proper performance.

According to [4], two types of arrangements are suggested for transmission above 500 kV in UHV: one and a half circuit breaker or simple double busbar 4 switch circuit breaker. The basic arrangement considered here is the one and a half circuit breaker. However, the single double busbar circuit breaker will also be examined.

Both alternatives, GIS and HGIS (hybrid) should be considered, and the decision as to which to adopt should be made after evaluating the cost in the life cycle (investments, maintenance, and operating costs), where the construction, maintenance, and land cost are part of the cost equation.

In all the substations, there is line input with series compensation, and parallel compensation. The line reactors may be connected to the side of the busbar or to the side of the series capacitor line, and may impact the costs.

11. Expansion of the Reference Alternative

This item presents the studies related to the expansion of the reference alternative. This evolution consists of the expansion up to the Ribeirão das Neves substation (Minas Gerais), distant 300 km from Pirapora, and the construction of another 1,000 kV circuit between Ourolândia and Ribeirão das Neves. Figure 11.1 presents this expansion.

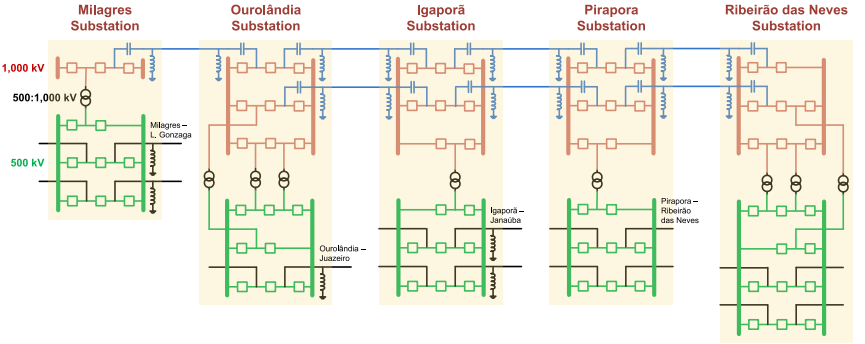

Figure 11.1: Expansion of the reference alternative

Figure 11.2 shows the single line diagram of the expanded system.

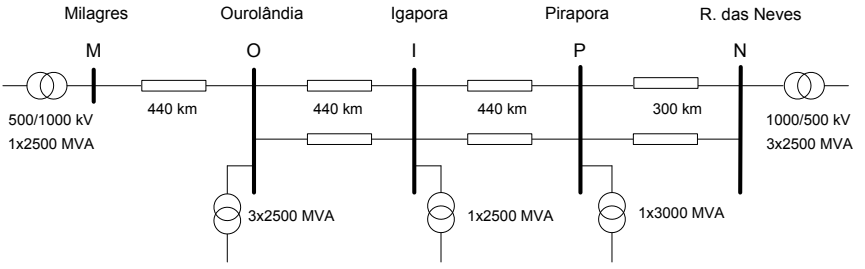

Figure 11.2: Single line diagram of the 1,000 kV expanded system

For this expansion, only the following verification studies were performed:

- Load rejection, and surge arrester effect;
- Transmission line energization;
- Fault application;
- Single-phase residual load;
- Single-pole reclosing;

- Three-pole reclosing;
- TRV;
- Calculation of series MOV.

11.1 Load Rejection and Surge Arrester

Load rejection tests were performed with and without single-phase fault, in addition to single-pole and three-pole reclosing for analysis both of overvoltage and energy absorbed in the surge arresters, with the latter test being performed with 4 types of surge arresters.

It is important to mention that, in the expanded system, the worst case of overvoltage in simple load rejection in the line occurred in the Ourolândia – Igaporã line, with 1.66 pu (1,355 kV peak) in the open terminal of the line, for opening via Igaporã.

With regards to energy absorption, 4 types of surge arresters were analyzed in the most critical case, the unsuccessful three-pole reclosing (after fault), as shown in Figure 11.3.

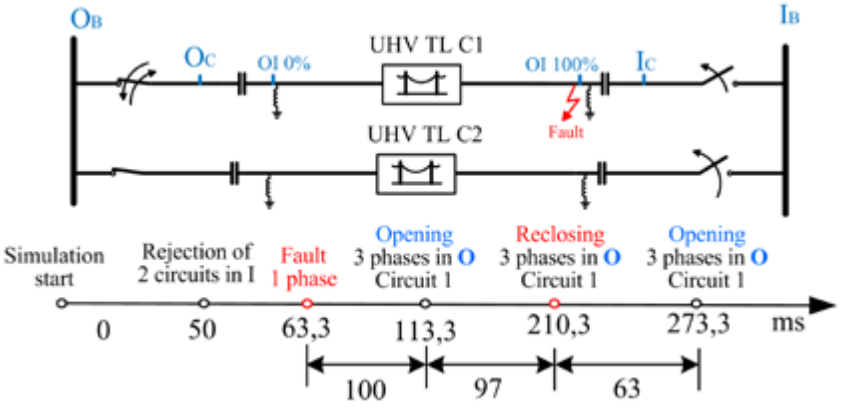

Figure 11.3: Single line diagram of the O-I section with rejection, short, three-pole opening, unsuccessful three-pole reclosing, and three-pole opening, and time line of the events

Table 11.1 presents the overvoltages and energy absorbed in the surge arresters analyzed. The different types of surge arresters were allocated to Bus I.

Table 11.1: Overvoltages and energy in the surge arrester

Type of surge arrester, value of the rated voltage (kV)	Maximum withstand energy (MJ)	Simulation results	
		Maximum voltage measured in the SA (pu)	Energy absorbed by the SA (MJ)
828	12.75	2.06	6.98
788	12.14	1.97	8.53
828 x 4 Columns	51.00	1.97	8.40
828 x 6 Columns	32.29	1.86	11.39

It was seen that the energy absorbed by the surge arresters did not exceed their rated capacity in any of the tests performed. On the other hand, the residual voltage value should be at 1.92 and 1.97 pu for a margin of 10 to 15% (insulation of 1,800 kV), regarding the insulation of the equipment.

Some other details are presented in Annex 9.

11.2 Line Energization

This study compared the reference system to the expanded system. The energization of the line was done in the Ourolândia – Igaporã section, energizing via Ourolândia (the most critical case reported in the reference system studies). The maximum overvoltage values obtained in the simulation of the expanded system occurred at the end of the O-I line, as presented in Table 11.2.

The overvoltages obtained in this study are lower than those obtained in the reference system for the same case. In the case of the phase-to-ground overvoltage, there was a reduction of 17.0% and, in the case of the phase-phase voltage, of 21.04%, related to the values obtained in the reference alternative.

Table 11.2: Result of the statistic energization

Overvoltage location	Phase-to-ground and Phase-to-phase	Average overvoltage (pu)	Standard deviation (pu)	Maximum overvoltage (pu)
0% of the TL	Phase A	1.137	0.030	1.135
	Phase B	1.187	0.030	1.182
	Phase C	1.141	0.046	1.198
	Phase B – Phase C	2.054	0.051	2.131
	Phase A – Phase C	1.944	0.067	2.071
	Phase A – Phase B	2.019	0.069	2.039
25 % of the TL	Phase A	1.231	0.043	1.227
	Phase B	1.293	0.039	1.290
	Phase C	1.214	0.041	1.203
	Phase B – Phase C	2.186	0.040	2.325
	Phase A – Phase C	2.066	0.072	2.161
	Phase A – Phase B	2.200	0.075	2.320
50% of the TL	Phase A	1.274	0.047	1.251
	Phase B	1.361	0.048	1.373
	Phase C	1.250	0.047	1.285
	Phase B – Phase C	2.253	0.059	2.331
	Phase A – Phase C	2.131	0.079	2.211
	Phase A – Phase B	2.288	0.074	2.438
75 % of the TL	Phase A	1.290	0.054	1.246
	Phase B	1.393	0.050	1.459
	Phase C	1.258	0.051	1.312
	Phase B – Phase C	2.265	0.070	2.314
	Phase A – Phase C	2.142	0.092	2.226
	Phase A – Phase B	2.327	0.076	2.484
100% of the TL	Phase A	1.290	0.064	1.250
	Phase B	1.394	0.062	**1.534**
	Phase C	1.245	0.058	1.302
	Phase B – Phase C	2.241	0.077	2.336
	Phase A – Phase C	2.120	0.108	2.216
	Phase A – Phase B	2.319	0.083	**2.565**

Some other details are presented in Annex 10.

11.3 Fault Application

Regarding the study involving single-phase faults (start of the fault) and consequent occurrence of overvoltages in the healthy phases, it was observed that in the expanded system these overvoltages are not high. These overvoltages proved to be lower than the values obtained when of the study of other types of phenomena such as, for example, line energization, lower even than those related to the fault application simulations in the reference alternative.

The results of the overvoltages in the phases are presented in Table 11.3. The maximum overvoltage value obtained is of 1.461 pu, which is 4.3% lower when compared to the values obtained in the reference alternative, which was of 1.526 pu.

Table 11.3: Overvoltages in the healthy phases of the Ourolândia – Igaporã section for single-phase fault at OI_{50}

	Peak values (pu) in the section Ourolândia – Igaporã				
Fault application instant (ms)	**OI_0**	**OI_{25}**	**OI_{50}**	**OI_{75}**	**OI_{100}**
14.7	1.091	1.254	1.461	1.291	1.107

Additional details are presented in Annex 11.

11.4 Single-phase Residual Load

In this case, with the 1,000 kV system operating "on-load", the secondary arc current (I_{ARC}) and recovery voltage (V_{REC}) values are slightly lower than the critical values obtained when of the same study in the reference alternative, in all the points of the sections where the fault was applied.

The influence of the system frequency variation in the arc extinction was analyzed. The reference values evaluated according to the guidelines established in [5] are 56 and 66 Hz.

Figure 11.4 presents the curve that relates the secondary arc current and grid frequency in the MO section, with short location 0%. It can be seen the nearly linear dependency of the secondary arc current and the frequency of the network.

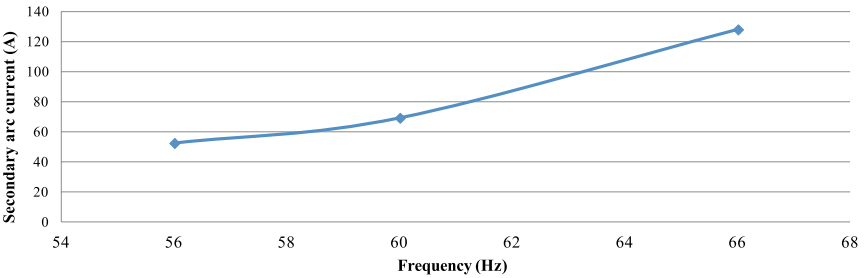

Figure 11.4: Secondary arc peak current versus frequency

Additional details are presented in Annex 12.

11.5 Single-pole Reclosing

For the single-pole reclosing simulations (Figure 11.5), it was selected the Milagres – Ourolândia section of the 1,000 kV line, because this section presented the highest overvoltage in the reference system.

The result obtained in the single-pole reclosing was a phase overvoltage of 1.838 pu, when the reclosing occurs via Milagres. This voltage value is slightly lower than the value obtained in the reference system, which was equal to 1.853 pu. This implies that changes in the expanded grid do not generate overvoltages higher than those obtained in the reference system in face of events with single-pole reclosing.

Figure 11.5 presents the main components represented in the Milagres – Ourolândia section used for the sequence of tests. The same figure also shows the timeline of the events.

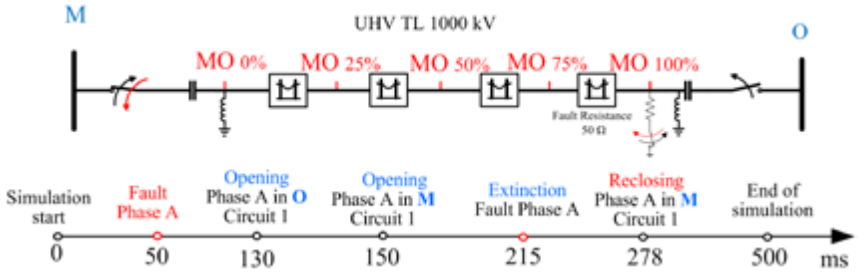

Figure 11.5: Detail of the Milagres – Ourolândia section

The worst case is presented in Figure 11.6, which is based on the statistic simulations performed.

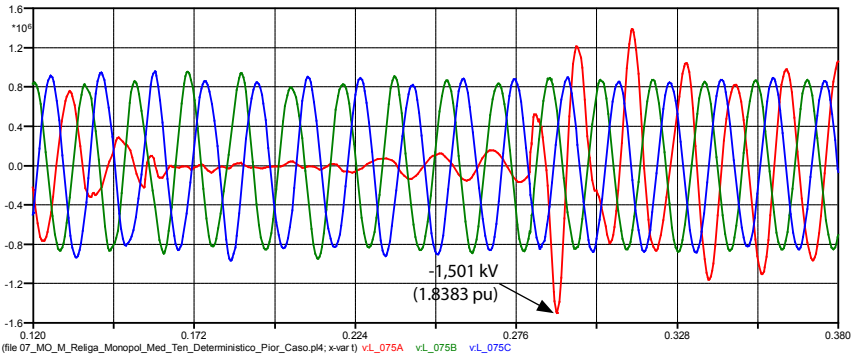

Figure 11.6: Worst case of maximum overvoltage at 75% of the M-O section, reconnected via M

Some other details are presented in Annex 13.

11.6 Three-pole Reclosing

Based on the information collected in the reference system, the worst case was registered in the Milagres – Ourolândia section, reconnected via Milagres. During the simulations for the expanded system for this same section, we verified that the maximum overvoltage in the reference system was of 1.791 pu, and in the expanded system it was of 1.804 pu, for the same condition, successful three-phase reclosing.

To analyze the impact on the expanded system in face of unsuccessful three-pole reclosing, a sequence of events was applied to the Milagres – Ourolândia section, with reclosing via Milagres, as presented in the timeline of Figure 11.7.

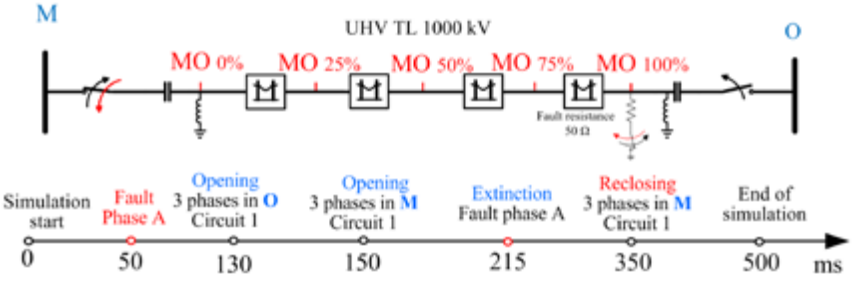

Figure 11.7: Milagres – Ourolândia section with sequence of reclosing events

Figure 11.8 shows one of the instants simulated when using systematic switches. It can be observed the highest overvoltage after the opening of the circuit breaker located at Ourolândia, which is much higher than the value obtained during the reclosing analysis. This behavior was observed in all the tests performed.

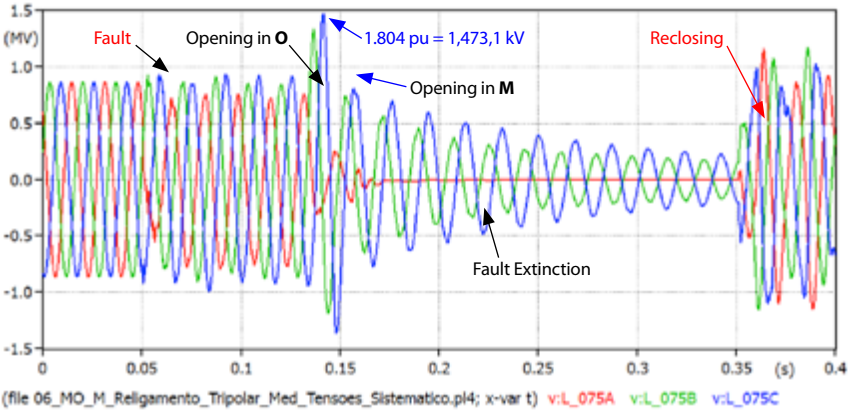

Figure 11.8: Voltage measured at 75% of the Milagres – Ourolândia section for reclosing via Milagres

Some other details are presented in Annex 14.

11.7 Transient Recovery Voltage (TRV)

The circuit breaker TRV studies were also conducted in the worst cases obtained on the "reference system" for the following conditions:

- Short-line fault applied to 2 km, 10 km, 50%, and 90% of the length.
- Three-phase "grounded" and "ungrounded" terminal fault on both sides of the circuit breaker.

The opening of the circuit breaker is done only in the line of the affected section, with the parallel healthy line connected.

It was observed that, for the short-line faults close (for ex. 2 km to 10 km), the effect of the series capacitor bypass is important, since, if it did not occur, the RRRV values and the TRV magnitude would surpass the limit values of the T-100 curve.

In all the cases analyzed, for short-line faults occurring at 50% and 90% of the length in the sections analyzed, the T-100 curve was not surpassed.

The circuit breaker in the Ourolândia – Igaporã section, in the Igaporã side, proved to be more critical, because the wavefront of the envelope curve (T-100) was surpassed even considering the magnitude of the T-60, T-30, and T-10 curves (phase B). This surpass is approximately 12.5% above the T-10 curve.

The Igaporã – Pirapora section also presented critical TRV conditions, because, mainly for Short-Line Faults at a distance of 2 km from the Pirapora terminal (with the series capacitor bypass performed via VCS - Voltage Controlled Switches), the TRV of the T-100 curve, and even the T-10 curve, were surpassed in their RRRV.

None of the TRVs corresponding to grounded and ungrounded terminal faults surpassed the specific curve obtained via fault current through the circuit breaker. Even the T-100 curve was not surpassed.

The inclusion of more than one circuit increased the power transmission capacity, in addition to the number of transformers. This led to an increase of fault currents. However, this additional parallel circuit contributed to a performance improvement regarding the TRV.

Additional details are presented in Annex 15.

11.8 Series Capacitor

The series capacitors must present the following characteristics:

- Protection system with *gaps* and varistors (MOV);
- 35 Ω/phase;
- 250 Mvar per phase;
- rated current of 2.7 kA;
- overload current for 30 minutes: 3.6 kA.

The power capacity should be determined by the vendor, considering the occurrence of short-circuits in different points in and out the line. Additionally, the action or not of the bypass switches should be considered; thus, the rating of the MOV may be altered.

Additional details are presented in Annex 16.

12. References

[1] EPRI. *Transmission Line Reference Book* - 345 kV and Above, Electric Power Research Institute (EPRI), Palo Alto, California.

[2] CIGRE TB 32. *Final report of the UHV ad hoc group*, 1972.

[3] DUFOURNET, D. Standardization Aspects of UHV Networks. In: *Second International Symposium on Standards for Ultra High Voltage Transmission, IEC-CIGRE*, 2008.

[4] IEC. UHV Transmission Systems. *Information on the Basic Construction of TC 122 Standard*, 2015.

[5] OPERADOR NACIONAL DO SISTEMA ELÉTRICO. *Submódulo 23.3 - Diretrizes e critérios para estudos elétricos*. Rio de Janeiro, p. 97, March 25, 2002.

[6] JARDINI J. A. *et al . Relatório 4500083056-RT-07-R8*. São Paulo, 2017.

[7] JARDINI J. A. *et al. Alternativas não Convecionais para Transmissão de Energia Elétrica - Estudos Técnicos e Econômicos*, Brasília: Goya, 2012.

[8] OPERADOR NACIONAL DO SISTEMA ELÉTRICO. *Diretrizes para Elaboração de Projetos Básicos para Empreendimentos de Transmissão*. Rio de Janeiro, 2013.

[9] XIAN, Zutao; LIN, Jiming; BAN, Liangeng; ZHENG, Bin. Investigation of TRV across Circuit-Breaker of Series Compensated Double-Circuit UHV Transmission Lines.In:*2010 International Conference on Power System Technology*, Hangzhou, 2010.

[10] OPERADOR NACIONAL DO SISTEMA ELÉTRICO. Órgão Nacional do Sistema, Submódulo 23.3 - Diretrizes e critérios para estudos elétricos, 2002.

[11] JARDINI J. A. *et al. Relatório 4500083056-NT 07-R0_Modelagem (R2)* – Estudos de Detalhamento de Transitórios Eletromagnéticos. São Paulo, 2016.

[12] CIGRÉ. WG_C4_307. *Transformer Energization in Power Systems: A Study Guide*. n.º 568, 2014. Paris.

[13] LIU, Zhenya. *Ultra-High Voltage AC/DC Grids*. London: Academic Press (Elsevier), 2015.

[14] OPERADOR NACIONAL DO SISTEMA ELÉTRICO. *Diretrizes para a Elaboração de Projetos Básicos para Empreendimentos de Transmissão – Estudos Elétricos, Especificação das Instalações, de Equipamentos e de Linhas de Transmissão*, Rio de Janeiro: ONS, 2013, p. 97.

[15] FASSBINDER, S. *Application Note Efficiency and Loss Evaluation of Large Power Transformers*, pp. 13. European Copper Institute, March 2013. [Online]. Available at: <http://www.leonardo-energy.org/sites/leonardo-energy/files/documents-and-links/Cu0144_Efficiency%20and%20Loss%20Evaluation%20of%20Large%20Power%20Transformers_v1.pdf.>. Accessed on: April 25, 2016.

[16] HARKER, K. *Power System Commissioning and Maintenance Practice*. London: IEE (The Institution of Electrical Engineers), pp. 229, 1998.

[17] ABB. *Controlled Switching Buyer's and Application Guide*. [Online]. Available at: <https://library.e.abb.com/public/d85e18212da04bb9c1257bcc001f2d5e/ABB%20B.G.%20Controlled%20Switching%20Ed4.pdf>.

[18] BRUNKE, John H.; FRÖHLICH, Klaus J. Elimination of Transformer Inrush Currents by Controlled Switching – Part I: Theoretical Consideration. *IEEE Transactions on Power Delivery,* vol. 16, n. 2, pp. 276-280, 2001.

[19] BRUNKE, John H.; FRÖHLICH, Klaus J. Elimination of Transformer Inrush Currents by Controlled Switching – Part II: Application and Performance Considerations. *IEEE Transactions on Power Delivery,* vol. 16, n. 2, pp. 281-285, 2001.

[20] HAYWARD, C. D. Prolonged Inrush Currents With Parallel Transformers affect Differential Relaying. *AIEE Transactions,* vol. 60, p. 1.096 – 1.101, 1941.

[21] WANG, Y.; YIN, X.; YOU, D.; XU, T. Analysis on the influencing factors of transformer sympathetic inrush current. In: *Power And Energy Society General Meeting*, Pittsburgh, 2008, DOI:10.1109/PES.2008.4596469.

[22] IEC, 826.*Loading and Strength of Overhead Transmission Lines*. 2nd Edition. Geneva, 1991.

[23] SEVES. *Sediver Toughened Glass Suspension Insulator Catalog,* 1996.

[24] CIGRE. *TB 048 - Tower Top Geometry,* 1995.

[25] CIGRÉ. *WG B2/B4/C1.17 Impacts of HVDC Lines on the Economics of HVDC Projects,* 2009.

[26] FDTE/ITAEE. *Modelagem do Sistema e Cálculo do Reator de Neutro*. São Paulo, 2016.

[27] NICOLA, G. L. C.; JARDINI, J. A. *Alternativas não Convencionais para Transmissão de Energia Elétrica*. Brasília - DF: Goya, 2010.

[28] BALOSSI, A. M. M. O. P. Laboratory full-scale tests for determination of the secondary arc extinction time in high-speed reclosing. *IEEE Summer Power Meeting,* New Orleans, 10-15 July 1966.

[29] O. OLIVEIRA FILHO, D. R. MELO, J. A. CARDOSO, R. M. DE AZEVEDO, W. A. S. Cruz, e S. G. Carvalho, *Performance Evaluation of 800 kV Porcelain Multicone Type Insulators Under Heavy Rain Based on Laboratory Tests*, International Conference on High Voltage Engineering and Application, Chongqing, China, November 2008.

[30] AZEVEDO, R. M., CARVALHO, F. M. S., CRUZ, W. A. S. AND S. G. *Estudo de Coordenação de Isolamento Baseado em Sobretensões Provocadas por Aplicação e Eliminação de Defeitos, e sua Relação com Chuvas Intensas*, XX SNPTEE, GDS – Grupo de Estudos de Desempenho de Sistemas Elétricos, Recife, 2009.

ATTACHMENTS – CHAPTER 5

ATTACHMENT 1 – Line Energization

1.1 Objective

Presenting the results obtained for the energization of the 1,000 kV AC transmission line that connects the Milagres III, Ourolândia III, Igaporã IV, and Pirapora III substations. Each section between the substations represents a length of 440 km.

1.2 General Description of the Calculation

The 1,000 kV transmission line is divided into three sections of 440 km each. The energization of the line was done via both terminals, in each of the three sections.

Since the sections of the 1,000 kV line present series compensation, the energization should also be possible with the series capacitor bank bypassed.

First, systematic energizations were done in all the sections. The systematic energization consists of determining for established instants by sweeping a cycle that causes greater overvoltage.

After determining the instant of higher overvoltage, the statistic energization is done, which consists of 200 switchings around this instant of higher overvoltage; Among these 200 switchings, the worst case of overvoltage is identified and repeated separately to obtain overvoltage graphs.

Sensitivity analyses were performed. One was the verification of the position of the line reactor related to the series capacitor; and the other regards verifying the energization with synchronized closing.

1.3 Systematic Energization

The transient energization overvoltage depends on the instant (in the voltage wave) in which the closing of the circuit breaker contact occurs. Thus, the first step is to explore, in an interval of half a cycle, which is the least favorable region (systematic energization). Next, a study should be elaborated with several instants (considering the dispersion of the closing of the poles), obtaining the statistic distribution. The systematic energization can be done dividing the time into several values, or using a random method (based on an equiprobable distribution), and on the worst case, to elaborate the statistic calculation.

To determine the worst energization instant of each of the transmission lines, systematic energizations were done consisting of energizing the line during a cycle of the 60 Hz grid (16.66 ms) with interval of 0.694 ms (15º electric), which means that 24 cases were performed.

Table A1.1, below, presents the highest overvoltages obtained by means of systematic energization, with 400 Ω pre-insertion resistor inserted for 8 ms, and bypassed series capacitor.

Table A1.1: Overvoltages for systematic energization

TL Sections	SS where the switching occurred	Voltages (pu)*				
		TL_0	TL_{25}	TL_{50}	TL_{75}	TL_{100}
Milagres – Ourolândia	Milagres	1.395	1.501	1.634	1.659	1.648
	Ourolândia	1.327	1.462	1.574	1.664	1.689
Ourolândia – Igaporã	Ourolândia	1.410	1.526	1.700	1.749	1.751
	Igaporã	1.178	1.335	1.400	1.431	1.419
Igaporã – Pirapora	Igaporã	1.253	1.357	1.399	1.499	1.506
	Pirapora	1.189	1.303	1.379	1.454	1.437

* Vbase = 816.5 kV

Note:

TL_0 is the start of the line from the substation where the switching occurs.

TL_{25} corresponds to 25% of the length of the line from the substation where the switching occurs.

TL_{50} is the corresponds to middle of the line from the SS where the switching occurs.

TL_{75} corresponds to 75% of the length of the line from the substation where the switching occurs.

TL_{100} corresponds to the end of the line from the substation where the switching occurs

We observe that the highest line energization overvoltage occurred in the second section (Ourolândia – Igaporã), energized via Ourolândia, and its value was 1.751 pu.

1.4 Statistic Energization

Based on the systematic energization instants that cause higher overvoltage in each section of the line, statistic energizations were performed.

Due to the randomness of the closing instants of the circuit breaker poles, the energization switching study should be evaluated in a statistic manner, considering, at least, a sample of two hundred switchings.

The following closing standard deviation values were considered for the circuit breaker: 0.75 ms for insertion of the pre-insertion resistor, and 1.25 ms for bypass of the resistor.

Table A1.2, below, presents the phase-to-ground overvoltage results for the statistic energization of the transmission line.

Table A1.2: Statistical Energization

Segment of Transmission Line	Substation where the maneuver occurred	Average and standard deviation	LT_0			LT_{25}			LT_{50}			LT_{75}			LT_{100}		
			A	B	C	A	B	C	A	B	C	A	B	C	A	B	C
Milagres – Ourolândia	Milagres	Average	1.242	1.315	1.323	1.345	1.426	1.393	1.411	1.522	1.446	1.431	1.566	1.471	1.427	1.564	1.464
		Deviation	0.046	0.057	0.079	0.056	0.087	0.084	0.068	0.115	0.087	0.075	0.127	0.097	0.083	0.134	0.104
	Ourolândia	Average	1.228	1.238	1.300	1.313	1.343	1.429	1.365	1.417	1.520	1.379	1.448	1.560	1.361	1.442	1.555
		Deviation	0.050	0.043	0.042	0.062	0.045	0.061	0.077	0.055	0.078	0.086	0.066	0.096	0.094	0.072	0.105
Ourolândia – Igaporã	Ourolândia	Average	1.379	1.286	1.281	1.501	1.420	1.381	1.592	1.495	1.453	1.632	1.517	1.487	1.623	1.507	1.476
		Deviation	0.039	0.049	0.041	0.060	0.079	0.042	0.081	0.110	0.045	0.097	0.128	0.055	0.107	0.142	0.058
	Igaporã	Average	1.124	1.137	1.144	1.239	1.252	1.248	1.303	1.308	1.314	1.332	1.338	1.348	1.325	1.343	1.349
		Deviation	0.031	0.032	0.026	0.051	0.082	0.050	0.063	0.104	0.066	0.073	0.117	0.077	0.079	0.122	0.088
Igaporã - Pirapora	Igaporã	Average	1.224	1.171	1.181	1.320	1.285	1.292	1.346	1.322	1.348	1.359	1.339	1.390	1.356	1.335	1.405
		Deviation	0.043	0.039	0.027	0.061	0.057	0.067	0.066	0.056	0.091	0.073	0.063	0.118	0.090	0.071	0.139
	Pirapora	Average	1.106	1.151	1.107	1.239	1.229	1.213	1.313	1.294	1.266	1.355	1.329	1.293	1.360	1.319	1.285
		Deviation	0.029	0.030	0.033	0.065	0.046	0.053	0.085	0.057	0.062	0.099	0.068	0.071	0.112	0.078	0.077

For the case of the energization of the Ourolândia – Igaporã line, energized via Ourolândia, we obtained the phase-to-ground and phase-to-phase voltage values. Table A1.3, below presents the values for this case.

Table A1.3: Results of the statistic energization (worst case)

Overvoltage location	Phase-to-ground and Phase-to-phase	Average overvoltage (pu)	Standard deviation (pu)	Maximum overvoltage (pu)
Start of the TL	Phase A	1.3786	0.0393	1.4533
	Phase B	1.2857	0.0489	1.4273
	Phase C	1.2805	0.0415	1.3957
	Phase A – Phase B	2.3240	0.0744	2.5750
	Phase B – Phase C	2.1741	0.0850	2.4195
	Phase A – Phase C	2.3064	0.0827	2.5339
25% of the TL	Phase A	1.5001	0.0596	1.6550
	Phase B	1.4197	0.0794	1.6351
	Phase C	1.3813	0.0419	1.5358
	Phase A – Phase B	2.5850	0.0932	2.8542
	Phase B – Phase C	2.3433	0.1175	2.7067
	Phase A – Phase C	2.4858	0.0810	2.6875
Middle of TL	Phase A	1.5920	0.0808	1.7551
	Phase B	1.4947	0.1105	1.7891
	Phase C	1.4531	0.0452	1.6064
	Phase A – Phase B	2.7522	0.1244	2.9948
	Phase B – Phase C	2.4539	0.1409	2.9151
	Phase A – Phase C	2.6057	0.0732	2.8700
75 % of the TL	Phase A	1.6316	0.0970	1.8305
	Phase B	1.5167	0.1276	1.8416
	Phase C	1.4872	0.0555	1.7042
	Phase A – Phase B	2.8334	0.1526	3.1747
	Phase B – Phase C	2.4782	0.1581	3.0326
	Phase A – Phase C	2.6579	0.0817	2.9276
End of TL	Phase A	1.6231	0.1069	1.8456
	Phase B	1.5070	0.1421	**1.8579**
	Phase C	1.4759	0.0581	1.7100
	Phase A – Phase B	2.8260	0.1667	**3.2780**
	Phase B – Phase C	2.4634	0.1719	3.1131
	Phase A – Phase C	2.6435	0.0976	2.9956

1.5 Determining the Worst Case

Figures A1.1 to A1.3, below, present the phase-to-ground overvoltages for the worst case (Ourolândia – Igaporã section, energized via Ourolândia).

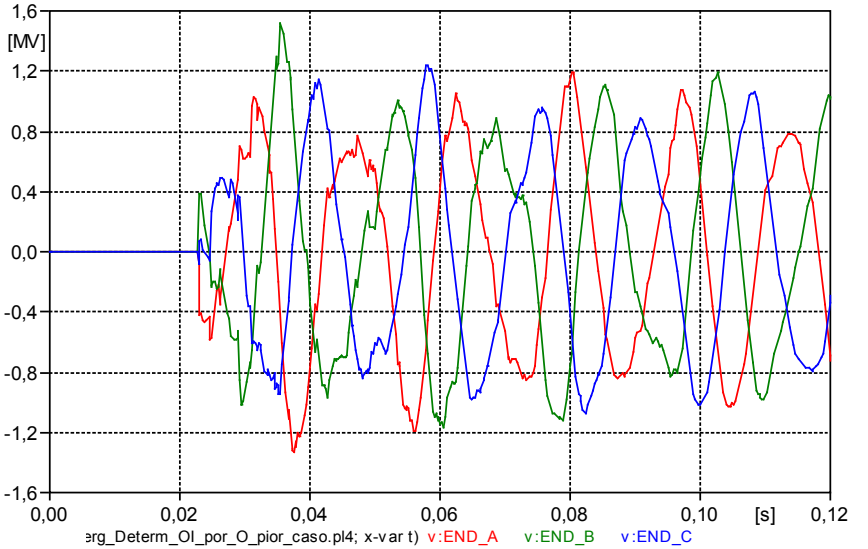

Figure A1.1: Phase-to-ground voltage at the end of the line (Igaporã)

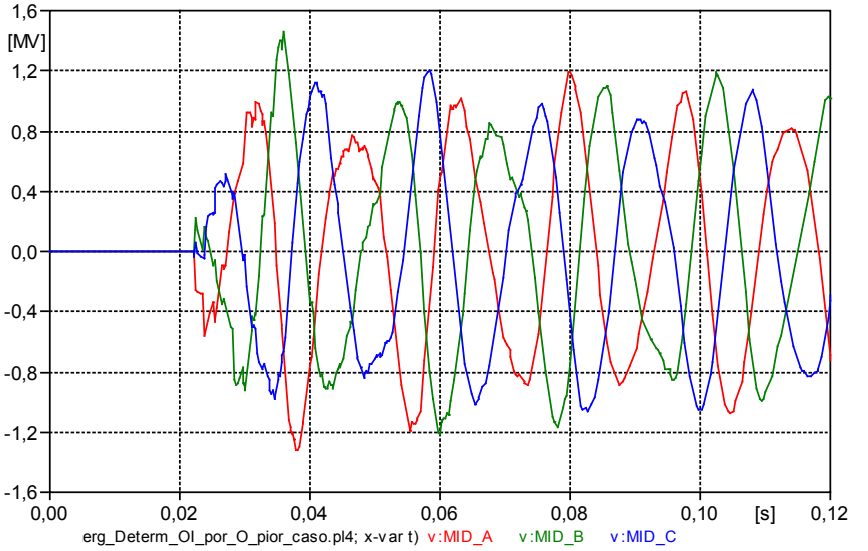

Figure A1.2: Phase-to-ground voltage in the middle of the line

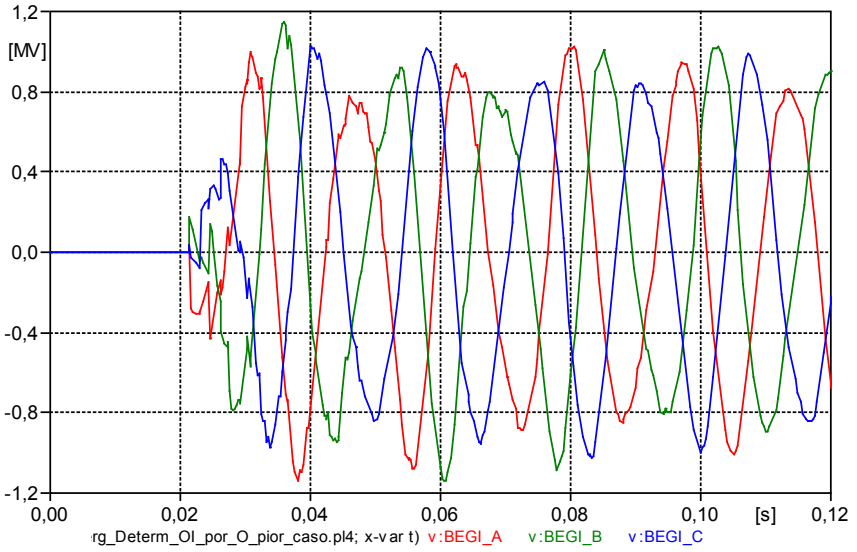

Figure A1.3: Phase-to-ground voltage at the start of the line (Ourolândia)

1.6 Sensitivities

Sensitivity analyses were performed for energization: energization with series capacitor, varying the position of the line reactor, and synchronized energization.

1.6.1 Position of the line reactor and series capacitor inserted

In general, the energizations were done with the capacitor bypassed. However, to evaluate the effect of the position of the line reactor, the energization was done with the series capacitor inserted.

Figure A1.4 presents these two cases.

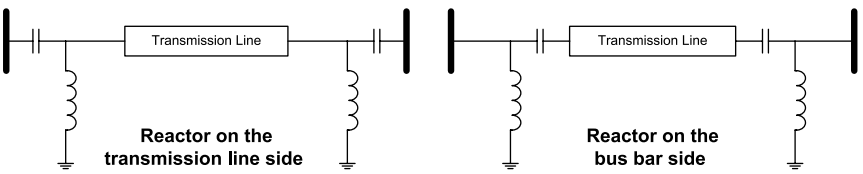

Figure A1.4: Reactor position

Table A1.4 presents the results for energization with bypassed capacitor, and two cases with capacitor connected, varying the position of the reactor.

Table A1.4: Comparison for energization of the Ourolândia – Igaporã line via Ourolândia

	Bypassed capacitor (pu)			Reactor on TL side (pu)			Reactor on bus side (pu)		
	Phase A	Phase B	Phase C	Phase A	Phase B	Phase C	Phase A	Phase B	Phase C
Mean	1.623	1.507	1.476	1.610	1.510	1.491	1.569	1.476	1.461
Standard deviation	0.108	0.142	0.058	0.116	0.113	0.052	0.105	0.119	0.053

With the values presented in Table A1.4, we verify that the energization bypassing the series capacitor results in higher average values, and that by energizing with the connected series capacitor, and the line reactor connected to the bus side of the series capacitor, the average values obtained are lower.

1.6.2 Synchronized energization

Some studies were conducted to verify the feasibility of using a synchronizer to obtain lower overvoltages during the energization of the transmission line. The synchronized energization consists of determining circuit breaker pole closing instants that result in lower overvoltage values resulting of the switching. The synchronizer estimates the instant when it should release the pole of the circuit breaker so it closes in the point of the wave where the lowest overvoltage occurs.

For the case of line energization, the best instant occurs when the voltage on the source side in passing through zero voltage. To verify efficiency, initially, two simulations were performed. The first consists of performing the statistic energization at zero voltage of one of the phases. The other two phases are 120º out of phase. The second consists of performing the statistic energization with the three phases at zero voltage.

Table A1.5 presents the phase-to-ground voltage values for the end of the line, which results for the synchronized energization

Table A1.5: Synchronized energization

	Synchronization 1			Synchronization 2		
	Phase A	Phase B	Phase C	Phase A	Phase B	Phase C
Mean	1.430	1.513	1.651	1.522	1.653	1.437
Standard deviation	0.093	0.054	0.112	0.060	0.111	0.102

Comparing the values of Table A1.5 with the values of Table A1.4, we verify that there is no significant gain in the synchronized energization in these two situations. Analyses were performed with a reduction of the switches closing standard deviation, and increase of the insertion time. The switch that connects the pre-insertion resistor had its standard deviation reduced to 0.50 ms, and the one that bypasses the resistor had the deviation reduced to 1.0 ms. The second analysis consisted of increasing the time of permanence of the pre-insertion resistor to 16 ms. Table A1.6 present the results of these two analyses.

Table A1.6: Synchronized energization sensitivity

	Reduction of standard deviation			Pre-insertion resistor to 16 ms		
	Phase A	Phase B	Phase C	Phase A	Phase B	Phase C
Mean	1.536	1.692	1.416	1.272	1.264	1.256
Standard deviation	0.035	0.092	0.068	0.025	0.066	0.031

Table A1.6 shows that the reduction of the circuit breaker standard deviation did not result in significant improvement in the overvoltage values. However, in the case in which the pre-insertion resistor is maintained for a longer time, there was a significant reduction in the overvoltage values at the end of the line, but that results in an increase in the requirement of energy dissipated by the resistor.

Therefore, simulations were performed to verify the increase of energy dissipated by the pre-insertion resistor (in the worst phase-to-ground overvoltage case).

The results are presented in Figures A1.5 and A1.6.

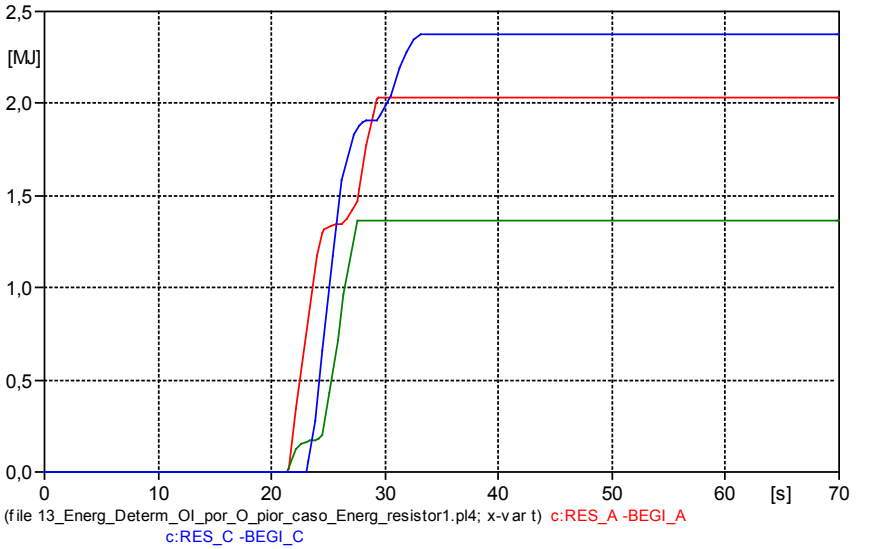

Figure A1.5: Energy dissipated through the resistor for 8 ms

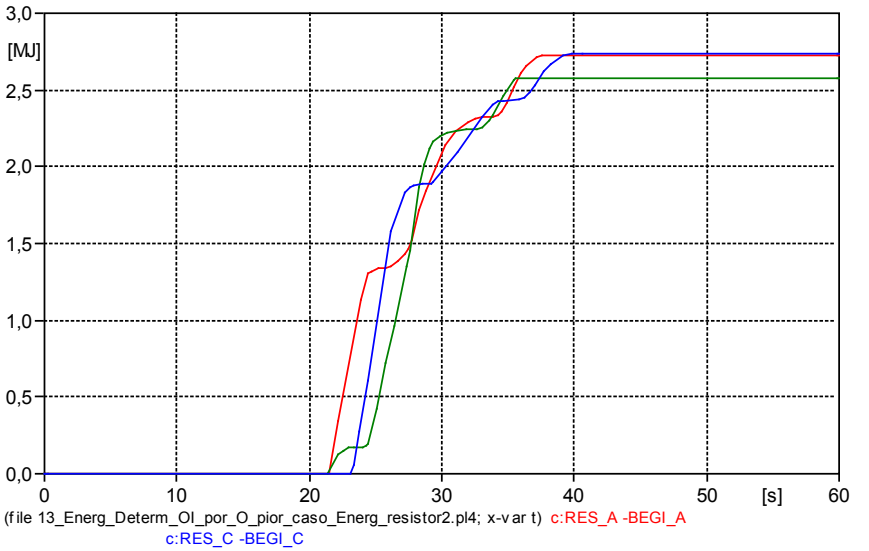

Figure A1.6: Energy dissipated through the resistor for 16 ms

We verify that there was an average increase of 40% in the energy dissipated by the resistor.

ATTACHMENT 2 – Single-pole Reclosing

2.1 Objective

Most faults that occur in power systems are of a temporary nature, affecting only one of the phases. Thus, it is interesting to evaluate the single-pole reclosing alternative, since this way there would be no need for interrupting the power flow in the healthy phases.

During the single-pole reclosing studies for new projects, the secondary arc current that appears after the opening of the circuit breakers at both ends of the line must be considered. The link between the secondary arc and the electric grid happens through the capacitive coupling between the healthy phases and the faulty phase. This secondary arc current is proportional to the length of the line, and is almost independent of the loading of the line. Therefore, the loading of the line (inductive coupling) has less influence than the capacitive one.

2.2 Methodology

The calculation of the transient overvoltages related to the single-pole reclosing was done considering the sequence described as follows:

a. Previous simulations were performed in the three sections of the 1,000 kV line, considering the complete sequence of events present in the single-pole reclosing process: starting of the system operating in normal "state", application of short in Phase A, and subsequent opening of the circuit breakers in this phase, allowed for observing that, after a certain time has elapsed since the opening of the circuit breakers, a stationary current flows through the fault switch, resulting of the coupling with the healthy phases. Thus, in the subsequent simulations for single-pole reclosing, the line starts with the short switch connected, which allows for reducing the simulation time. The curve in Figure A2.1 represents the recovery voltage and the residual load (at the short location) after the opening of the short switch.

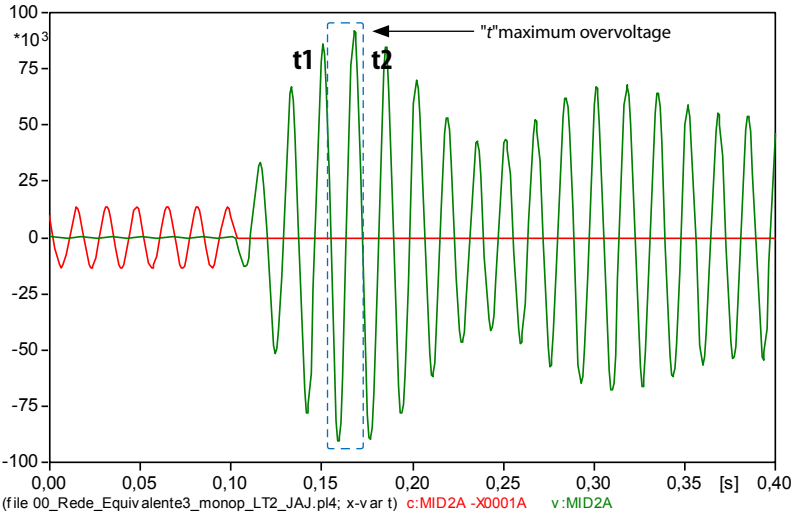

Figure A2.1: I_{ARC} (red) and residual load (green) in the fault point

b. The single-pole reclosing simulations were done considering the least favorable conditions. We considered that the worst instant, after the extinction of the secondary arc current, would be the instant "*t*" when the recovery voltage reaches its maximum value. The t_1 and t_2 times of the window shown in Figure A2.1 are obtained (during the passage through the zero of the complete wave). These times determine the frequency of this transient voltage wave, and the instant for the closing of the systematic switch in the calculation.
c. In the systematic switch, the sinusoidal wave scan was specified every 15° of the 360° period, which results in a total of 24 cases. In this switch, we defined the t_1 time to start the scan. The opening of both circuit breakers at the extremities of the line occur at t = 0.05s. If the fault occurs in another point of the line, and not in the middle, the circuit breaker closer to the fault will be the first to open, establishing a delay (~20 ms) for the opening of the other circuit breaker.
d. We highlight that, after completing the tests, the maximum transient overvoltages simulating the short switch closed, to be soon opened considering the respective times normally used in the project guidelines, and with them already open, were practically the same. Thus, a more exhaustive analysis with these keys was performed considering the "open" short switch.

e. Only the successful reclosing simulations are analyzed, because, in the cases of unsuccessful reclosing, the fault would still not have been eliminated, and the overvoltage in the phase in short would not have been expressive.
f. After the completion of all the simulations with systematic switches, the system ran with statistic switches (for 200 switchings), only for the case in which maximum overvoltage was obtained with systematic switch.

2.3 Results of the Milagres-Ourolândia line

2.3.1 Reclosing via Milagres

2.3.1.1 With systematic switch

Table A2.1 shows the values using the systematic switches. Reclosing via Milagres (worst case) and short in different points of the line.

Table A2.1: Reclosing with systematic switch via Milagres

Measurement point L = 440 km	Phase	Overvoltages (pu)		
		Short at the start (Milagres)	Short in the middle	Short at the end (Ourolândia)
0% (Milagres)	A	1.340	1.335	1.336
	B	1.165	1.166	1.166
	C	1.119	1.118	1.118
25%	A	1.478	1.478	1.476
	B	1.194	1.189	1.190
	C	1.163	1.156	1.158
50%	A	1.582	1.580	1.580
	B	1.194	1.192	1.193
	C	1.201	1.204	1.204
75%	A	**1.670**	**1.668**	**1.669**
	B	1.168	1.170	1.170
	C	1.208	1.204	1.205
100% (Ourolândia)	A	1.650	1.657	1.655
	B	1.100	1.101	1.100
		1.166	1.166	1.166

2.3.1.2 With statistic switch

Table A2.2 shows the reclosing values of the Milagres – Ourolândia section, using statistic switch, reclosing via Milagres, and short at the start of the line.

Table A2.2: Reclosing with statistic switch via Milagres

Overvoltage location	Phase	Average (pu)	Standard deviation (pu)	Maximum overvoltage (pu)
0% of TL (Milagres)	A	1.275	0.051	1.389
	B	1.150	0.025	1.198
	C	1.081	0.017	1.121
25% of the TL	A	1.402	0.087	1.542
	B	1.175	0.000	1.192
	C	1.125	0.000	1.140
50% of the TL	A	1.499	0.119	1.647
	B	1.149	0.025	1.185
	C	1.125	0.004	1.155
75% of the TL	A	1.567	0.125	1.690
	B	1.128	0.012	1.155
	C	1.125	0.000	1.149
100% of TL (Ourolândia)	A	1.576	0.125	**1.700**
	B	1.079	0.013	1.108
	C	1.125	0.000	1.131

In the case of the Milagres – Ourolândia section, the maximum overvoltage with statistic switch was equal to 1.70 pu at the open extremity (Ourolândia).

Figure A2.2 presents the phase-ground voltages at the Ourolândia terminal.

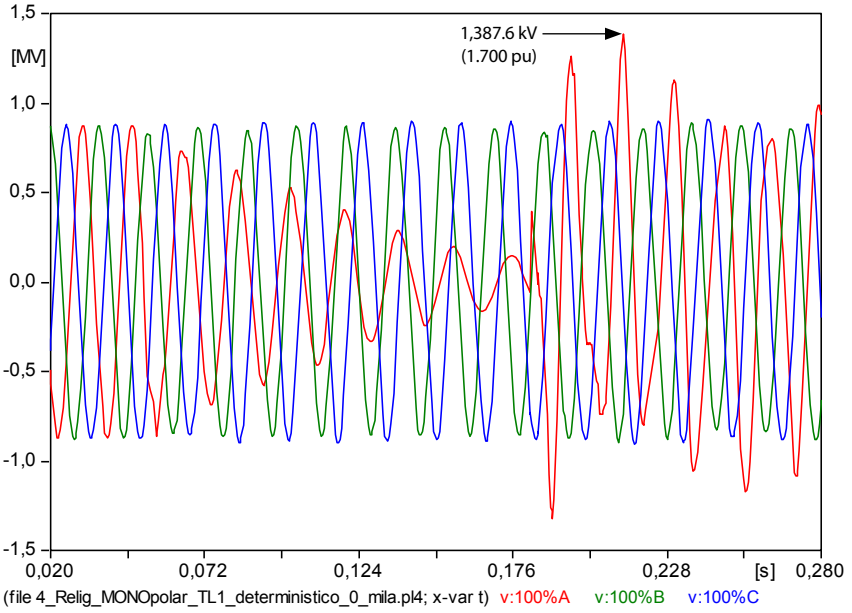

Figure A2.2: Voltages at the open extremity of the Milagres – Ourolândia section, reclosing via Milagres

2.3.2 Reclosing via Ourolândia

The cases of reclosing with systematic switch were done and the results were lower than the reclosing via Milagres. Thus, the values with statistic switch were not calculated.

2.4 Results of the Ourolândia – Igaporã line

2.4.1 Reclosing via Ourolândia

2.4.1.1 With systematic switch

Table A2.3 shows the reclosing values of the Ourolândia – Igaporã section, via Ourolândia, using systematic switches.

Table A2.3: Reclosing with systematic switch via Ourolândia

Measurement points	Phase	Overvoltages (pu)		
		Short at the start (Ourolândia)	Short in the middle (pu)	Short at the end (Igaporã)
0% (Ourolândia)	A	1.368	1.362	1.366
	B	1.184	1.178	1.181
	C	1.158	1.153	1.153
25%	A	1.529	1.527	1.529
	B	1.192	1.190	1.191
	C	1.176	1.171	1.172
50%	A	1.703	1.707	1.709
	B	1.176	1.170	1.173
	C	1.196	1.194	1.189
75%	A	1.781	1.776	1.774
	B	1.149	1.152	1.154
	C	1.202	1.193	1.197
100% (Igaporã)	A	**1.785**	**1.787**	**1.782**
	B	1.096	1.104	1.103
	C	1.164	1.156	1.158

2.4.1.2 With statistic switch

Table A2.4 shows the results.

Table A2.4: Reclosing with statistic switch via Ourolândia

Overvoltage location	Phase	Average (pu)	Standard deviation (pu)	Maximum overvoltage (pu)
0% of TL (Ourolândia)	A	1.341	0.040	1.474
	B	1.166	0.022	1.205
	C	1.122	0.039	1.169
25% of the TL	A	1.517	0.043	1.644
	B	1.188	0.022	1.241
	C	1.151	0.026	1.206
50% of the TL	A	1.662	0.056	1.764
	B	1.182	0.017	1.223
	C	1.160	0.026	1.206
75% of the TL	A	1.741	0.056	1.840
	B	1.134	0.019	1.182
	C	1.160	0.029	1.202
100% of TL (Igaporã)	A	1.745	0.064	**1.853**
	B	1.075	0.004	1.101
		1.133	0.018	1.164

Figure A2.3 presents the voltages close to the Igaporã busbar (100% of the TL) when the Ourolândia – Igaporã section is energized via Ourolândia.

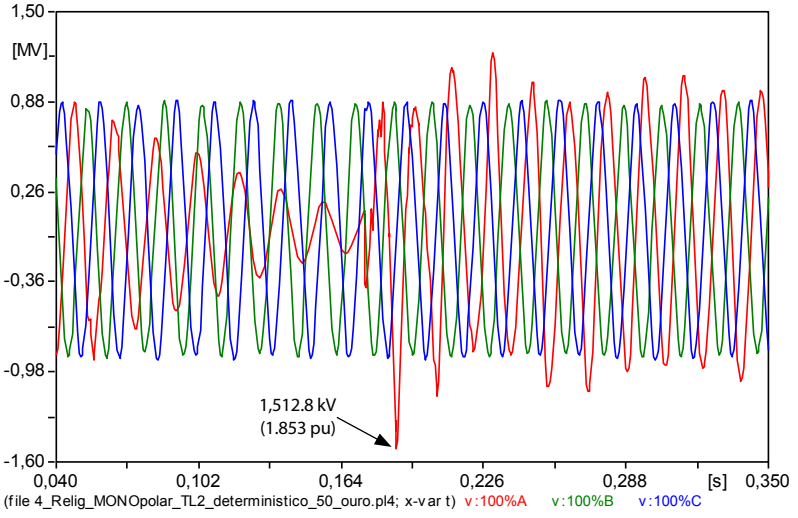

Figure A2.3: Voltages in the open extremity of the Ourolândia – Igaporã section, reclosing via Ourolândia

2.4.2 Reclosing via Igaporã

The cases of reclosing with systematic switch were done and the values were lower than the reclosing via Ourolândia. Thus, the values with statistic switch were not calculated.

2.5 Results of the Igaporã – Pirapora Line

2.5.1 Reclosing via Igaporã

2.5.1.1 With systematic switch

Table A2.5 shows the reclosing values of the Igaporã – Pirapora section, via Igaporã.

Table A2.5: Reclosing with systematic switch via Igaporã

Measurement point L = 440 km	Phase	Overvoltages (pu)		
		Short at the start (Igaporã)	Short in the middle (pu)	Short at the end (Pirapora)
0% (Igaporã)	A	1.528	1.529	1.525
	B	1.097	1.085	1.087
	C	1.229	1.230	1.228
25%	A	**1.545**	**1.542**	**1.548**
	B	1.099	1.101	1.100
	C	1.208	1.210	1.212
50%	A	1.503	1.502	1.494
	B	1.121	1.116	1.122
	C	1.207	1.207	1.216
75%	A	1.423	1.425	1.428
	B	1.141	1.137	1.143
	C	1.204	1.203	1.198
100% (Pirapora)	A	1.282	1.281	1.283
	B	1.128	1.128	1.127
		1.174	1.175	1.171

2.5.1.2 With statistic switch

Table A2.6 shows the results.

Table A2.6: Reclosing with statistic switch via Igaporã

Overvoltage location	Phase	Average (pu)	Standard deviation (pu)	Maximum overvoltage (pu)
0% of TL (Igaporã)	A	1.486	0.115	**1.694**
	B	1.125	0.004	1.124
	C	1.128	0.012	1.171
25% of the TL	A	1.480	0.112	1.689
	B	1.129	0.013	1.159
	C	1.147	0.034	1.216
50% of the TL	A	1.433	0.109	1.636
	B	1.123	0.024	1.158
	C	1.167	0.021	1.207
75% of the TL	A	1.353	0.098	1.567
	B	1.092	0.024	1.120
	C	1.161	0.023	1.191
100% of TL (Pirapora)	A	1.232	0.055	1.356
	B	1.077	0.009	1.120
		1.153	0.025	1.194

Figure A2.4 presents the voltages close to the Igaporã busbar (0% of the TL).

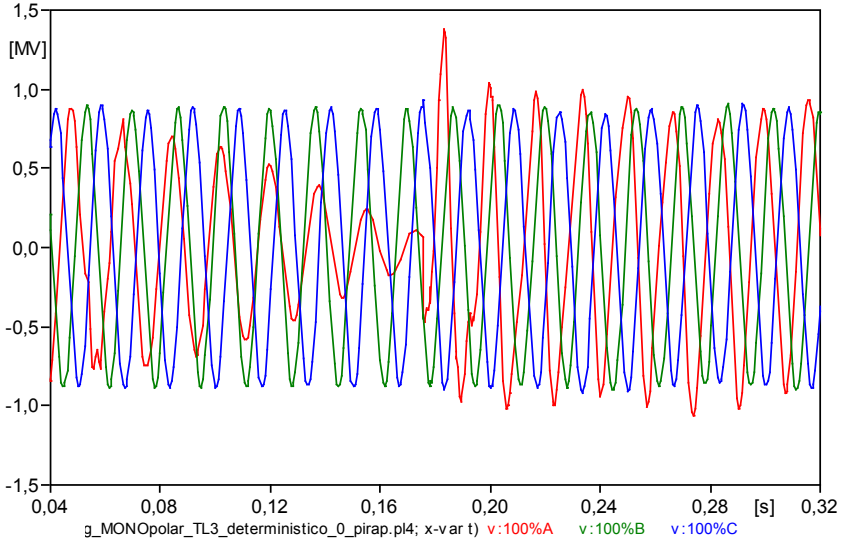

Figure A2.4: Voltages at the close extremity of the Igaporã section when the reclosing via Igaporã (deterministic simulation)

2.5.2 Reclosing via Pirapora

The cases of reclosing with systematic switch were done and the values were lower than the reclosing via Igaporã. Thus, the cases with statistic switch were not calculated.

2.6 Findings

After completing the single-pole reclosing simulations for the three sections of the 1,000 kV line (Milagres – Ourolândia, Ourolândia – Igaporã, and Igaporã – Pirapora), it was possible to compare the overvoltages obtained. The average value and maximum voltage obtained for each of these sections (reclosing with statistic switch) were of:

- Milagres – Ourolândia: V_{μ}= 1.576 pu, V_{max} = 1.700 pu
- Ourolândia – Igaporã: V_{μ}= 1.745 pu, V_{max} = 1.853 pu
- Igaporã – Pirapora: V_{μ}= 1.486 pu, V_{max} = 1.694 pu

ATTACHMENT 3 – Three-pole Reclosing

3.1 Objective

Presenting the studies and detailing of the switching overvoltages resulting of three-pole reclosing in the 1,000 kV transmission system, so as to evaluate the statistic distributions for the overvoltages along the proposed transmission lines, for subsequent sizing of the surge arresters and coordination of the insulation of lines and substations.

Presented here are the EMT (*Electromagnetic Transients*) studies referring to three-pole reclosing of the following sections:

- Milagres – Ourolândia.
- Ourolândia – Igaporã.
- Igaporã – Pirapora.

A sensitivity analysis was also performed considering the following configurations, so as to identify the worst operating conditions:

- Use of fast grounding switch (reduction of trapped charge).
- Positioning of the shunt compensation reactor.
- Series capacitor bypass during reclosing.
- Length of the line.

To perform the three-pole reclosing studies, first, the line was divided into five equidistant points, at intervals of 25% of the length of the line. Thus, the voltages were analyzed at 0%, 25%, 50%, 75%, and 100% of the line.

3.2 With and Without Bypass of the Series Capacitor – Reclosing

The simulations considered the three-pole opening at the two extremities of the line, without prior short, to obtain the highest residual load after opening.

Next, the processing with systematic switch was done to find the least favorable region for reclosing, 200 ms after the opening. The study considered that the circuit breaker has a 400 Ω pre-insertion resistor, average insertion time of 8 ms (as in the line energization study). Finally, the distribution represented with statistic switch at the closing was calculated.

First, studies were conducted to verify if the presence of the series capacitor has significant influence during reclosing.

The distributions with the presence of the series capacitor are presented in Table A3.1.

With the capacitor bypassed during reclosing, the overvoltages are those presented in Table A3.2. In both situations, the overvoltages are of the same magnitude.

Table A3.1: Worst overvoltage case. Milagres – Ourolândia section, via Milagres. Capacitor inserted during reclosing

Milagres – Ourolândia	Phase-to-ground and phase-to-phase	Average (pu)	Standard deviation (pu)	μ + 3σ (pu)
Start of the TL	Phase A	1.239	0.065	1.435
	Phase B	1.295	0.040	1.414
	Phase C	1.291	0.056	1.459
	Phase A – Phase B	2.168	0.093	2.448
	Phase B – Phase C	2.249	0.069	2.457
	Phase A – Phase C	2.198	0.104	2.509
25% of the TL	Phase A	1.304	0.082	1.551
	Phase B	1.388	0.048	1.531
	Phase C	1.396	0.073	1.616
	Phase A – Phase B	2.287	0.089	2.554
	Phase B – Phase C	2.423	0.095	2.710
	Phase A – Phase C	2.358	0.147	2.798
Middle of TL	Phase A	1.357	0.093	1.635
	Phase B	1.445	0.054	1.606
	Phase C	1.469	0.089	1.737
	Phase A – Phase B	2.361	0.088	2.627
	Phase B – Phase C	2.527	0.114	2.870
	Phase A – Phase C	2.469	0.179	3.005
75 % of the TL	Phase A	1.378	0.099	1.674
	Phase B	1.464	0.061	1.646
	Phase C	**1.497**	0.097	1.788
	Phase A – Phase B	2.383	0.097	2.674
	Phase B – Phase C	2.561	0.128	2.945
	Phase A – Phase C	2.509	0.194	**3.092**
End of TL	Phase A	1.362	0.099	1.660
	Phase B	1.452	0.063	1.640
	Phase C	1.491	0.106	**1.809**
	Phase A – Phase B	2.355	0.100	2.656
	Phase B – Phase C	2.542	0.137	2.952
	Phase A – Phase C	2.480	0.200	3.081

Table A3.2: Worst overvoltage case. Milagres – Ourolândia section, via Milagres. Capacitor bypassed during reclosing

Ourolândia – Igaporã	Phase-to-ground and phase-to-phase	Average (pu)	Standard deviation (pu)	μ + 3σ (pu)
Start of the TL	Phase A	1.260	0.033	1.360
	Phase B	1.304	0.026	1.383
	Phase C	1.233	0.023	1.301
	Phase A – Phase B	2.259	0.065	2.453
	Phase B – Phase C	2.188	0.050	2.337
	Phase A – Phase C	2.139	0.041	2.261
25% of the TL	Phase A	1.354	0.031	1.447
	Phase B	1.417	0.042	1.543
	Phase C	1.320	0.036	1.428
	Phase A – Phase B	2.416	0.073	2.635
	Phase B – Phase C	2.371	0.068	2.577
	Phase A – Phase C	2.278	0.046	2.417
Middle of TL	Phase A	1.412	0.031	1.505
	Phase B	1.494	0.058	1.669
	Phase C	1.369	0.047	1.511
	Phase A – Phase B	2.518	0.082	2.764
	Phase B – Phase C	2.478	0.087	2.740
	Phase A – Phase C	2.367	0.052	2.523
75 % of the TL	Phase A	1.436	0.037	1.546
	Phase B	**1.524**	0.071	1.739
	Phase C	1.379	0.054	1.542
	Phase A – Phase B	2.551	0.090	2.820
	Phase B – Phase C	2.514	0.106	2.831
	Phase A – Phase C	2.396	0.057	2.567
End of TL	Phase A	1.418	0.040	1.539
	Phase B	1.509	0.080	**1.748**
	Phase C	1.359	0.057	1.530
	Phase A – Phase B	2.524	0.100	2.824
	Phase B – Phase C	2.484	0.121	**2.848**
	Phase A – Phase C	2.364	0.059	2.540

3.3 Sensitivity Regarding the Length of the Sections

The choosing of the electric and geographical location of the new substations may be subject to changes, and it is important to evaluate the length of the sections regarding overvoltage during three-pole reclosing. The chosen base solution standardizes the lengths at 440 km each, leveling performance from a switching perspective. Below, the overvoltage

distributions of the worst reclosing case are presented, but with the 550 km section between Sobradinho and Igaporã, maintaining the same shunt and series compensation percentages. The Sobradinho substation was disregarded for other access reasons, as well as for the distance to the Igaporã substation, having been replaced with a substation closer to Ourolândia.

Table A3.3: Worst overvoltage case. Sobradinho – Igaporã section, via Igaporã. 550 km section adopted in preliminary studies

Overvoltage location	Phase-to-ground and phase-to-phase	Average (pu)	Standard deviation (pu)	Maximum overvoltage (pu)
Start of the TL	Phase A	1.240	0.065	1.450
	Phase B	1.321	0.057	1.550
	Phase C	1.355	0.084	1.550
	Phase A – Phase B	2.181	0.083	2.550
	Phase B – Phase C	2.335	0.091	2.650
	Phase A – Phase C	2.251	0.157	2.650
25% of the TL	Phase A	1.416	0.089	1.750
	Phase B	1.517	0.084	1.800
	Phase C	1.529	0.116	1.800
	Phase A – Phase B	2.449	0.120	2.850
	Phase B – Phase C	2.666	0.138	3.050
	Phase A – Phase C	2.565	0.183	3.000
Middle of TL	Phase A	1.511	0.101	1.850
	Phase B	1.624	0.095	2.000
	Phase C	1.661	0.134	2.000
	Phase A – Phase B	2.608	0.143	3.050
	Phase B – Phase C	2.889	0.159	3.300
	Phase A – Phase C	2.769	0.211	3.200
75 % of the TL	Phase A	1.544	0.109	1.900
	Phase B	1.648	0.093	1.950
	Phase C	1.715	0.132	1.950
	Phase A – Phase B	2.649	0.153	3.200
	Phase B – Phase C	2.944	0.152	3.300
	Phase A – Phase C	2.845	0.221	3.300
End of TL	Phase A	1.530	0.119	1.950
	Phase B	1.644	0.111	1.950
	Phase C	**1.730**	0.155	2.200
	Phase A – Phase B	2.610	0.158	3.300
	Phase B – Phase C	2.939	0.185	3.350
	Phase A – Phase C	2.830	0.247	**3.400**

The overvoltages were significantly higher.

3.4 Use of Fast Grounding Switch

We observed that the use of fast grounding switches would not be necessary to reduce the residual load in the line, since there is margin for application of a longer dead time before reclosing. Also, the three-pole reclosing overvoltages are comparable to those of other switchings (energization), and did not cause impact on the insulation coordination.

3.5 Statistic Distributions

As indicated, the worst overvoltages were observed with the series capacitor inserted for all the sections, because the dispersions are larger in this case. Thus, the results of the statistic simulations are presented for this condition.

3.5.1 Milagres – Ourolândia

a) Via Milagres

a1) Phase-to-ground

	0% L (start)			25% L			50% L		
	A	B	C	A	B	C	A	B	C
Average value (pu)	1.239	1.295	1.291	1.304	1.388	1.396	1.357	1.445	1.469
Standard deviation (pu)	0.065	0.040	0.056	0.082	0.048	0.073	0.093	0.054	0.089
Simulated peak (pu)	1.400	1.450	1.450	1.550	1.550	1.550	1.650	1.650	1.650
μ + 3σ (pu)	1.435	1.414	1.459	1.551	1.531	1.616	1.635	1.606	1.737

	75% L			100% L (end)		
	A	B	C	A	B	C
Average value (pu)	1.378	1.464	1.497	1.362	1.452	1.491
Standard deviation (pu)	0.099	0.061	0.097	0.099	0.063	0.106
Simulated peak (pu)	1.650	1.650	1.700	1.650	1.650	1.750
μ + 3σ (pu)	1.674	1.646	1.788	1.660	1.640	**1.809**

a2) Phase-to-phase

	0% L (start)			25% L			50% L		
	A–B	B–C	C–A	A–B	B–C	C–A	A–B	B–C	C–A
Average value (pu)	2,168	2,249	2,198	2,287	2,423	2,358	2,361	2,527	2,469
Standard deviation (pu)	0,093	0,069	0,104	0,089	0,095	0,147	0,088	0,114	0,179
Simulated peak (pu)	2,450	2,500	2,450	2,550	2,650	2,650	2,700	2,850	2,850
μ + 3σ (pu)	2,448	2,457	2,509	2,554	2,710	2,798	2,627	2,870	3,005

	75% L			100% L (end)		
	A–B	B–C	C–A	A–B	B–C	C–A
Average value (pu)	2.383	2.561	2.509	2.355	2.542	2.480
Standard deviation (pu)	0.097	0.128	0.194	0.100	0.137	0.200
Simulated peak (pu)	2.750	2.950	2.950	2.700	2.950	3.000
μ + 3σ (pu)	2.674	2.945	**3.092**	2.656	2.952	3.081

b) Via Ourolândia

b1) Phase-to-ground

	0% L (start)			25% L			50% L		
	A	B	C	A	B	C	A	B	C
Average value (pu)	1.244	1.264	1.269	1.322	1.363	1.340	1.377	1.426	1.382
Standard deviation (pu)	0.029	0.067	0.029	0.028	0.078	0.033	0.034	0.088	0.040
Simulated peak (pu)	1.350	1.450	1.350	1.400	1.550	1.450	1.500	1.650	1.550
μ + 3σ (pu)	1.331	1.464	1.357	1.407	1.598	1.439	1.479	1.688	1.503

	75% L			100% L (end)		
	A	B	C	A	B	C
Average value (pu)	1.397	1.446	1.388	1.379	1.430	1.367
Standard deviation (pu)	0.039	0.094	0.041	0.043	0.099	0.046
Simulated peak (pu)	1.500	1.650	1.550	1.500	1.650	1.550
μ + 3σ (pu)	1.515	**1.730**	1.512	1.507	1.726	1.505

b2) Phase-to-phase

	0% L (start)			25% L			50% L		
	A–B	B–C	C–A	A–B	B–C	C–A	A–B	B–C	C–A
Average value (pu)	2.168	2.249	2.198	2.287	2.423	2.358	2.361	2.527	2.469
Standard deviation (pu)	0.093	0.069	0.104	0.089	0.095	0.147	0.088	0.114	0.179
Simulated peak (pu)	2.450	2.500	2.450	2.550	2.650	2.650	2.700	2.850	2.850
μ + 3σ (pu)	2.448	2.457	2.509	2.554	2.710	2.798	2.627	2.870	3.005

	75% L			100% L (end)		
	A–B	B–C	C–A	A–B	B–C	C–A
Average value (pu)	2.401	2.496	2.373	2.372	2.465	2.335
Standard deviation (pu)	0.100	0.108	0.060	0.104	0.116	0.065
Simulated peak (pu)	2.650	2.750	2.600	2.650	2.750	2.600
μ + 3σ (pu)	2.701	**2.819**	2.554	2.685	2.812	2.529

3.5.2 Ourolândia – Igaporã

a) Via Ourolândia

a1) Phase-to-ground

	0% L (start)			25% L			50% L		
	A	B	C	A	B	C	A	B	C
Average value (pu)	1.317	1.212	1.217	1.423	1.302	1.290	1.495	1.355	1.345
Standard deviation (pu)	0.026	0.030	0.057	0.039	0.047	0.054	0.050	0.063	0.053
Simulated peak (pu)	1.400	1.350	1.400	1.550	1.500	1.500	1.650	1.600	1.500
μ + 3σ (pu)	1.395	1.301	1.388	1.540	1.444	1.453	1.643	1.544	1.503

	75% L			100% L (end)		
	A	B	C	A	B	C
Average value (pu)	1.523	1.370	1.368	1.507	1.353	1.352
Standard deviation (pu)	0.060	0.070	0.052	0.067	0.076	0.053
Simulated peak (pu)	1.700	1.650	1.600	1.700	1.700	1.550
μ + 3σ (pu)	1.702	1.582	1.524	**1.709**	1.580	1.511

a2) Phase-to-phase

	0% L (start)			25% L			50% L		
	A–B	B–C	C–A	A–B	B–C	C–A	A–B	B–C	C–A
Average value (pu)	2.213	2.048	2.238	2.405	2.186	2.362	2.517	2.277	2.453
Standard deviation (pu)	0.045	0.059	0.081	0.070	0.066	0.096	0.094	0.067	0.107
Simulated peak (pu)	2.350	2.250	2.450	2.600	2.400	2.600	2.800	2.500	2.700
μ + 3σ (pu)	2.347	2.225	2.481	2.616	2.383	2.649	2.799	2.477	2.773

	75% L			100% L (end)		
	A–B	B–C	C–A	A–B	B–C	C–A
Average value (pu)	2.554	2.312	2.482	2.525	2.285	2.451
Standard deviation (pu)	0.115	0.070	0.119	0.129	0.073	0.124
Simulated peak (pu)	2.850	2.550	2.800	2.900	2.500	2.800
μ + 3σ (pu)	2.900	2.521	2.840	**2.913**	2.506	2.822

b) Via Igaporã

b1) Phase-to-ground

	0% L (start)			25% L			50% L		
	A	B	C	A	B	C	A	B	C
Average value (pu)	1.246	1.133	1.180	1.358	1.226	1.231	1.422	1.272	1.262
Standard deviation (pu)	0.033	0.027	0.024	0.045	0.045	0.043	0.048	0.048	0.055
Simulated peak (pu)	1.400	1.300	1.300	1.500	1.400	1.500	1.550	1.450	1.500
μ + 3σ (pu)	1.345	1.214	1.253	1.494	1.361	1.360	1.565	1.416	1.427

	75% L			100% L (end)		
	A	B	C	A	B	C
Average value (pu)	1.439	1.285	1.273	1.424	1.276	1.259
Standard deviation (pu)	0.047	0.051	0.064	0.051	0.055	0.071
Simulated peak (pu)	1.600	1.500	1.550	1.600	1.500	1.600
μ + 3σ (pu)	**1.579**	1.439	1.466	1.577	1.440	1.472

b2) Phase-to-phase

	0% L (start)			25% L			50% L		
	A–B	B–C	C–A	A–B	B–C	C–A	A–B	B–C	C–A
Average value (pu)	2.069	1.987	2.096	2.250	2.108	2.221	2.362	2.173	2.296
Standard deviation (pu)	0.053	0.034	0.067	0.068	0.054	0.121	0.074	0.072	0.134
Simulated peak (pu)	2.300	2.100	2.300	2.450	2.300	2.500	2.600	2.400	2.600
μ + 3σ (pu)	2.227	2.090	2.297	2.454	2.270	2.585	2.583	2.390	2.698

	75% L			100% L (end)		
	A–B	B–C	C–A	A–B	B–C	C–A
Average value (pu)	2.403	2.191	2.333	2.382	2.167	2.305
Standard deviation (pu)	0.073	0.088	0.135	0.075	0.099	0.137
Simulated peak (pu)	2.650	2.550	2.600	2.600	2.600	2.600
μ + 3σ (pu)	2.622	2.454	**2.739**	2.606	2.465	2.715

3.5.3 Igaporã – Pirapora

a) Via Igaporã

a1) Phase-to-ground

	0% L (start)			25% L			50% L		
	A	B	C	A	B	C	A	B	C
Average value (pu)	1.175	1.231	1.236	1.237	1.316	1.336	1.273	1.352	1.396
Standard deviation (pu)	0.034	0.024	0.040	0.047	0.037	0.069	0.060	0.043	0.084
Simulated peak (pu)	1.300	1.350	1.350	1.450	1.500	1.500	1.550	1.550	1.550
μ + 3σ (pu)	1.277	1.303	1.355	1.378	1.425	1.542	1.451	1.481	1.647

	75% L			100% L (end)		
	A	B	C	A	B	C
Average value (pu)	1.284	1.358	1.422	1.274	1.339	1.412
Standard deviation (pu)	0.072	0.050	0.093	0.088	0.055	0.102
Simulated peak (pu)	1.600	1.500	1.600	1.600	1.500	1.650
μ + 3σ (pu)	1.500	1.507	1.702	1.538	1.503	**1.720**

a2) Phase-to-phase

	0% L (start)			25% L			50% L		
	A–B	B–C	C–A	A–B	B–C	C–A	A–B	B–C	C–A
Average value (pu)	2.028	2.164	2.091	2.139	2.322	2.216	2.178	2.410	2.283
Standard deviation (pu)	0.051	0.063	0.057	0.082	0.092	0.098	0.085	0.093	0.126
Simulated peak (pu)	2.250	2.350	2.300	2.450	2.550	2.600	2.500	2.650	2.650
μ + 3σ (pu)	2.181	2.353	2.261	2.386	2.599	2.509	2.433	2.690	2.663

	75% L			100% L (end)		
	A–B	B–C	C–A	A–B	B–C	C–A
Average value (pu)	2.178	2.439	2.304	2.156	2.407	2.282
Standard deviation (pu)	0.095	0.098	0.151	0.112	0.099	0.162
Simulated peak (pu)	2.500	2.700	2.650	2.550	2.700	2.650
μ + 3σ (pu)	2.463	2.735	2.757	2.491	2.704	**2.768**

b) Via Pirapora

b1) Phase-to-ground

	0% L (start)			25% L			50% L		
	A	B	C	A	B	C	A	B	C
Average value (pu)	1.158	1.227	1.244	1.226	1.299	1.314	1.267	1.335	1.357
Standard deviation (pu)	0.047	0.037	0.048	0.070	0.051	0.059	0.084	0.053	0.071
Simulated peak (pu)	1.350	1.350	1.400	1.500	1.500	1.500	1.550	1.500	1.550
μ + 3σ (pu)	1.300	1.337	1.387	1.436	1.454	1.489	1.519	1.494	1.571

	75% L			100% L (end)		
	A	B	C	A	B	C
Average value (pu)	1.274	1.350	1.364	1.257	1.338	1.349
Standard deviation (pu)	0.090	0.058	0.077	0.093	0.063	0.085
Simulated peak (pu)	1.600	1.500	1.600	1.600	1.550	1.600
μ + 3σ (pu)	1.544	1.524	1.596	1.535	1.528	**1.605**

b2) Phase-to-phase

	0% L (start)			25% L			50% L		
	A–B	B–C	C–A	A–B	B–C	C–A	A–B	B–C	C–A
Average value (pu)	2.032	2.154	2.091	2.147	2.264	2.216	2.194	2.322	2.299
Standard deviation (pu)	0.070	0.057	0.089	0.087	0.077	0.118	0.085	0.081	0.147
Simulated peak (pu)	2.300	2.350	2.350	2.500	2.500	2.550	2.600	2.600	2.650
μ + 3σ (pu)	2.243	2.325	2.358	2.407	2.496	2.570	2.448	2.566	2.738

	75% L			100% L (end)		
	A–B	B–C	C–A	A–B	B–C	C–A
Average value (pu)	2.205	2.337	2.313	2.179	2.307	2.277
Standard deviation (pu)	0.094	0.094	0.159	0.104	0.099	0.164
Simulated peak (pu)	2.650	2.700	2.750	2.700	2.650	2.750
μ + 3σ (pu)	2.487	2.620	**2.789**	2.491	2.604	2.768

3.5.4 Transient oscillograms

Figures A3.1 and A3.2 show the overvoltage oscillograms in the line reclosing cases of the Milagres – Ourolândia section, via Milagres, which presented the highest overvoltages.

3.5.5 Milagres – Ourolândia (via Milagres)

Maximum overvoltages: 1,717 pu phase-to-ground and 2,679 pu phase-to-phase.

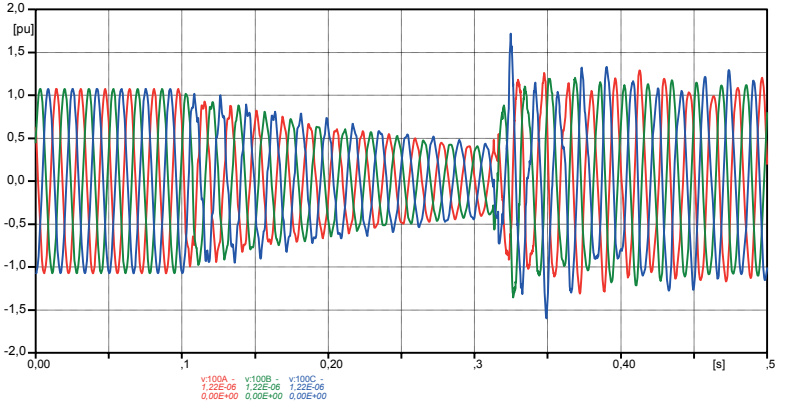

Figure A3.1: Phase-to-ground overvoltage during the three-pole reclosing of the Milagres – Ourolândia section, when done via Milagres (100% TL, Line Terminal)

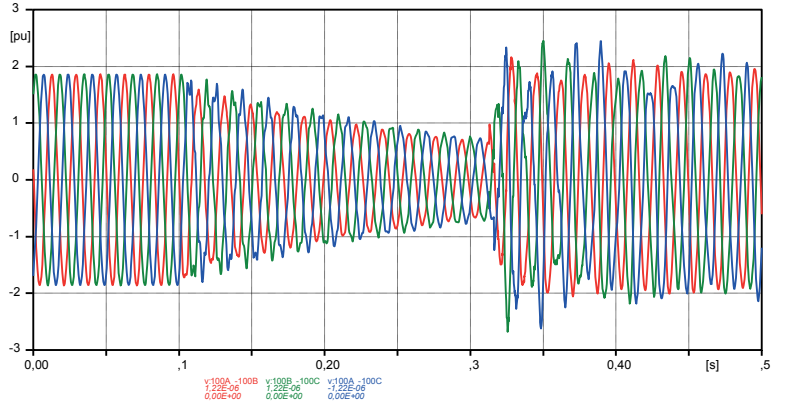

Figure A3.2: Phase-to-phase overvoltage during the three-pole reclosing of the Milagres – Ourolândia section, when done via Milagres (100% TL, Line Terminal)

ATTACHMENT 4 – Fault Application and Clearing, and Load Rejection

4.1 Objective

Presenting the results obtained in the studies of the 1,000 kV AC transmission line connecting the Milagres (A), Ourolândia (B), Igaporã (C), and Pirapora (D) substations. Each section between the substations presents a length of 440 km. The studied conducted are:

- Fault application
- Fault clearing
- Load rejection

In the fault application, the overvoltages generated during the start of the fault (*fault inception*), and the requests at line insulation level should be observed. The overvoltages for the single-phase faults occurring at 0%, 25%, 50%, 75%, and 100% of the length of each section will be evaluated.

In the fault clearing, we observed the overvoltages resulting of the opening of the line sections for the case of single-phase fault in the middle, at 75% from the start of the line, and at the end of the line. Single-pole and three-pole openings, the current opening sequence, the influence of line surge arresters, and the healthy system were considered.

In load rejection, we observe the overvoltages and energy passing through the line surge arresters on both sides of the line, and if, during load rejection, there is no overvoltage and energy higher than the surge arrester can withstand.

4.2 Fault application

The overvoltages produced during the start of the fault (*fault inception)* are also phenomena of the EMT (*Electromagnetic Transients*) type. After the start of the fault (single-phase or three-phase), traveling waves are injected into the system, which, after some reflexes on the substations, can add up at some specific points resulting in higher overvoltages. These overvoltage values can impact the sizing of the insulation of the line and substations because of their magnitude. Usually, these are short-term wave forms when compared, for example, to overvoltages resulting of line energization. These

overvoltages are influenced by factors such as the number of lines that go in or out of the substation, reactive compensation, and the action of surge arresters.

The series capacitors protection system (bypass), usually done by MOV (*Metal Oxide Varistor*), influence the overvoltages and must be represented in the system. Thus, in the 1,000 kV system, the simulations were done considering series capacitors inserted, and their protection against overvoltage (bypass). This equipment (MOV) was chosen based on the voltage (rated) in the capacitor terminals (bank). In the case of faults close to the capacitor, the MOV protection system should operate and do its bypass in a short time interval.

With the objective of analyzing the worst instants that will originate overvoltages in the healthy phases, the fault (phase A) will be applied in the following instants (Figure A4.1):

- Fault occurring at the peak of the positive cycle.
- On the instant of crossing through wave zero.
- Fault occurring at the peak of the negative cycle.

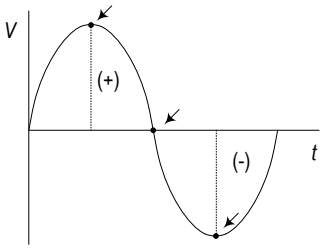

Figure A4.1: Voltage wave instants in which the faults were applied

Single-phase faults were simulated, and the voltages were read at points at 0%, 25%, 50%, 75%, and 100% of the length of each section (Figure A4.2). The fault resistance considered was equal to 50 Ω.

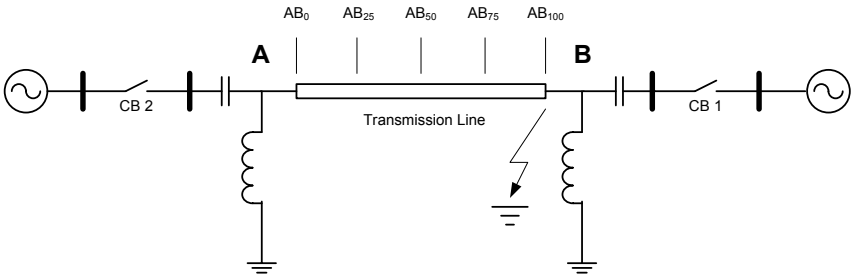

Figure A4.2: Simulated system

Tables A 4.1, A4.2, and A4.3 show the overvoltages in the healthy phases (B and C), resulting of the occurrence of single-phase faults (phase A) in the middle of each section. The highest overvoltage value (peak value) found was in the Ourolândia – Igaporã section, and was equal to 1.52 pu.

The overvoltage values for faults in other point of the sections considered were lower than the ones shown in these tables. Overvoltage measurements in the sections next to the fault section presented low values.

Table A4.1: Overvoltages in the healthy phases (B and C) of the Milagres – Ourolândia section for the single-phase fault in the AB_{50} point (middle of the Milagres – Ourolândia section)

		Overvoltage (pu) in the Milagres – Ourolândia section				
Position in the voltage wave, fault application	Fault application instant (s)	AB_0	AB_{25}	AB_{50}	AB_{75}	AB_{100}
Cycle peak (+)	0.0967	1.103	1.299	1.448	1.297	1.148
Crossing by zero	0.0846	1.091	1.206	1.345	1.216	1.118
Cycle peak (-)	0.0884	1.101	1.298	**1.451**	1.297	1.149

Table A4.2: Overvoltages in the healthy phases (B and C) of the Ourolândia – Igaporã section for the single-phase fault in the BC_{50} point (middle of the Ourolândia – Igaporã section)

		Overvoltage (pu) in the Ourolândia – Igaporã section				
Position in the voltage wave, fault application	Fault application instant (s)	BC_0	BC_{25}	BC_{50}	BC_{75}	BC_{100}
Cycle peak (+)	0.0974	1.115	1.328	1.517	1.344	1.129
Crossing by zero	0.0933	1.110	1.199	1.378	1.237	1.106
Cycle peak (-)	0.0892	1.133	1.323	**1.522**	1.346	1.143

Table A4.3: Overvoltages in the healthy phases (B and C) of the Igaporã – Pirapora section for the single-phase fault in the CD_{50} point (middle of the Igaporã – Pirapora section)

		Overvoltage (pu) in the Igaporã – Pirapora section				
Position in the voltage wave, fault application	Fault application instant (s)	BC_0	BC_{25}	BC_{50}	BC_{75}	BC_{100}
Cycle peak (+)	0.0813	1.133	1.244	1.399	1.265	1.113
Crossing by zero	0.0772	1.113	1.187	1.336	1.204	1.118
Cycle peak (-)	0.0897	1.134	1.244	**1.400**	1.266	1.119

We can observe that the worst instants for the fault to occur are when the voltage in the defective phase is at the wave peak.

Figure A4.3 shows the instant overvoltages for the worst condition presented in Table A4.3 (Ourolândia - Igaporã section).

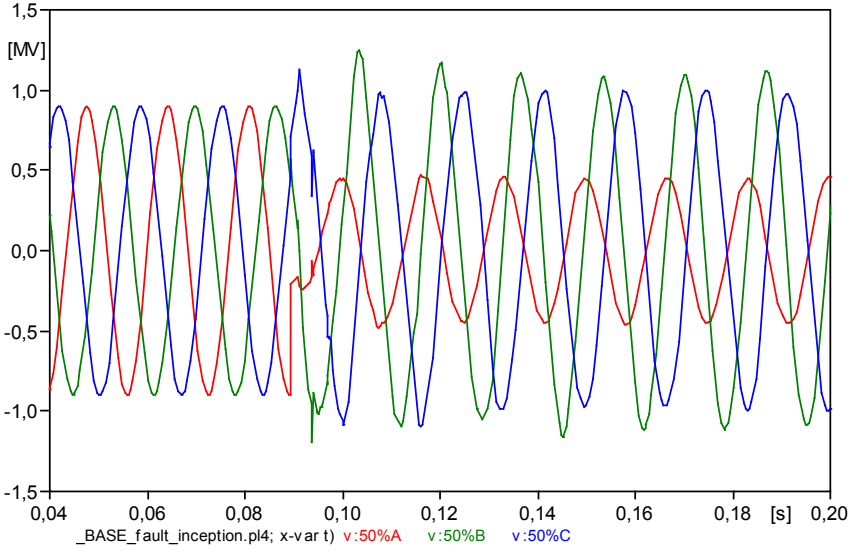

Figure A4.3: Highest overvoltage obtained due to the start of the fault (phase A)

However, this highest overvoltage value shown is lower than the values obtained in the energization of the lines. As Figure A4.4 shows, this overvoltage establishes a very low energy value (lower than 70 Joules) to be absorbed in the surge arresters (of rated value 828 kV_{rms}), not imposing significant stress on this equipment.

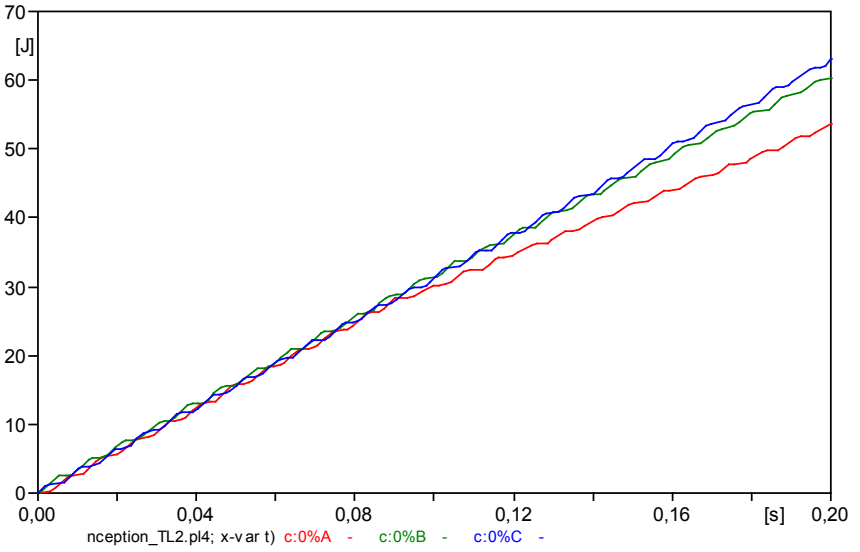

Figure A4.4: Energy in the surge arresters in the Ourolândia busbar

4.3 Fault Clearing

For the study of this phenomenon, we analyze the overvoltages resulting of the opening of a transmission line after the occurrence of a single-phase fault in some points of the line.

4.3.1 Results obtained

The 1,000 kV transmission line is composed of three sections of approximately 440 km each. The study of the three-pole and single-pole fault clearing was performed in each of the sections, according to the following procedure: a single-phase fault was applied along a section of the line (25% of the length of the line section), the closest circuit breaker opens after approximately 50 ms, after another 50 ms another circuit breaker opens isolating the line. In the case of the fault in the middle of the line, two sequences of line circuit breaker opening were studied.

a) Three-pole opening of the line

The results of the simulations performed with the three-pole opening of the feeder circuit breaker are presented in Table A4.4, below.

Table A4.4: Overvoltages for the three-pole opening of the line

Failure location	Overvoltages (pu)		
	TL_0	TL_{50}	TL_{100}
MO_{100}	1.43	1.77	1.87
MO_{75}	1.48	1.69	1.79
MO_{50}	1.41	1.67	1.76
MO_{25}	1.58	1.51	1.27
MO_0	1.58	1.43	1.24
OI_{100}	1.48	1.77	1.87
OI_{75}	1.49	1.74	1.83
OI_{50}	1.42	1.73	1.81
OI_{25}	1.59	1.49	1.30
O_{I0}	1.58	1.46	1.38
IP_{100}	1.39	1.83	**1.92**
IP_{75}	1.35	1.76	1.84
IP_{50}	1.35	1.80	1.82
IP_{25}	1.68	1.64	1.25
IP_0	1.85	1.68	1.44

The highest overvoltage (1.92 pu) occurred in the Igaporã - Pirapora section, with the short-circuit applied in Pirapora. Figure A4.5 presents the voltage at the Pirapora terminal for this case.

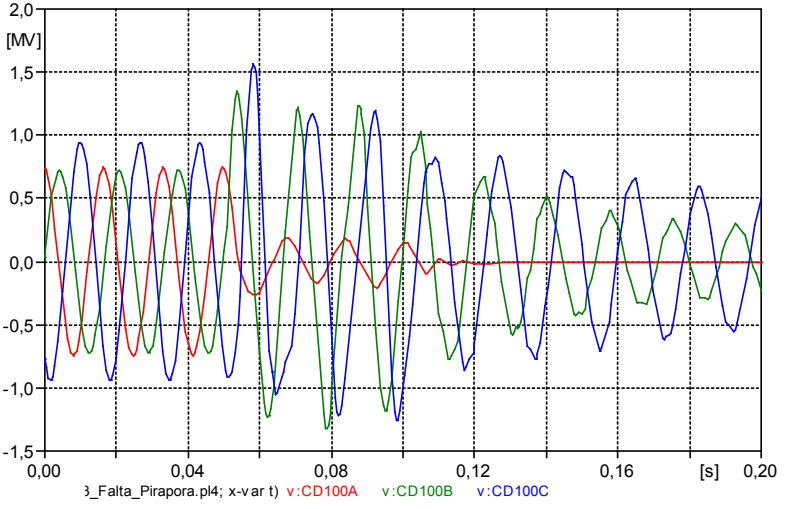

Figure A4.5: Voltage at Pirapora

b) Single-pole opening of the line

The same procedure was adopted for the single-pole opening of the feeder circuit breakers. Table A4.5, below, presents the results for this study.

Table A4.5: Overvoltages for the single-pole opening of the line

TL Section	Failure location	Overvoltages (pu)		
		TL_0	TL_{50}	TL_{100}
Milagres – Ourolândia (MO)	MO_{100}	1.17	1.31	1.32
	MO_{75}	1.15	1.23	1.18
	MO_{50}	1.20	1.32	1.15
	MO_{25}	1.22	1.29	1.23
	MO_0	**1.35**	1.34	1.28
Ourolândia – Igaporã (OI)	OI_{100}	1.24	1.30	1.23
	OI_{75}	1.19	1.24	1.16
	OI_{50}	1.21	**1.35**	1.15
	OI_{25}	1.24	1.28	1.15
	O_{I0}	1.31	1.34	1.17
Igaporã – Pirapora (IP)	IP_{100}	1.18	1.24	1.15
	IP_{75}	1.15	1.23	1.15
	IP_{50}	1.14	1.34	1.15
	IP_{25}	1.15	1.25	1.14
	IP_0	1.23	1.19	1.21

c) Comparison of the results

Comparing the overvoltage values of Table A4.4 and Table A4.5, we verify that the highest overvoltages occurred in the case of the three-pole opening of the line, and that the highest overvoltage occurs as a result of the opening of the first circuit breaker, the one closest to the fault.

4.3.2 Sensitivity analysis

The highest overvoltage occurred in the Igaporã – Pirapora section, with the short-circuit applied in Pirapora, and three-pole opening of the line. For this case, some sensitivity studies were conducted.

a) Influence of the line surge arresters

The line surge arrester current conduction threshold is of 1.87 pu.

The highest value of 1.92 pu indicated in Table A4.4 occurred in the end of the Igaporã – Pirapora section, with fault at the Pirapora terminal, and surge arrester connected. Without the surge arrester, the overvoltage goes up to 1.99 pu. In this case, however, the energy absorbed by the surge arrester was low, much lower than admissible.

b) Influence of the current opening sequence

The instant of opening changes the current interruption sequence. Figure A4.6, below, presents two current interruption sequences.

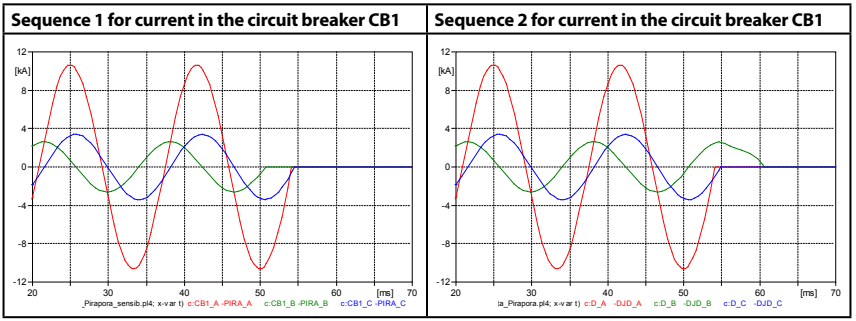

Figure A4.6: Current opening sequence

For sequence 1 (BAC), maximum overvoltage was 1.92 pu, and for sequence 2 (ACB) maximum overvoltage was 1.96 pu. Therefore, we verify that the current extinction sequence has little influence on the overvoltages resulting of fault clearing.

4.3.3 Overvoltages in the healthy system

The overvoltages in the busbars isolated by the line in fault were analyzed. The maximum overvoltages occurred in the opening of the Igaporã – Pirapora line, with fault in the line at Pirapora.

For this case, the voltages at Pirapora and Igaporã were observed after the circuit breaker, that is, the voltage in the healthy busbars. The maximum overvoltage at Igaporã was of 1.34 pu, and at Pirapora was of 1.59 pu. Figures A4.7 and A4.8, below, presents these voltages.

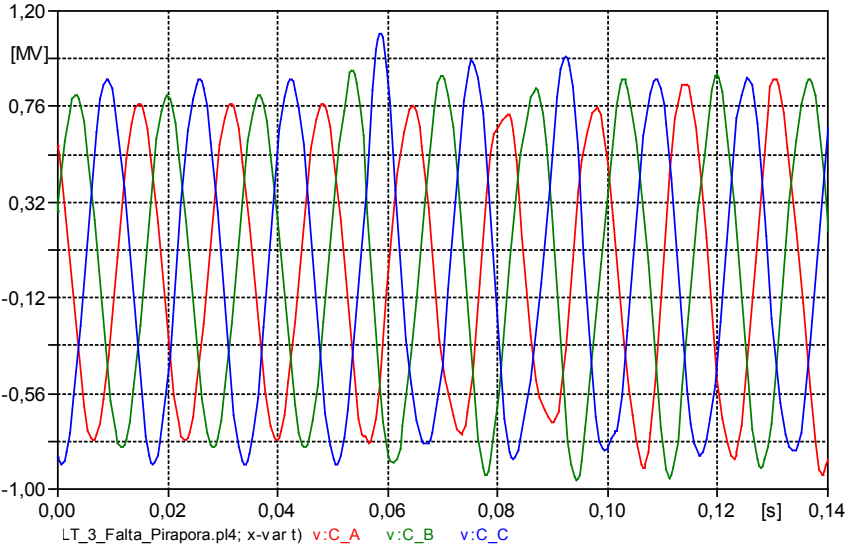

Figure A4.7: Voltages at Igaporã

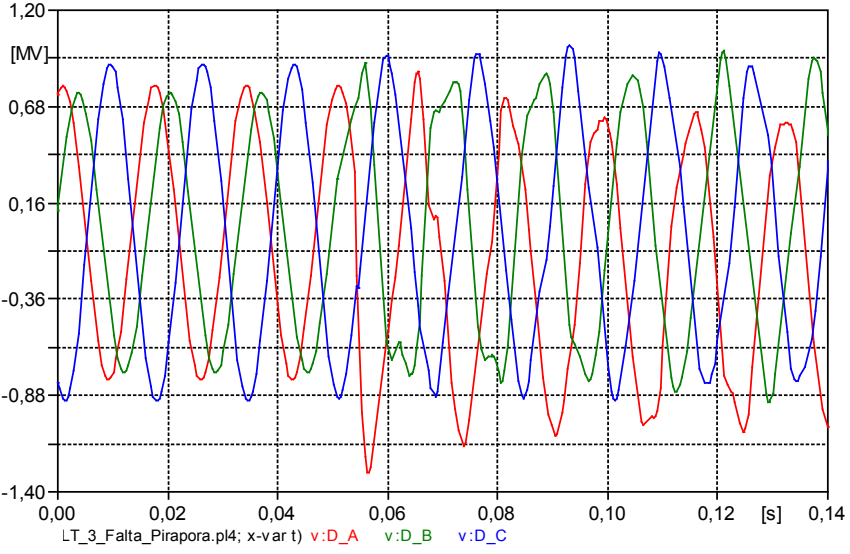

Figure A4.8: Voltages at Pirapora

The healthy system did not suffer severe impacts due to the short-circuit and opening of the transmission line.

4.4 Load Rejection

The load rejection study was conducted as follows:

- Open one of the sides of the line sections at 50 ms.
- Analyze which line section presents higher overvoltage, in which point of the line the overvoltage occurs, and if this will cause the surge arrester to operate.
- Analyze the overvoltages with the occurrence of short-circuit (before the opening of one of the sides of the line) and after the opening. Analyze, also, the voltages and energy in the surge arresters.

4.4.1 Opening without short

All the sections of the line were tested by performing, one at a time, the opening of one of the sides of the line, with the system in state, and analyzing the voltages in the 0% and 100% points of the line sections, without the inclusion of surge arresters.

The worst overvoltage case occurs in the Igaporã – Pirapora line, when the opening occurs via Pirapora. The values are described in Table A4.6.

Table A4.6: Phase-to-ground voltages (pu) in the Igaporã – Pirapora line, with opening via Pirapora

Phase	Pirapora (pu)	Igaporã (pu)
A	**1.68**	1.27
B	1.34	1.28
C	1.67	1.24

None of the tests showed voltage enough to trigger surge arrester operation. The voltage oscillograms at Pirapora are shown in Figure A4.9.

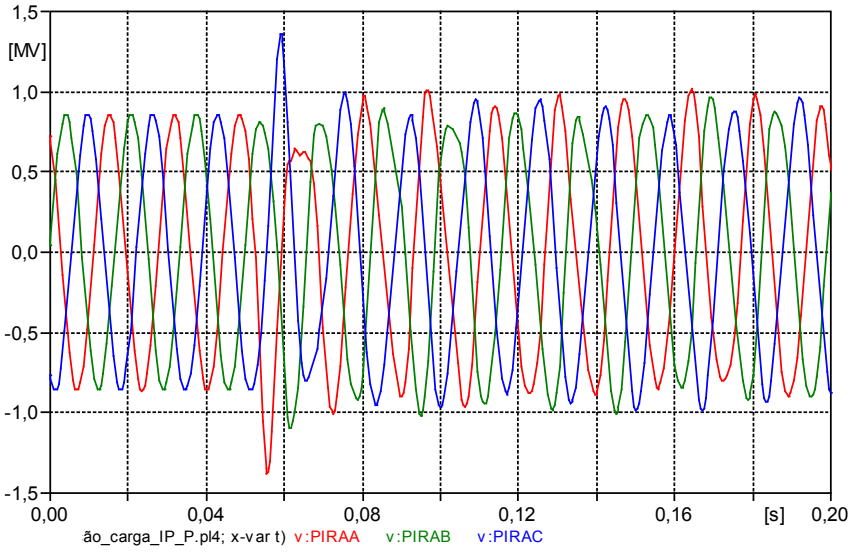

Figure A4.9: Voltages at Pirapora, rejection at Pirapora

4.4.2 Short followed by opening

In this case, one of the sides of the line is opened, and the voltages are analyzed at the extremities of the line in short circuit, having pre-opening at the points 0%, 50% or 100%. The worst case occurs in the Igaporã – Pirapora line, when the short is inserted at the 100% point (on the Pirapora side). The results are presented in Table A4.7.

Table A4.7: Phase-to-ground voltages (pu) in the Igaporã – Pirapora line, with short at Pirapora

Phase	Igaporã (pu)	Pirapora (pu)
A	1.17	1.05
B	1.18	1.63
C	1.39	**2.08**

The voltage oscillograms at Pirapora are shown in Figure A4.10.

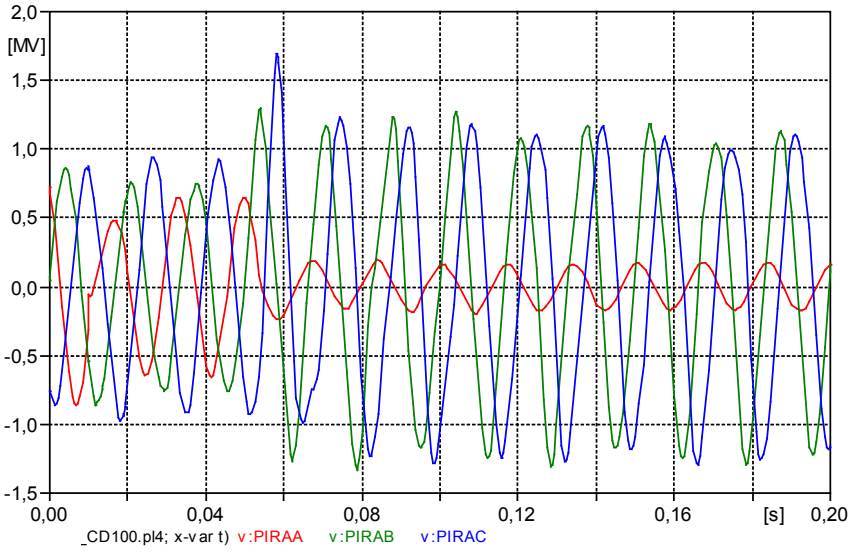

Figure A4.10: Voltages at Pirapora, rejection at Pirapora with short circuit

In this case, we observe that now it is possible for the surge arrester to operate on the Pirapora side. Thus, we repeated the case including the surge arresters in the lines, and analyzed the energy conducted by them (Figure A4.11).

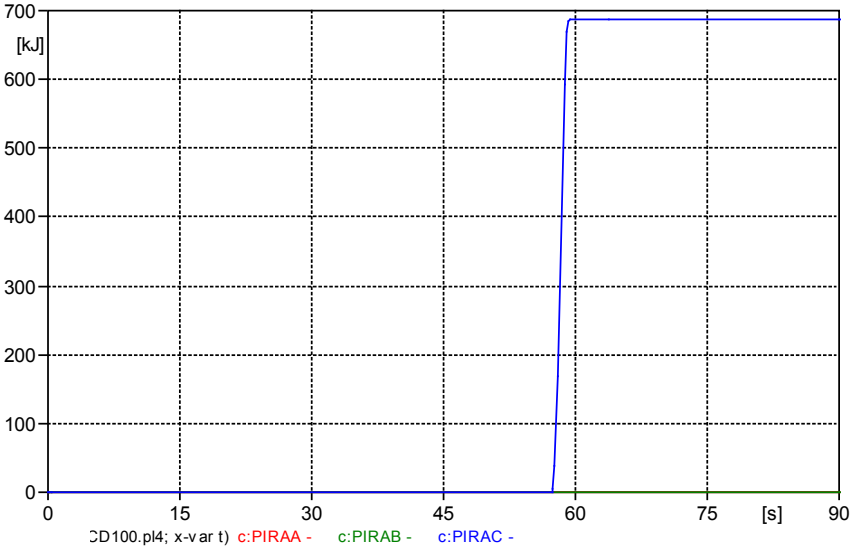

Figure A4.11: Energy absorbed by the surge arrester at Pirapora

From the rated values of the surge arrester used, we have that the maximum energy to be absorbed by it will be 16kJ/kV · 828 kV = 13.2 MJ.

4.4.3 Opening followed by short

In this case, the line is opened in one of the sides and, next, a single-phase short is applied (on the 50 to 60 ms instants). The most severe case occurred with the Ourolândia – Igaporã line.

The results are presented in Table A4.8.

Table A4.8: Phase-to-ground overvoltage (pu) without surge arrester

Phase	Ourolândia (pu)	Igaporã (pu)
A	1.33	1.61
B	1.32	**2.27**
C	1.24	1.92

Figure A4.12 presents the voltage oscillograms.

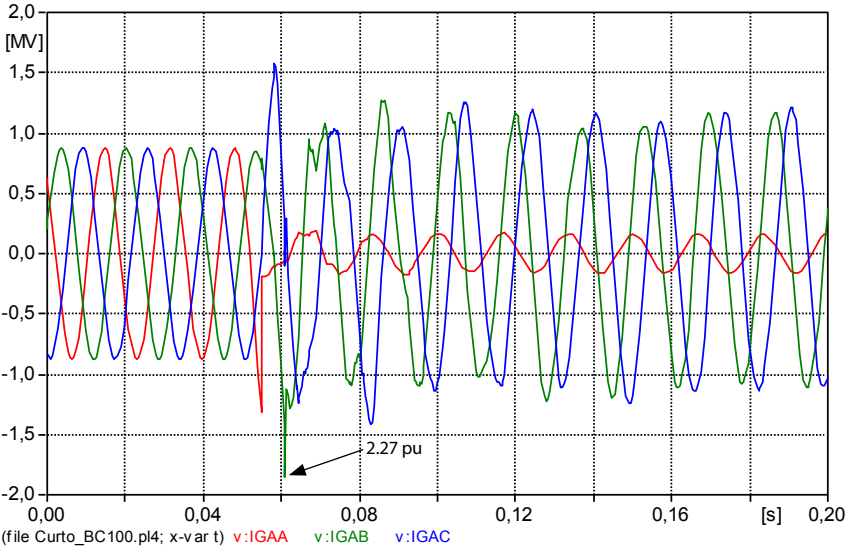

Figure A4.12: Voltages at Igaporã, rejections at Igaporã, and occurrence of short circuit without surge arrester

In this case, overvoltage capable of triggering the action of the surge arrester also occurs. Figure A4.13 presents the energy in the surge arresters at Igaporã.

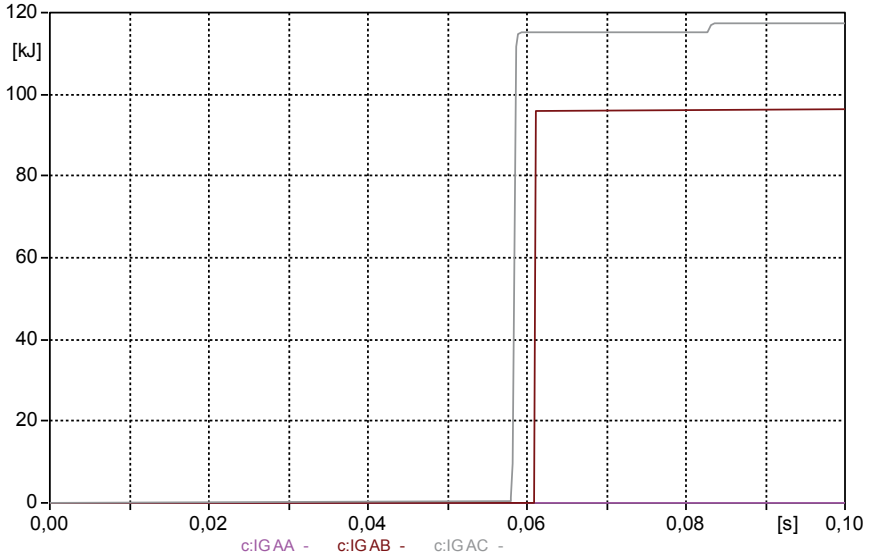

Figure A4.13: Energy absorbed by the surge arrester at Pirapora

ATTACHMENT 5 – Residual Load and Arc Extinction

5.1 Objective

This attachment presents the detailed studies of single-phase and three-phase residual load, and the conditions for extinction of the secondary arc.

The 1,000 kV line simulated was divided into three sections of equal length.

The faults were applied to the sections at 0%, 25%, 50%, 75%, and 100% along the line.

5.2 Single-phase Residual Load

5.2.1 General conditions

Following, we present the studies of the simulations obtained in the ATP program, considering the following conditions:

- 1,000 kV line modeled with distributed parameters.
- Parallel compensation of the sections in each of the extremities of the TL: ~ 85%.
- Single-phase short in Phase A: The simulation starts already in short, with the short switch opened at t = 0,1 s. Under this condition, we consider that the system has already reached the steady state value of the fault current.
- Short resistance: 50 Ω.
- Position of the short in the TL: 0%, 25%, 50%, 75%, and 100% of the line.
- We will obtain the values for the arc extinction current and the first peak of the recovery voltage at the point in fault. These values will be lower than 50 A (effective), 70 Ap (peak), and 100 kVp. The conditions that govern arc extinction are: the value of the last peak of the arc current, and the value of the first peak of the recovery voltage (post-arc).
- The voltage and current limiting values for the secondary arc, referred to above, were defined in Sub module 23.3 (Guidelines and Criteria for Electric Projects Rev_1.1) of the ONS. Figures A5.1 and A5.2 show these waves.

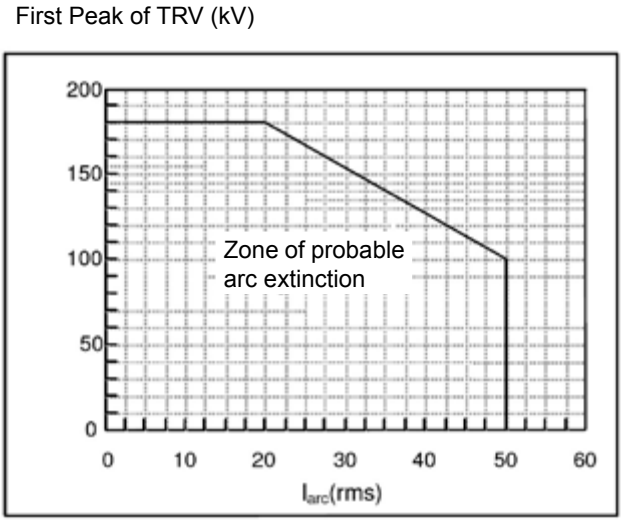

Figure A5.1: Indicative curve for analysis of secondary arc current extinction, for a dead time of up to 500 ms

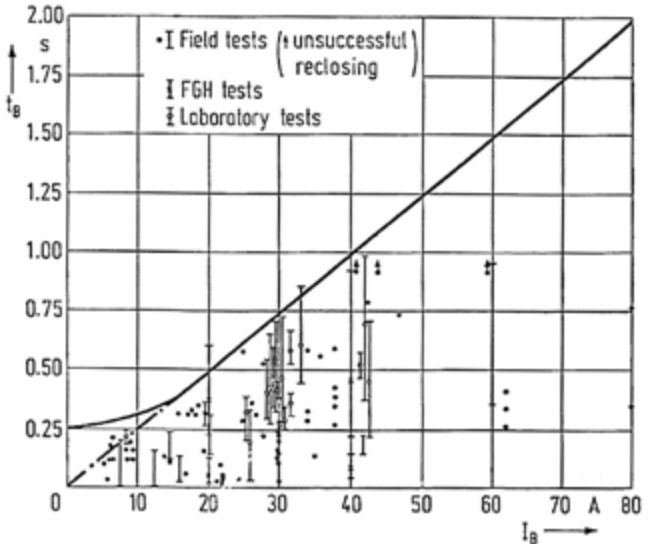

Figure A5.2: Indicative curve dead time for secondary arc extinction *versus* effective value of the secondary arc current, for voltages up to 765 kV

5.2.2 Arc extinction

During the single-pole opening, the electric arc (fault) goes through two stages. The first, called "primary arc," occurs when the circuit breakers in the extremities of the phase in fault are still closed. The second stage, "secondary arc," occurs after the opening of these circuit breakers, with the arc being fed by the inductive and capacitive coupling with the healthy phases.

Before the single-phase reclosing is performed, the secondary arc must be extinguished, and the post-arc voltage must be low. After the arc extinction, the air in the defect region continues ionized. If the secondary arc current, and/or the post-arc voltage are too high, the arc reignition may occur.

5.2.3 Arc extinction phenomenon

The results presented below show the arc current opening process in the Ourolândia-Igaporã section, with line operating on-load, and short occurring at the start of the line (Ourolândia).

The switch simulating the short-circuit (phase A) is closed at t = 0.03 s. In sequence, at t = 0.05 s, the circuit breakers are opened at both extremities of the line. The opening of the short switch occurs at t = 0.9 s. Figure A5.3 presents the entire phenomenon.

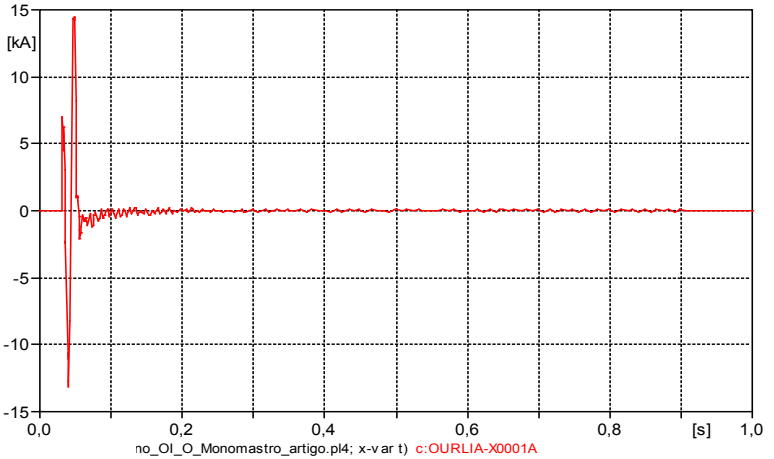

Figure A5.3: Short current (phase A) occurring in section 2 (Ourolândia side)

The peak value of the short current, before the opening of the circuit breakers is of the order of 14.5 kA. In Figure A5.4, we observe that, approximately in the period of t = 0.05 to 0.2 s, there is contribution of the current remaining in the phase in short, in addition to the contribution (inductive effect) of phases B and C. From this instant on, there is only the contribution of the healthy phases to the short, which is the reason this current is much lower, compared to the previously-mentioned period.

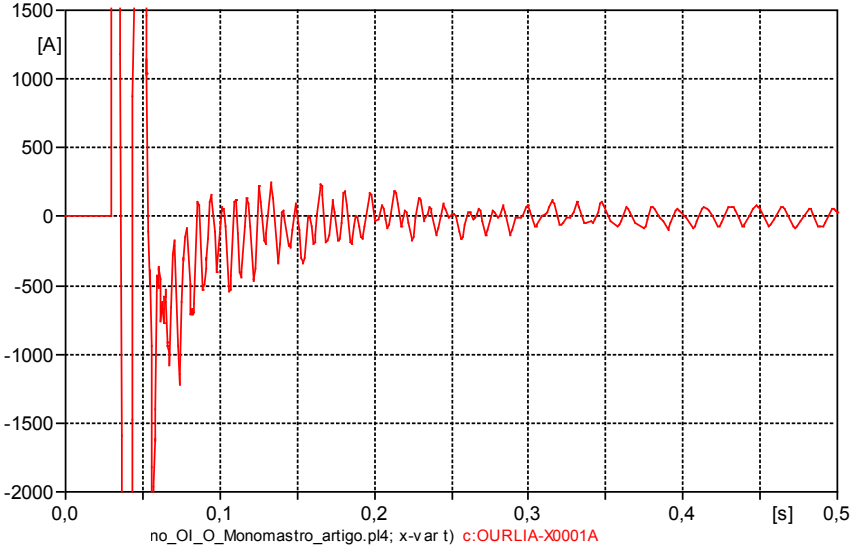

Figure A5.4: Fault current after the opening of the circuit breakers

Figure A5.5 presents the short current in the scale t = 0.5 to 1s, where we verify that in the instants prior to the opening of the short switch, the fault current reaches an almost constant value (short state). It is for this reason that, in the following simulations, we considered that the fault current is already at this state. It is worth mentioning that the simulation may start with the short switch closed, and the circuit breakers in the phase A opened. Figure A5.6 shows the recovery voltage in phase A, on the instant of opening of the short.

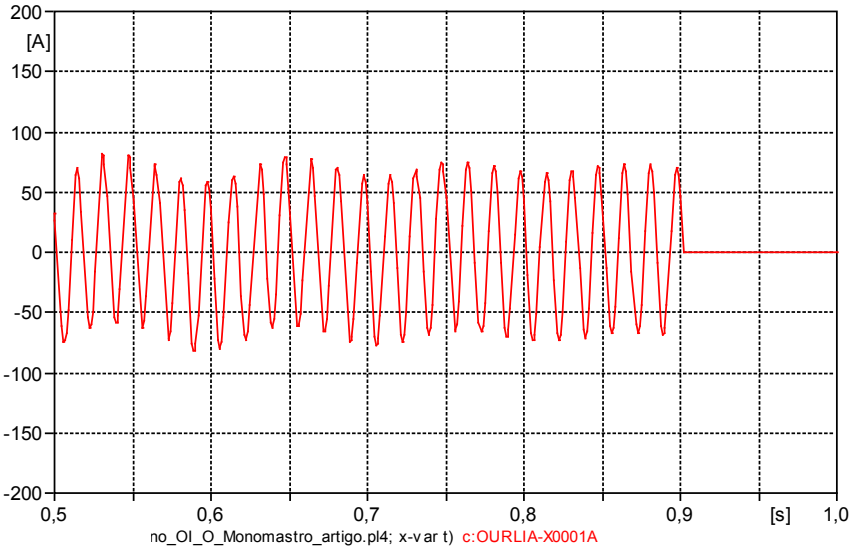

Figure A5.5: Fault current in phase A already reaching the state

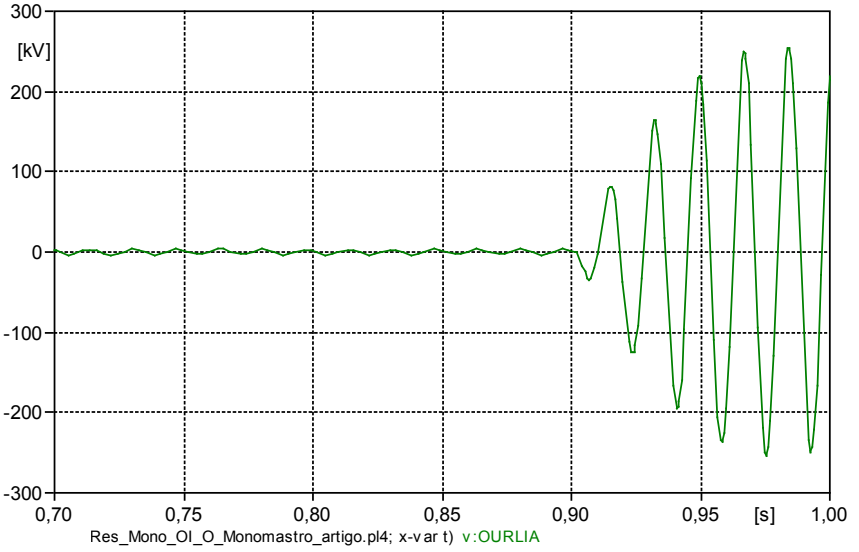

Figure A5.6: Recovery voltage in phase A on the instant of opening of the short

5.2.4 Arc extinction

The currents in the phases before the short and the single-pole opening are the same of the system in steady state (without fault).

It is important to note that in this calculation, a reactor (Xn1) was allocated to the neutral of the line reactors. The reactance of this neutral reactor depends on the capacitances between phases, and on the line reactor. The value chosen was of 250 Ω.

Table A5.1: Results of the Milagres – Ourolândia section

	Short point (TL = 440 km)	Peak values			
		I_{ARC} (A)	V_{REC} (kV)	$V_{REACTOR}$ neutral (kV)	
				Milagres	Ourolândia
Section 1 Milagres to Ourolândia Xn1 = Xn2 = 250 Ω	Milagres (0%)	68.0	33.3	125.3	126.8
	25%	52.5	27.4	125.5	124.5
	50%	41.9	22.3	126.5	123.6
	75%	35.5	18.5	128.4	123.7
	Ourolândia (100%)	34.2	16.7	131.2	125.1

Table A5.2: Results for Ourolândia – Igaporã section

	Short point (TL = 440 km)	Peak values			
		I_{ARC} (A)	V_{REC} (kV)	$V_{REACTOR}$ neutral (kV)	
				Ourolândia	Igaporã
Section 2 Ourolândia to Igaporã Xn1 = Xn2 = 250 Ω	Ourolândia (0%)	70.1	34.1	127.0	126.2
	25%	53.4	27.9	127.6	123.9
	50%	41.9	22.4	129.1	122.9
	75%	34.9	18.2	131.5	123.1
	Igaporã (100%)	33.7	16.4	134.7	124.5

Table A5.3: Results for the Igaporã – Pirapora section

	Short point (TL = 440 km)	Peak values			
		I_{ARC} (A)	V_{REC} (kV)	$V_{REACTOR}$ neutral (kV)	
				Pirapora	Igaporã
Section 3 Igaporã to Pirapora Xn1 = Xn2 = 250 Ω	Igaporã (0%)	70.8	34.4	125.0	125.2
	25%	53.3	27.8	122.5	126.1
	50%	41.1	21.9	121.4	127.8
	75%	33.4	17.4	121.4	130.4
	Pirapora (100%)	31.9	15.5	122.6	133.8

In the previous tables, we observe that both the arc currents and the recovery voltages simulated in the five points of the line are lower, or are at the limit of the specified values (50 A_{rms} or 70 A_p, and 100 kVp) in all the sections.

The maximum voltage on the neutral reactor of section 2 is equal to 135 kV (Ourolândia side), and 126 kV (Igaporã side). Values similar to those found in the remaining sections.

5.2.5 Bypass of the series capacitor on the instant of the fault

In the operation of electric systems, it is also common for the bypass of the series capacitor to operate on the instant of the fault to protect the capacitor. Thus, the series capacitors are normally protected with MOV (*Metal Oxide Varistor*) to reduce or minimize the overvoltages between the capacitor terminals and the bypass switch.

After simulating this condition (bypass of the series capacitor), we observe that the effect on the I_{ARC} and V_{REC} is negligible.

5.2.6 Extinction of the arc "on-load", case of tower with another geometry

Other types of towers with other geometries and conductors were evaluated in the project (8 x 954 MCM, 8 x 795 MCM), self-supporting or single mast guyed tower.

Thus, the values of the secondary arc current and recovery voltage were verified for the new geometries, and neutral reactors with value between 230 Ω and 280 Ω. The results obtained presented little variation (< 10 %).

5.2.7 Influence of system frequency variation in the arc extinction

The influence of system frequency variation in the arc extinction was analyzed in the arc extinction conditions. The analysis was performed considering the most critical case obtained, with the short applied in the second section of the 1,000 kV line, at the Ourolândia terminal.

In the simulations, we verified that, for frequencies lower than 60 Hz (for example, 56 Hz), the secondary arc currents and recovery voltages are lower than the previously presented values (when f = 60 Hz). Thus, there is

no problem regarding arc extinction under this condition.

For frequencies higher than 60 Hz, the secondary arc currents are higher than the previously presented values (when f = 60 Hz). For example, in the case of f = 66 Hz, the value of I_{ARC} can be seen in Table A5.4.

Table A5.4: I_{ARC} current varying with the system frequency

	Frequency	Current (Ap)
Section 2 Ourolândia to Igaporã Xn = 250 Ω	60 Hz	75.92
	66 Hz	130.0

As an alternative to contain a very high I_{ARC}, we can consider using grounding switches close to the terminal in fault, in this case the Ourolândia terminal. A grounding switch placed in parallel to the shunt reactor and neutral reactor was simulated. The switch closing time is equal to 0.05 s, with short already started at the start of the simulation.

The I_{ARC} results obtained with the grounding switch can be seen in Table A5.5. We observe that the I_{ARC} values decrease substantially when compared to those shown in Table A5.4.

Table A5.5: I_{ARC} current varying with the system frequency, with grounding switch

		Current (A) – Peak values	
	Frequency	Guyed single mast tower cable 8 x 954 MCM (Rail)	Guyed single mast tower cable 8 x 795 MCM (Tern)
With grounding switch at the Ourolândia terminal.	60 Hz	1.29	1.45
	66 Hz	2.57	2.82

It is important to note that, as the 1,000 kV line is distant from important generators, the frequencies did not vary much during the electromagnetic transients.

5.3 Three-Phase Residual Load

5.3.1 Results

In this case, with the line with single-phase short, we perform the three-pole opening in the two circuit breakers on both sides of the line.

The residual load obtained for each case and grid is described in Table A5.6, where all the values represent the voltage and peak current in fault. The voltage and current limiting values are respected in all the situations. The situation where there is higher overvoltage and arc current is in the Igaporã – Pirapora line, with short at 25% (110 km) of Pirapora.

Table A5.6: Igaporã – Pirapora

Failure location	I_{FAULT} (A_p)	V_{FAULT} (kV_p)
0%	0.89	0.29
25%	1.19	0.03
50%	0.77	0.41
75%	1.21	0.15
100%	1.1	0.43

The values are low, and the current and voltage oscillograms is presented in Figure A5.7.

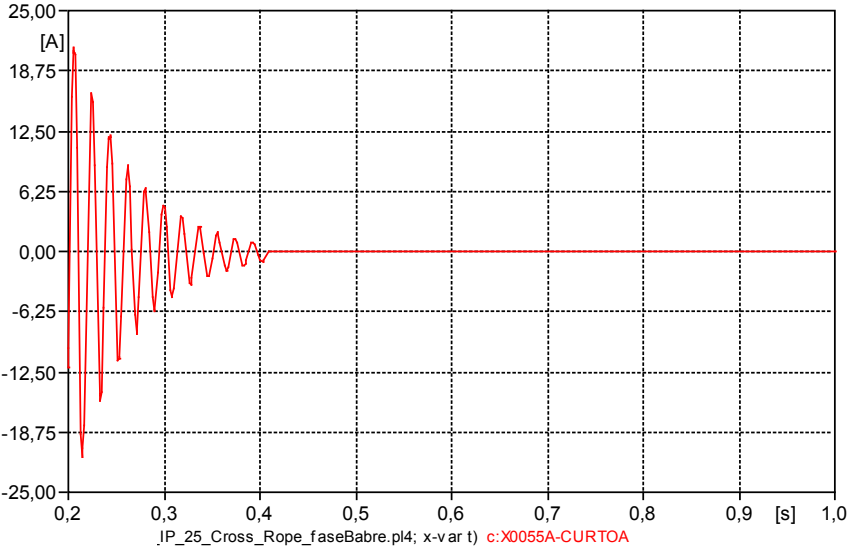

Figure A5.7: Current in the point of fault – Phase A

5.3.2 Position of the reactor

Here, we discuss the position of the line reactor, inserted on the busbar side of the series capacitor, or on the line side. That is because, in the first case, when of the opening of the line, the series capacitor is loaded and, subsequently, discharges through the reactor-capacitor-short circuit. The results are presented in Table A5.7, where we notice that the position of the reactor alters the values of the residual load study, but the voltage and current are low.

Table A5.7: Residual load voltages and current, for change in the reactor position

	Ia (A_p)	Va (kV_p)
Reactor on the series capacitor side.	1.72	0.86
Reactor on the series capacitor busbar side.	5.7	2

ATTACHMENT 6 – Transient Recovery Voltage (TRV)

6.1 General Procedure

The capacity of the line circuit breakers (for short-circuit) in the sections of the 1,000 kV line is equal to 63 kA (rms). Both in the case of the short-line fault and in the case of the terminal fault the system simulation (section) starts with the fault applied in the system.

The circuit breaker "opening" instants were adopted at: $t_A = 0.010818$ s; $t_B = 0.010818$ s; $t_C = 0.01740$ s; being that the phase in fault (phase C) is always the last one to open.

Parasitic capacitances were adopted in both sides of the circuit breaker, equal to 6.8 nF.

Table A6.1 shows the values of the envelope curves proposed by the IEC-CIGRÉ standards for short at the 1,100 kV circuit breaker terminals. The T-100, T-60, T-30, and T-10 curves are chosen based on the relation between the symmetrical short-circuit current through the circuit breaker, and the circuit breaker opening capacity (current). Similarly to the TRV curves for voltage levels lower than 1,000 kV, available in the standard, the T-100 and T-60 curves are four parameter curves, and T-30 and T-10 are 2 parameters.

Table A6.1: TRV parameters (terminal fault) for 1,100 kV circuit breakers

Test duty	kpp	kaf	Uc (kV)	t_2 or t_3 (µs)	U_1 (kV)	t_1 (µs)	RRRV (kV/µs)
T10	1.2	1.76	1,897	271	–	–	7
T30	1.2	1.54	1,660	332	–	–	5
T60	1.2	1.5	1,617	808	808	269	3
T100	1.2	1.5	1,617	1,212	808	404	2
TLF	1.3	1.7 x 0.9	1,786				–

In the program used (ATP), the TRV curves were obtained using an adequate integration step (0.08 ms).

Since the envelope curve for short-line short is not specified in the standard, TRVs for this type of fault are obtained using the T-100 curve.

Similarly to the other studies of the EMT type, the fault resistance was also considered to be equal to 50 Ω.

Along with the TRV curves for each analyzed case, a Table is presented with the notation T_A, T_B, and T_C, with these being the relation in % between the present short current, and the maximum value of the circuit breaker fault opening current (rms).

In these Tables, the type of surpassing of the circuit breaker is indicated by the letter $R_{A,B,C}$, if it is due to the RRRV (*Rate of Rise of Recovery Voltage*); or by the letter $M_{A,B,C}$, if it is because of the magnitude factor.

6.2 Results Ourolândia – Igaporã Section

Transient Recovery Voltages (TRV) were calculated for the following types of switching of the 1,000 kV circuit breakers:

- Single-phase short-line fault occurring at 2 km, 10 km, at 50%, and 90% of the length of the line from the point where the circuit breaker is located.
- Terminal fault on each side of the circuit breaker.

6.2.1 Short-Line Fault

The parameters of the envelope curve used in the short-line fault analysis are those corresponding to the T-100 curve. When there was surpassing of the curve, it was also verified for other values (T_{10}, T_{30}, T_{60}).

a) Fault at 2 km from Ourolândia (opening via Ourolândia)

In the case of the short-line faults, the series capacitor can be bypassed by means of *Metal Oxide Varistor* (MOV) devices and gaps, as a form of protection against high overvoltages during fault periods. In the initial simulation of this case (Figure A6.1), the capacitor bypass was represented by a short-circuit in this element.

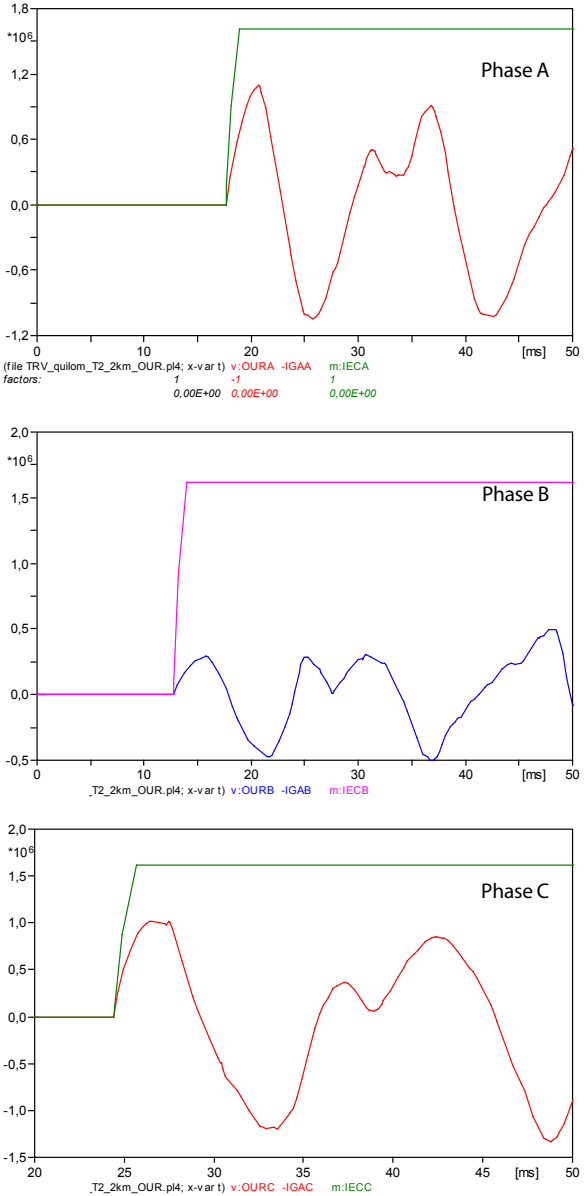

Phase	Icc via DJ (kA_p)	T (%)	Surpassed	Type of surpassing
A	3.55	3.98	No	–
B	0.97	1.09	No	–
C	15.17	17.03	No	–

Figure A6.1: Short-line fault at 2 km from Ourolândia

This case was also simulated using, for the bypass of the series capacitor, a switch with voltage control (*Voltage-Controlled Switch*). In this type of component, the switch will close every time the voltage over the series bank is higher than the established value ($V_{switch} = 3 \cdot 93.3$ kV). The result is presented in Figure A6.2, below:

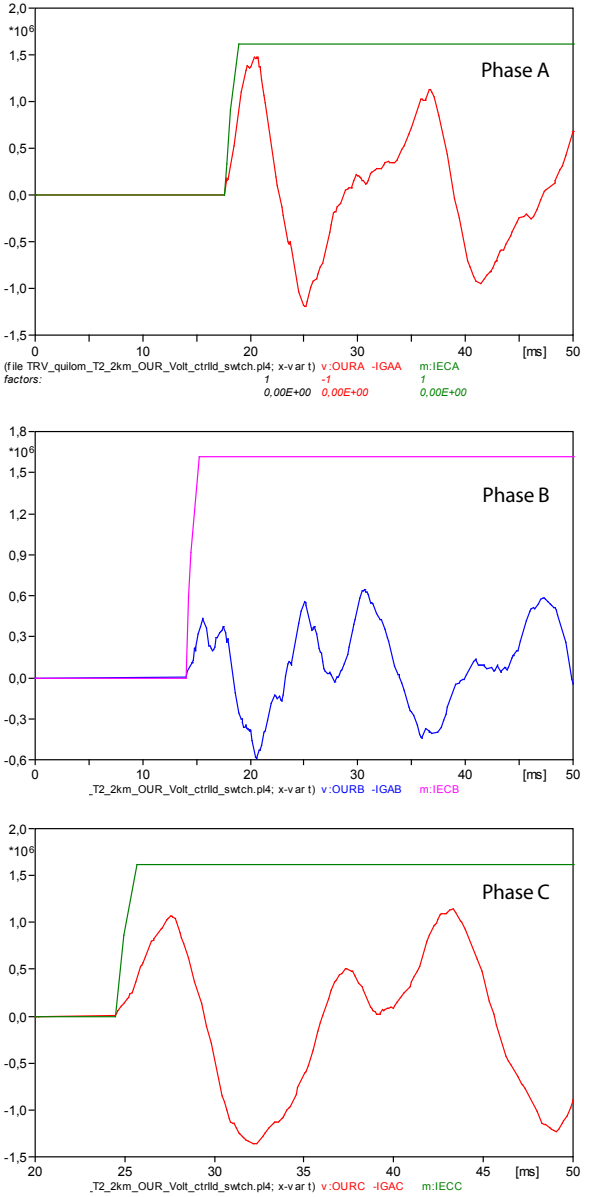

Phase	Icc via DJ (kA_p)	T (%)	Surpassed	Type of surpassing
A	4.4	4.94	No	–
B	1.18	1.32	No	–
C	28.6	32.10	No	–

Figure A6.2: Short-line fault at 2 km from Ourolândia

Note: We observed that, for this type of fault (short-line fault, 2 km), the TRV of the circuit breaker at Ourolândia, with the capacitor inserted (without the bypass), is surpassed both in the RRRV, and in its magnitude. However, in this situation, the current through the series capacitor will be high, and the series capacitor will be bypassed.

For the fault occurring right at the start of the section, soon after the series capacitor (from the Ourolândia side), the magnitude of the fault current through the circuit breaker, and the TRV values are very close to the values shown when the fault was applied at 2 km.

b) Fault at 10 km from Ourolândia (opening via Ourolândia)

The result of this simulation is shown in Figure A6.3.

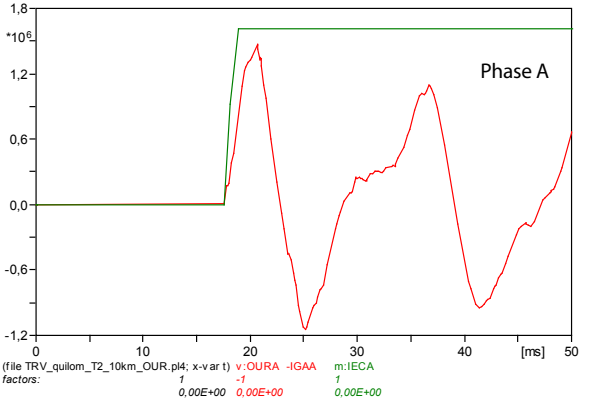

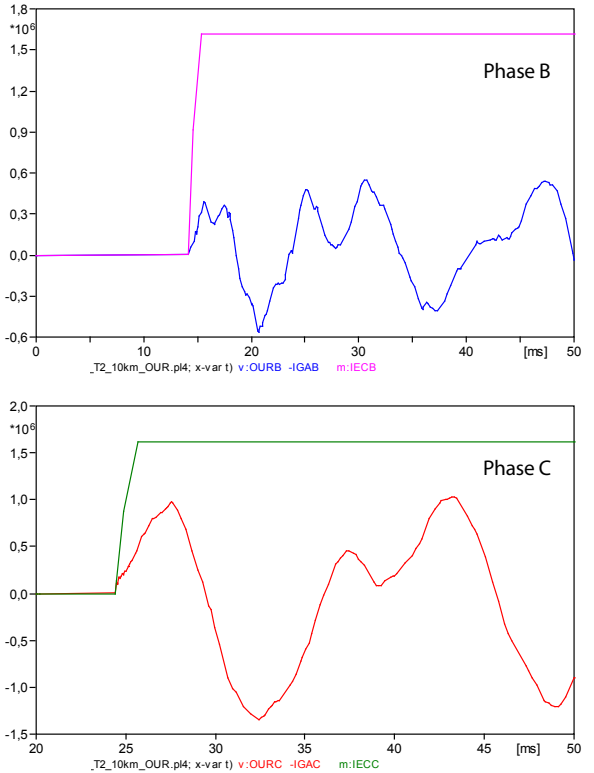

Phase	Icc via DJ (kA_p)	T (%)	Surpassed	Type of surpassing
A	4.08	4.58	No	–
B	1.23	1.38	No	–
C	23.4	26.26	No	–

Figure A6.3: Short-line fault at 10 km from Ourolândia (bypass with voltage-controlled switch)

c) Fault at 50% of the section (opening via Ourolândia)

The result of this simulation is shown in Figure A6.4.

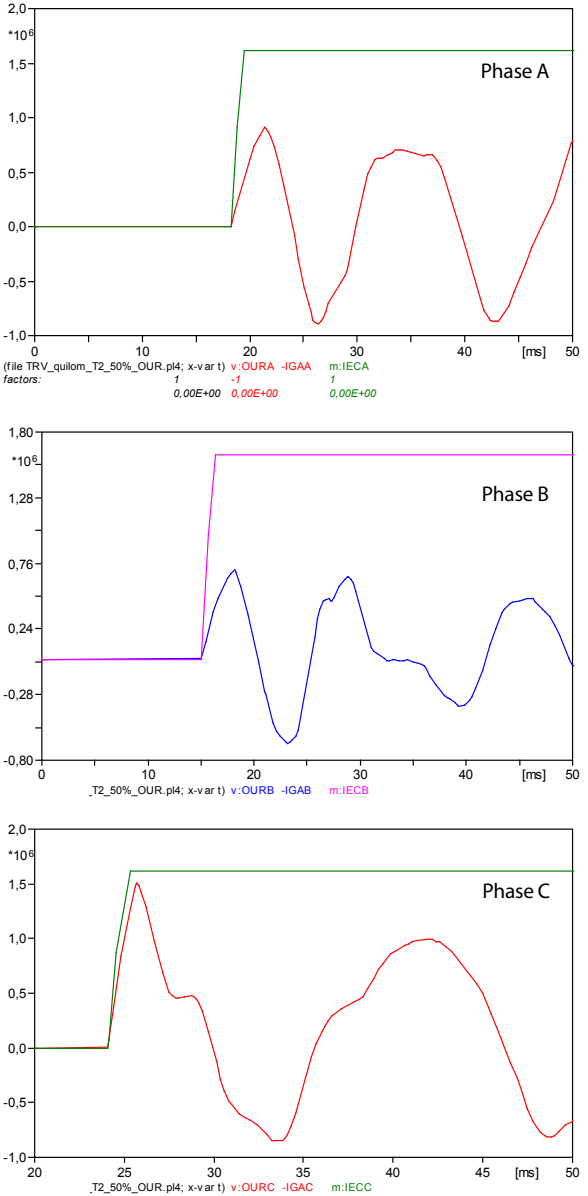

Phase	Icc via DJ (kA_p)	T (%)	Surpassed	Type of surpassing
A	2.73	3.06	No	–
B	2.07	2.32	No	–
C	6.4	7.18	No	–

Figure A6.4: Short-line fault at 50 km from Ourolândia (capacitor not bypassed)

d) Fault at 90% of the section (opening via Ourolândia)

Figure A6.5 shows the result of this simulation.

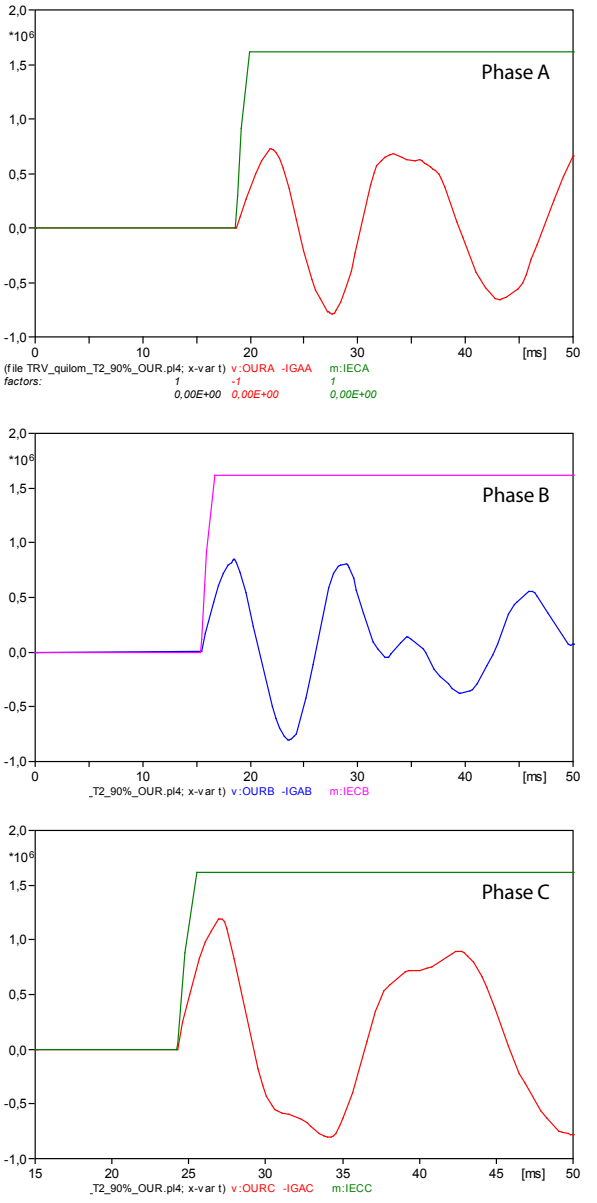

Phase	Icc via DJ (kA_p)	T (%)	Surpassed	Type of surpassing
A	2.24	2.51	No	–
B	2.52	2.83	No	–
C	4.25	4.77	No	–

Figure A6.5: Short-line fault at 90 km from Ourolândia (capacitor not bypassed)

a) Fault at 2 km from Igaporã (opening via Igaporã)

This case was more critical. There was surpassing at the wavefront of the envelope curve (T-100), used in this analysis, as well as in that of the T-60 and T-30 curves (Figure A6.6).

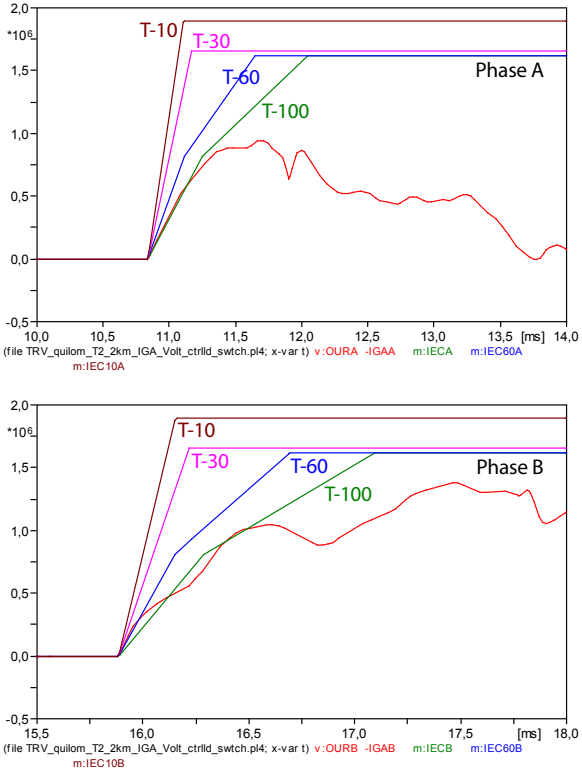

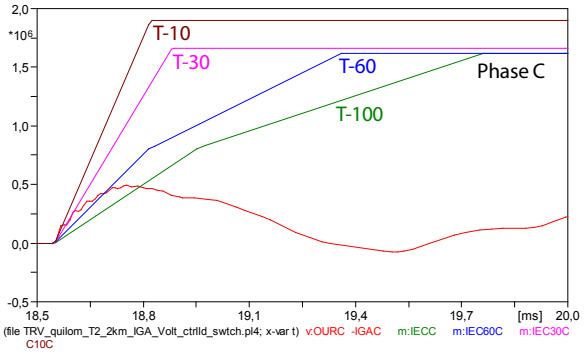

Phase	Icc via DJ (kA$_p$)	T (%)	Surpassed	Type of surpassing
A	3.1	3.48	No	–
B	3.8	4.27	Yes	Rb
C	33.0	37.04	Yes	Rc

Figure A6.6: Short-line fault at 2 km from Igaporã (with voltage-controlled switch)

The surpassing in phase B was in RRRV, with approximately 96 kV, above the 1st slope of the envelope T-100 curve, at approximately one third of said curve. The second surpassing in RRRV occurs at approximately one fourth of the second slope of the envelope curve, at approximately 14 kV.

The surpassing in phase C was also in RRRV, with approximately 176 kV above the 1st slope of the envelope T-100 curve. The T-10 curve is only marginally surpassed at the start of the RRRV.

Below, we present the results of the short-line fault at 2 km of the Igaporã terminal, with the series capacitor bypassed (without voltage-controlled switch).

With the series capacitor bypassed (which actually occurs), we observe in Figure A6.7 that none of the phases is surpassed in magnitude or at the wave front.

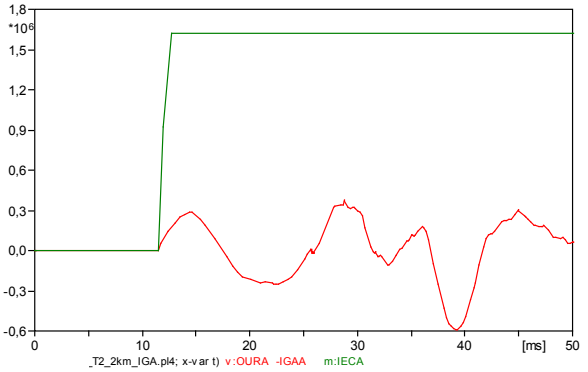

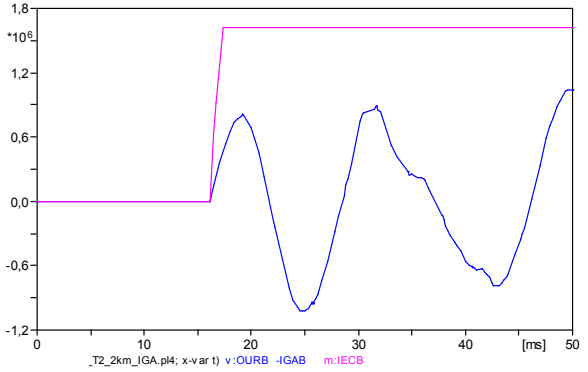

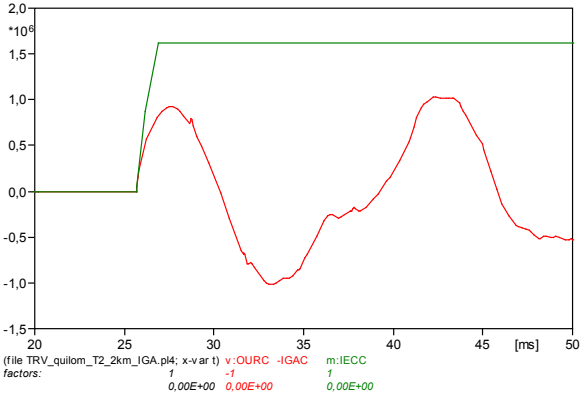

Phase	Icc via DJ (kA_p)	T (%)	Surpassed	Type of surpassing
A	1.05	1.18	No	–
B	2.90	3.25	No	–
C	19.93	22.37	No	–

Figure A6.7: Short-line fault at 2 km from Igaporã (without voltage-controlled switch)

a) Fault at 10 km from Igaporã (opening via Igaporã)

Figure A6.8 shows the result of this simulation.

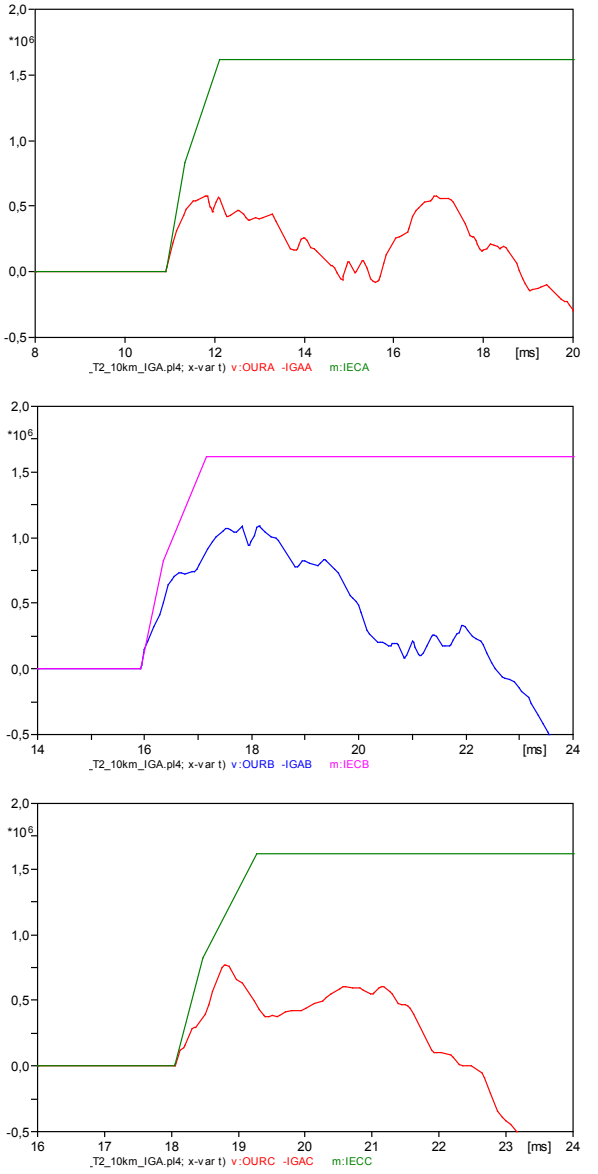

Phase	Icc via DJ (kA_p)	T (%)	Surpassed	Type of surpassing
A	1.5	1.68	No	–
B	3.4	3.82	No	–
C	23.9	26.83	No	–

Figure A6.8: Short-line fault at 10 km from Igaporã (capacitor bypassed with voltage-controlled switch)

g) Fault at 50% of the section (opening via Igaporã)

Figure A6.9 shows the result of this simulation.

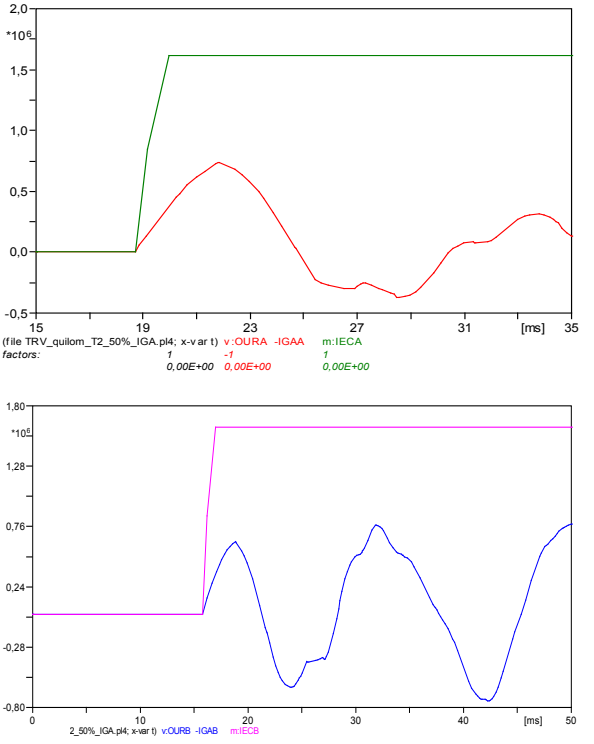

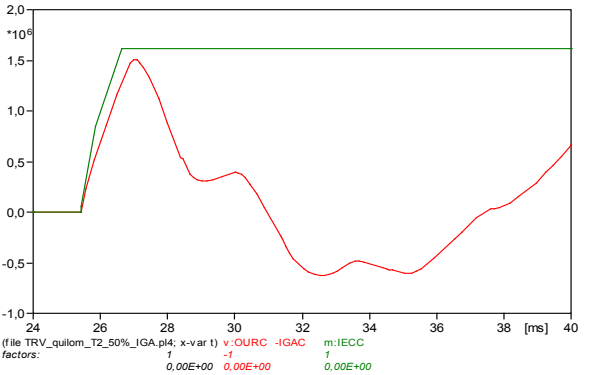

Phase	Icc via DJ (kA$_p$)	T (%)	Surpassed	Type of surpassing
A	2.4	2.69	No	–
B	2.09	2.35	No	–
C	6.8	7.63	No	–

Figure A6.9: Short-line fault at 50 km from Igaporã (capacitor not bypassed)

h) Fault at 90% of the section (opening via Igaporã)

Figure A6.10 shows the result of this simulation.

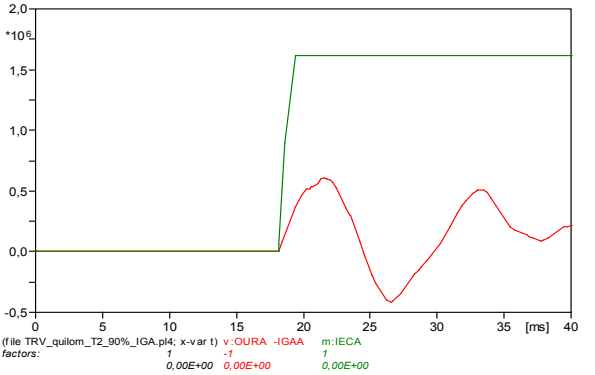

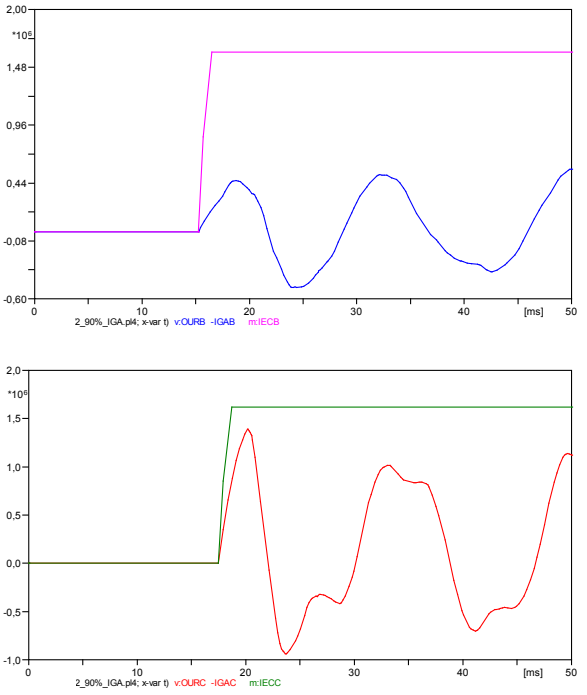

Phase	Icc via DJ (kA_p)	T (%)	Surpassed	Type of surpassing
A	3.2	3.59	No	–
B	1.2	1.35	No	–
C	4.8	5.39	No	–

Figure A6.10: Short-line fault at 90 km from Igaporã (capacitor not bypassed)

6.2.2 Terminal fault (Ourolândia side)

This item studies the circuit breaker opening with the contribution on the line side or on the transformer side.

a) Three-phase – insulated (feeder circuit-breaker)

The result obtained for this condition is shown in Figure A6.11.

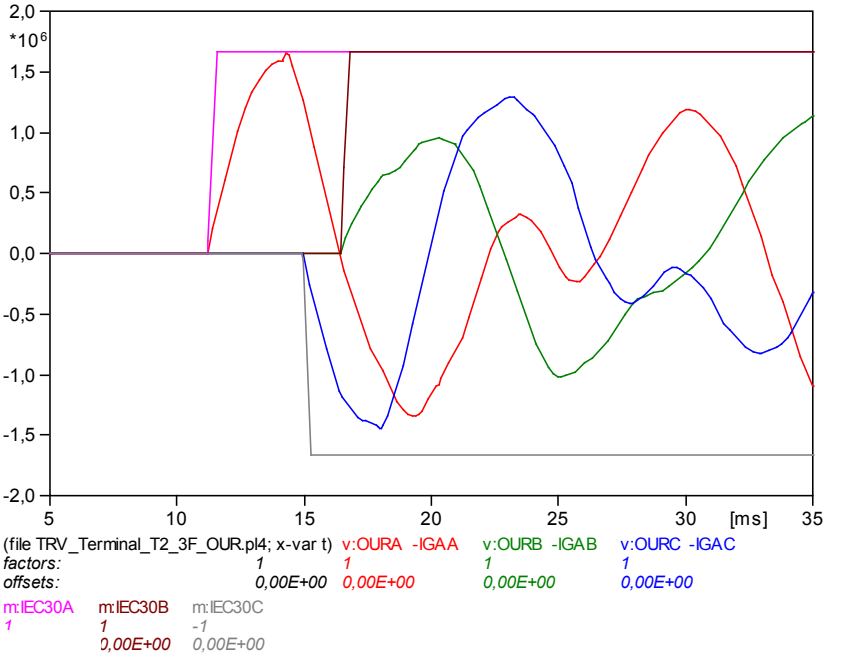

Phase	Icc via DJ (kA$_p$)	T (%)	Surpassed	Type of surpassing
A	9.84	11.04	No	–
B	9.84	11.04	No	–
C	9.84	11.04	No	–

Figure A6.11: Three-phase terminal fault insulated on the side of the line (Ourolândia)

Fault current (three-phase, insulated) via the circuit breaker = 9.84 kA.
For this fault current value, the envelope curve to be used will be:

$$T(\%) = \frac{9{,}84kA}{\sqrt{2}} \cdot \frac{100}{63kA} = 11{,}04\%\text{, T30 curve.}$$

b) Three-phase – grounded (line side)

The result obtained for this condition is shown in Figure A6.12.

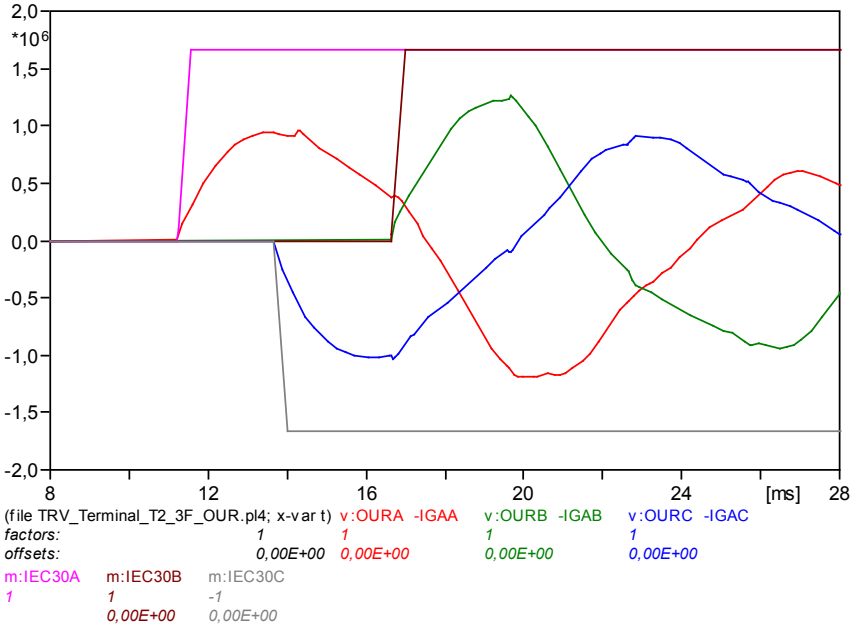

Phase	Icc via DJ (kA_p)	T (%)	Surpassed	Type of surpassing
A	9.84	11.04	No	–
B	9.84	11.04	No	–
C	9.84	11.04	No	–

Figure A6.12: Three-phase terminal fault grounded on the side of the line (Ourolândia)

c) Three-phase – insulated (transformer side)

The result obtained for this condition is shown in Figure A6.13.

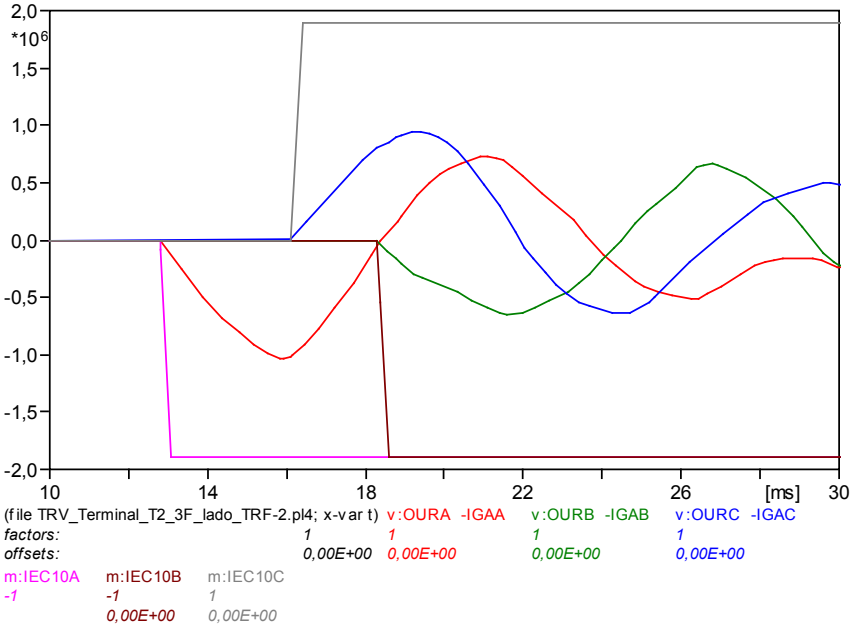

Phase	Icc via DJ (kA$_p$)	T (%)	Surpassed	Type of surpassing
A	3.63	4.07	No	–
B	3.63	4.07	No	–
C	3.63	4.07	No	–

Figure A6.13: Three-phase terminal fault insulated on the side of the transformer

For this fault current value, the envelope curve to be used will be:

$$T(\%) = \frac{3,63kA}{\sqrt{2}} \cdot \frac{100}{63kA} = 4,07\%\text{, T10 curve.}$$

d) Three-phase – grounded (transformer side)

The result obtained for this condition is shown in Figure A6.14.

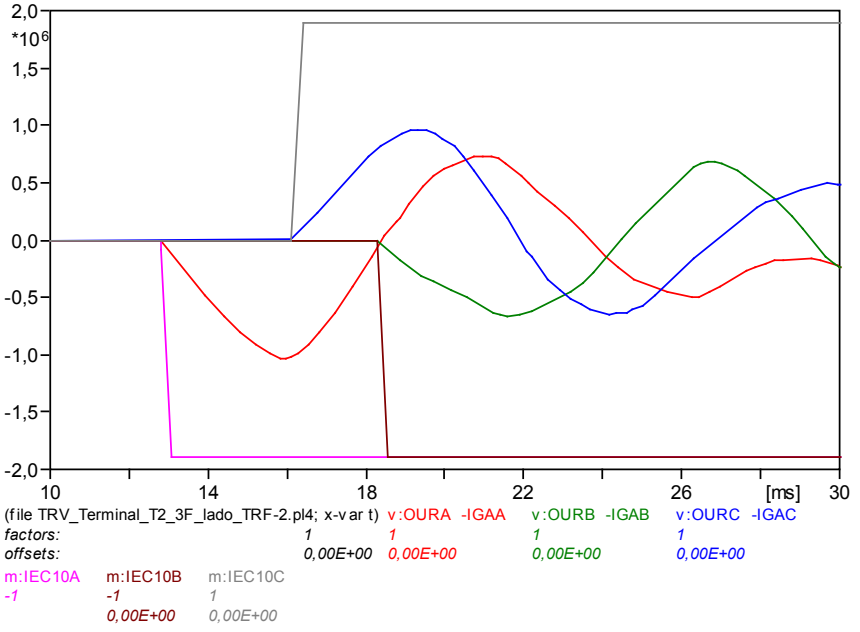

Phase	Icc via DJ (kA_p)	T (%)	Surpassed	Type of surpassing
A	3.63	4.07	No	–
B	3.63	4.07	No	–
C	3.63	4.07	No	–

Figure A6.14: Three-phase terminal fault grounded on the side of the transformer (Ourolândia)

6.2.3 Terminal fault (Igaporã side)

a) Three-phase – insulated (line side)

The result obtained for this condition is shown in Figure A6.15.

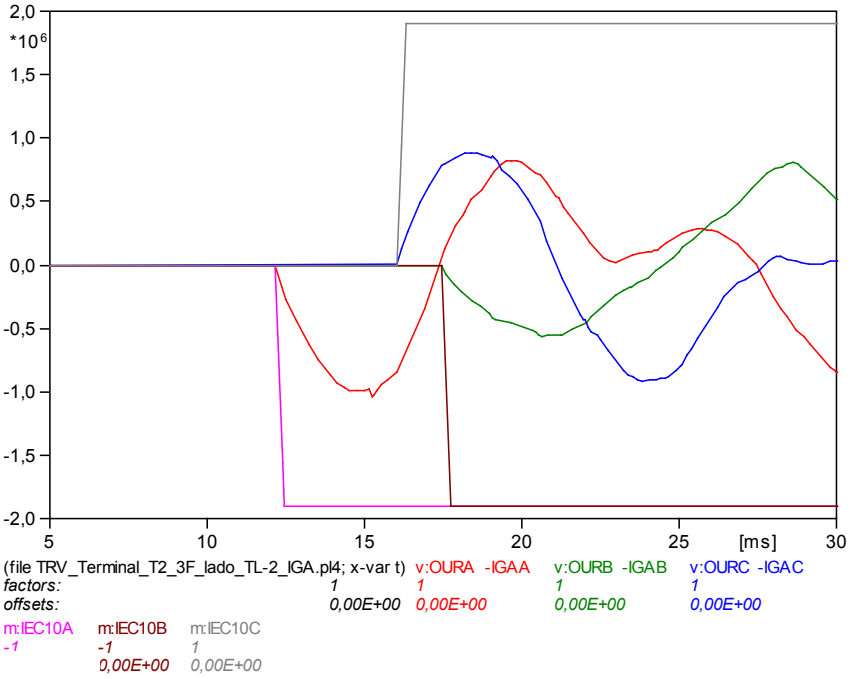

Phase	Icc via DJ (kA$_p$)	T (%)	Surpassed	Type of surpassing
A	8.85	9.93	No	–
B	8.85	9.93	No	–
C	8.85	9.93	No	–

Figure A6.15: Three-phase terminal fault insulated on the side of the line (Igaporã)

For this fault current value, the envelope curve to be used will be:

$$T(\%) = \frac{8{,}85kA}{\sqrt{2}} \cdot \frac{100}{63kA} = 9{,}93\%\text{, T10 curve.}$$

b) Three-phase – grounded (line side)

The result obtained for this condition is shown in Figure A6.16.

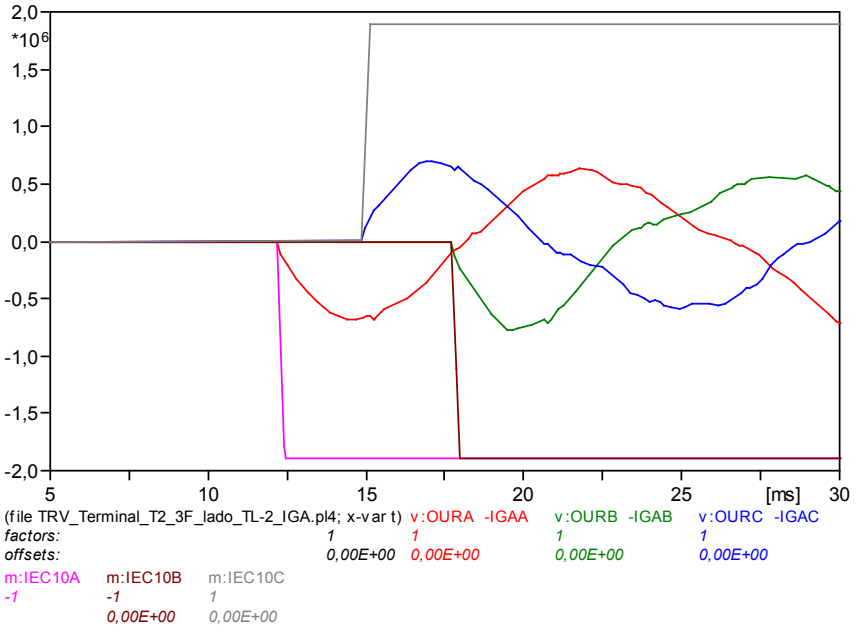

Figure A6.16: Three-phase terminal fault grounded on the side of the line (Igaporã)

For this case of grounded three-phase fault, the current values through the circuit breaker and envelope curve are the same as in the previous case. The magnitude of the voltages at the circuit breaker terminals falls to approximately half of the case with insulated three-phase fault.

c) Three-phase – insulated (transformer side)

The result obtained for this condition is shown in Figure A6.17.

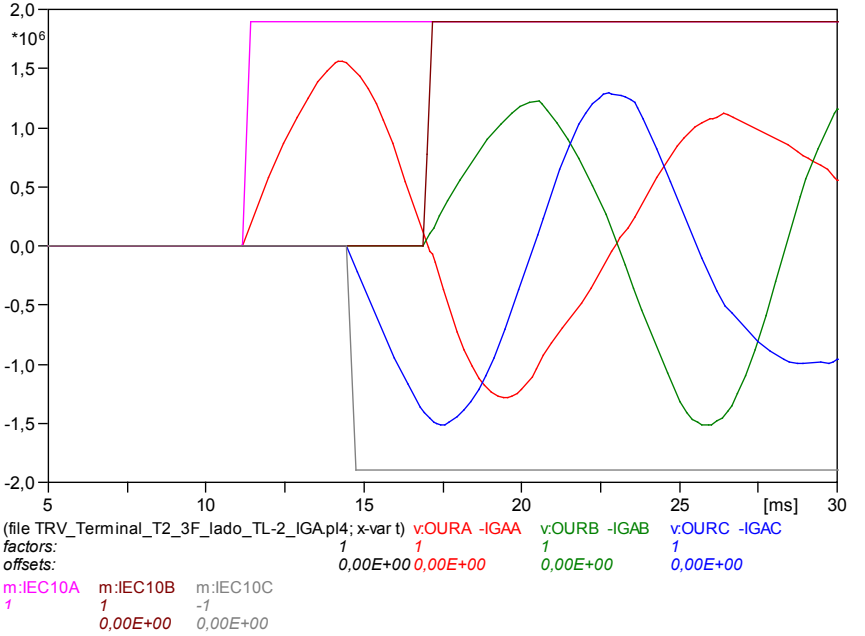

Phase	Icc via DJ (kA$_p$)	T (%)	Surpassed	Type of surpassing
A	5.56	6.24	No	–
B	5.56	6.24	No	–
C	5.56	6.24	No	–

Figure A6.17: Three-phase terminal fault insulated on the side of the transformer (Igaporã)

For this fault current value, the envelope curve to be used will be:

$$T(\%) = \frac{5,56kA}{\sqrt{2}} \cdot \frac{100}{63kA} = 6,24\%, \text{ T10 curve.}$$

d) Three-phase – grounded (transformer side)

The result obtained for this condition is shown in Figure A6.18.

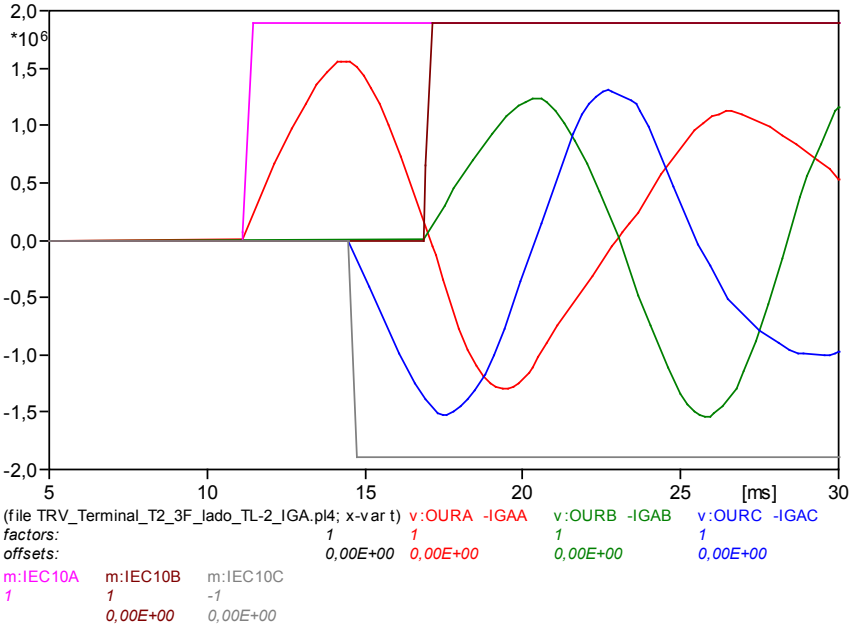

Figure A6.18: Three-phase terminal fault grounded on the side of the TRF-3 (Igaporã)

We verify that the TRV values, in the case of three-phase faults insulated and grounded in the transformer circuit breaker, are practically the same. Thus, the values of Table in the previous item are also valid for this case.

6.3 Other sections

The TRV values for other sections were similar.

ATTACHMENT 7 – Transformer Energization

7.1 Transformer Characteristics

The main characteristics of the auto-transformer to be modeled are:

- In the ATP program, the model used to represent the auto-transformer was the BCTRAN, which allows for specifying a transformer with 2 and 3 windings.
- The voltages and power (three-phase) used initially were:
  - Primary: 500 kV, 1,500 MVA, Y connection.
  - Secondary: 1,000 kV, 1,500 MVA, Y connection.
  - Tertiary: 69 kV, 500 MVA, D connection. This voltage value may be used for feeding local loads, or for connecting fixed reactive compensation.
- The transformer reactance, referred to the auto-transformer base itself, is: $X_{P\text{-}S} = 18\%$

These reactances were obtained from an auto-transformer with similar voltage and power characteristics in China. The values were then reviewed based on recommendations from the manufacturers. Thus, the cases were recalculated for three-phase power of 3,000 MVA, and reactance of 14%, with results obtained similar to the previous cases.

7.2 Energization Sequence

The energization is done via de 500 kV side. However, aiming at the possibility of energization via the 1,000 kV side, an analysis of this energization possibility is also conducted.

7.3 Energization of the Ourolândia Transformer – Results

7.3.1 Energization via the 500 kV side

To observe the behavior under this condition, a second transformer is energized at a random instant, in this case (simultaneous closing of the three phases) at t = 150 ms (Figure A7.1). We observe that the peak of the inrush

current (phase B) reaches a value of approximately 1.71 times the value of the rated current of the transformer (I_N = 1,732 A_{rms}).

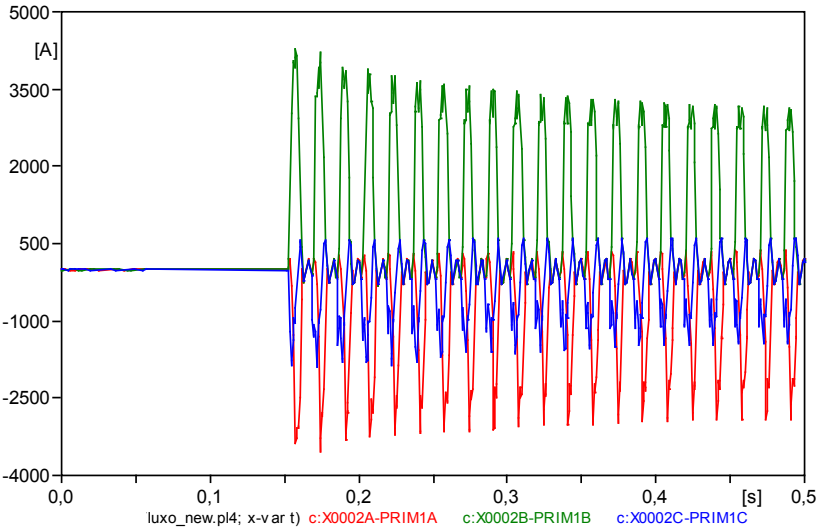

Figure A7.1: Inrush currents, energization via the 500 kV side

Figure A7.2, shows the inrush current spectrum of harmonics and their angles, in phase B. This spectrum belongs to the last cycle of the plotting period (t = 0.48 – 0.5 s).

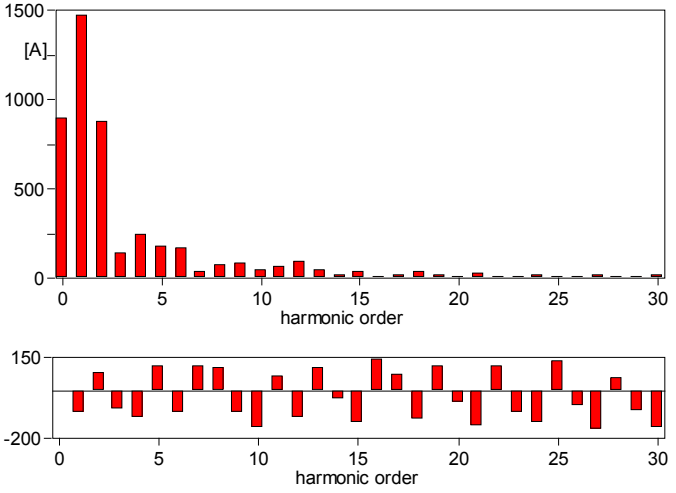

Figure A7.2: Harmonics composition of the inrush current for phase B

Figure A7.3 presents the voltage at the terminal on the 500 kV side. Maximum overvoltage also occurs in phase B, with its peak being equal to 673 kVp (1.65 pu at the 500 kV base).

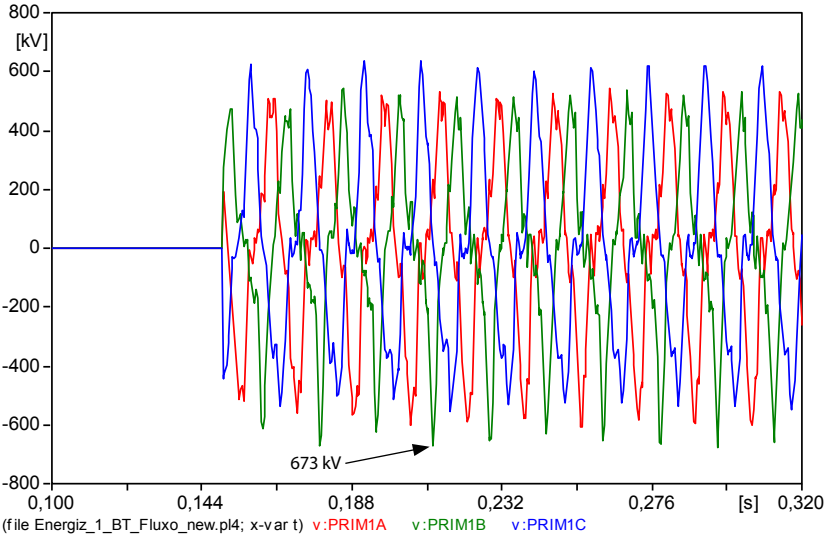

Figure A7.3: Voltage on the 500 kV side

The pre-energization voltage, on the 500 kV side of the transformer, to be applied to all the simulations, is equal to 1.086 pu (543 kV rms). This value is close to the maximum operating voltage (550 kV).

7.3.2 Controlled energization of the transformer via the 500 kV side

Depending on the type of core and arrangement of the windings, during energization any of the phases may, or may not, affect the others. The main factors for this to occur are: (i) condition of insulated neutral on the side to be energized, (ii) three-phase arrangement of the core (cores of phases A, B, and C not independent), connection in delta to the secondary or tertiary.

In steady state, the magnetic flux is delayed 90° related to the voltage. In the of the single-phase auto-transformer, for example, the relation between flux, voltage and current is shown in Figure A7.4.

If the auto-transformer presents residual flux, which is a case that usually occurs, and said transformer is energized (voltage is applied) at any instant, the inrush current may reach high values.

Among the most common methods to reduce these currents, such as the use of pre-insertion resistor and controlled energization, the latter proved to be a more effective alternative for this purpose. Controlled energization consists of closing the energization switches at specific instants to compensate the residual flux existing in the transformer core.

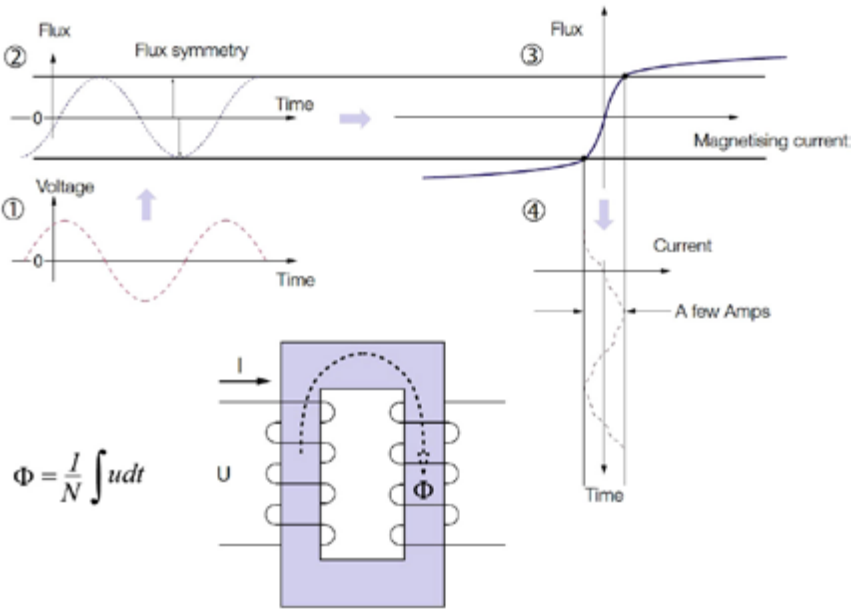

Figure A7.4: Operation of the single-phase transformer on empty

In Figure A7.4, the numbers in circles refer to:

1. Voltage in steady state applied to the transformer winding.
2. Flux in steady state generated by the application of voltage.
3. Symmetrical flux in steady state, which determines the form of the characteristic magnetization curve.
4. Resulting magnetization current (state) determined by the characteristic magnetization curve.

The best instant for energizing the transformer would be when the prospective flux ($\Phi_{prospective}$) is equal to the residual flux $\Phi_{residual}$ (points 1 or 2), as shown in Figure A7.5.

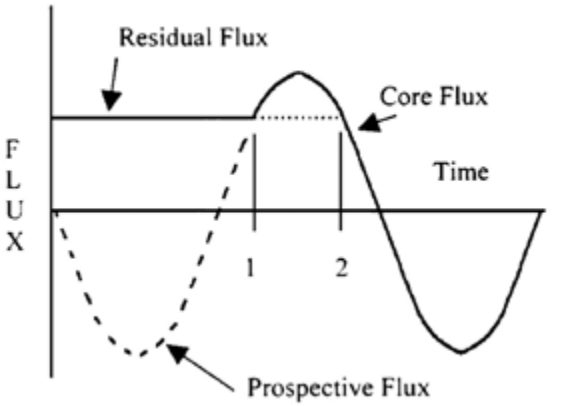

Figure A7.5: Example of ideal energization of a single-phase transformer

As the core of the chosen transformer (BCTRAN) is the *triplex*, there is no restriction to the application of this energization alternative.

Below, are presented the results considering the three proposed energization strategies:

- **Fast closing strategy:** Requires the reading of the residual flux in the three phases, and independent control of the poles in the circuit breaker. First, one phase is closed and, then, after approximately 90° (¼ of a cycle) the remaining phases are closed. This delay corresponds, approximately, to the time in which the $\Phi_{residual}$ crosses the $\Phi_{prospective}$ in the remaining phases. Knowing this crossing instant, it is possible to effectively reduce the inrush current in the remaining phases.
- **Delayed closing strategy:** Requires the reading of the residual flux in only one of the phases, and independent control of the poles in the circuit breaker. First, one phase is closed and, then, after 2 or 3 cycles, the remaining phases are closed.
- **Strategy of simultaneous closing of the three poles:** Requires the residual flux of the three phases, and that the magnitude of the residual flux in 2 phases are high, and follow the course of the traditional residual flux. Does not require independent control of the poles in the circuit breaker. In this strategy, the three phases are closed simultaneously in an optimum point of the residual flux.

7.3.2.1 Energization in the condition of residual flux = flux

a) Fast closing strategy

For the application of this technique, we inserted in the ATP a TACS (*Transient Analysis of Control Systems*) component to measure the residual flux existing in the transformer after its de-energization. The flux measured in this component results of the integral of the voltage in the winding. So, at a random instant t (in this case t = 0.05 s) after the interruption of the flux through the switches, the N switches are closed using the above-mentioned times. These times were obtained from the crossing of the residual flux and the prospective flux in the simulation. This technique assumes that the energization switches have independent controls.

The residual flux of the first pole to be closed (phase B) was the lowest (ideally it would be zero), and equal to 2.46% (20.5 Wb) of the maximum flux in state (847 Wb). In phase A, this flux was equal to 34.4%, and in phase C of 38.3%.

In Figure A7.6 we can observe the significant reduction of the inrush current after the application of the controlled energization technique, closing the first pole (phase B) at T_B = 0.20277s, and the remaining poles (phases A and C) at $T_A = T_C$ = 0.2062s; specifically, 73.4° after the beginnig of the opening. The maximum value of this current is equal to 25.7 A (phase C, peak value). Figure A7.7, shows the spectrum of harmonics (phase B) of the inrush current. There are no harmonics that deserve significant highlight.

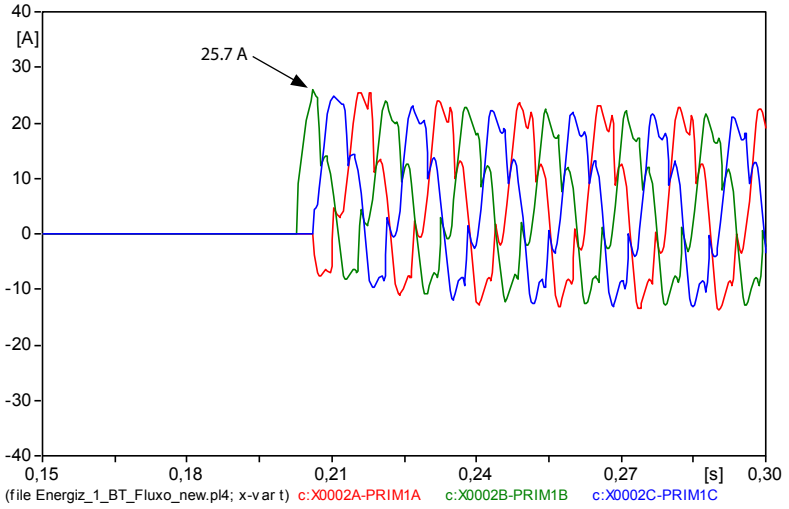

Figure A7.6: Inrush currents on the 500 kV side (fast closing strategy)

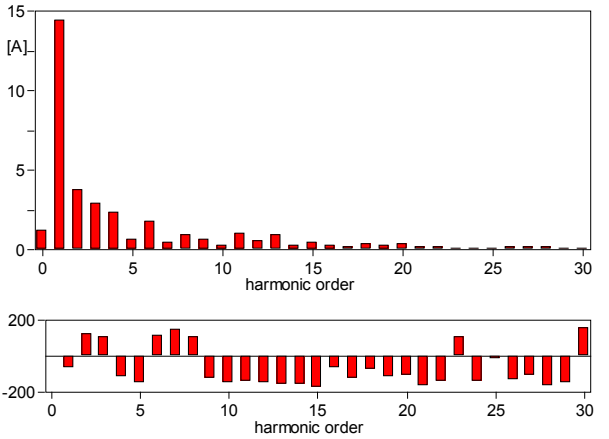

Figure A7.7: Harmonics decomposition of the inrush current for phase B

b) Delayed closing strategy

In this strategy, one phase is closed first, and after 2 or 3 cycles, the remaining phases are closed. In the case being analyzed (Figure A7.8), the closing of the first phase was done at t = 0.20277s (instant in which the residual flux of phase B is equal to its prospective flux, with this being the phase with lowest residual flux 20.15 Wb), and the remaining phases were closed 3 cycles after this time (t = 0.25277s).

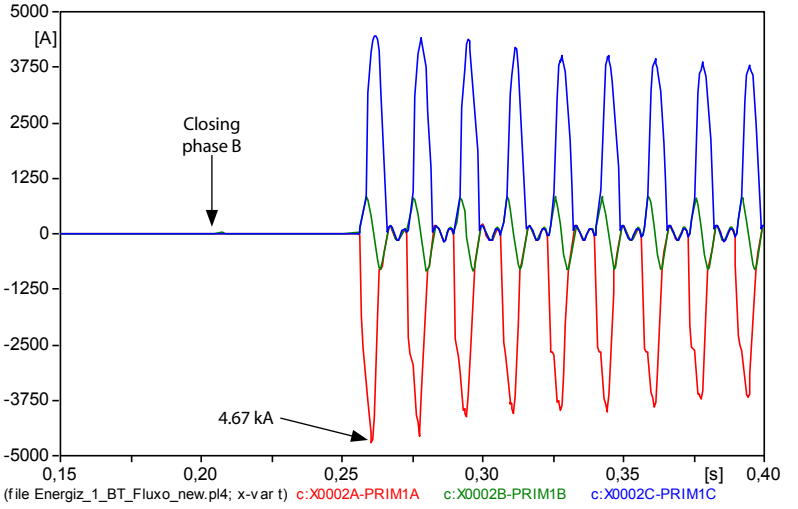

Figure A7.8: Inrush currents on the 500 kV side (delayed closing strategy)

We observe that although the inrush current in phase B (in green) was efficiently reduced, the remaining phases (A and C) present high values, since at the instant when they were closed, their fluxes were not equal ($\Phi_{residual} \neq \Phi_{prospective}$).

c) Strategy of simultaneous closing of the three poles

In this strategy, the three phases are closed simultaneously in an instant considered the best among the relation of residual and prospective fluxes. The lowest inrush currents occur when these fluxes have equal values. In this case, however, without independent control of the circuit breaker poles, this condition is relatively hard to find, because, while in one of the phases these fluxes approach, in the other phases they grow apart. Thus, it is necessary to find a point in the middle, which in the case being analyzed was at t = 0.2114 s. Under these conditions, the inrush currents are shown in Figure A7.9.

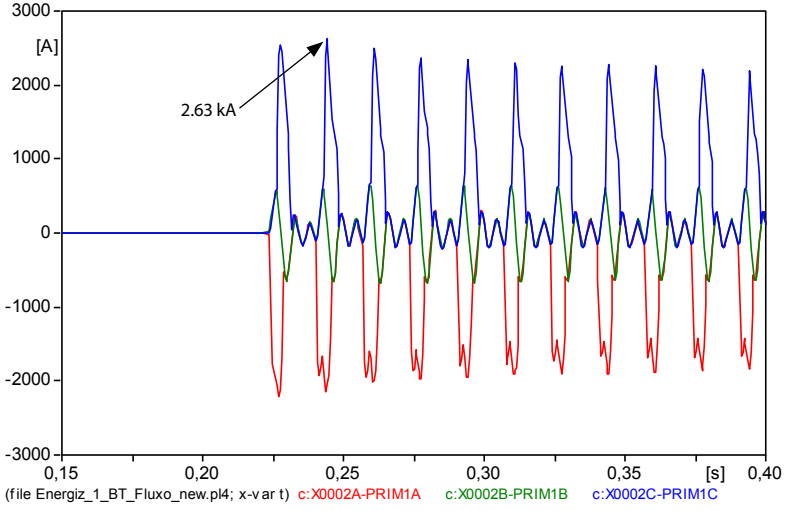

Figure A7.9: Inrush currents on the 500 kV side (strategy of simultaneous closing of the three poles)

We observe that the inrush currents of phases A and C are much higher than in phase B (green). The peak value of the current in phase C is relatively high (2,634 A, blue curve), and is higher than the value of the rated current of the transformer ($I = 1{,}500/(\sqrt{3} \cdot 500) = 1.730$ kA). Thus, this strategy does not ensure the reduction of the inrush currents during energization.

7.3.2.2 Energization at the instant of maximum prospective flux

To obtain this value, the energization was done in two instants:

- Simultaneous closing of the three poles at the maximum of the opposite flux.
- Closing of the two 90° phases after the first phase.

d) Simultaneous closing of the three poles at the maximum of the opposite flux

Energization is done at the instant in which the $\Phi_{residual}$ is at the opposed maximum. Specifically, the time corresponding to the maximum flux of the first pole chosen (phase B) was at t = 0.2068 s. Assuming the three-phase operation of the circuit breaker, the remaining phases (A and C) were also energized at this instant. Figure A7.10 shows the result of this simulation, in which the inrush current (peak value) in phase B is equal to 5.36 kA.

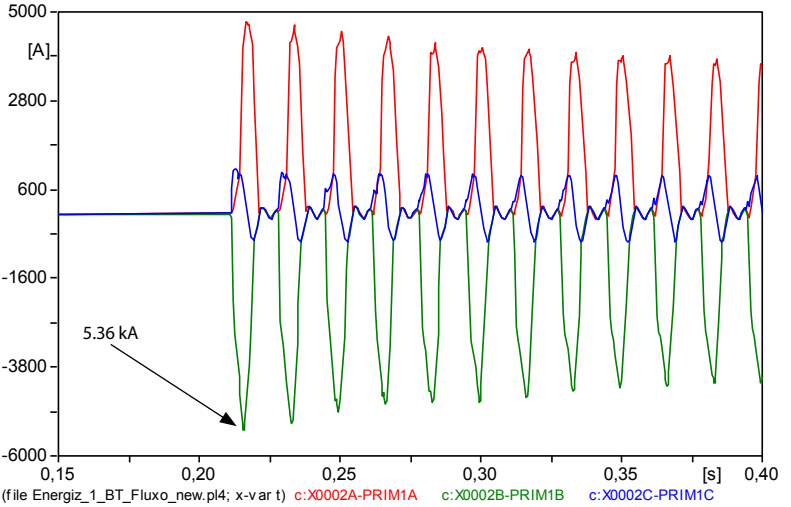

Figure A7.10: Inrush currents during energization at maximum flux of the opposed curve, simultaneous closing of phases A, B and C

e) Closing of the two 90° phases after the first phase

For the most severe demand (Figure A7.11), energization was also done with synchronized closing. In this case, the closing of the first pole (phase B), also occurs at the instant when the residual flux is at the opposed maximum (T_B = 0.2068 s). However, the closing of the two other phases (Phases A and C) occurs at 90º electric (t = 4.1667 ms) after the closing of the first pole. Under these conditions, the highest value of the inrush current occurs in phase A, being equal to 9.06 kA (peak value). This current (3.7 pu at the base of 1,732 A) represents the worst transformer energization condition and, thus, the statistic closing will be processed.

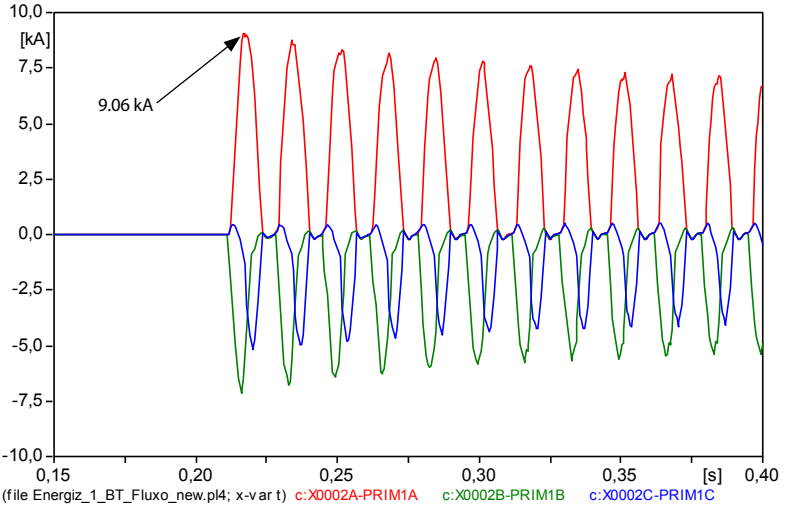

Figure A7.11: Inrush currents during energization at maximum flux of the opposed curve, closing of phases A and C at 90°, after phase B

7.3.2.3 Statistic closing for the worst case

Based on the previously-presented results, simulations of the statistic closing were performed (sample of 200 switchings), of the three (3) phases of the circuit breaker. For this, were considered the instants in which we obtained the highest inrush currents (T_B = 0.2068 s, $T_A = T_C$ = 90° after). This energization instant corresponds to zero voltage in the switching busbar, ensuring the worst transformer energization condition. The maximum flux under these conditions was of 1,520 Wb (Figure A7.12).

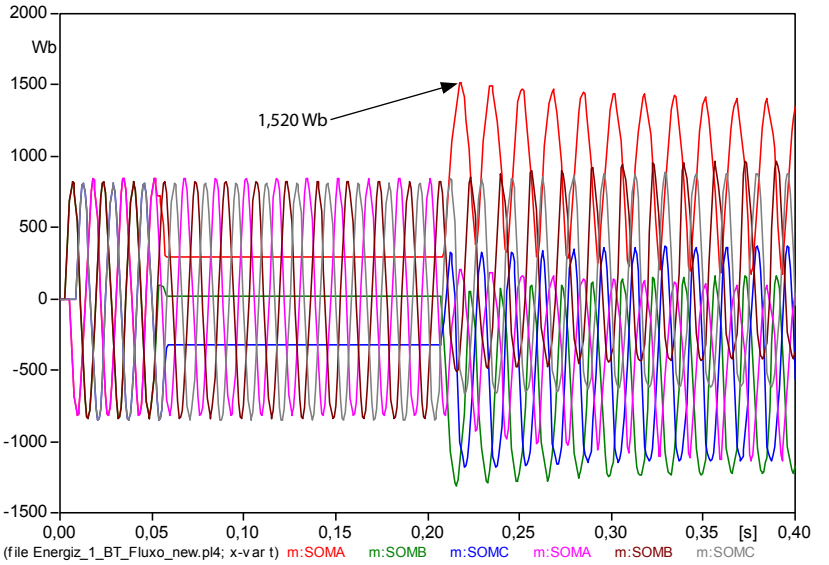

Figure A7.12: Condition of the prospective flux for maximum voltage

Normal distribution was assumed for the closing of the three points, truncated at ±2σ. According to the guidelines of the ONS, the value of the standard deviation was defined at 1.0 ms. The times used in statistic switches were: T_B = 0.2068s (first pole to be closed), $T_A = T_C$ = 0.21097s (90° after phase B).

Tables A7.1 and A7.2 show the values referring to the closing with statistic switches, for inrush current and overvoltage, considering the worst energization case presented in Figure A7.12.

Table A7.1: Worst current condition during energization via the 500 kV side

Phase	Imed (pu)	σ (pu)	Imax measured (pu)
A	1.924	0.8024	5.007
B	2.944	0.2510	4.787
C	2.213	0.9516	7.293

$I_{base} = (1{,}500{,}000/(\sqrt{3} \cdot 500)) \cdot \sqrt{2} = 2{,}449.5$ Ap

Table A7.2: Worst voltage condition during energization via the 500 kV side

Phase	Imed (pu)	σ (pu)	Imax measured (pu)
A	1.462	0.0877	1.687
B	1.394	0.0999	1.704
C	1.464	0.0750	1.583

$V_{base\ (ATP)} = 421\ kV_{(phase,\ peak)}$

The highest inrush current value resulting of the statistic closing is equal to 7.29 pu that occurs in phase C, which also presents the highest standard deviation.

The highest overvoltage value resulting of the statistic closing is equal to 1.70 pu that occurs in phase B, standard deviation equal to 0.0999.

The demand identified as the most severe in the statistic simulation was reproduced in deterministic manner. The response is shown in Figure A7.13.

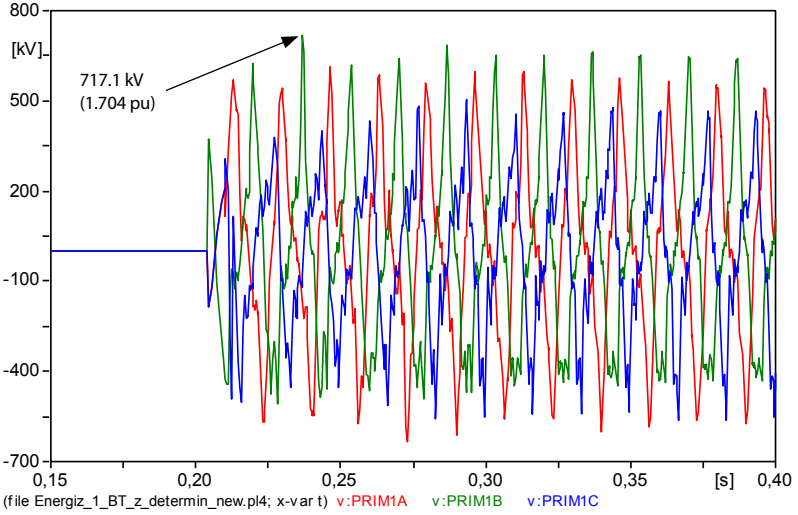

Figure A7.13: Voltage on the BT side (worst case) obtained with deterministic switch

7.3.2.4 System resonance frequency during energization

Figure A7.14 presents the variation of impedance with the frequency seen through the transformer terminal. To obtain this result, all equivalent sources of the system were subject to short-circuit and grounded, and transformer was replaced by a current source with magnitude equal to 1.0 A, and zero degree of lag angle.

The red curve corresponds to the system without any contingency, while the green curve includes one line (500 kV Ourolândia – Juazeiro) out. Seen from the transformer switching point, the most significant resonances in the grid occur:

- Without contingency (red curve): for a frequency of 510 Hz, close to the order 8 harmonics, with magnitude in the order of 2,507 Ω.
- With contingency (green curve, output of the Ourolândia – Juazeiro line): for a frequency of 540 Hz, corresponding to the order 9 harmonics, with magnitude in the order of 2,703 Ω.

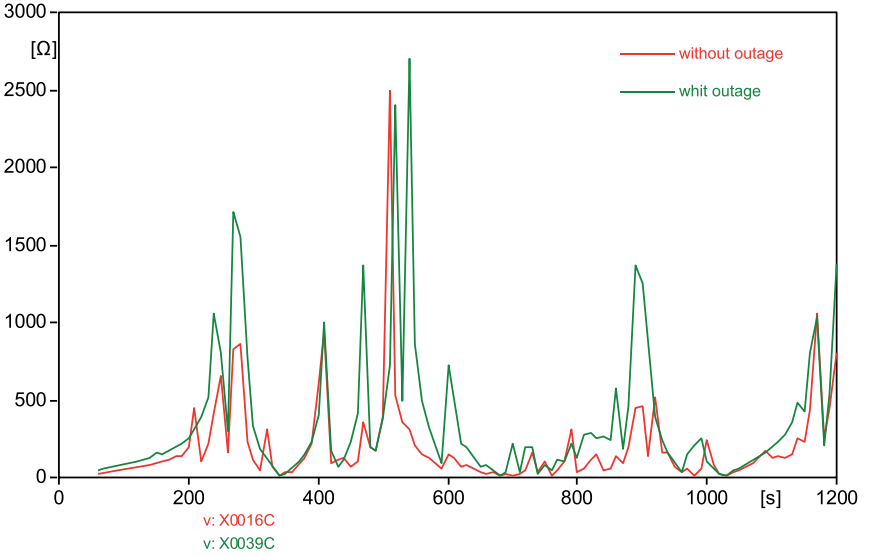

Figure A7.14: Response in frequency (Ω x f) seen from the transformer

This analysis is important because, during energization, if there are frequencies close to 510 Hz (and 540 Hz during contingency), there would be overvoltages due to these harmonics (of order 8º and 9º). As in the case without contingency, the prevailing order of the harmonics is of 510 Hz/60 Hz = 8.5 (not integer), so the probability of these overvoltages occurring is low. Other frequencies in which resonance could occur, in the case with contingency, would be in the range of 270 Hz and 900 Hz.

7.3.2.5 Use of pre-insertion resistors

This item presents the results referring to the possibility of the use of pre-insertion resistors during the energization of the transformer via the 500 kV side. Figure A7.15 shows the arrangement of switches (controlled by time) used in the simulation. The objective is the reduction of the inrush currents, and for that the t_1 switch is opened at an arbitrary instant leaving a residual flux in the transformer. At the instant when the transformer needs to be energized, the t_2 switch is closed (for example, t_2 = 202.7 ms), inserting the pre-insertion resistor that should cut the inrush current for, finally, this switch (t_2) to be bypassed by switch t_3. After the connection of the last switch, the t_2 switch can be opened.

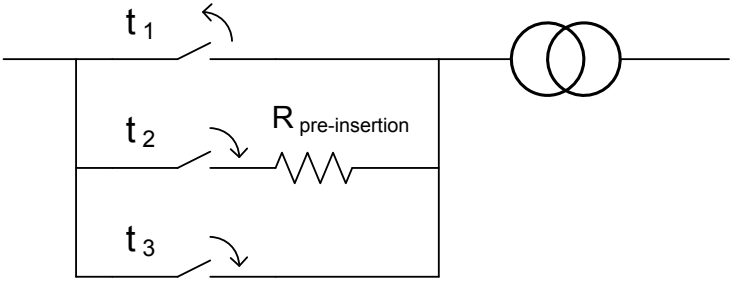

Figure A7.15: Use of pre-insertion resistor

Table A7.3 presents the results (deterministic normal switches) obtained for the different pre-insertion resistor values, and the respective inrush currents (first peak value), as well as the peak value of the highest overvoltage. The peak voltage value per phase (at state) is of 445 kV.

Table A7.3: Use of pre-insertion resistor during energization via the 500 kV side

	R pre-insertion (Ω)	I_{inrush} peak (A)	V_{inrush} peak (kV)
1	200	856.7	493.3
2	400	564.8	465.0
3	800	334.0	453.0
4	1,000	277.2	449.4

We verify that the pre-insertion resistor significantly reduces the inrush current, including during the first cycles. After its insertion, the inrush currents are lower than the rated current of the transformer.

For example, 800 Ω resistors would reduce the first peak of the inrush current to approximately 334 A, as shown in Figure A7.16. Other (smaller) pre-insertion resistor values (see Table A7.3) presented the same behavior, but being less effective.

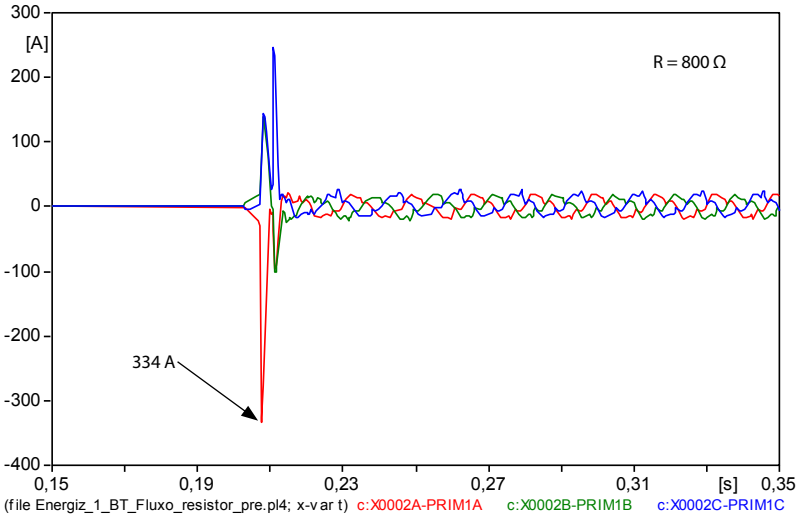

Figure A7.16: Inrush current for pre-insertion resistor = 800 Ω

The simultaneous closing of the three phases of the t_2 switch (containing the pre-insertion resistor) occurred when the $\Phi_{residual} = \Phi_{prospective}$ in phase A. The closing of this t_2 switch at other instants, for example, when the flux is at the maximum of the opposed semi-wave, generated higher inrush currents, but these (peak value) were lower than the rated current of the transformer.

7.3.2.6 Energization during contingency

The possibility of energizing transformers during contingency periods was also analyzed. In the specific analysis case, the output of the Juazeiro – Ourolândia line, close to the 500 kV terminal through which the transformer is being energized was simulated. Under this condition, two cases were simulated:

1. Best closing condition.
2. Worst closing condition.

In both cases, only the fast closing strategy will be illustrated.

1. Best closing condition.
   We considered the condition $\Phi_{residual} = \Phi_{prospective}$ for closing of the first pole (that has lower residual flux), and approximately 90° after, or at the instant when the fluxes (residual and prospective) cross in these phases, the remaining poles are closed. In this case, phase C was the one that presented highest residual flux (34.9 Wb) and, therefore, this phase was the first to be closed ($T_C = 0.20854$s), soon followed by the remaining phases ($T_A = T_B = 0.2119$s). The highest inrush current (peak value) was of approximately 26.6 A (phase A), as shown in Figure A7.17.

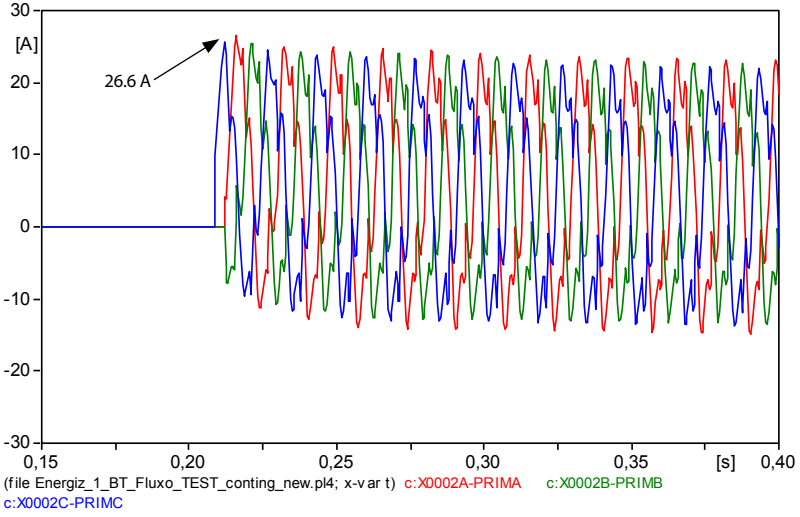

Figure A7.17: Best inrush current for the case with contingency (fast closing strategy)

2. Worst closing condition.
   Phase C is closed at the maximum point of its prospective flux (T_C = 0.2126s), and 90° later the remaining phases are closed ($T_A = T_B$ = 0.21677s). The inrush current (peak value) in phase B (maximum) was equal to 6.92 kA (Figure A7.18).

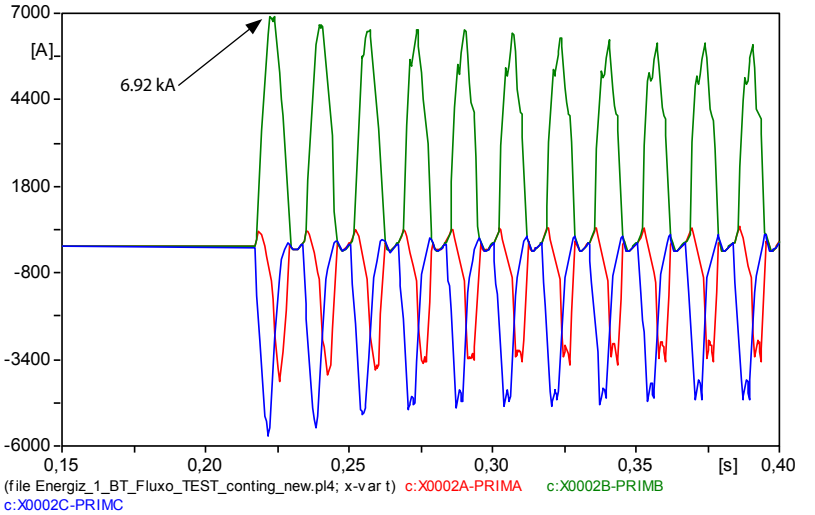

Figure A7.18: Worst inrush current for the case with contingency (fast closing strategy)

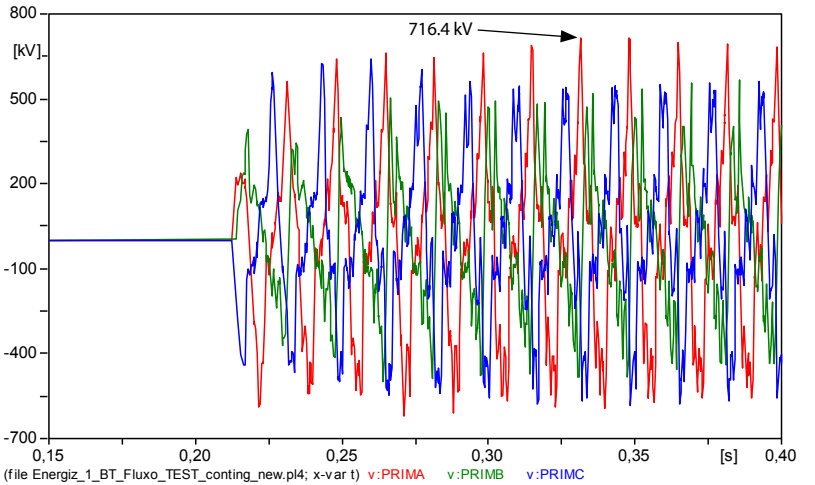

Figure A7.19: Terminal voltage of transformer (500 kV side) for the worst inrush current

The highest voltage in the transformer terminal (500 kV side), in the worst energization condition, was of 716.4 kV (1.755 pu) as shown in Figure A7.19.

7.3.3 Energization via the 1,000 kV side

Similarly to the study of the energization via the 500 kV side, in this case we will also present the results for the best and worst instant for energization of the Ourolândia transformer, via the 1,000 kV side.

The pre-energization voltage at the transformer input was equal to 1.066 pu. The residual fluxes after the opening of the transformer (at t = 0.05s in the three M switches), for the transformer soon to be re-energized, were equal to: Φ_{A_resid} = 535.6 Wb, Φ_{B_resid} = 82.8 Wb (lowest residual flux), and Φ_{C_resid} = -604.4 Wb.

In the previous section (energization via the 500 kV side), we could observe that the fast energization strategy, in which one needs to know the residual flux in the three phases, offered the best results in terms of the best and worst energization conditions. Therefore, in this section only this strategy will be used.

7.3.3.1 Best closing instant – fast energization strategy

Figure A7.20 presents the inrush current for energization on the 1,000 kV side, with the series capacitors inserted in the line. In this case, the N switches are being closed at T_B = 0.2030s ($\Phi_{prospective} = \Phi_{residual}$), $T_A = T_C$ = 0.2064s, which means, approximately 73° after closing phase B (Figure A7.20), instant in which the residual and prospective fluxes of these phases intersect. We observe that the maximum magnitude of the first peak is of only 12.9 A. This value is half the value of the inrush current presented for this same strategy on the 500 kV side. As can be expected, for this case, the voltage at the transformer terminals (1,000 kV) does not present any overvoltage.

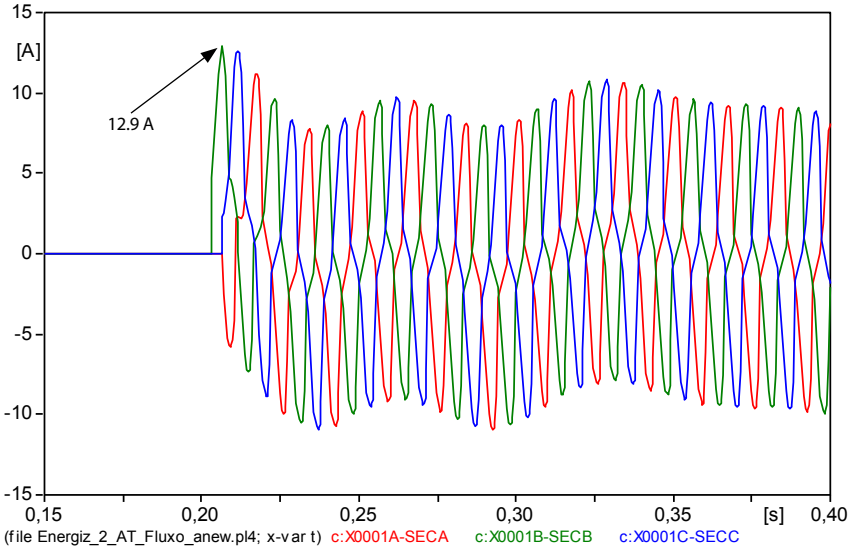

(a)

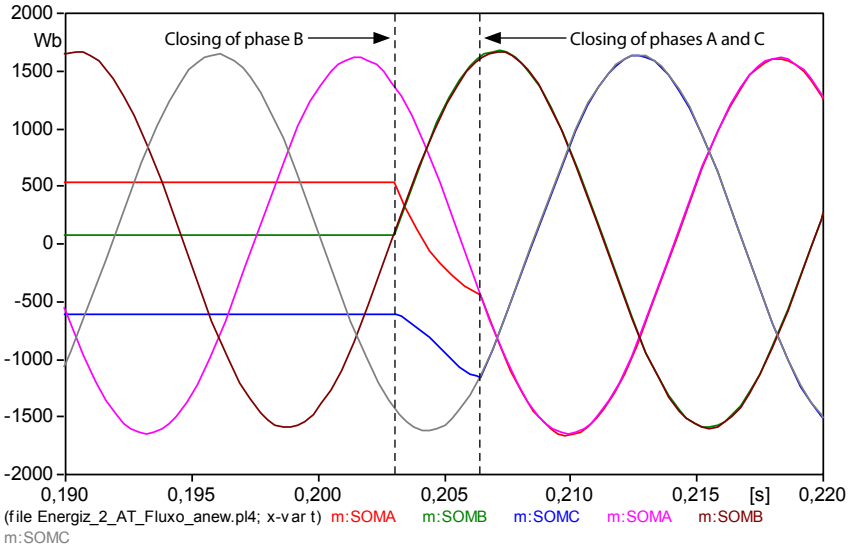

(b)

Figure A7.20: (a) Inrush current for the fast energization strategy, (b) closing instants of the prospective and residual fluxes

7.3.3.2 Worst closing instant

For the "most severe demand," energization was also done with synchronized closing. In this case, the closing of the first pole (phase B), occurs at the instant when the residual flux is at the "opposed maximum" (T_B = 0.2154 s). However, the closing of the two other phases (Phases A and C) occurs at 90º electric (t = 4.1667 ms) after the closing of the first pole. Under these conditions, the highest value of the inrush current occurs in phase A, being equal to 3.57 kA (peak value).

Observe that this maximum current value is lower than the value obtained in the case of the worst inrush current, when the energization was done via the 500 kV side, without contingency.

We have observed that the (alternating) form of the inrush current, shown in Figure A7.21, is due to the series capacitors located in the neighboring lines, since, when one or both capacitors close to the transformer is bypassed, the current form approached the typical form of inrush in transformers.

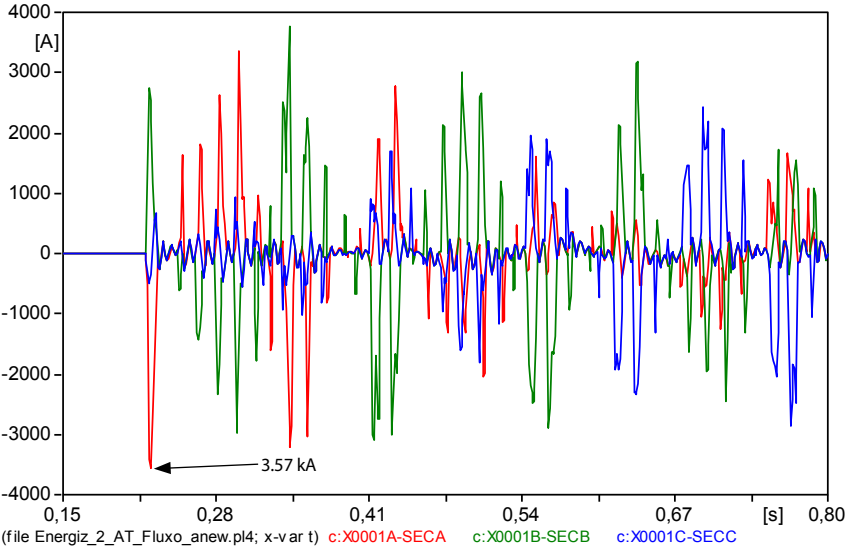

Figure A7.21: Worst inrush current during energization at maximum flux of the opposed curve

Figure A7.22 shows the inrush current considering "one" of the series capacitors bypassed. The capacitor closer to the transformer (1,000 kV side) was bypassed. Both responses present near peak values, with the difference that the dampening in the case of Figure A7.22 is more evident, though the highest peak (4.26 kA) appears in this response.

This inrush current in phase A represents the worst transformer energization condition, and this will be the condition with which the statistic closing will be processed (with at least one series capacitor bypassed).

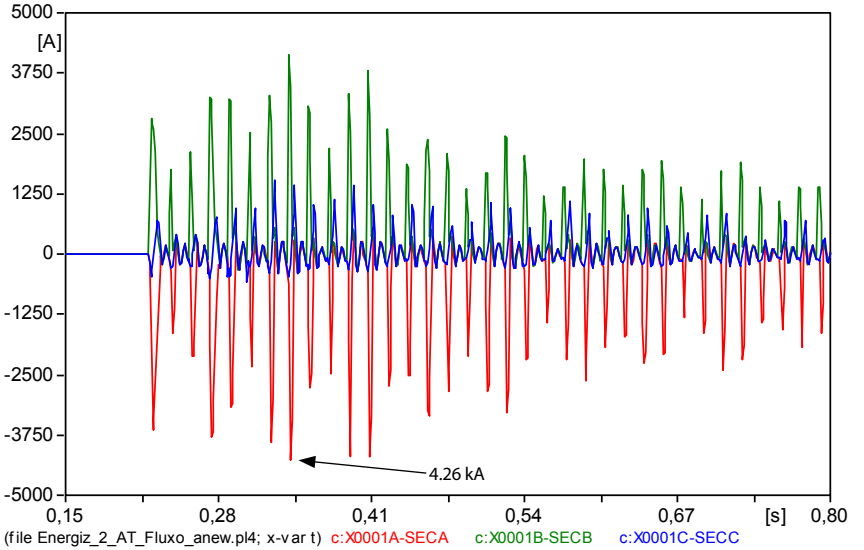

Figure A7.22: In rush currents with the capacitor (close) to the Ourolândia – Igaporã section bypassed

Table A7.4 presents the values referring to the closing with statistic switches (voltage) considering the worst case of the inrush current presented in Figure A7.22.

Table A7.4: Statistic energization (worst case) via the 1,000 kV side

Phase	Vmed (pu)	σ (pu)	Vmax measured (pu)
A	2.035	0.3255	2.011
B	1.691	0.0600	1.785
C	1.778	0.2453	1.837

The demand identified as the most severe in the statistic simulation was also reproduced in deterministic manner. This response is shown in Figure A7.23.

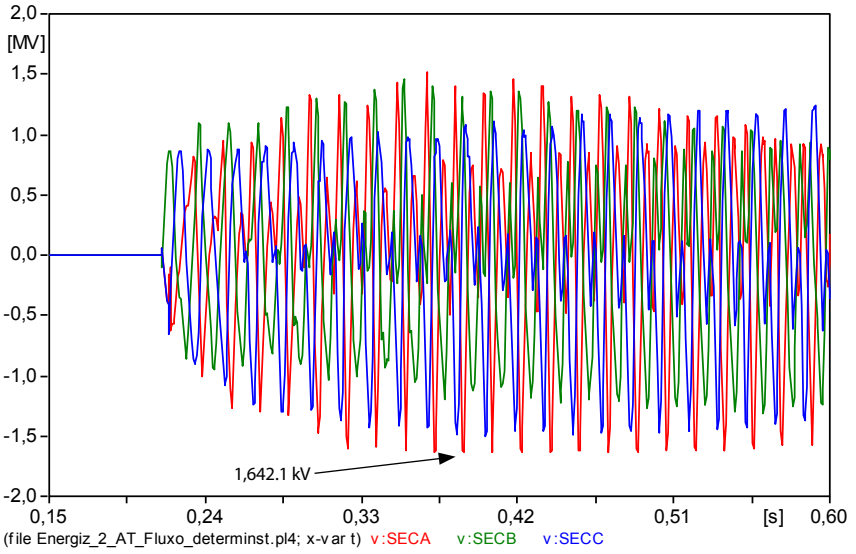

Figure A7.23: Voltage on the AT side (worst case) obtained with deterministic switch (2.01 pu)

7.3.3.3 Use of pre-insertion resistors

Similarly to the use of pre-insertion resistors performed for the 500 kV side, simulations were also done considering this energization alternative via the 1,000 kV side. In this case, the focus was observing the responses with the bypass of the series capacitor near the Ourolândia busbar, be it for the Ourolândia – Igaporã section or for the Milagres – Ourolândia section.

Table A7.5 presents the results (deterministic normal switches) obtained for the different pre-insertion resistor values, and the respective inrush currents (first peak value), as well as the peak value of the highest overvoltage. The peak voltage value per phase (at state) is of 875 kV.

Table A7.5: Use of pre-insertion resistor during energization via the 1,000 kV side

	R pre-insertion (Ω)	I_{inrush} peak (A)	V_{inrush} peak (kV)
1	800	660.0	925.0
2	1,000	548.0	907.0
3	1,500	392.6	896.0
4	2,000	306.6	888.0

Observe that 2,000 Ω resistors, for example, have reduced the first peak of the inrush current to approximately 306.6 A (Figure A7.24). Other (lower) pre-insertion resistor values (see Table A7.5) presented lower effectiveness and originated components such as the ones showed in Figure A7.25, but with magnitude lower than the first peak value.

The simultaneous closing of the three phases of the t_2 switch (containing the pre-insertion resistor) also occurred when $\Phi_{residual} = \Phi_{prospective}$ in phase B ($t = 0.20307$s). The closing of this t_2 switch at the instants, for example, when the flux is at the maximum of the opposed semi-wave, generated higher inrush currents, but these (peak value) were lower than the rated current of the transformer.

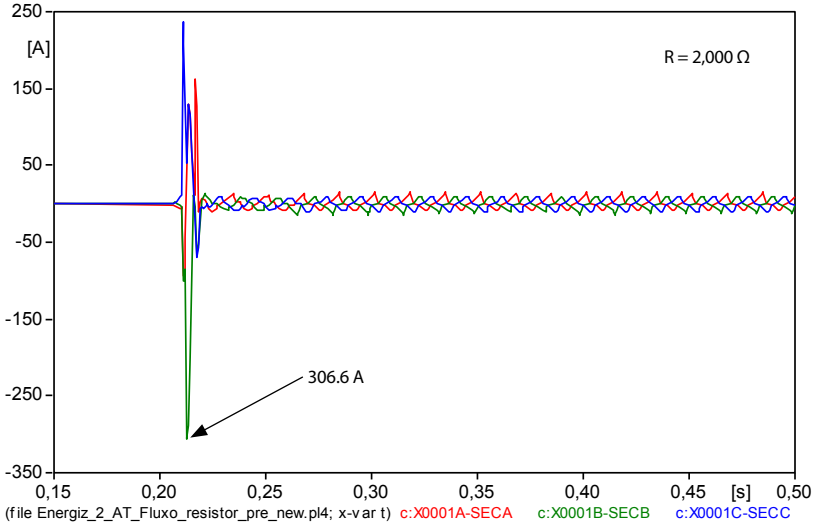

Figure A7.24: Inrush current for pre-insertion resistor = 2,000 Ω, with the series capacitor near the Ourolândia terminal bypassed

Figure A7.25 shows the inrush current "without" any series capacitor bypassed. We observe that after the closing of the t_3 switch (that bypasses the pre-insertion resistor) periodic inrush current components appear.

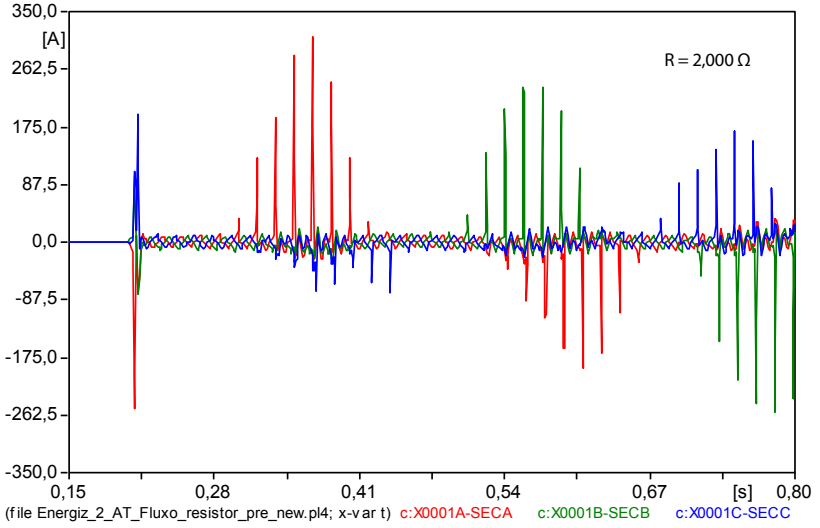

Figure A7.25: Inrush current with all the series capacitors inserted

7.4 Displacement of ±1 ms at the Closing

The possibility of displacement of ±1 ms during the closing of the first pole, both in the case of the best and of the worst condition was also analyzed. These results are shown only in Table form, including those values in which the closing was at the exact instant.

The maximum values (peak) of the inrush current, and of the overvoltage resulting of this current are presented. We highlight that these overvoltage values do not correspond to the statistic closing, but only to the overvoltage originated by the inrush current. This error in the closing will be applied only on the fast closing strategy. This means that in the best and worst condition, the closing of the first pole and of the remaining phases will be advanced/delayed in ±1 ms.

Tables A7.6 and A7.7 present the results of the simulations for the cases in which the transformer is energized via the 500 kV and 1,000 kV sides, respectively.

Table A7.6: Dispersion at the time of the closing of the 1st pole (500 kV)

Case (condition)	Dispersion of the 1st pole	I_{inrush_peak} (A)	V_{peak} (kV)	Phase (I_{inrush})	Phase (overvoltage)
Best	-1 ms	2,017.4	583.0	A	B
	0	25.7	443.6	B	A, B, C
	+1 ms	2,318.9	586.2	A	B
Worst	-1 ms	8,259.1	633.7	A	B
	0	9,060.0	582.0	A	B
	+1 ms	7,966.6	640.8	A	B

Table A7.7: Dispersion at the time of the closing of the 1st pole (1,000 kV)*

Case (condition)	Dispersion of the 1st pole	I_{inrush_peak} (A)	V_{peak} (kV)	Phase (I_{inrush})	Phase (overvoltage)
Best	-1 ms	1,564.4	1,139.5	A	A
	0	12.9	870.4	B	A, B, C
	+1 ms	1,921.3	1192.1	A	A
Worst	-1 ms	3,993.4	1487.4	A	B
	0	4,260.0	1,519.2	A	B
	+1 ms	4,020.7	1,491.9	A	B

(*) Ourolândia-Igaporã series capacitor bypassed.

For the case of the best condition, in both Tables, we observe that small closing errors (±1 ms) originate high inrush currents. We observe an increase in overvoltages because of the closing errors.

On the other hand, closing errors in the case of the "worst" condition reduce the inrush currents, although not significantly. The overvoltages are not significantly affected.

7.5 Transformers Connected in Parallel (Ourolândia)

Another similar phenomenon that produces differential currents are the so called sympathetic energizations. This phenomenon occurs when a transformer T_{II} is energized in the proximities of another transformer T_I, which was already energized. In this case, the overvoltages that appear due to the energization of the transformer T_{II} cause overvoltages to appear also in transformer T_I.

The inrush current of a transformer usually decays within a few cycles, but in this case, this current may persist for a longer period (of even a few seconds), which can also affect the operation of the differential protection of the transformers.

7.5.1 Assumptions for analysis of sympathetic energization

The assumptions for analysis of this phenomenon were the following:

- Both T_I and T_{II} transformers, to be connected in parallel, are exactly alike, same power 1,500 MVA (500 kV/1,000 kV), and present the same electric parameters (saturation curve with the component *L(i) type* 96 of the ATP, reactance between phases, etc.).
- The pre-energization voltage with the first transformer already energized was equal to 1.09 pu (545 kVrms), a value close to the maximum operating voltage (550 kV).

Two cases will be presented:

- Energization of the transformer T_{II} in the presence of a synchronizer (controlled switching) to obtain the lowest inrush current.
- Energization of the transformer T_{II} (with synchronizer) at the maximum (opposed) point of the residual flux.

7.5.2 Best connection instant of the transformer in parallel, 500 kV side (with synchronizer)

Following, we present the results of the simulation considering the "fast closing strategy." Which means, the condition $\Phi_{prospective} = \Phi_{residual}$ in phase C, with lower residual flux (37.8 Wb) is met at $T_C = 0.1997$s, instant in which the energization switch is closed in this phase. The closing instants of phases A and B occur at $T_A = T_B = 0.2035$s, approximately 82° after). We observe that the inrush current of the transformer T_{II} being energized is low (33.8 A). There was practically no overvoltage on the 500 kV side of transformer T_{II}.

The inrush current (peak) of the transformer T_I already energized was of approximately 23.2 A. Very little change was observed in the magnitude of this current. The first transformer (T_I), already energized, is sympathetic absorbing part of the phenomenon of the second transformed (T_{II}), thus the name sympathetic energization.

7.5.3 Worst connection instant of the transformer in parallel (with synchronizer)

We studied the inrush current of the transformer T_{II} for the worst condition, that is, closing of the phase C switch at the opposed maximum of its flux, also for the "fast closing strategy." In this case, the closing times were: $T_C = 0.2041$s, and $T_A = T_B = 0.20827$s (90° after the closing of phase C).

The inrush current (value of the first peak) of the transformer T_{II} being energized is equal to 7.44 kA, lower than the 9,06 kA obtained when only one transformer was energized. This fact shows the contribution (sympathy) of transformer T_I in the reduction of the inrush current of transformer T_{II}.

The maximum value (peak) of the voltage on the 500 kV side, resulting of this inrush current, was equal to 587 kV, equivalent to 1.44 pu.

7.6 3,000 MVA Transformer

Because of the possibility of the 1,000 kV line also being connected to the 500 kV grid by means of 3,000 MVA transformers, a study of the energization of this alternative was also performed.

7.6.1 Energization via the 500 kV side

a) Best closing instant

The maximum peak value of this current is equal to 52.63 A_p (phase A). We observed that, though the wave form contains almost all the harmonics up to the order of 30° of the requested spectrum, their magnitude is relatively low.

b) Worst closing instant

The maximum peak value of this current was equal to 12,380 A_p (phase A).

For this case, the statistic closing was also performed. For this, were considered the instants in which we obtained the highest inrush currents. This energization instant corresponds to zero voltage in the switching busbar, ensuring the worst transformer energization condition. Table A7.8 shows the overvoltage values referring to the closing with statistic switches for the worst energization condition.

Table A7.8: Worst voltage condition during energization via the 500 kV side

Phase	Vmed (pu)	σ (pu)	Vmax (pu)
A	1.535	0.0816	1.745
B	1.582	0.1162	1.972
C	1.592	0.1188	1.806

The highest overvoltage value resulting of the statistic closing is equal to 1.972 pu that occurs in phase B, standard deviation equal to 0.1162.

7.6.2 Energization via the 1,000 kV side

a) Best closing instant

The maximum peak value of this current is equal to 25.70 A (phase B). In the case of the best closing instant, there is practically no overvoltage on the transformer terminals (low inrush current).

b) Worst closing instant

In this case, the maximum peak value of this current is equal to 6.06 kA (phase A).

c) Worst closing instant with series capacitor bypassed

Table A7.9 presents the values referring to the closing with statistic switches (voltage) considering the worst case of the inrush current.

Table A7.9: Statistic energization (worst case) via the AT (1,000 kV)

Phase	Vmed (pu)	σ (pu)	Vmax measured (pu)
A	1.999	0.3364	2.048
B	1.922	0.0249	1.987
C	1.818	0.3257	2.006

The demand identified as the most severe in the statistic simulation was also reproduced in deterministic manner. The response is shown in Figure A7.26.

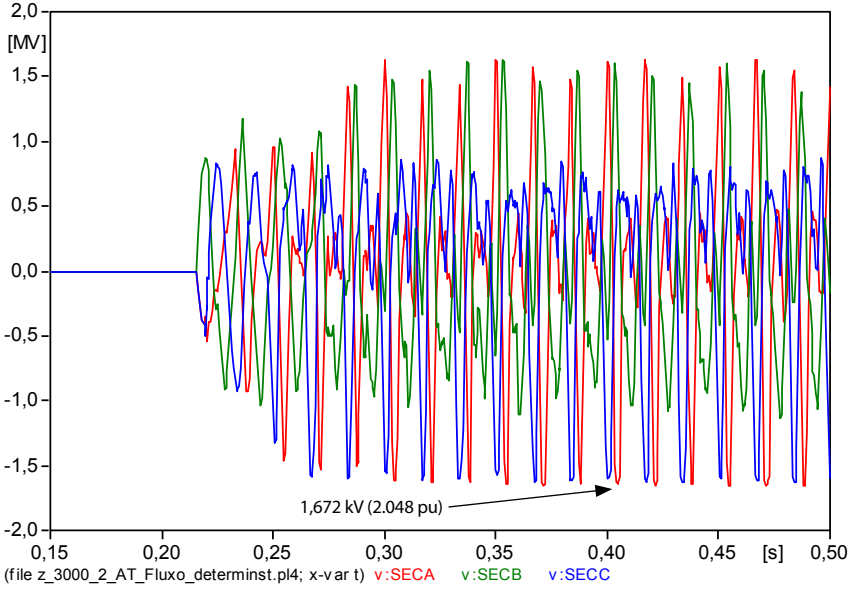

Figure A7.26: Voltage on the AT side (worst case) obtained with deterministic switch (2.051 pu)

ATTACHMENT 8 – Resonance Analysis - Line and Parallel Reactor

8.1 Objective

For better operation of very long transmission lines, it is common practice to insert reactive compensations, both capacitive (series) and inductive (parallel), in order to reduce the equivalent length of the line, interfering in the short and transient currents, and other parameters affected by the length of the line. However, it is necessary to properly size this equipment.

In this item, the objective is to evaluate the response in transmission line frequency with parallel compensation, when of the opening of one phase or two phases, since the coupling between phases may present resonance frequencies with consequent overvoltages. Resonances may occur due to the series or parallel association between the sequence impedances, as seen in Figures A8.1 and A8.2:

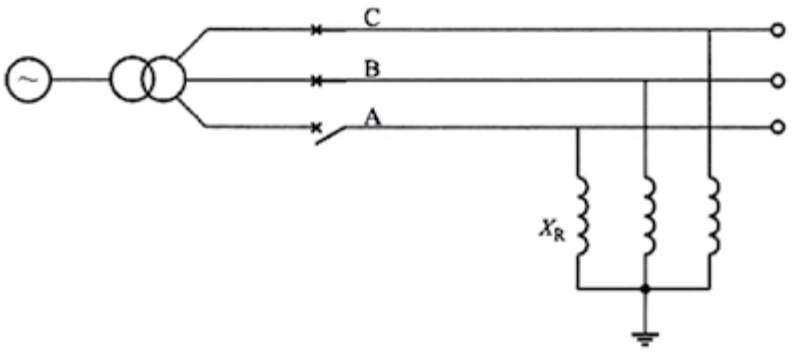

Figure A8.1: Circuit with parallel reactor and one phase open

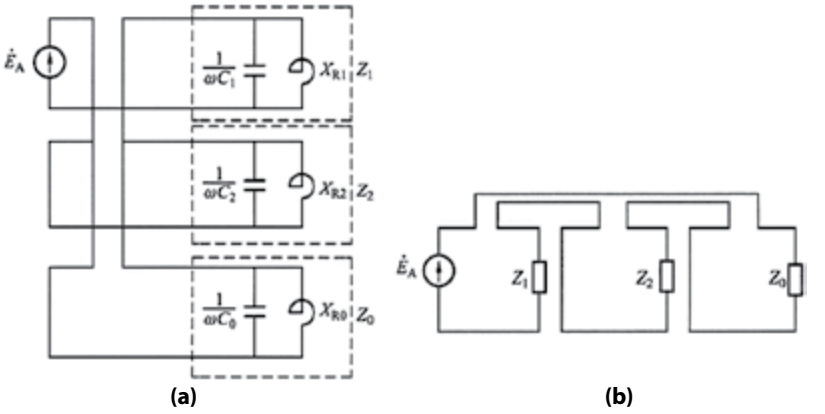

Figure A8.2: Association of the equivalent networks for the line with parallel reactors and open phases. (a) Only one phase open, (b) two phases open

To simplify the analysis, the internal impedance of the equivalent sources, and the series impedance of the line were disregarded. Thus, the equivalent circuit is formed only by the impedances of the parallel reactor, neutral reactor, and capacitive coupling between the phases.

With only one phase open, the induced voltage in the open phase to ground, Ua, will be:

$$\dot{U}_A = \dot{E}_A \frac{Z_1 - Z_0}{Z_1 + 2Z_0}$$

With two phases open, the induced voltage in the open phases to ground, Ub and Uc, will be:

$$\dot{U}_B = \dot{U}_C = \dot{E}_A \frac{Z_0 - Z_1}{Z_0 + 2Z_1}$$

Since the lines are usually undercompensated, the positive sequence impedance will be capacitive. If the frequency is between

$$\frac{1}{\sqrt{L_1 C_1}} < \omega < \frac{1}{\sqrt{L_1 C_0}}$$

Then, the zero sequence impedance will be overcompensated, and Z_1 and Z_0 will have opposite signs and there might be resonance. There will be no resonance if there is no parallel compensation in the line, or if the zero sequence is undercompensated.

A way to mitigate resonance is to use neutral reactors, which make the line undercompensated for the zero sequence, and also act to reduce the secondary arc currents during fault.

8.2 Results of the System with 1,000 kV Line

Considering the equations presented and using the parameters of the 1,000 kV TL of Table A8.1, and of the reactors.

Table A8.1: Line sequence parameters (60 Hz, 1,000 kV, 440 km)

Positive sequence		Zero sequence		Unit
C_1	14.2E-09	C_0	8.65E-09	nF/km
Q_{C1}	2353.8	Q_{C0}	1,430	Mvar
X_{C1}	424.8	X_{C0}	697	Ω

Parallel Reactors

L1	1.326 H	Ln	0.663 H
Qr	2000 Mvar	Xn	250 Ω
		Lo =	3.31 H

With neutral reactor equal to Xn = 250 Ω, we have the following response in frequency (Figure A8.3):

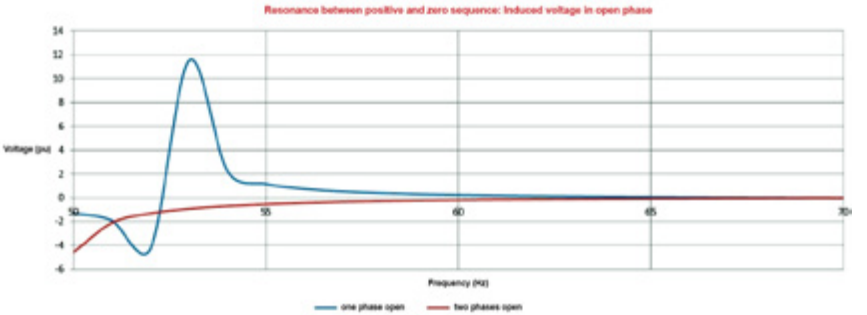

Figure A8.3: Resonance between positive and zero sequence: Induced voltage in open phase. 250 Ω neutral reactor

If the dimensioned neutral reactor was not used, the overvoltage profile due to resonance would be as presented in Figure A8.4.

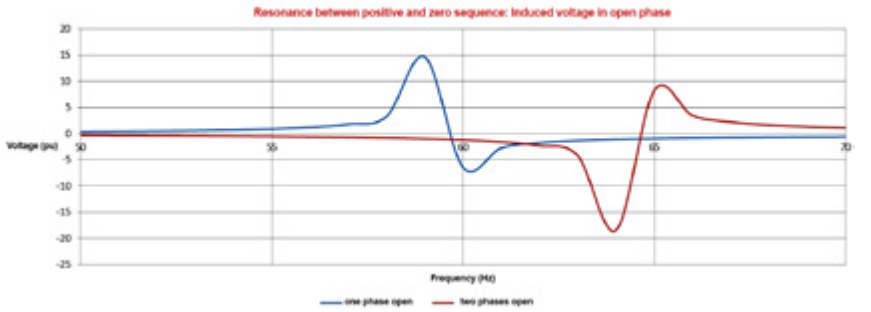

Figure A8.4: Resonance between positive and zero sequence: Induced voltage in open phase. Without neutral reactor

Resonance frequencies are verified both for one and for two open phases, within the frequency range of 56 Hz to 66 Hz. The sizing of the 250 Ω neutral reactor proved to be adequate also for mitigation of parallel resonance.

8.3 Resonance of the system in two circuits per 1,000 kV section

To verify if there is resonance in the range of 56 Hz to 66 Hz, when of a future entry of a second 1,000 kV circuit, a modeling in PSCAD was done (Figure A8.5).

Figure A8.6 presents the impedance in frequency of two circuits at 1,000 kV, with opening of one or two phases of a same circuit. We see that the result is similar to the result obtained with one circuit.

The sensitivity analysis was performed varying the reactance of the neutral reactor from 250 Ω to 350 Ω, corroborating the non-existence of resonance in the 56 to 66 Hz range between the positive and zero sequence, during the opening of the TL, be it with one or two phases, with only one circuit or with two 1,000 kV circuits.

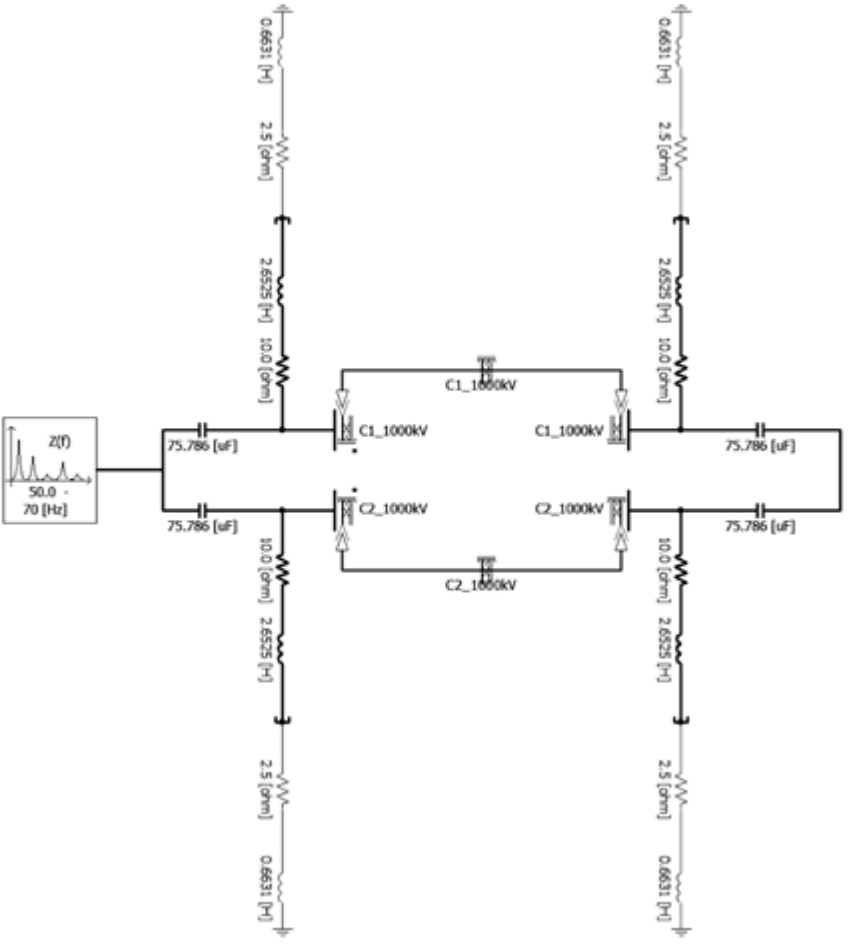

Figure A8.5: Single line diagram with two circuits in 1,000 kV

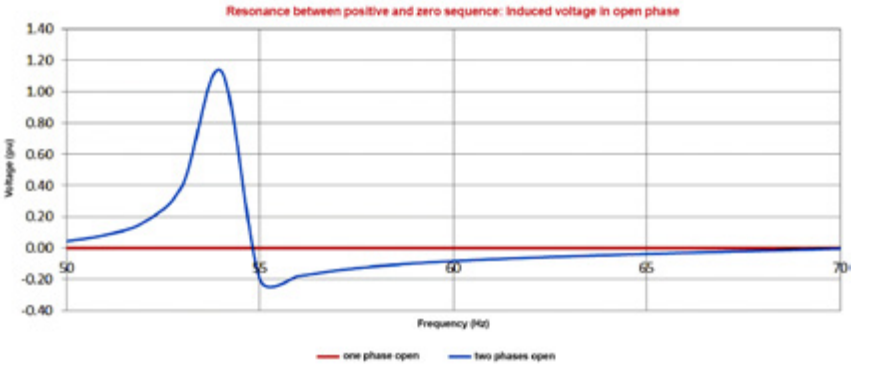

Figure A8.6: Resonance between positive and zero sequence: Induced voltage in open phase. 250 Ω neutral reactor

ATTACHMENT 9 – Load Rejection and Surge Arrester Effect (Expanded System)

9.1. Objective

Presenting and analyzing the overvoltages resulting of switchings due to load rejection and three-pole and single-pole reclosing, as well as the energy absorbed in the line surge arresters, considering the evolution of the 1,000 kV system by the addition of a fourth section (Pirapora – Ribeirão das Neves), and of a second circuit from Ourolândia to Ribeirão das Neves.

From the analysis performed for the reference alternative (one circuit), we concluded that the voltage elevations were not significant and did not lead to high energy in the surge arresters.

Similarly, a study was conducted for the expanded system and its results and analyses are presented below for the following events:

a. Rejection with opening of both lines on one side.
b. Similar to (a), followed by single-phase short in one of the circuits.
c. Single-phase short in one circuit, followed by rejection of the two circuits in one side.
d. Similar to (b), but with opening and "single-pole" reclosing of the line in short, followed by permanent three-pole opening of this line.
e. Similar to (b), with opening and "three-pole" reclosing of the circuit in short, followed by permanent three-pole opening of the line in short.

9.1.1 Load rejection (Case a)

The load rejection study was conducted according to the following sequence:

- Open one of the sides of the two lines at t = 50 ms, for all the sections, one at a time in each simulation. The total time of the simulation is 500 ms.
- Analyze in which line the highest overvoltage occurred, with the measurement placed at the terminals, where the surge arresters will be installed, and on the busbars.
- Observe the value of the overvoltage, which is compared to the start of the nonlinearity of the I-V curve of the surge arrester ≈ 1.91 pu.

Figure A9.1 shows the voltage measurement points (Busbar_A_C, AB_0%, AB_100%, and Busbar_B_C) and the timeline of the events. The measurements are the same both in circuit 1 (C1) and in circuit 2 (C2).

The lines and busbars are named with the initial letter of the busbar.

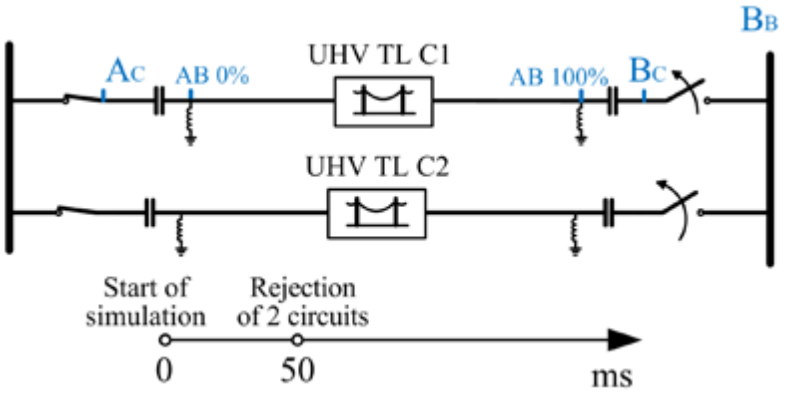

Figure A9.1: Simplified single line diagram of one sections of the 1,000 kV line and the event timeline

The results of the maximum voltages during the transient are described in Table A9.1.

Table A9.1: Maximum voltage values during rejection in the transient Vo(+)

Test	TL Section	Open terminal	Measurement	Busbar AC	AB0 0%	AB100 100%	Busbar BC
1	MO	M	Vo(+)	1.28	1.25	1.15	1.16
2	MO	O	Vo(+)	1.32	1.33	1.59	1.67
3	OI	O	Vo(+)	1.45	1.40	1.31	1.33
4	OI	I	Vo(+)	1.50	1.46	1.66	1.67
5	IP	I	Vo(+)	1.45	1.39	1.28	1.31
6	IP	P	Vo(+)	1.33	1.32	1.55	1.63
7	PN	P	Vo(+)	1.42	1.46	1.28	1.33
8	PN	N	Vo(+)	1.39	1.42	1.58	1.65

The values are in pu. $V_{base} = 1.000 \cdot \frac{\sqrt{2}}{\sqrt{3}} = 816{,}5\,\text{kV}$

Nomenclature:

The maximum voltage values can be obtained at three significant instants, being:

- Vo(+) = Highest voltage during transient.
- Vo(-) = Voltage at pre-occurrence state.
- Vo(Sust) = Sustained voltage after transient.

In all the tests the series capacitors were bypassed according to the guidelines of the ONS (Submodule 23.3).

The worst overvoltage case occurs in the Ourolândia – Igaporã line, with 1.66 pu (1,355 kV peak) at 100% of the length of the line (AB100), with opening on the Igaporã side. In the reference alternative, the highest overvoltage was of 1.68 pu, Igaporã – Pirapora section, for opening via the Pirapora side.

We highlight that in Table A9.1, all the voltage values in the final busbar (BC) are slightly higher than the location of the 100% of the line (AB100), due to the voltage stored in the series capacitor.

The triggering of the surge arresters is based on a voltage threshold of ≈ 1.9 pu, which implies the overvoltages in this case do not affect them.

Figure A9.2 presents the graph of the voltages measured at the end of the Ourolândia – Igaporã section (AB100). It also shows three significant instants where the maximum values are identified.

As a complement, Table A9.2 presents the Vo(-) and Vo(Sust) values.

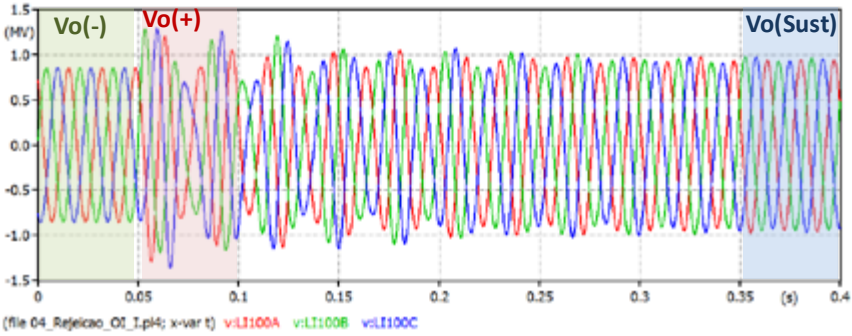

Figure A9.2: Voltage at the end of the Ourolândia – Igaporã line (AB100), with opening at Igaporã

Proceeding with the case studies, simulations will be done only in the most critical case (Ourolândia – Igaporã, rejection on the Igaporã side). The simulations with short-circuit will always be of the single-phase type, in the C1 circuit, at the end of the OI line (AB100). The rejections happen always in the two circuits, simultaneously.

Table A9.2: Pre-event Vo(-) and Sustained Vo(Sust) values

TL Section	Open terminal	Measurement	Busbar AC	AB0 0%	AB100 100%	Busbar BC
MO	M	Vo(-)	1.03	1.03	1.04	1.03
		Vo(Sust)	1.15	1.07	1.04	1.05
MO	O	Vo(-)	1.03	1.03	1.04	1.03
		Vo(Sust)	1.11	1.10	1.13	1.21
OI	O	Vo(-)	1.03	1.03	1.04	1.04
		Vo(Sust)	1.19	1.12	1.09	1.11
OI	I	Vo(-)	1.03	1.03	1.04	1.04
		Vo(Sust)	1.15	1.14	1.17	1.22
IP	I	Vo(-)	1.04	1.04	1.02	1.02
		Vo(Sust)	1.17	1.09	1.06	1.08
IP	P	Vo(-)	1.04	1.04	1.02	1.02
		Vo(Sust)	1.13	1.12	1.15	1.21
PN	P	Vo(-)	1.02	1.03	1.00	1.01
		Vo(Sust)	1.14	1.08	1.06	1.06
PN	N	Vo(-)	1.02	1.03	1.00	1.01
			1.14	1.13	1.14	1.20

9.1.2 Load rejection followed by short circuit (Case b)

This test was performed in the Ourolândia – Igaporã line, using short resistances of 5 Ω and 50 Ω. Initially, simulations were performed without surge arresters. Figure A9.3 shows the simplified single line diagram of the test.

The overvoltages at the substations and at the extremities of the line were observed. The opening of the circuit breakers of the two circuits occur at 50 ms, and the single-phase short in circuit 1 at 63.3 ms (phase A); this instant was chosen because this is when the highest overvoltage occurs. The short was inserted at the end of the line, on the side where the rejection occurs (Igaporã).

If the phase overvoltage exceeds 1.9 pu, the case is repeated, the surge arrester is inserted and, in addition to voltage, absorbed energy is also measured.

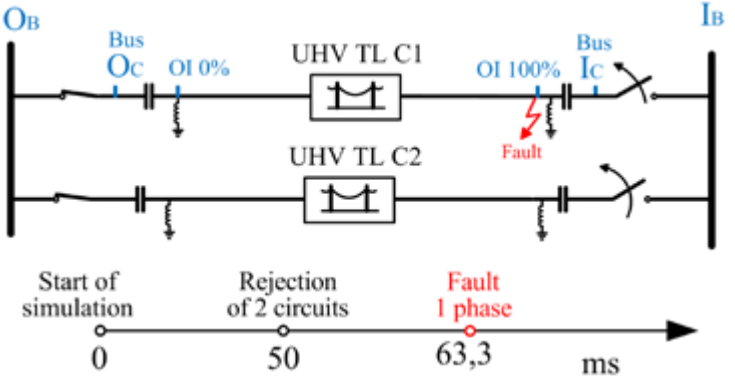

Figure A9.3: Single line diagram of the OI section with rejection, single-phase fault, and event timeline

a) Without surge arrester

The maximum value found is of 2.60 pu and occurs at the end of the line. Thus, it is necessary to examine the effect of the surge arrester on the overvoltage, and the energy it absorbs.

Table A9.3 presents the results of the overvoltages for short resistances of 5 Ω and 50 Ω. Figure A9.4 presents the behavior of the voltage measured at the end of the line, with short resistance of 5 Ω.

Table A9.3: Overvoltages produced by rejection, followed by short along the line, without surge arrester

Short resistance (Ω)	Initial busbar AC	AB0 0%	AB100 100%	Final busbar BC
5	1.64	1.58	2.60	2.53
50	1.61	1.54	2.50	2.44

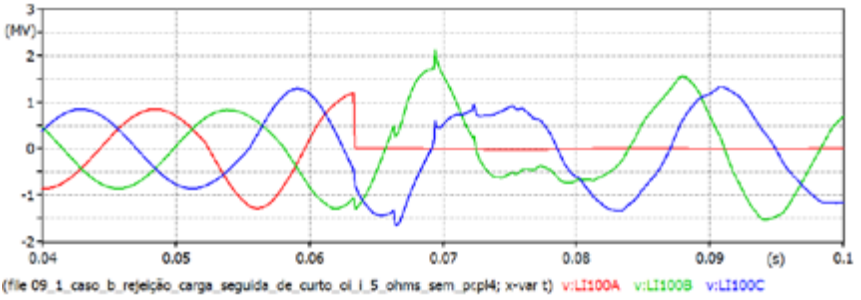

Figure A9.4: Voltage measured at the 100% location of the OI line, short resistance of 5 Ω, without surge arrester

b) With surge arrester

Table A9.4 presents the overvoltages after inserting the surge arrester at the end of the line (between the series capacitor and the circuit breaker), with short resistances of 5 Ω and 50 Ω. Figure A9.6 presents the voltage and energy absorbed by the surge arrester, for short resistance of 5 Ω.

Table A9.4: Overvoltages before short in phase A measured along the line with surge arrester

Short resistance (Ω)	Initial busbar AC	AB0 0%	AB100 100%	Final busbar BC
5	1.63	1.57	2.02	1.95
50	1.60	1.54	2.01	1.94

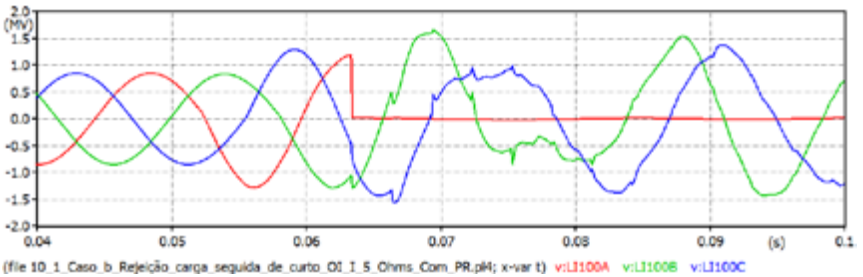

Figure A9.5: Voltage measured at the 100% location of the OI line, short resistance of 5 Ω, with surge arrester

The energy absorbed by the surge arrester allocated to the end of the line (AC100) is of 1.64 MJ.

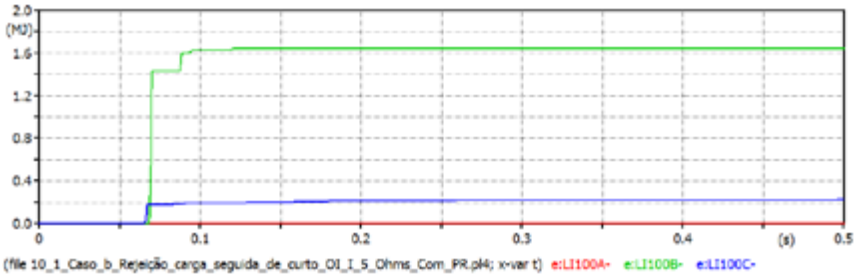

Figure A9.6: Energy absorbed in the surge arrester in the OI section

The maximum energy permissible through the surge arrester is 16 kJ/kV · 828 kV = 13.2 MJ and, therefore, the value of 1.64 MJ is much lower than the surge arrester absorption capacity.

9.1.3 Short followed by rejection (Case c)

In this test, the short occurred before the rejection. Similarly to the previous case, the tests use short resistances of 5 Ω and 50 Ω. The tests are performed, initially, without line surge arrester, and subsequently the surge arresters are inserted. Figure A9.7 shows the simplified single line diagram of the test, and the respective event timeline.

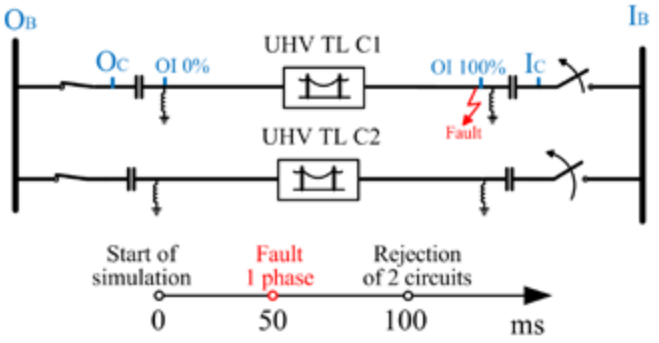

Figure A9.7: Single line diagram of the OI section with single-phase fault and subsequent rejection, and the event timeline

a) Without surge arrester

Table A9.5 presents the results of the overvoltages for short resistances of 5 Ω and 50 Ω. Figure A9.8 presents the graph of the voltage measured at the end of the line, with short resistance of 50 Ω.

Table A9.5: Overvoltages produced by short, followed by rejection along the line, without surge arreste

Short resistance (Ω)	Initial busbar AC	AB0 0%	AB100 100%	Final busbar BC
5	1.45	1.41	1.93	1.93
50	1.49	1.44	2.21	2.39

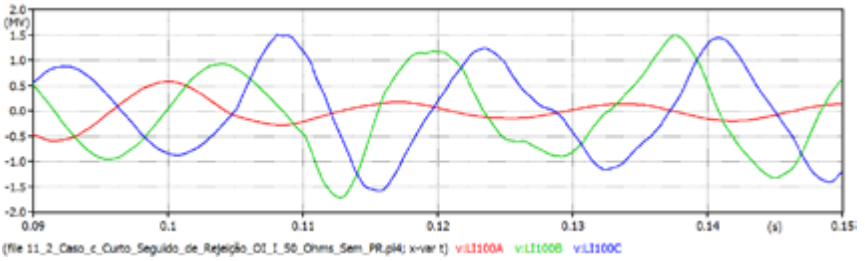

Figure A9.8: Voltage measured at the 100% location of the OI line

b) With surge arrester

Table A9.6 presents the behavior of the overvoltages measured after the insertion of the surge arrester at the end of the line, with short resistances of 5 Ω and 50 Ω.

Table A9.6: Overvoltages with short, followed by rejection along the line, with surge arrester

Short resistance (Ω)	Initial busbar AC	AB0 0%	AB100 100%	Final busbar BC
5	1.44	1.41	1.85	1.85
50	1.40	1.40	1.91	1.91

Figures A9.9 and A9.10 show the voltage and energy absorbed in the surge arrester for short resistance of 50 Ω, with energy equal to 0.8 MJ.

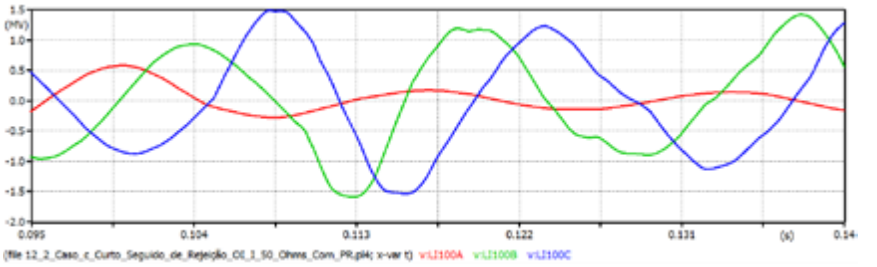

Figure A9.9: Voltage measured at the 100% location of the OI line

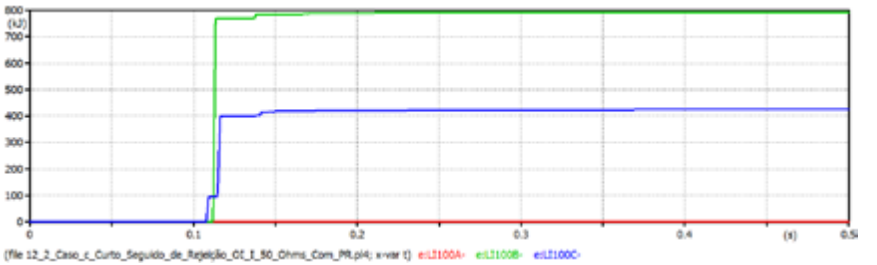

Figure A9.10: Energy absorbed in the surge arrester at 100% of the OI line, in the OI section

Considering the overvoltages obtained in the various cases, it was possible to observe that the highest overvoltage was produced in the case of rejection, followed by short with 2.60 pu.

Thus, the next tests will be based on this configuration, and with short resistance of 5 Ω.

The following tests correspond to three-pole and single-pole reclosing. The sequence of events of the following tests are continuation of the previous case, adding only the reclosings. This type of event proved to be the most critical, thus, the tests will be performed including the surge arresters.

9.1.4 Unsuccessful single-pole reclosing (Case d)

Figure A9.11 presents the single line diagram of the OI section with rejection of the 3 phases in the two circuits, single-phase short in circuit 1 (C1), single-pole opening in circuit 1 on the O side, single-pole reclosing in C1 on the O side, and, finally, three-pole opening at this same location. This figure also shows the timeline, showing each of the events already described.

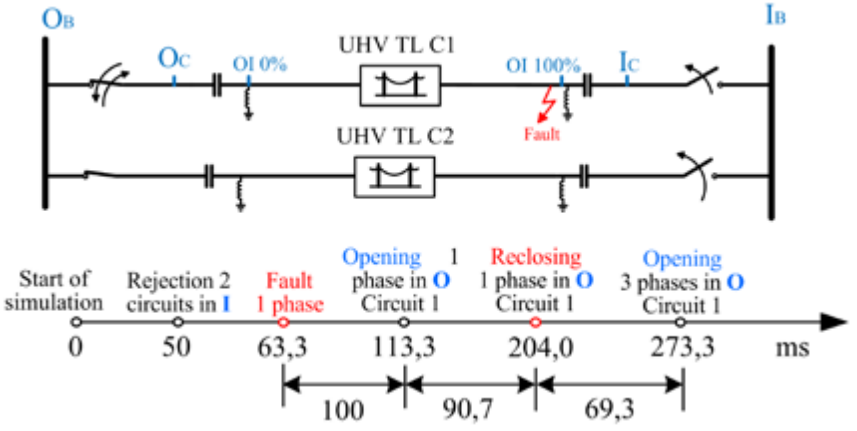

Figure A9.11: Single line diagram of the OI section with rejection, short, single-pole opening, single-pole reclosing, and three-pole opening, including timeline of the events

The reclosing time observed in the timeline of Figure A9.11 was obtained from the analyses of systematic and statistic closing.

a) Systematic Test

Aiming at locating the instant of the single-pole reclosing with greater impact on energy absorption by the line surge arresters, a series of systematic tests is developed. For this, we used the switch (allocated at O) with switching start time at t = 200 ms, and a spacing of 0.6944 ms, equivalent to 15º, resulting in 24 steps to comprise one wave cycle.

Table A9.7 presents the highest result after the insertion of only one surge arrester at position 100% (OI100) and at the Busbar I (IC), operating one at a time, separately.

Table A9.7: Energy absorbed in the surge arrester during unsuccessful single-pole reclosing

Measurement location	Energy absorbed (MJ)	Switch closing time (ms)
OI100	1.65	204.17
IC	1.25	204.17

The circuit breaker closing time is the same in both cases, and the energy in the surge arrester located at OI100 of the line is higher, compared to the surge arrester located at IC.

b) Statistic test

Starting from the switch closing time obtained in the systematic test, we can proceed to the statistic tests. For this, we use a single-phase statistic switch with the following characteristics:

- Average time 204.1665 ms.
- Deviation of 0.75 ms.
- Gaussian distribution with 100 shots.

Table A9.8 presents the result of the simulation for each surge arrester. The maximum energy absorbed at 100% (OI100) of the line is higher if compared to the energy absorbed at Busbar_I. The switch (circuit breaker) closing times are similar.

Table A9.8: Energy absorbed in the surge arresters during unsuccessful single-pole reclosing (statistic closing)

Measurement location	Energy absorbed (MJ)	Switch closing time (ms)
OI100	1.65	204.15
IC	1.25	204.18

The single-phase reclosing time chosen was 204.15 ms, because this was the instant in which the highest energy absorbed value was obtained, in this case by the surge arrester at 100% (OI100) of the line.

Voltages and energy in the surge arresters are presented in Figures A9.12 and A9.13.

The highest voltage was of 2.04 pu at (OI100).

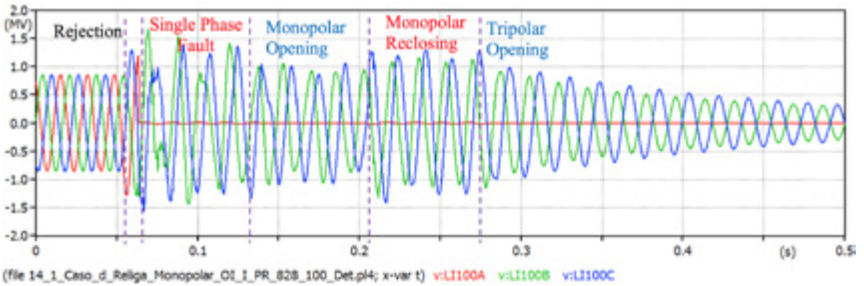

Figure A9.12: Voltage measured at the 100% of the OI section

The energy absorbed by the surge arrester located at 100% (OI100) of the line is of 1.65 MJ.

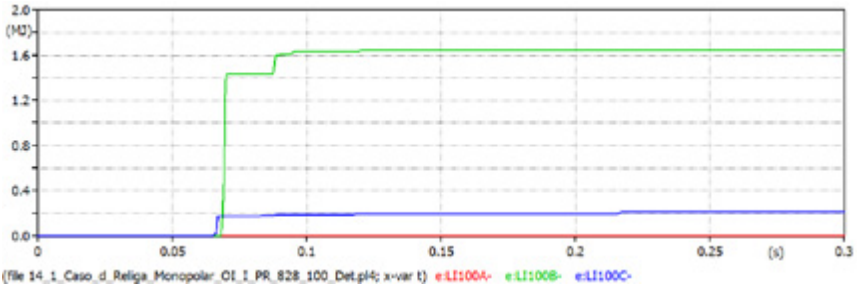

Figure A9.13: Energy absorbed by the surge arrester at 100% (OI100.)

9.1.5 Unsuccessful three-pole reclosing (Case e)

Figure A9.14 presents the single line diagram of the OI section with rejection of the 3 phases in the two circuits, single-phase short in C1, three-pole opening in C1 on the O side, three-pole reclosing in C1 on the O side, and, finally, three-pole opening at this same location. This same figure also shows the timeline, showing each of these events.

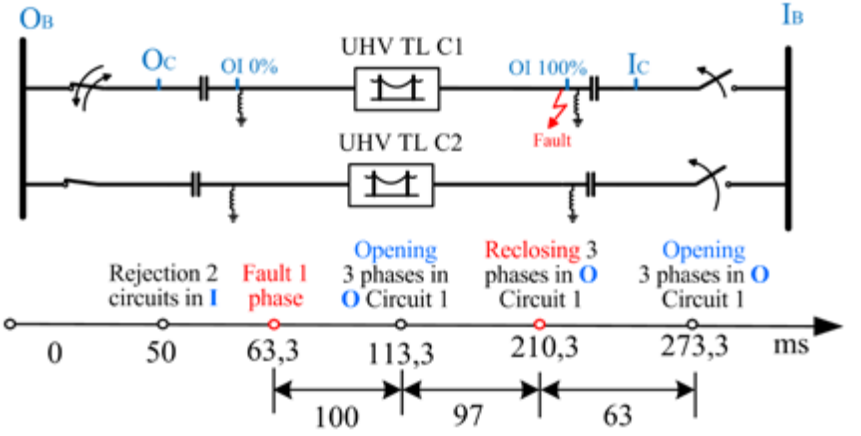

Figure A9.14: Single line diagram of the OI section with rejection, short, three-pole opening, three-pole reclosing, and three-pole opening, and timeline of the events

a) Systematic test

Table A9.9 presents the result for the insertion of only one surge arrester allocated at position 100% (OI100) and at the Busbar I, operating one at a time, separately.

Table A9.9: Energy absorbed in the surge arresters during unsuccessful three-pole reclosing (systematic closing)

Measurement location	Energy absorbed (MJ)	Switch closing time (ms)
100%	6.93	210.42
Bus_I	7.50	210.42

The circuit breaker closing time is the same in both cases, and energy is higher in the surge arrester at Busbar_I (IC).

b) Statistic test

Starting from the circuit breaker closing time obtained in the systematic test, we can proceed to the statistic tests. For this, we use a statistic switch with the following characteristics:

- Average time 210.41624 ms.
- Deviation of 0.75 ms.
- Gaussian distribution with 100 shots.

Table A9.10 presents the result of the simulation for each surge arrester. We observe that the energy values are the same, and the circuit breaker pole closing times are very close, however, any of the time instants obtained can be used for the deterministic test.

Table A9.10: Energy in the surge arresters and pole closing times

Measurement location	Energy absorbed (MJ)	Switch closing time (ms)		
		Pole A	Pole B	Pole C
OI100	7.9	210.72	209.63	210.06
IC	7.9	210.71	209.60	210.58

9.1.6 Line and busbar surge arrester simulations

Both the line and the busbar surge arresters were subject to overvoltages that would lead to them conducting energy.

Simulating the two surge arresters in the worst case (Table A9.11), the highest energy in one of them went down to 6.98 MJ.

9.1.7 Analysis with different types of surge arresters

Four types of surge arresters were analyzed in the most critical case (unsuccessful three-pole reclosing). Table A9.11 presents the overvoltages and energy absorbed in the surge arresters analyzed. The different types of surge arresters were allocated to the busbar side of the series capacitor, as this is the most critical location according to the results presented above.

Table A9.11: Overvoltages and energy for unsuccessful three-pole reclosing

Type of surge arrester, value of rated voltage (kV)	Maximum withstand energy (MJ)	Simulation results	
		Maximum voltage measured in the SA (pu)	Energy absorbed by the SA (MJ)
828	12.75	2.06	7.90
788	12.14	1.97	8.53
828 x 4 Columns	51.00	1.97	8.40
828 x 6 Columns*	32.29	1.86	11.39

*Special surge arrester under development

Below, are presented the voltages and energy absorbed by the surge arresters presented in Table A9.11.

Figures A9.15 and A9.16 present the voltages and energy absorbed by the 828 kV surge arrester, respectively.

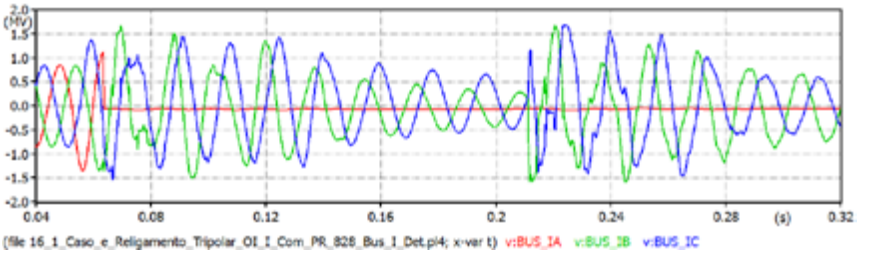

Figure A9.15: Voltage measured at Busbar_I, 828 kV surge arrester

The energy absorbed in the 828 kV surge arrester is of 6.98 MJ.

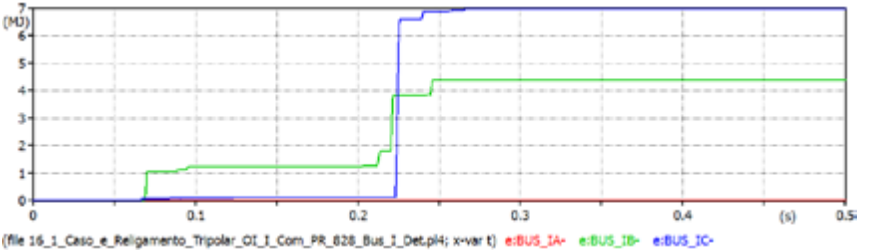

Figure A9.16: Energy absorbed in the 828 kV surge arrester at Busbar_I

Figures A9.17 and A9.18 present the voltages and energy absorbed by the 788 kV surge arrester.

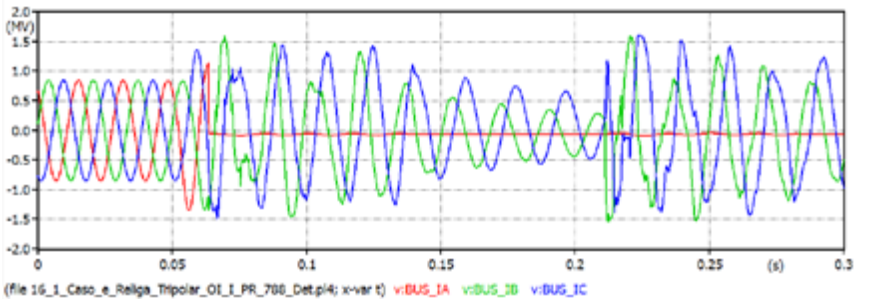

Figure A9.17: Voltage measured at Busbar_I, with three-pole reclosing with 788 kV surge arrester

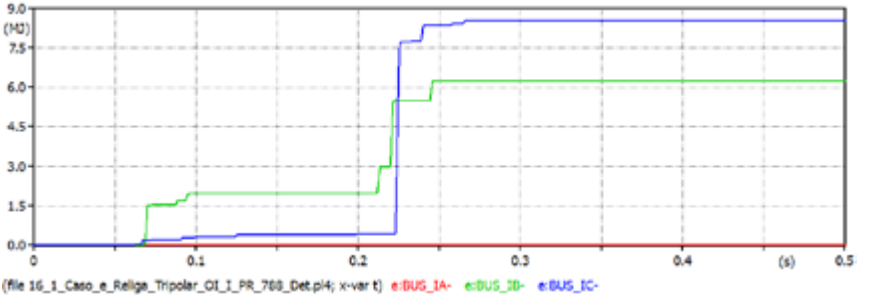

Figure A9.18: Energy absorbed in the 788 kV surge arrester at Busbar_I

Figure A9.19 presents the energy absorbed by the 828 kV surge arrester with 4 columns.

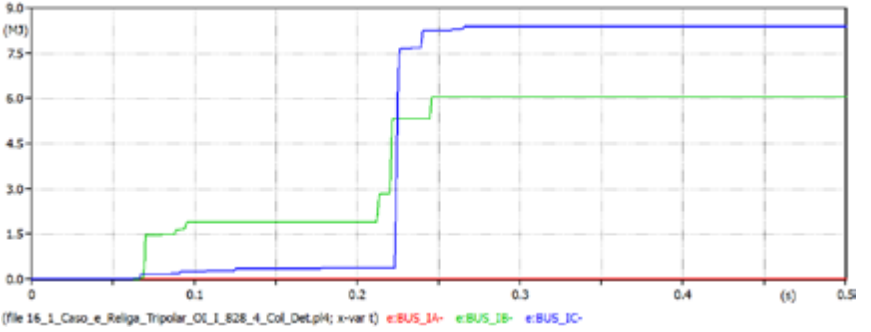

Figure A9.19: Energy absorbed in the 828 kV surge arrester with 4 columns

Figure A9.20 presents the energy absorbed by the 828 kV surge arrester with 6 columns.

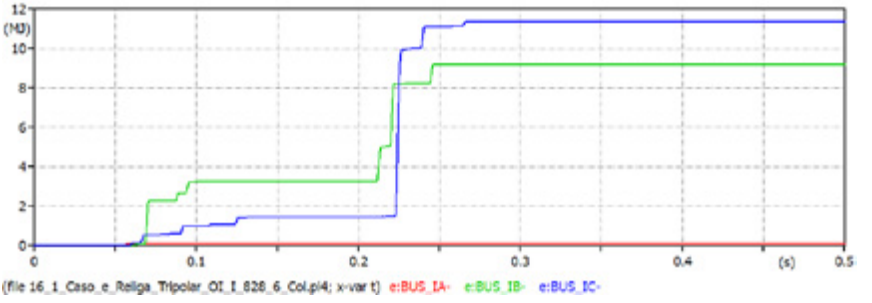

Figure A9.20: Energy absorbed in the 828 kV surge arrester with 6 columns

ATTACHMENT 10 – Line Energization (Expanded System)

10.1 Objective

Presenting the results obtained for the energization of the expanded 1,000 kV AC transmission line (1,620 km) connecting the substations of Milagres, Ourolândia, Igaporã, Pirapora, and Ribeirão das Neves, with two circuits in the last three sections.

Since, in the study of the reference system, the Ourolândia – Igaporã section presented the highest overvoltages, the line energization study will be performed in this same section to verify additional impacts.

We highlight that, in this case, one of the circuits of the section in question is considered already energized, while the second circuit will be energized on one of the sides.

10.2 Findings

Energizations were performed in the second section of the 1,000 kV line, Ourolândia – Igaporã, energized via Ourolândia. The energizations performed were systematic (24 switchings), statistic (200 switchings), and deterministic for the worst case.

We verified that, comparing the reference system to the expanded system, the overvoltages obtained in the latter were lower in approximately 16.7%.

10.3 Transmission Line Energization

First, systematic energizations were performed. The purpose of the systematic energization is determining the energization instant that causes higher overvoltage in a grid cycle, in a series of circuit breaker closing instants along a cycle.

After determining the instant of higher overvoltage, the statistic energization is performed, which consists of the random application of 200 switchings around this instant. Among these 200 switchings, the worst case of overvoltage is identified and presented in a deterministic manner.

10.3.1 Systematic energization

The systematic energization consisted of energizing the line during a 60 Hz grid cycle (16.66 ms), with intervals of 0.69 ms (15º electric), which means, 24 energizations were performed via the O terminal, of the 1,000 kV line OI section. The three phases are closed simultaneously, as well as the pre-insertion resistor bypass.

Table A10.1, below, presents the highest overvoltages in the OI section, obtained by means of systematic energization.

Table A10.1: Overvoltages resulting of systematic energization in the OI section

TL Sections	Energized via	Voltages (pu)				
		TL_0	TL_{25}	TL_{50}	TL_{75}	TL_{100}
Ourolândia – Igaporã	Ourolândia	1.179	1.283	1.372	1.458	1.441

TLx corresponds to x% of the length of the line from the terminal through which energization is done

We observe that the highest line energization overvoltage occurred at 75% of the OI line section energized via O, with a value of 1.458 pu. The value obtained in the reference system was of 1.791 pu. This represents a reduction of 16.7% of the overvoltage related to the reference system.

The circuit breaker closing time corresponding to the maximum overvoltage is 20.853 ms. Based on this time obtained, the statistic energization simulations were performed as follows.

10.3.2 Statistic energization

Due to the randomness of the closing instants of the circuit breaker poles, the energization switching study should be done in a statistic manner, considering a sample of two hundred switchings.

The following standard deviation values were considered for the circuit breaker: 0.75 ms for insertion of the pre-insertion resistor, and 1.25 ms for bypass of the resistor.

For the case of the Ourolândia – Igaporã section (energization via the Ourolândia side), we obtained phase-to-ground and phase-to-phase voltage values for five points of the line. Table A10.2 presents the values for this case.

Table A10.2: Result of the statistic energization

Overvoltage measurement location	Phase-to-ground and phase-to-phase	Average overvoltage (pu)	Standard deviation (pu)	Maximum overvoltage (pu)
0% of the TL	Phase A	1.137	0.030	1.135
	Phase B	1.187	0.030	1.182
	Phase C	1.141	0.046	1.198
	Phase B – Phase C	2.054	0.051	2.131
	Phase A – Phase C	1.944	0.067	2.071
	Phase A – Phase B	2.019	0.069	2.039
25% of the TL	Phase A	1.231	0.043	1.227
	Phase B	1.293	0.039	1.290
	Phase C	1.214	0.041	1.203
	Phase B – Phase C	2.186	0.040	2.325
	Phase A – Phase C	2.066	0.072	2.161
	Phase A – Phase B	2.200	0.075	2.320
50% of the TL	Phase A	1.274	0.047	1.251
	Phase B	1.361	0.048	1.373
	Phase C	1.250	0.047	1.285
	Phase B – Phase C	2.253	0.059	2.331
	Phase A – Phase C	2.131	0.079	2.211
	Phase A – Phase B	2.288	0.074	2.438
75 % of the TL	Phase A	1.290	0.054	1.246
	Phase B	1.393	0.050	1.459
	Phase C	1.258	0.051	1.312
	Phase B – Phase C	2.265	0.070	2.314
	Phase A – Phase C	2.142	0.092	2.226
	Phase A – Phase B	2.327	0.076	2.484
100% of the TL	Phase A	1.290	0.064	1.250
	Phase B	1.394	0.062	**1.534**
	Phase C	1.245	0.058	1.302
	Phase B – Phase C	2.241	0.077	2.336
	Phase A – Phase C	2.120	0.108	2.216
	Phase A – Phase B	2.319	0.083	2.565

The maximum overvoltage values obtained in the simulation of the expanded system occurred at the end of the OI line. These values are lower than those obtained in the reference system for the same case. In the case of the phase-to-ground overvoltage, there was a reduction of 17.4% and, in the case of the phase-phase voltage, of 21.7%.

10.3.3 Deterministic of the worst case

Based on the closing times of the circuit breaker poles for the worst overvoltage obtained in the statistic simulation, the deterministic simulation is performed. Figure A10.1 presents the graph of the phase-to-ground overvoltage. Figure A10.2 presents the phase-to-phase overvoltages, measured at 100% (TL100) of the OI line, energized via O.

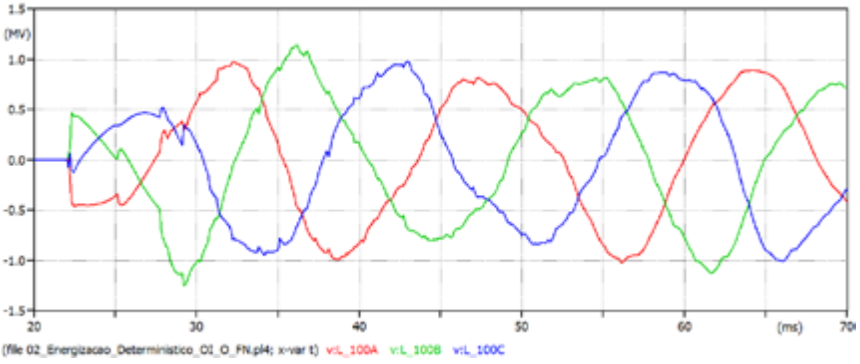

Figure A10.1: Phase-to-ground voltage at the end of the line (Igaporã – TL100)

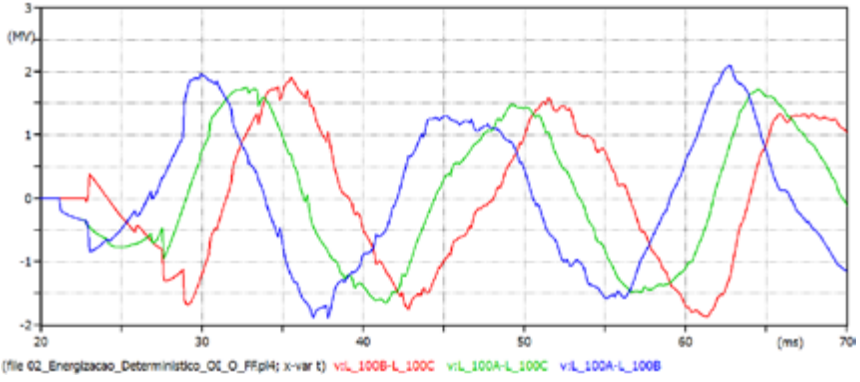

Figure A10.2: Phase-to-phase voltage at the end of the line (Igaporã – TL100)

ATTACHMENT 11 – Fault Application (Expanded System)

11.1 Objective

In the fault application, the overvoltages generated during the start of the fault, and the possible stress caused on the line insulation level should be observed. In previous studies, the overvoltages for the single-phase faults occurring at 0%, 25%, 50%, 75%, and 100% of the length of each section were evaluated. The worst case, at the time of this study, occurred in the Ourolândia – Igaporã section, for single-phase fault at the OI_{50} point (in the middle of the section).

11.2 Results

To perform this study, as well as the subsequent studies presented in this document, the systems and components described in the case studied in the reference system were used. Figure A11.1 shows the four sections (Milagres – Ourolândia – Igaporã – Pirapora – Ribeirão das Neves) of the 1,000 kV system, called expanded system. In this Figure are defined the sections with the initial letters of the substations (MO – OI – IP – RN).

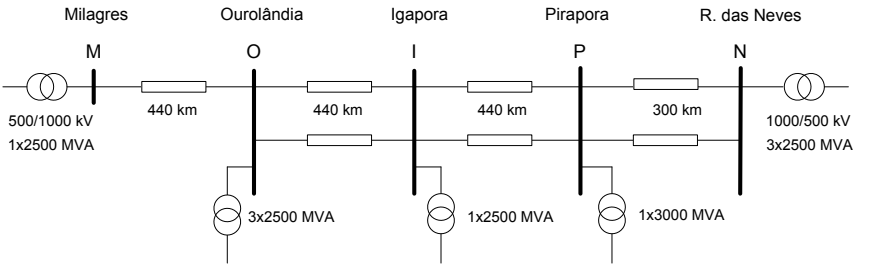

Figure A11.1: Single line diagram of the 1,000 kV expanded system

Figure A11.2 shows the main components used in each section. The neutral reactor (250 Ω) was placed at the neutral point of the line reactor. This is a conventional configuration aimed at suppressing secondary arc currents.

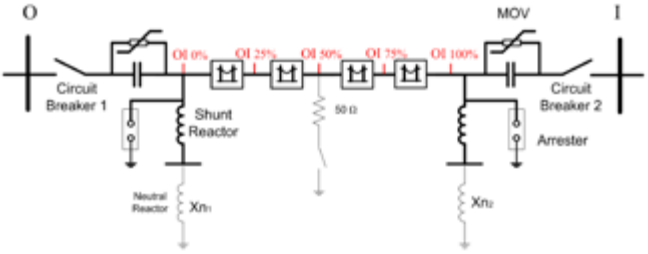

Figure A11.2: Main Components, fault location

A single-phase fault was simulated at the OI_{50} point (in the middle of the Ourolândia – Igaporã section), and the voltages were read at points at 0%, 25%, 50%, 75%, and 100% of the length of each section. The fault resistance considered was equal to 50 Ω.

The results of the overvoltages in the phases are presented in Table A11.1.

Table A11.1: Overvoltages in the healthy phases of the Ourolândia – Igaporã section for single-phase fault at OI_{50}

		Peak values (pu) in the Ourolândia – Igaporã section				
Position in the voltage wave, fault application	**Fault application instant (ms)**	**OI_0**	**OI_{25}**	**OI_{50}**	**OI_{75}**	**OI_{100}**
Cycle peak (+)	14.7	1.091	1.254	**1.461**	1.291	1.107
Cycle peak (-)	23.0	1.090	1.253	1.457	1.291	1.135

Observe that the maximum overvoltage value obtained in the expanded system when the fault is applied at the peak of the positive semi-cycle is of 1.461 pu, which is 4.3% lower when compared to the value obtained in the reference alternative, which was of 1.526 pu. This overvoltage occurs for the fault at 50% of the length of the section, which is the same point analyzed in the reference alternative.

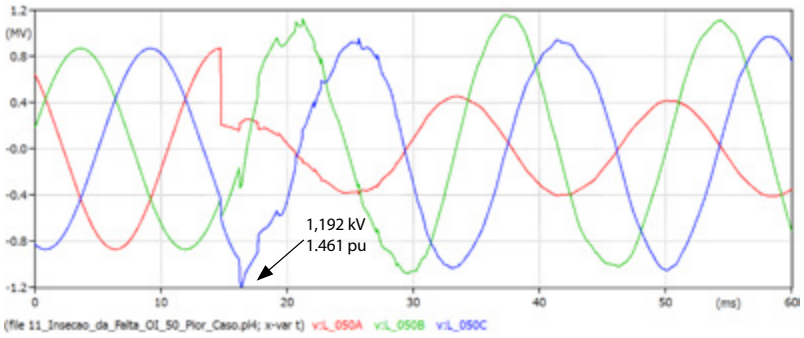

Figure A11.3: Worst overvoltage obtained due to the start of the fault (phase A)

ATTACHMENT 12 – Single-Phase Residual Load (Expanded System)

12.1 Objective

Presenting the overvoltage results of the application of single-phase faults applied to three points at 0%, 50%, and 100% of each section of the line.

12.2 Results

The results of the simulations were obtained considering the following conditions:

- "Phase A" remains open on the two extremities of the line during the entire simulation (200 ms).
- Single-phase short in "Phase A:" The simulation starts already in short, with the short switch opened at t = 100 ms. Under this condition, we consider that the system has already reached the state value of the fault current.
- Neutral reactor $Xn_1 = Xn_2 = 250\ \Omega$.
- Position of the short in the line: 0%, 50%, and 100% of the line.
- We will obtain the values for the arc extinction current and the first peak of the recovery voltage at the point in fault. These values will be lower than 50 A (effective), and 100 kVp phase-to-ground (thresholds). The conditions that govern arc extinction are: the value of the last peak of the arc current, and the value of the first peak of the recovery voltage (post-arc).
- The voltage and current limiting values for the secondary arc, referred to above, were defined in Submodule 23.3 (Guidelines and Criteria for Electric Projects Rev_2.0) of the ONS.

12.3 Extinction of the secondary arc

We obtained and analyzed mainly the secondary arc currents (I_{ARC}) and recovery voltage (V_{REC}), in addition to the neutral reactor voltages. The time interval when the measurements are obtained is: half a cycle before for the current, and half a cycle after the opening of the short switch, for the voltage.

Each of the sections are simulated, and will be called by their respective initials: MO, OI, IP, and PN, as explained in the beginning of this document.

a) Milagres – Ourolândia (MO) line section

Table A12.1 presents the results of the voltage and peak current measurements for the Milagres to Ourolândia line section, when the single-phase short occurs at 0%, 50%, and 100% of the line.

Table A12.1: Voltages and currents of the MO line

	Short location	Peak values			
		I_{ARC} (A)	V_{REC} (kV)	$V_{REACTOR}$ neutral (kV)	
				0%	100%
Section 1 MO	MO 0%	**69.5**	**33.7**	**115.5**	**113.6**
	MO 50%	46.2	24.6	121.8	119.5
	MO 100%	30.8	14.9	125.8	121.1

On one side, we observe that the secondary arc current I_{ARC} is 69.5 A_p when the short occurs at the start of the line.

The recovery voltage obtained is of 33.7 kV, the maximum obtained among the 4 sections. In the reference system, this voltage value, in this same section, was of 33.3 kV, very similar.

Figures A12.1 and A12.2 present the secondary arc current (I_{ARC}) and recovery voltage ($V_{RE}C$), respectively.

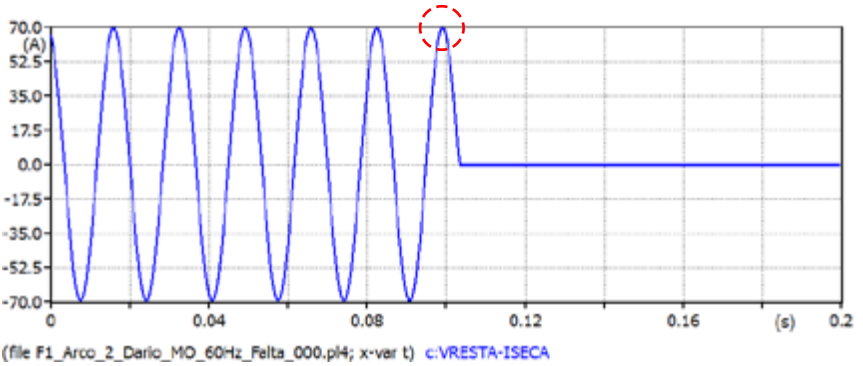

Figure A12.1: Secondary arc current in the MO line, short location 0%

Similarly, Figure A12.2 shows, with a dashed circle in blue, the recovery voltage value. This value is measured at the absolute maximum point in the first half cycle after the opening of the short switch at 100 ms.

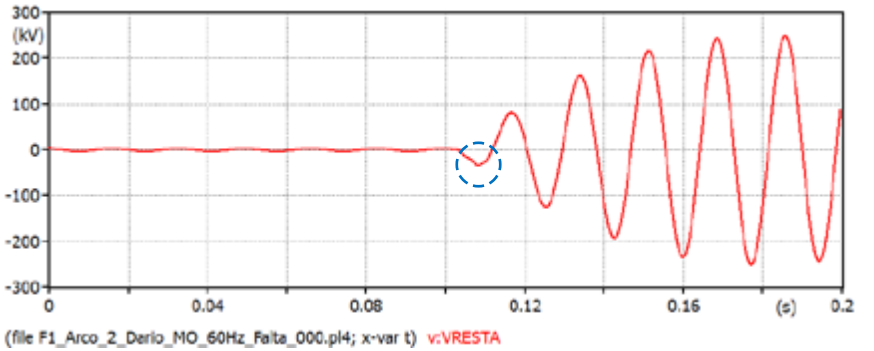

Figure A12.2: Recovery voltage in the MO line, short location 100%

Similarly, Figure A12.3 presents the voltages in the neutral reactor located at 0% and 100% of the MO line.

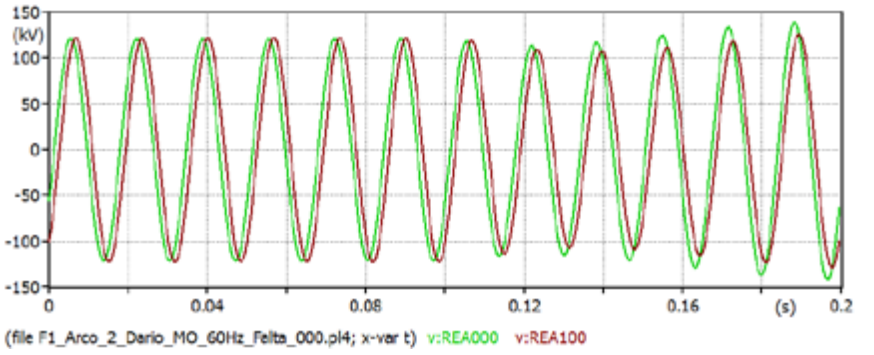

Figure A12.3: Voltages in the neutral reactors at the 0% and 100% locations of the line

b) Ourolândia – Igaporã (OI) line section

Table A12.2 presents the results of the voltage and peak current measurements for the Ourolândia – Igaporã line section, when the single-phase short occurs at the locations 0%, 50%, and 100%. This Table shows that the values obtained when the short occurs at 0% of the line are higher than the remaining ones. Despite that, these values are lower than those obtained in the MO section.

Table A12.2: Voltages and currents of the MO line

	Short location	Peak values			
		I_{ARC} (A)	V_{REC} (kV)	$V_{REACTOR}$ neutral (kV)	
				0%	100%
Section 2 OI	OI 0%	**61.94**	**30.11**	**118.16**	**121.54**
	OI 50%	46.08	24.71	117.37	119.29
	OI 100%	38.03	18.56	119.71	121.01

c) Igaporã – Pirapora (IP) line section

Table A12.3 presents the results of the voltage and peak current measurements for the Igaporã – Pirapora line section, when the single-phase short occur at the locations 0%, 50%, and 100%.

Table A12.3: Voltages and currents of the IP line

	Short location	Peak values			
		I_{ARC} (A)	V_{REC} (kV)	$V_{REACTOR}$ neutral (kV)	
				0%	100%
Section 3 IP	IP 0%	**61.6**	**29.9**	**119.8**	**118.3**
	IP 50%	46.0	24.7	119.4	116.7
	IP 100%	38.0	18.5	122.8	118.9

d) Pirapora – Ribeirão das Neves (PN) line section

Table A12.4 presents the results of the voltage and peak current measurements for the Pirapora – Ribeirão das Neves line section, when the single-phase short occurs at the locations 0%, 50%, and 100%.

Table A12.4: Voltages and currents of the PN line

	Short location	Peak values			
		I_{ARC} (A)	V_{REC} (kV)	$V_{REACTOR}$ neutral (kV)	
				0%	100%
Section 4 PN	Pirapora (0%)	**34.7**	**25.1**	**125.5**	**122.1**
	50%	26.7	20.1	125.9	121.6
	Ribeirão das Neves (100%)	20.9	15.2	127.8	123.1

Next, we present the influence of the grid frequency variation in the secondary arc current and voltages already analyzed.

12.3.1 Influence of system frequency variation in the line arc extinction, worst case

This item analyzes the influence of the system frequency variation in arc extinction. The 56 and 66 Hz frequency values are evaluated according to the established guidelines.

Figure A12.4 presents the curve that relates the secondary arc current and grid frequency in the MO section, with short location 0%. We can observe the almost linear increase of the secondary arc current when the grid frequency increases.

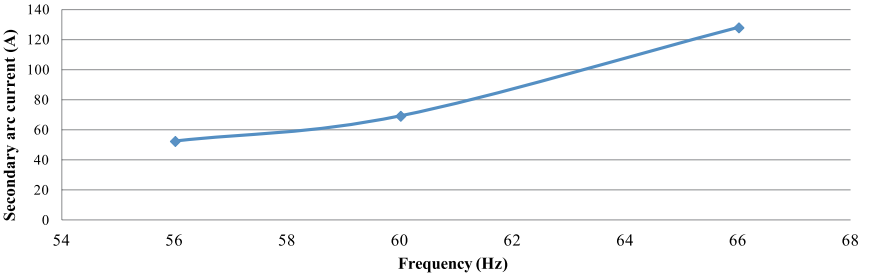

Figure A12.4: Secondary arc current (peak value) *versus* frequency in the MO section, with short location 0%

Tables A12.5 and A12.6 present the results for the 56 and 66 Hz frequencies, respectively.

Table A12.5: Voltages and currents in the sections of the 1,000 kV line for 56 Hz

Section	Short location	Peak values			
		I_{ARC} (A)	V_{REC} (kV)	$V_{REACTOR}$ neutral (kV)	
				0%	100%
Milagres to Ourolândia	MO 0%	**52.8**	**26.5**	**117.7**	**118.4**
	MO 50%	33.9	9.9	116.7	112.5
	MO 100%	34.5	11.7	120.5	113.4
Ourolândia to Igaporã	OI 0%	39.9	26.9	110.5	113.7
	OI 50%	33.7	27.0	110.3	111.8
	OI 100%	34.7	9.0	112.4	112.9
Igaporã to Pirapora	IP 0%	39.4	20.9	111.5	111.4
	IP 50%	33.6	22.1	111.5	109.8
	IP 100%	35.0	25.1	113.9	111.2
Pirapora to Ribeirão das Neves	PN 0%	25.3	22.7	116.7	116.5
	PN 50%	22.9	23.8	117.1	115.6
	PN 100%	22.9	26.1	118.6	116.4

In Table A12.6, the current and voltage values are higher, if compared to the results obtained for the 60 Hz frequency. This same response was reported in the previous case of this phenomenon, with the reference system.

Table A12.6: Voltages and currents in the sections of the 1,000 kV line for 66 Hz

Section	Short location	Peak values			
		I_{ARC} (A)	V_{REC} (kV)	$V_{REACTOR}$ neutral (kV)	
				0%	100%
Milagres to Ourolândia	MO 0%	**128.4**	**61.7**	**132.3**	**137.1**
	MO 50%	98.4	51.2	132.9	132.9
	MO 100%	79.5	38.2	138.2	135.8
Ourolândia to Igaporã	OI 0%	118.3	56.9	132.3	136.3
	OI 50%	99.8	52.1	131.5	133.7
	OI 100%	85.9	41.4	134.8	136.6
Igaporã to Pirapora	IP 0%	120.3	57.9	135.3	131.4
	IP 50%	100.0	52.5	135.5	129.7
	IP 100%	82.2	39.3	139.0	133.4
Pirapora to Ribeirão das Neves	PN 0%	71.5	50.8	141.8	131.4
	PN 50%	58.9	43.7	142.6	132.0
	PN 100%	47.3	33.7	145.6	134.9

It is important to highlight that, since the 1,000 kV system is inserted in the middle of the SIN, distant from synchronous generators, the frequency variation of the electromechanical transients is not large.

ATTACHMENT 13 – Single-Pole Reclosing (Expanded System)

13.1 Objective

The study of single-pole reclosing is a continuation of the "single-phase residual load" study, where I_{ARC} and V_{REC} must be lower than the threshold values defined in the grid modules of the ONS (Electric System National Operator).

To perform the single-pole reclosing simulations, we selected the Milagres – Ourolândia section of the 1,000 kV line, because this section presented the highest overvoltage during the recovery voltage test in the reference system. Based on this, we performed systematic (24 switchings), statistic (200 switchings) and, finally, deterministic simulations with the worst case of the statistic simulation.

The result obtained in the single-pole reclosing was a phase overvoltage of 1.84 pu (with statistic switch), when the reclosing occurs via Milagres. This voltage value is slightly lower than the value obtained in the reference system, which was equal to 1.85 pu. This implies that changes in the expanded grid do not generate overvoltages higher than those obtained in the reference system, in face of events with single-pole reclosing.

a) Statistic analysis

After the completion of all the simulations with systematic switches, the system ran with statistic switches (for 200 switchings), only for the case in which maximum overvoltage was obtained with systematic switch.

The result obtained is presented in Table A13.1. We can observe that the maximum value is of 1.838 pu, which is much closer to the value obtained in the reference system, which was of 1.853 pu. This implies that changes in the expanded grid did not generate overvoltages higher than those obtained in the reference system, in face of events with single-pole reclosing.

Table A13.1: Overvoltages in the MO section (statistic switch)

Measurement location	Maximum overvoltage (pu*)					
	Phase A	Phase B	Phase C	Phases B – C	Phases A – C	Phases A – B
0%	1.433	1.136	1.177	1.783	2.163	2.196
25%	1.628	1.159	1.249	1.825	2.322	2.326
50%	1.772	1.170	1.248	1.841	2.337	2.494
75%	**1.838**	1.167	1.214	1.831	2.294	2.626
100%	1.799	1.143	1.192	1.794	2.196	**2.667**

* Base voltage (peak) = 816.5 kV

We also observe that the highest phase-to-phase overvoltage occurs at the opposed extremity of the reclosing terminal, and is equal to 2.667 pu.

The times obtained in statistic switches 1 and 2 for the highest phase-to-ground overvoltages were of 279.17 ms and 284.86 ms, respectively. With these times, we proceed to the deterministic simulation.

b) Deterministic Analysis (worst case)

The worst case registered in the statistic simulation is presented in a determining manner in Figure A13.1.

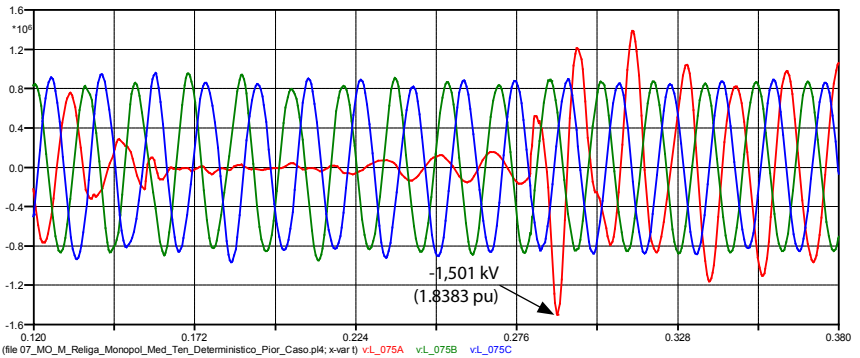

Figure A13.1: Worst case of maximum overvoltage at 75% of the MO section, reconnected via M

ATTACHMENT 14 – Three-pole Reclosing (Expanded System)

14.1 Objective

Based on the results obtained in the study of the reference system, the worst case was registered in the Milagres – Ourolândia section, reclosing via Milagres. During the simulations for the expanded system for this same section, we verified that the maximum overvoltage in the reference system was of 1.792 pu, and in the expanded system it was of 1.804 pu, for the same condition, successful three-phase reclosing.

To analyze the impact on the expanded system in face of the unsuccessful three-pole reclosing, a sequence of events was performed in the Milagres – Ourolândia section, with reclosing at M, as presented in the timeline of Figure A14.1:

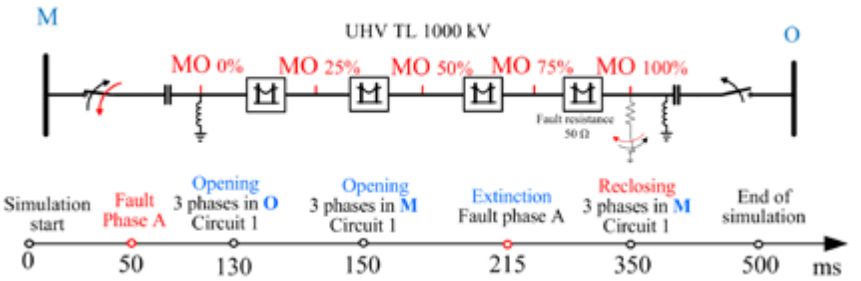

Figure A14.1: MO section with sequence of reclosing events

14.2 Systematic Analysis:

The results presented in Table A14.1 correspond to simulations using systematic switches that operate in an interval of 360° (every 15°), with a total of 24 shots. Simulations were performed with and without fault. In this Table, we observe that the overvoltages with fault were higher than those obtained without fault.

Table A14.1: Overvoltages obtained in the MO section

	Peak values (pu) in the section Milagres – Ourolândia				
Condition of reclosing/fault	**MO_0**	**MO_{25}**	**MO_{50}**	**MO_{75}**	**MO_{100}**
Successful reclosing	1.459	1.626	1.757	1.804	1.792
Unsuccessful reclosing	1.459	1.626	1.757	1.804	**1.808**
Reclosing without fault	1.330	1.450	1.570	1.623	1.589

The maximum overvoltage value with fault was of 1.804 pu, measured at 75% of the MO section. The value obtained in the reference system was of 1.792 pu.

In the simulations, we could observe that the overvoltages occurred during the opening of the circuit breakers, still during the short-circuit. Right after the reclosing, the overvoltages were always lower.

Figure A14.2 shows one of the instants simulated with systematic switch. In this figure, we can observe the highest overvoltage after the opening of the circuit breaker located at O, which is much higher than the value obtained in the reclosing. This behavior was observed in all the tests performed.

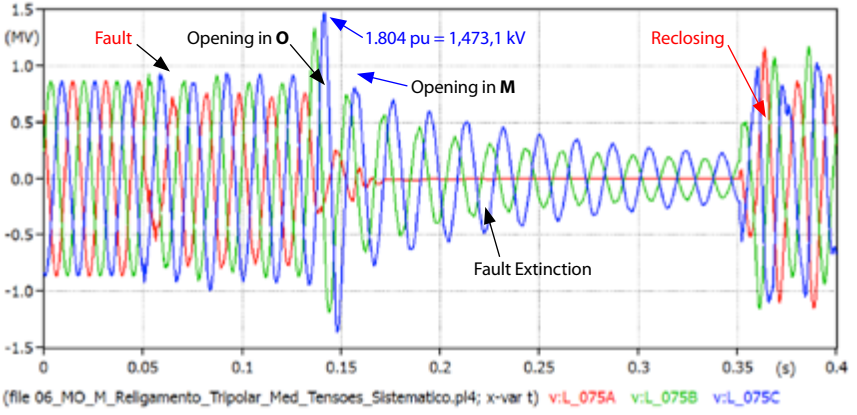

Figure A14.2: Voltage measured at 75% of the MO section for reclosing via M

Figure A14.3 presents the unsuccessful three-pole reclosing, where the fault switch remains connected until the end of the simulation. In this figure, we can observe the maximum overvoltage is still after the opening of the switch closest to the fault. The measurement is at the end of the line, and the overvoltage is slightly higher than the previous one.

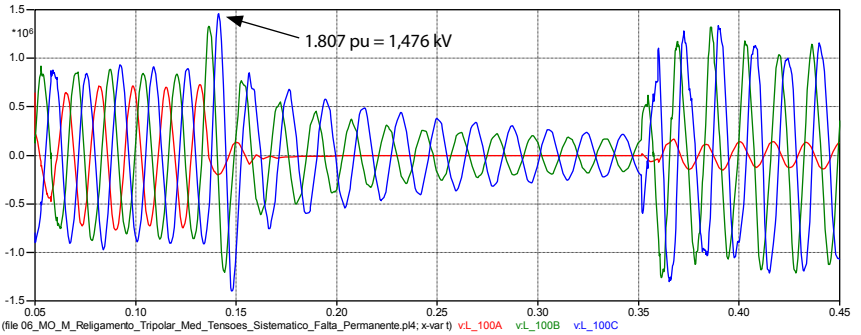

Figure A14.3: Voltage measured at the 100% of the MO section, unsuccessful reclosing via M (permanent fault)

Finally, Figure A14.4 presents the three-pole reclosing without fault. In this figure, we observe that the maximum overvoltage presents smaller magnitude than the case of Figure A14.3.

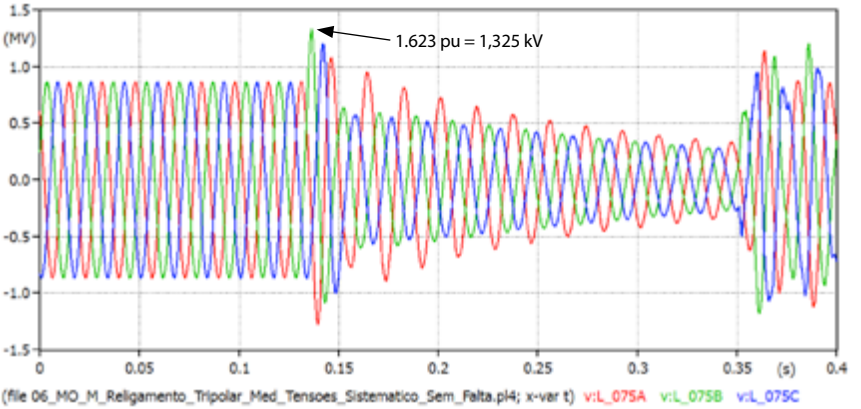

Figure A14.4: Voltage measured at the 75% of the MO section, reclosing via M, without fault

ATTACHMENT 15 – Transient Recovery Voltage (Expanded System)

15.1 Objective

Following, we present a synthesis of Transient Recovery Voltage (TRV) study.

TRV studies of the circuit breakers were performed for the following conditions:

- Short-line fault applied to 2 km, 10 km, 50%, and 90% of the length.
- Terminal three-phase fault insulated and grounded on both sides of the circuit breaker.

Specifically, the sections of Ourolândia – Igaporã and Igaporã – Pirapora were analyzed for showing more critical TRV values in the reference system.

We highlight that in the tests performed, the opening of the circuit breaker is done only in the line of the affected section, with the parallel healthy line staying connected.

15.2 Main Results

Following are presented the most critical results of the study. Those cases where there was no surpassing of the TRV are not included in this section.

15.2.1 Ourolândia – Igaporã Section

The most critical case was the short-line fault at 2 km from the Igaporã terminal. In this case, the bypass of the series capacitor was done via voltage-controlled switch.

a) Short-line fault at 2 km from Igaporã

The result is presented in Figure A15.1, below:

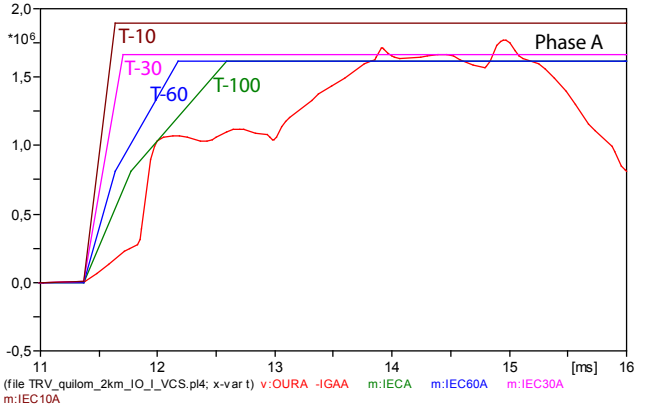

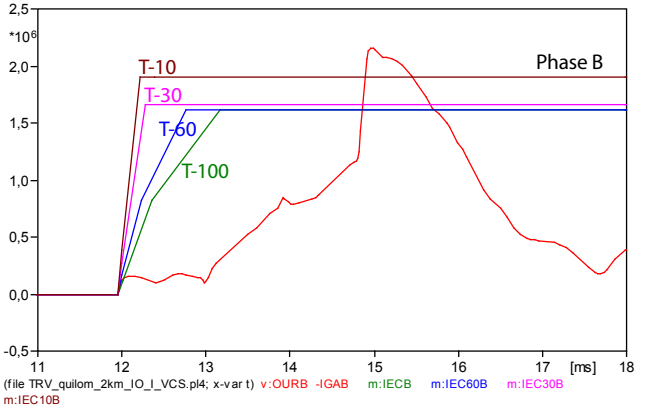

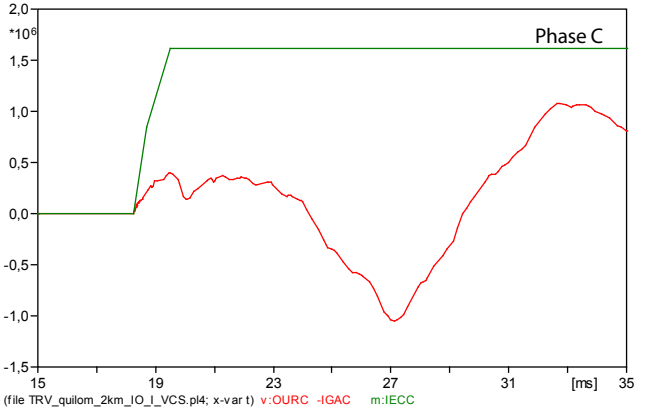

Phase	Icc via DJ (kA_p)	T (%)	Surpassed T-100	Type of surpassing
A	5.9	6.62	Yes	Ma
B	3.4	3.82	Yes	Mb
C	67.6	75.87	No	--

Figure A15.1: Short-line fault at 2 km from Igaporã

The circuit breaker on the Igaporã side proved to be more critical, because the wave front of the envelope curve (T-100) was surpassed, as well as the magnitude of the T-60, T-30, and T-10 curves (phase B). This magnitude surpassing is of approximately 12.5% above the T-10 curve (phase B).

For faults occurring right at the start of the section (for ex. 0.5 km), right after the series capacitor, the magnitude of the fault current through the circuit breaker, and the TRV values are very close to the values shown when the fault is applied at 2 km.

b) Short-line faults at 10 km, 50%, and 90% from the Ourolândia and Igaporã terminals

There was no surpassing in any of the cases for short-line faults at 10 km, 50%, and 90% of the length of the section.

c) Terminal three-phase fault insulated and grounded

None of the TRVs corresponding to insulated or grounded (three-phase) terminal faults surpassed the specific curve determined by the relation of fault current and its current interruption capacity (63 kA rms). Even the T-100 curve was not surpassed.

15.2.2 Results for the Igaporã – Pirapora section

a) Short-line fault at 2 km from Pirapora

The series capacitor on the Pirapora side was bypassed, the results are shown in Figure A15.2.

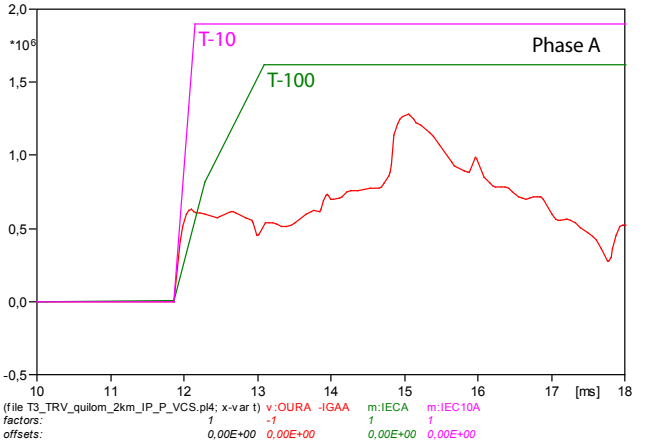
2,0
*10^6
1,5
1,0
0,5
0,0
-0,5
T-10
T-100
Phase A
10
11
12
13
14
15
16
17
[ms]
18
(file T3_TRV_quilom_2km_IP_P_VCS.pl4; x-var t) v:OURA -IGAA m:IECA m:IEC10A
factors: 1 -1 1 1
offsets: 0,00E+00 0,00E+00 0,00E+00 0,00E+00

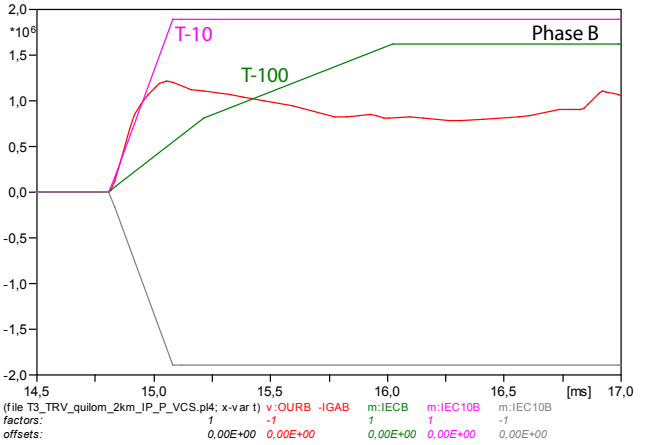
2,0
*10^6
1,5
1,0
0,5
0,0
-0,5
-1,0
-1,5
-2,0
T-10
T-100
Phase B
14,5
15,0
15,5
16,0
16,5
[ms]
17,0
(file T3_TRV_quilom_2km_IP_P_VCS.pl4; x-var t) v:OURB -IGAB m:IECB m:IEC10B m:IEC10B
factors: 1 -1 1 1 -1
offsets: 0,00E+00 0,00E+00 0,00E+00 0,00E+00 0,00E+00

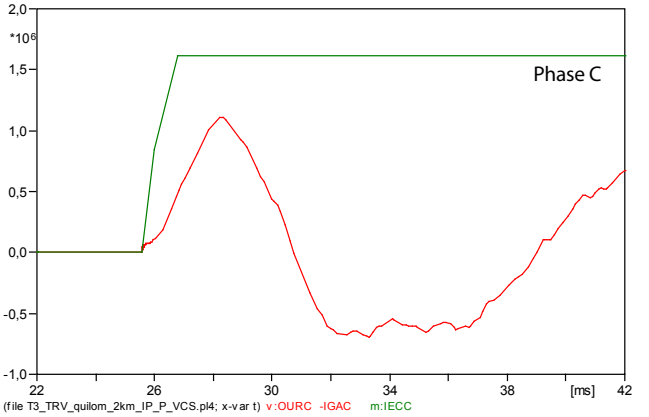
2,0
*10^6
1,5
1,0
0,5
0,0
-0,5
-1,0
Phase C
22
26
30
34
38
[ms]
42
(file T3_TRV_quilom_2km_IP_P_VCS.pl4; x-var t) v:OURC -IGAC m:IECC

Phase	Icc via DJ (kA_p)	T (%)	Surpassed T-100	Type of surpassing
A	4.40	4.94	Yes	Rc
B	3.20	3.60	Yes	Rc
C	36.17	40.60	No	--

Figure A15.2: Short-line fault at 2 km from Pirapora (section 3)

There was surpassing at the wave front (RRRV) of the (T-100) curve, as shown in Figure A15.2. Even the T-10 curve was surpassed in its RRRV, although marginally.

b) Short-line faults at 50%, and 90% from the Igaporã – Pirapora terminals

There was no surpassing in any of the cases for short-line faults at 50%, and 90% of the length of the section.

c) Terminal three-phase fault insulated and grounded (Igaporã – Pirapora)

None of the TRVs corresponding to insulated or grounded three-phase terminal faults surpassed the specific curve (T-10 or T-30). Even the T-100 curve was not surpassed.

ATTACHMENT 16 – Analysis of the Series Capacitor (Expanded System)

16.1 Objective

Presenting the procedure followed for analysis of the series capacitor requirements, including the protection system provided of MOV (*Metal Oxide Varistor*).

Usually, MOVs are installed in parallel to the series bank, and their function is protecting it, be it during faults in the line itself, or as a result of demands imposed by a line parallel to the line with series bank.

The calculations presented in this item were based on the recommendations of IEC-143, as well as in experiences in projects listed in the reference section, and considering the emergency condition of the 1,000 kV system.

16.2 1,000 kV System

Figure A16.1 presents the single line diagram of a line section with one circuit, where we observe the elements that compose it, and the voltage measurement locations (in red).

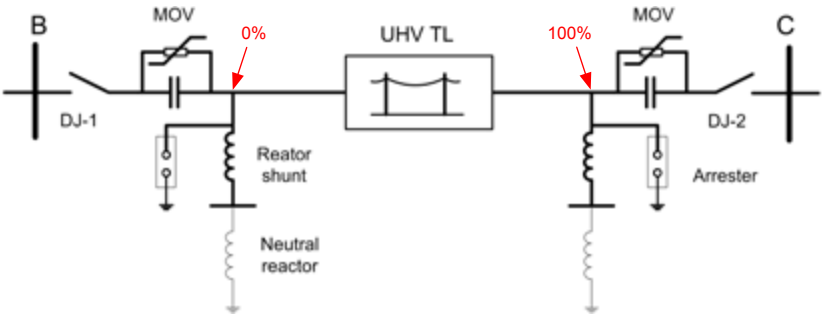

Figure A16.1: Single line diagram of a line section of a 1,000 kV circuit

Figure A16.2 shows the main components of the series bank protection. They are: the MOV, bypass gap, the dampening reactor, and the bypass circuit breaker.

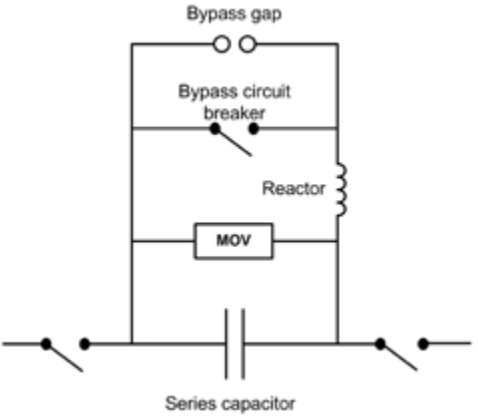

Figure A16.2: Main components of the series bank protection

The MOV offers protection against overvoltages during line faults. The bypass gap is triggered during excess energy conditions in the varistor, while the bypass circuit breaker operates automatically in the case of prolonged conduction of the gap, or during other contingencies in the bank platform. The dampening reactor limits the capacitor discharge current that would result in discharges in the gap, or closing of the bypass circuit breaker. Both the MOV and the gap operate independently in each phase, while the bypass circuit breaker operates simultaneously in the three phases.

16.3 Determining series compensation characteristics

16.3.1 Fluxes during emergency

From the power flux studies (heavy load, humid North scenario), in the case of the expanded system, we determined that in the worst contingency (outage of a circuit), the healthy line with heavier load (Ourolândia – Igaporã), would have flux of approximately 5,929 MW and 1,870 MVAr, which implies current equal to:

$$I_{emerg} = \frac{6217MVA}{\sqrt{3} \cdot 1.000} = 3,6kA$$

The I_{emerg} value corresponds to the current value with duration of up to 30 min.

Table A16.1: flux in the expanded system during emergency

Line	Side	MW	Mvar	MVA	Emergency
Milagres – Ourolândia	Milagres	2865	53.2	2871	Output of the reinforcement made, second 500 kV TL, Juazeiro – Ourolândia 3
	Ourolândia	2834	-514	2880	
Ourolândia – Igaporã	Ourolândia	5929	1870	**6217**	Output of the second 1,000 kV TL, Ourolândia – Igaporã
	Igaporã	5792	-1984	6123	
Igaporã – Pirapora	Igaporã	5550	1769	5825	Output of the second 1,000 kV TL, Igaporã – Pirapora
	Pirapora	5426	-1691	5684	
Pirapora – Neves	Pirapora	5640	1582	5858	Output of the second 1,000 kV TL, Pirapora – Neves
	Neves	5559	-743	5609	

16.3.2 Calculation of state currents and transients.

The state current may be estimated according to the concept expressed in Figure A16.3.

With the overload capacity of the series capacitor (I_{emerg}) being for 30 min, this value must be 35% of the steady state current (I_{rated}).

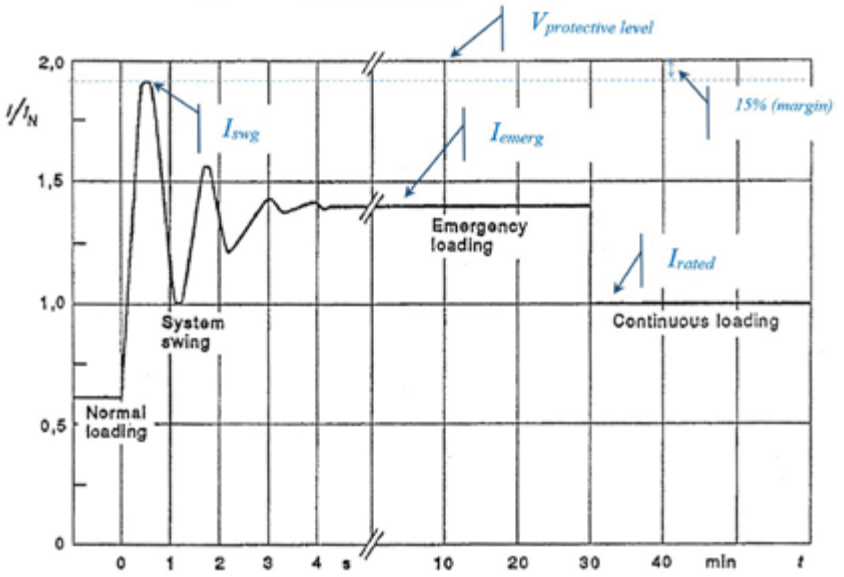

Figure A16.3: Typical swing current for insertion of the series capacitor after the fault and loss of the parallel line

$$I_{emerg} = 1.35 \cdot I_{rated}$$

$$I_{rated} = \frac{3{,}60}{1{,}35} = 2{,}67\ kA$$

The current for an overload with duration of 10 min. (I_{10}) would be:

$$I_{10} = 1.5 \cdot 2,\ 67 = 4\ \text{kA}$$

The transient oscillation during energization is shown in Figure A16.4.

Therefore, adopting a margin of 15% for the swing current (I_{swg}) for up to 10s:

I_{swg} = 1.15 · 4 = 4.6 kA, with this value being based on an additional margin of 15% over the 10 min value.

16.3.3 Voltages and power

The state voltage over the series capacitor considering reactance of the bank Xc = 35 Ω.

$$V_C = Xc \cdot I_{rated}$$
$$V_C = 35 \cdot 2.67 = 93.4\ \text{kV}$$

The continuous reactive power, MVAr per series capacitor phase, would be:

$$Q_C = Xc \cdot (I_{rated})^2$$
$$Q_C = 35 \cdot (2.67)^2 = 250\ \text{Mvar (per phase)}$$
$$Q_{C\_3F} = 3 \cdot 249.5 = 750\ \text{Mvar (three-phase)}$$

Voltage during current swing:

$$V_{swg} = Xc \cdot I_{swg}$$
$$V_{swg} = 35 \cdot 4.6 = 161\ \text{kV}$$

Voltage during emergency (V_{emerg}),

$$V_{emerg} = Xc \cdot I_{emerg}$$
$$V_{emerg} = 35 \cdot 3.6 = 126\ \text{kV}$$

16.3.4 MOV Requirements

The MOV is defined considering the protection level (*protective level*) adopted 15% above the 10s voltage and swing. This protection level is used to determine the short-term insulation level requirements.

Thus, the protection level of the bank (*protective level*, V_{pl}) will be:

$$V_{pl} = 1.15 \cdot V_{swg}\,(\text{rms})$$
$$V_{pl} = 1.15 \cdot 161 = 185.2\ \text{kV}$$

The peak value of which is,

$$V_{pl\_pk} = \sqrt{2} \cdot 185{,}2\ kV = 261{,}1\ kVp$$

The insulation withstand voltage (*power frequency bank withstand voltage of the insulation*), V_{ipf}, is calculated based on the following expression:

$$V_{ipf} = 1{,}2 \cdot \frac{V_{pl}}{\sqrt{2}} \cdot K_a$$

- For altitudes of up to 1,000 m, the value of $K_a = 1.0$.

$$V_{ipf} = 1.2 \cdot 185.2\ \text{kV} = 222.2\ \text{kV (rms)}$$

On the other hand, the MOV rated voltage related to the capacitor varies between:

$$V_{MOV} = (2.5\text{-}3.0)\ V_c$$
$$V_{MOV} = 2.5 \cdot 93.4 = 233.5\ \text{kV (rms)}$$

- The highest value (rms) between V_{ipf} and V_{MOV} is: $V_{MOV} = 233.5$ kV.
- Peak value $V_{MOV} = \sqrt{2} \cdot 233.5 = 330$ kV.

The MOV characteristics can be obtained based on the characteristics of ZnO surge arresters.

To calculate the residual voltage (peak) in the surge arrester catalog (wave of 30/60 ms), we consider a 2 kA current, for the *IR* voltage value in the surge arrester.

Using this value in the catalog of ABB surge arresters, for example, we have:

- V_{rated} = 162 kV (rms)
- IR at 2 kA would be 336 kV.
- Energy absorption capacity = 12.0 kJ/kV
- Maximum residual voltage (Table A16.2):

Table A16.2: Maximum residual voltage of the MOV

I (kA)	V (kV_{peak})
0.5	316
1	328
2	336

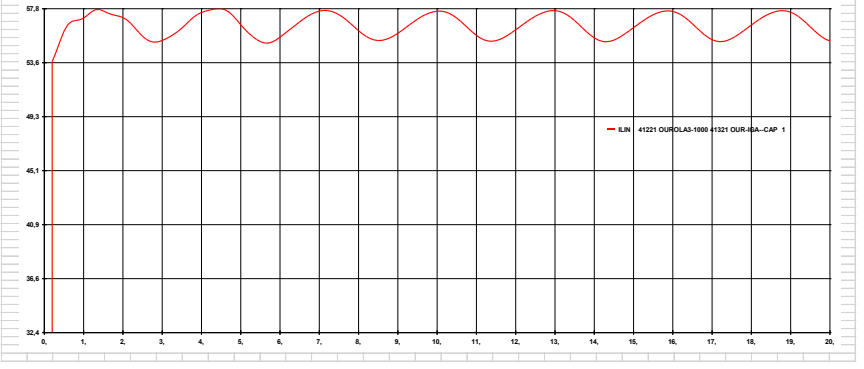

Figure A16.4: Current (pu) in the capacitor during contingency, with dynamic representation of the new machines

ATTACHMENT 17 – Studies and Development of Polymeric Surge Arrester and Insulator Prototypes for the UHV Transmission System

17.1 Objective

Balestro, a Brazilian surge arrester and insulator manufacturing company, was integrated to the project for the conceptual definition and presentation of prototypes of this equipment for the lines and substations of the 1,000 kV System.

The system is unprecedented in Brazil, but similar systems are being developed in other countries [13]. Thus, materials and equipment solutions emerge for substations and transmission lines.

Following, from this perspective, we present a synthesis of the development of these two types of equipment.

17.2 Surge arrester for the 1,000 kV System

For the rated and maximum operating voltage levels (U_M = 1,100 kV) of the proposed system, based on the surge arrester sizing recommendation of the IEC 60099-5 standard, the most adequate surge arrester for this system should have maximum continuous operating voltage $U_C > U_M$ phase-to-ground of the system.

Thus, the U_R = 828 kV rated voltage was considered the most adequate, since in this case, we have U_C = 662 kV, meeting the above-mentioned requirement. The same sizing solution was chosen for the similar systems in operation and under construction in China.

The 1,000 kV transmission systems require the use of surge arresters with better protective characteristics than those used for lower voltages, to ensure that minimum insulation coordination margins are maintained with the substation equipment, thus ensuring such equipment meets the supportabilities foreseen for these systems according to the IEC 60071-1 standard.

Therefore, in 1,000 kV transmission system projects, the performance required from the surge arresters renders mandatory the use of surge arrester solutions with multiple columns, so as to reduce the density of the discharge currents on the varistor blocks, thus, also reducing the residual voltages of atmospheric and switching surges to acceptable factors.

As the goal for this project, the following withstand values for the equipment (in conformity with IEC 60071-1), and respective minimum protection margins were defined.

a. Minimum protection margin of 15% for withstand switching surges of 1,800 kVp in the equipment, which implies residual voltage for switching surges to 2 kA, maximum of 1,530 kVp;
b. Minimum protection margin of 25% for atmospheric discharge surges of (NBI) = 2,400 kVp, in the which implies residual voltage for atmospheric surges to 20 kA, maximum of 1,800 kVp.

The definition of these electrical requirements allowed us to maintain the substation equipment at supportability levels already developed by the equipment manufacturers.

Based on a more in depth analysis of the Chinese and Indian solutions, we observed that the surge arresters, in general, were developed with 4 columns of class 5 varistors, thus, aiming at obtaining much higher protection characteristics, with higher safety margins.

Evaluating said solutions, and the requirements set forth for the system proposed in Brazil, we chose to propose a prototype surge arrester with intermediate electrical characteristics between: a) the solution with only one class 5 column (which this project proved to be inadequate, requiring higher supportability levels for the substation equipment); and b) the Chinese and Indian proposal. The comparison presented in Table A17.1, below, with values in p.u. for the rated voltage of the surge arresters, illustrates the protection levels proposed for the prototype.

Table A17.1: Values proposed for the electric performance of the surge arrester

Estimated protection level values of the surge arresters (U_R pu)			
Atmospheric surge		**Switching surge**	
Relation between Ures at 20 kA/U_R		Relation between Ures at 2 kA/U_R	
Projection: 1 column class 5	2.38	Projection: 1 column class 5	1.984
Indian	2.00	Indian	1.765
Chinese	1.96	Chinese	1.763
Balestro's proposal: 6 columns class 3	2.17	Balestro's proposal: 6 columns class 3	1.845

For this project, we aimed at making feasible times and costs in obtaining a viable concept prototype, in order to meet the deadlines defined in the project. Therefore, naturally, we would need to use technology already existing in Brazil. Thus, the project has the following characteristics that make it different and innovative related to the compared proposals:

- Manufacturing using electrical modules of the class 3 surge arrester, already developed and being regularly offered in the market, designed with 6 columns in parallel;
- Use of polymeric insulation, a solution more in tune with the future;
- Open concept electromechanical design (the columns do not share heat);
- Optimized electrical values, defined by the supportability of the equipment, aiming at an intermediate alternative regarding the initial concept.

Based on these assumptions, the design of the prototype surge arrester is illustrated in Figure A17.1.

Figure A17.1: Illustration and photo of the project prototype surge arrester

In the building of a surge arrester with this configuration, some aspects deserve special attention, since they are object of intense work:

- The asymmetry of voltage distribution along the length of the height of the surge arrester should be controlled by capacitive equalization elements. In the case of this project, all the compensation is external to the surge arrester, resulting in the intricate ring geometry seen in Figure A17.1.
- The current distribution between columns was assumed with maximum asymmetry of ±10 %, as project goal. Special attention was dedicated to the asymmetry in the region of the switching surge currents, since the highest electrical demands this surge arrester will be subject to in operation occurring in switching surges, therefore, in temporary overvoltage conditions, as confirmed by the electrical studies in this project.

According to a recent publication at CIGRÉ level, the transmission systems at U_M = 1,100 kV AC will demand from the surge arresters a thermal energy absorption capacity, W_{TH}, higher than the current class 5 of transmission lines discharge, remembering that the line discharge classes are a concept in extinction in the new edition of the IEC 60099-4 standard. The class 5 surge arresters dissipate on average 15 kJ/kV of emergency U_R, and are normally used in AC systems up to 765 kV. However, the mentioned article points to specific thermal energies between 25 kJ/kV and 50 kJ/kV of U_R.

Thus, considering the above-mentioned asymmetries of the project, and in conformity with the IEC 60099-4 standard, the guaranteed characteristics of this surge arrester are:

- Repetitive load transfer capacity Q_{RS} = 6.8 C;
- Maximum rated thermal energy W_{TH} = 39 kJ/kV of U_R;
- Supportability to short-circuit I_{SC} = 63 kA.

The specific thermal energy above, which considers the asymmetries, proved to be adequate in the simulations performed during the transient studies of the proposed transmission system, with the surge arresters having dissipated maximum energy of 11.39 MJ in the worst transient situation evaluated (unsuccessful three-pole reclosing after the occurrence of load rejection, and single-phase short-circuit).

The specific thermal energy dissipated in the surge arrester reached 13.76 kJ/kV of U_R, approximately 35% of its maximum capacity, thus, properly sized.

17.3 Manufacturing

To ensure compliance with the above-mentioned requirements, a detailed electric control was performed in the 1,020 ZnO varistors, manufactured by Balestro for building the prototype. The electrical characterization included an additional stage in the routine electrical testing, to properly select these varistors. A statistic distribution criterion was applied to the electrical values to identify those that could operate in parallel, complying with the established current and energy asymmetry criteria.

Mathematical studies of the validity of varistor selection were implemented in ATP, and showed an even better distribution than the one defined as goal, as illustrated in Figure A17.2. In this simulation, the electric performance of six columns of U_R = 30 kV in parallel was evaluated, with the varistors as used in the actual manufacturing.

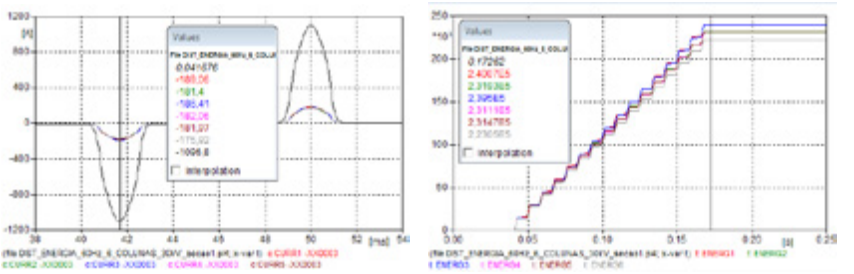

Figure A17.2: Asymmetries of currents in power frequency overvoltage between 6 columns, and respective energies per columns, values according to Table 3, total current = 1,097 Apk

Table A17.2: Asymmetries of currents and energies U_R 30 kV, 6 columns in parallel

Module	1	2	3	4	5	6
Current (Ap)	189.09	181.4	186.41	182.06	181.97	175.92
Asymmetry over average (%)	3.42	-0.77	1.97	-0.41	-0.46	-3.77
Energy (J)	240,070	231,930	239,500	231,110	231,470	223,050
Percentage of the maximum (%)	100.03	96.64	99.79	96.30	96.45	92.94
∑ Energy (J)	240,070	472,000	711,500	942,610	1,174,080	1,397,130

17.4 Laboratory Tests

To validate the above-mentioned studies, some electrical tests were performed at the Cepel (Figure A17.3), in a pioneer work in Brazil, and a very good compliance between the values of routine trials and simulations was finally verified when confronted with the measured results.

Figure A17.3: UHV surge arrester testing arrangement, with power frequency

Illustrated here only as an example, the verification of current distribution between columns showed great conformance of results with equivalent simulation in ATP. The verification was performed in the lower electric section of the surge arrester, the rated voltage U_R of which is 90 kV.

The ATP model was fed with the electrical values obtained in the routine testing of the equivalent columns. The laboratory measurement was done directly under the columns, using the Marx current pulse generator, with 8/20 μs wave form, in an also unprecedented testing arrangement.

Figure A17.4 illustrates the pulse generator circuit implemented in the ATP, with the 6 columns of the electric section inserted with its routine testing electrical values.

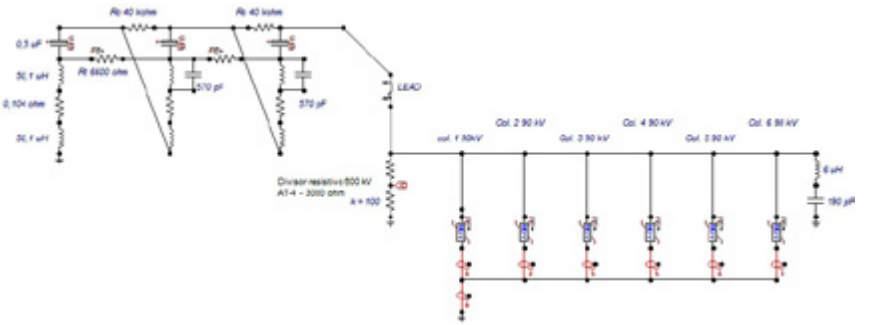

Figure A17.4: Pulse generator circuit implemented in the ATP

For a determined applied current impulse (total current of 4.65 kAp), the equivalent in the simulation is presented in Figure A17.5, resulting in a maximum asymmetry of these currents of +4.2% and -7.3% over the average value.

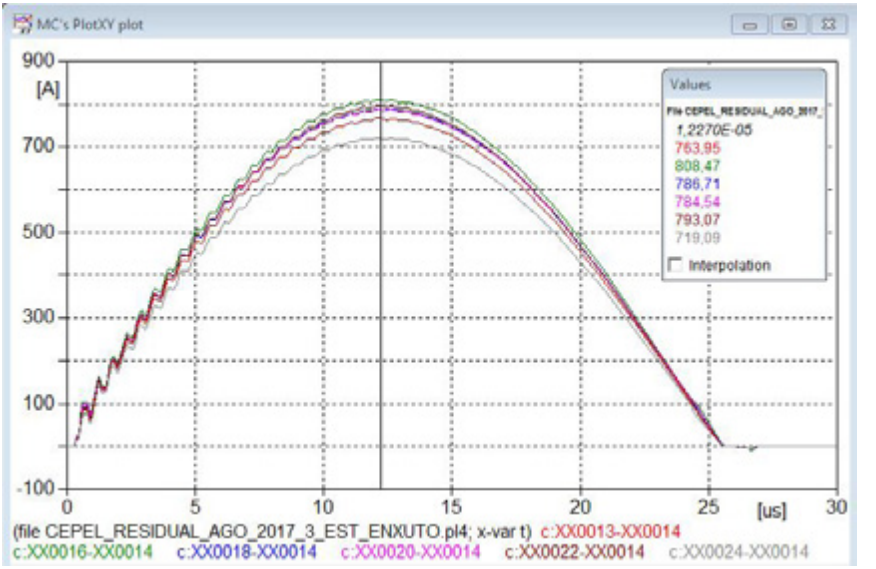

Figure A17.5: Asymmetry between the 6 columns currents for atmospheric impulse 8/20 μs, total current = 4.68 kAp, average current between columns = 776 Ap (simulation)

In the same situation, the values of this asymmetry calculated in the laboratory measurements were according to Table A17.3, and Figure A17.6 shows the currents measured, indicating great conformance with those of the simulation (Figure A17.5).

Table A17.3: Current asymmetry between columns measured in the Cepel.

Surge arrester column	I total kAp	I column Ap	I average Ap	Deviation %
1	4.68	782.34	781.52	0.10
2	4.68	802.56		2.69
3	4.68	797.20		0.73
4	4.68	766.10		-1.97
5	4.72	806.70		**3.22**
6	4.72	744.20		**-4.78**

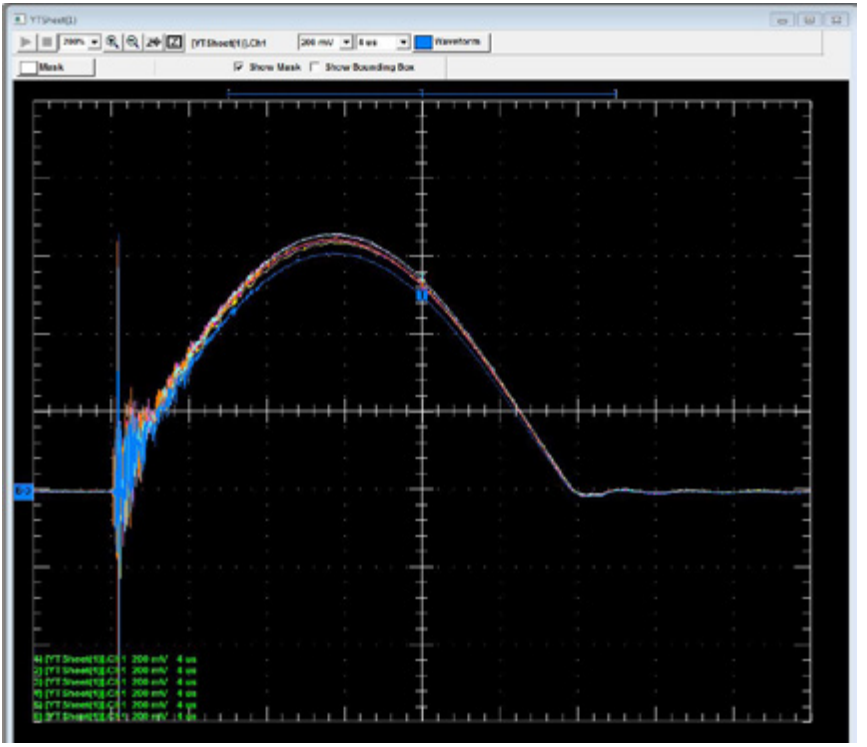

Figure A17.6: Record of the currents of all the columns measured in the Cepel

17.5 Polymeric Insulators for the 1,000 kV System

In this project, Balestro also manufactured prototypes of polymeric insulators with electrical characteristics deemed adequate to the working conditions in 1,000 kV AC transmission lines.

The initial basis for the sizing was the step indicated by the insulation coordination studies of the project, which recommended an equivalent string of 51 glass disks, therefore a step of 8,670 mm.

Such projection, when transferred to the project polymeric insulator, implies insulators with the following basic characteristics, assumed by projection:

- Insulator with arc distance of 7,670 mm.
- Atmospheric impulse withstand voltage, dry: 4,100 kVp.
- Power frequency withstand voltage, dry: 2,290 kV.
- Power frequency withstand voltage, under rain: 1,770 kV.
- Switching impulse withstand voltage, under rain: 1,950 kV.
- Creepage distance: 42,858 mm.

An initial view of the designed insulators is presented in Figure A17.7.

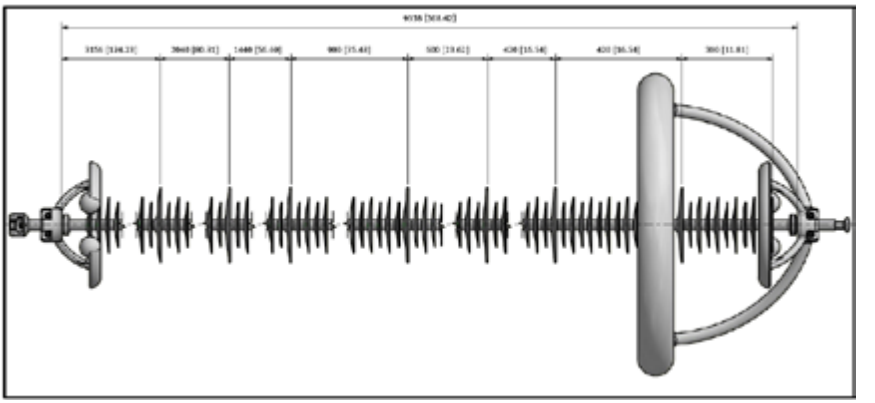

Figure A17.7: Illustration of one of the insulators for this project

Because there is currently an advanced stage in the development of the state-of-the-art in polymeric insulators for transmission systems, the main challenge of this project lies in the high operating voltage level and in its inherent difficulties.

Thus, following we present two topics of main importance and degree of difficulty in the design and manufacturing of these insulators.

17.6 Control of the Electric Field

As is generally known, the polymeric insulators must be provided of rings for control of the electric field, so as to prevent high stresses, especially in the region of the triple point, where the three materials that compose the insulator meet. The most severe concern is in the terminal of the energized side, and in the region up to the first sheds of this same side, regions that are naturally subjected to greater power gradients.

An effective control action of the superficial electric field in insulators of this magnitude, and for operating voltage levels at 1,000 kV, requires rings of large dimensions, and very distant from the triple point. Thus, in the draft in Figure A17.7, we can verify the use of combined equipotentiation and corona effect rings on the side of the phase, using the two ring configuration, to reduce the electric field gradient in the critical area of the insulator, and also mitigate the corona effect at the triple point (close to the line terminal fixing hardware). In Figures A17.8 and A17.9, we can observe the dimensions of the combined rings on the phase side, and a projection of their installation in the insulators.

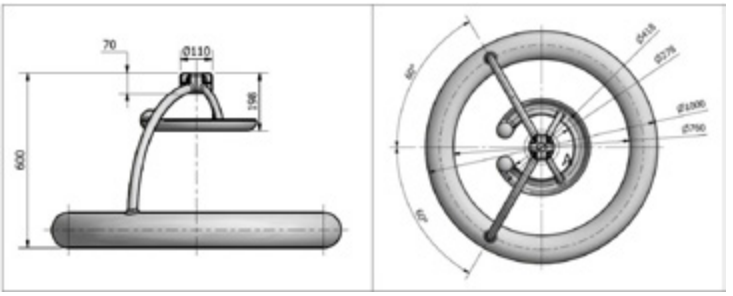

Figure A17.8: Dimensions of the combined rings used in this project

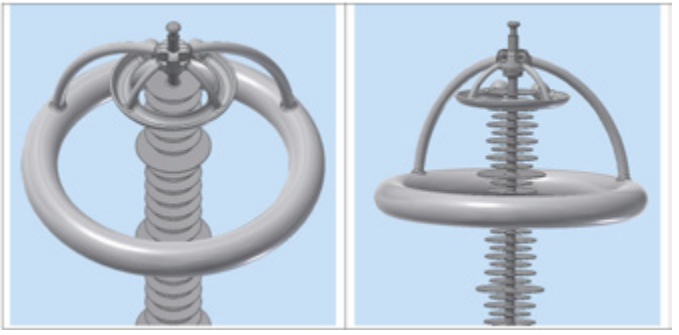

Figure A17.9: Projection of the installation of the rings combined in the insulator

17.7 Electrical Behavior under Rain

Taking as basis an insulator profile already in use in 500 kV systems, of rated mechanical load CMN = 240 kN, and adequate to pollution level "e" (very heavy, according to ABNT IEC/TS 60815-3), a prototype of this insulator was developed, which, due to its very long length, is the object of concern at this voltage level when positioned in the suspended installation position in "I."

It is important to emphasize that the project indicates medium pollution level along the route foreseen for the line (level "c" according to ABNT IEC/TS 60815-3), but chose its EAPX profile, already developed for CMN = 240 kN, so as to make feasible the manufacturing of the prototypes in during the duration of this project. The design of this profile is illustrated in Figure A17.10.

We also highlight that the objective of the prototype was its electrical characterization and sizing, since the electromechanical design of the line points to insulators of CMN = 420 kN, still under development by Balestro, therefore, this solution was chosen so as not to compromise the project deadlines.

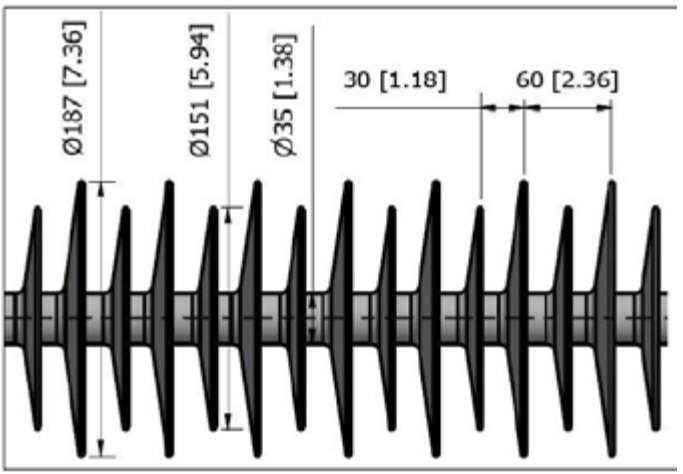

Figure A17.10: Configuration of the sheds in the EAPX profile

Adopting this profile for the insulator, the resulting leakage distance of 42,858 mm represents a specific leakage distance (according to ABNT/IEC 60815-3):

$$specific\ leakage\ distance = \frac{leakage\ distance}{system\ maximum\ voltage/\sqrt{3}}$$

Thus, we have:

$$specific\ leakage\ distance_{profileEAPX} = \frac{42{,}858}{1.1 \cdot 1{,}000 / \sqrt{3}} = 67.48 \text{mm / kV}$$

Although the concern with pollution level is not a relevant factor in face of all that was presented above, a rising concern is associated to the momentary reduction of the electric performance of insulators installed in vertical position in conditions of intense rains [29][30].

In the insulators under study of great length in vertical position, a standardized incident rain produces a flow of water to the edges of the sheds, which from that edge precipitate vertically. Water precipitation from a shed joins the precipitation of the shed immediately below and, thus, successively until the last shed, which in the case of suspension insulators is the shed closest to the line power.

Thus, the volume of water running through the edges of the sheds is progressively increased in a way that, in the lower portion of the insulator closer to the phase terminal, the phenomenon of bridging of these fins, i.e., water bridges are formed, which form conductive branches in the lower regions of the insulators, and the longer the insulator, larger will be the "waterfall" formed in its lowest position.

In this condition, the preceptor arches (*streamers*) caused by the intense electric field applied begin to develop in higher portions of the insulating column height of the suspension insulators in "I", promoting the occurrence of flashover in voltage levels much lower than the dry condition. Studies conducted at Cepel combining intense rainfalls and the observation of electric activity with UV cameras (Daycor) show, visually, the large increase of electric activity associated with this phenomenon. Similarly, in this same condition, there is a drastic reduction of the supportability to switching surges under rain.

Aiming at mitigating this problem, this project presented insulators equipped with special larger diameter sheds, distributed along its length, as shown in Figure A17.11.

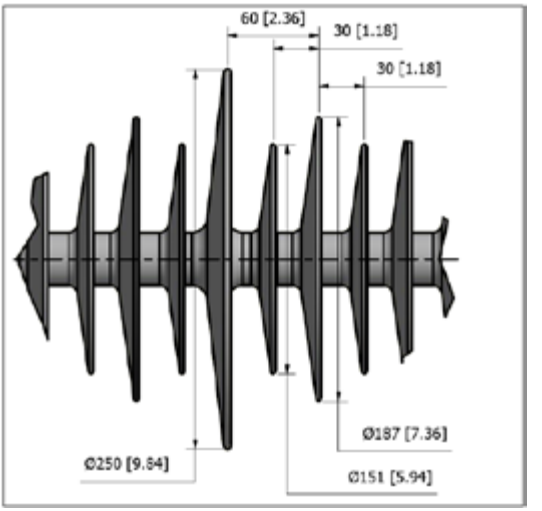

Figure A17.11: EAPX profile insulator with the inclusion of the special shed

These sheds, called "anti-rain sheds," are intended to spread the accumulated water, sending it away from the edges of the sheds in the portion immediately below them in a non-linear configuration along the length of the insulator; thus, the water that cumulatively flows around the edges of the sheds of an insulator section is projected further off-axis by the anti-rain sheds, and tends to disperse in drops until it reaches the anti-rain sheds further below.

Figure A17.12 shows the prototype insulators being manufactured, still prior to the application of special anti-rain sheds. In the 8670 mm step insulator, with 273 sheds (alternated according to Figure A17.10), 6 anti-rain sheds were applied.

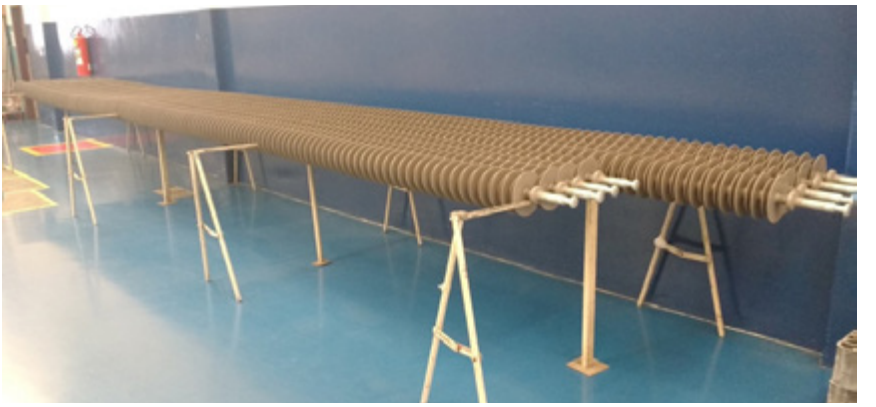

Figure A17.12: Insulator prototypes for the 1,000 kV AC during manufacturing

Figure A17.13 shows a ring manufactured and applied to an insulator during the routine tests in the factory.

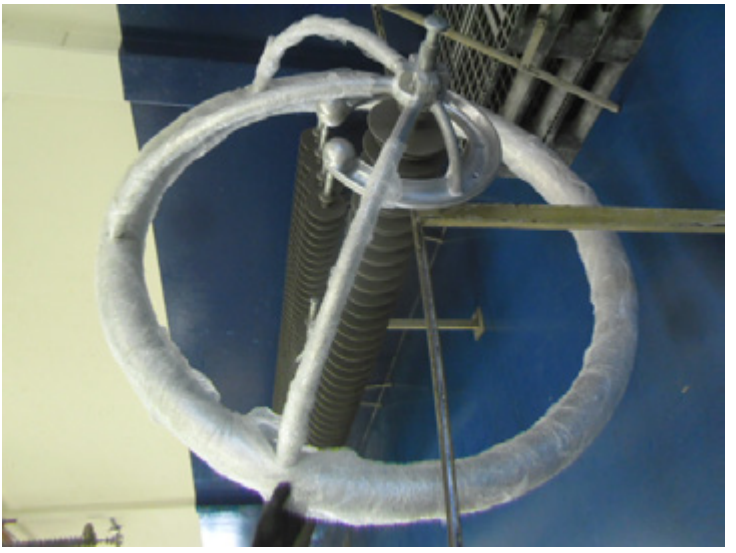

Figure A17.13: Experimental assembly of a ring in a prototype insulator

Balestro manufactured samples of the same insulator without the anti-rain sheds, so a comparison study can be conducted in laboratory. We verified that these isolators have electric supportability values that exceed the testing limits in the Cepel laboratory (AT-1).

ATTACHMENT 18 – Mechanical Design of the UHV Line

18.1 Objective

The objective of this present attachment is to present the loading hypotheses that will be used in determining the weight of the 1,000 kV structure, foundations, and the definition of the bases for the mechanical design.

18.2 General Data

18.2.1 Cables

The conductor used in this present study was of the CAA "Aluminum-Steel Cable" type, the characteristics of which are shown in Table A18.8.

The ground wire used in the calculations was of galvanized steel, 3/8" EAR, and its data is indicated in Table A18.1.

Table A18.1: Characteristics of the cables used

Description	MCM	795	∅ 3/8"
Code		Tern	
Type of cable		CAA	EAR
Rated diameter of the wire	mm	3.38-Al 2.25-steel	3.05
Number of wires	37 wires	45x7	7
Rated diameter of the cable	mm (")	27.03	9.52 (3/8)
Minimum failure load	kgf	10025	6990
Approximate weight	kgf/m	1.366	0.406

18.2.2 Tower

Table A18.2 presents the general characteristics of the basic tower.

Table A18.2: Characteristics of the basic tower

Tower type	Maximum spans (m)	
	Wind	Weight
Guyed/self-supporting	500	750

18.3 Reference Wind

For the purposes of calculation, we present the values referring to winds with return period of 250 years (10-min integration), which is ANEEL's requirement for lines with voltage higher than 230 kV.

Data from NBR 5422 were used to define the wind speed to be used in this present study: the alfa parameter (α) of the Gumbel distribution equal to 0.3 (m/s); and the beta parameter (β) of the Gumbel distribution equal to 11 m/s.

The wind speed value for the return period (T) of 250 years is obtained by the expression:

$$V_T = \beta - \frac{\ln\left[-\ln\left(1-\frac{1}{T}\right)\right]}{\alpha}$$

$$V_T = 29.4 \text{ m/s or } 105.8 \text{ km/h}$$

In face of the objective of this project, we will use as starting point the wind value equal to 105.8 km/h (integration period of 10 min, at 10 m from the ground).

18.4 Conditions Studied

Using the methodology of the IEC-60826 standard, we determined the wind loads and pressures in the various elements of the line.

Will be considered:

- Basic span: 500 m.
- Average altitude: 300 m.
- Return period: 250 years.

18.5 Loadings Due to Extreme Wind

18.5.1 Dynamic reference pressure

Following the IEC 60826 standard, we obtain:

$$q_0 = \left(\frac{1}{2}\right) \cdot VR^2 \cdot \mu$$

Where:
q_0 is the dynamic reference pressure, in kgf/m².
μ is the specific air mass: 1.1635 kgf/m³.
VR is the extreme wind speed, in m/s.
q_0 = 51.24 kgf/m².

18.5.2 Extreme wind pressure on the cables

According to the IEC 60826 standard, we obtain:

$$A_C = q_0 \cdot C_{XC} \cdot G_C \cdot G_L \cdot \mathrm{d} \cdot \mathrm{L} \cdot \sin^2\Omega$$

Where:
C_{XC} = 1.00
G_C is the combined wind factor for cables, obtained in the IEC 60826 standard as a function of the average height of the external conductor (33.6 m), or internal conductor (51.6 m), or ground wire (63 m), equal to 2.288 (external conductor), 2.448 (internal conductor), and 2.523 (ground wire).
G_L is the span factor as a function of the span adopted for calculation (500 m) equal to 0.9153.
d is the diameter.
L the length of the span.
Ω is the angle formed by the direction of the wind with the direction of the cables. For winds acting in the transverse direction (Ω = 90°), result in the following pressures:

- Pcond external = 107.3 kgf/m².
- Pcond internal = 114.8 kgf/m².
- Psurge arrester = 118.3 kgf/m².

18.5.3 Extreme wind pressure on the insulator strings

From the IEC 60826 standard, we obtain:

$$Ai = q_0 \cdot Cxi \cdot Gt \cdot Si$$

Where:
q_0 = see item 18.5.1
C_{xi} = 1.20.
G_t is the combined wind factor, obtained from the standard as a function of the heights.
Si is the area of the insulator string.
Resulting in:

- Pisol external conductor = 157.7 kgf/m².
- Pisol internal conductor = 161.1 kgf/m².

The summary of the values obtained in found in Table A18.3, below.

Table A18.3: Summary of wind pressure for speed with return time of 250 years

Phase	Proj. V	In the conductors		In the insulators		In the surge arresters	
	V_T	P_c(Pa)	P_c(kgf/m²)	P_{vi}(Pa)	P_{vi}(kgf/m²)	P_{PR}(Pa)	P_{PR}(kgf/m²)
External	29.40	1053	107.3	1546	157.7	1160.6	118.3
Internal	29.40	1126	114.8	1580	161.1		

Extreme wind pressure on the structures acting on the direction of the wind, from the IEC 60826 standard, we obtain:

$$A_t = q_0(1 + 0.2 \cdot sin^2 2\theta) \cdot (S_{t1} \cdot C_{xt1} \cdot cos^2\theta) + S_{t2} \cdot C_{xt2} \cdot sin^2\theta)\, G_t$$

Where:
G_t is the combined wind factor, obtained from of the IEC 60826 standard as a function of the height relative to the ground of the gravity center of the panel being considered.
S_{t1} and S_{t2} are the net areas of faces 1 and 2 do of the panel being considered, in m².
C_{xt1} and C_{xt2} are the drag coefficients of faces 1 and 2 of the panel being considered, obtained from of the IEC 60826 standard.
θ is the angle formed by the direction of the wind with the perpendicular to face 1, as per of the IEC standard.

Table A18.4: Summary of the pressure on the structure

θ	A_t (kgf)	Direction of the wind
0°	$51.24 \cdot G_t \cdot S_{t1} \cdot C_{xt1}$	Transverse wind
45°	$30.7 \cdot G_t \cdot S_{t1} \cdot C_{xt1}$	Wind at 45°

18.6 High Intensity Winds

There is no internationally accepted and standardized criterion for defining the wind speed resulting of electric storms (high intensity wind). In the absence of specific data about wind speeds during this type of storms, it has been customary to increase the extreme gust wind (t = 3 s) for the return period of the design by a factor close to 20%, with a narrow acting front. Thus, next, we will determine the high intensity wind for the return period of 250 years, to be adopted in the design.

Considering the extreme wind speed for the return period of T = 250 years, we obtain the following value for the high intensity wind (V_{ai}):

$$V_{ai} = 29.4 \cdot 1.39 \cdot 1.2 = 49.0 \text{ m/s or } 176.4 \text{ km/h}$$

The factor 1.39 is applied to the 10-minute wind to obtain the gust at 3 seconds.

18.6.1 Pressure of the high intensity wind on the cables and strings

Considering also that this type of wind has a very reduced front, acting on a maximum of 1/4 of the span, a wind pressure equal to 1/4 of the total pressure is considered on the conductor and the ground wire, acting evenly along the span.

Thus, the pressure of the high intensity wind on the conductor and ground wire will be equal to 37.5 kgf/m².

18.6.2 Pressure of the high intensity wind on the structures and strings

Dynamic reference pressure:

$$q_0 = 150 \text{ kgf/m}^2$$

For different θ values, we have on the structures:

Table A18.5: Summary of the pressure on the structures

θ	A_v (kgf)	Direction of the wind
0°	$150.0 \cdot S_{t1} \cdot C_{xt1}$	Transverse wind
45°	$90.0 (S_{t1} \cdot C_{xt1} + S_{t2} \cdot C_{xt2})$	Wind at 45°

For the strings the pressure is the reference pressure.

18.7 Tension on Cables and Sags

Following, we present the tensions and sags on the cables to be used in the various representative conditions.

Table A18.6: Tensions for the external conductor

Condition	θ (°C)	Wind pressure (kgf/m²)	Tf (kgf)	Tf (%)	Ti (kgf)	Final sag (m)
EDS	24	0	2005	20.0	2145	20.83
Vmax	20	107.3	4434	44.2	4542	22.54
V45	20	53.65	2889	28.8	3049	21.35
V_{ai90}	20	37.5	2493	24.9	2649	21.03
V_{ai45}	20	18.75	2152	21.5	2299	20.76
θmin	7	0	2080	20.7	2233	20.06
θmax	75	0	1819	18.1	1927	22.97

Tf – final tension; **Ti** – initial tension

Table A18.7: Tensions for the internal conductor

Condition	θ (°C)	Wind pressure (kgf/m²)	Tf (kgf)	Tf (%)	Ti (kgf)	Final sag (m)
EDS	24	0	2005	20.0	2145	20.83
Vmax	20	114.8	4656	46.4	4747	22.69
V45	20	57.4	2989	29.8	3149	21.42
V_{ai90}	20	37.5	2493	24.9	2649	21.02
V_{ai45}	20	18.75	2152	21.5	2299	20.75
θmin	7	0	2080	20.7	2233	20.06
θmax	75	0	1818	18.1	1927	22.96

Tf – final tension; **Ti** – initial tension

Table A18.8: Tensions on the ground wire 3/8 EHS

SW	θ (°C)	Wind pressure (kgf/m²)	Tf (kgf)	Tf (%)	Ground wire sag (m)	Fcond (m)
EDS	24	0	680	9.7	18.68	20.83
Vmax	20	107.3	1700	24.3	21.28	22.69
V45	20	53.65	1076	15.4	19.66	21.42
V_{ai90}	20	37.5	871	12.5	19.10	21.02
V_{ai45}	20	18.75	737	10.5	18.73	20.75
θmin	7	0	697	10.0	18.23	20.06
θmax	40	0	666	9.5	19.10	22.96

Tf – final tension; **Ti** – initial tension

The cables should be sized to withstand tension states – basic, and normal tension, defined based on the combination of climate and cable aging conditions as follows.

a) Basic state

- For minimum temperature conditions, the maximum axial tension must be limited to 33% of the cable failure tension.
- For wind conditions with the return period of 50 years, the maximum axial tension must be limited to 50% of the cable failure tension.
- For extreme wind conditions, the maximum axial tension must be limited to 70% of the cable failure tension.

b) Normal tension state (EDS everyday stress)

- In the final settlement, at average temperature, no wind, the average tension level of the cables must comply with the definitions in the NBR 5422 standard. Additionally, the average tension of the cables must be compatible with the mechanical performance with regards to the stress along the life period of the transmission line. The values of 20% was chosen for the conductor EDS, and of 9.7% for the surge arresters EDS.

18.8 Calculation of the Stress on the Towers

This item presents the general expressions for the calculation of the vertical, transverse, and horizontal stresses.

18.8.1 Vertical loads

$V = CS[(n \cdot g \cdot ag) + Pci]$ – Normal hypotheses.
$V = CS[(n \cdot g \cdot ag) + Pci + 0{,}3162 \cdot (Tc \cdot n)]$ – Hypotheses cables anchored to the ground.
$V = CS[(n \cdot g \cdot ag) + Pci] + CS1 \cdot CM$ – Assembly hypotheses.
CS is the coefficient used in the hypothesis.
n = number of subconductors per phase or surge arrester.
g = weight of the surge arrester or conductor cable.
ag = span weight.
Pci = weight of the insulator string.
Tc = tension of the surge arrester or conductor cable.
CS1= safety coefficient.
CM = load due to the fitters.

18.8.2 Transverse loads

$T = CS[(((n \cdot d \cdot av \cdot pvc) + (Aci \cdot pvi)) \cdot (sen2(i + a/2)))cos(a/2) + ((Acj/2) \cdot pvi) \cdot sen(i) + (2T \cdot n \cdot sen(a/2))]$ – Normal hypotheses with wind.
CS is the coefficient used in the hypothesis.
n = number of subconductors per phase or surge arrester.
d = diameter of the surge arrester or conductor cable.
av = wind span.
pvc = wind pressure on the surge arrester or conductor cable.
Aci = area exposed to the wind of the insulator string of the conductor or surge arrester.
pvi = wind pressure on the insulator string of the conductor or surge arrester.
a = line deflection angle.
i = wind incidence angle.
Acj = area exposed to the wind of the conductor jumper string.
T = tension of the surge arrester or conductor cable.

18.8.3 Longitudinal loads

$T = CS[(((n \cdot d \cdot av \cdot pvc) + (Aci \cdot pvi)) \cdot (sen^2(i + 90 + a/2))) \, sen(a/2) + ((Acj/2) \cdot pvi) \cdot cos(i + 90) + (T \cdot n \cdot cos(a/2))]$ – Normal hypotheses with wind.

18.9 Loading Trees

The following Figures present the illustrative loading trees referring to some of the hypotheses below, which were used in the calculations.

- EDS condition (predominant): E1 and E1R.
- Extreme transverse wind: V1 and V1R.
- Extreme oblique wind at 45°: V4 and V4R.
- Transverse electrical storm wind: W1 and W1R.
- Electrical storm wind at 45°: W3 and W3R.
- Rupture of 1 ground wire: R1 and R1R.
- Rupture of the external conductor cable bundle: R4 and R4R.
- Rupture of the internal conductor cable bundle: R5 and R5R.
- Cascade contention: D1 and D1R.
- Ground wire assembly: M1 and M2.
- Conductor assembly: M4 and M5.

The conditions above with termination in “R” are for hypotheses considering the minimum span weight.

Árvore de Carregamento

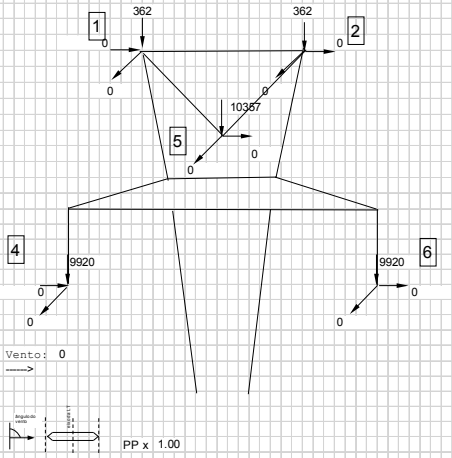

Deflexão / aplicação da Torre =			0	º
Pressão de Vento na torre [kgf/m2] :				
pvt(h) =		0		kgf/m²
Ângulo de incidência do vento:		i =	0	º
Pressão Vento [kgf/m2]	fase	P. Raio	Condut.	Isolador
	externa	118.30	107.30	157.70
	interna		114.80	161.10
Coeficientes de Segurança / Fator de Carga				
- Verticais	máximas			1.15
-	mínimas			0.90
- Transversais	máximas			1.00
-	mínimas			1.00
- Longitudinais	máximas			1.00
-	mínimas			1.00
Fator de resistência da torre:				0.930

Hipótese E1

EDS - Vertical Máxima

HVAC 1100 KV - 8 x TERN (ACSR 795 MCM)	ESTAIADA	Nº	0	Folha	1	de 27
	TORRE DE SUSPENSÃO	Revisão	2	Data	3/23/2016	

Árvore de Carregamento

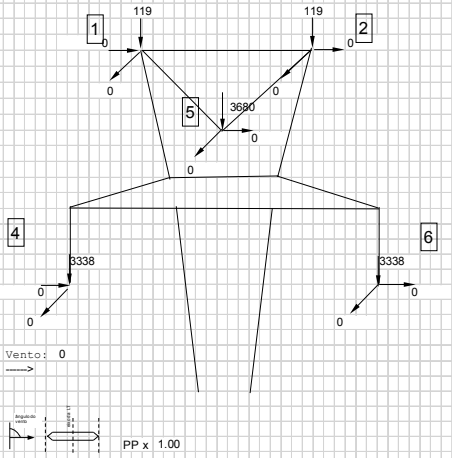

Deflexão / aplicação da Torre =			0	º
Pressão de Vento na torre [kgf/m2] :				
pvt(h) =		0		kgf/m²
Ângulo de incidência do vento:		i =	0	º
Pressão Vento [kgf/m2]	fase	P. Raio	Condut.	Isolador
	externa	118.30	107.30	157.70
	interna		114.80	161.10
Coeficientes de Segurança / Fator de Carga				
- Verticais	máximas			1.15
-	mínimas			0.90
- Transversais	máximas			1.00
-	mínimas			1.00
- Longitudinais	máximas			1.00
-	mínimas			1.00
Fator de resistência da torre:				0.930

Hipótese E1R

EDS - Vertical Mínima

HVAC 1100 KV - 8 x TERN (ACSR 795 MCM)	ESTAIADA	Nº	0	Folha	2	de 27
	TORRE DE SUSPENSÃO	Revisão	2	Data	3/23/2016	

Árvore de Carregamento

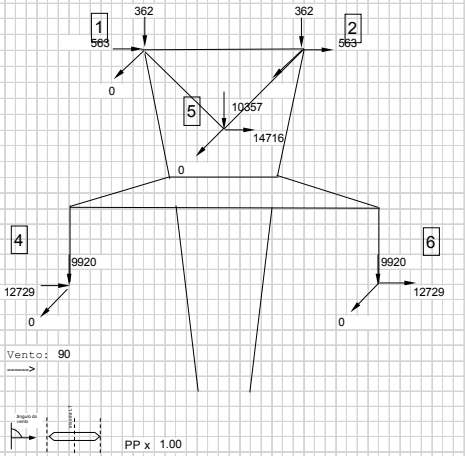

Deflexão / aplicação da Torre =			0	°
Pressão de Vento na torre [kgf/m2] :				
pvt(h) =	51,24*Gt(IEC)			kgf/m²
Ângulo de incidência do vento:		i =	90	°

Pressão Vento	fase	P. Raio	Condut.	Isolador
[kgf/m2]	externa	118.30	107.30	157.70
	interna		114.80	161.10

Coeficientes de Segurança / Fator de Carga		
- Verticais	máximas	1.15
-	mínimas	0.90
- Transversais	máximas	1.00
-	mínimas	1.00
- Longitudinais	máximas	1.00
-	mínimas	1.00
Fator de resistência da torre:		0.930

Hipótese	V1
Vento Extremo 90°	

HVAC 1100 KV - 8 x TERN (ACSR 795 MCM)	ESTAIADA	Nº	0	Folha	3	de 27
	TORRE DE SUSPENSÃO	Revisão	2	Data	3/23/2016	

Árvore de Carregamento

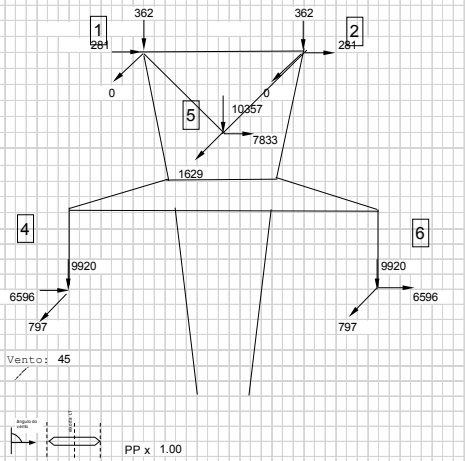

Deflexão / aplicação da Torre =			0	°
Pressão de Vento na torre [kgf/m2] :				
pvt(h) =	42,7*Gt(IEC)			kgf/m²
Ângulo de incidência do vento:		i =	45	°

Pressão Vento	fase	P. Raio	Condut.	Isolador
[kgf/m2]	externa	118.30	107.30	157.70
	interna		114.80	161.10

Coeficientes de Segurança / Fator de Carga		
- Verticais	máximas	1.15
-	mínimas	0.90
- Transversais	máximas	1.00
-	mínimas	1.00
- Longitudinais	máximas	1.00
-	mínimas	1.00
Fator de resistência da torre:		0.930

Hipótese	V4
Vento Extremo 45°	

HVAC 1100 KV - 8 x TERN (ACSR 795 MCM)	ESTAIADA	Nº	0	Folha	5	de 27
	TORRE DE SUSPENSÃO	Revisão	2	Data	3/23/2016	

Árvore de Carregamento

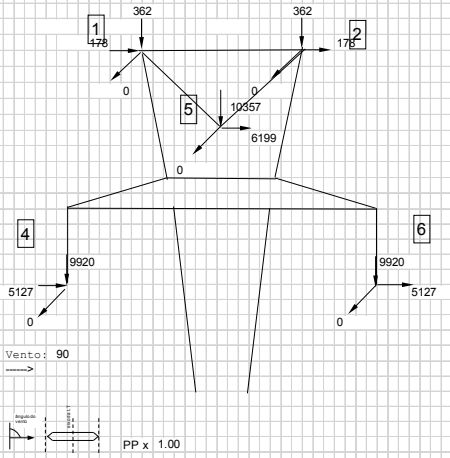

Deflexão / aplicação da Torre =	0	°
Pressão de Vento na torre [kgf/m2] :		
pvt(h) =	150	kgf/m²
Ângulo de incidência do vento:	i = 90	°

Pressão Vento	P. Raio	Condut.	Isolador
[kgf/m2]	37.50	37.50	150.00

Coeficientes de Segurança / Fator de Carga		
- Verticais	máximas	1.15
-	minimas	0.90
- Transversais	máximas	1.00
-	minimas	1.00
- Longitudinais	máximas	1.00
-	minimas	1.00
Fator de resistência da torre:		0.930

Hipótese W1

Vento de Alta Intensidade 90°

HVAC 1100 KV - 8 x TERN (ACSR 795 MCM)	ESTAIADA	Nº 0	Folha 7 de 27
	TORRE DE SUSPENSÃO	Revisão 2	Data 3/23/2016

Árvore de Carregamento

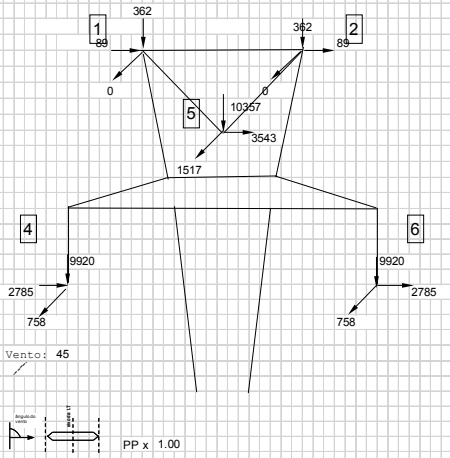

Deflexão / aplicação da Torre =	0	°
Pressão de Vento na torre [kgf/m2] :		
pvt(h) =	150	kgf/m²
Ângulo de incidência do vento:	i = 45	°

Pressão Vento	P. Raio	Condut.	Isolador
[kgf/m2]	37.50	37.50	150.00

Coeficientes de Segurança / Fator de Carga		
- Verticais	máximas	1.15
-	minimas	0.90
- Transversais	máximas	1.00
-	minimas	1.00
- Longitudinais	máximas	1.00
-	minimas	1.00
Fator de resistência da torre:		0.930

Hipótese W3

Vento de Alta Intensidade 45°

HVAC 1100 KV - 8 x TERN (ACSR 795 MCM)	ESTAIADA	Nº 0	Folha 9 de 27
	TORRE DE SUSPENSÃO	Revisão 2	Data 3/23/2016

Árvore de Carregamento

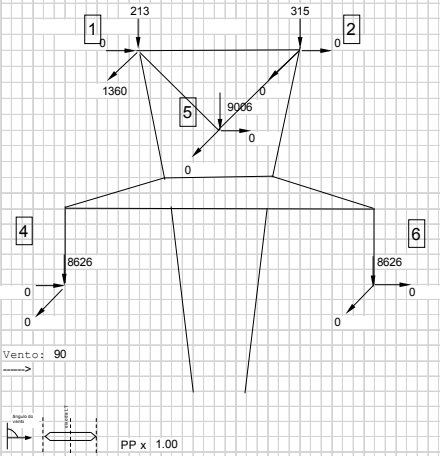

Deflexão / aplicação da Torre =	0	°
Pressão de Vento na torre [kgf/m2] :		
pvt(h) =	0	kgf/m²
Ângulo de incidência do vento:	i = 90	°

Pressão Vento [kgf/m2]	P. Raio	Condut.	Isolador
	0.00	0.00	0.00

Coeficientes de Segurança / Fator de Carga		
- Verticais	máximas	1.00
-	mínimas	0.90
- Transversais	máximas	1.00
-	mínimas	1.00
- Longitudinais	máximas	1.00
-	mínimas	1.00
Fator de resistência da torre:		1.000

Hipótese	R1
Rupt. Pr 1 s/ Vento	

HVAC 1100 KV - 8 x TERN (ACSR 795 MCM)	ESTAIADA	Nº 0	Folha 11 de 27
	TORRE DE SUSPENSÃO	Revisão 2	Data 3/23/2016

Árvore de Carregamento

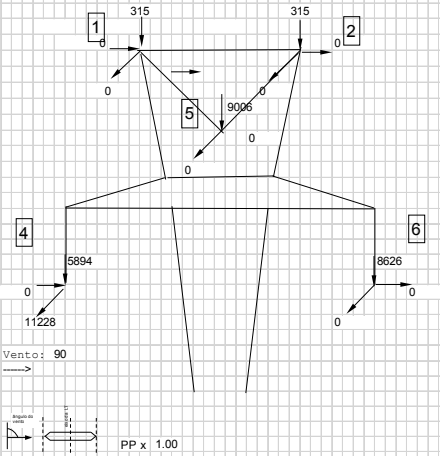

Deflexão / aplicação da Torre =	0	°
Pressão de Vento na torre [kgf/m2] :		
pvt(h) =	0	kgf/m²
Ângulo de incidência do vento:	i = 90	°

Pressão Vento [kgf/m2]	P. Raio	Condut.	Isolador
	0.00	0.00	0.00

Coeficientes de Segurança / Fator de Carga		
- Verticais	máximas	1.00
-	mínimas	0.90
- Transversais	máximas	1.00
-	mínimas	1.00
- Longitudinais	máximas	1.00
-	mínimas	1.00
Fator de resistência da torre:		1.000

Hipótese	R4
Rupt. Fase em 4 s/ Vento	

HVAC 1100 KV - 8 x TERN (ACSR 795 MCM)	ESTAIADA	Nº 0	Folha 15 de 27
	TORRE DE SUSPENSÃO	Revisão 2	Data 3/23/2016

CHAPTER 6

Socio-environmental Characterization and Analysis of the Project (R3)

Maíra Dzedzej
Alex da Silva Sousa
Mauricio George Miguel Jardini
Gerson Yukio Saiki

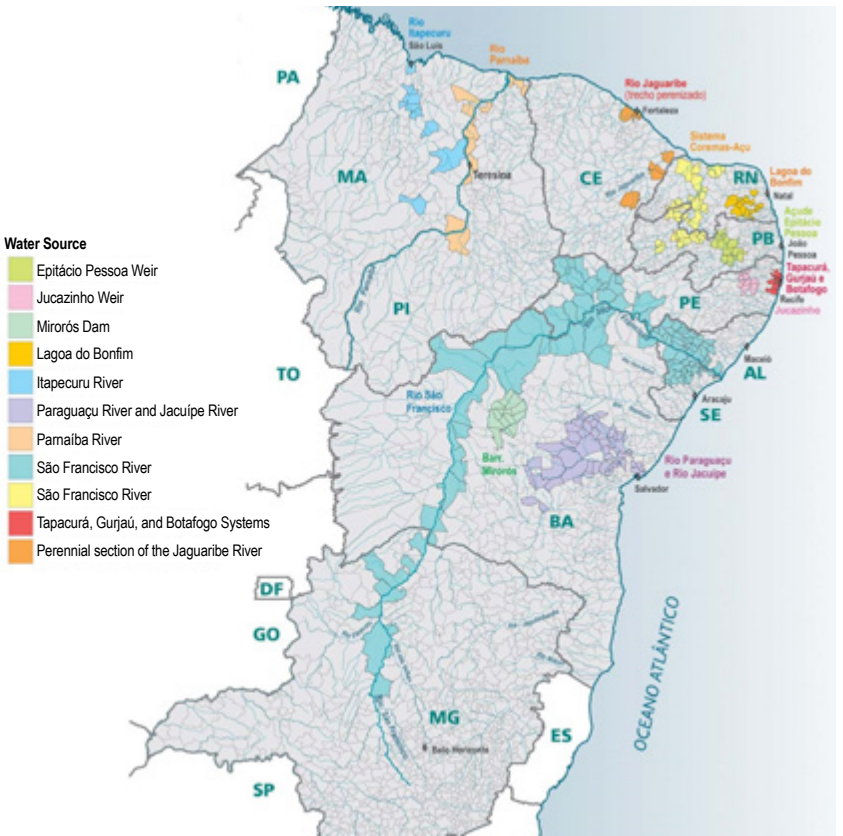

1. Introduction

The purpose of the R3 Report – Socio-environmental Characterization and Analysis of the Project – is to present the socio-environmental characteristics of the path corridor selected. This item presents the socio-environmental characteristics related to the physical, biotic, and socioeconomic environments in which the path corridor of the line between the substations of Milagres (Ceará), Ourolândia (Bahia), Igaporã (Bahia), and Pirapora (Minas Gerais) is inserted.

The scope includes the approximate length of the transmission line, the criteria for elaboration of the defined route, the foreseen crossings, and other information relevant to this characterization.

This chapter presents the socio-environmental characterization and analysis of the path corridor, as well as the preferred route proposed in the R3; it provides an analysis of the physical, biotic, and socioeconomic environments (Technical Note n. 0203/2013-SCT-SRT/ANEEL).

Thus, this item comprises the socio-environmental aspects and will be presented by section between the Substations, divided as follows:

- **Section 1 (T1)** – Milagres (Ceará) to Ourolândia (Bahia);
- **Section 2 (T2)** – Ourolândia (Bahia) to Igaporã (Bahia);
- **Section 3 (T3)** – Igaporã (Bahia) to Pirapora (Minas Gerais).

The total path formed by the three sections is located in the states of Ceará, Pernambuco, Bahia, and Minas Gerais, with the largest part located in Bahia and within the caatinga biome. Figure 1.1 illustrates the location of the substations and sections T1, T2, and T3.

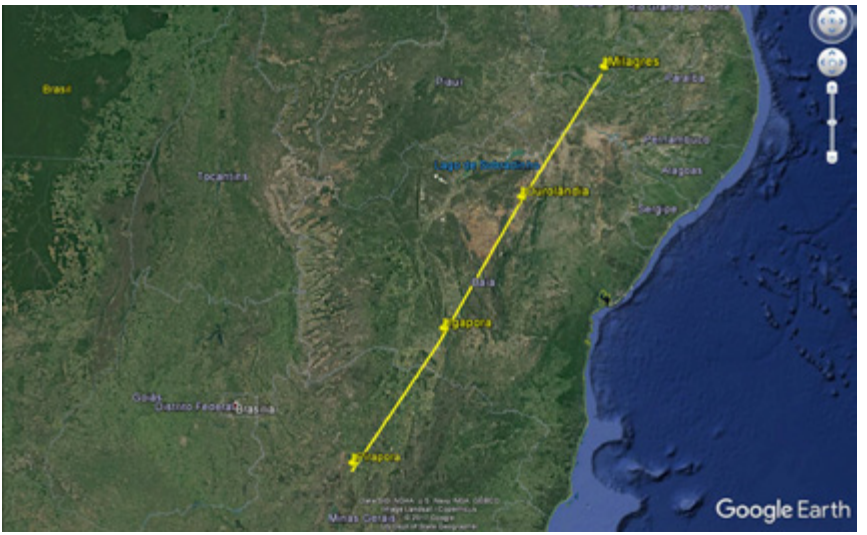

Figure 1.1: Location of the transmission line and substations

2. Justification

In this item, the objective is to present the elaboration of the socio-environmental analyses made for each of the sections of the transmission lines that connects the various substations and their respective corridors, which are 3 km wide.

For this, an analysis was carried out considering the variables of the physical, biotic, and socioeconomic environment, which together form the socio-environmental environment. The purpose of understanding it is describing the natural and anthropic interaction and dynamics in the project area, demonstrating the most and least fragile areas of the natural and anthropic environment, with regards to the implementation of projects of this magnitude.

The variables of the physical environment comprise of the components of Earth's natural systems, considering elements such as the climate, relief, geology, soils, and water resources.

With regards to the biotic environment, its variables comprise of the living beings and their presence on Earth, the use of the soil, vegetation, fauna, special ecosystems, and protected areas. The objective is to provide an overview of the biotic environment, the importance of which is demonstrated by the types of use, ecosystems, and protection areas existing in the project implementation area.

The analysis of the variables of the socioeconomic and cultural environment involves aspects related to the qualification of the predominant types of uses in the region, and of demographic, economic, cultural, and structural aspects. For this, information will be collected regarding the population, regional economy, road and power infrastructure, land property structure and conflict areas, Human Development Index (HDI), indigenous population, archaeological, geological, and cultural heritage. The purpose of this assessment is to demonstrate the land and economic uses existing in the area, and possible conflict areas for the implementation of the project.

Once the socio-environmental assessment is consolidated, the most and least sensitive areas according to various aspects are listed, and presented in the form of a map validated on-site.

This study is important because it provides a regional overview of the impacts and benefits the line will bring to the areas where it will be implemented, as well as a more adequate overview for the evaluation of the actual costs of the project.

With the possible implementation of this new and modern line structure, it will be possible to establish a more efficient integration of the Northeastern and Southeastern power poles, making the SIN (Brazilian Interconnected Power System) more dynamic and stable for these regions, and the economic development of these areas more promising.

The line will allow for improving the integration of the wind farms in the Northeastern region, thus, transferring the power to areas where there is demand for it, and also improving the infrastructure of a region that lacks investments, so that conditions for heating the economy are created.

3. General Characterization of the Project Area

The area of implementation of the line crosses great part of the Brazilian semiarid area, and stretches of the north mesoregion of Minas Gerais, which coincides with the limits of the semiarid in some portions. The semiarid region (Figure 3.1) is inserted in nine Brazilian states, eight of which are in the Northeastern region. These states are: Ceará, Piauí, Rio Grande do Norte, Paraíba, Pernambuco, Alagoas, Sergipe, and Bahia, and also the state of Minas Gerais, in the Southeastern region of Brazil.

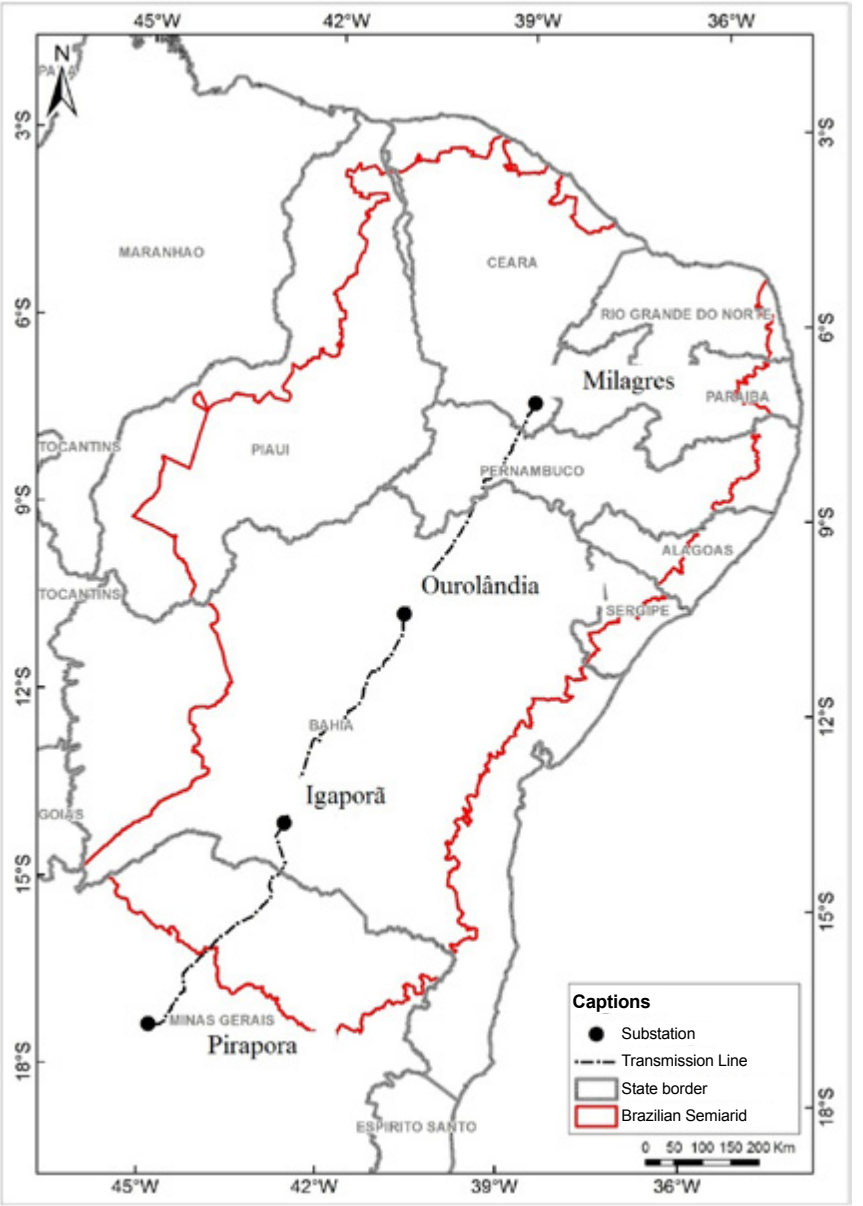

Figure 3.1: Limits of the brazilian semiarid area. Source: Sudene, 2016

According to Sudene (2016), the characteristics of the physical environment of the semiarid are: annual rainfalls lower than 800 mm; high average hours of sunshine per year; annual average temperatures between 23 °C and 27 °C; seasonal rains; predominance of the caatinga; poor soils in terms of organic matter, predominantly sandy and litholic; predominantly crystalline substrate, with portions of clastic rocks; large number of intermittent rivers, and groundwater associated with sedimentary basins.

In socioeconomic terms, the semiarid (Sudene, 2016) is characterized for composing 57.53% of the Northeastern region territory, and concentrating 40.54% of its population, and despite that, being responsible for only 21.6% of its GDP. It is an underdeveloped region, with low population density and stagnant economy that presents subsistence family agriculture, and extensive livestock farming as predominant activities.

Along the area which the line will cross, there are settlements, quilombolic and indigenous lands, as well as caves, geological sites, and archaeological sites, so these areas must be detailed, aiming at their preservation when of line implementation.

The availability of water resources insufficient for the existing demand, the climate severity, where the occurrence of desertification processes and low nutrient soils are common, are factors that hinder the adequate development of the region. Variables like these are responsible for factors such as low population density, which in the 70's was of 12.4 people/km² and in 2000 went to 21.6 people/km².

4. Procedures and Research Source

Two levels of socio-environmental analyses were made aiming at identifying and evaluating the elements of the physical, biotic, and socioeconomic environments that might interfere in the line facilities, and/or be affected by the impacts caused by this project, configuring socio-environmental factors that hinder or prevent the implementation of the project. The first level consists of a general diagnostic of the physical, biotic, and socioeconomic environments of the area of the path, in the context of the Brazilian semiarid area, and mesoregion north of Minas Gerais, where the path will be inserted.

The second level represents a qualitative and quantitative socio-environmental analysis of each section of the path and their respective 30 km wide corridor paths, and the preferred route for line installation. This more detailed characterization was based on the spatial analysis of official secondary data, and on the data collected and validated in the field, by means of a Geographic Information System (GIS). Several socio-environmental indicators were considered in the characterization of each section of the path. These indicators were built based on the spatial analysis of official secondary data, and interpreted based on multidisciplinary knowledge. The width of the path for detailing of the results is of 30 km, 15 km to each side from the central axis of the corridor, and the preferred route for installing the line is inserted in this corridor. The results obtained are presented by means of maps and descriptive texts.

To elaborate the socio-environmental characterization we used secondary data from official state and federal sources, such as the CPTEC/Inpe (Center for Weather Forecasting and Climate Studies) for climatological information; the Brazilian Geological Survey (CPRM) to obtain Geological and Geomorphologic data; Brazilian Institute of Geography and Statistics (IBGE) for socioeconomic, physical, and biotic data; Brazilian Agricultural Research Corporation (Embrapa) for soil data; National Water Agency (ANA) for the assessment of water resources and water uses; Chico Mendes Institute for Biodiversity Conservation (ICMBio) and Project for the Conservation and Sustainable Use of Brazilian Biological Diversity (Probio) for data related to the protected areas; National Institute of Colonization and Agrarian Reform (INCRA) for data regarding the quilombolic communities and settlements, and the Pastoral Land Commission's (CPT) Land Conflicts Report; Brazilian National Indian Foundation (Funai) for data on indigenous reserves; Institute of National Historical and Artistic Heritage (Iphan) for data on archeological sites; the National Center for Research and Conservation of Caves (Cecav) for the information on caves; and the Brazilian Commission of Geological and Paleobiological Sites (Sigep) for information on paleontological and geological sites in general. Also researched were the EEZs (Ecological Economic Zoning) of the states involved.

Data from bibliographic surveys made on academic articles and publications was also used. To help in the analysis, images from the Landsat 8 made available by the for free U.S. Geological Survey (USGS) will be used.

5. Socio-environmental Characterization

Next are described elements of the physical, biotic, and socioeconomic environments, considering aspects related to the characteristics of the physical environment, terrestrial ecosystems, indigenous and traditional populations, population density, and urban concentrations. This diagnosis supports the project location and socio-environmental feasibility analysis through the identification of sustainability indicators for the corridor, delimiting areas of greater and lesser socio-environmental sensitivity.

5.1 Physical Environment

The physical environment comprises the variables that compose the Earth's natural systems. It takes into consideration elements such as the climate, relief, geology, soils, and water resources. Understanding it is important because it demonstrates the natural interaction and dynamics that exist in the environment to be analyzed. Its description in this project is important because it demonstrates the most fragile and least fragile areas of the natural environment in the project implementation area.

5.1.1 Climatology

The project implementation area is inserted mainly in the semiarid region, where the Ministry of the Environment (MMA) develops a series of projects via the Superintendence for the Development of the Northeast (Sudene).

It is an area where droughts are frequent, and which is characterized by the following climatic factors (Sudene, 2016):

- Average annual rainfall equal to or lower than 800 mm;
- Average hours of sunshine 2,800 h/year;
- Average annual temperatures 23 ºC to 27 ºC;
- Rain regimen marked by irregularity (space / time).

To meet the project needs, the available climatic normal information was researched. The climatic normal is obtained by means of the averages of a series of 30 years of climatological surveys. The Inmet has generated a

series of mappings based on the information generated from the climatic normal for the period of 1961-1990. Next, is presented a characterization of the project area based on this information.

The line will be implemented mostly on semiarid domain area, in a transect that crosses the states of Ceará, Pernambuco, Bahia, and Minas Gerais. As can be observed, Figure 5.1 presents the intensity of winds at a height of 10 meters. The area referring to Section 1 is under medium to high intensity winds. Section 2 crosses an area where the average wind speeds are lower. Section 3 will cross areas of medium to high intensity winds.

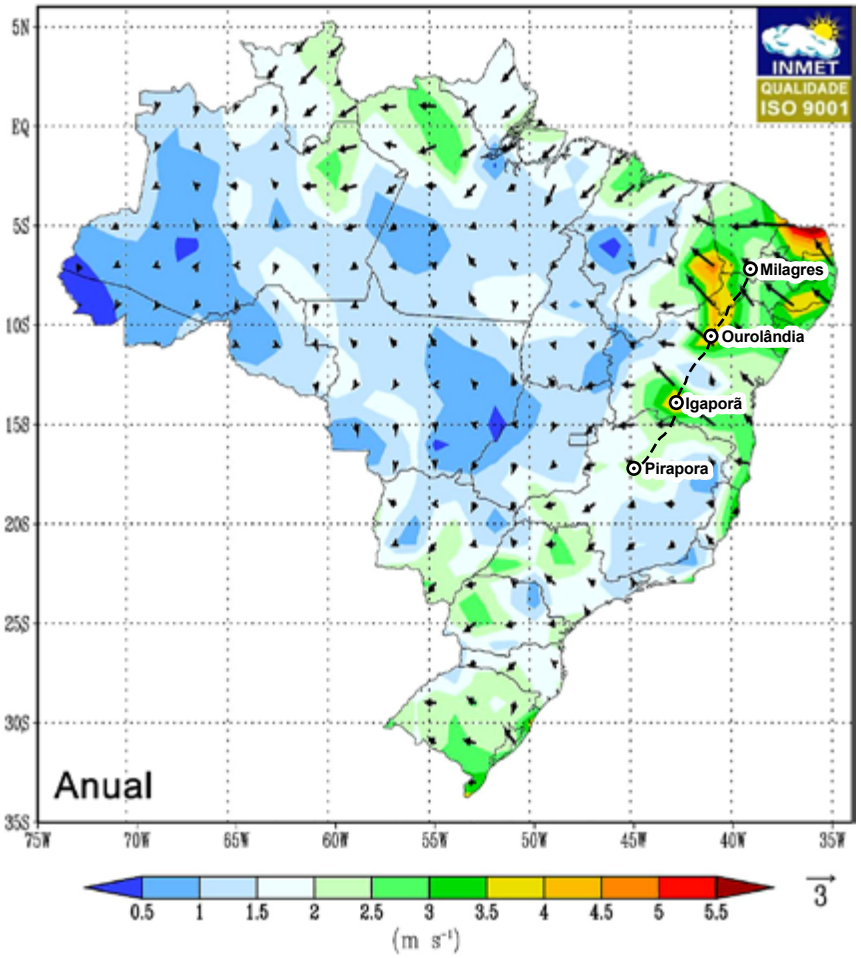

Figure 5.1: Climatic normal (1961-1990) for winds at a height of 10 meters.
Source: adapted from Inmet, 2016

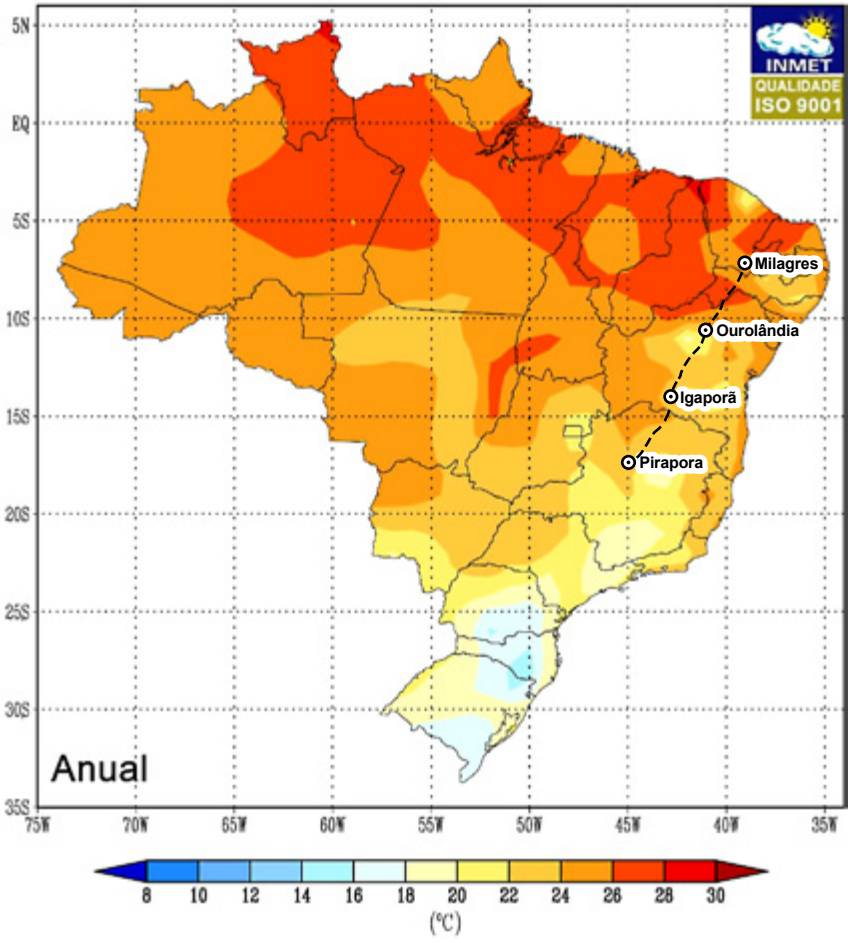

Figure 5.2: Temperature compensated average (ºC) for 1961-1990.
Source: adapted from Inmet, 2016

Temperature presented higher averages in the area of section 1, with milder values in section 2, and in section 3, values slightly higher than in section 2, but lower than in section 1.

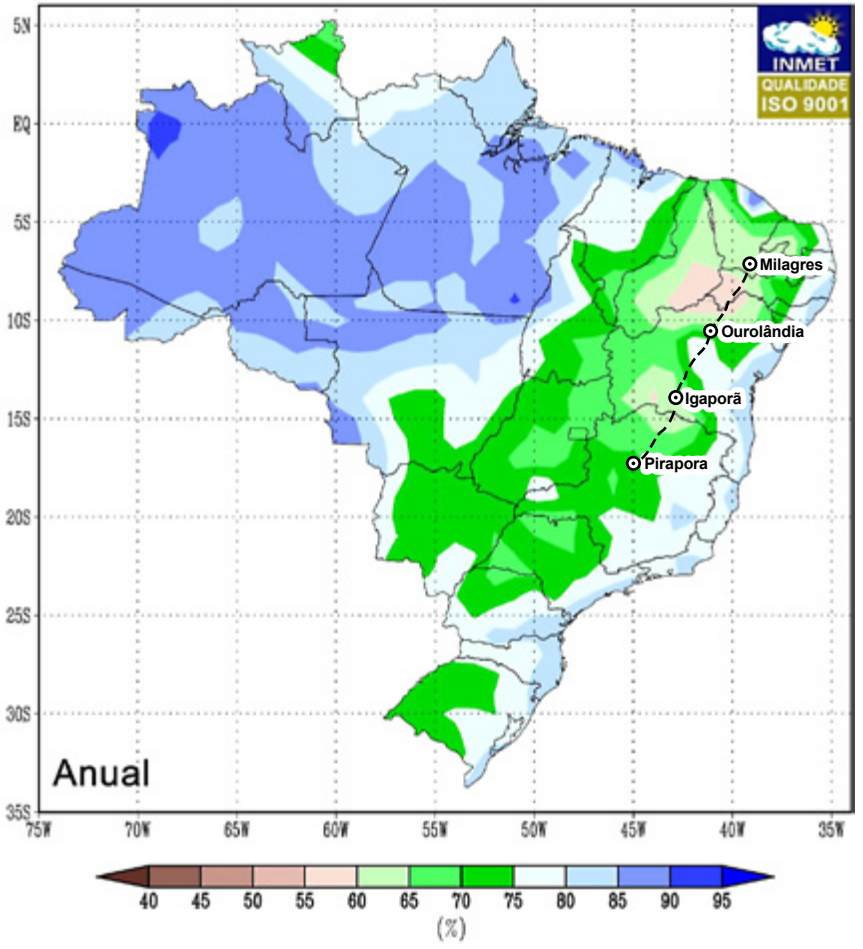

Figure 5.3: Compensated relative humidity (%) for 1961-1990.
Source: adapted from Inmet, 2016

Relative humidity (Figure 5.3) in the project area, in percentages, is significantly reduced in the area of section 1, increases a little in portions of section 2, and drops again in the area of section 3, but still remaining higher than in section 1.

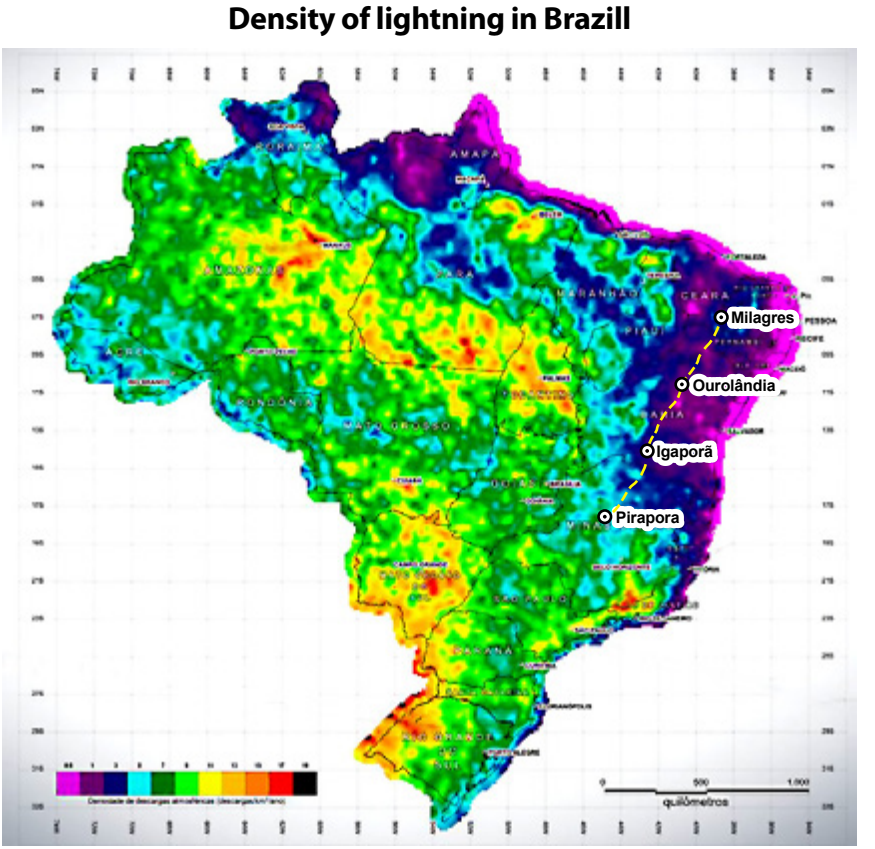

Figure 5.4: Density of lightning in Brazil. Source: adapted from CPTEC, 2016

The line area presents the lowest values for density of lightning in Brazil (Figure 5.4), mainly in section 2 of the project.

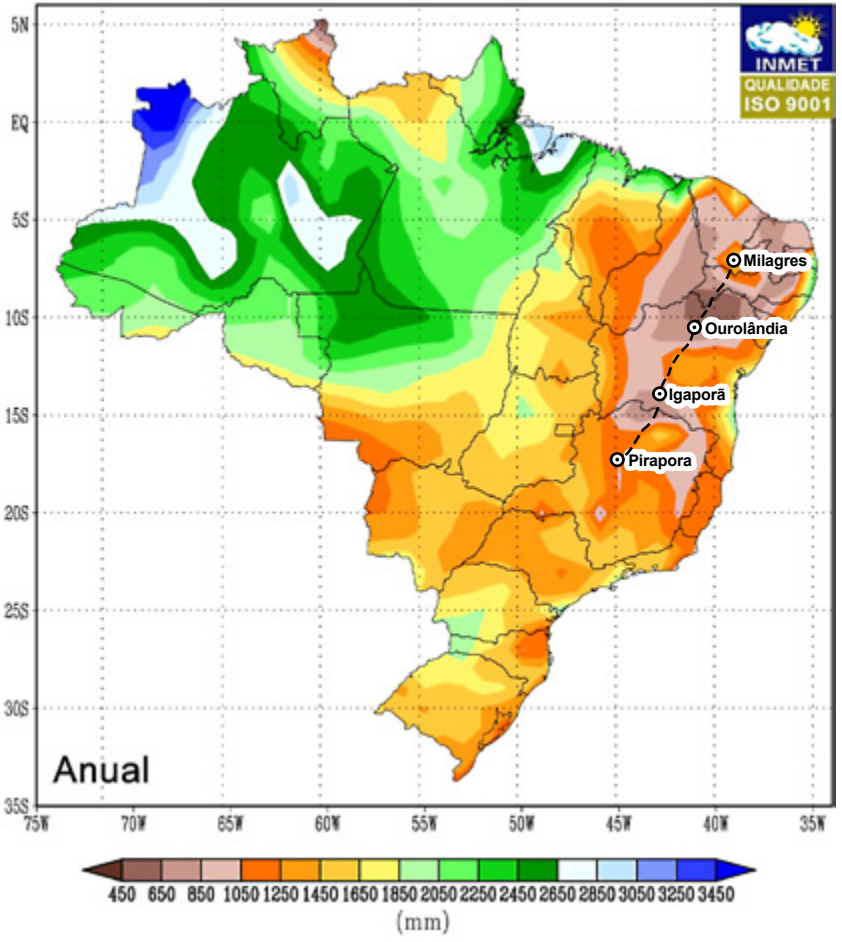

Figure 5.5: Monthly and annual accumulated precipitation (mm) for 1961-1990.
Source: adapted from Inmet, 2016

As it is located in the semiarid region, rainfall in the project implementation area (Figure 5.5) is lower when compared to the rest of the Brazilian territory. The smallest number of millimeters of rain is concentrated in the area of section 1, with areas with less than 450 mm/year. Section 2 presents a portion where the index is a little higher, and section 3 presents a decrease in the average annual precipitation volumes, although it does not decrease as much as in section 1.

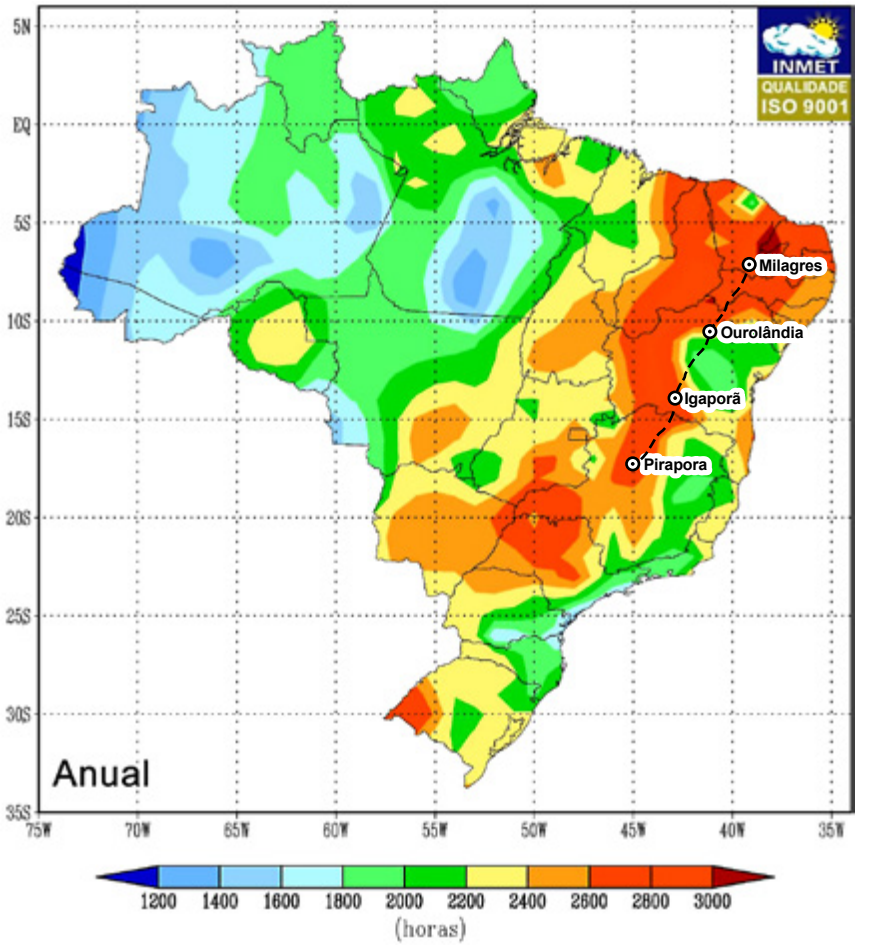

Figure 5.6: Total hours of sunshine (hours) for 1961-1990. Source: Inmet, 2016

Regarding hours of sunshine, most of the project area is located in territories with high incidence of total hours of sunshine (Figure 5.6), with the most significant territories located in sections 1 and 3.

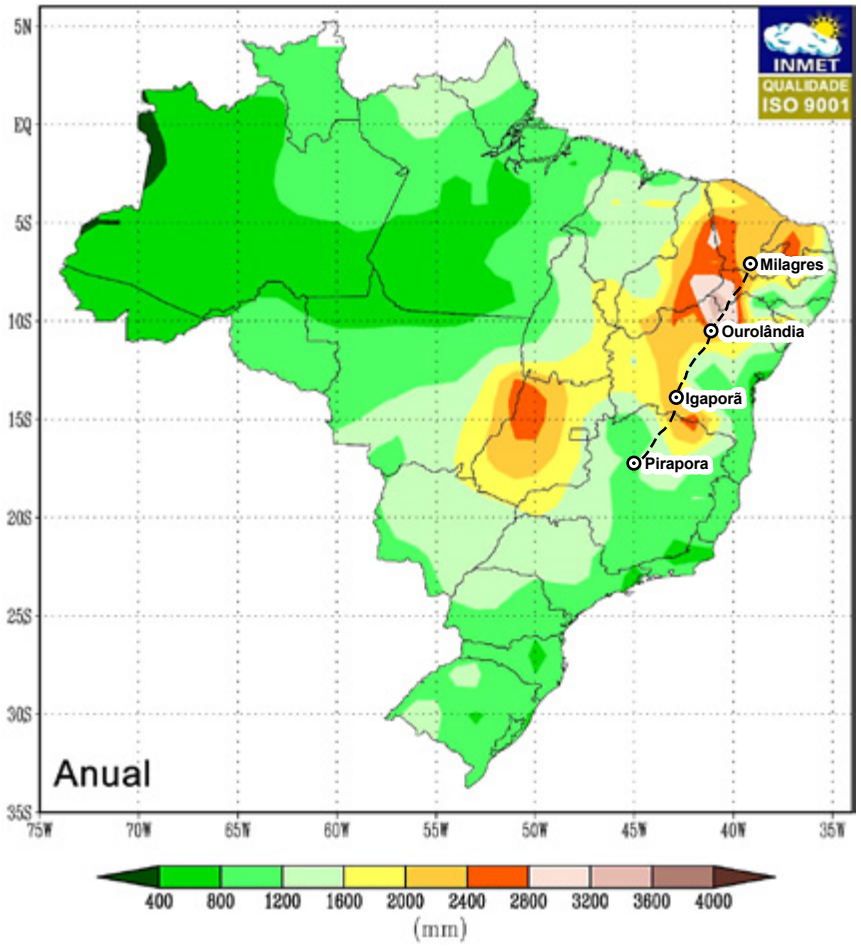

Figure 5.7: Total evaporation (mm) for 1961-1990. Source: adapted from Inmet, 2016

The line implementation area presents the highest rate of total evaporation of the Brazilian territory in the normal climatic period (Figure 5.7). The portion that presents the highest evaporation rate is the area of section 1. Next, we have the area of section 3, with total evaporation a little lower and, finally, the area of section 2 with a portion of the territory presenting values closer to the national average.

5.1.2 Geomorphology/Geology/Mining Resources/Geotechnics

The region presents a predominance of crystalline basement rocks, such as granitoids and metamorphic rocks of different degrees of metamorphism. There are portions of areas with clastic basement, with occurrence of caves, mainly in the central area of the state of Bahia, and the north of the state of Minas Gerais. These are clastic sedimentary rocks that give rise to caves, so these are areas that require greater attention. There are also sandstones, sometimes metamorphosed, and siltstone.

The relief of Section 1 is composed mainly of Planation Surfaces, which is a type of relief eroded by erosive processes of preferably flat areas, and that sometimes present residual reliefs in the form of hills and mountain alignments of varied altitude composed of more resistant rocks, such as granitoids and rocks of high metamorphism.

Section 2 presents compartmentation of tablelands, low plateaus and plateaus, with predominance of hills and mountain alignments. In its most northern portion, the predominant basement is sedimentary with clastic, silty, and clayey terrains presenting a more flattened relief, with some more elevated residual soil supported by more resistant lithology. We highlight the presence of Parque Estadual do Morro do Chapéu with a more irregular relief. The portion more to the south presents crystalline basement with igneous and metamorphic rocks, and a relief composed of hills and mountain alignments, thus presenting an area with greater natural obstacles for the implementation of the line.

Section 3 presents areas with tablelands, planation surfaces, and environments with more hills, with a variety of lithological metamorphic and sedimentary material. It presents areas with a more flattened relief, and areas with a more irregular relief, with differences in altitude level related to the lithological diversity.

In general, the project implementation area is located in areas with certain ecodynamic stability, that is, the predominance is of pedogenic processes, which make the environment more stable in general.

The library of relief patterns, elaborated by Dantas (2016), contains the definitions for this relief compartments found in the area of study, which will be presented in this work so as to better geomorphologically characterize the project area.

The tablelands are degradation reliefs in sedimentary rocks. They present slightly dissected form with flat and elongated tops, as well as rectilinear slopes associated to U-shaped valleys between hills, due to recent river dissection. These are areas where pedogenesis predominates.

Low plateaus, as well as tablelands, are degradation reliefs in sedimentary rocks. These are surfaces higher than the surrounding soils and little dissected in tabular form. They present a main drainage system with weak weathering and predominance of pedogenic processes.

Tablelands and plateaus, or elevated surfaces, are degradation reliefs in sedimentary rocks, which may be presented as elevated tabular surfaces, or elevated flat or flattened and slightly dissected reliefs. Their ridge areas are positioned at high altitudes, delimited by steep to precipitous slopes. Predominance of pedogenesis processes with thick and well drained soils, and significant morphogenesis processes on the ridges of the erosive escarpments, through the lateral retreat of the slopes.

Flattened surfaces are flat to slightly undulated, without being wide enough to constitute hills, developed by the general leveling of the lands, being a representation of great extensions of the interplanaltic depressions of the Brazilian territory. As these are very flat surfaces, there is a predominance of pedogenic processes with shallow and rocky soils.

Inselbergs and other residual reliefs are the isolated peaks, residual hills, pontoons, monoliths, low amplitude and small extension mountain alignments. These are residual reliefs characterized by presenting greater resistance to the erosion processes, thus, standing out in the landscape.

Degraded escarpments, structural steps, and erosive ridges are reliefs consisting of predominantly rectilinear to concave slopes, sloping and slightly rounded tops. It is common for them to contain sedimentation of colluvium and talus deposits. The drainage system is more active in these areas, causing the weathering of the slopes. It is the compartmentation that represents the transition between two different surfaces. There is a predominance of morphogenesis processes.

Hills are degradation reliefs that can be found in any lithology. They present convex or concave slopes and broad tops, their morphology is elongated or rounded. They present low amplitudes, inferior to 50m. Drainage density varies from low to medium, with predominantly dendritic pattern. There is a predominance of pedogenesis processes.

Low hills are a relief typical of the domain of "seas of hills," sometimes presenting dissected hills, with convex or concave slopes and rounded tops. The slopes present declivity with mild to moderate gradient. The drainage density is moderate, with dendritic or subdendritic pattern. They are subject to both pedogenesis and morphogenesis processes.

High hills are contained in all lithologic typologies and are degradation reliefs. They present hills with convex or concave geometry, well dissected,

and with rounded or pointed tops. They present sedimentation of colluvium, alluvium, and talus deposits. The slopes are characterized by medium to elevated gradients, the tops are rounded or pointed. They present moderate to high drainage, with subdendritic to trellis patterns, with a predominance of morphogenesis.

Isolated crests and low ridges are degradation reliefs with varied lithology. They are composed by small isolated ridges, with predominance of predominantly rectilinear slopes and aligned, pointed or slightly rounded crests, with topographical highlight compared to its surroundings They present high relief amplitudes, with the occurrence of very steep slopes, and sub-vertical rocky walls. The drainage density is incipient, with clear structural control. There is predominance of morphogenesis.

Ridge domain is a degradation compartment in any lithologic type, with predominance in igneous and metamorphic types. It presents a mountainous aspect, with rectilinear and concave slopes, and with aligned crest, pointed and slightly rounded tops. It presents sedimentation of colluvium and talus deposits. The slopes present steep declivity, and occurrence of sub-vertical rocky walls and sugar loaves. The main drainage in plain carving process with trellis to rectangular pattern, under strong structural control. There is a predominance of morphogenesis processes.

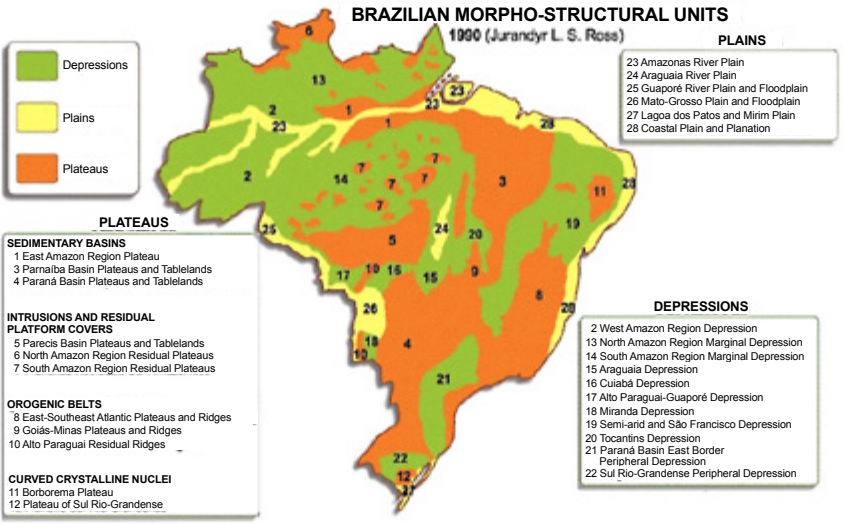

Figure 5.8: Geomorphologic compartmentation of the Brazilian territory according to Ross, 1990

According to Ross (1990), the project implementation area (Figure 5.8) is under two morpho-structural units, "19 – Semi-arid and São Francisco Depression", and "08 – East-Southeastern Atlantic plateaus and ridges."

The plateaus are the elevated and flattened relief forms, where there is predominance of altitude higher than 3000 meters, characterized by escarpments in which the processes of erosion prevail over sediment accumulation ones. This type of compartment can be found in any type of geological structure. In sedimentary basins, the plateaus are characterized by the formation of escarpments in areas that border the depressions. They also form the tableland and low plateau compartments, which are characterized by a flatter relief in areas of higher altitudes. The plateaus are considered residual forms, since they remain in higher altitudes due to the greater resistance they offered to past erosive processes.

The depressions are areas depressed due to the erosive processes that occurred in the limit of sedimentary basins with the old massifs, that is, limits between areas of plains and plateaus. With this, there was a depression of the reef, mainly during the Cenozoic era. The São Francisco depression is characterized by being an interplanar depression, that is, it is a sunken area compared to the surrounding plateaus.

From the hypsometry (Figure 5.9), we can see that the area with the greatest variation is located in section 2, in the central area of the state of Bahia; and in section 3 of the project, to the south of the state of Bahia, and north of the state of Minas Gerais.

These more elevated areas are composed of plateaus, tablelands and mountainous domains. They occur due to the lithologic composition being more resistant to the erosive processes, so they are residual reliefs that, with the passing of geological time, remained at a higher altitude elevation compared to the lower areas, in general, related to past lithologies that were less resistant to relief denudation processes.

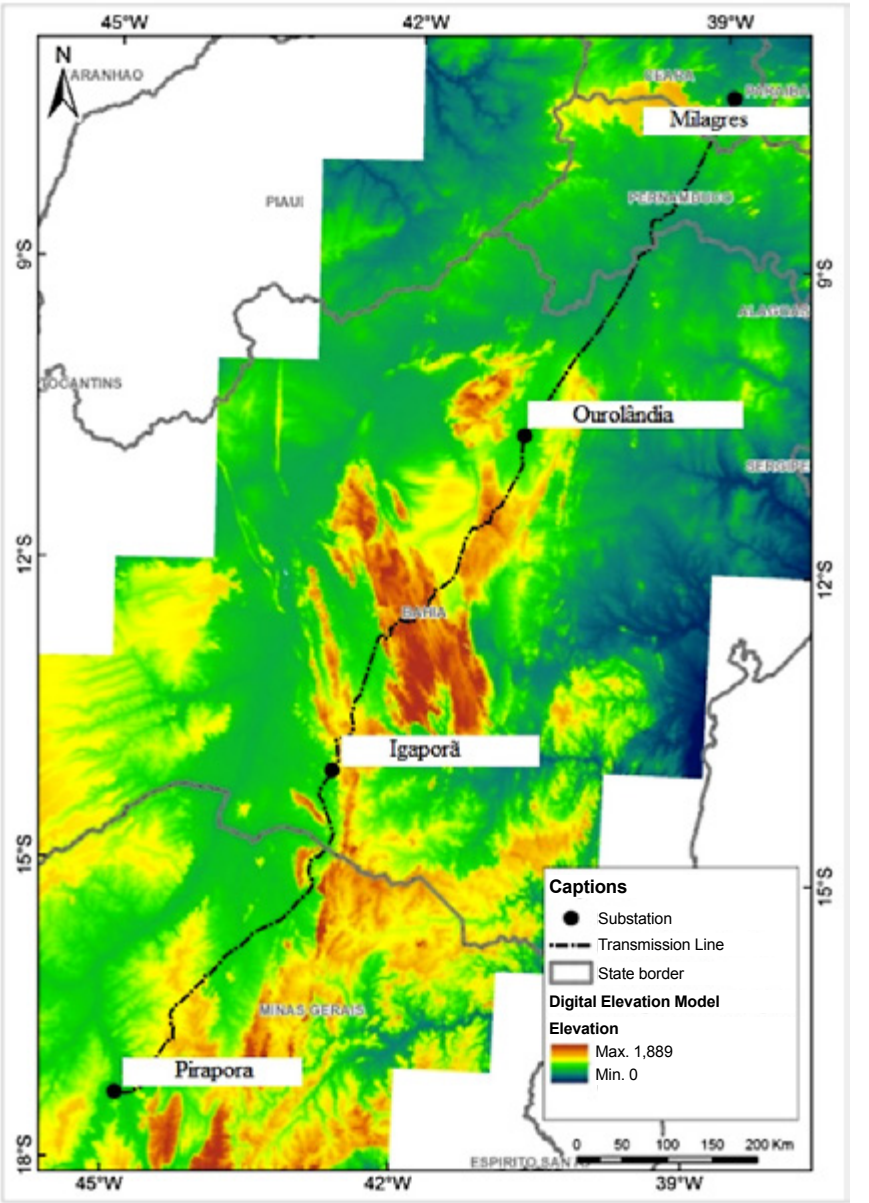

Figure 5.9: Hypsometry presenting the altimetric variation of the TL implementation area. Source: adapted from SRTM, 2016

Based on the Agrometeorological Zoning of the Northeast (Figure 5.10), we observe the great geological and morphological complexity existing in the line implementation area, being that formations like plateaus and ridges are more common in areas of crystalline and tableland basement, continental dunes and sedimentary basins are constituted predominantly of sedimentary material.

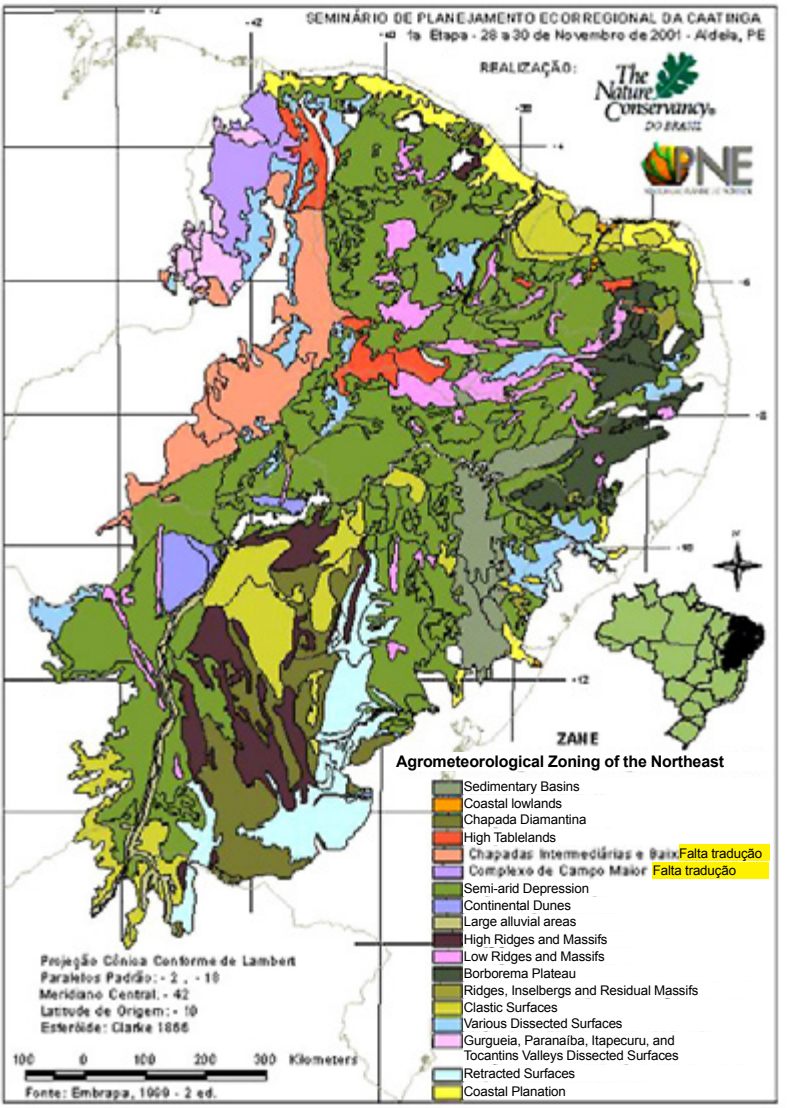

Figure 5.10: Agrometeorological Zoning of the Northeast elaborated by Embrapa, 1999. Source: The Nature Conservancy of Brazil, 2001

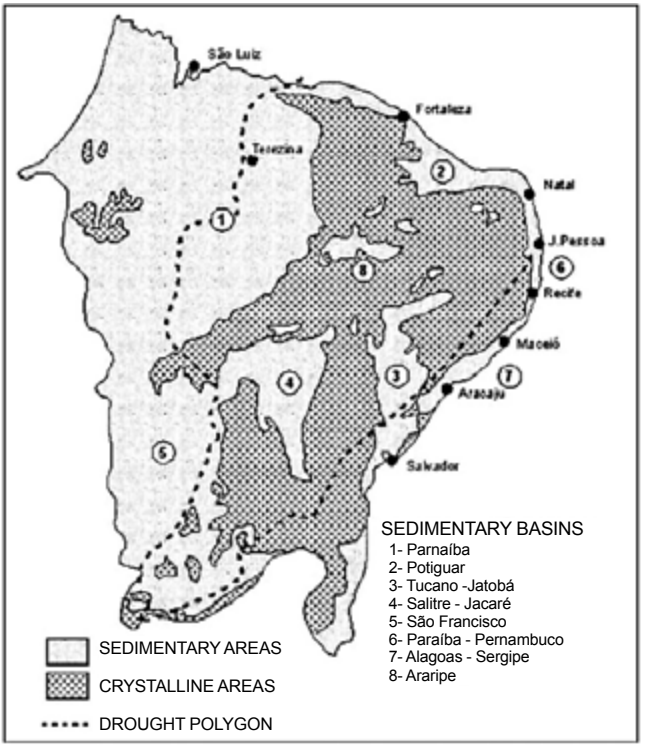

Figure 5.11: Distribution of sedimentary and crystalline rocks in the area comprised by the drought polygon defined by Sudene. Source: Demetrio *et al.,* 2007

Figure 5.11 with the distribution of sedimentary and crystalline rocks provides an overview of the lithologic variation present in the project implementation area. The line crosses the areas of the Tucano-Jatobá, Salitre-Jacaré, and São Francisco Sedimentary Basins.

For mineral exploration there are quarries, areas of extraction of sandy material, and karst rocks in certain areas.

5.1.3 Soils

The soils in the region (Figure 5.12) present mostly a clayey-sandy constitution, and are poor in organic matter (Sudene, 2016). There is also a large amount of planosols, characteristic of the semiarid regions, and also shallow soils of the litholic neosol, quartzarenic neosol, and fluvic neosol, in addition to the luvisols.

The shallow depth of the soils and their pedregosity are a result of the more arid climate prevailing in the region, which does not allow the formation of deeper soil profiles.

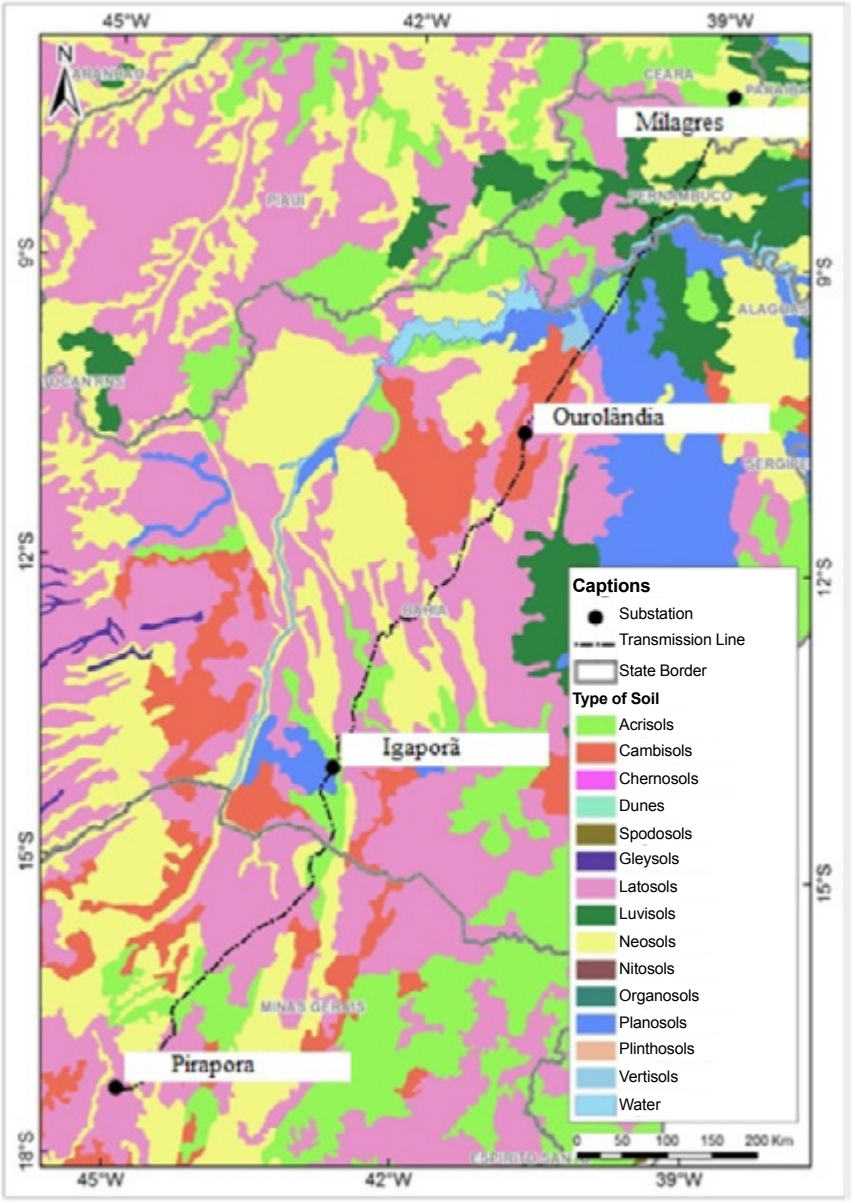

Figure 5.12: Pedologic cover. Source: adapted from Embrapa, 2011

According to Embrapa's mapping (2011), in the scale of 1: 5,000,000 (Figure 5.12), the area presents a predominance of the following types of soils: latosols, cambisols, acrisols, neosols, planosols, and luvisols. Next, we present the definition of these types of soils in their first order, as presented in Embrapa's Brazilian Soil Classification System (2006).

5.1.3.1 Acrisols

According to Embrapa's definition (2006), these are soils composed of mineral material with presence of agric textural B horizon of low activity clay, or high activity clay combined with low base saturation or allytic character.

In general, this soil category presents increased clay in the B horizon, related to the superficial, with clear, abrupt or gradual transition between the A and Bt horizons. They present variable depth, going from strong to perfectly drained. The colors are reddish or yellowish and, in rare cases, brownish or grayish.

They present texture from sandy to clayey in the horizon A and from medium to very clayey in the horizon Bt, with concentration of clay. They have high or low base saturation, vary from strongly to moderately acidic, and are predominantly kaolinitic with Ki ranging from 1.0 to 3.3.

The acrisols are soils previously classified as red-yellow podzolics, high or low activity clay; part of them were also classified as structured reddish-purple soil, structured reddish-purple soil similar to structured brown earth, structured brown earth similar, with most presenting textural gradient required for textural B; they are eutrophic, dystrophic or allelic. They are part of the brown grayish podzolic, dark red podzolic, yellow podzolic, grayish podzolic, and the alisols that present textural B.

5.1.3.2 Cambisols

They are defined by Embrapa (2006) as being soils composed of mineral material, with incipient B horizon subjacent to any type of superficial horizon, provided that in any of the horizons the B horizon does not present the characteristics established to be classified in the classes of the other soils, being vertisols, chernozem, plinthosols, and organosols.

The cambisols present sequence of A or hystic, Bi, C horizons, with or without R. They are soils that present heterogeneous material of origin, relief forms, and climatic conditions for its formation, thus, being a class that comprises soils that go from strongly to imperfectly drained, and vary from shallow to deep. Their color varies from brown, to yellowish brown to dark red. They have high to low base saturation and chemical activity of the clay fraction.

Their incipient B horizon (Bi) presents a loamy to a more clayey texture, and the solum usually presents uniform clay contents, and may present a slight decrease or a small increase of clay from horizon A to Bi.

The structure of the Bi horizon may be in blocks, granular or prismatic, with cases of soils with absence of aggregates, structure in simple or massive grains. Their horizon may present plinthite or gleying. They can also be similar to the latosols, being distinguished from those for presenting, in the B horizon, one or more characteristics not compatible with very evolved soils.

Are part of this class, the soils previously classified as cambisols, including those developed in alluvial sediments. Soils with chernozemic A horizon and incipient B horizon with high base saturation and high activity clay are not part of this class.

5.1.3.3 Latosols

Latosols, according to Embrapa's definition (2006), are the soils consisting of mineral material and latosolic B horizon located below any of the superficial diagnostic horizon types, except for the hystic.

This is a type of soil in an advanced stage of weathering, which are well developed resulting from energetic transformations in the constituent material. They are virtually devoid of primary or secondary minerals that exhibit less resistance to weathering. They present low CEC of the clay fraction, with variations ranging from predominantly kaolinitic soils, with higher Ki values, to extremely low Ki oxidic soils.

They also present variation from strongly to well drained, moderate drainage, or even imperfectly drained with a certain degree of gleying.

In general, they are very deep, with solum thickness rarely inferior to one meter. They present horizon sequence with little differentiation of sub-horizons, and transitions usually diffuse or gradual. The A horizon presents darker colors, while the B horizon presents more lively colors, varying from yellow, grayish-brown, to dark-grayish-red, in 2.5YR to 10YR shades, varying according to the nature, form, and quantity of the mineral constituents. In the C horizon, the chromatic expression is very variable and even heterogeneous, given its more saprolite nature.

There is little clay increase from horizon A to B, and the textural relationship between B/A does not satisfy the requirements for textural B and, in general, the clay fraction contents in solum gradually increase with depth, or remain constant throughout the profile. The mobility of clays in the B horizon is low, except for soils developed from materials with sand-quartz composition.

Are part of this class all old latosols, except some previously identified modalities identified as plinthic latosols.

5.1.3.4 Luvisols

According to Embrapa (2006), luvisols are mineral soils, non-hydromorphic, with textural B horizon with high activity clay and high base saturation, located immediately below horizon A or horizon E.

They vary from imperfectly drained, usually presenting (60 to 120 cm), with sequence of A, Bt, and C horizons, and clear differentiation between the A and Bt horizons, due to the texture, color, and/or structure contrast between them.

They present a clear or abrupt transition to the textural B horizon, with most of this class of soils presenting abrupt textural change. In the superficial part, they may present pedregosity, solodic or sodic character in the superficial part.

The coloring of the Bt horizon is reddish, yellowish and, less frequently, brownish or grayish. Their structure is in blocks, moderately or strongly developed, or prismatic, composed of angular or sub-angular blocks.

These are moderately acid to slightly alkaline soils, with low or zero extractable aluminum contents, and high values for the molecular relation Ki in the Bt horizon, with variable but expressive amount of 2:1 type clay minerals.

Soils that have been classified as non-calcium brown, eutrophic red-yellow podzolic, high-activity clay, and eutrophic grayish-brown podzolic, with some eutrophic red-dark podzolics, with high activity clay, are included in this class of soils.

5.1.3.5 Neosols

According to Embrapa's definition (2006), these are soils composed of mineral material, or thin organic material, and which do not present expressive changes regarding the material of their parent rock, due to the low intensity of the pedogenetic processes. This can occur because of the characteristics inherent to the material of origin, (greater resistance to weathering or chemical-mineralogical composition), or due to influences of exogenetic factors that might prevent or limit soil evolution.

The sequence of horizons is A-R, A-C-R, A-Cr-R, A-Cr, A-C, O-R or H-C, without meeting the requirements established to be classified as chernosols, vertisols, plinthosols, organosols, or gleysols.

In this class, there might be several types of superficial horizons, such as the O that is less than 20 cm thick and is over the parent rock, and the A horizon humic or prominent, which is more than 50 cm thick over the R, C or Cr layer.

This class of soils may present thin B horizon without meeting enough requirements to characterize any type of diagnostic B horizon. The C horizon may present diagnostic characteristics for other classes, but the position where they are located prevent them from being classified in the classes of the gleysols, vertisols or plinthosols.

Are part of this class soils previously called lithosols, and litholic, regosols, alluvial soils, and quartzous sands (dystrophic, marine and hydromorphic). They also include soils with A horizon humic or prominent A, and thickness higher than 50 cm in contact with the rock, or those that present sequence of horizons A, C or ACr.

5.1.3.6 Planosols

Embrapa (2006) defines planosol as imperfectly or poorly drained mineral soils that have an eluvial surface or subsurface horizon, and have a lighter texture, with abrupt contract with the B horizon (or with an abrupt transition), immediately subjacent and thickened, and usually marked concentration of clay, with slow to very slow permeability, and sometimes constituting a pan horizon, which allows for the formation of suspended water sheets of variable presence during the year.

This soil may present any type of A or E horizon, with the E-albic horizon being less frequent, followed by planic B. The sequence of horizons presented is A, AB or A, E (albic or not) or Eg, followed by Bt, Btg, Btn or Btng. When dry, the parallel contact of horizons A or E and B is remarkable, configuring a very clear fracturing.

The B horizon presents a strong structure in angular blocks, often with a cubic aspect, or a prismatic or columnar structure in the upper part of the referred horizon. The colors tend to be grayish or darkened, with or without occurrences and even predominance of neutral reduction colors, with or without mottles.

It is also possible that the soils present a calcic horizon, with carbonate, duripan, sodic, solodic, saline or salic character. They may present plinthite, provided they are not located in a plinthosols diagnostic horizon, or in enough quantity for that diagnostic.

They are predominant in areas of flat or slightly undulating areas, where environmental conditions favor the annual periodic excess of water, even for short duration, especially in regions subject to prolonged drought, such as semiarid areas.

5.1.4 Water resources and water uses

The transect (Figure 5.13) of the line passes over the water divide of the hydrographic regions of the São Francisco and Eastern Atlantic. The São Francisco plain is more expressive in the region and the line is intended to be installed, in general, parallel to the axis of the São Francisco River.

Figure 5.13: Hydrographic regions of the project area. Source: ANA, 2006

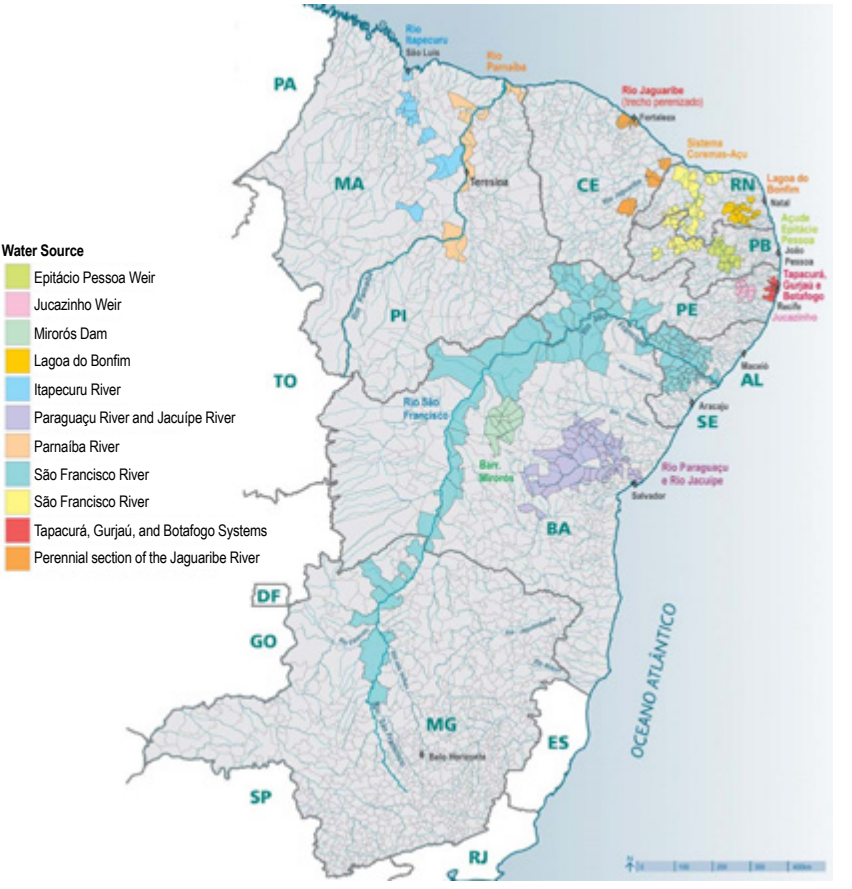

Figure 5.14: Water catchment areas of the main rivers and springs of the project area. Source: ANA, 2006

We observe that the line will cross the water source areas of the São Francisco River in the areas of the state of Pernambuco, and north of the state of Bahia, area of section 1; this area is the one that will require greater attention when of the implementation of the project, aiming at preserving the water dynamics of the São Francisco River (Figure 5.14).

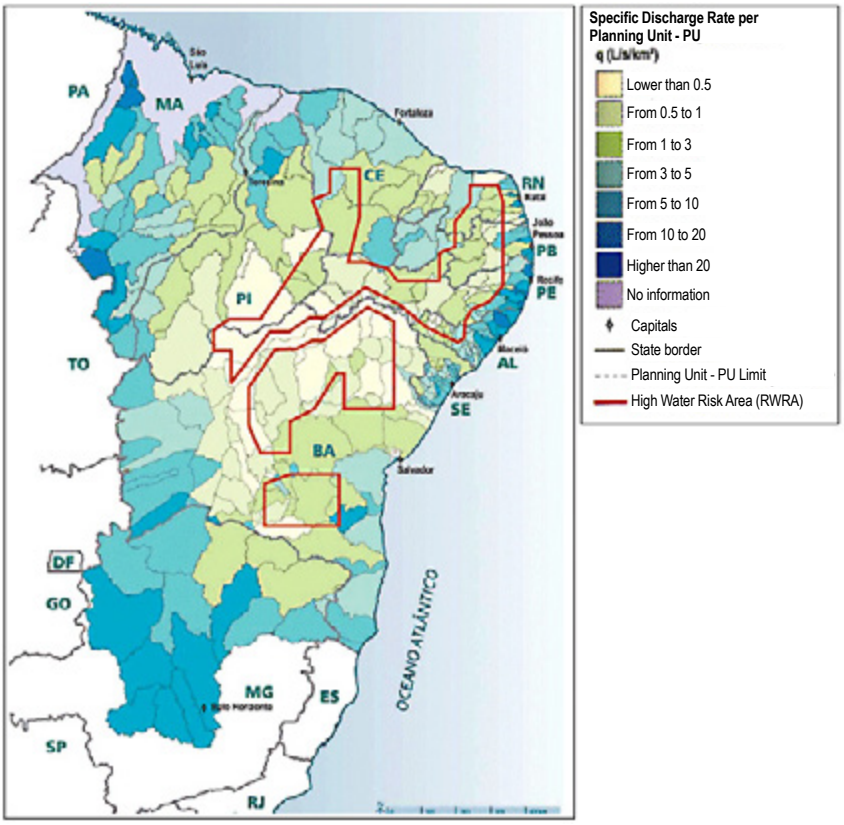

Figure 5.15: Medium specific discharges and areas of high water risk. Source: ANA, 2005

The area in which the line is to be implemented presents a very low specific discharge rate (Figure 5.15), with sections 1 and 2 having most of their territory delimited with a high-water risk area.

Domain	Description	Water Potential
Porous Sedimentary Basins and Cenozoic Coverings	Variable extension free aquifers, formed by non-consolidated clastic sediments of Tertiary-Quaternary age. Water chemical quality, in general, good. Exploration, frequently via shallow wells.	Low to Medium
	Aquitards, and aquicludes formed by consolidated clastic sediments, predominantly shales, argillites, and siltstones, of Mesozoic age. Locally may constitute aquifers.	Low
	Limited regional extension free or confined aquifers, formed by consolidated clastic sediments, predominantly sandy, of Mesozoic age. Water chemical quality, in general, good.	Medium to High
	Regional extension free or confined aquifers, formed by consolidated clastic sediments, predominantly sandy, of Mesozoic age. Water chemical quality, in general, good. Possibility of salinization of water in the confined parts of the Parnaíba Basin.	High
Fractured - Clastic Limestone Rocks	Aquifers associated to the fractured and dissolution zones, represented by sediments, metasediments, and limestones. Localized water hardness problems due to the contribution of limestone rocks.	Medium
Fractured Crystalline	Aquifers restricted to fractured zones, represented by metasediments, and meta-igneous, of Archaean to Proterozoic age, associated to the presence of thick weathering mantle. Water chemical quality, in general, good.	Low to Medium
	Aquifers restricted to fractured zones, represented by metasediments and meta-igneous, of Archaean to Proterozoic age, associated to the presence of thin weathering mantle (3 to 5 m), located in the semi-arid region. Water salinization problems.	Low

Figure 5.16: Lithologic domains, types of aquifers, and water potential. Source: ANA, 2006

Figure 5.6 presents the various geological domains existing in the area, showing that there is a variation of crystalline (predominant) to clastic materials, to Cenozoic coverings. To each type of domain, there are different types of associated aquifers and their respective water potentials.

The area where the line is to be implemented is characterized, predominantly, by crystalline substrate, with low water potential, and portions of limestone areas of medium water potential. With regards to the karst areas, geological surveys must be made to assess the risk of land subsidence due to the presence of dolines, with the occurrence of caves being common in this type of basement. There is also an expanse between the border of the states of Ceará and Pernambuco, with sedimentary basins and variation from low to high water potential, and attention should be given to this issue when of the line implementation in this area.

5.2 Biotic Environment

The biotic environment comprises the variables related to living beings and their presence on Earth. The use of the soil and vegetation, the fauna and special ecosystems, and the protected areas are considered. Understanding it is important for providing an overview regarding existing living beings and their relationship with the ecosystem where they are inserted, and which is being studied. For the current project, the description and understanding of the biotic environment is relevant to demonstrate the current types of land use and occupation, the ecosystems, and protection areas existing in the project implementation area.

5.2.1 Land use and vegetation

As presented in the map (Figure 5.17), there is a predominance of areas of steppic-savannas (caatinga) and anthropic use in the project implementation area.

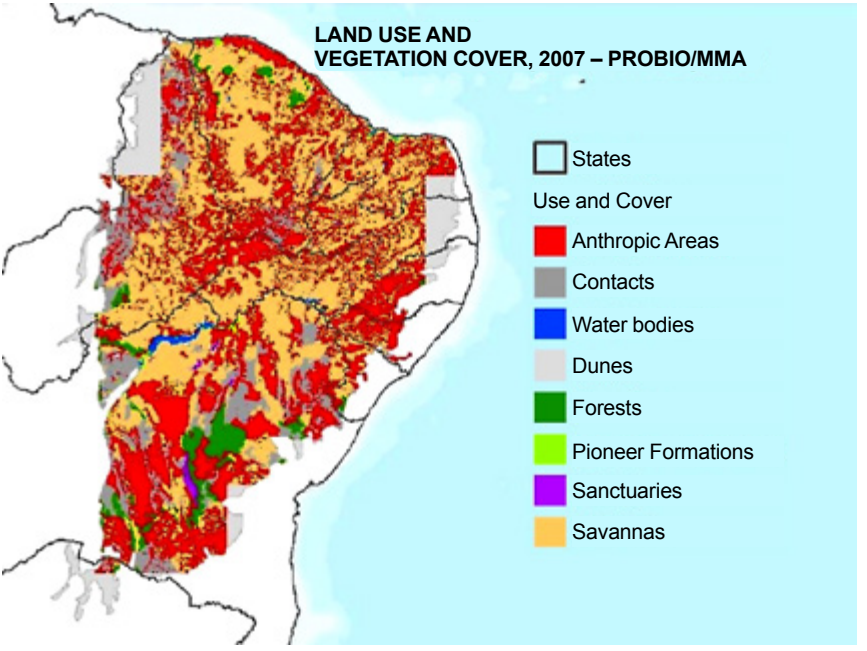

Figure 5.17: Land use and vegetation cover. Source: Probio/MMA, 2007

There are occurrences of large fragments of forested areas of caatinga, and seasonal forest that require attention. The line also crosses areas of campo rupestre (rocky fields), mainly in sector 2. The areas of campo rupestre must be highlighted for presenting endemic vegetation. Thus, the regions where the line crosses areas with this physiognomy will require more attention. Section 3, from Igaporã to Pirapora, is a stretch that presents caatinga and savanna physiognomies, which may make identifying some fragments of natural vegetation more difficult because of the transition areas. In the area along the line, we notice various areas of contact between different types of vegetation.

In the areas of anthropic use, agricultural uses and areas for urban settlement stand out.

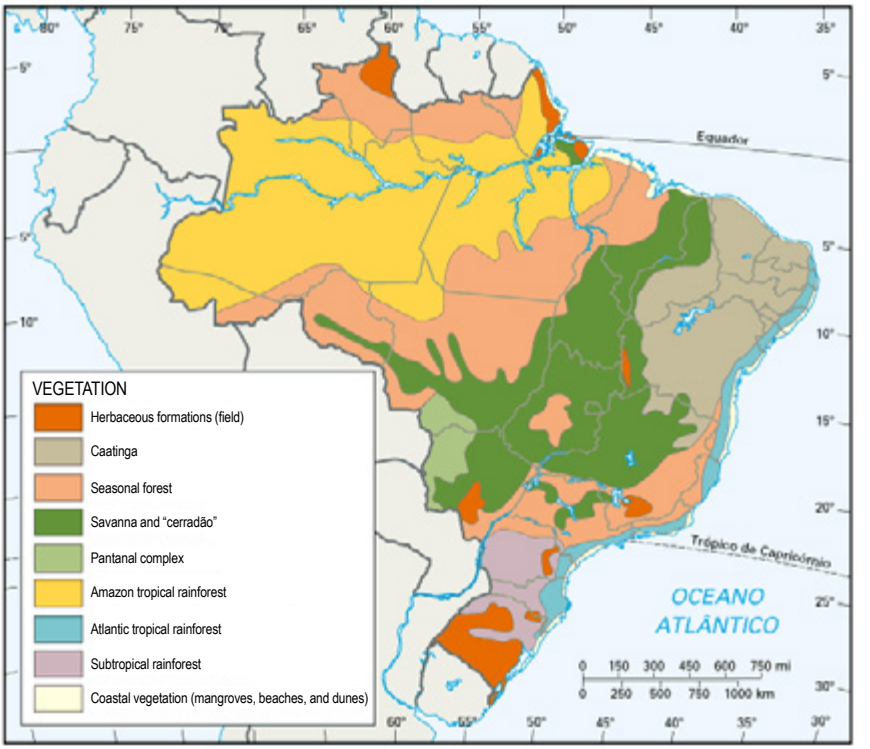

Figure 5.18: Different types of vegetation in the Brazilian territory. Source: IBGE, 2012

The line area is inserted predominantly in the caatinga biome, with some stretches of savanna, cerradão, and seasonal forest (Figure 5.18).

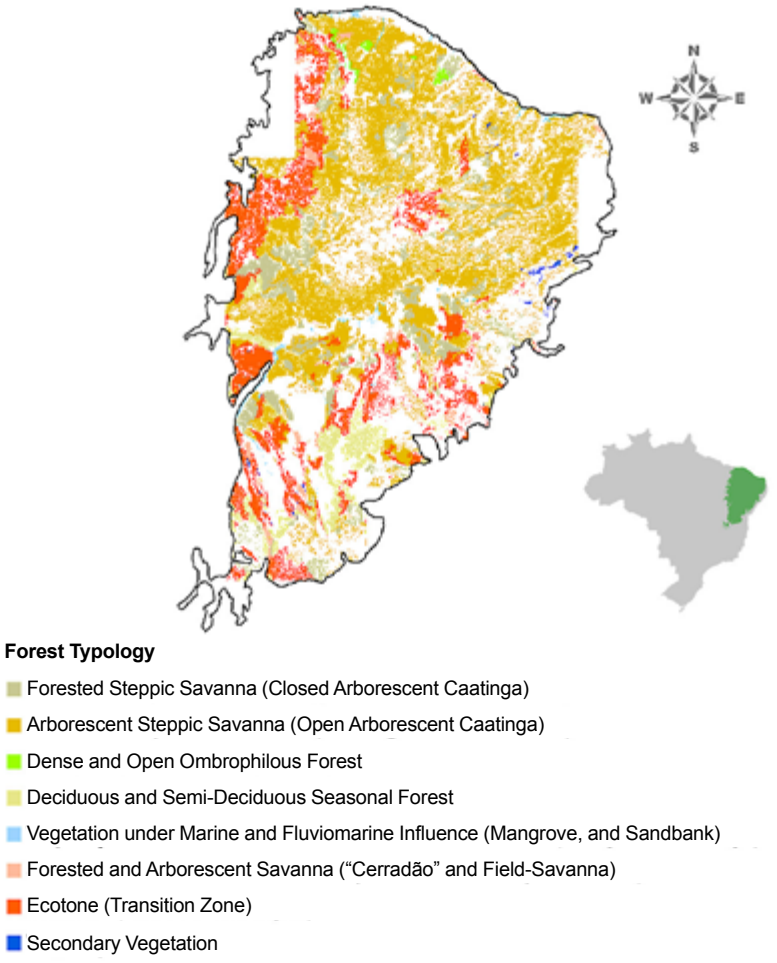

Figure 5.19: Detailing of the vegetation found in the project area. Source: MMA, 2009

The caatinga vegetation is xerophytic ("drought friendly"), deciduous, and thorny vegetation, exclusive of warm climates, and adapted to the ecologic condition of the semiarid tropics, with light rains followed by long dry periods (BRASIL, 1973; 1981; CASTRO and CAVALCANTE, 2010). There is a predominance of rocky soils and intermittent rivers. During rain periods, its aspect changes significantly with the emergence of abundant herbaceous vegetation.

The caatinga is a vegetation complex where a large variety of physiognomic shapes and structures can be observed. Among the typical physiognomies (Figure 5.19), we have the arborescent closed caatinga (forested), and the arborescent open caatinga (wooded), park and grassy-woody (IBGE, 2012).

(a) **(b)** **(c)** **(d)**

Figure 5.20: Schematic profile of the core caatinga area, also called steppic-savanna. (a) Forested; (b) Wooded; (c) Park; and (d) Grassy-woody.
Source: Veloso, Rangel, and Lima (1991) adapted by IBGE (2012)

There are also some areas with fragments of deciduous and semi-deciduous seasonal forest, as well as transition areas, as previously mentioned.

Semi-deciduous

Semi-deciduous

Deciduous

Deciduous

Figure 5.21: Typical forms of seasonal forest manifestations

5.2.2 Ecosystem and fauna

Figure 5.22 shows the areas of biologic importance found in the line implementation region. The areas have been categorized according to their biological importance, varying from high, very high, and extremely high biological importance.

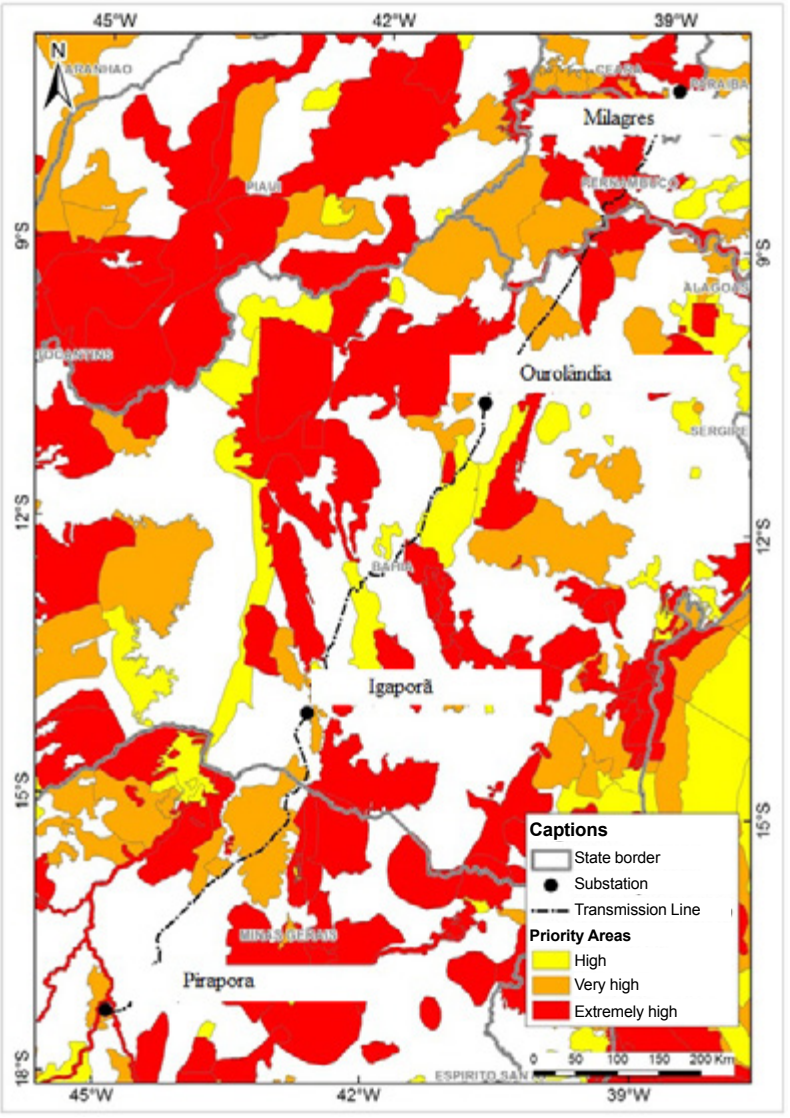

Figure 5.22: Areas of biological importance. Source: Probio, 2000

The path crosses some portions of areas of extremely high biological importance, and is close to areas of very high and high biological importance, according to the Probio methodology. The proximity to areas of biological importance highlights the need of attention to the path of the line, thus, special care should be dedicated to these portions, aiming at deviating the implementation of the Transmission Line, whenever possible.

The biological importance presented in the map is associated to the great diversity and endemism of the flora and fauna of the caatinga, which is adapted to the xerophytic vegetation, to varied habitats of semiarid climate, and with little water during most of the year. Additionally, due to the large anthropogenic pressure, in many regions there are great threats to the extinction of many species, some of which may not even be known for lack of study in the biome. For this reason, attention should be given to the areas considered as of biological importance in the proximity of the line.

The avifauna is one of the fauna groups of great importance to the balance of the ecosystem and which can influence the drawing of the line, because the project can negatively affect some migration routes of this group. In this sense, among the areas of biological importance, we must understand the areas that are related to the avifauna and its migration routes, so that the line path does not damage the bird community, or so that, if necessary, possible changes are made in the path.

5.2.3 Protected areas

The creation of Nature Conservation Units (CUs) has been a more effective global strategy for the biodiversity conservation *in situ*.

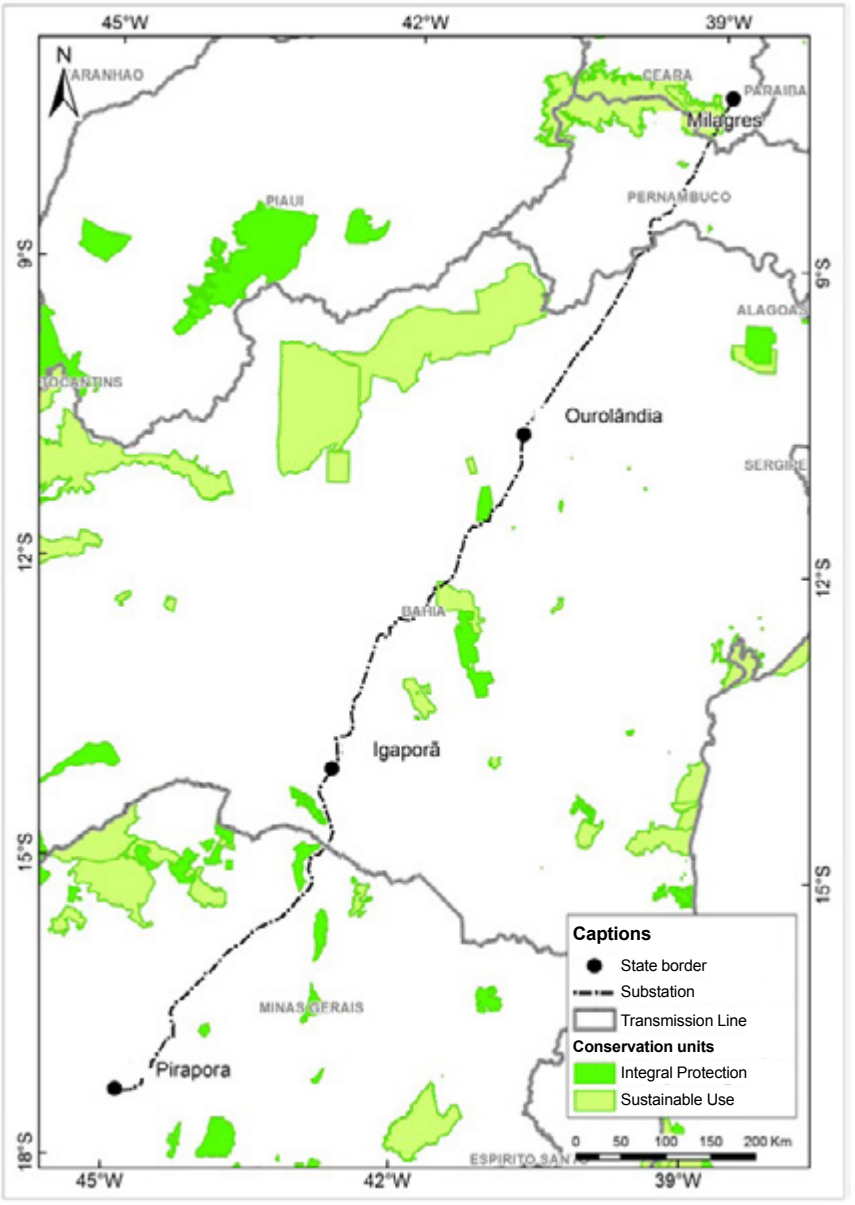

Figure 5.23: Protected areas: Federal, state, and municipal.
Source: adapted from MMA, 2007

The CUs refer to the areas that are especially important for environmental conservation and preservation, with essential function in maintaining ecological biodiversity. Thus, the CUs not only perform environmental conservation and preservation functions, but also promote environmental services of carbon fixation and carbon stocks regularization, biodiversity gene flow, biologic control, landscape maintenance, thermal comfort, leisure areas, recreation, education and research, and water and air purification. In addition to these, they improve the preservation of cultural values of traditional communities, historical, architectural and archaeological values, and develop region integration social functions (RODRIGUES and BONONI, 2008).

These different interrelationships related to the diversity of CU environments create the need for having different types or categories of CUs. Thus, the National System of Conservation Units (SNUC - law 9,985/2000) created the CUs, according to their forms of protection and permitted uses, which can be Integral Protection and Sustainable Use. Inside Integral Protection CUs only the indirect use of its natural resources is allowed (for example: ecological tourism and scientific research) for nature conservation, and the areas cannot be inhabited by man. On the other hand, in the Sustainable Use CUs, the presence of man is allowed, and the natural resources can be used in a sustainable manner.

The map (Figure 5.23) presents the federal and state Integral Protection and Sustainable Use CUs present in the TL area. These limits were obtained from the ICMBio (Chico Mendes Institute for Biodiversity Conservation) site, and by means of researches in the state information databases of the states of Ceará, Pernambuco, Bahia, and Minas Gerais, via their respective environmental agencies: Semace (Superintendence of the Environment of the State of Ceará), CPRH (State Environmental Agency), Inema (Institute of Environment and Water Resources), and IEF (State Forestry Institute).

In the line path, there are some points that require attention regarding their proximity to CUs. In section 2, it was necessary to divert the trajectory of the path due to the existence and limits of Parque Estadual do Morro do Chapéu. While, in section 3, it was necessary to divert the trajectory of the path due to the existence of three Integral Protection CUs: Parque Estadual Caminho dos Gerais, Parque Estadual da Serra dos Montes Altos, and Serra dos Montes Altos Wildlife Refuge. These trajectory deviations were necessary because in Integral Protection CUs no type of use is permitted, be it anthropic or sustainable; only the indirect use of their area is permitted.

On the other hand, regarding Sustainable Use CUs, the line corridor path crosses the APA Chapada do Araripe in section 1, and APA Marimbus/ Iraquará in section 2.

The corridor being studied also crosses a Private Reserve of Natural Heritage (RPPN): RPPN Fazenda Chacrinha, in the municipality of Coração de Jesus, in the state of Minas Gerais.

Also regarding biodiversity conservation, another aspect that may be relevant for the line corridor path is in the areas where it crosses rivers or lakes, because present APP (permanent preservation) areas that must be preserved for their importance as areas of connectivity and ecological corridor formation. A very critical area for the caatinga region is the crossing of the line over the São Francisco River, in the area close to Orocó and Riacho Seco, in Bahia. In these areas, removal of APP vegetation might occur, and that will require environmental compensation studies for the region. This might also occur in other crossings, such as the crossing of Rio das Velhas, and other smaller rivers.

In 2004, the Ministry of the Environment (MMA) defined rules for identifying priority areas for conservation, sustainable use, and distribution of biodiversity benefits via decree n. 5092. In addition to this decree, the MMA published a map of Priority Areas for Conservation, which was revised in 2007, defining which are priority areas for the elaboration and implementation of public policies, programs, projects, and activities under the responsibility of the Federal Government for in situ conservation of biodiversity, sustainable use, and distribution of biodiversity benefits.

The Priority Areas for Conservation crossed by the corridor path being studied are presented in Table 5.1, as follows:

Table 5.1: Priority Areas for Biodiversity Conservation (PABC) in the corridor being studied

Name of PABC	Code	Importance	Priority action
Jaíba	Ca001	Extremely high	Inventory
Jacaraci	Ca002	Insufficiently known	Recovery
Guanambi	Ca004	Insufficiently known	Promote Sustainable Use
Igaporá	Ca008	Insufficiently known	Recovery
Riacho de Santana	Ca010	Insufficiently known	Create CU - Undefined
Paramirim	Ca015	High	Recovery
Oliveira dos Brejinhos	Ca019	Insufficiently known	Create CU - Undefined
Marimbus/Iraquara	Ca020	Extremely high	Create CU - PI
Dois Riachos	Ca022	Insufficiently known	Inventory
Morro do Chapéu Region	Ca023	Extremely high	Mosaic/corridor
Serra do Tombador	Ca030	High	Recovery
Corredor dos Brejões	Ca033	Extremely high	Very High
Umburanas	Ca037	High	Very high
Region of Carrancas	Ca047	Very High	Recovery
Rio Curuçá e Serras	Ca053	Extremely high	Create CU - Undefined
Channel of the São Francisco River	Ca054	Extremely high	Create CU - PI
Baixo da Melância	Ca062	Extremely high	Create SU - CU
Petrolina	Ca064	Very High	Create CU - PI
Cabrobó	Ca079	Very High	Recovery
Chapada do Araripe (East)	Ca093	Extremely high	Create CU - PI
Kariris	Ca100	Extremely high	Create CU - Undefined
Morro do Chapéu State Park	Ca233	Extremely high	Protected Area
TI Truka	Ca254	Extremely high	Protected Area
APA Chapada do Araripe - Catolé	Ca258	Extremely high	Protected Area
APA Chapada do Araripe - Catolé	Ca259	Extremely high	Protected Area
Buritizeiro	Ce098	High	Recovery
Alto - Médio São Francisco	Ce106	Extremely high	Recovery
Northern Ridge	Ce123	Extremely high	Recovery
São João da Ponte	Ce124	Very High	Promote Sustainable Use
Verdelândia - Varzelândia	Ce126	Very High	Recovery
Rio Pardo - Santo Antônio do Retiro	Ce130	Extremely high	Inventory
Verdelândia - Varzelândia	Ce134	Extremely high	Recovery

5.3 Socioeconomic Environment

The characterization of the socioeconomic and cultural environment involves the analysis of aspects related to the qualification of the predominant types of uses in the region, focusing on demographic, economic, cultural, and structural aspects. Information is collected referring to demographics, population, regional scale economy, road and power infrastructure, land property structure and conflict areas, Human Development Index, indigenous population, archaeological heritage, and cultural history. This information is important for this project because it demonstrates the types of land and economic uses existing in the area, and possible conflict areas for the implementation of the project.

5.3.1 Demographics aspects

The project implementation area is located mostly within the Brazilian semiarid area. This region is characterized by presenting 57.53% of the area of the Northeastern region of Brazil, and 40.54% of the population of this same region (Sudene, 2016). Its GDP represents only 21.6% of the GDP of the Northeastern region (Sudene, 2016), although its territory occupies almost 60% of the region's territory, which highlights the area's low economic development aspect. In addition to being in the Northeastern semiarid region, the project area is also in the semiarid region of the state of Minas Gerais, which presents the same socio-economic aspects of the Northeastern semiarid region.

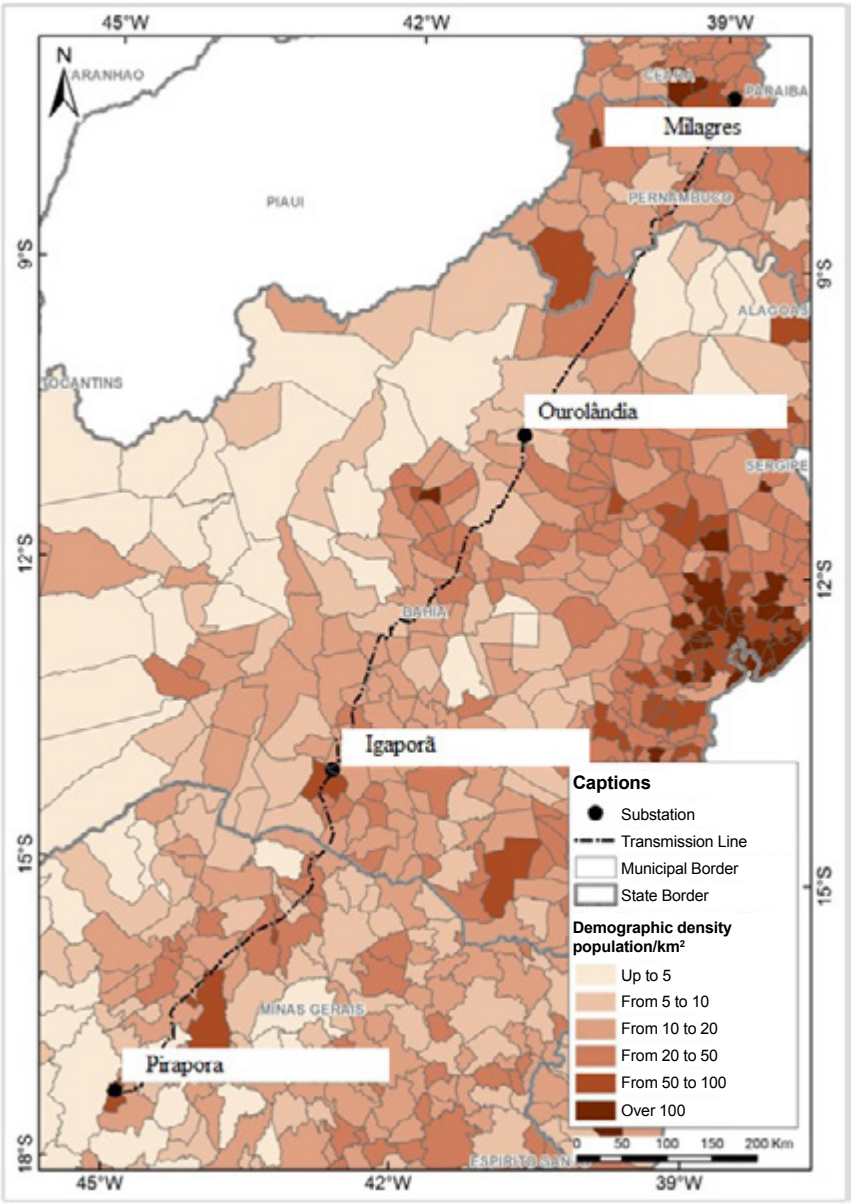

Figure 5.24: Population density per municipality. Source: adapted from IBGE, 2010

Figure 5.24 shows that the population density in the municipalities involved in the project implementation area is lower than 100 inhabitants, being higher than 50 inhabitants only in some rare cases.

The average population density in the municipalities crossed by the line corridor path is of about 10 to 50 people/km². In general, the line will be implemented in a region of low population density.

Regarding the per capita GDP (Figure 5.25), we observe that most municipalities the line is going to cross is in the range of 5 to 10 thousand Reais (R$) *per capita*.

There is a group of municipalities in the central-southern region of the state of Bahia where the GDP is lower than 5 thousand Reais *per capita*.

In very few cases, the line corridor path crosses the territory of municipalities where the GDP value is higher than 10 thousand Reais *per capita*.

The MDHI (Figure 5.26) of most of the municipalities range from very low to low, especially in the municipalities of the states of Pernambuco, and Bahia. In the state of Ceará, there is a predominance of municipalities with medium MHDI. In Minas Gerais, the index varies between medium and high.

In general, the municipalities present MHDIs low. compared to the national context. This is a result of the low economic dynamics of these regions, which ends up being reflected in this indicator.

The line will be implemented in an area that presents low population density, low per capita GDP, and reduced human development index, that is, it is a sparsely inhabited area, with low economic development, and an insufficient standard of living.

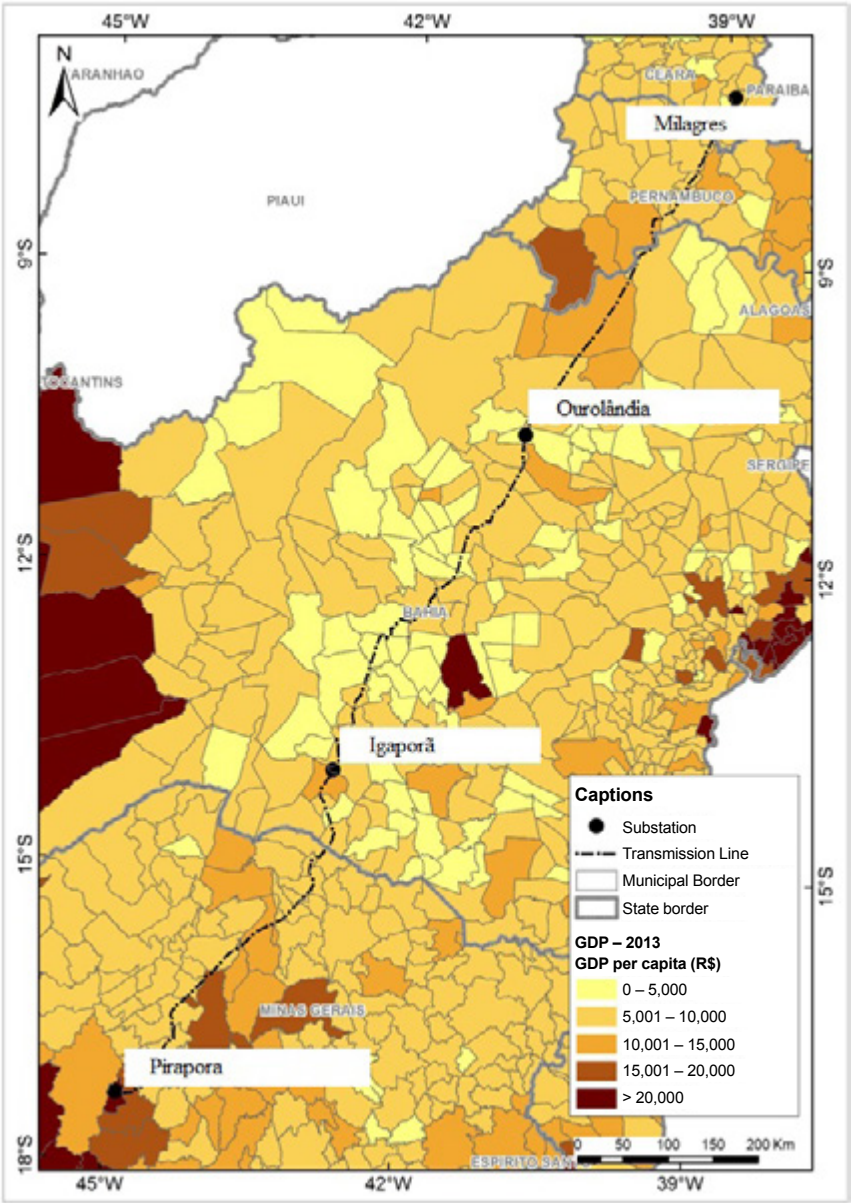

Figure 5.25: Municipal per capita GDP and current prices in R$. Source: IBGE, 2013

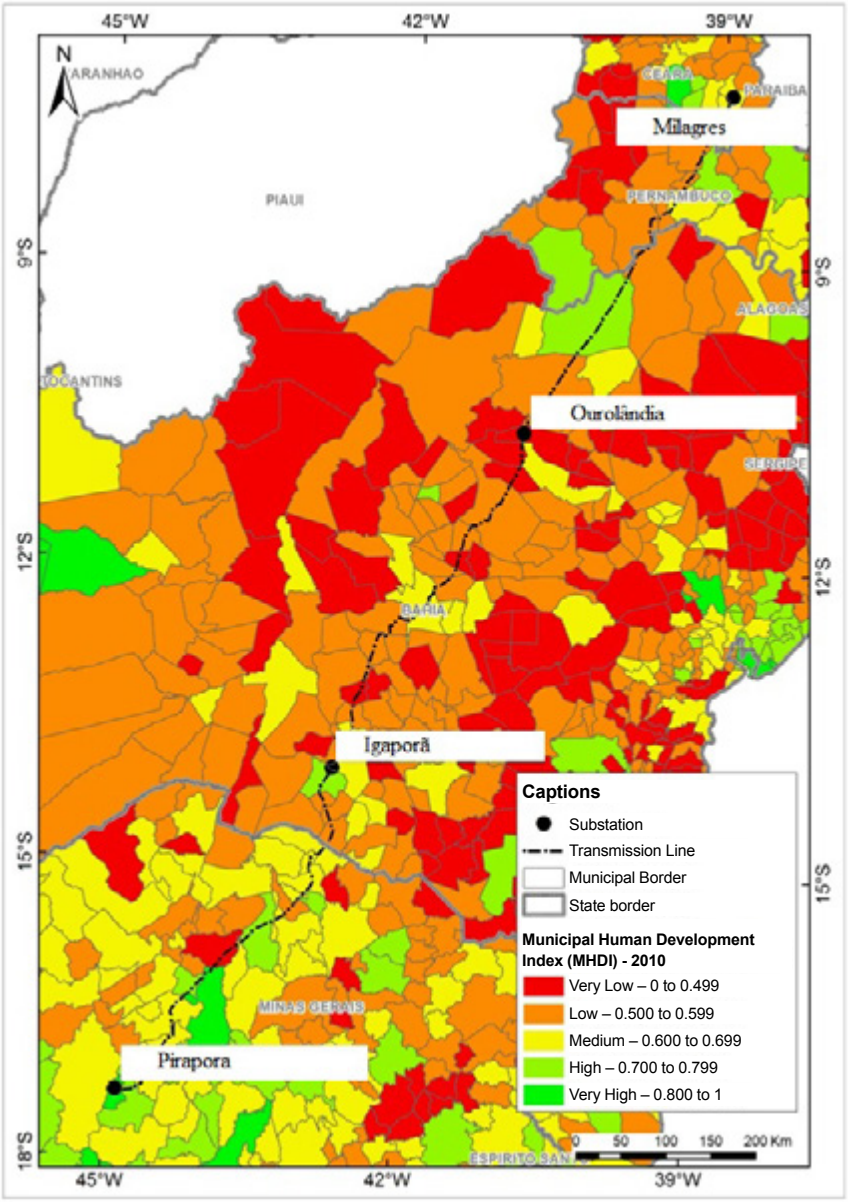

Figure 5.26: Municipal Human Development Index. Source: IBGE, 2010

5.3.2 Territorial organization and regional structure

The area where the line is to be implemented crosses a significant part of the Brazilian semiarid area, where, at times, the infrastructure is precarious, the roads are not paved, or are paved with poor quality asphalt. Thus, we understand that the project may, to a certain extent, contribute to promote regional development.

The areas that concentrate the greater quantity and better quality of infrastructure in the states involved in the installation of the line are located on the coast, where the capitals of the states of Ceará, Pernambuco, and Bahia are located. Except for the state of Minas Gerais, which does not present a coastal area. For this state, it is important to mention that the line will be implemented to the north, which is the state's least developed region.

Figure 5.27 presents the road, railway, and airfield/runway structures in the project area, as well as the preferred route for implementation of the line and its substations. The areas between the states of Ceará and Pernambuco concentrate a large number of roads. There is an axis between roads also in the central region of the state of Bahia, and in the north of the state of Minas Gerais.

With regards to railroads, there is a larger concentration in the south of the state of Bahia, in the north of Minas Gerais and Pernambuco.

As for the airfields/runways, there is a larger concentration in the state of Minas Gerais, and in the state of Pernambuco, being the most critical area for implementation of the line

5.3.3 Land property structure, settlements and conflict areas

According to Incra's definitions, rural settlements are *"a set of agricultural units independent from each other, installed by Incra where originally there was a rural property that belonged to a single owner."*

They are divided into parcels, patches or lots and delivered to families with no economic conditions to buy land on their own account. Their sizes, sometimes, are associated to the support capacity that involves the geography of the terrain, and the production capacity is associated to the number of settled families.

With regards to the project implementation area (Figure 5.28), we observe that there is greater concentration of rural settlements in Pernambuco, central area of Bahia, and north of Minas Gerais. These

settlement areas that the line will in fact cross, must be analyzed in greater depth to evaluate possible conflicts that might arise from the implementation of the project.

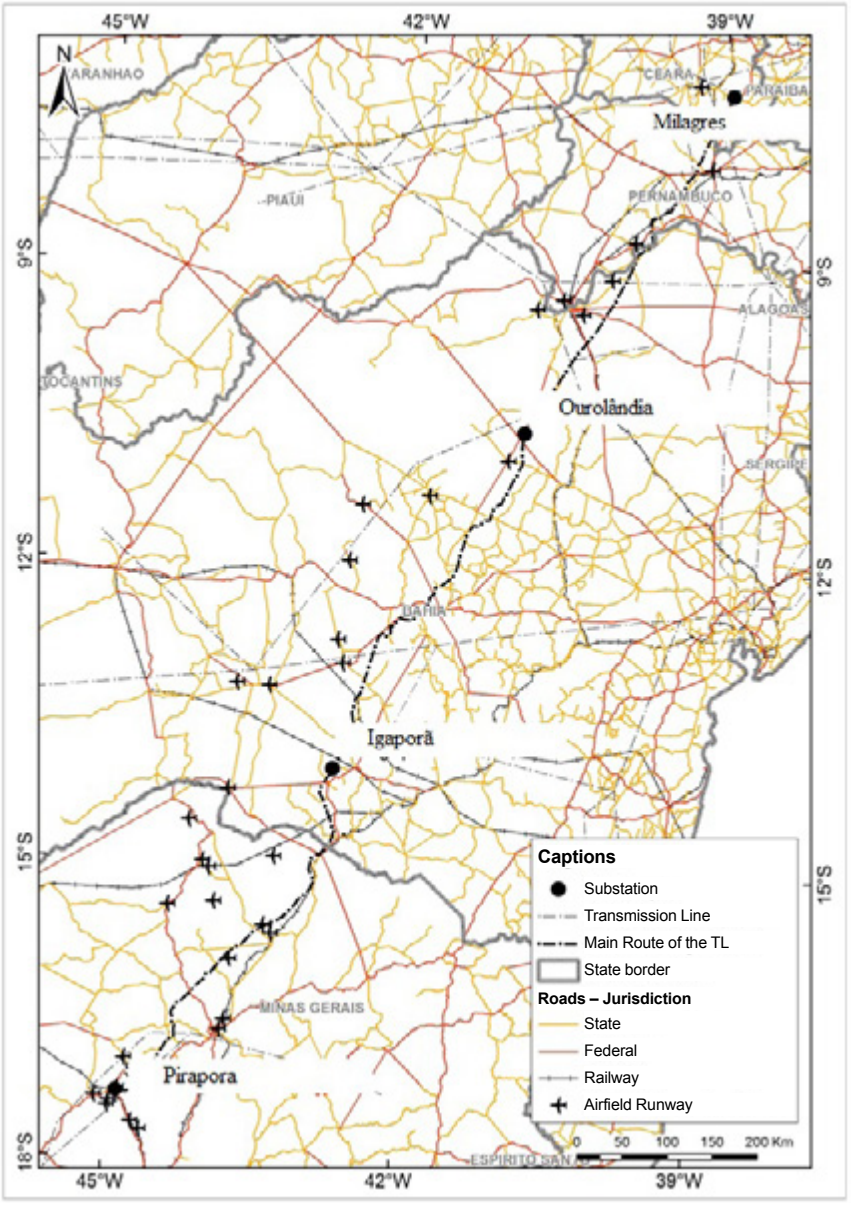

Figure 5.27: Regional infrastructure. Source: adapted Ministry of Transportation, 2010

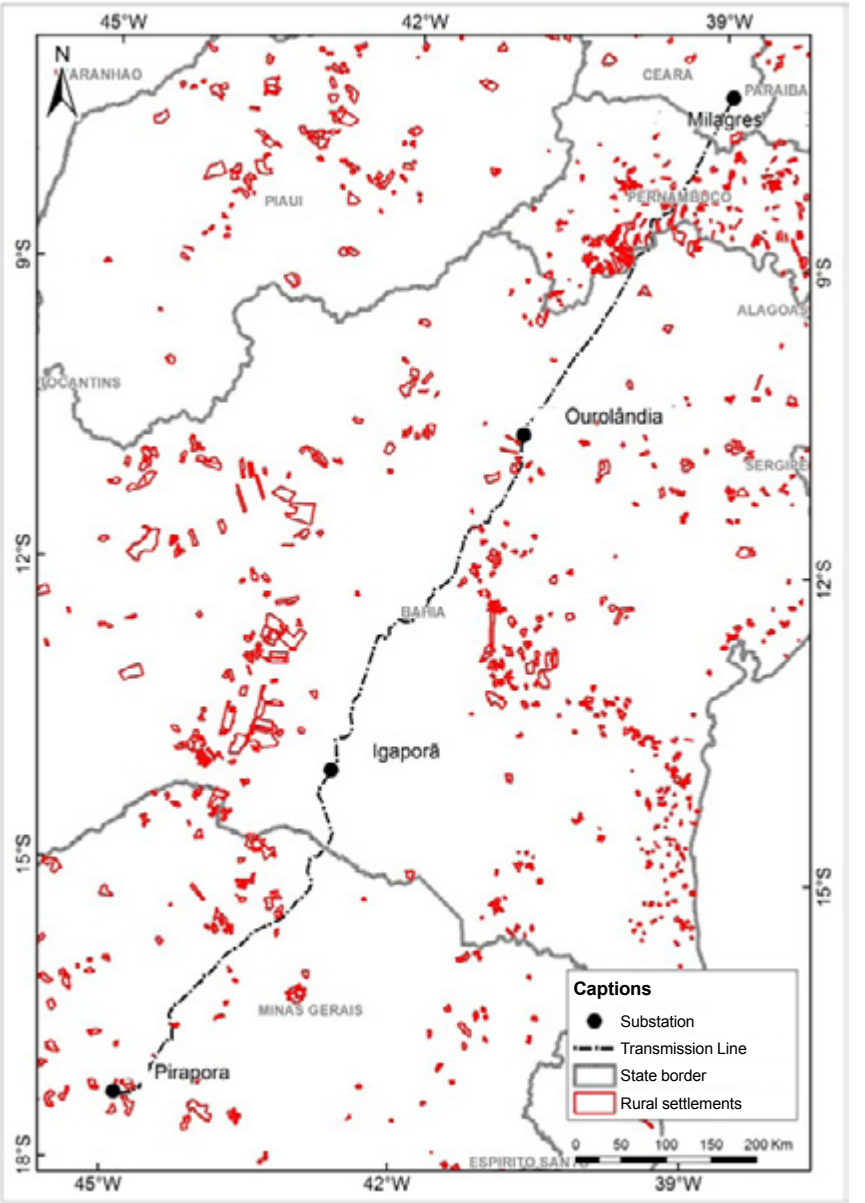

Figure 5.28: Rural settlements existing in the project implementation region. Source: adapted from Incra, 2015

The proposed line will not cross any agricultural settlement areas. However, there are some settlements located within the 30 km wide corridor. Following is a list of the communities existing in this corridor, so that during the implementation of the line, greater attention is given to these areas (Table 5.2:

Table 5.2: Agricultural settlements in the municipalities crossed by the corridor path being studied. Source: Incra, Sep/2016

State	Municipality	Community	Area (ha)	Capacity*	Creation
PE	Cabrobó	PA Juventude	1389.90	40	12/08/2005
PE	Orocó	PA Bom Jesus	361.50	60	08/13/1999
PE	Santa Maria da Boa Vista	PA Caraúbas II	392.92	40	10/24/2001
PE	Lagoa Grande	PA Madre Paulina	1733.57	62	10/02/2003
PE	Orocó	PA Várzea Grande	171.15	12	02/27/2007
PE	Cabrobó	PA Santana	166.43	5	09/12/1989
PE	Santa Maria da Boa Vista	PA Poço do ICG	893.23	26	12/27/1989
PE	Santa Maria da Boa Vista	PA Safra	3496.62	220	12/02/1996
PE	Santa Maria da Boa Vista	PA Vitória	4626.94	264	05/27/1997
PE	Santa Maria da Boa Vista	PA Boqueir	1695.27	105	06/30/1997
PE	Lagoa Grande	PA Jatobá	701.73	40	10/29/1997
PE	Lagoa Grande	PA Ouro Verde	547.84	100	12/19/1997
PE	Santa Maria da Boa Vista	PA Catalunha	6865.55	600	12/16/1998
PE	Santa Maria da Boa Vista	PA Aquarius	2889.97	150	12/27/1999
PE	Orocó	PA Alegre	3133.80	100	05/25/2000
PE	Santa Maria da Boa Vista	PA Brilhante	1794.74	55	05/25/2000
PE	Lagoa Grande	PA Riacho Fundo	483.12	35	06/12/2002
PE	Cabrobó	PA Poço da Umburana	873.05	20	07/17/2008
PE	Santa Maria da Boa Vista	PA Maristela Medrado	347.09	6	11/19/2002
PE	Parnamirim	PA Antônio de Linda	839.80	20	12/05/2002
PE	Santa Maria da Boa Vista	PA Chapada do Peba	246.03	10	12/5/2002
PE	Orocó	PA Maria Carolina	127.84	8	03/11/2003
PE	Cabrobó	PA Salãozinho	261.03	7	07/22/2004
PE	Santa Maria da Boa Vista	PA Denis Santana	1031.92	30	11/05/2008
PE	Santa Maria da Boa Vista	PA José Ivaldo	364.64	25	07/13/2005
PE	Santa Maria da Boa Vista	PA José Ivaldo I	804.44	50	08/23/2005
PE	Terra nova	PA Mororo dos Peixotos	2106.42	30	01/03/2007
PE	Orocó	PA Santo Antônio da Mandassaia	935.32	17	02/27/2007
PE	Orocó	PA Olho D'Água	130.47	6	02/27/2007
PE	Orocó	PA Vitorino	115.49	15	02/27/2007
PE	Lagoa Grande	PA Abreu e Lima I	1911.07	50	10/26/2007
PE	Santa Maria da Boa Vista	PA Nossa Senhora da Conceição	4237.62	140	08/13/1999
PE	Orocó	PA Casa Nova	121.22	4	11/30/2007
PE	Orocó	PA Gilda Gomes	1044.69	25	08/25/2008
PE	Terra Nova	PA Quilombola - Contendas	2177.71	46	02/07/2006
PE	Orocó	PA Demétrius	1558.88	30	01/15/2001
PE	Cabrobó	PA Varzinha	316.78	8	09/12/1989
PE	Cabrobó	PA Eloita Pereira	854.47	30	10/19/2007

State	Municipality	Community	Area (ha)	Capacity*	Creation
PE	Santa Maria da Boa Vista	PA Progresso	721.81	12	08/20/2010
PE	Santa Maria da Boa Vista	PA Portelinha	160.42	-	-
BA	Morro do Chapéu	PA Pachola	406.34	-	-
BA	Morro do Chapéu	PA Morrinhos	2118.80	63	02/23/1995
BA	Ourolândia	PA Lagoa de Dentro I e II	2320.04	40	12/19/2003
BA	Ourolândia	PA Vila Nova	2592.01	52	09/22/2005
BA	Campo Formoso	PA Moka	638.23	18	12/17/2008
BA	Bonito	PA Central	2993.59	150	12/18/1998
BA	Ourolândia	PA Santa Luzia	4862.58	64	12/22/2002
BA	Morro do Chapéu	PA Recreio	556.14	23	11/26/2002
BA	Jacobina	PA Pedra Vermelha	1896.08	-	-
BA	Morro do Chapéu	PA Fazenda Santa Ernestina	10873.01	300	08/14/1987
BA	Iraquara	PA Fazenda Reunidas FS	3196.46	120	08/10/2004
BA	Morro do Chapéu	PA Lagoinha e Boa Vista	1788.99	74	01/20/2004
BA	Bonito	PA Eugênio Lyra	1366.62	60	12/30/1996
MG	Nova Porteirinha	PA Dom Mauro	1876.53	46	04/22/2009
MG	Pirapora	PA Floresta/Viveiros	4745.22	60	09/18/2002
MG	Janaúba	PA Jacaré Grande	11227.97	200	09/22/1998
MG	Coração de Jesus	PA Irmã Doroty II	1737.79	30	11/12/2007
MG	Capitão Enéas	PA Darcy Ribeiro	1164.89	25	04/17/2007
MG	Porteirinha	PA João Paulo II	1154.44	20	09/13/2005
MG	Porteirinha	PA União	3138.62	49	03/20/2006
MG	Sao João da Lagoa	PA Posto Agropecuário	107.61	15	06/21/2006
MG	Várzea da Palma	PA M3E D'	4345.69	56	12/05/2007
MG	Várzea da Palma	PA Correntes	11628.38	238	08/10/2000
MG	Pirapora	PA Paco Paco	452.30	42	08/10/2000
MG	Várzea da Palma	PA Tanque/Rompe Dia	7911.82	94	03/07/2007

* Capacity: indicate the total agricultural areas that the settlement can support

The Comissão Pastoral da Terra elaborated the report on "Land Conflicts" every year. Thus, based on the analysis of the report for the year 2015, we were able to identify the information regarding land conflict that exist in the states where the project is located.

Table 5.3: Land conflicts in Brazil and in the states where the project is located. Source: adapted from CPT, 2016

	Land conflicts		Occupations		Encampments		Total	
	Occurrences	Families	Occurrences	Families	Occurrences	Families	Occurrences	Families
Northeast	255	26,280	60	6,413	2	255	317	32,948
CE	3	3,065	1	65	-	-	4	3,130
PE	20	3,493	13	1,870	0	0	33	5,363
BA	63	8,874	34	3,666	2	255	99	12,795
Southeast	73	5,264	36	3,071	3	575	112	8,910
MG	48	3,005	12	1,122	1	500	61	4,627
Brazil	**771**	**81,602**	**200**	**31,293**	**27**	**7,763**	**998**	**120,658**

As can be observed, the state that presents the largest number of land conflicts is Bahia, with almost one third of the total conflicts that occurred in the Northeast region in the year 2015, followed by Minas Gerais, Pernambuco, and Ceará. Regarding the total number of families involved in the conflicts, Bahia is again the state that involved the largest number of families, followed by Pernambuco, Minas Gerais, and Ceará, where, although only four conflicts occurred during that year, they involved over three thousand families.

5.3.3 Cultural and natural heritage

Caves are formed as a result of a series of geological processes involving chemical reactions, atmospheric and biological conditions. They have specific, and sometimes endemic, ecosystems adapted to the conditions presented, such as absence of light and vegetation. Some of them present vestiges of populations of old, since they are safe refuge areas, with a great variety of archaeological evidences and rock art. They present specific formations such as stalactites that work as evidence of past climatic conditions. They can also present fossils and testimonies of past geological processes.

The geological sites are areas that, due to their geologic, mineral or paleontological singularity are of interest to scientific, didactic or touristic studies. The set of geological sites found in a same region may be established as geoparks, conservation units, and protection areas. Their preservation is important due to their value for geoscience studies and their potential for tourism, and didactics activities. Thus, attention should be given to these areas when of the implementation of the project, since these areas could improve the development of certain regions, either for their potential for scientific studies or as a tourist attraction.

It is important to identify caves and geological sites to preserve their characteristics as much as possible, and to be careful when implementing certain types of projects in areas like these. That is the case for clastic terrains because, as they present a series of caves, some types of projects could cause land subsidence processes. Therefore, the geological assessment is extremely important.

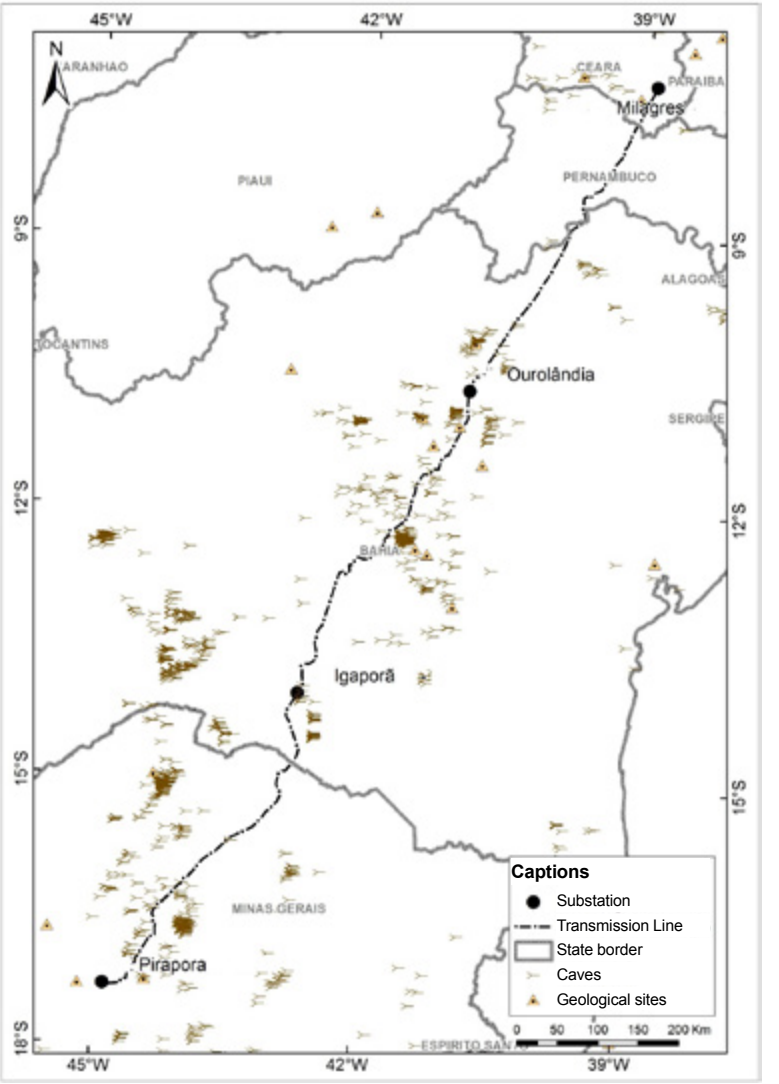

Figure 5.29: Caves and geological sites present in the project implementation region. Source: adapted from Cecav, 2015, and MMA, 2006

Figure 5.29 shows the caves and geological sites present in the project implementation area. We observe that there is greater concentration of caves in section 2. In the central area of the state of Bahia, an area that stands out for presenting clastic geology, and in section 3, in the state of Minas Gerais.

With regards to geological sites, there is a concentration of them in section 2, close to the Ourolândia substation and half way through the path. There are also some other geological sites close to the Pirapora substation.

5.3.4 Indigenous and quilombolic lands

The quilombolic lands or remaining territories of quilombolic communities are ethnic-racial territories, with collective occupation based on ancestry, kinship, and their own cultural traditions. These territories reflect the victory of the resistance to various forms of historical domination suffered, where the community recognizes itself as "remnant from quilombos," and the regularization of these territories is guaranteed by the Federal Constitution of 1988 (SILVA, 2015; ISA, 2016).

The assessment of the quilombolic territory is aimed at ensuring their social, physical, economic, and cultural integrity is maintained. The purpose of the regularization is to provide historical compensation aiming at ensuring the dignity and continuity of these ethnical groups.

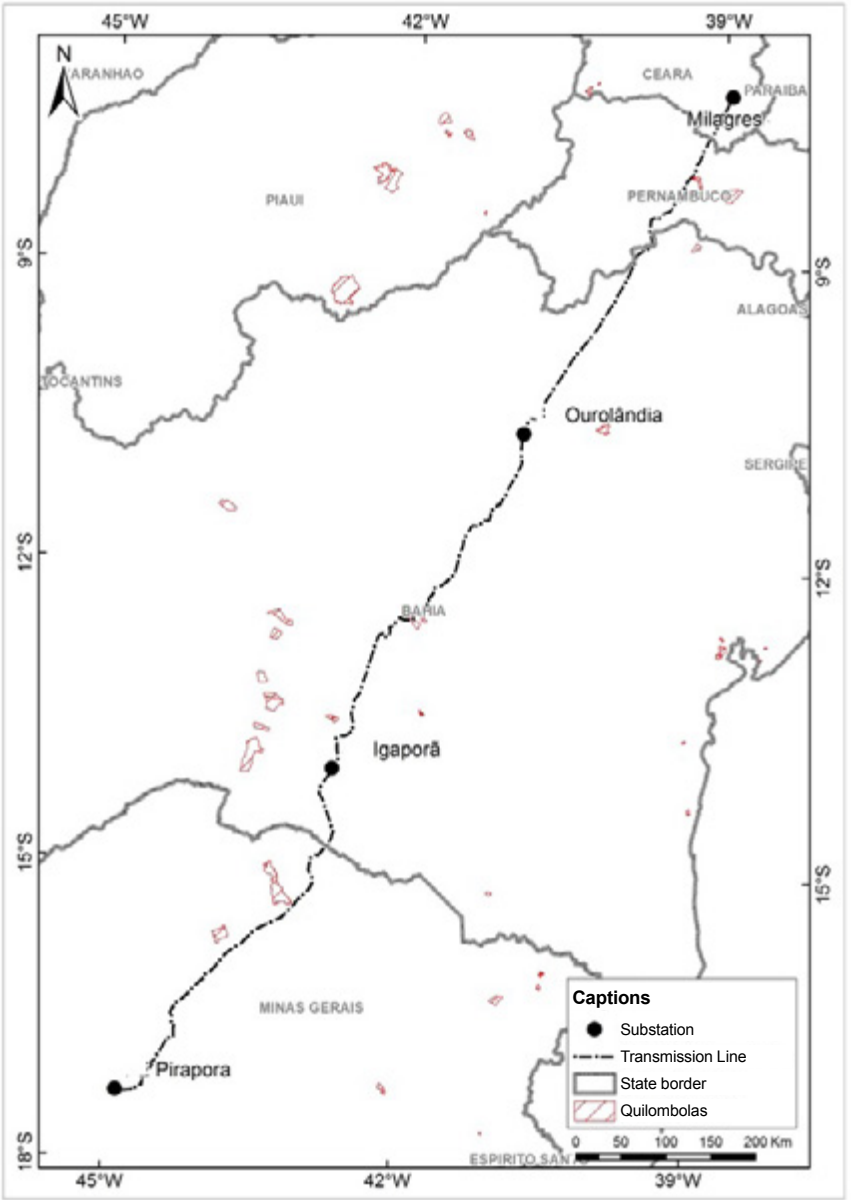

Figure 5.30: Quilombolic communities in the project implementation area.
Source: adapted from Incra, 2015

Table 5.4: Quilombolic communities in the municipalities crossed by the corridor path being studied. Source: Incra, Sep. 2016

State	Municipality	Community	Area (ha)	# of families	Date it was acknowledged	RTID Notice in DOU
BA	Seabra	Morro Redondo	5,068.79	67	04/03/2012	
BA	Seabra	Capão das Gamelas	1,316.16	60	10/25/2011	
BA	Seabra	Agreste	2,341.54	74	10/18/2010	
BA	Seabra	Olhos D'água do Basílio	4,842.41	73	11/26/2009	12/24/2010
MG	São João da Ponte/ Varzelândia/ Verdelândia	Brejo de Crioulos	17,302.69	387	12/24/2007	02/24/2011
MG	Jaíba/Gamaleiras /Porteirinha / Paipedro	Gurutuba	45,589.21	891		
PE	Salgueiro e Terra Nova	Contendas	2,128.20	43	10/27/2008	
PE	Salgueiro	Santana III	2,336.56	85	01/02/2011	

On the other hand, the indigenous populations are descendant from peoples who lived in what today is the Brazilian territory, before the arrival and settlement of the European peoples. This process of occupation by the Europeans resulted in the extinction of several indigenous peoples, and the reduction of the population of the communities that still exist.

According to Funai data, in the year 2010, the indigenous population was of less than one million inhabitants, and corresponded to 0.3% of the total population of Brazil. Therefore, the purpose of the indigenous territories is maintaining these remaining communities, thus, respecting their cultural and social characteristics, and their dignity.

Figure 5.31 shows the indigenous land areas regionally with regards to the line implementation area. As can be observed, the route of the main line does not cross any indigenous land area. However, near the corridor path being studied are the Truká Indigenous Territory (TI), in the municipality of Cabrobó-PE, and the TI Tumbalalá, in the municipalities of Abar and Curaçá, in Bahia.

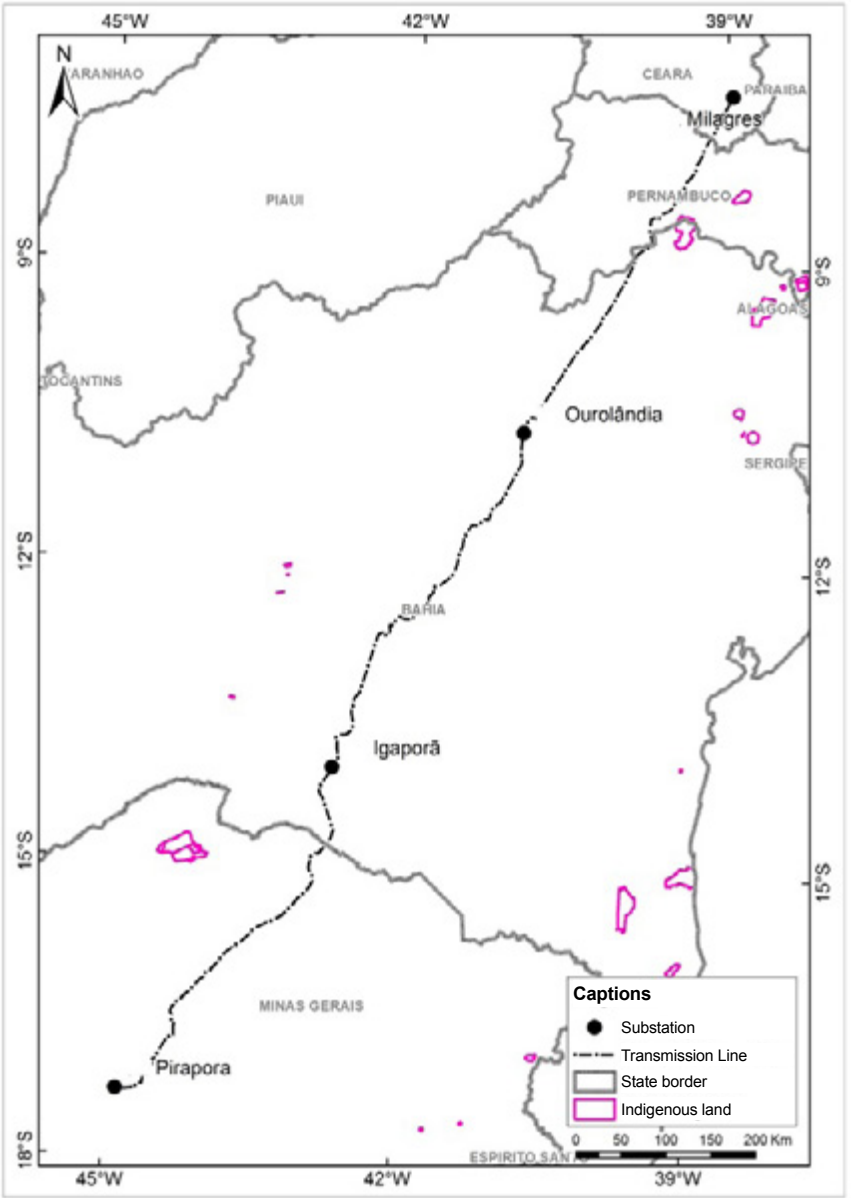

Figure 5.31: Indigenous lands in the project implementation area.
Source: adapted from Funai, 2015

5.4 Ecolgical Economic Zoning (EEZ)

We also collected information on the EEZs of the states involved in the project, so as to evaluate the areas that will be crossed by the line, and the possible existing constraints. Therefore, the states of Ceará, Pernambuco, Bahia, and Minas Gerais were evaluated.

In Ceará, the area where the line is to be implemented was covered by the "ecological economic zoning of the caatinga biome and wet ridges of the state of Ceará," which presents two distinct zones, the ZUSssc, and the ZUSsuc. Next is a description of both according to the EEZ technical report [48].

Sustainable Use and Natural Balance Conservation Zone of the Sertões do Salgado and Sertões do Cariri (ZUSssc) – Moderately Stable - It is the partially dissected pediplane surface area of the high Sertões do Salgado and Sertões do Cariri, in Ceará. It presents eco-dynamically moderately stable environments.

Sustainable Use and Natural Balance Conservation Zone of the Sertões Úmidos do Cariri (ZUSsuc) – Moderately Fragile – It is the flat surface area with swash and coalescence of alluvial plains in the foothills of the Chapada do Araripe. These environments are eco-dynamically moderately stable, where care must be taken when considering occupying these areas for the risks of biodiversity impoverishment caused by disorderly deforestation, deforestation in spring areas, and chemical contamination of soils and water resources.

For the state of Pernambuco, there is no Ecological Economic Zoning that covers the areas that the line will cross.

Bahia has established an EEZ that divides the state into thirty six zones. These zones are based on the relief compartments of the state, elaborated in the RADAM Brazil project, which compartmented the relief based on radar images elaborated in the 70s. For the entire stretch of the line, an analysis was conducted considering the relief compartments. In Bahia, the line will cross the zones defined with the following numbers: 17, 7, 15, 10, 9, 11, 8, and will come close to zone 5.

Following is a summarized description of each of these zones, comprising the geomorphological, vegetation, and socio-economic aspects presented in the EEZ report ZEE [33]:

Area 17 – Depressão Sertaneja de Curaçá – Curaçá semi-arid depression, in the heart of the caatinga, with goat breeding and copper mining. Indigenous population. Existence of historical and cultural heritage (Canudos).

Area 7 – Lowlands of the Salitre and Verde/Jacaré rivers – Lowlands of the Salitre and Verde/Jacaré rivers, in an area of arborescent caatinga, with temporary crops (castor bean) and permanent crops (sisal), irrigated agriculture, mining (ornamental rocks - Bege Bahia), and quilombolic communities (Campo Formoso).

Area 15 – Chapada de Morro do Chapéu – Morro do Chapéu tableland with savanna, seasonal forest, and caatinga. Protected area at Morro do Chapéu (Park). Agriculture and livestock farming with polycultures, irrigated crops, and cattle farming, as well as mining. Quilombolic communities and pastures. Tourism at Morro do Chapéu.

Area 10 – Chapada de Irecê – Irecê tableland in the middle of caatinga, and with activities related to temporary grain crops, livestock farming, strutioculture (ostrich), mining (phosphate – Irecê), urban concentration (Irecê), and quilombolic communities (São Gabriel, Jussara, Ibititá, and Canarana).

Area 9 – Chapada Diamantina and Serra do Espinhaço – Diamantina tableland and Serra do Espinhaço with savanna and mountain forest preserved, Agriculture, highlight for mining, especially in Caetité, production of cachaça (sugarcane liquor) in Abaíra, and wind power generation. Quilombolic communities, pastures, indigenous population, and fishermen. In addition to mining, tourism stands out (Lençóis, Palmeiras, Mucugê, and Rio de Contas).

Area 11 – Gerais da Diamantina – Gerais da Diamantina in the middle of savanna, and contact between savanna/seasonal forest/caatinga, with agriculture and livestock farming, and irrigated crops. Highlighting the coffee production at Piatã.

Area 8 – Guanambi and Paramirim Depressions – Guanambi and Paramirim Depressions in the middle of caatinga, with productive arrangements of cotton, corn and cassava, livestock farming, mining (lead, zinc, silver, and ornamental rocks). Urban concentrations (Guanambi and Bom Jesus da Lapa), and religious tourism (Bom Jesus da Lapa).

Area 5 – Médio São Francisco Depression – Médio São Francisco Depression in area of seasonal forest, with agricultural production of cassava and other products, irrigated agriculture, fruit farming, livestock farming, rural settlements, mining (rare earths), quilombolic communities (Bom Jesus da Lapa, Malhada, Sítio do Mato, and Muquém de São Francisco).

In the state of Minas Gerais in the EEZ-MG (2007), Areas for Development were defined. The line is concentrated mainly in areas defined as areas for development 5 and 6, also crossing some stretches of areas for development 1 and 2. The areas for development were defined based on an integrated analysis of natural vulnerabilities and social potential.

Following is a description of each of the Areas for Development (EEZ-MG 2007) that are crossed by the line:

- Area for Development 1: This area is composed of class AA (Lands of low vulnerability in places of high social potential) of the Ecological Economic Index (EEI). These are areas of high social potential, which assume conditions for management of larger projects that might cause greater socio-environmental impacts. They are characterized for their capacities at strategic, tactic, and operational levels, and being easily stimulated to leverage local sustainable development. In this area, the locations are less environmentally vulnerable, the entrepreneurs have better conditions for implementing impact preventative and mitigation actions.

- Area for Development 2: This area is composed of class AB (Lands of high vulnerability in places of high social potential) of the EEI. These are areas of high social potential, which assume conditions for management of larger projects that might cause greater socio-environmental impacts. They are characterized for their capacities at strategic, tactic, and operational levels, and being easily stimulated to leverage local sustainable development. In this area, the locations are more environmentally vulnerable, the entrepreneurs should seek to implement a wider variety of impact preventative and mitigation actions.

- Area for Special Development 5: This area is composed of class BB (Lands of high vulnerability in places of medium social potential) of the EEI. These are areas of intermediate social potential and high natural vulnerability, which require actions that promote development, considering that the environment presents low resilience capacity, reducing the effectiveness of mitigation actions, or rendering them unfeasible.

- Area for Special Development 6: This area is composed of class CB (Lands of high vulnerability in places of low social potential) of the EEI. These are areas of low social potential and high natural vulnerability, depending on direct and constant assistance from the state or federal government in basic areas of development, considering that the natural environment is a limiting element.

In addition to these, there is also the EEZ of the Basin of the São Francisco River, but maps were elaborated only on a regional scale, with no standardization of the use of the areas.

6. Integrated Analysis and Definition of Areas of Greater and Lesser Socio-environmental Sensitivity

The integrated analysis of the variables considered for the socio-environmental assessment and field work developed by the multidisciplinary team (with knowledge of archeology, cultural and social heritage, physical and biotic environments), on August 2016, allowed for the elaboration of a characterization that considers the main socio-environmental factors, and their respective sensitivity level.

Based on secondary data from specialized official databases, a sensitivity map was elaborated considering the areas of greater and lesser criticality, with the purpose of indicating the areas of greater and lesser sensitivity for implementation of the project.

Thus, by means of a Geographic Information Systems (GIS), sensitivity values were assigned to the different types of socio-environmental variables, so that they could compose the sensitivity mapping for the area under analysis. These values were evaluated in the field work conducted.

To elaborate the mapping, the variables were characterized as presented in Table 6.1.

Table 6.1: Variables and sensitivity

Socio-environmental variable	Data source	Application	Sensitivity
Rural Settlements	Incra	Polygon classification	High
Quilombolic Areas	Incra	Polygon classification	High
Indigenous Lands	Funai	Polygon classification	High
Built Areas	IBGE	Polygon classification	High
Caves	Cecav	300 m Buffer	High
Geological Sites	Sigep	300 m Buffer	High
Archaeological sites	Iphan	300 m Buffer	High
Railways	IBGE	50 m Buffer to each side	High
Roads	IBGE	50 m Buffer to each side	High
Transmission Lines	Aneel	50 m Buffer to each side	High
Airports/Airfields	IBGE	1000 m Buffer	High
Relief Compartmentation	CPRM	Polygon classification	High/Medium/Low
Priority Areas for Conservation	Probio	Polygon classification	High/Medium/Low
Integral Protection Conservation Unit	ICMBio	Polygon classification	High
Sustainable Use Conservation Unit	ICMBio	Polygon classification	Medium

Based on the characterization of the variables, the sensitivity mapping was elaborated. Since this is a map that integrates various types of socio-environmental information available, it is an essential instrument that synthesizes the context in which the line will be implemented.

The representation of these variables in the sensitivity mapping was achieved with the use of polygons, lines, and dots, with or without a buffer area. Buffers were used to give more adequate emphasis to the areas of lesser spatial expression.

High, medium, and low classes were used for sensitivity, and the areas classified as high sensitivity should be avoided, since they are more critical for the implementation of the line. The areas of medium sensitivity require special attention for the implementation of the line. The areas of low sensitivity present fewer problems and obstacles to the installation of the line.

The mapping was elaborated considering a 30 km wide corridor from a central axis that connects all the substations involved, and the preferred route for the installation of the line.

The areas of rural settlements, quilombolic, indigenous lands, and built areas were represented in the form of polygons, which are classified of high sensitivity areas in their entirety. They were represented colored in red (See Figure 6.1). They were classified as high sensitivity due to the existing conflicts for the use of these lands. The consolidation of these areas involves a conflict and historical context, and it is preferable to divert from these areas to prevent problems for the development of the project, and conflicts with the communities already settled in the area where the line is to be implemented.

The areas of caves, geological and archaeological sites were represented with dots and, from these dots, a buffer of 300 meters was generated, with these areas being classified as high sensitivity areas, represented in the color red. These areas are classified as high sensitivity areas due to their historical and scientific value, and the tourism potential they present, thus, it is preferable to divert from these areas.

The areas of railroads, roads, and transmission lines are represented by lines, and for those, a buffer of 50 meters was generated. These areas were classified as high sensitivity areas due to the difficulties that involved their crossing by the transmission line. It is important to highlight that it is preferable to implement the line in the proximity of roads, so as to make the logistics easier, both for installation and maintenance of their structures. As for airports and airfields, we considered a buffer of 1,000 meters, with the sensitivity of these areas considered as high.

For the entire area of the 30 km corridor in which the line is to be implemented, the relief was characterized in terms of sensitivity classes. This procedure was performed using the geomorphological compartment classification of the CPRM mapping (2010, 2014), indicated in classes of low, medium, and high sensitivity (Table 6.2). The compartmentation of the relief expresses a synthesis of the predominant types of soils, and the lithological pattern. Thus, this is an extremely relevant variable in the studies for the implementation of the line. Some areas were classified with more than one sensitivity class, because in the field we observed that some places were more sensitive than others. Therefore, the sensitivities of these compartments were defined differently, and based on observations made on the field.

Table 6.2: Sensitivity values for the various geomorphological compartmentations

Geomorphological compartmentation	Sensitivity
Tablelands and plateaus	Low
Structural steps and erosive ridges	Medium
Mostly wide and gentle slopes	Low
Mostly dissected slopes and low hills	Medium
Mostly low hills and ridges	High
Mostly mountains	High
Ridge escarpments	Medium
Inselbergs	High
Plateaus	Low
Plateaus and low plateaus	Low/Medium
Fluvial or fluvial-lacustrine plains	High
Preserved flattened surfaces	Low
Degraded flattened surfaces	Low/High
Tablelands	Low
Dissected tablelands	Low
U-shaped valleys	High
Slopes covered with slope deposits	Low

The priority areas for conservation defined by Probio (2016) were also characterized. This mapping classifies the areas according to their degree of biological importance, varying between high, very high, and extremely high. The classes were validated by means of field work, and these areas were classified into sensitivity classes, varying between high, medium, and low sensitivity, as presented in Table 6.3.

Table 6.3: Sensitivity classification of the priority areas existing in the project area

Biological importance	Sensitivity	Characteristics of the priority area
Extremely high	Medium	Threatened deciduous forest in priority area.
Extremely high	High	Fauna and flora endemism, remnants of Atlantic Forest, creation of CU.
Extremely high	High	Limit of distribution of the Lear's macaw and reintroduction of the little blue macaw (extinct in nature).
Extremely high	Low	Vegetable and ecotone fragments of caatinga and savanna.
Extremely high	High	Flora endemism, physiognomy diversity, ecotone of caatinga and savanna.
Extremely high	High	Discovery of new species, concentration of caves, creation of CU.
Extremely high	Low	Ecotone with area of high altitudes and thermal waters.
Extremely high	High	Areas with well-preserved vegetation cover, and presence of indigenous community (Kariris).
Extremely high	Medium	Presence of settlement, and fragments of preserved natural vegetation.
Extremely high	High	Presence of riverside community.
Extremely high	High	Remnants of preserved vegetation, and presence of one of the world's largest fossiliferous deposits.
Extremely high	High	Fauna and flora endemism. State UC, rocky field.
Extremely high	High	Revitalization of the São Francisco (riparian woods), for starting the transposition.
Extremely high	High	Protection of rocky fields.
Extremely high	High	Remnants of vegetation with high fauna and flora diversity, aquifer recharging.
Extremely high	High	Studies related to the reintroduction of the little blue macaw.

The Conservation Units (CUs) polygons were also classified. The CUs (ICMBio, 2016) are classified into two main types: "Integral Protection" and "Sustainable Use." Thus, the Integral Protection CUs were classified as high sensitivity because these are areas where no type of use is permitted, while the Sustainable Use CUs were classified as medium sensitivity, because these are areas where some types of use are permitted.

Based on the variables presented, and on the weight attributed to them, next, we present an analysis of each of the three sections were the line is to be implemented, with detailing of the higher sensitivity areas.

To make the description and location of the area analyzed easier, we created points in each vertex of the preferred route of the line indicated in this study. The vertices were named according to the section in which they are located, and in increasing numbers from north to south. There are 98 points in section 1, 102 in section 2, and 107 in section 3.

6.1 Milagres (Ceará) to Ourolândia (Bahia) Section

The first section (Figure 6.1) corresponds to the connection between the Milagres substation, located in the state of Ceará, and the Ourolândia substation, located in the state of Bahia, and presents 98 vertices that were named T1-1 to T1-98, with T1-1 being located closest to Milagres, and T1-98 closest to Ourolândia. In the portion of the territory in the state of Ceará, the higher sensitivity is associated with a large number of archaeological sites to the north, in the proximities of the municipality of Milagres. There is also the occurrence of river plains (T1-4, T1-6, and T1-18) with the presence of hydromorphic soils that, present higher sensitivity, since the crossing at these points would require greater care and costs.

More to the south, there is an area with mostly low hills and ridges between vertices T1-28 and T1-37, which is approximately 7 km long, and presents greater sensitivity to the implementation of the transmission line because, in addition to having vegetation cover that is slightly better preserved, is at the limit of the Chapada do Araripe Sustainable Use Conservation Unit, a CU that is crossed again on the border of the states of Ceará and Pernambuco, between points T1-41 and T1-42.

There are also some road crossings, the route and buffer area of which are defined as high sensitivity areas.

In the state of Pernambuco, we highlight the presence of agricultural settlements as high sensitivity points. In the north of Pernambuco, there is an area of dissected slopes and low hills that is approximately 20 km long, and part of the T1-48 to T1-51 stretch and presents medium sensitivity. To the south, the line will cross some areas that present small mountain alignments, composed of inselbergs and witness hills, with these areas being characterized as high sensitivity due to the difficulties in crossing it, and frequent presence of endemic species, or better preserved vegetation fragments, so these stretches of the line should be diverted (T1-65 to T1-69).

In the limit of the states of Pernambuco and Bahia is the crossing of the São Francisco River, which consists in a critical stretch, presenting high sensitivity because of the technical difficulties for crossing this large river (T1-75 to T1-79).

In the north of Bahia, we also highlight the priority area where the little blue macaw is being reintroduced in nature; this is an endangered species and care must be taken in this area not to advance over the more preserved areas, thus this area is classified as high sensitivity (T1-76 to T1-84).

Finally, we highlight an extensive area of plateaus and low plateaus, which extends from 100 km before the Ourolândia substation (T1-91 to T1-98), up to 70 km after this same substation (T2-1 to a little before T2-5). This area presents a more flattened relief, but with clastic basement that gives rise to caves as can be observed in the Cecav cave information base, where we verify a large concentration of caves in this compartment. Therefore, this variable should be considered when of the implementation of the line in this medium sensitivity stretch.

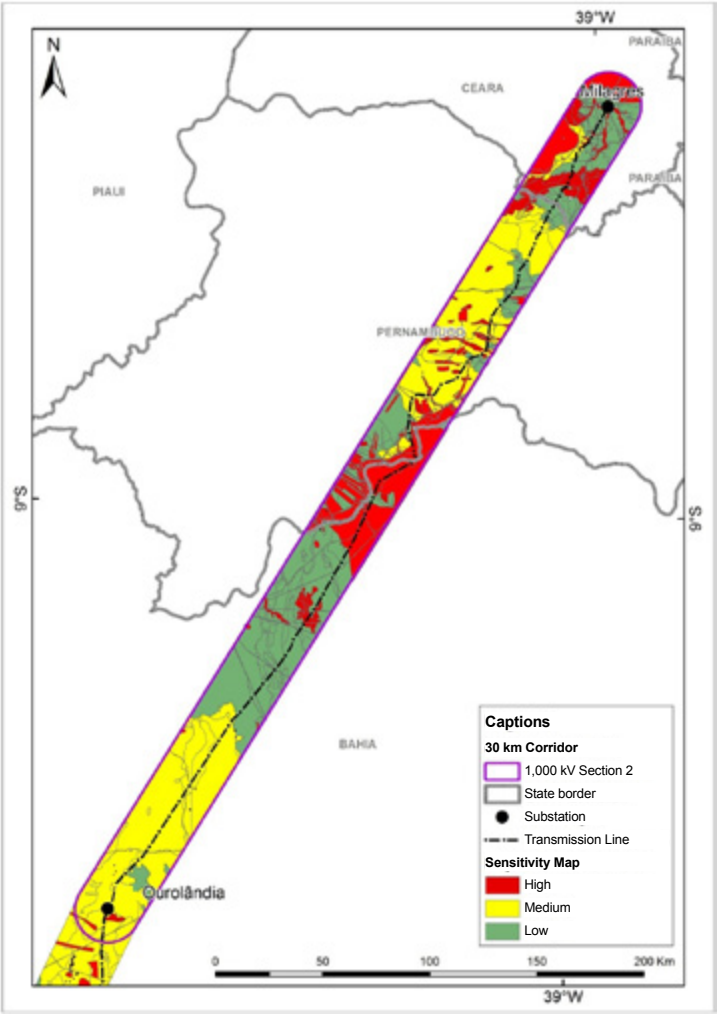

Figure 6.1: Sensitivity map elaborated based on the variables analyzed. Section 1: Milagres (Ceará) to Ourolândia (Bahia)

6.2 Ourolândia (Bahia) to Igaporã (Bahia) Section

The second section (Figure 6.2) corresponds to the connection between the Ourolândia substation and the Igaporã substation, both located in the state of Bahia, and presents 102 vertices that were named T2-1 to T2-102, with T2-1 being located closest to Ourolândia, and T2-102 closest to Igaporã.

In the proximity of the Ourolândia substation, to the south, there are some agricultural settlements that present high sensitivity, and to the west of the area between vertices T2-3 to T2-4 there is a set of caves that, with their buffer, present high sensitivity. The caves are associated to the clastic basement of the plateaus and low plateaus relief compartment, as described in the previous sub item.

In this section, there is also the Morro do Chapéu State Park (T2-13 to T2-15), an Integral Protection Conservation Unit, which means no intervention is permitted, and it is marked as high sensitivity in the mapping. The line will pass near this CU, in an area that presents low ridges and hills and is approximately 3 km long. To the south of the CU there are also some agricultural settlements.

In the central portion of this stretch of the line, there is the Marimbus/ Iraquara Sustainable Use Conservation Unit, the sensitivity of which is medium (T2-32 to T2-36). Within the limits of this CU, there are several high sensitivity caves and the limits of an environmental protection area related to these caves, the limits of which have been classified as high sensitivity. Sections of this CU are inserted in an area with mostly low hills and ridges, and the extension of this area to be crossed by the TL is of approximately 7.5 km, between vertices T2-32 to T2-39. At approximately 20 km from the end of this stretch, there is another segment of the same low hills and ridges domain that is approximately 6.5 km long, starting a little before vertex T2-50, and ending a little after vertex T2-53, and which presents high sensitivity because of the difficulties the crossing of these stretches implies.

A little more to the southeast, there are high sensitivity quilombolic communities (T2-52 to 2-59). The quilombolic communities are delimited based on the historical relationship of the community with the territory in which they are located and, thus, they present high sensitivity for the implementation of the line, since the line would interfere in a historically consolidated space.

After the areas of these quilombos, there is a long stretch of mostly mountainous domain to be crossed by the line, with a length of approximately 37 km (T2-59 to T2-84), and presenting high sensitivity because of the relief obstacles it imposes to the installation of the line. Closer to the Igaporã substation, there is another stretch of mostly mountainous domain going from vertex T2-86 to T2-101, with the most critical part being from vertex T2-94 to

T2-97 and a length of approximately 8 km, and ending close to the urban area of the municipality of Igaporã. This alignment of high hills presents a complex of aero generators installed in its ridge line, and so this complex will require attention when of the implementation of the line.

To the east of the Igaporã substation, there are several archaeological sites associated to a section of the geomorphological compartment of higher altitude, but more flattened, consolidating an area of high sensitivity for the implementation of the line.

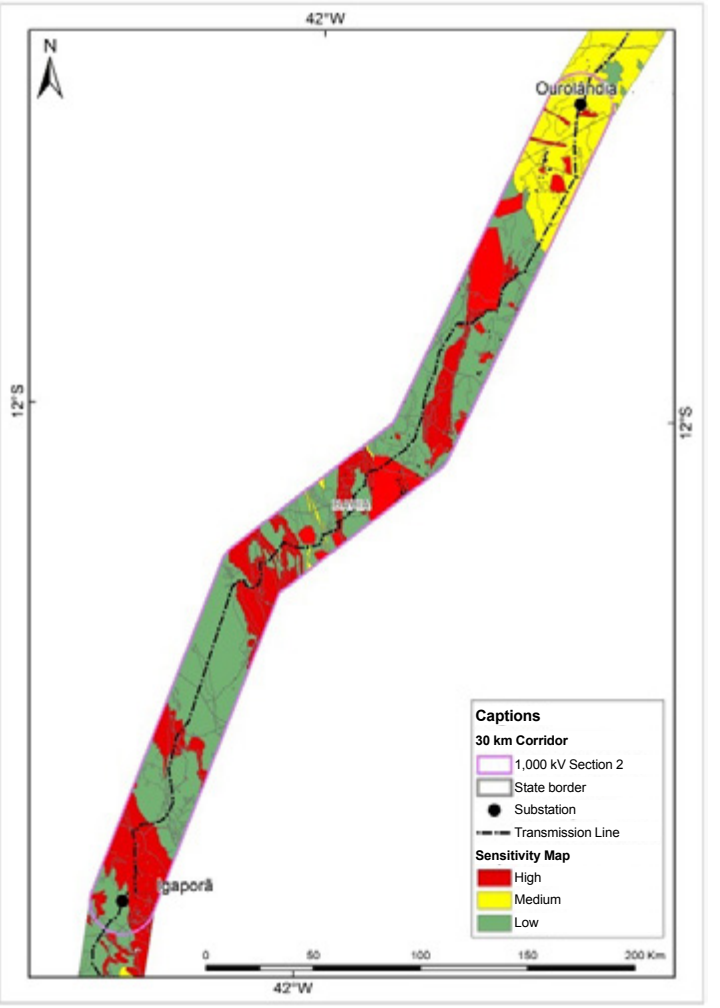

Figure 6.2: Sensitivity map elaborated based on the variables analyzed. Section 2: Ourolândia (Bahia) to Igaporã (Bahia)

6.3 Igaporã (Bahia) to Pirapora (Minas Gerais) Section

The third section (Figure 6.3) corresponds to the connection between the Igaporã substation, located in the state of Bahia, and the Pirapora substation, located in the state of Minas Gerais, and presents 107 vertices that were named T3-1 to T3-107, with T3-1 being located closest to Igaporã, and T3-107 closest to Pirapora.

To the south of the Igaporã substation, starting from the urban area of the municipality of Guanambi, the main axis of the line extends over a stretch of approximately 100 km (T3-4 to T3-44), alternating areas of fluvial plains with presence of hydromorphic soils, and areas of dissected hills and low hills. There are also two Integral Protection Conservation Units to the west of this axis: Serra dos Montes Altos State Park (to the west of stretch T3-6 to T3-7), and the Caminho das Gerais State Park (to the west of stretch T3-16 to T3-44), and an area of mountainous domain and high amplitude to the east, with this stretch consisting of a critical area for the installation of the line.

Starting from vertex T3-44, starts a flatter stretch, parallel to the Ferrovia Centro-Atlântica S.A. and BR 122, and which presents areas of fluvial plains with hydromorphic soils. To the west of T3-46, there is the Gurutuba quilombolic community and, close to this community, there is an agricultural settlement, with both areas being classified as high sensitivity. There is a larger concentration of agricultural settlements and quilombolic communities in the stretch of the line that goes from T3-46 to T3-56.

From the section where the main axis of the line crosses state highway MG-401 (T3-49), there are some high sensitivity clusters of caves in the corridor of the axis of the line. Some of these caves are close to settlements and quilombos.

When approaching the urban area of the municipality of Coração de Jesus (located to the west of T3-82), it is advised that the main axis of the line is diverted to the east of the urban area, seeking to avoid passing through the degraded flattened surface relief located in this portion closest to Pirapora. The work developed in the field showed that in this portion of flattened surfaces there is little logistics access, a large number of veredas, paleontological and archaeological sites, and caves, thus being a critical and highly sensitive area that should be avoided.

When approaching the Pirapora substation, it is recommended to maintain this detour more to the east, since at approximately 2.5 km to the north there is an airport, the São Francisco River plain, and an extensive agricultural settlement, located mostly on a tableland compartment (west of the stretch that goes from T3-98 to T3-104).

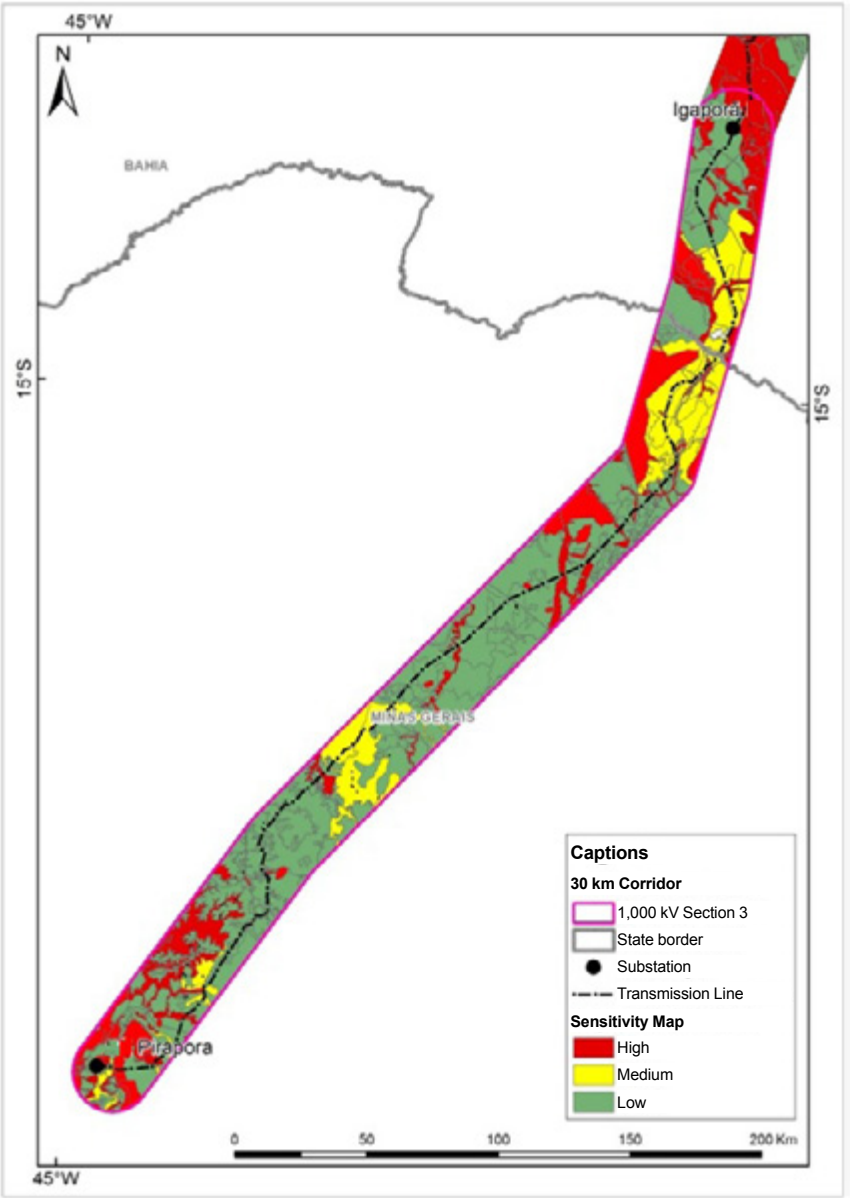

Figure 6.3: Sensitivity map elaborated based on the variables analyzed. Section 3: Igaporã (Bahia) to Pirapora (Minas Gerais)

7. Recommendations and Preferred Route for the Line Path

Base on the data assessment conducted in this work, the analyses and validations performed during field work, and the sensitivity mapping, we have elaborated a proposal for the preferred route for implementation of the transmission line, considering all the socio-environmental issues.

This proposal was made using secondary data obtained from official federal and state databases related to the socio-environmental themes, and also through on-site validation performed by means of field work.

To support the definition of the main route of the line, we used the sensitivity mapping that presents an integrated analysis of the variables used. The analysis of the socio-environmental sensitivity categorization allowed for better understanding of the context in which the line will be inserted, establishing conditions for the definition of the preferred route for its implementation.

To consolidate the preferred route, we elaborated a preliminary path based on the secondary data from the official databases available, which constitute socio-environmental variables as presented in Table 7.1.

Table 7.1: Secondary data from official databases used in the study

Socio-environmental variable	Data source	Data format
Rural Settlements	Incra	Polygon
Quilombos	Incra	Polygon
Indigenous Lands	Funai	Polygon
Built Areas	IBGE	Polygon
Caves	Cecav	Dot
Geological Sites	Sigep	Dot
Archaeological sites	Iphan	Dot
Railways	IBGE	Line
Roads	IBGE	Line
Transmission Lines	Aneel	Line
Airports/Airfields	IBGE	Dot
Relief Compartmentation	CPRM	Polygon
Priority Areas for Conservation	Probio	Polygon
Integral Protection Conservation Unit	ICMBio	Polygon
Sustainable Use Conservation Unit	ICMBio	Polygon

We analyzed the presence of these variables in a 30 km wide corridor, from a central axis that starts at the municipality of Milagres, and goes all the way to the municipality of Pirapora, intermediately connecting the other two substations of Ourolândia and Igaporã, both in the state of Bahia.

Thus, the purpose was defining a line path that would deviate from conservation units, indigenous lands, priority areas for conservation, presence of caves, remnants of vegetation, proximity to urban areas, agricultural settlements, quilombos, geological sites, archaeological sites, hydromorphic soil areas, ridge areas, high hills, and the crossing of large rivers, mainly the São Francisco River.

Based on this preliminary path, we assessed the critical points to be observed and validated on the field. As an ancillary tool, we used the Google Earth software that, in addition to allowing for a pre-evaluation with some adjustments, also contributed to the planning of the field work logistics.

With the preliminary path in hand, the next stage was the verification on-site, so as to validate the path. During the field work, the purpose was to travel the area of this preliminary path, evaluating the following aspects:

- Evaluation of the access to the line implementation area;
- Evaluation of the existing logistic support in the proximities of the line implementation area;
- Validation of socio-environmental variables obtained from secondary data;
- Evaluation of points of doubts;
- Evaluation of vegetation fragments to be crossed by the line, and their conservation state;
- Evaluation of the areas of fluvial plains to be crossed by the line, to verify their extension and the hydromorphic soils;
- Evaluation of the archaeological sites close to the line implementation area;
- Evaluation of the hills and ridge stretches to be crossed by the line, to identify the most adequate locations for the line to pass;
- Existence of aero generators field in the line path, and deviation points;
- Evaluation of the existence of airports and airfields in the proximity of the line;
- Evaluation of the existence of villages in the path elaborated for the line;
- Evaluation of the Priority Areas crossed by the line;
- Evaluation of the best stretches for crossing Roads and Railroads;
- Verification of the existence of any settlements, quilombolic, or indigenous lands that might not be present in the official databases;
- Observation of existing patterns of crop and pasture areas.

Based on the information collected on the field, it was possible to make new adjustments on the existing path, taking into account the socio-environmental factors.

We sought to make the adjustments in the preliminary path within the 30 km wide corridor initially characterized. However, in the field, we observed that for some areas a greater detour was necessary, thus optimizing the route, and preventing increased costs and bureaucratic issues that would have to be resolved for implementation of the line.

Along the path, some occasional adjustments were made, aiming at diverting the path of the overhead lines from areas of fluvial plains with hydromorphic soils, diverting from some existing residual hills and inselbergs, trying to have the line pass along its side to avoid unnecessary altimetric variations in the terrain. We also sought to divert from urban areas and small villages, and areas with greater archeological potential. In the areas composed of vegetation fragments, we tried to adjust the path to areas with less preserved vegetation fragments, and, in the ridge areas, we looked for points that were more adequate for the line to cross.

Table 7.2 shows the vertices of the preferred route of the line, with respective coordinated, partial and progressive distances, and deflections in degrees. The start is at the Milagres substation (Ceará), with T1-1 being the first vertex after leaving the substation.

Table 7.2: Table of Vertices of the TL Route

SE MILAGRES (CE)						
Vertices	Time zone	Coordinates UTM Datum SIRGAS 2000		Distance (m)		Deflections (decimal degree)
		E	N	Partial	Progressive	
T 1-1	24	507,129.583	9,192,138.149	581.18	581.18	-
T 1-2	24	507,115.339	9,191,557.142	655.41	1,236.60	25,446 D
T 1-3	24	506,819.312	9,190,972.391	680.32	1,916.91	5,816 E
T 1-4	24	506,575.121	9,190,337.408	403.56	2,320.47	9,587 E
T 1-5	24	506,495.021	9,189,941.875	653.36	2,973.83	44,526 D
T 1-6	24	505,953.526	9,189,576.277	11,709.56	14,683.39	28,813 E
T 1-7	24	500,608.097	9,179,158.017	378.40	15,061.79	8,899 E
T 1-8	24	500,489.518	9,178,798.678	555.42	15,617.22	10,211 D
T 1-9	24	500,224.722	9,178,310.438	1,358.22	16,975.43	5,164 E
T 1-10	24	499,687.294	9,177,063.073	384.23	17,359.66	10,266 E
T 1-11	24	499,600.585	9,176,688.760	173.88	17,533.54	65,788 D
T 1-12	24	499,429.997	9,176,655.078	369.63	17,903.17	29,025 E
T 1-13	24	499,147.652	9,176,416.524	453.36	18,356.53	5,763 E
T 1-14	24	498,832.480	9,176,090.637	651.01	19,007.53	32,496 E

SE MILAGRES (CE)						
Vertices	Time zone	Coordinates UTM Datum SIRGAS 2000		Distance (m)		Deflections (decimal degree)
		E	N	Partial	Progressive	
T 1-15	24	498,702.176	9,175,452.804	752.94	19,760.48	6,132 D
T 1-16	24	498,473.531	9,174,735.416	1,666.49	21,426.97	32,248 D
T 1-17	24	497,198.315	9,173,662.565	1,274.37	22,701.33	8.41 D
T 1-18	24	496,113.656	9,172,993.594	974.82	23,676.15	9,874 E
T 1-19	24	495,383.998	9,172,347.164	1,214.94	24,891.09	4,364 E
T 1-20	24	494,538.560	9,171,474.637	2,260.82	27,151.90	4,259 E
T 1-21	24	493,090.260	9,169,738.629	670.59	27,822.49	42,255 E
T 1-22	24	493,118.547	9,169,068.636	786.57	28,609.06	5.65 D
T 1-23	24	493,074.196	9,168,283.320	1,653.96	30,263.02	10,035 D
T 1-24	24	492,694.623	9,166,673.504	1,399.86	31,662.88	10,047 D
T 1-25	24	492,140.586	9,165,387.954	1,447.26	33,110.14	1.74 D
T 1-26	24	491,527.701	9,164,076.872	1,142.22	34,252.36	21,322 E
T 1-27	24	491,453.350	9,162,937.070	1,302.90	35,555.26	3,195 D
T 1-28	24	491,296.205	9,161,643.679	1,028.68	36,583.94	24,751 E
T 1-29	24	491,611.070	9,160,664.377	1,245.83	37,829.77	43,163 D
T 1-30	24	491,077.874	9,159,538.417	948.14	38,777.90	10,837 D
T 1-31	24	490,518.203	9,158,773.086	1,096.10	39,874.00	1,254 D
T 1-32	24	489,851.982	9,157,902.694	2,470.55	42,344.55	26,122 E
T 1-33	24	489,367.507	9,155,480.118	1,408.59	43,753.14	5,467 E
T 1-34	24	489,224.135	9,154,078.840	1,655.05	45,408.19	76.23 D
T 1-35	24	487,584.908	9,153,850.552	3,255.79	48,663.98	54,895 E
T 1-36	24	486,097.864	9,150,954.196	216.89	48,880.87	18,127 D
T 1-37	24	485,943.688	9,150,801.649	348.69	49,229.56	29,284 E
T 1-38	24	485,847.456	9,150,466.503	1,206.03	50,435.58	11,159 D
T 1-39	24	485,296.575	9,149,393.642	483.05	50,918.64	8,946 E
T 1-40	24	485,145.435	9,148,934.841	439.32	51,357.95	18,793 D
T 1-41	24	484,880.889	9,148,584.108	4,573.57	55,931.53	9,844 E
T 1-42	24	482,791.582	9,144,515.648	1,298.84	57,230.37	6,142 D
T 1-43	24	482,078.024	9,143,430.374	1,257.62	58,487.98	3,252 D
T 1-44	24	481,328.611	9,142,420.435	1,001.68	59,489.66	14,233 E
T 1-45	24	480,947.801	9,141,493.963	640.06	60,129.72	1,401 D
T 1-46	24	480,690.067	9,140,908.088	724.29	60,854.02	7,839 E
T 1-47	24	480,491.567	9,140,211.526	584.87	61,438.88	2,995 D
T 1-48	24	480,302.106	9,139,658.195	5,718.76	67,157.65	8,293 D
T 1-49	24	477,688.579	9,134,571.575	840.11	67,997.75	33,665 E
T 1-50	24	477,783.251	9,133,736.820	918.41	68,916.16	25.69 D
T 1-51	24	477,480.928	9,132,869.600	806.97	69,723.12	20,539 D
T 1-52	24	476,964.828	9,132,249.246	980.19	70,703.32	13,023 D
T 1-53	24	476,184.269	9,131,656.366	2,238.42	72,941.74	38,859 E
T 1-54	24	475,645.697	9,129,483.700	2,048.82	74,990.56	3,546 D
T 1-55	24	475,030.703	9,127,529.363	3,265.54	78,256.10	7,127 D
T 1-56	24	473,671.581	9,124,560.096	3,754.07	82,010.17	3,581 E
T 1-57	24	472,325.409	9,121,055.692	3,142.07	85,152.23	12,563 D

SE MILAGRES (CE)						
Vertices	Time zone	Coordinates UTM Datum SIRGAS 2000		Distance (m)		Deflections (decimal degree)
		E	N	Partial	Progressive	
T 1-58	24	470,587.679	9,118,437.891	3,699.86	88,852.09	4,667 D
T 1-59	24	468,297.449	9,115,532.067	4,420.69	93,272.79	37,508 E
T 1-60	24	468,240.701	9,111,111.740	4,176.07	97,448.86	16,903 D
T 1-61	24	466,975.334	9,107,131.987	5,691.71	103,140.57	23,157 D
T 1-62	24	463,256.619	9,102,823.069	7,053.00	110,193.57	0,228 D
T 1-63	24	458,627.309	9,097,501.952	2,902.47	113,096.05	7,068 E
T 1-64	24	457,006.169	9,095,094.410	4,352.71	117,448.76	18,614 E
T 1-65	24	455,854.620	9,090,896.788	11,517.10	128,965.86	8,992 E
T 1-66	24	454,581.018	9,079,450.320	2,033.47	130,999.33	10,362 D
T 1-67	24	453,996.311	9,077,502.724	7,444.69	138,444.03	52,684 D
T 1-68	24	447,027.872	9,074,882.742	10,974.14	149,418.16	39,056 E
T 1-69	24	441,484.675	9,065,411.491	7,832.60	157,250.76	38,112 D
T 1-70	24	434,199.535	9,062,534.639	5,297.69	162,548.44	38,877 E
T 1-71	24	431,584.842	9,057,927.160	2,775.87	165,324.31	51,049 D
T 1-72	24	428,846.068	9,057,474.891	5,230.00	170,554.31	13,153 D
T 1-73	24	423,627.421	9,057,819.294	3,414.74	173,969.05	42,247 E
T 1-74	24	420,953.949	9,055,694.915	13,639.01	187,608.06	46,853 E
T 1-75	24	419,842.140	9,042,101.294	9,640.76	197,248.82	22,555 E
T 1-76	24	422,801.920	9,032,926.115	3,061.29	200,310.10	13.92 D
T 1-77	24	423,013.295	9,029,872.135	2,157.14	202,467.24	47,687 E
T 1-78	24	424,704.906	9,028,533.593	1,561.63	204,028.87	67,807 D
T 1-79	24	424,270.255	9,027,033.675	5,411.42	209,440.28	50,937 D
T 1-80	24	419,285.416	9,024,927.776	6,836.17	216,276.45	9,704 E
T 1-81	24	413,526.661	9,021,244.041	7,233.20	223,509.65	1,152 D
T 1-82	24	407,356.334	9,017,469.625	9,311.52	232,821.17	41,064 E
T 1-83	24	404,559.075	9,008,588.197	19,859.35	252,680.51	5,268 D
T 1-84	24	396,879.274	8,990,273.880	26,171.84	278,852.36	5.01 D
T 1-85	24	384,689.163	8,967,114.289	9,339.51	288,191.87	0,111 E
T 1-86	24	380,355.029	8,958,841.337	17,382.63	305,574.50	5,108 D
T 1-87	24	370,949.504	8,944,223.129	3,799.24	309,373.74	16,681 E
T 1-88	24	369,897.403	8,940,572.468	8,786.42	318,160.17	15.4 D
T 1-89	24	365,309.558	8,933,078.942	30,718.76	348,878.93	5,551 D
T 1-90	24	346,810.761	8,908,554.733	2,930.00	351,808.92	13,481 D
T 1-91	24	344,549.634	8,906,691.352	75,106.80	426,915.72	19,395 E
T 1-92	24	305,740.128	8,842,388.527	7,233.07	434,148.79	12,245 D
T 1-93	24	300,774.234	8,837,129.519	3,497.48	437,646.27	1,428 E
T 1-94	24	298,437.148	8,834,527.522	2,589.74	440,236.00	0,265 E
T 1-95	24	296,715.571	8,832,592.864	4,419.49	444,655.49	0,784 E
T 1-96	24	293,823.106	8,829,251.379	9,574.14	454,229.63	29,195 E
T 1-97	24	291,884.091	8,819,875.644	3,439.02	457,668.65	15,755 D
T 1-98	24	290,299.319	8,816,823.543	0.00	457,668.65	-

SE OUROLÂNDIA (BA)						
Vertices	Time zone	Coordinates UTM Datum SIRGAS 2000		Distance (m)		Deflections (decimal degree)
		E	N	Partial	Progressive	
T 2-1	24	290,278.507	8,816,786.307	4,442.72	4,442.72	-
T 2-2	24	288,725.980	8,812,623.682	14,901.96	19,344.68	17,897 E
T 2-3	24	288,061.132	8,797,736.562	13,525.25	32,869.93	8,011 E
T 2-4	24	289,346.627	8,784,272.541	47,749.36	80,619.29	31,871 D
T 2-5	24	268,103.098	8,741,509.080	1,756.33	82,375.62	17,777 E
T 2-6	24	267,839.272	8,739,772.675	1,292.90	83,668.52	41.8 D
T 2-7	24	266,842.514	8,738,949.223	2,090.42	85,758.95	31,777 D
T 2-8	24	264,771.356	8,738,666.096	1,400.17	87,159.11	27,714 E
T 2-9	24	263,631.427	8,737,853.060	1,501.96	88,661.07	35,293 E
T 2-10	24	263,137.259	8,736,434.720	2,159.71	90,820.78	53.25 D
T 2-11	24	261,077.971	8,735,783.824	3,202.65	94,023.43	38,252 E
T 2-12	24	259,277.478	8,733,135.205	2,670.04	96,693.47	0,992 D
T 2-13	24	257,738.393	8,730,953.384	10,115.63	106,809.10	25,005 E
T 2-14	24	255,947.994	8,720,997.457	5,270.33	112,079.43	80,192 D
T 2-15	24	250,677.788	8,721,032.981	4,005.64	116,085.06	60,103 E
T 2-16	24	248,657.878	8,717,573.923	1,885.64	117,970.71	48,996 D
T 2-17	24	246,805.152	8,717,223.133	1,980.83	119,951.54	44,982 E
T 2-18	24	245,688.998	8,715,586.705	2,010.95	121,962.49	22.3 D
T 2-19	24	244,010.221	8,714,479.621	4,318.64	126,281.13	33,981 D
T 2-20	24	239,691.802	8,714,523.165	1,243.99	127,525.12	1,861 D
T 2-21	24	238,448.942	8,714,576.105	1,383.30	128,908.42	30,548 E
T 2-22	24	237,228.800	8,713,924.353	14,787.45	143,695.87	32,318 E
T 2-23	24	229,930.749	8,701,063.282	9,525.73	153,221.60	20.15 E
T 2-24	24	228,371.193	8,691,666.081	2,548.86	155,770.46	6,896 D
T 2-25	24	227,655.027	8,689,219.903	2,456.87	158,227.33	14,108 D
T 2-26	24	226,410.775	8,687,101.404	5,336.37	163,563.70	13,302 E
T 2-27	24	224,839.455	8,682,001.615	4,170.44	167,734.14	5.46 E
T 2-28	24	223,996.282	8,677,917.301	6,708.22	174,442.36	5,377 E
T 2-29	24	223,261.633	8,671,249.433	10,725.15	185,167.51	8,507 D
T 2-30	24	220,522.894	8,660,879.859	6,444.62	191,612.12	23,725 D
T 2-31	24	216,509.300	8,655,837.621	6,760.29	198,372.42	11.24 D
T 2-32	24	211,348.904	8,651,470.484	9,251.97	207,624.39	0,302 D
T 2-33	24	204,255.126	8,645,531.012	558.53	208,182.92	37,909 D
T 2-34	24	203,696.943	8,645,511.234	1,140.68	209,323.61	6,064 D
T 2-35	24	202,559.088	8,645,591.501	1,646.59	210,970.19	28,335 E
T 2-36	24	201,058.383	8,644,913.911	1,138.44	212,108.63	3,424 D
T 2-37	24	199,994.680	8,644,508.226	1,192.98	213,301.61	32,039 E
T 2-38	24	199,275.325	8,643,556.531	2,759.62	216,061.23	20,962 E
T 2-39	24	198,508.979	8,640,905.451	1,467.38	217,528.61	7,947 E
T 2-40	24	198,300.297	8,639,452.985	780.39	218,309.00	29,482 E
T 2-41	24	198,583.848	8,638,725.933	422.47	218,731.47	26,082 D
T 2-42	24	198,548.673	8,638,304.929	7,120.59	225,852.06	39,006 D

SE OUROLÂNDIA (BA)						
Vertices	Time zone	Coordinates UTM Datum SIRGAS 2000		Distance (m)		Deflections (decimal degree)
		E	N	Partial	Progressive	
T 2-43	24	193,621.858	8,633,163.992	3,087.53	228,939.59	44,418 E
T 2-44	24	193,656.145	8,630,076.652	2,564.68	231,504.27	12,222 E
T 2-45	24	194,226.888	8,627,576.280	1,071.45	232,575.72	12,938 D
T 2-46	24	194,225.388	8,626,504.833	2,485.47	235,061.19	70,348 D
T 2-47	24	191,883.517	8,625,672.244	1,962.33	237,023.52	51,734 E
T 2-48	24	191,254.554	8,623,813.440	2,088.50	239,112.02	39,473 D
T 2-49	24	189,480.185	8,622,711.881	1,375.64	240,487.66	4,335 D
T 2-50	24	188,259.947	8,622,076.731	1,356.41	241,844.08	20,741 E
T 2-51	24	187,356.525	8,621,064.957	3,630.99	245,475.06	43,967 E
T 2-52	24	187,496.210	8,617,436.658	2,817.59	248,292.65	75,211 D
T 2-53	24	184,801.644	8,616,613.184	2,525.28	250,817.93	10,227 E
T 2-54	24	182,556.019	8,615,458.096	2,639.56	253,457.49	2,604 D
T 2-55	24	180,156.347	8,614,358.616	4,516.23	257,973.73	51.23 E
T 2-56	24	179,052.011	8,609,979.482	3,422.65	261,396.38	64,382 D
T 2-57	24	175,697.647	8,609,299.196	2,489.87	263,886.26	9,818 E
T 2-58	23	825,395.731	8,608,409.463	2,971.65	266,857.90	12,672 D
T 2-59	23	822,448.194	8,608,031.678	3,500.71	270,358.62	17,483 D
T 2-60	23	819,002.581	8,608,650.338	5,287.28	275,645.90	11,069 D
T 2-61	23	814,074.742	8,610,566.509	4,663.17	280,309.07	78,284 E
T 2-62	23	811,537.452	8,606,654.048	2,150.18	282,459.25	8,264 D
T 2-63	23	810,120.347	8,605,036.927	2,992.31	285,451.55	8,155 E
T 2-64	23	808,487.391	8,602,529.467	2,871.70	288,323.26	19,693 D
T 2-65	23	806,201.000	8,600,791.913	548.24	288,871.49	9,527 D
T 2-66	23	805,715.622	8,600,537.018	871.69	289,743.19	72,402 D
T 2-67	23	805,095.979	8,601,150.120	1,573.10	291,316.29	58,585 E
T 2-68	23	803,568.867	8,600,772.520	3,275.59	294,591.88	81,639 E
T 2-69	23	803,884.410	8,597,512.161	1,467.34	296,059.23	3,355 D
T 2-70	23	803,940.051	8,596,045.874	906.89	296,966.12	35,328 E
T 2-71	23	804,492.149	8,595,326.400	1,191.44	298,157.56	51,629 D
T 2-72	23	804,201.344	8,594,170.998	1,723.73	299,881.29	4,392 E
T 2-73	23	803,909.876	8,592,472.086	360.45	300,241.74	36,308 D
T 2-74	23	803,650.403	8,592,221.895	916.45	301,158.19	41,388 E
T 2-75	23	803,576.015	8,591,308.469	1,261.54	302,419.72	45,158 D
T 2-76	23	802,612.262	8,590,494.431	1,457.34	303,877.07	11,658 D
T 2-77	23	801,331.863	8,589,798.429	903.49	304,780.56	14,318 E
T 2-78	23	800,669.438	8,589,184.027	968.46	305,749.02	40.14 D
T 2-79	23	799,702.056	8,589,138.309	1,324.66	307,073.68	24,992 D
T 2-80	23	798,476.350	8,589,640.677	2,156.91	309,230.59	20,804 D
T 2-81	23	796,901.220	8,591,114.185	1,127.51	310,358.10	43,256 D
T 2-82	23	796,829.377	8,592,239.407	381.37	310,739.47	34,383 E
T 2-83	23	796,594.393	8,592,539.785	3,481.69	314,221.16	64,509 E
T 2-84	23	793,195.822	8,591,783.564	2,831.31	317,052.47	33,851 E
T 2-85	23	791,243.141	8,589,733.362	66,009.37	383,061.83	26.97 E

SE OUROLÂNDIA (BA)						
Vertices	Time zone	Coordinates UTM Datum SIRGAS 2000		Distance (m)		Deflections (decimal degree)
		E	N	Partial	Progressive	
T 2-86	23	772,346.879	8,526,486.483	8,133.48	391,195.31	22,768 D
T 2-87	23	767,183.979	8,520,201.746	15,890.19	407,085.51	27,092 E
T 2-88	23	763,795.948	8,504,676.942	12,800.48	419,885.99	22.48 E
T 2-89	23	766,055.830	8,492,077.526	2,816.58	422,702.57	5,744 D
T 2-90	23	766,273.136	8,489,269.340	4,504.83	427,207.40	29.67 D
T 2-91	23	764,351.863	8,485,194.762	2,512.35	429,719.75	0,761 D
T 2-92	23	763,250.278	8,482,936.792	3,318.27	433,038.02	21,425 D
T 2-93	23	760,806.474	8,480,692.076	3,372.69	436,410.71	16,425 D
T 2-94	23	757,778.841	8,479,205.987	5,663.53	442,074.25	24.18 D
T 2-95	23	752,118.634	8,479,011.903	3,462.14	445,536.38	49,367 E
T 2-96	23	749,955.430	8,476,308.765	2,211.83	447,748.21	39,753 D
T 2-97	23	747,788.609	8,475,864.848	6,125.09	453,873.30	90,396 E
T 2-98	23	749,059.394	8,469,873.033	7,444.38	461,317.68	11,411 D
T 2-99	23	749,132.582	8,462,429.013	8,104.85	469,422.53	7,959 E
T 2-100	23	750,333.606	8,454,413.643	13,074.18	482,496.71	37,148 D
T 2-101	23	744,069.850	8,442,937.599	0.00	482,496.71	-

SE IGAPORÃ (BA)						
Vertices	Time zone	Coordinates UTM Datum SIRGAS 2000		Distance (m)		Deflections (decimal degree)
		E	N	Partial	Progressive	
T 3-1	23	744,058.807	8,442,911.185	7,107.47	7,107.47	-
T 3-2	23	742,005.323	8,436,116.452	3,643.42	10,750.89	44,218 D
T 3-3	23	738,821.939	8,434,354.319	15,369.21	26,120.10	29,673 E
T 3-4	23	730,834.737	8,421,249.168	7,289.95	33,410.05	32.08 E
T 3-5	23	730,926.027	8,413,970.611	6,103.61	39,513.66	32,967 E
T 3-6	23	734,306.412	8,408,899.256	37,614.92	77,128.58	14,103 D
T 3-7	23	746,897.153	8,373,506.935	4,897.98	82,026.56	40,005 D
T 3-8	23	745,190.188	8,368,922.447	977.75	83,004.32	45,718 E
T 3-9	23	745,607.456	8,368,039.543	975.16	83,979.48	47,068 D
T 3-10	23	745,246.198	8,367,135.064	1,168.43	85,147.91	7,201 D
T 3-11	23	744,680.918	8,366,114.143	2,190.02	87,337.92	3.89 E
T 3-12	23	743,753.659	8,364,133.158	6,931.91	94,269.83	1,488 E
T 3-13	23	740,982.535	8,357,788.974	454.13	94,723.96	0,353 D
T 3-14	23	740,798.435	8,357,374.486	368.18	95,092.14	14,784 D
T 3-15	23	740,568.369	8,357,087.658	992.33	96,084.47	7,428 D
T 3-16	23	739,853.552	8,356,401.247	1,554.64	97,639.11	12,895 E
T 3-17	23	739,001.906	8,355,103.101	1,512.51	99,151.62	35.57 D
T 3-18	23	737,593.317	8,354,557.773	760.71	99,912.33	40,764 E
T 3-19	23	737,235.821	8,353,887.473	678.26	100,590.59	40,646 D
T 3-20	23	736,604.674	8,353,641.640	491.70	101,082.29	7,994 D
T 3-21	23	736,126.796	8,353,528.793	936.64	102,018.93	57,914 E
T 3-22	23	735,825.374	8,352,643.348	280.10	102,299.03	16.54 D
T 3-23	23	735,663.583	8,352,415.180	1,777.47	104,076.50	12.22 D

SE IGAPORÃ (BA)						
Vertices	Time zone	Coordinates UTM Datum SIRGAS 2000		Distance (m)		Deflections (decimal degree)
		E	N	Partial	Progressive	
T 3-24	23	734,353.682	8,351,217.377	631.98	104,708.48	25,412 E
T 3-25	23	734,115.763	8,350,632.856	1,694.40	106,402.89	20,745 D
T 3-26	23	732,964.135	8,349,393.266	3,195.93	109,598.81	0,426 E
T 3-27	23	730,809.456	8,347,039.184	2,687.42	112,286.23	60,527 D
T 3-28	23	728,194.752	8,347,642.564	2,967.60	115,253.83	39,605 E
T 3-29	23	725,545.557	8,346,315.356	2,187.43	117,441.25	12,018 E
T 3-30	23	723,839.372	8,344,951.971	2,220.15	119,661.40	28,351 E
T 3-31	23	722,972.500	8,342,911.877	1,740.83	121,402.23	24,104 E
T 3-32	23	723,005.324	8,341,174.126	624.63	122,026.86	42,952 D
T 3-33	23	722,589.083	8,340,709.722	1,588.24	123,615.10	32,095 E
T 3-34	23	722,319.889	8,339,147.041	3,573.90	127,189.00	5,997 D
T 3-35	23	721,350.078	8,335,713.204	803.59	127,992.59	38,024 E
T 3-36	23	721,653.902	8,334,970.664	239.15	128,231.74	24,059 D
T 3-37	23	721,646.374	8,334,732.014	3,349.09	131,580.83	15,346 D
T 3-38	23	720,660.251	8,331,537.059	5,768.92	137,349.75	33,273 E
T 3-39	23	722,259.466	8,326,003.906	2,953.59	140,303.34	30,968 E
T 3-40	23	724,419.296	8,323,996.098	5,477.21	145,780.55	32,064 D
T 3-41	23	725,837.007	8,318,714.336	3,063.95	148,844.50	24,177 D
T 3-42	23	725,350.401	8,315,694.052	2,395.66	151,240.17	39,671 D
T 3-43	23	723,550.021	8,314,119.265	2,417.16	153,657.32	54,422 E
T 3-44	23	723,785.447	8,311,717.415	17,156.40	170,813.72	47,882 D
T 3-45	23	712,261.711	8,299,045.785	1,829.41	172,643.13	32,536 D
T 3-46	23	710,499.251	8,298,567.582	7,375.76	180,018.89	40,195 E
T 3-47	23	706,315.955	8,292,509.098	20,221.67	200,240.56	7,669 D
T 3-48	23	692,734.660	8,277,580.131	31,441.11	231,681.67	21,361 D
T 3-49	23	664,623.216	8,263,658.879	22,949.85	254,631.52	18.46 E
T 3-50	23	648,382.988	8,247,528.338	17,578.01	272,209.53	10.08 D
T 3-51	23	633,977.166	8,237,543.624	8,746.29	280,955.82	12,357 E
T 3-52	23	628,039.391	8,231,157.737	11,307.49	292,263.32	6,304 E
T 3-53	23	621,316.492	8,222,109.710	6,536.26	298,799.58	4,562 D
T 3-54	23	617,027.017	8,217,205.614	1,263.99	300,063.57	8,562 D
T 3-55	23	616,065.599	8,216,391.358	1,505.11	301,568.67	32,211 E
T 3-56	23	615,613.811	8,214,960.789	3,212.84	304,781.51	27,623 D
T 3-57	23	613,343.503	8,212,702.341	3,000.05	307,781.56	48,054 D
T 3-58	23	610,358.061	8,212,869.450	1,017.08	308,798.64	83,487 E
T 3-59	23	610,186.975	8,211,870.308	1,396.46	310,195.09	8,911 D
T 3-60	23	609,742.404	8,210,551.434	3,732.41	313,927.50	11,618 D
T 3-61	23	607,868.621	8,207,337.964	694.92	314,622.42	58,284 D
T 3-62	23	607,176.281	8,207,320.206	1,608.98	316,231.40	57.76 E
T 3-63	23	606,355.912	8,205,942.426	2,681.44	318,912.84	38,557 D
T 3-64	23	603,855.689	8,204,999.038	2,737.13	321,649.97	38,632 E
T 3-65	23	602,463.265	8,202,653.513	695.72	322,345.69	3,513 E

SE IGAPORÃ (BA)						
Vertices	Time zone	Coordinates UTM Datum SIRGAS 2000		Distance (m)		Deflections (decimal degree)
		E	N	Partial	Progressive	
T 3-66	23	602,146.539	8,202,036.771	2,853.28	325,198.97	29,254 D
T 3-67	23	599,777.252	8,200,464.794	3,492.59	328,691.57	26,194 E
T 3-68	23	598,024.361	8,197,458.126	11,934.01	340,625.57	14,885 D
T 3-69	23	589,597.412	8,189,068.481	1,118.57	341,744.14	27,942 D
T 3-70	23	588,531.245	8,188,743.924	2,155.41	343,899.56	42,025 E
T 3-71	23	587,423.799	8,186,904.023	4,686.16	348,585.72	13,564 D
T 3-72	23	584,145.160	8,183,580.203	1,859.97	350,445.69	57,115 D
T 3-73	23	582,330.821	8,183,956.700	3,781.00	354,226.69	64,677 E
T 3-74	23	580,061.536	8,180,950.327	2,608.31	356,835.00	2,115 D
T 3-75	23	578,420.647	8,178,935.643	1,550.78	358,385.79	21,318 E
T 3-76	23	577,947.264	8,177,465.117	4,885.82	363,271.61	27,074 D
T 3-77	23	574,510.722	8,174,018.753	5,852.91	369,124.51	26,335 E
T 3-78	23	572,652.813	8,168,492.640	4,375.66	373,500.18	52,473 E
T 3-79	23	575,083.164	8,164,874.495	3,712.91	377,213.09	46,635 D
T 3-80	23	574,267.195	8,161,267.127	2,713.98	379,927.06	10,369 E
T 3-81	23	574,155.077	8,158,566.024	4,068.11	383,995.17	46,067 E
T 3-82	23	576,954.300	8,155,635.799	5,217.13	389,212.31	49,861 D
T 3-83	23	576,395.647	8,150,468.836	7,883.72	397,096.03	10,787 E
T 3-84	23	577,027.744	8,142,640.880	3,205.18	400,301.20	73,202 D
T 3-85	23	574,055.353	8,141,475.145	1,890.06	402,191.27	19,848 D
T 3-86	23	572,173.355	8,141,423.686	3,242.54	405,433.81	69,813 E
T 3-87	23	571,142.043	8,138,362.928	2,774.79	408,208.60	52,836 D
T 3-88	23	568,521.689	8,137,483.986	5,398.28	413,606.88	43,078 E
T 3-89	23	565,966.060	8,132,753.410	13,130.77	426,737.65	3,363 D
T 3-90	23	559,085.987	8,121,632.007	6,644.92	433,382.57	5,846 E
T 3-91	23	556,195.855	8,115,679.015	2,318.57	435,701.14	36,246 D
T 3-92	23	554,154.514	8,114,600.128	1,443.40	437,144.54	25,482 E
T 3-93	23	553,296.301	8,113,447.113	3,320.80	440,465.34	54.18 E
T 3-94	23	554,291.771	8,110,293.605	1,475.87	441,941.21	57,663 D
T 3-95	23	553,344.256	8,109,170.126	4,000.97	445,942.18	5,888 E
T 3-96	23	551,101.658	8,105,877.107	5,840.89	451,783.07	21,045 D
T 3-97	23	546,320.027	8,102,566.265	9,651.99	461,435.06	40.3 E
T 3-98	23	543,832.549	8,093,283.461	4,973.10	466,408.16	6,935 E
T 3-99	23	543,137.772	8,088,380.928	2,103.07	468,511.24	86,868 D
T 3-100	23	541,051.629	8,088,561.016	2,269.86	470,781.10	35,845 E
T 3-101	23	539,112.718	8,087,400.102	2,227.27	473,008.37	0,159 E
T 3-102	23	537,213.413	8,086,255.722	1,277.36	474,285.73	12,571 E
T 3-103	23	536,293.124	8,085,378.087	2,179.80	476,465.53	34,468 E
T 3-104	23	535,845.963	8,083,254.564	13,709.37	490,174.90	70,815 D
T 3-105	23	522,309.568	8,081,522.085	3,556.67	493,731.57	26.03 D
T 3-106	23	518,957.204	8,082,659.192	4,998.41	498,729.98	18,027 E
T 3-107	23	513,982.979	8,082,720.807	0.00	498,729.98	0
SE PIRAPORA (MG)						

7.1 Adjustments to the Preliminary Path and Final Route

For the field work, we designed a preliminary path. This path was subject to some changes after the validations performed on the field. In addition to some minor adjustments, some more significant adjustments were made. These adjustments are detailed in this sub item.

The first more significant adjustment (Figure 7.1) was made in the portion of the line that will cross the São Francisco River, in Section 1. In the preliminary path, the line would pass through an area that is defined as indigenous land, but which, in the field we observed that it is in fact a settlement, Projeto Brígida (Figure 7.2), so the path should be diverted a little more to the west (T1-69 to T1-71). From the area of Projeto Brígida to the northern margin of the São Francisco river, one needs to cross an area with higher hills and the proximity to some other agricultural settlements (T1-71 to T1-75). Thus, the path was directed to a portion that presents a more consolidated river island, which may help make the crossing of this large river that divides the states of Pernambuco and Bahia (T1-75 to T1-79).

After crossing the São Francisco River, we tried to maintain the path parallel next to state highway BA 210 (T1-79 to T1-84), for better logistic access, and because in the region there is a priority area associated to an endangered species (little blue macaw), with various projects under development related to this matter, and to the southeast of said road there is a more preserved vegetation area. It is important to highlight that there is an installed line that runs parallel to the axis of the new TL to be implemented, at approximately 12 km southeast from state highway BA 210.

When approaching federal highway BR 235, the line will cross a series of other lines that run towards Petrolina (Pernambuco) and Juazeiro (Bahia) (associated mainly to the stretch from T1-85 to T1-87).

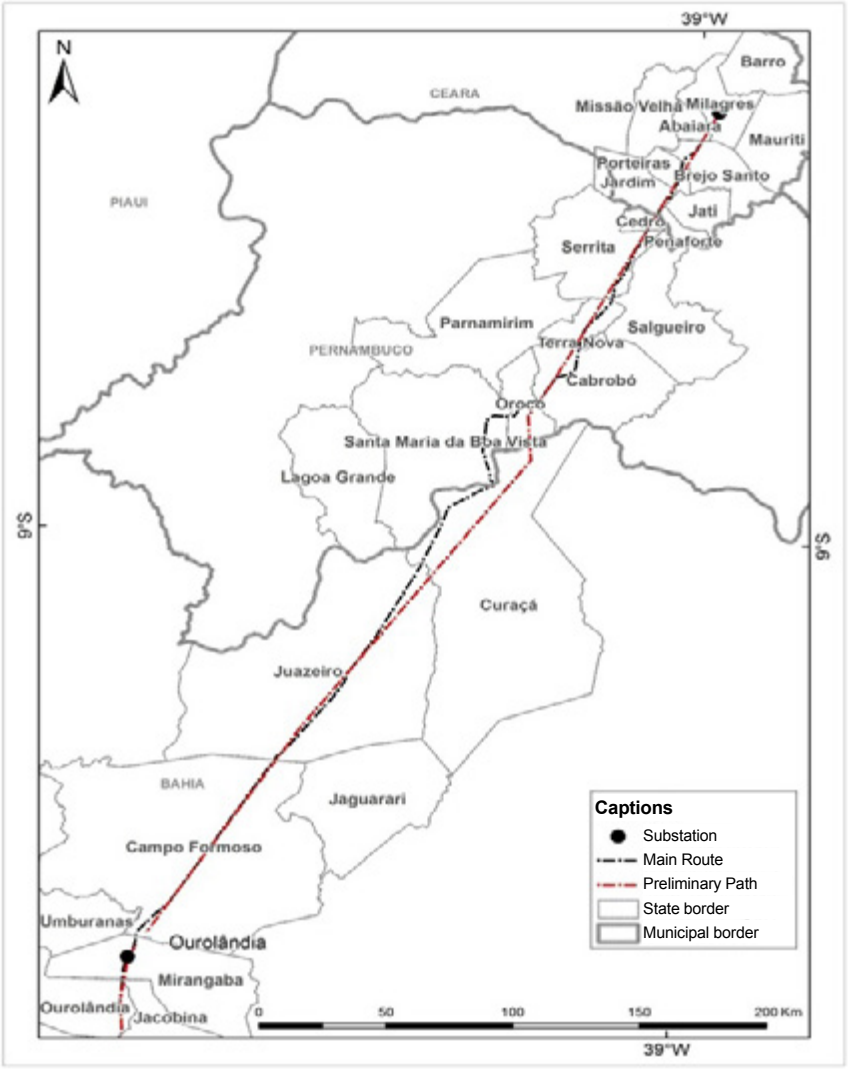

Figure 7.1: Changes in the main route of the line in Section 1

Figure 7.2: Settlement of Projeto Brígida in the state of Pernambuco

The second area (Figure 7.3), where there was a more significant adjustment to the preliminary path, starts at the region close to the municipality of Morro do Chapéu, located in Section 2. In this section, the path was diverted a little more to the west to steer away from the urban area of this municipality and from the airport (T2-8 to T2-14). The path more to the west also avoids a stretch of relief that presents altimetric variations associated with drainage dissection. In this section, the path was designed on the margin of the Integral Protection Conservation Unit Morro do Chapéu State Park (T2-13 to T2-15).

Close to the alignment of hills of the Morro do Chapéu Geological Unit, a detour was made to the west to prevent the line from crossing an aero generator field, and also to divert it from the Pachola Settlement Project (T2-19 to T2-22). After crossing the settlement, the line path is maintained parallel to the alignment of hills of Morro do Chapéu, to detour it from some urban centers and fluvial plains areas, where there are areas of crops and hydromorphic soils (T2-23 a T2-32).

Next, the installation of the line will cross some areas of mountain alignments with a more pronounced amplitude. Aiming at presenting fewer difficulties to the implementation of the line, we recommend that, as demonstrated by the line path, a detour is made so that the first ridge section is crossed exactly to the west of the urban area of the municipality of Iraquara, parallel to state highway BA-848, going next towards the north of the urban area of the municipality of Seabra (T2-33 to T2-39). In this section, the line will cross the northwestern portion of the Sustainable Use Conservation Unit Marimbus/Iraquara. After crossing federal highway BR-122, the line will cross an alignment of high hills that is part of the same geological complex of the first mountain alignment, mentioned in this paragraph (T2-49 to T2-53).

Next, the line will pass through a section where there are some quilombolic communities, and will have to cross another mountain alignment. This next alignment is more extensive and presents greater altimetric variation compared to the first one. It presents an extension of approximately 35 km. Thus, we sought to design the line route in areas that present accesses, and a relief with lower altimetric variation, so as to make implementation easier in this more critical stretch (T2-59 to T2-85). Since the line route has been defined based on the lower sections of the mountain alignment, attention should be paid to the areas of hydromorphic soils.

There is still another mountain alignment to be crossed, which is located between the urban areas of the municipalities of Tanque Novo and Igaporã. We recommend that the line crosses this area close to the latitude of the urban area of Igaporã (T2-94 to T2-97), because of the greater number of accesses, and to avoid crossing an extensive field of aero generators that extends from this point to the south (Figure 7.4).

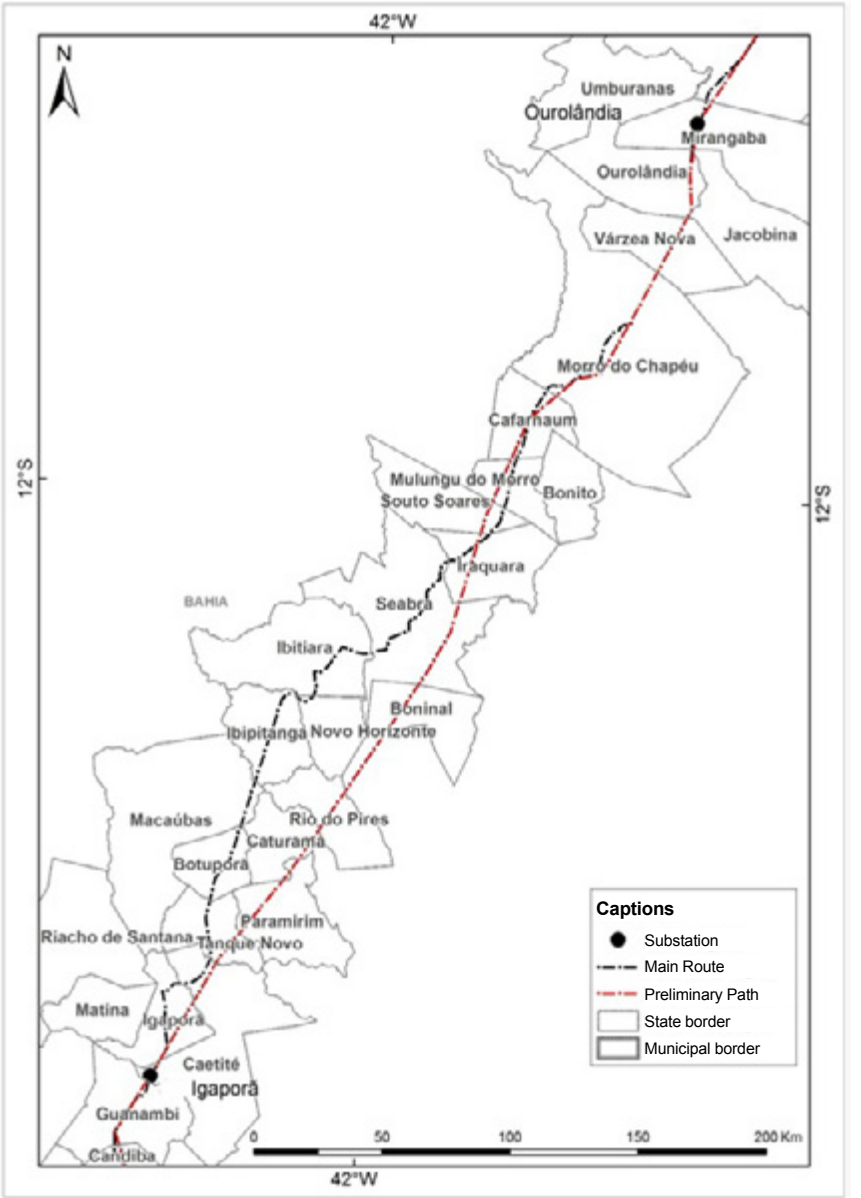

Figure 7.3: Changes in the main route of the line in Section 2

Figure 7.4: Field of aero generators close to Igaporã

The third area (Figure 7.5), where the preliminary path was altered after the completion of the field work, is located near the border of the states of Minas Gerais and Bahia, located in Section 3. The preliminary path crossed a mountain alignment with pronounced amplitude. To avoid this area, the route was adapted and diverted to the west from a point close to the urban area of the municipality of Urandi (T3-7), maintaining the path parallel to the west of federal highway BR 122 (T3-44).

Attention should be paid to this stretch, since this area presents a series of areas of humid soils between the urban areas of the municipalities of Urandi (T3-8) and Espinosa (T3-21). Near the urban area of Espinosa (T3-24), approximately 10 km to the south of the urban area of the municipality of Monte Azul (T3-44), the stretch is composed of low and high hills located close to the urban area of the municipality of Mamomas, between vertices T3-35 and T3-37 (Figure 7.6). And for the entire stretch, going from Urandi to the south of Monte Azul, the area is located between a large amplitude mountain alignment to the east, and two large Integral Protection Conservation Units to the west, Serra dos Montes Altos State Park and Caminho dos Gerais State Park.

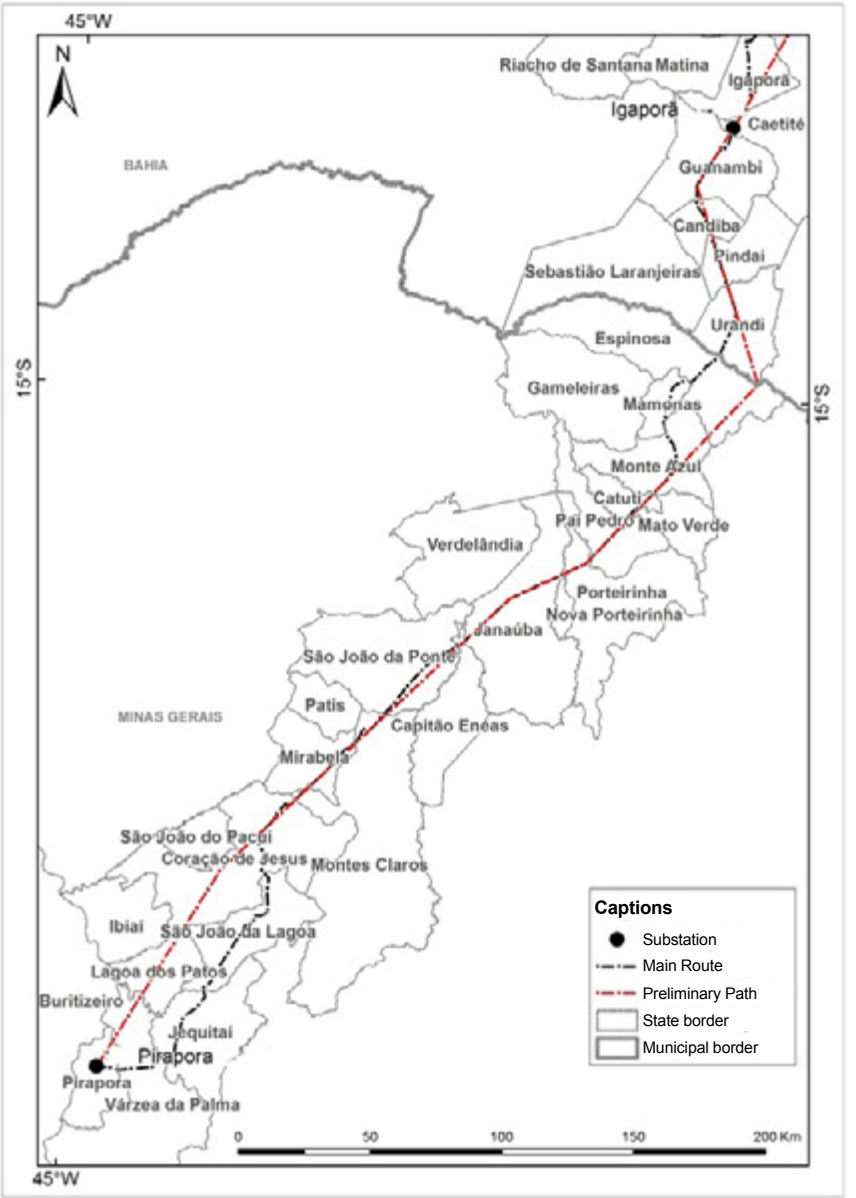

Figure 7.5: Changes in the main route of the line in Section 3

Figure 7.6: Area of low and high hills close to the urban area of the municipality of Mamomas

The forth more significant detour (Figure 7.7) was made starting from vertex T3-77, near the urban area of the municipality of Coração de Jesus, in Section 3 of the line. The detour was made because the preliminary path crossed an area that proved to provide little logistic access, a large number of veredas, paleontological and archeological sites, caves, the presence of an airport, proximity to areas with extensive fluvial plains, and agricultural settlements.

The detour was made starting from a point located approximately 19 km north of the urban area of the municipality of Coração de Jesus (T3-77), where an adjustment was made to the east. Starting from the point where the main route of the line crosses state highway MGT 251 (T3-85), the path continues approximately 15 km away from federal highway BR 365, running parallel to it up to stretch T3-97 to T3-98 of the line, where the road converges toward the line and crosses it. We sought to maintain the tracts in the altimetrically higher portions and close to rural roads, in order to cause less impact to the silviculture areas, and avoid areas dissected by hydrography in general.

After crossing federal highway BR 365, the preferred route for the line continues for approximately 16 km towards the southwest, to then (T3-104) be directed towards the west, in the direction of the Pirapora substation. This area requires attention because there is a series of other transmission lines crossing the area towards the same substation. We must highlight that, in this stretch between federal highway BR-365 and the Pirapora substation, there are two stretches of plateaus and low plateaus to be crossed (T3-100 to T3-103 and T3-106), these being two points of greater sensitivity due to the altimetric variation.

Figure 7.7: Buritis in a vereda close to the urban area of the municipality of Coração de Jesus

Figure 7.8 shows the preliminary path and the final path, with the main route indicated in this project for the implementation of the line, taking into consideration the socio-environmental variables for the entire project area.

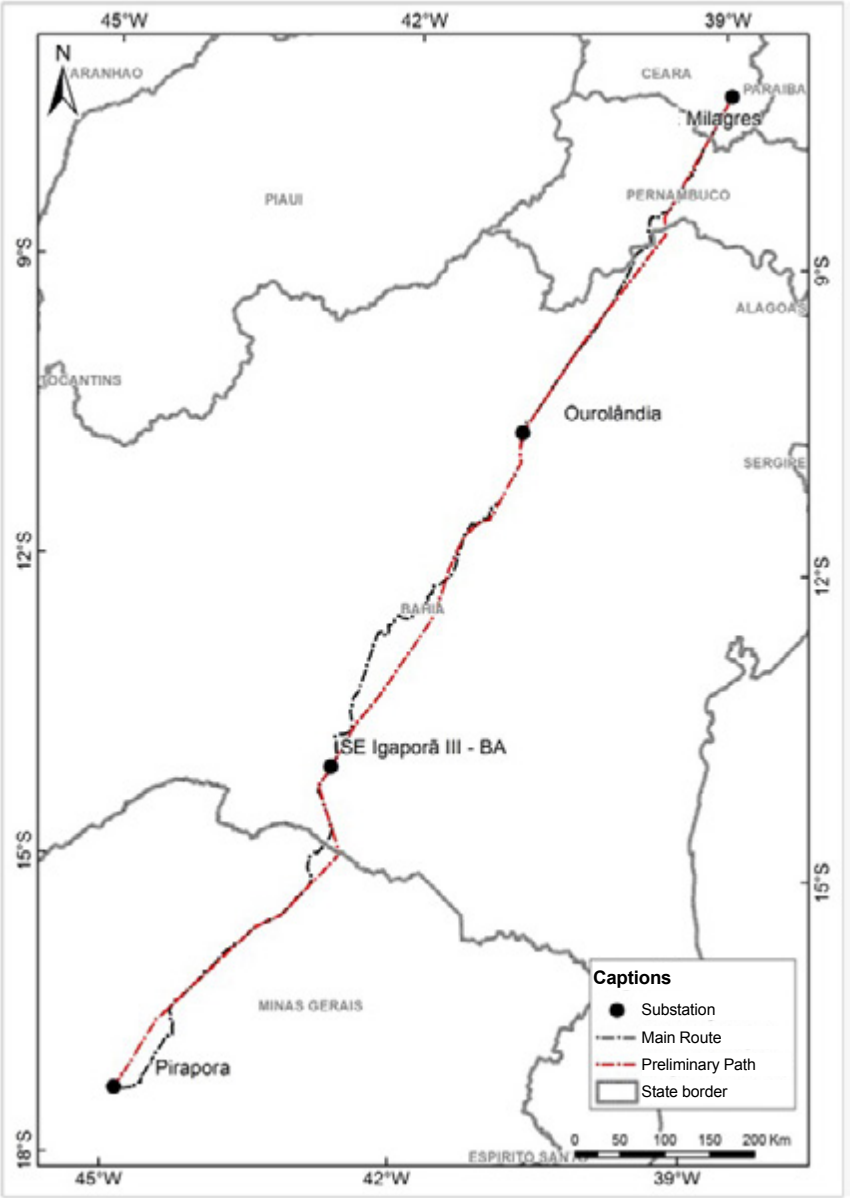

Figure 7.8: Preliminary path and preferred route for line implementation

8. Socio-environmental Characterization of the Corridor of the Main Route of the Line

The purpose of the socio-environmental analysis of the sections of the path is obtaining a characterization of various socio-environmental aspects of the 30 km corridor and main route of the line, and evaluating its interference in the implementation of the Transmission Line. For this, elements that reflect the impacts on the physical, biotic, and socioeconomic environments, considering aspects related to terrestrial ecosystems, indigenous and traditional populations, population density, and urban concentrations are taken into account. This diagnosis supports the evaluation and decision making in the projects through the identification of sustainability indicators for the path.

8.1 Variables Considered in the Socio-environmental Characterization

The quality-quantitative characterization of the sections of the path, and their respective 30 km corridors was developed using the evaluation of relevant socio-environmental indicators built from the spatial analysis of official secondary data. The indicators were elaborated based on the variables selected considering their interference in legally protected areas and regions of great environmental and social relevance, in addition to the impact on different types of land uses and covers. Secondary databases from Probio (2007) and IBGE (2012) were used, among others.

During these evaluations, the following socio-environmental variables were observed:

- Integral Protection Conservation Units (IPCU);
- Sustainable Use Conservation Units (SUCU);
- Caves;
- Quilombolic communities;
- Indigenous lands (TIs);
- Settlements;
- Priority Areas for Biodiversity Conservation (PABC);
- Land use and cover;

The Conservation Units are defined by the National System of Conservation Units (SNUC) as legally protected areas with relevant natural characteristics, the purpose of which is to promote conservation, biodiversity preservation, and sustainable development. The Conservation Units (CUs) are subdivided into Integral Protection Conservation Units (IPCU), and Sustainable Use Conservation Units (SUCU).

In the IPCU, only the indirect use of natural resources is allowed, that is, without consuming, collecting, damaging or destroying them. Among the IPCUs are Ecological Stations (Esec), Biological Reserves (Rebio), National Parks (Parna), Natural Monuments (MN), and Wildlife Sanctuaries (Revis) (ICMBio 2015).

The objective of the SUCUs is to make nature conservation compatible with the sustainable use of its natural resources, reconciling the use of the environment and guaranteeing the conservation of renewable natural resources. Among the SUCUs there are Environmental Protection Areas (APA), Areas of Relevant Ecological Interest (Arie), National Forests (Flona), Extractive Reserves (Resex), Fauna Reserves (Refau), Sustainable Development Reserves (RDS), and Private Reserve of Natural Heritage (RPPN) (IMCBio, 2015).

The CUs data used to compose the indicators was extracted from the National Register of Conservation Units (2015), and from the Ministry of the Environment (MMA).

The data on caves was obtained from the ICMBio's National Center for Research and Conservation of Caves (Cecav) (2015), and from the Ministry of the Environment (2006), respectively. The geological sites were compiled by the MMA from the Geodiversity Map of Brazil, conducted by CPRM.

In delimiting the path corridor, it was tried to avoid areas with indigenous lands, settlements and quilombolic communities. The information referring to the indigenous areas, quilombolic communities, and rural settlements was obtained from Funai (2015) and Incra (2015), respectively.

The data related to the land use and its cover was obtained from various fonts, namely:

- Deforestation data from the Satellite Deforestation Monitoring of the Brazilian Biomes Project (PMDBBS), from the MMA, from 2008 to 2010;
- Built Areas, by IBGE (2015);
- Hydrography, by IBGE (2015),
- Land Use and Coverage Map, by IBGE (2012).

To determine the Priority Areas, data from the Ministry of the Environment (2007) was used. These areas represent locations of considerable importance for conservation, sustainable use, and distribution of biodiversity benefits.

The data about roads was obtained from the IBGE database (2015), and the National Plan of Logistics and Transportation (PNLT) of the Ministry of Transportation (2010). State, federal, and municipal roads were evaluated, regardless of being paved, because of their significance in choosing the TL path. Similarly, the data about Railways from the PNLT (2010), and IBGE (2015) were used.

8.2 Description of the Path and 30 km Wide Corridor

The path analyzed is formed by three sections that connect four substations. The total length of the path is of 1,438.89 km that stretch through 55 municipalities, 17 of which are in the state of Minas Gerais, 7 in the state of Pernambuco, 6 in the state of Ceará, and 25 in the state of Bahia. The 30 km wide corridor was defined based on a route, so that the path chosen is fully contained within the corridor. The corridor has an area of 39,939.2 km2, 76.97% of which lie within the caatinga biome, and 23.03% in the savanna biome. The analyses are presented per section between the substations, as seen in Figure 8.1.

- **Section 1 (T1)** – Milagres (CE) to Ourolândia (BA) – 457.67 km;
- **Section 2 (T2)** – Ourolândia (BA) to Igaporã (BA) – 482.49 km;
- **Section 3 (T3)** – Igaporã (BA) to Pirapora (MG) – 498.73 km.

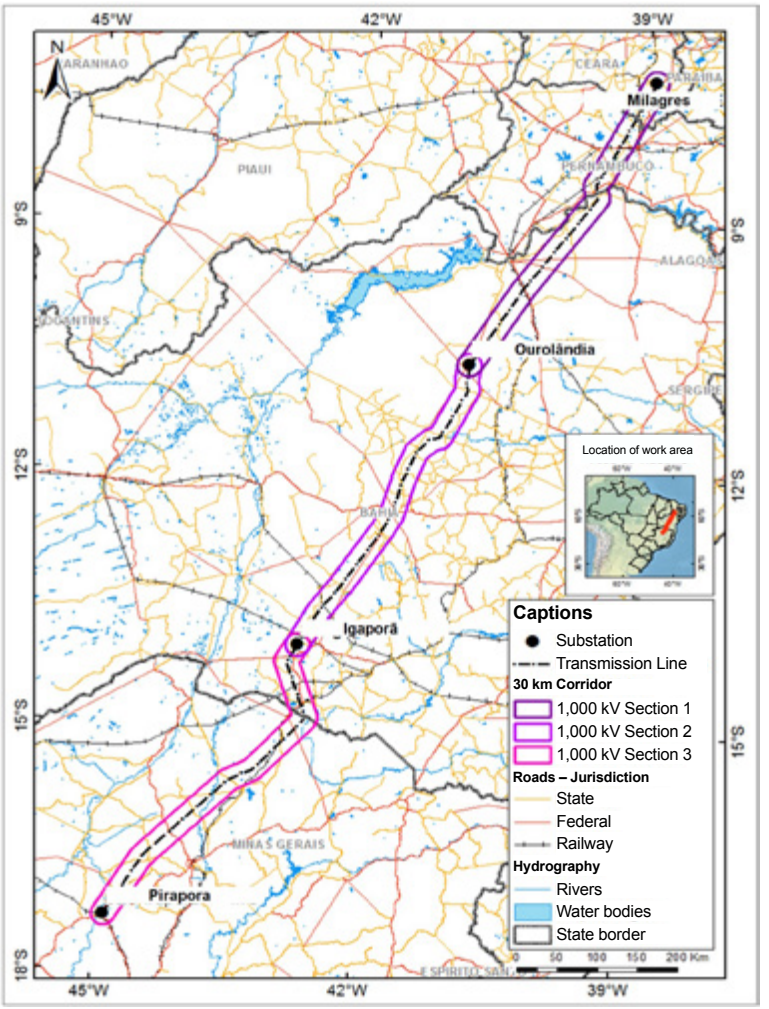

Figure 8.1: Location of the 30 km wide corridors divided by sections

Along the alternative route defined, there is a crossing of the São Francisco River, in the central portion of the Section 1 corridor, and a crossing of the Rio das Velhas river, close to the Pirapora substation, in Section 3. We also highlight the existence of 54 crossings of Federal, State, and Municipal roads, and important cart paths, and 4 crossings of railways in traffic.

In the corridor of the path, natural vegetation, anthropic areas, and water bodies correspond to 36.36%, 61.12%, and 0.63% of the total area, respectively. In this corridor, there are significant areas of agriculture and silviculture, which together represent 1.67% of the total length of the corridor. The main areas of

agriculture and silviculture are located in the municipalities of: Brejo Santo (Ceará), Porteiras (Ceará), Cedro (Ceará), and Penaforte (Ceará), in the north portion of Section 1; Santa Maria da Boa Vista (Pernambuco), Curaçá (Bahia), Juazeiro (Bahia), and Orocó (Pernambuco), in the central region of Section 1; Várzea Nova (Bahia), to the north of Section 2; Urandi (Bahia), and Sebastião Laranjeiras (Bahia), to the north of Section 3; Nova Porteirinha (Minas Gerais), Capitão Enéas (Minas Gerais), and Janaúba (Minas Gerais), in the central region of Section 3; and Jequitaí (Minas Gerais), São João da Lagoa (Minas Gerais), and Coração de Jesus (Minas Gerais), in the south portion of Section 3.

Cities, towns and villages correspond to 0.21 % of the area of the corridor of the chosen route. Among the built areas present in the corridor, we highlight those of the main offices of the municipalities of Brejo Santo (Ceará) and Milagres (Ceará), to the north of Section 1; Seabra (Bahia), in the central region of Section 2; Guanambi (Bahia), Espinosa (Minas Gerais), and Mamomas (Minas Gerais) in the north of Section 3; Nova Porteirinha (Minas Gerais), in the central region of Section 3; and Coração de Jesus (Minas Gerais) and Pirapora (Minas Gerais), to the south of Section 3.

With regards to special and/or protected areas, in the corridor of the chosen route there are 8 Conservation Units, and 6 quilombolic communities. The path chosen does not pass through any indigenous territories or quilombolic communities, and passes through 2 CUs, as presented in Table 8.1, and in the summary of the main socio-environmental interferences in the designed route and in its 30 km wide corridor. Figure 8.1 presents the location of the route and of the 30 km wide corridors for each section.

Table 8.1: Main socio-environmental interferences along the line route

Description	Quantitative	
Length of the line (km)	1,437.39	
Conservation Units (#)	Corridor Axis	Corridor (30 km)
	2	7
Native vegetation (km^2) in the 30 wide corridors	14,484.01	
Agriculture (km^2)	666.79	
Indigenous lands (#)	Corridor Axis	Corridor (30 km)
	0	0
Quilombolas (#)	Corridor Axis	Corridor (30 km)
	0	7
Incra Settlements (#)	Corridor Axis	Corridor (30 km)
	0	65
Caves (#) in the 30 wide corridors	199	
Municipalities crossed	Corridor Axis	Corridor (30 km)
	55	79
Urban areas (km^2)	84.66	

8.3 Macro-characterization of the Section Milagres (Ceará) to Ourolândia (Bahia)

Section 1 (T1) comprises the area of the corridor that starts at the Milagres substation, located in the city of Milagres, in the Southeast of the state of Ceará. This is a 13,707.81 km² area. The São Francisco River crosses the south part of the T1 corridor, which should be carefully evaluated for the location of the main route of the line, so as to choose the best crossing point.

The municipalities crossed by T1 and their respective population densities are described in Table 8.2, and shown in Figure 8.2.

Table 8.2: List of municipalities crossed by corridor T1 – Milagres (CE) to Ourolândia (BA)

State	Mesoregion	Microregion	Municipality	Population	Population density (people/km²)
Ceará	South of Ceará	Barro	Barro	21,479	20 to 50
			Mauriti	44,167	20 to 50
		Brejo Santo	Jati	7,632	20 to 50
			Penaforte	8,196	50 to 100
			Abaiara	10,474	50 to 100
			Brejo Santo	45,162	50 to 100
			Milagres	28,262	20 to 50
			Jardim	26,646	20 to 50
			Missão Velha	34,206	50 to 100
			Porteiras	15,052	20 to 100
Pernambuco	São Francisco in Pernambuco	Petrolina	Terra Nova	9,257	20 to 50
			Cabrobó	30,775	10 to 20
			Lagoa Grande	22,698	20 to 50
			Orocó	13,129	20 to 50
			Santa Maria da Boa Vista	39,393	10 to 20
			Cedro	10,774	50 to 100
	Semi-arid area of Pernambuco	Salgueiro	Parnamirim	20,167	5 to 10
			Salgueiro	56,050	20 to 50
			Serrita	18,323	10 to 20
Bahia	Vale São-Franciscano da Bahia	Juazeiro	Juazeiro	197,397	20 to 50
			Curacá	32,134	up to 5
	Central-North of Bahia	Jacobina	Jacobina	79,112	20 to 50
			Mirangaba	16,270	5 to 10
			Ourolândia	16,389	10 to 20
		Senhor do Bonfim	Campo Formoso	66,441	5 to 10
			Jaguarari	30,281	10 to 20
			Umburanas	16,908	5 to 10

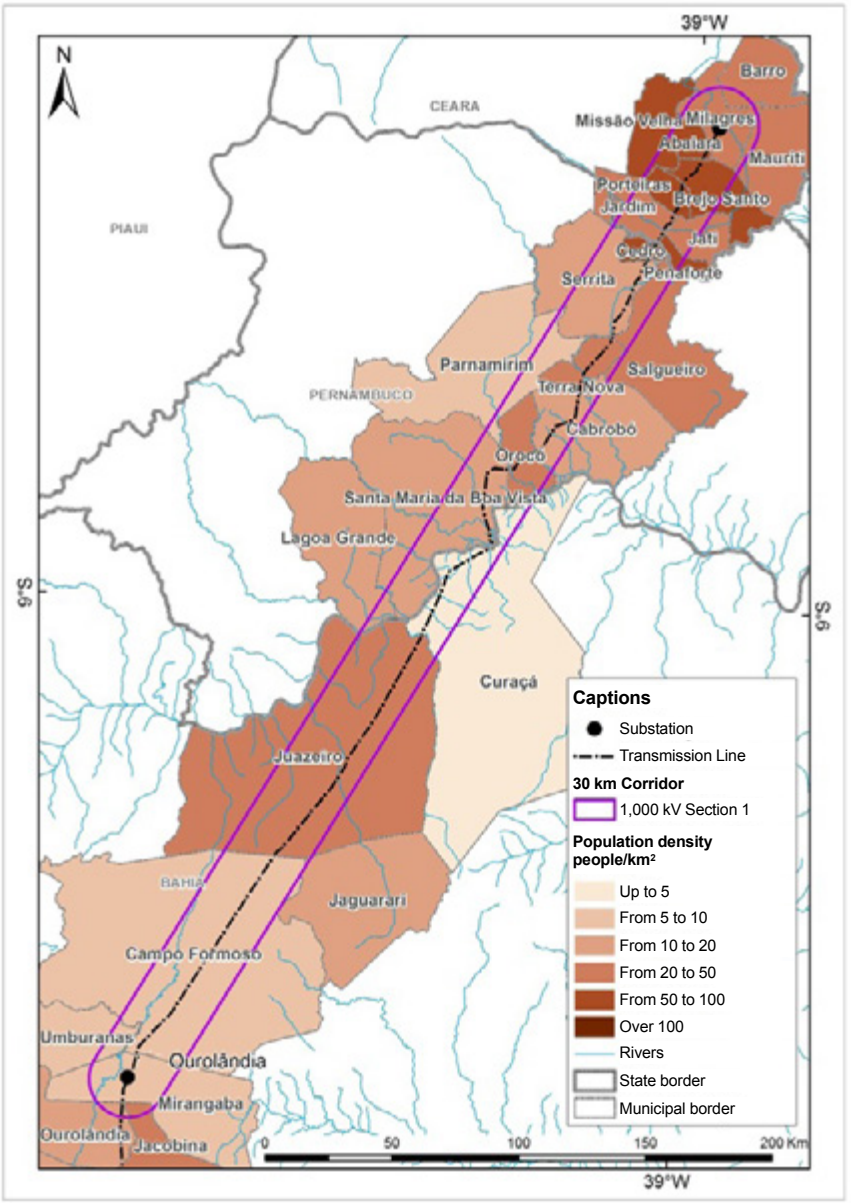

Figure 8.2: Location of T1 – Milagres (Ceará) to Ourolândia (Bahia)

According to the Land Use and Coverage Map published by IBGE, in 2012, T1 presents significant agricultural areas (Table 8.3), located mainly in the municipalities of Brejo Santo (Ceará), Porteiras (Ceará), Cedro (Ceará), and Penaforte (Ceará), in the northern area; Santa Maria da Boa Vista (Pernambuco), Curaçá (Bahia), Juazeiro (Bahia), and Orocó (Pernambuco), in the central region.

The T1 corridor is fully comprised in the caatinga biome. The vegetation cover and land use classes of this section are listed in Table 8.3. In Figure 8.3, the distribution of the vegetation cover and the occupation within the T1 corridor are shown.

Table 8.3: Vegetation cover and land use in the T1 corridor - Milagres (Ceará) to Ourolândia (Bahia)

Dominant classes	Area in the corridor (km2)	%
Agricultural area	435.04	3.174
Other uses (such as pasture)	6,933.42	50.580
Built area	16.82	0.123
Water bodies	186.57	1.361
Natural vegetation	6135.97	44.763
Total	13,707.81	100

Within the region comprised by the T1 corridor, there are only sustainable use conservation units, which are listed in Table 8.4. One of these CUs is a public sustainable use forest managed by ICMBio. Even with the existing sustainable CUs, the axis of the chosen corridor was designed avoiding these areas, as much as possible. In the Section 1 corridor there are no Indigenous Lands (Figure 8.4).

Table 8.4: Conservation Units in the T1 corridor T1 – Milagres (Ceará) to Ourolândia (Ceará)

CU name	Group	Category	Sphere
Environmental Protection Area Chapada do Araripe	SU	Environmental Protection Area	Federal
Floresta Nacional de Negreiros	SU	Forest	Federal

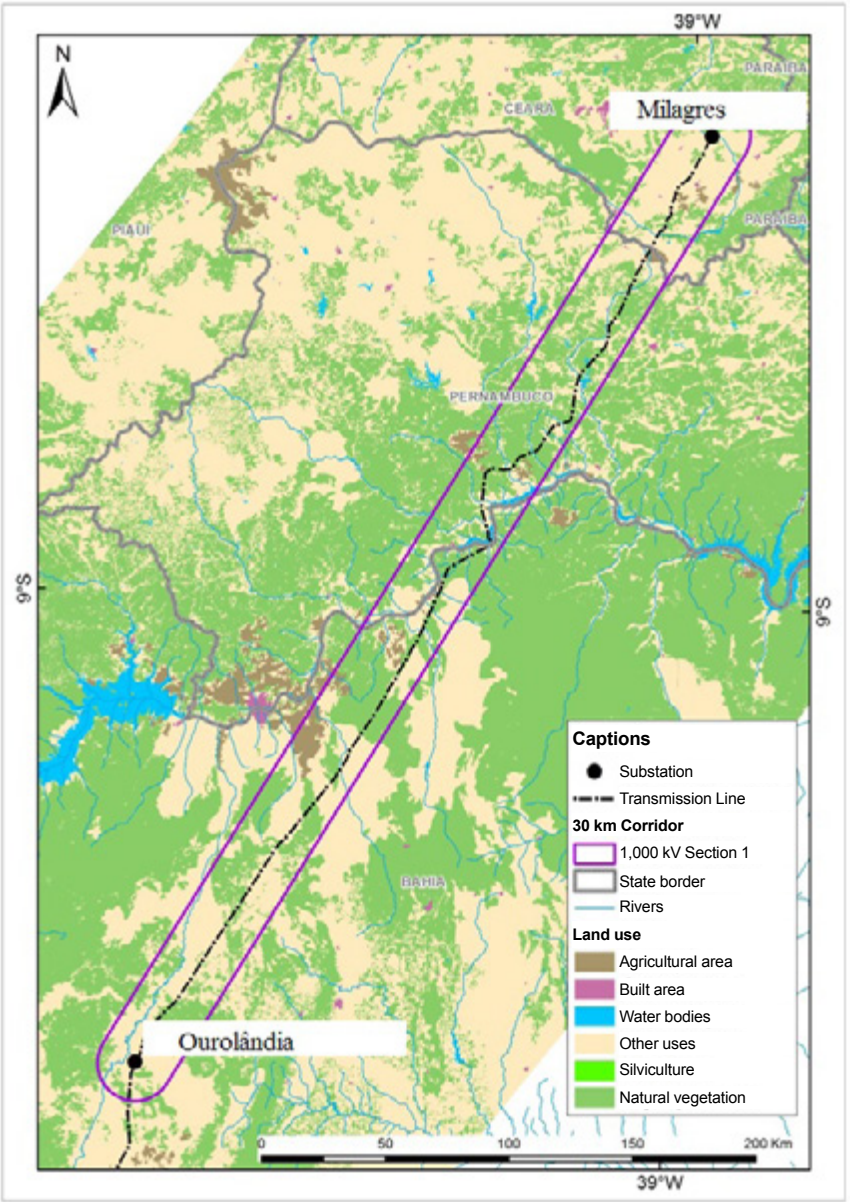

Figure 8.3: Vegetation cover and land use in the T1 corridor - Milagres (Ceará) to Ourolândia (Bahia)

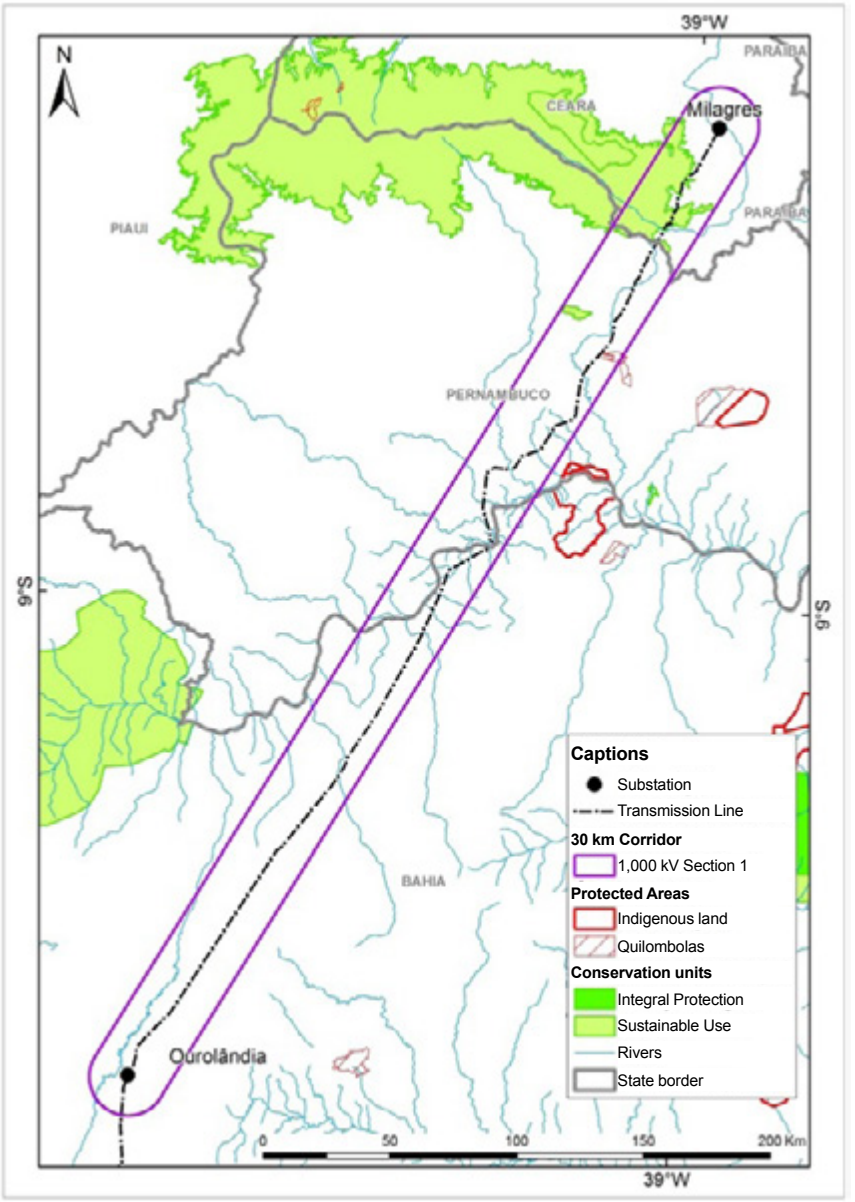

Figure 8.4: Conservation units, indigenous lands and quilombolic communities in the T1 corridor – Milagres (Ceará) a Ourolândia (Ceará)

There are several Priority Areas for Biodiversity Conservation (PABC) comprised in the T1 corridor. Table 8.5 describes these priority areas, their degree of importance, and priority action, according to the MMA criteria. The priority areas comprised in the T1 corridor are shown in Figure 8.5.

Table 8.5: Priority Areas for Biodiversity Conservation in the T1 corridor – Milagres (Ceará) to Ourolândia (Bahia)

Name of PABC	Code	Importance	Priority action
Rio Curaçá e Serras	Ca053	Extremely high	Create CU - Undefined
Region of Carrancas	Ca047	Very High	Recovery
Channel of the São Francisco River	Ca054	Extremely high	Create CU - PI
Petrolina	Ca064	Very High	Create CU - PI
Baxio da Melância	Ca062	Extremely high	Create SU - CU
Cabrobó	Ca079	Very High	Recovery
Chapada do Araripe (East)	Ca093	Extremely high	Create CU - PI
Kariris	Ca100	Extremely high	Create CU - Undefined
APA Chapada do Araripe - Catolé	Ca258	Extremely high	Protected Area
APA Chapada do Araripe - Catolé	Ca259	Extremely high	Protected Area

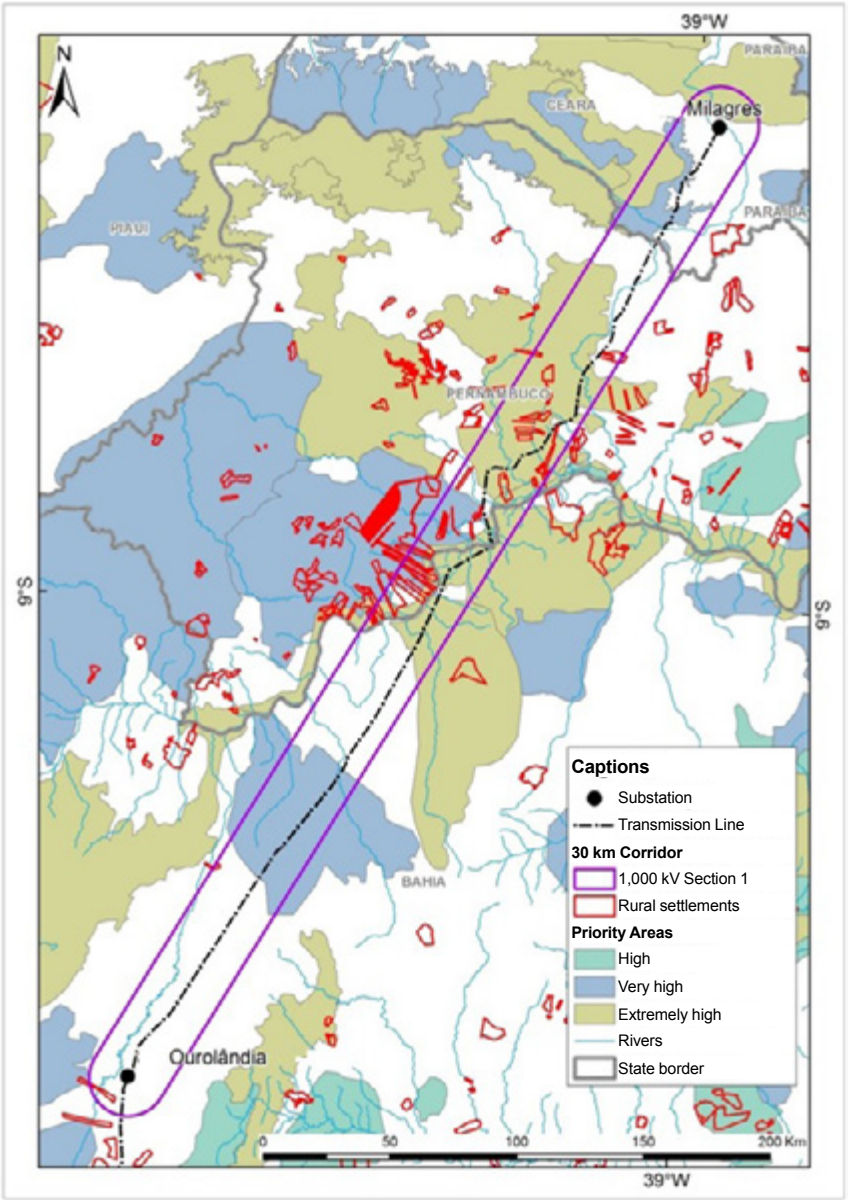

Figure 8.5: Priority Areas for Biodiversity Conservation and rural settlements in the T1 corridor – Milagres (Ceará) to Ourolândia (Bahia)

The area of the T1 corridor comprises 42 rural settlement projects, most of them in the State of Pernambuco, and 7 in the state of Bahia. The settlement projects (PAs) are concentrated mainly in the municipalities of Lagoa Grande, Orocó, Santa Maria da Boa Vista, and Terra Nova. We were able to divert the path chosen from all the settlements. Among the rural settlement projects (PA) inserted in the T1 corridor, there is the PA of the Contendas quilombolic community, located in the municipality of Terra Nova - Pernambuco. Table 8.6 lists the number of PAs per municipality.

Table 8.6: Rural settlement projects found in the T1 corridor - Milagres (Ceará) to Ourolândia (Bahia)

Municipality	Settlement projects
Cabrobó (Pernambuco)	6
Campo Formoso (Bahia)	1
Lagoa Grande (Bahia)	5
Mirangaba (Bahia)	1
Orocó (Pernambuco)	10
Parnamirim (Pernambuco)	1
Santa Maria da Boa Vista (Pernambuco)	16
Terra Nova (Pernambuco)	2

Next, Table 8.7 presents a summary of the main socio-environmental information found in the T1 corridor - Milagres (Ceará) to Ourolândia (Bahia).

Table 8.7: Summary of the main socio-environmental information found in the T1 corridor - Milagres (Ceará) to Ourolândia (Bahia)

Description	Quantitative
Length of the line (km)	457.67
Conservation Units (#)	2
Native vegetation (km^2)	6,135.97
Agriculture (km^2)	435.04
Indigenous lands (#)	0
Quilombolas (#)	1
Incra Settlements (#)	42
Caves (n°)	9
Municipalities crossed	27
Urban areas (km^2)	16.82

8.4 Macro-characterization of the Section Ourolândia (Bahia) to Igaporã (Bahia)

Section 2 (T2) of the transmission line comprises the area of the corridor that starts at Ourolândia, located in the municipality of Mirangaba, in the north of the state of Bahia, and stretches up to Igaporã, located in the municipality of Caetité, in the central-western region of the state of Bahia. This is a 13,684.00 km² area. The municipalities crossed by T2 and their respective population densities are described in Table 8.8, and shown in Figure 8.6.

Table 17: List of municipalities crossed corridor T2 – Ourolândia (Bahia) to Igaporã (Bahia)

State	Mesoregion	Microregion	Municipality	Population	Population density (people/km²)
Bahia	Central-North of Bahia	Irecê	Cafarnaum	17,169	20 to 50
			Iraquara	22,569	20 to 50
			Mulungu do Morro	12,212	20 to 50
			Souto Soares	15,855	10 to 20
		Jacobina	Jacobina	79,112	20 to 50
			Mirangaba	16,270	5 to 10
			Morro do Chapéu	35,065	5 to 10
			Ourolândia	16,389	10 to 20
			Várzea Nova	13,049	10 to 20
		Senhor do Bonfim	Campo Formoso	66,441	5 to 10
			Umburanas	16,908	5 to 10
	Central/South of Bahia	Guanambi	Caetité	47,368	10 to 20
			Guanambi	78,644	50 to 100
			Igaporã	15,183	10 to 20
			Matina	11,135	10 to 20
			Riacho de Santana	30,597	5 to 10
		Livramento do Brumado	Paramirim	20,967	10 to 20
			Rio do Pires	11,909	10 to 20
		Seabra	Boninal	13,683	10 to 20
			Bonito	14,816	10 to 20
			Seabra	41,714	10 to 20
		Boquira	Botuporã	11,143	10 to 20
			Caturama	8,838	10 to 20
			Ibipitanga	14,166	10 to 20
			Ibitiara	15,490	5 to 10
			Macaúbas	47,017	10 to 20
			Novo Horizonte	10,500	10 to 20
			Tanque Novo	16,108	20 to 50

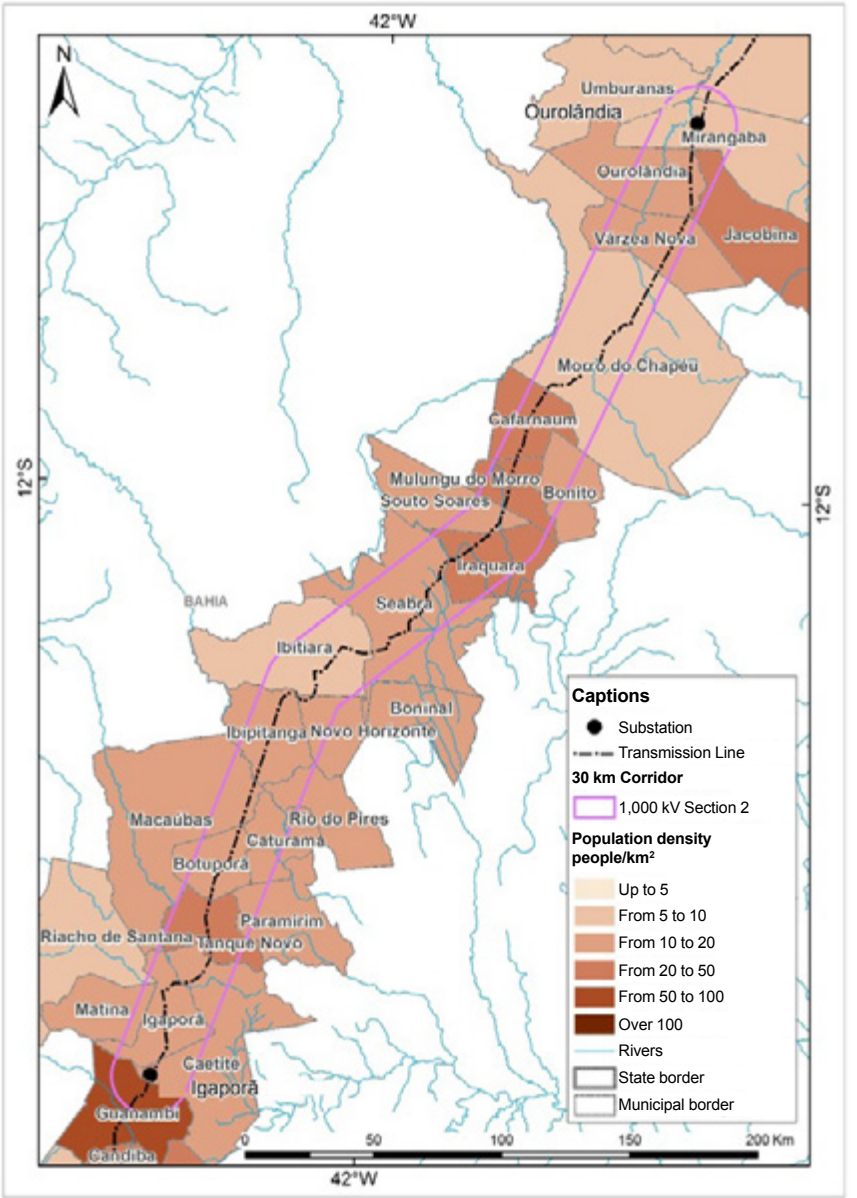

Figure 8.6: Location of T2 – Ourolândia (Ceará) to Igaporã (Bahia)

According to data from the Satellite Deforestation Monitoring of the Brazilian Biomes Project (PMDBBS), in T2 there is a predominance of other uses, such as pastures (67.483% of the area of the Section 2 corridor). In T2 there are no expressive agricultural areas. The main urban/built areas are located to the extreme north of the municipalities of Ourolândia (Bahia), and Morro do Chapéu (Bahia), as well as in the center of T2, in the municipality of Seabra (Bahia), and to the south of the corridor in the municipalities of Igaporã (Bahia), Botuporã (Bahia), Tanque Novo (Bahia), and Guanambi (Bahia). The T2 corridor is fully comprised in the caatinga biome. The vegetation cover and land use classes of this section are listed in Table 8.9. In Figure 8.7, the distribution of the vegetation cover and its occupation within the T2 corridor are shown.

Table 8.9: Vegetation cover and land use in the T2 corridor - Ourolândia (Ceará) to Igaporã (Bahia)

Dominant classes	Area in the corridor (km²)	%
Agricultural area	2.95	0.022
Other uses (such as pasture)	9,234.34	67.483
Built area	16.37	0.120
Water bodies	6.37	0.047
Natural vegetation	4423.97	32.330
Total	13,684.00	100

Table 8.10: Conservation Units in the T2 corridor – Ourolândia (Bahia) to Igaporã (Bahia)

CU name	Group	Category	State
Environmental Protection Area Marimbus/Iraquara	SU	Environmental Protection Area	Bahia
Morro do Chapéu State Park	PI	State Park	Bahia

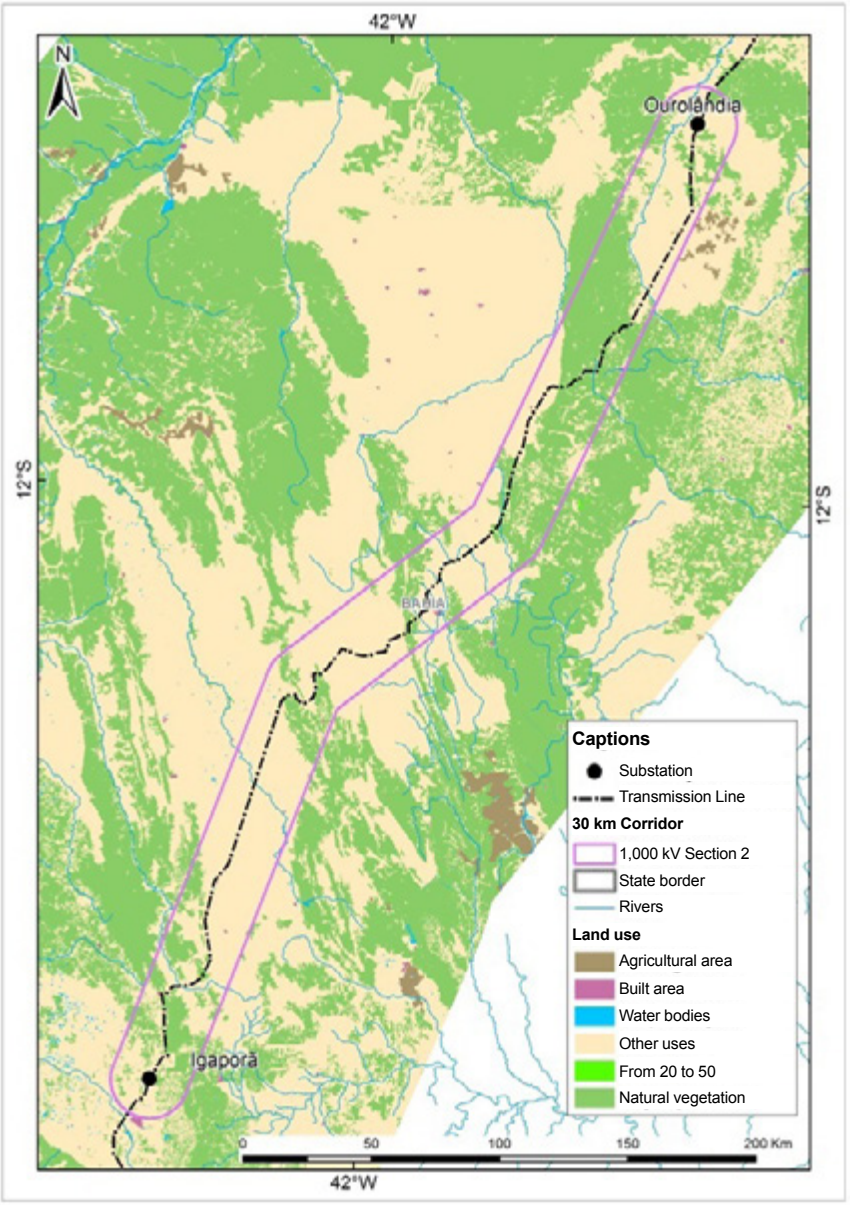

Figure 8.7: Vegetation cover and land use in the T2 corridor - Ourolândia (Bahia) to Igaporã (Bahia)

Within the region comprised by the T2 corridor, there is a sustainable use conservation unit, and an integral protection conservation unit, listed in Table 8.8. On the other hand, there are no indigenous lands in T2. Figure 8.8 illustrates the distribution of Conservation Units (CUs) and quilombolic communities in the region of the T2 corridor.

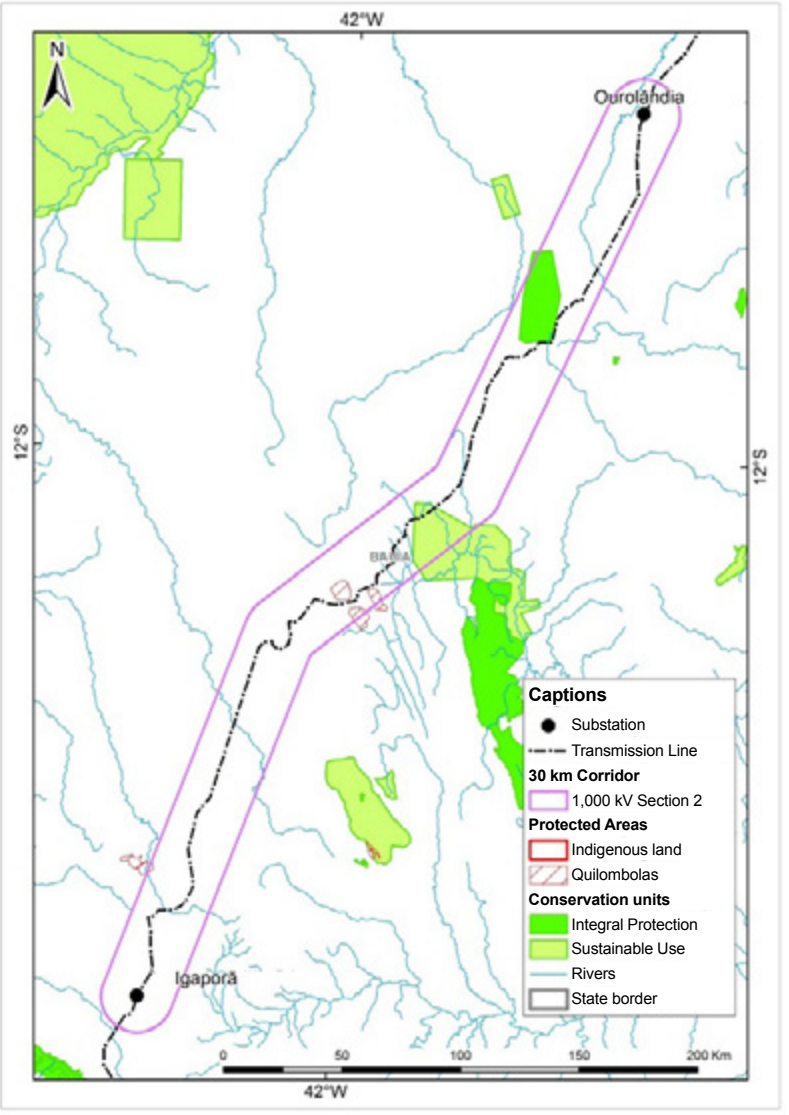

Figure 8.8: Conservation units, indigenous lands and quilombolic communities in the T2 corridor – Ourolândia (Bahia) to Igaporã (Bahia)

There are several Priority Areas for Biodiversity Conservation comprised in the T2 corridor. Table 8.11 describes these priority areas, their degree of importance, and priority action, according to the MMA criteria. The priority areas comprised in the T2 corridor or even located close to it are shown in Figure 8.9.

Table 8.11: Priority Areas for Biodiversity Conservation in the T2 corridor - Ourolândia (Bahia) to Igaporã (Bahia)

Name of PABC	Code	Importance	Priority action
Guanambi	Ca004	Very High	Promote Sustainable Use
Igaporá	Ca008	High	Recovery
Paramirim	Ca015	High	Recovery
Corredor dos Brejões	Ca033	Very High	Create CU - Undefined
Marimbus/Iraquara	Ca020	Extremely high	Create CU - PI
Dois Riachos	Ca022	High	Inventory
Oliveira dos Brejinhos	Ca019	Extremely high	Create CU - Undefined
Morro do Chapéu Region	Ca023	Extremely high	Mosaic/Corridor
Riacho de Santana	Ca010	Very High	Create CU - Undefined
Morro do Chapéu State Park	Ca233	Extremely high	Protected area
Umburanas	Ca037	High	Recovery

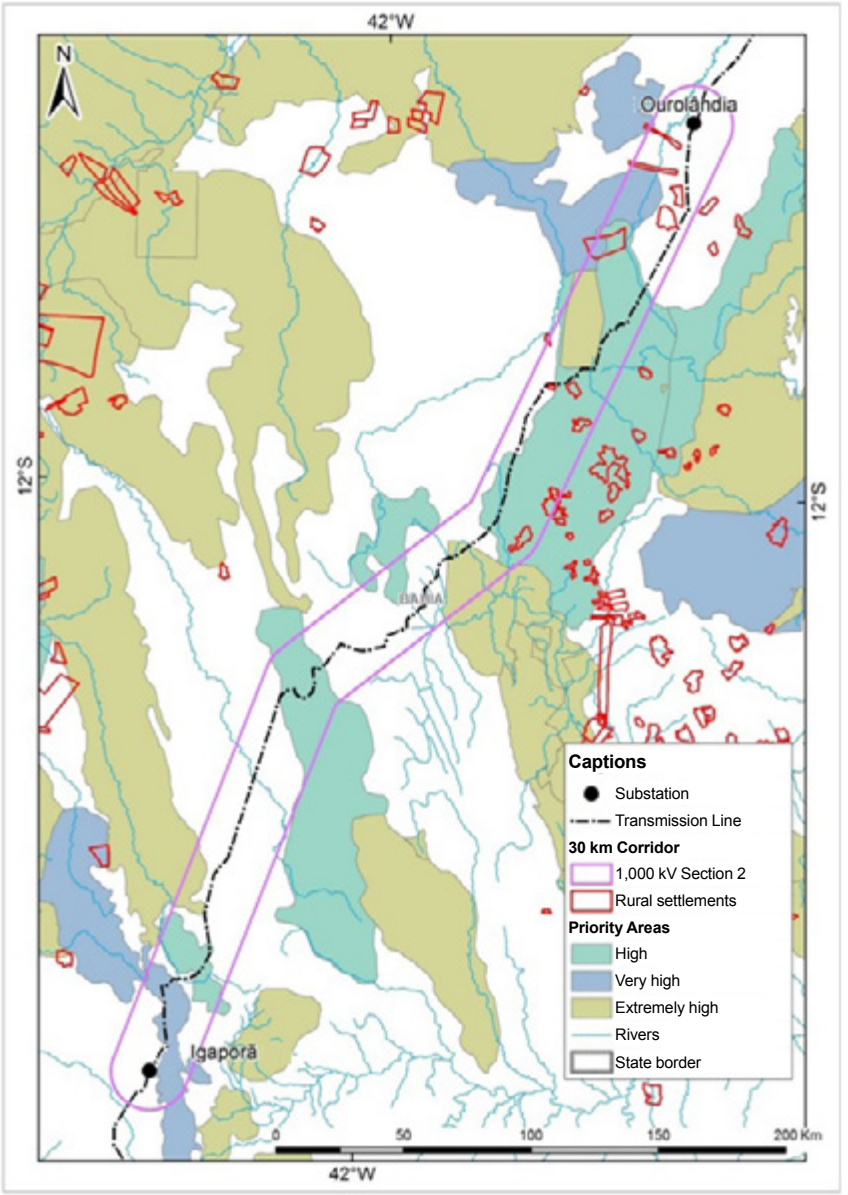

Figure 8.9: Priority Areas for Biodiversity Conservation and rural settlements in the T2 corridor - Ourolândia (Bahia) to Igaporã (Bahia)

The area of the T2 corridor comprises 12 rural settlement projects. In this section there is a smaller concentration of settlement projects (PAs), which allowed for greater flexibility in the definition of the path so as to steer clear of these settlement projects. Table 8.12 lists the number of PAs per municipality.

Table 8.12: Rural settlement projects found in the T2 corridor - Juazeiro (Bahia) to Bom Jesus da Lapa (Bahia)

Municipality	Settlement projects
Bonito - Bahia	2
Iraquara - Bahia	1
Morro do Chapéu - Bahia	5
Ourolândia - Bahia	3
Mirangaba - Bahia	1

Next, in Table 8.13, a summary of the main socio-environmental information found in the T2 corridor - Juazeiro II (Bahia) to Bom Jesus da Lapa II (Bahia) is presented.

Table 8.13: Summary of the main socio-environmental information found in the T2 corridor - Ourolândia (Bahia) to Igaporã (Bahia)

Description	Quantitative
Length of the line (km)	482.49
Conservation Units (#)	2
Native vegetation (km^2)	4,423.97
Agriculture (km^2)	2.95
Indigenous lands (#)	0
Quilombolic Areas (#)	5
Incra Settlements (#)	12
Caves (#)	123
Municipalities crossed	28
Urban areas (km^2)	16.37

8.5 Macro-characterization of the Section Igaporã (Bahia) to Pirapora (Minas Gerais)

Section 3 (T3) comprises the area of the corridor that starts at Igaporã, located in the municipality of Caetité, central-southern region of the state of Bahia, and goes to Pirapora, located in the municipality of Pirapora, State of Minas Gerais. This is a 13,857.35 km^2 area. The São Francisco and Rio das Velhas rivers cut the south part of T3. In this section, crossing the Rio das

Velhas, close to Pirapora will be unavoidable. The municipalities crossed by the T3 corridor, and their respective population densities, are described in Table 8.14, and shown in Figure 8.10.

Table 8.14: List of municipalities crossed by T3 corridor – Igaporã (Bahia) to Pirapora (Minas Gerais)

State	Mesoregion	Microregion	Municipality	Population	Population density (people/km²)
Bahia	Central/South of Bahia	Guanambi	Caetité	47,368	10 to 20
			Candiba	13,201	20 to 50
			Guanambi	78,644	50 to 100
			Igaporã	15,183	10 to 20
			Matina	11,135	10 to 20
			Pindaí	15,616	20 to 50
			Sebastião Laranjeiras	10,340	5 to 10
			Urandi	16,447	10 to 20
Minas Gerais	North of Minas	Montes Claros	Capitão Enéas	14,151	10 to 20
			Coração de Jesus	25,918	10 to 20
			Mirabela	13,003	10 to 20
			Montes Claros	360,405	50 to 100
			Patis	5,565	10 to 20
			São João da Lagoa	4,651	up to 5
			São João da Ponte	25,293	10 to 20
			São João do Pacuí	4,056	5 to 10
			Verdelândia	8,281	5 to 10
		Janaúba	Catuti	5,094	10 to 20
			Espinosa	31,028	10 to 20
			Gameleiras	5,114	up to 5
			Janaúba	66,495	20 to 50
			Mamomas	6,311	20 to 50
			Mato Verde	12,657	20 to 50
			Monte Azul	21,936	20 to 50
			Nova Porteirinha	7,371	50 to 100
			Pai Pedro	5,917	5 to 10
			Porteirinha	37,492	20 to 50
		Pirapora	Buritizeiro	26,774	up to 5
			Ibiaí	7,803	5 to 10
			Jequitaí	7,917	5 to 10
			Lagoa dos Patos	4,218	5 to 10
			Pirapora	52,929	50 to 100
			Várzea da Palma	35,699	10 to 20

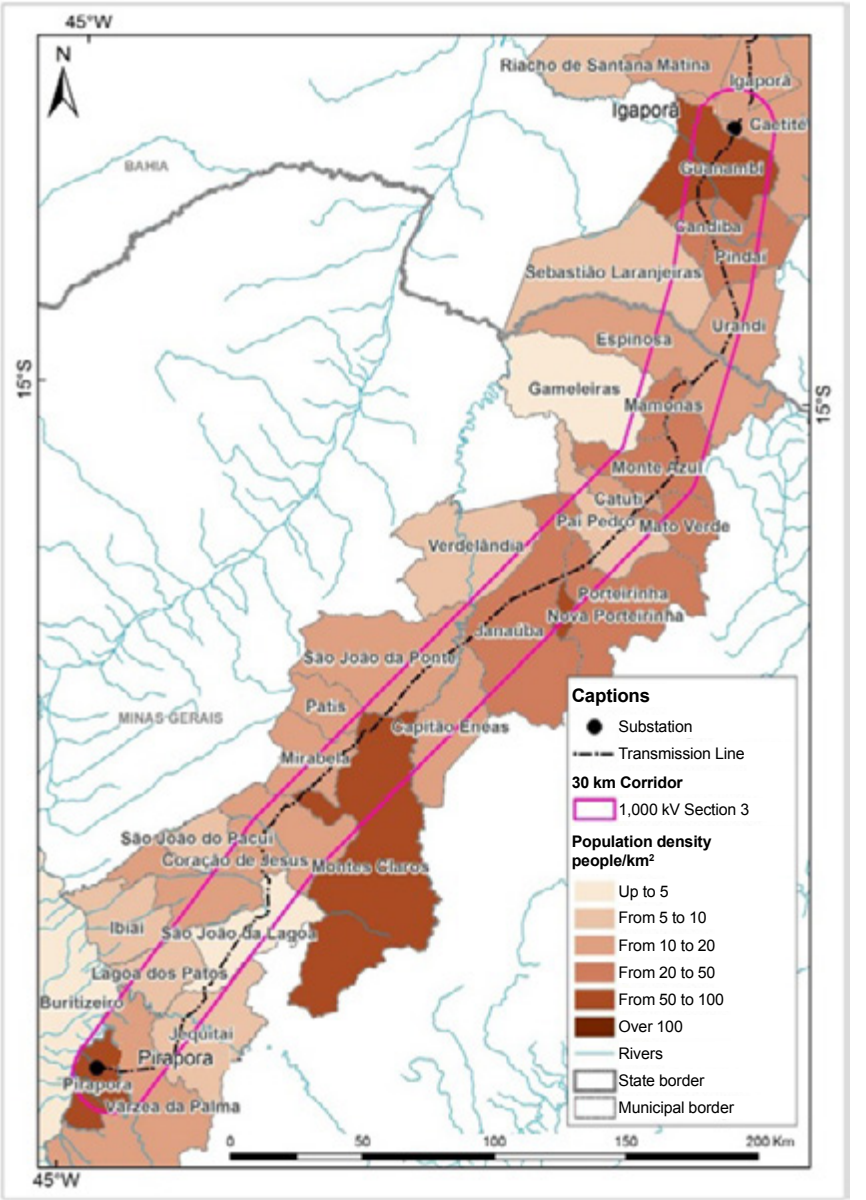

Figure 8.10: Location of the T3 corridor – Igaporã (Bahia) to Pirapora (Minas Gerais)

According to data from the Satellite Deforestation Monitoring of the Brazilian Biomes Project (PMDBBS), in T3 there is a predominance of other uses, such as pastures (66.60% of the area of the Section 3 corridor). The more expressive agricultural areas are concentrated in the municipalities of Porteirinha (Minas Gerais), Nova Porteirinha (Minas Gerais), and Janaúba (Minas Gerais), located in the central portion of T3, and in the municipalities of Jequitaí (Minas Gerais), and São João da Lagoa (Minas Gerais), located in the south region of the corridor. In the T3 corridor there are also important silviculture areas T3 that spread through the municipalities of Sebastião Laranjeiras (Bahia), and Urandi (Bahia), located in the north of the corridor, Janaúba (Minas Gerais), Verdelândia (Minas Gerais), and Coração de Jesus (Minas Gerais), located in its central portion. About 66.22% of the T3 corridor is comprised in the savanna biome, and only 33.78% in the caatinga biome. The vegetation cover and land use classes of this section are listed in Table 8.15. In Figure 8.11, the distribution of the vegetation cover and the occupation within the T3 corridor are shown.

Table 8.15: Vegetation cover and land use in the T3 corridor - Igaporã (Bahia) to Pirapora (Minas Gerais)

Dominant classes	Area in the corridor (km²)	%
Agricultural area	134.94	0.974
Other uses	9,229.02	66.600
Built area	52.12	0.376
Water bodies	62.15	0.449
Forestry	93.83	0.677
Natural vegetation	4285.29	30.924
Total	13,857.35	100

Within the region comprised by the T3 corridor, there are only integral protection conservation units, which are listed in Table 8.16. The path alternative was designed so as to avoid these areas. On the other hand, there are no indigenous lands in the T3, with the closest Indigenous lands, the TI Xacriabe, located about 100 km from the corridor (Figure 8.12).

Table 8.16: Conservation Units in the T3 corridor – Igaporã (Bahia) to Pirapora (Minas Gerais)

CU name	Group	Category	State
Caminho dos Gerais State Park	PI	State Park	Minas Gerais
Serra dos Montes Altos State Park	PI	State Park	Bahia
Serra dos Montes Altos Wildlife Refuge	PI	Wildlife Refuge	Bahia

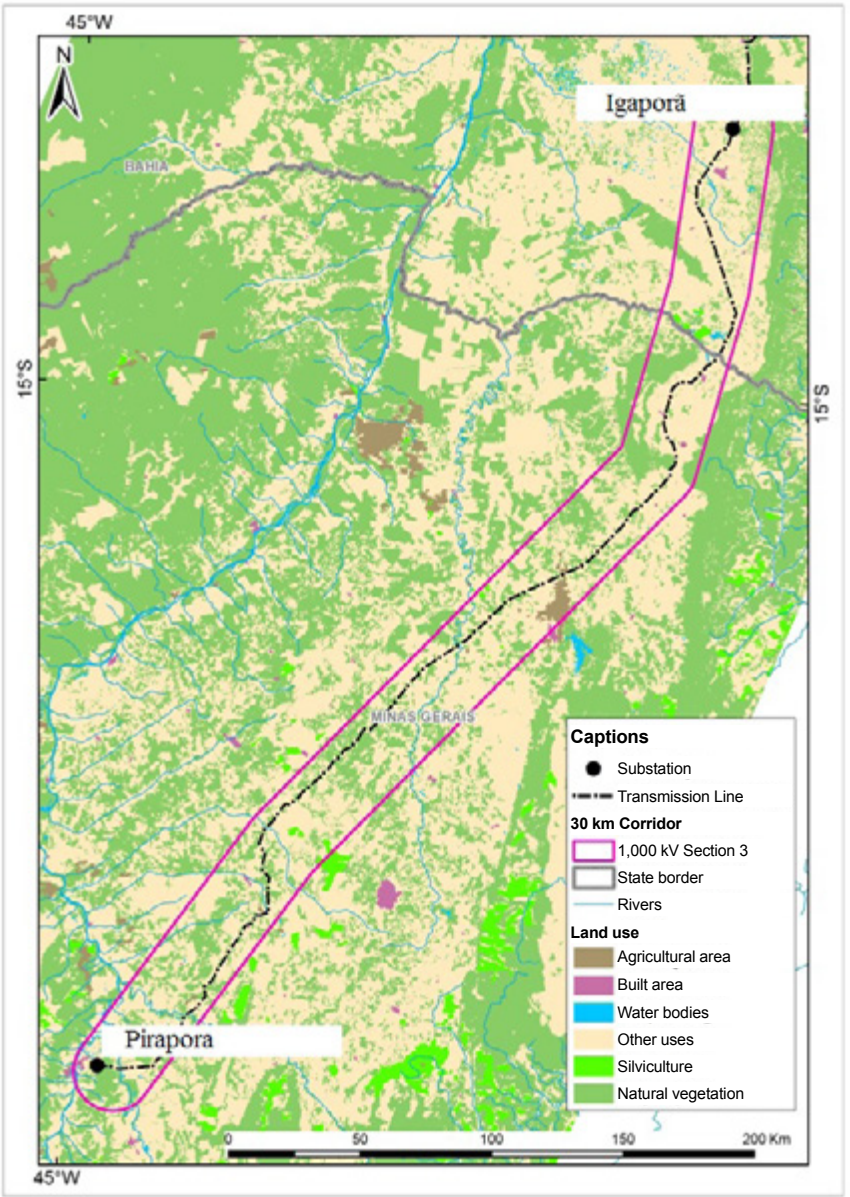

Figure 8.11: Vegetation cover and land use in the T3 corridor - Igaporã (Bahia) to Pirapora (Minas Gerais)

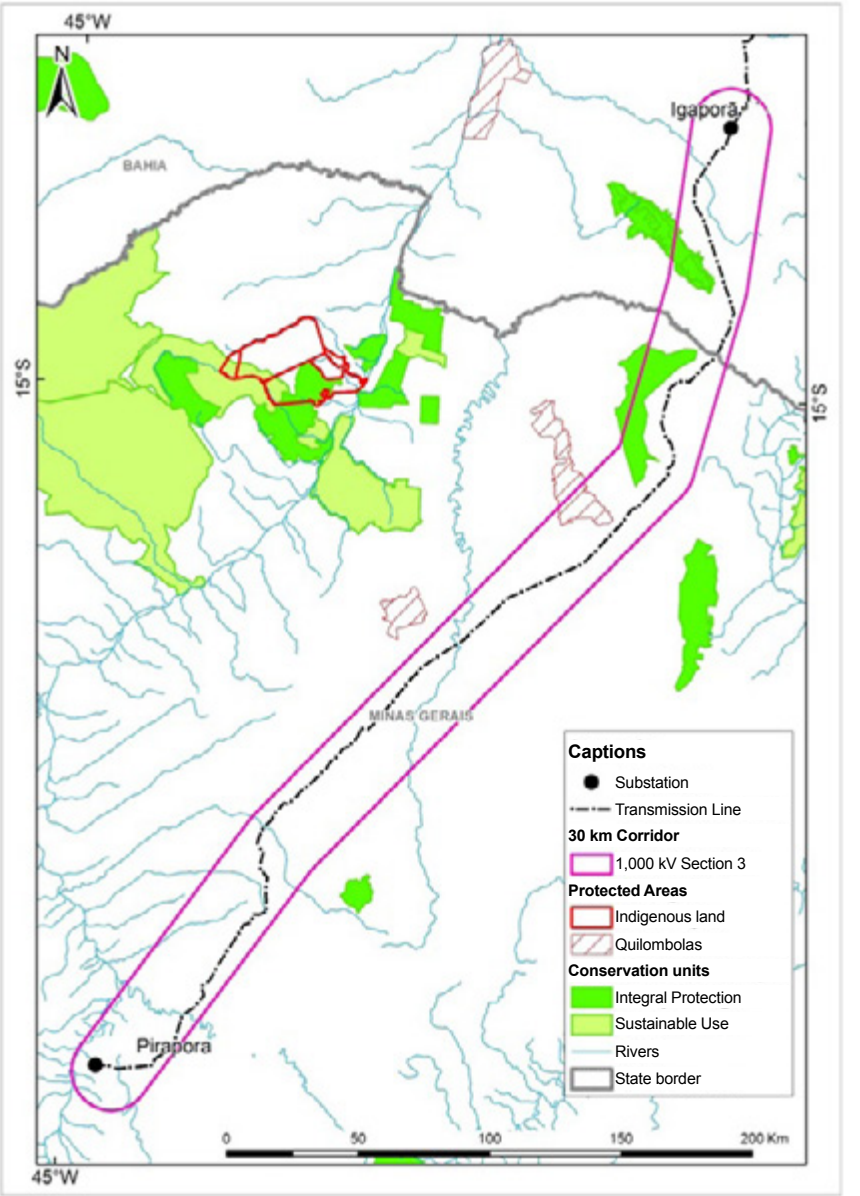

Figure 8.12: Conservation units, indigenous lands, and quilombola communities in the T3 corridor – Igaporã (Bahia) to Pirapora (Minas Gerais)

There are several Priority Areas for Biodiversity Conservation comprised in the T3 corridor. Table 8.17 describes these priority areas, their degree of importance, and priority action, according to the MMA criteria. The priority areas comprised in the T3 corridor or even located close to it are shown in Figure 8.13.

Table 8.17: Priority Areas for Biodiversity Conservation in the T3 corridor - Igaporã (Bahia) to Pirapora (Minas Gerais)

Name of PABCå	Importance	Priority action
Alto - Médio São Francisco	Extremely high	Recovery
Buritizeiro	High	Recovery
Northern Ridge	Extremely high	Recovery
Jaíba	Extremely high	Inventory
Jacaraci	Insufficiently known	Recovery
São João da Ponte	Very High	Promote Sustainable Use
Verdelândia	Extremely high	Recovery
Verdelândia – Varzelândia	Very High	Recovery
Guanambi	Insufficiently known	Promote Sustainable Use

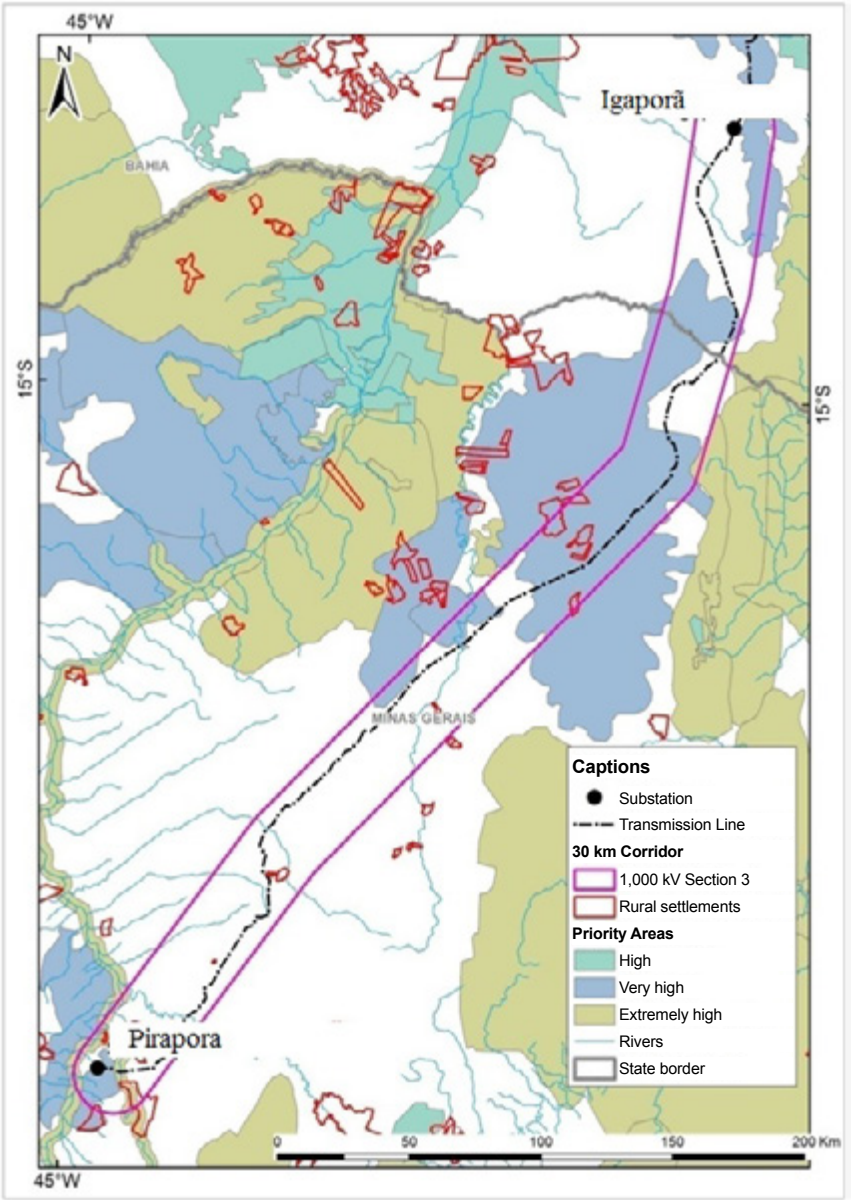

Figure 8.13: Priority Areas for Biodiversity Conservation and rural settlements in the T3 corridor - Igaporã (Bahia) to Pirapora (Minas Gerais)

The area of the T3 corridor comprises 12 rural settlement projects. The path was modeled so as to divert from all the settlements. Table 8.18 presents the number of PAs per municipality.

Table 8.18: Rural settlement projects found in the T3 corridor – Igaporã (Ceará) to Pirapora (Minas Gerais)

Municipality	Settlement projects
Capitão Enéas (Minas Gerais)	1
Coração de Jesus (Minas Gerais)	1
Janaúba (Minas Gerais)	1
Nova Porteirinha (Minas Gerais)	1
Pirapora (Minas Gerais)	2
Porteirinha (Minas Gerais)	2
São João da Lagoa (Minas Gerais)	1
Várzea da Palma (Minas Gerais)	3

Next, Table 8.19 presents a summary of the main socio-environmental information found in the T3 corridor - Igaporã (Bahia) to Pirapora (Minas Gerais).

Table 8.19: Summary of the main socio-environmental information found in the T3 corridor – Igaporã (Bahia) to Pirapora (Minas Gerais)

Description	Quantitative
Length of the line (km)	498.73
Conservation Units (#)	3
Native vegetation (km^2)	4,285.29
Agriculture (km^2)	134.94
Indigenous lands (#)	0
Quilombolas (#)	1
Incra Settlements (#)	12
Caves (#)	75
Municipalities crossed	33
Urban areas (km^2)	52.12

Based on the evaluations proposed here, it is recommended that a more in-depth study is conducted on the more critical areas, prior to the implementation of the line

9. General Recommendations for Future Actions

This chapter provides support for the implementation of the transmission line and its preferred route. However, it is recommended that a more detailed evaluation of the socio-environmental variables is made, mainly regarding those related to the more critical points listed in the sensitivity mapping.

It is important to consider a more detailed analysis of the vegetation fragments to be crossed and their current conservation state, assessing the possible impacts with the implementation of the project. We should seek to assess the areas where there will be lower vegetation suppression.

The ecosystems should be studied in more detail, seeking to identify the more fragile systems to prevent impacts that would bring risk to the natural operating dynamics.

It is also necessary to make a more in-depth assessment of the potential areas with regards to the presence of archaeological sites, so as to obtain more consistent information on existing sites and, thus, of the potential impact that might be caused. This requires a more specific and detailed work, since the secondary data indicate a concentration of archaeological sites in certain regions, such as the municipalities of Abaiara (Ceará), and Guanambi (Bahia).

It is also necessary to conduct a more detailed assessment of the mountain alignments to be crossed, so as to detail the difficulties and possible specific needs for the implementation of the project. These alignments present natural altimetric barriers and make the line implementation more difficult. They often present associated vegetation fragments that may present endemism, due to the isolation they present from the general context. In the lower parts of the mountain alignments, there are hydromorphic, and sedimentary alluvial and colluvial deposit areas. Thus, a more detailed evaluation of the points where the line towers are to be installed is necessary.

The areas of plateaus and tablelands sometimes present ridges that must be crossed. These compartments are more sensitive and their material more consolidated, so special care should be taken in these areas.

The presence of airports and airfields is another aspect that requires attention, and the line should be kept as far as possible from these areas so as to prevent accidents.

It is also important to steer away from areas of quilombos, agricultural settlements, and indigenous lands, since these areas have been consolidated after land conflicts. A more in-depth study is required on the influence the line might cause for being near some of these areas.

The areas where medium and large rivers will be crossed also deserve special attention, such as the case of Rio das Velhas and the São Francisco River. In the addition of hydromorphic soils, and river margin APPs (Areas of Permanent Protection), there are also technical difficulties to be overcome regarding the crossing, as well as the issue of navigation, as in the case of the São Francisco River.

Special care should be dedicated to silviculture areas due to the high costs they represent, so greater detailing should be made of the more adequate areas for the line to pass.

Some areas require a more detailed geological assessment, mainly those that present clastic lithology, due to the existence of caves, as is the case in the central area of the state of Bahia. We highlight the region of the municipality of Iraquara (Bahia), and also the regions of the municipalities of Campo Formoso (Bahia), and Várzea Nova (Bahia).

In the proximity of the municipality of Coração de Jesus, in the state of Minas Gerais, attention should be given to the presence of paleontological sites, which will also require a more specific assessment. The area also presents a series of veredas, and archeological potential.

It is important to highlight that most of the territory to be crosses is composed of rural areas, so an assessment should be made of the rural occupation registers, listing the owners and the situation of the properties. Thus, a study is recommended to evaluate the average value of the properties and agricultural potential.

As many hills, ridges, and rivers will be crossed, a more detailed evaluation of the existing Areas of Permanent Protection in the stretch were the line is to be implemented is necessary, so as to prevent the construction of the transmission line over areas of spring APP, or river margin APPs, thus respecting the legislation in effect.

10. References

[1] AGÊNCIA NACIONAL DE ÁGUAS (ANA). 2006. Atlas Nordeste de Abastecimento Urbano de Água. Available at: <http://www.ana.gov.br/bibliotecavirtual/arquivos/20061213161802_atlas.pdf> Accessed on: 07/11/2016.

[2] AHP. Available at: <http://ppegeo.igc.usp.br/scielo.php?pid=S0101-90822009000400006&script=sci_arttext&tlng=es>. Accessed on: Jan. 04, 2015.

[3] AGÊNCIA NACIONAL DE ENERGIA ELÉTRICA (ANEEL). 2013. Technical Note n. 0203/2013-SCT-SRT/ANEEL. Available at: <http://www.aneel.gov.br/aplicacoes/audiencia/arquivo/2013/081/documento/nt_n%C2%BA_203_sct_e_srt.pdf>. Accessed on: Dec 18, 2015.

[4] BRAZIL, 1981. Ministério das Minas e Energia. Secretaria Geral. Projeto RADAMBRASIL: Sheet SD. 24 Salvador. Rio de Janeiro, 1981. 620 p. (Levantamento de Recursos Naturais, v. 24).

[5] BRAZIL, 1973. Ministério das Minas e Energia. Secretaria Geral. Projeto RADAMBRASIL: Sheet SA. 23 São Luis and part of Sheet SA. 24 Fortaleza. Rio de Janeiro, 1973. 331 p. (Levantamento de Recursos Naturais, v. 3)

[6] CASSETI, V. *Geomorfologia*. [S.I]. Available at: <http://www.funape.org.br/geomorfologia/>. Accessed on: Oct 2016.

[7] CASTRO, A.S.; CAVALCANTE, A. *Flores da caatinga*. Campina Grande: Instituto Nacional do Semiárido, 2010. 116p.

[8] CHRISTOFOLETTI, A. Geomorfologia. 2 ed. Editora Edgard Blüncher Ltda, 1980.

[9] COFINS. *Desenvolvimento rural do semiárido brasileiro: transformações recentes, desafios e perspectivas*. Available at: <https://confins.revues.org/8633>. Accessed on: Jul 11, 2016.

[10] COMISSÃO PASTORAL DA TERRA (CPT). *Conflitos no Campo Brasil*. Comissão Pastoral da Terra. Goiânia, 2016. 240p.

[11] DANTAS, M.E. *Biblioteca de Padrõ*es de Relevo: Carta de Suscetibilidade a Movimentos Gravitacionais de Massa e Inundação. Rio de Janeiro: CPRM, 2016. Available at: <http://www.cprm.gov.br/suscetibilidade/Biblioteca_Padroes_Relevo_Suscetibilidade_31mar2016.pdf>. Accessed on: Mar 2016.

[12] MACHADO, M.F. ; SILVA, S.F. (Org). In: *Geodiversidade do estado de Minas Gerais*. CPRM, 2010. 131p.

[13] CAVALHO, L.M; RAMOS, M.A.B (Org.). In: *Geodiversidade do estado da Bahia*. CPRM, 2010. 184p.

[14] TORRES, F.S. de M. & PFALTZGRAFF, P.A. dos S. (Org). In: *Geodiversidade do estado de Pernambuco*. CPRM, 2014. 214p.

[15] BRANDÃO, R.L.; FREITAS, L.C.B. (Org) In: *Geodiversidade do estado do Ceará*. Fortaleza, CPRM, 2014. 282p.

[16] EMBRAPA. *Sistema Brasileiro de Classificação de Solos*. Centro Nacional de Pesquisa de Solos. Rio de Janeiro, RJ, 2016. 306p. 2nd Edition.

[17] EMBRAPA. *O novo mapa de solos do Brasil: legenda atualizada*. Scale 1: 5,000,000. 2011.

[18] EMBRAPA SOLOS. Available at: https://www.embrapa.br/solos/busca-de-publicacoes/-/publicacao/920267/o-novo-mapa-de-solos-do-brasil-legenda-atualizada (Accessed on data missing).

[19] FLORENZANO, T.G. *Geomorfologia: conceitos e tecnologias atuais*. Editora Oficina de Textos, São Paulo. 2008.

[20] FUNDAÇÃO NACIONAL DO ÍNDIO (FUNAI). *Dados de Terras indígenas*. Available at: <www.funai.gov.br/index.php/shape> Accessed on: Dec 14, 2015.

[21] GUERRA, A.J.T.; CUNHA, S.B. *Geomorfologia: uma atualizaçã*o de base e conceitos. 9 ed. Editora Bertrand Brasil, 2009.

[22] GUERRA, A.T.; GUERRA, A.J.T. *Novo dicionário geológico-geomorfológico*. 7 ed. Editora Bertrand Brasil, 2009.

[23] IBGE (INSTITUTO BRASILEIRO DE GEOGRAFIA E ESTATÍSTICA), 2012. *Dados de uso do solo e cobertura vegetal*. Available at: <www.ibge.gov.br/home/geociencias/recursosnaturais> Accessed on: Dec 15, 2015.

[24] INSTITUTO BRASILEIRO DE GEOGRAFIA E ESTATÍSTICA (IBGE). *Hidrografia*. Available at: <www.ibge.gov.br/home/geociencias/recursosnaturais> Accessed on: Aug 2016.

[25] INSTITUTO BRASILEIRO DE GEOGRAFIA E ESTATÍSTICA (IBGE). *Rodovias*. Available at: <www.ibge.gov.br/home/geociencias/recursosnaturais> Accessed on: Aug 2016.

[26] INSTITUTO BRASILEIRO DE GEOGRAFIA E ESTATÍSTICA (IBGE). *Manual técnico da vegetação brasileira*. 2nd. ed. (rev. and enhanced). Rio de Janeiro: Manuais Técnicos em Geociências – number 1, 2012. 275p.

[27] INSTITUTO BRASILEIRO DE GEOGRAFIA E ESTATÍSTICA (IBGE). Portal Cidades. Available at: <http://cidades.ibge.gov.br/xtras/home.php> Accessed on: Aug 2016.

[28] INSTITUTO BRASILEIRO DE GEOGRAFIA E ESTATÍSTICA (IBGE). Portal Estados. Available at: <http://www.ibge.gov.br/estadosat/> Accessed on: Aug 2015.

[29] INSTITUTO CHICO MENDES DE BIODIVERSIDADE (ICMBio). *Unidades de conservação*. Available at: <http://www.icmbio.gov.br/portal/biodiversidade/unidades-de-conservacao/grupos.html and http://www.florestal.gov.br/snif/recursos-florestais/sistema-nacional-de-unidades-de-conservacao?print=1&tmpl=component>. Accessed on: Dec 14, 2015.

[30] INSTITUTO CHICO MENDES DE BIODIVERSIDADE (ICMBio). *Unidades de conservação*. Available at: <http://www.icmbio.gov.br/portal/biodiversidade/unidades-de-conservacao/grupos.html> and <http://www.florestal.gov.br/snif/recursos-florestais/sistema-nacional-de-unidades-de-conservacao?print=1&tmpl=component>. Accessed on: Dec 21, 2015.

[31] INSTITUTO CHICO MENDES DE BIODIVERSIDADE (ICMBio). *Dados de cavernas*. Available at: <www.icmbio.gov.br/cecav/downloads/mapas.html>. Accessed on: Dec 14, 2015.

[32] INSTITUTO NACIONAL DE COLONIZAÇÃO E REFORMA AGRÁRIA (INCRA). *Dados de assentamentos*. Available at: <acervofundiario.incra.gov.br> Accessed on: Dec 14, 2015.

[33] INEMA *Zoneamento ecológico econômico do estado da Bahia*, 2013. Available at: <http://www.zee.ba.gov.br/> Accessed on: Jan 2017.

[34] INSTITUTO NACIONAL DE METEREOLOGIA (INMET). *Normas climatológicas do Brasil 1961-1990*. Available at: <http://www.inmet.gov.br/portal/index.php?r=clima/normaisClimatologicas>. Accessed on: Jul 11, 2016.

[35] INPE (Instituto Nacional de Pesquisas Espaciais), 2016 . *Infográfico - Densidade de raios no Brasil*. Available at: <http://www.inpe.br/webelat/homepage/menu/infor/infografico.-.densidade.de.raios.no.brasil.php>. Accessed on: Jul 11, 2016.

[36] IPHAN, 2016 – *Base de dados de Sitios Georreferenciados*. Available at: <http://portal.iphan.gov.br/pagina/detalhes/1227/> Accessed on: Aug 2016.

[37] JÚNIOR, E.C.; COUTINHO, B.H.; FREITAS, L.E., 2009 *Gestão da Biodiversidade e Áreas protegidas*. In: GUERRA, A.T.; COELHO, M.C.N. (Org). *Unidades de Conservação: Abordagens e características geográficas*. Rio de Janeiro: Bertrand Brasil, 2009.

[38] LEPSCH, I.F., 2010. *Formação e Conserva*ção dos solos. 2 ed. São Paulo: Oficina de Textos, 2010.

[39] LUZ, S.; SELLITTO, M. ; GOMES, L. *Medição de desempenho ambiental baseada em método multicriterial de apoio à decisão: estudo de caso na indústria automotiva*. Gestão & Produção, v.13, n.3, p.557-570, 2006.

[40] MINISTÉRIO DO MEIO AMBIENTE (MMA). *Dados de desmatamento do Projeto de Monitoramento do Desmatamento dos Biomas Brasileiros por Satélite (PMDBBS), 2008*. Available at: <mapas.mma.gov.br/i3geo/datadownload.htm>. Accessed on: Dec 18, 2015.

[41] MINISTÉRIO DO MEIO AMBIENTE (MMA). Probio, 2007. Available at: <mapas.mma.gov.br/mapas/aplic/probio/datadownload.htm>. Accessed on: Aug 2016.

[42] MINISTÉRIO DO MEIO AMBIENTE (MMA). *Sítios arqueológicos*. Available at: <mapas.mma.gov.br/i3geo/datadownload.htm>. Accessed on: Dec 15, 2015.

[43] MINISTÉRIO DOS TRANSPORTES (MT). *Dados de Ferrovias do Plano Nacional de Logística e Transportes (PNLT), 2010*. Available at: <http://www.transportes.gov.br/conteudo/61-relatorios/2822-base-de-dados-georreferenciados-pnlt-2010.html>. Accessed on: Dec 14, 2015.

[44] PNUD Índice de Desenvolvimento Humano Municipal Brasileiro. In: *Atlas do Desenvolvimento Humano do Brasil*. Brasília: PNUD, Ipea, 2013.

[45] PROBIO, 2016 – *Informações sobre Áreas Prioritárias*. Available at: <http://www.mma.gov.br/biodiversidade/biodiversidade-brasileira/%C3%A1reas-priorit%C3%A1rias> Accessed on: Aug 2016.

[46] ROSS, J.L.S. *Geomorfologia, Ambiente e Planejamento*. Editora Contexto, São Paulo, 1990.

[47] SAATY, T.L. *Axiomatic foundation of the analytic hierarchy process*. Management Science, v. 32, n.7, p. 841-855, July 1987.

[48] SEMACE. *Zoneamento Ecológico Econômico do Bioma Caatinga e Serras Úmidas do estado do Ceará*. Superintendência Estadual do Meio Ambiente do Ceará. 2007.

[49] SIGEP. *Informações sobre os sítios geológicos e áreas de proteção Paleontológica*. Available at: <http://sigep.cprm.gov.br/> Accessed on: Aug 2016

[50] SOTCHAVA, V.B. *O estudo de geossistemas*. In: Instituto Geográfico do Estado de São Paulo, Série Métodos em Questão, São Paulo, p. 1-51, 1978.

[51] SUDENE. *Semiárido*. Available at: <http://www.sudene.gov.br/acesso-a-informa%C3%A7%C3%A3o/institucional/area-de-atuacao-da-sudene/semiarido>. Accessed on: Jul 2016.

[52] ZEE-MG. *Zoneamento Ecológico Econômico do Estado de Minas Gerais*, 2007. Available at: <http://www.zee.mg.gov.br/> Accessed on: Jan 2017.

CHAPTER 7

Characterization of the Existing Grid for Integration of the 1,000 kV AC System

José Antonio Jardini
José William de Medeiros
Ricardo Leon Vasquez Arnez
Sergio de Oliveira Frontin

1. Introduction

Based mainly on the Ten-Year Plan and on the Transmission Expansion Program, detailed studies are conducted for the projects to be indicated for transmission auctions. These studies are consolidated in what we call R1, R2, R3, and R4 reports.

The R1, R2, and R3 reports are presented in chapters 4, 5, and 6, respectively. This chapter presents the general aspects of the R4 Report (Characterization of the Existing Grid), specified by EPE as follows:

> *This report contains the basic technical requirements and characteristics of the installations necessary for the new project to come to operate in accordance with the provisions of the design studies, and in a harmonious manner with the surrounding system. [1].*

2. R4 Elaboration Process

Once the transmission project necessary for the expansion of the Interconnected Power System is approved, the Ministry of Mines and Energy (MME) formally requests that transmission concessionaires, owners of facilities that will be shared, or which are adjacent to a new substation, elaborate the R4 Report.

EPE also suggests that, although the situations in which these facility sharing might occur are various, the R4 Report should contain at least the following information considered more common:

- Protection analysis to define the philosophy and basic characteristics of the protection system associated to the new project.
- Identification of works at adjacent substations, regarding the adjustment of its communications and protection system to make it compatible with the new facilities.
- Characteristics of the lines to be sectioned.
- Telecommunication requirements identifying the facilities/operations centers with which voice communication and data transmission channels will be necessary.
- Facility supervision and control requirements.
- Operational restrictions for the sectioning of the existing lines.

As already mentioned, for this project we chose the 1,000 kV AC transmission alternative connecting the south region of Ceará to the central region of Minas Gerais, passing through the central region of Bahia. This transmission system will have new 1,000/500 kV substations operating as collectors for the region's renewable energy, located close to the current 500 kV substations: Milagres II, Ourolândia II, Igaporã III, and Pirapora 2.

3. General Conditions for the Sectioning of Transmission Lines

In this context, the connection of the 1,000 kV system to the existing system will occur through the sectioning of the 500 kV lines that run close to the 1,000/500 kV substations. It is important to emphasize that the equipment and line sections necessary for this connection will be transferred, with no additional charge, to the owners of the lines to be sectioned, who continue to be responsible for their operation and maintenance.

Thus, some R4 Reports elaborated for situations equivalent to this project present important requirements that the Transmission company who wins the auction will have to meet, such as, for example:

- For the implementation of line sections associated to the sectioning and corresponding switching modules, the Transmission company should comply with the technical norms and standards of the line owners. Considering that the referred line sections will become extensions of the original lines, they must have electrical, mechanical, and performance characteristics equal or superior to those of the existing lines.
- Before starting the first tests, the Transmission company should provide the owners with a list containing a schedule of all the tests to be performed in the equipment, materials, and systems that will be transferred to the owners, including, necessarily, the tests required by the Brazilian Association of Technical Standards (ABNT). For the cases in which the ABNT is not applicable, the tests performed should include those required by the corresponding International Technical Standards. Owners will have the prerogative to witness any trial runs and tests performed on the equipment, materials, and systems to be transferred to them.

- A certificate should be issued for each test. Routine tests should be performed in all the equipment supplied, including the equipment to be provided to remote substations.
- The commissioning of the facilities will be performed jointly by the Transmission company and the owners.
- The Transmission company should acquire the equipment, materials, and systems necessary for the adjustments resulting of the sectioning of the transmission line at the terminal substations mentioned above.
- The transfer of the facilities and equipment associated to the Transmission function of the sectioned lines will occur with no charges to the Transmission Concessionaire of the sectioned line. The assigning Transmission company should allocate, as an additional contracted concession cost, the acquisition and construction costs effectively incurred for the facilities and equipment to be transferred.
- The assigning Transmission company should inform the owners of the sectioned lines of the costs of registering them as fixed assets, having as counterpart the "Obligations Related to the concession of the Public Power Service (Special Obligations)".
- For the equipment, materials, and systems associated to the sectioning of the transmission lines, the Transmission company should provide the owners with sufficient spare parts to provide the stability required for the system, and comprising the equipment necessary for replacing a complete phase of a Line Input module (breaker pole, section switch, power transformer, current transformer, and surge arrester). The list of spare parts to be transferred should be approved by the owners.
- The Transmission company will be responsible for providing all documentation (designs, manuals, catalogs, etc.), tools, and accessories necessary for the commissioning, operation, and maintenance of the equipment transferred.
- The Transmission company should provide proper training covering the equipment transferred, if the equipment is different from the one used by the owners in the sectioned transmission line.
- All instruments, panels, and other equipment for the protection, command, supervision, telecommunications, and ancillary service systems to be transferred should be installed in a Control House to be used exclusively by the owners.
- The Transmission company should provide independent AC and DC ancillary service systems for its facilities, and for the facilities to be transferred to the owners.

4. Connection of the 1,000 kV System to the Existing System

Next, we present the existing and planned 500 kV transmission lines that will be sectioned at the 1,000/500 kV collector substations called: Milagres III, Ourolândia III, Igaporã IV, and Pirapora III, as shown in Figure 4.1.

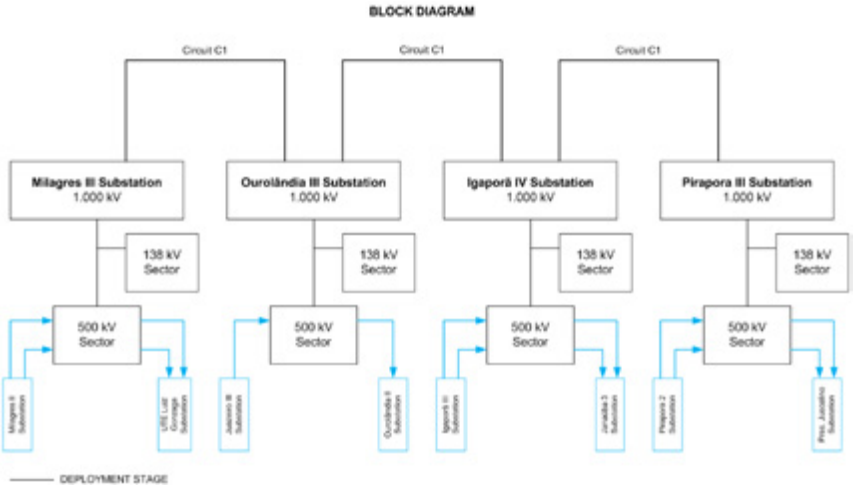

Figure 4.1: Connection of the 1,000 kV System to the Existing System

4.1 Sectioning at the Milagres III – 1,000/500 kV Substation

The transmission lines indicated below will be sectioned close to the Milagres III 1,000/500 kV substation, located about 20 km south of the Milagres II 500 kV Substation, with the following (approximate) coordinates: Latitude: 10°28'27.30" S and Longitude: 38°52'25.16" W:

- 500 kV Milagres / US. Luiz Gonzaga C-1 TL, Pernambuco/Ceará (PE/CE) – Owner Chesf (date foreseen for entry in operation: 02/28/2019).
- 500 kV Milagres II / US. Luiz Gonzaga C-2 TL, Pernambuco/Ceará (PE/CE) – Owner Abengoa (no date foreseen for entry in operation).

The two single circuits Milagres – Luiz Gonzaga are about 220 km long and have 4 ACSR 954 MCM conductor bundles.

4.2 Sectioning at the Ourolândia III – 1,000/500 kV Substation

The transmission line indicated below will be sectioned at the Ourolândia III 1,000/500 kV Substation, located 20 km north of the Ourolândia II 500 kV Substation (towards Juazeiro), with the following (approximate) coordinates: Latitude: 10º41'27.73" S and Longitude: 40º55'03.54" W:

- 500 kV Juazeiro III / Ourolândia II C-1 TL, Bahia (BA) – Owner BJL SPE Transmissora de Energia Elétrica S.A (date foreseen for entry in operation: 06/27/2020).

This line is about 224 km long and has a 4 ACSR 954 MCM conductor bundle.

4.3 Sectioning at the Igaporã IV – 1,000/500 kV Substation

The transmission lines will be sectioned at the Igaporã IV 1,000/500 kV Substation, located 40 km to the South the Igaporã III 500 kV Substation (towards Janaúba), with the following (approximate) coordinates: Latitude: 14°04'16.62" S and Longitude: 42°44'31.12" W.

- 500 kV Igaporã III / Janaúba 3 C-1/C-2 TL, Bahia/Minas Gerais (BA/MG) – Owner Equatorial Transmissora (date foreseen for entry in operation: 02/09/2022).

This line is being planned with two single circuits and to be about 245 km long.

4.4 Sectioning at the Pirapora III – 1,000/500 kV Substation

The transmission line indicated below will be sectioned at the Pirapora III 1,000/500 kV Substation, located 20 km southeast of the Pirapora II – 500 kV Substation (towards PresidenteJuscelino), with the following (approximate) coordinates: Latitude: 17°29'55.04" S and Longitude: 44°46'48.31" W:

- 500 kV Pirapora II/Presidente Juscelino C-1/C-2 TL, Minas Gerais (MG) – Owner Mantiqueira Transmissora de Energia S/A (date foreseen for entry in operation: 03/04/2021).

This line is about 170 km long with a ACSR 4 x 954 MCM bundle.

5. Substations of the 1,000 kV System

The location chosen for the new 1,000/500 kV substations favor a possible expansion of the system at 1,000 kV, and also the connection to the wind and solar power potential of the Northeastern region of Brazil.

The area to be occupied by each of the 1,000/500 kV substations, with a one and a half circuit breaker arrangement, is estimated at about 1 km^2.

5.1 Milagres III – 1,000/500 kV Substation

The Milagres II 500 kV substation was assigned to Abengoa, and its entry in operation has not yet been scheduled. The Luiz Gonzaga 500 kV substation, however, is owned by Chesf [2] [3] [4].

The existing Milagres II substation was implemented to integrate the set of expansion works of the Basic Grid of the Brazilian Interconnected Power System (SIN), and make the outflow of the wind power generation from new projects in the state of Ceará possible. Additionally, its construction was necessary in view of the impossibility of expanding the current Milagres 500/230 kV substation, after the installation of the third 500/230 kV - 600 MVA auto-transformer, and of the 180 Mvar - 500 kV bus reactor.

The Milagres III 1,000/500 kV substation is a new facility to be implemented to the south of Ceará, distant about 400 km from Fortaleza, Ceará (CE), 430 km from Natal, Rio Grande do Norte (RN), and 20 km to the south of the Milagres II 500 kV substation, with the following coordinates: Latitude: 10°28'27.30" S and Longitude: 38°52'25.16" W.

The respective line input and reactor connection modules to be moved, and which should be installed and transferred to the owners of the lines to be sectioned are the following:

- four transmission line sections in 500 kV single circuit;
- four 500 kV line input modules;
- one line reactor connection module;
- equipment, materials, and systems necessary for the adjustments resulting from the sectioning of the lines at the terminal substations of Milagres II and Luiz Gonzaga.

5.2 Ourolândia III – 1,000/500 kV Substation

The Ourolândia II 500 kV substation is owned by Transmissora José Maria Macedo de Eletricidade S.A (TJMME) (date foreseen for entry in operation: 03/27/2018). The Juazeiro III 500 kV substation, however, is owned by Chesf [5] [6], and its main stages are:

- In 2018:
  - Installation of a 500 kV TL feeder bay and associated equipment for the implementation of the new 500 kV Ourolândia – Morro do Chapéu II CS TL;
  - Installation of a 500 kV TL feeder bay and associated equipment for the implementation of the new 500 kV Gentio do Ouro II – Ourolândia CS TL;
  - Installation of two 230 kV TL feeder bays and associated equipment for the implementation of the connection, in two single circuits, with the sectioning of the 230 kV Irecê – Senhor do Bonfim II TL;
  - Installation of two 500/230-13.8 kV, 3x300 MVA auto-transformer banks;

- In 2021:
  - Installation of a 500 kV TL feeder bay and associated equipment for the implementation of the new 500 kV Ourolândia – Juazeiro III CS TL;
  - Installation of a 500/230-13.8 kV, 3x300 MVA auto-transformer bank.

The Ourolândia III 1,000/500 kV substation is a new facility to be implemented in the central region of Bahia, 20 km north of the Ourolândia II 500 kV substation (towards Juazeiro), with the following coordinates: Latitude: 10º41'27.73" S and Longitude: 40º55'03.54" W.

The respective line input and reactor connection modules to be moved, and which should be installed and transferred to the owners of the lines to be sectioned are the following:

- two transmission line sections in 500 kV single circuit;
- two 500 kV line input modules;
- one line reactor connection module;
- equipment, materials, and systems necessary for the adjustments resulting from the sectioning of the lines at the terminal substations of Ourolândia 500 kV and Juazeiro 500 kV.

5.3 Sectioning at the Igaporã IV – 1,000/500 kV Substation

The Igaporã III 500 kV substation is a property of Chesf since 11/15/2015. The Janaúba III 500 kV substation, however, is owned by Taesa [7] [8].

The Igaporã IV 1,000/500 kV substation is a new facility to be implemented in the south region of Bahia, 40 km south of the Igaporã III 500 kV substation (towards Janaúba), with the following coordinates: Latitude: 14°04'16.62" S Longitude: 42°44'31.12" W.

The respective line input and reactor connection modules to be moved, and which should be installed and transferred to the owners are the following:

- two transmission line sections in 500 kV duplex circuit;
- two 500 kV line input modules;
- one line reactor connection module;
- equipment, materials, and systems necessary for the adjustments resulting from the sectioning of the lines at the terminal substations of Igaporã IV 500 kV and Janaúba III 500 kV.

5.4 Pirapora III – 1,000/500 kV Substation

The Pirapora II – 500/345/138 kV substation is owned by Serra Paracatu Transmissora de Energia S.A (SPTE) and is located at the margins of the Highway BR-496, approximately 14 km south of the city of Pirapora, state of Minas Gerais, with the following coordinates: Latitude 17°20'21.96' S and Longitude 44°52'12.53" W. The Presidente Juscelino 500 kV substation is owned by Taesa Transmissora Aliança S.A [9][10].

The Pirapora III – 1,000/500 kV substation is a new facility to be implemented in the state of Minas Gerais, 20 km southeast of the Pirapora 2 – 500 kV substation (towards Presidente Juscelino), with the following coordinates: Latitude 17°29'55.04" S and Longitude 44°46'48.31" W.

The respective line input and reactor connection modules that should be installed and transferred to the owners of the lines are the following:

- two transmission line sections in 500 kV single circuit;
- two 500 kV line input modules;
- equipment, materials, and systems necessary for the adjustments resulting from the sectioning of the lines at the terminal substations of Pirapora 2 – 500 kV and Presidente Juscelino 500 kV.

6. Conclusions

- The requirements necessary for the connection of the 1,000 kV system through sectioning of the 500 kV lines at the 1,000/500 kV substations should be defined in R4 Reports to be elaborated by the line owning concessionaires.
- The equipment, line sections, protection and communication systems, etc. necessary for the sectioning, after implemented, will be transferred at no charge to the owners of the lines, who will remain responsible for their operation and maintenance.
- Thus, the owners must present, along with the R4 Reports, their project, construction, and commissioning standards, and protection, control, measurement, and telecommunications philosophy.
- It is equally essential that the owners monitor all the implementation phases of the sectioning, up to the final delivery of the equipment, with associated projects and designs.

7. References

[1] EMPRESA DE PESQUISA ENERGÉTICA (EPE). *Diretrizes para Elaboração dos Relatórios Técnicos Referentes às Novas Instalações da Rede Básica*, nº EPE-DEE-RE-001/2005-R1, of May 16, 2005.

[2] CHESF. Empreendimento Entrada de Linha de 500 kV SE Paulo Afonso IV – *Características e Requisitos Básicos das Instalações – Subestação de Luiz Gonzaga.*

[3] POWERCONSULT. *SE Milagres II 500 kV e Sistema de Transmissão Associado. Relatório R4 – Características e Requisitos das Instalações.*

[4] MARTE ENGENHARIA. ATE XVII, *SE Milagres II 500 kV. Relatório R4 – Caracterização da Rede Existente.* June 3, 2015.

[5] ODOYÁ TRANSMISSORA DE ENERGIA. *Subestações Sapeaçu, Morro do Chapéu, Juazeiro da Bahia III e Juazeiro da Bahia I. Relatório de Caracterização da Rede Existente e Descritivo do Empreendimento.* April 2015.

[6] POWERCONSULT and NEOENERGIA. *SE Ourolândia II 500/230 kV e Sistema de Transmissão Associado, Relatório R4 – Características e Requisitos das Instalações*. May 2014.

[7] CHESF - *Empreendimento – 2 EL 500 kV em função das LT 500 kV Janaúba III – Igaporã III C1 e C2 – Características e requisitos básicos das instalações – SE Igaporã III. Oficion.º 034/2015 – SPE-MME.*

[8] LEME ENGENHARIA. Taesa – *Subestação Janaúba 3 500 kV – Relatório R4 – Características Básicas das Instalações.*

[9] SERRA PARACATU TRANSMISSORA DE ENERGIA S.A AND POWERCONSULT. *SE Pirapora 2 500/345/138 kV Instalação de duas Saídas de LT 500 kV Para Interligação com a Nova SE Presidente Juscelino*. September 2014.

[10] TAESA. *Subestação Presidente Juscelino 500/345 kV. Relatório R4 – Características Básicas das Instalações*. March 10, 2014.

CHAPTER 8

Transmission Project Auction Process

Sergio de Oliveira Frontin
Geraldo Luiz Costa Nicola

1. Introduction

The implementation of power transmission projects in the current model of the Brazilian power sector starts with the identification of the need in view of the expansion of the electric system. Overall, the steps required in this process can be named as follows:

- Conducting the studies for the expansion of the transmission system;
- Holding the auctions for the identified assets;
- Formalizing the commitments of the transmission company who wins the auction, by means of the signing of a power transmission public service Concession Agreement and other related agreements.
- Elaborating the projects to meet the requirements of the Notice;
- Building and commissioning the projects;
- Operating and maintaining the facilities;
- Receiving compensation for the availability of the transmission assets.

This chapter addresses the process for holding the transmission system auction, presenting and analyzing the following documents:

- Auction notice, containing the legal and commercial clauses.
- Attachment with the draft of the Concession Contract.
- Attachments containing the standard agreements: CPST, CUST, CCT, and CCI (see item 7 below).
- Technical attachment containing the basic requirements and characteristics of the project to be auctioned.
- Technical reports R1, R2, R3 and R4 (see item 3 below).

Next, it will be presented the general aspects of each of these documents, starting with the Ten-Year Energy Expansion Plan and the National Energy Plan, in which, the projects necessary for the expansion of the interconnected system, and which will be subsequently be offered in auctions, are identified.

2. The Ten-Year Energy Expansion Plan and the National Energy Plan

The Ten-Year Energy Expansion Plan and the National Energy Plans are important documents for the planning of the Brazilian power and energy sector under the responsibility of Empresa de Pesquisas Energéticas (EPE).

The National Energy Plan (PNE) represents another instrument for the planning of the energy sector in Brazil. It presents guides for the expansion, trends and strategies for the long term (horizon of 30 years in the future), and supports the elaboration of short and medium-term studies of the system.

The planning of the power sector includes the assessment of the energy potential, highlighting the hydrographic basin hydroelectric inventory studies, and technical, economic, and environmental feasibility studies.

Regarding the transmission systems, in these energy studies, the areas of interest in the long term are, naturally, the large interconnection trunks between subsystems. Given the distances involved and the amount of power to be transmitted in such systems, the reference considered for estimating the investment costs are the 500 or 765 kV voltages, and the average power levels equal to 1,500, 2,250, and 3,000 MW. To simplify, the studies did not consider electric aspects like stability related flow constraints or reliability criteria that might result in additional costs.

The expansion of the generation and transmission system is planned by Empresa de Pesquisa Energética (EPE), and presented in the Ten-Year Energy Plan (PDE), and in the Transmission Expansion Program (PET).

The Operador Nacional do Sistema (ONS - Electric System National Operator), based on studies for the horizon of up to five years may, in turn, identify the need for expansions and reinforcements in the current system, which are presented in the Expansion and Reinforcement Plan (PAR).

The PET, elaborated by EPE after long term planning studies, and the PAR, elaborated by ONS after short term studies of the electric grid, are analyzed and consolidated, resulting in a set of transmission projects necessary to lodge the load of the Brazilian Interconnected Power System (SIN), and for the proper operation of the system.

To define the power system expansion alternatives, studies related to power flow, short-circuit, stability, and transient overvoltage are carried out in the planning phase.

These and other specific studies related to the economic and environmental issues are performed by Empresa de Pesquisa Energética (EPE), which, based on the knowledge of the power demand in the planning horizon, and on the generation alternatives, determines the solutions that are technically and economically more adequate for the expansion of the power system. In addition to other parameters, the transmission alternatives should be identified by their transmission modality (alternating current or direct current), transmission line voltage level, loading level under normal and emergency operation conditions, their substations, and the date required to start its operation.

The results of the studies are combined for the Ten-Year Power Expansion Plan, which presents the main aspects that guide the definition of the reference configuration of the generation and transmission system and its evolution along the 10-year period.

The Power Generation item of this Ten-Year Expansion Plan presents the hypotheses for the generation expansion, and the various analyses performed, such as: deficit risks, marginal operation costs, flow evolution in the interconnections, estimated total investments, analyses of sensitivity to longer times for obtaining environmental licenses, etc.

The Power Transmission item describes transmission expansion per geo-electric region of the Brazilian Interconnected Power System (SIN), and per state of these regions. In addition to investment estimates, it indicates: evaluation of the interconnected system electromechanical stability, projection of the evolution of the tariffs for the use of the transmission system, evaluation of the power grid reliability indexes, and the evolution of the short-circuit levels on the busbars.

The Socio-environmental Analysis of the Power System item presents an overview of these issues related to the configurations proposed for the generation and transmission expansion.

Based on the Ten-Year Expansion Plan, EPE, as indicated, elaborates the Transmission Expansion Program (PET), which indicates the transmission lines and substations necessary for the proper rendering of power transmission services by the Basic Grid (RB) of the Brazilian Interconnected Power System (SIN).

With this information, ANEEL (Agência Nacional de Energia Elétrica) prepares and publishes the auctions notices for the new generation sources and transmission facilities. In the case of the works indicated at PAR, ANEEL sends the proper authorizations to the facility holding companies.

In this process, the generation and transmission agents are responsible for the investments, and the distribution agents are responsible for contracting the power portion, early enough to supply the demand in their concession area.

The studies performed both by ONS and EPE indicate that the projects entering in the generation and transmission auctions are selected considering, among others, the following factors: whether they are considered feasible and attractive solutions for the entrepreneurs; if the maturity of the technology recommended is assured; whether they have the potential for application in the short term; if the costs are consistent with those practiced in the market; and if they are in compliance with the current legislation.

3. Technical Reports R1, R2, R3, and R4

Based on the Ten-Year Expansion Plan, detailed studies are conducted for each of the projects, before they are indicated for the transmission auctions. These studies are consolidated in what we call R1, R2, R3, and R4 reports [1], described next:

- R1 Report (technical, economic and socio-environmental feasibility study): it analyzes the technical feasibility of the project, taking into account the preliminary socio-environmental conditions, to demonstrate its competitiveness in view of other alternatives, and define the basic preliminary characteristics of the project's facilities, as well as expectations regarding its costs, based on modular cost references used in the planning.
- R2 Report (detailing of the reference alternative): it provides the information necessary for defining the technical characteristics of the new transmission facilities, and adjusting the existing facilities of the Basic Grid.
- R3 Report (socio-environmental characterization and analysis): it provides the socio-environmental analysis of the path corridor selected in the studies conducted for the elaboration of the R1 report. The analysis of the environmental aspects of the corridor should allow for the identification of the highlights from a socioeconomic and environmental perspective, which might bring greater complexity to the transmission facilities, resulting in higher environmental costs and longer deadlines to the project's licensing process.
- R4 Report (characterization of the existing grid): this report must contain the basic technical requirements and characteristics necessary for the new project to come to operate in accordance with the provisions of the design studies, and in a harmonious manner with the surrounding system.

4. The Transmission Auction Process

According to the current model of the electric power sector, once the need for a transmission project is established, the corresponding notice is published aiming at the holding of an auction for the interested entrepreneurs. The following events are part of the process for holding the auction:

- Publishing of the Auction Notice in draft form for Public Audience, with availability of information and studies;
- Public Audience for clarifications for the entrepreneurs interested;
- Definition of dates for requesting clarification and responses;
- Publication of the Auction Notice;
- Visits to the existing facilities to be integrated to the assets to be auctioned;
- Registration and provision of guarantees;
- Holding of the auction in a public session.

The Ministry of Mines and Energy (MME), among its legal powers, has been delegating to ANEEL the bidding process, in the auction mode, for the selection of proposals for the contracting of a public transmission service, through concessions, including the construction, assembly, operation, and maintenance of transmission facilities.

According to the provisions set by art. 18A of Law n. 8,987/1995, the notices define that the auction will be carried out in the modality called "inversion of the order of qualification and judgement phases." In this modality there is no pre-qualification phase for the companies interested in participating in the auction, there is only the requirement to present a proposal guarantee for the registration in the event. Subsequently, only the winning proponents will present the respective qualification documents, according to the schedule presented in the notice.

For each lot, each participant will present in a sealed envelope, the financial proposal with the value of the Permitted Annual Revenues (RAP). The participant who presents the highest discount in relation to the maximum Permitted Annual Revenue (RAP) wins. If the difference between the lowest offer and the other proposals is higher than 5%, the participant who offers the lowest proposal wins. If the difference is equal to or lower than 5%, or if the best offers are tied, there will be an open live bidding (verbal), in which the auctioneer can set minimum values to be offered between one bid and another. The proponent who presents the lowest value wins. In the event no proponent makes a live offer, the winner will be the proponent who presented the lowest value via envelope. If there is a tie in the values presented via envelope, without the presentation of live offers, the winner will be determined by means of a drawing promoted by the session director.

Thus, as already mentioned, according to the current auction regulations, the participant who offers the financial proposal with the highest discount in relation to the predefined maximum Permitted Annual Revenues (RAP)

will be awarded the corresponding lot offered in the auction. In this case, the revenue associated with the entrepreneurs with the exploitation of the assets will be lower than expected, which will contribute to reduce the energy tariff.

In the period of 2000 – 2016, 43 auctions were held, with 356 lots composed of transmission lines, equipment, and substations, with the following main indicators:

- Total length of transmission lines – 85,037.85 km.
- Sum of the maximum RAP of the notices – R$ 6.46 trillion.
- Sum of RAP of the proposals awarded – R$ 5.16 trillion.
- Average discount – 20 %.

The average discount considers the reduction of the total Permitted Annual Revenues (RAP) foreseen by ANEEL, defined in the notice with the total RAP resulting of the bids from the various winners of the auctions.

In the first auctions, in 2001 and 2002, the average discount was relatively low, lower than 10%. As of 2003, with the participation of the state-owned power companies, and the evident increase of the competition, there was a greater number of bids. Thus, from the beginning of 2003 to December 2014, the average discount value grew, exceeding the 50% level in some cases.

During 2003 to 2011, the only auction that presented a relatively small average discount value for its lots (7.15%) was auction 007/2008, corresponding to the facilities of the direct current system for the plants in the Madeira River. It should be noted, however, that auction 011/2013, regarding the direct current transmission for the Belo Monte plant, presented a discount of 38%, and auction 007/2015, related to the second bipole of the Belo Monte plant, presented a discount of 19%.

5. The Transmission Auction Notice

The Auction Notice (Edital) is the main document for holding an auction for a transmission project and is composed of several volumes, appendices, and attachments, which present the drafts of the concession and transmission service agreements, in addition to commercial and legal clauses, such as, for example:

- Object;
- General Rights and Obligations;
- Permitted Annual Revenues for the Rendering of the Transmission Service;

- On the Document Presentation Form;
- On the Registration to Participate in the Auction;
- On the Proposal Warranty;
- On the Auction Session;
- On the Qualification;
- On the Guarantee of Full Performance of the Agreement;
- Awarding of the Object;
- Penalties; and
- Signing of the Concession Agreement.

6. The Concession Agreement

The legal basis for the awarding of the transmission concession is based on Law n. 8,987/1995 – "Service Rendering Concession and Permission Regimen," which in its 4th, 5th, and 14th articles defines that:

> *Art. 4th. The concession of public services, preceded or not by the execution of public works, will be formalized by means of an agreement, which will comply with the terms of this Law, of the relevant regulations, and of the bidding notice.*
> *Art. 5th. The granting authority will publish, prior to the bidding notice, an act justifying the convenience of granting a concession or permission, characterizing its purpose, area, and term.*
> *Art. 14th. Any concession of public service, whether or not preceded by the execution of public works, will be the object of prior bidding, under the terms of the applicable legislation, and in compliance with the principles of legality, morality, publicity, equality, judgment by objective criteria, and bound to the invitation to bid.*

In addition to the clauses contained in this law, law n. 10,848/2004 defined as the granting authority's privileges the following points:

> *I - Elaborate the grant plans, define the guidelines for the bidding procedures, and promote the bidding processes for contracting public service concessionaires for the production, transmission, and distribution of electric-power, and for granting concessions to potential hydroelectric schemes.*
> *II - Signing the agreements for the concession or permission for*

electric-power public services, for the concession of use of public assets, and issuing authorizing acts.
§ 1st In the exercise of the powers referred to in item IV of art. 29 of Law No. 8,987, of February 13, 1995, and of the powers referred to in items I and II of the caput of this article, the Granting Authority will first listen to ANEEL.
§ 2nd In the exercise of the powers referred to in item I of the «caput» of this article, the Granting Authority will delegate to ANEEL the operation of the bidding procedures.
§ 3rd The signing of agreements and issuing of authorizing acts addresses in item II of the «caput» of this article can be delegated to ANEEL.
§ 4th The exercise by ANEEL of the powers referred to in items VIII and IX of art. 29 of Law n. 8,987, of February 13, 1995, will depend on the express delegation of the Granting Authority.

Considering these requirements, the concession agreement to be signed by the auction winners is elaborated according to the following stages:

- Reception of the documentation for qualification of the proponents who win the auction.
- Publication of the results.
- Definition of deadlines for appeals.
- Confirmation of the result and awarding of the concession.
- Delivering on schedule and budget for the construction of the transmission facilities.
- Delivering of the documents required for the concession awarding and agreement.
- Granting of the concession.
- Delivering to ANEEL of the guarantee of full performance.
- Signing of the concession agreement.

The awarded proponents must prove that they are in compliance with their obligations to the Brazilian government, especially regarding taxes, and that they have equity and technical qualification to build, maintain, and operate the facilities, for which they have offered a proposal that won the auction. The Qualification documentation comprises:

- Legal Qualification;
- Technical Qualification;
- Economic-financial Qualification;
- Fiscal Compliance.

Once the procedural requirements indicated in the auction notice have been met the awarded transmission company signs the Concession Agreement: an agreement with a term of 30 (thirty) years, to be signed by and between the transmission company and the Federal Government, through ANEEL, governing the concession of the public transmission service. This agreement contains, among others, the following main clauses:

- Definitions;
- Conditions for the rendering of the service;
- Transmission company obligations and charges;
- Prerogatives of the Transmission company;
- Transmission services revenues;
- Review of the permitted annual revenues;
- Inspection of the services;
- Penalties;
- Intervention on the concession;
- Extinction of concession and reversal of related assets;
- Term of the concession.

7. Agreements Related to Transmission Services

The compensation for the availability of the asset [2] will be made through the payment of the Permitted Annual Revenue (RAP) in 12 (twelve) monthly installments, as provided for in the Concession Agreement, and established in the following contracts related to the use of the transmission system, and to the provision of transmission system services:

- Transmission Service Provision Agreement (CPST).
- Transmission System Use Agreement (CUST).
- Transmission System Connection Agreement (CCT).
- Facility Sharing Agreement (CCI).

The transmission company will join ONS as a transmission agent, with the responsibilities and costs of the sponsoring institution defined under terms of the ONS Bylaws and other applicable standards.

The transmission company, to fulfill its function in the Brazilian Interconnected Power System, and to allow the connection of users or other transmission concessionaires, will:

- Make available the studies, designs and technical standards used in its facilities;

- Promote, according to the accessing concessionaire, the assignment of use or transfer of goods and facilities, with the objective of optimizing investments and better characterizing the respective responsibilities for operation and maintenance; and
- Share existing facilities and infrastructure, and allowing for construction in available areas, without compensation, if they are already receiving compensation at the permitted annual revenues.

More details about these agreements are presented next:

7.1 Transmission Service Provision Contract (CPST)

The transmission company, on the same day or within 60 (sixty) of the signing of the Concession Contract, will sign the Transmission Service Provision Agreement (CPST) with ONS, thus, substantiating the technical and commercial conditions regarding the availability of the transmission facilities for interconnected operation.

This agreement established the terms and conditions for the provision of the public power transmission service to the users by a concessionaire that owns transmission facilities that are part of the basic grid, under the administration and coordination of the ONS.

The CPST is also the granting instrument through which the transmission concessionaire authorizes ONS to perform all acts necessary and sufficient to represent it before the users in the Transmission System Use Agreements (CUST) and their warranty mechanisms.

By means of the CPTS, ONS is authorized to check out, manage the collection and settlement of charges for the use of the transmission system resulting of the application of the Transmission System Usage Tariff (TUST), as well as the sector charges.

7.2 Transmission System Use Contract (CUST)

The CUST, to be signed by ONS, the transmission concessionaire and the users, has the purpose to define the terms and conditions that will regulated the use of the Basic Grid by the users, and the provision of the transmission services by the transmission concessionaires, under the control and supervision of the ONS; as well as establishing the provision,

by the ONS, of the coordination and control services for the operation of interconnected electric-power systems and international interconnections, and administration of the transmission services provided by the transmission concessionaires.

It is also the purpose of CUST the management, by the ONS, of the collection and settlement of the charges for the use of the transmission and the performance of the warranty system, acting on account and under the order of the transmission concessionaires.

By means of the CUST, the users contract the Transmission System Usage Amounts (MUST), according to the current regulation, which corresponds to the maximum average paid-in power in 15 minutes that will be withdrawn or injected by users at the regulatory connection points.

7.3 Transmission System Connection Contract (CCT)

The transmission company, according to the Concession Agreement, must provide free access to its transmission facilities, signing Transmission System Connection Contracts (CCT) with the prospective users who are connected to it. These users accept the connection charges under the terms of Law n. 9,074 of 1995, regulated by ANEEL Resolution n. 281, of October 1, 1999, as amended by Resolution No. 208, of June 7, 2001.

The CCT is signed between the transmission concessionaires and the users of its facilities, with the intervention of the ONS, and is aimed at establishing the conditions, procedures, technical, operational, and commercial responsibilities that will regulate the connection of the users to the transmission facilities.

The CCT presents the detailed list of connection equipment owned by the concessionaires and users, and also issues provisions regarding operational requirements, payment of connection charges, civil liabilities, and resolution of disputes.

ONS participates in the CCT as an intervenor, with the purpose of ensuring that the rights and obligations established for the connection facilities do not impact the other members of the Basic Grid.

7.4 Facility Sharing Contract (CCI)

The CCI is signed between the transmission concessionaires that own interdependent equipment, with the intervention of the ONS. The purpose of the CCI is to establish technical and operational procedures and commercial and civil responsibilities that will regulate the sharing of such equipment.

The CCI presents the detailed list of the interdependent equipment that is part of the Basic Grid and belong to each of the transmission concessionaires, and also issues provisions regarding the security and safety of the facilities; implementation, commissioning, operation, and alterations in the facilities; patrimonial surveillance, conservation, and cleaning of the facilities; reimbursement of costs; facility conservation fees; and payments.

8. Transmission System Rates – RAP – TUST

8.1 Permitted Annual Revenues (RAP)

The power transmission services will be paid for through the Permitted Annual Revenues (RAP) to the concessionaries and authorized agents. These revenues are the compensation owed based on the contracting of the services provided, according to the Transmission Service Provision Agreement (CPST), and are defined during the biding process, or when of the authorizing acts by the Granting Authority. The RAP is apportioned by all users of the grid, power generation and distribution companies, free consumers, power importers and exporters, in the proportion of 50% paid by generation class, and 50% paid by consumption class.

Every year, ANEEL publishes the resolutions that regulate the RAP for the transmission facilities of the existing system and new projects that will start operations during the period. Such RAP together with the ONS budget and eventual differences from the previous year, define the total Basic Grid RAP for each rate period, which begins on July 1st of the year of publication of the Resolution, and extends until June 30th of the following year.

The definition of the permitted revenues considers as basis the unit costs elaborated by Eletrobras, used in the planning studies by the sector companies. The revenues are updated annually using the readjustment index defined in the concession agreement (IGP-M or IPCA), and added of the values associated to the new projects (bid or authorized) incorporated to the SIN.

8.2 Transmission System Usage Fee (TUST)

The $TUST_{RB}$ (for basic grid) refers to the apportionment of the Basic Grid RAP. This fee generates charges applicable to all users, since it pays for the facilities that compose the basic grid, except for the border transformers, and including the interconnections used to promote the optimization of the electric-power resources of the SIN [3].

The calculation of the $TUST_{RB}$ uses the Nodal method, which uses the concept of locational rates, whereby each system user pays system usage charges according to the connection point (node) of the network in which it is located.

The transmission system usage charges paid by an agent are the contracted values multiplied by the usage fees, and the fees depend on the location and on the impact they cause to the system at that point.

8.3 Technical Calculation of Transmission Services and Charges

The transmission company is responsible for maintaining the transmission facilities to ensure higher availability, providing the ONS with the necessary information, defined in the Grid Procedures, so as to allow the ONS to perform its coordination, supervision, and control actions.

The maintenance of the lines and terminal substations is extremely important, as the unavailability is accounted for and directly affects the company's billing.

These accounting procedures are detailed in the Transmission Service Provision Contract (CPST), in which the Concession is divided into Transmission Functions (FTs), based on the availability and the operative capacity of the transmission installation. Thus, it becomes relevant to indicate the following items:

- **Base Payment (PB)**
  Portion equivalent to one twelfth of the Permitted Annual Revenues (RAP) associated with the full availability of transmission facilities that compose a transmission function. This RAP is divided into monthly Base Payments, which are received in full by the transmission agents if their FT are fully available for operation by the ONS 100% of the month.

- **Variable Portion due to Delay for Entering into Service (PVA)**
  Portion to be deducted from the Base Payment of an FT due to the delay for entering into service.
- **Variable Portion for Unavailability (PVI)**
  Portion to be deducted from the base payment due to scheduled outages, or other outages resulting of events involving the main and/or complementary equipment of the transmission function, which are the responsibility of the transmission company (RN 270). It is important to note that PVI may lead to a discount 10 times the Base Payment for Programmed Disconnections and 150 times the Base Payment for Other type of Disconnections, except those foreseen in a specific Resolution.
- **Variable Portion for Operative Restriction (PVRO)**
  Portion to be deducted from the base payment of an FT for reducing the operative capacity of the FT that is responsibility of the transmission company.

For the PVI and PVRO application purposes as well as for the recording of disconnections, disconnections and operative restrictions occurring 6 (six) months after the initial commercial operation of a new TF or a new main equipment of an existing FT it will not be considered.

The transmission company shall send to the ONS its Maintenance Plans, contemplating the maintenance services that influence the system. ONS is responsible for making them compatible with the Maintenance Plans of the other transmission, generation, and distribution concessionaires, so as to adjust them to operational conveniences and system safety, also according to the grid procedures.

Currently, the ANEEL's Regulatory Resolution n. 729/2016 establishes the validation criteria of the PVA, PVI and PVRO portions.

9. Auction Notice Technical Attachment

The Auction Notice is composed of several volumes, appendices, and attachments, which present the drafts of the various agreements previously cited, and also of an attachment containing the general technical requirements and characteristics of the facilities object of the auction.

This technical attachment consolidates the results of the studies conducted, indicating the minimum technical requirements of the transmission lines, substations, equipment, protection, supervision, and control systems, and telecommunication systems, in addition to other information, so as to ensure the safety and reliability of the projects.

10. Relevant Points for the Ultra-High Voltage System Auction

Considering the novelty of an Ultra-High Voltage system in Brazil, it is considered timely to indicate some relevant points whose inclusion in the transmission project notices should be analyzed by the responsible agencies.

The bases for the presentation of this point was the Notice for Auction 007/2015 – ANEEL, published in June 2015, which refers to the Belo Monte ±800 kV DC direct current transmission system. Similarly to the UHVAC system, this ±800 kV DC system is a pioneering transmission system in Brazil [4].

10.1 Reimbursement of Expenses (items 4.6 and 4.7 of the Auction Notice)

This item indicates, under the terms of the Concession Agreement, that the Transmission Company should reimburse the companies that incurred expenses in the elaboration of the technical documentation.

In this case, in addition to other expenses that might occur, we will have the investments of approximately R$ 5.6 million made in the R&D project.

Considering that this investment is mandatory for the proposing companies, resulting from the obligations taken on under the R&D program, these funds do not need to be reimbursed and, therefore, represent a reduction in the investment made by the auction winning transmission company.

10.2 Deadline for the Presentation of the Basic Design (item 4.8 of the Auction Notice)

The transmission company must present to ANEEL the basic design for the transmission facilities within 180 days of the signing of the Concession Agreement.

For most projects, the time for the delivery of the basic design is of 120 days. The extension of the deadline to 180 days is be justifiable due to the inovation of this transmission system.

10.3 Entry into Commercial Operations (item 4.13 of the Auction Notice)

For the ±800 kV DC system, it was indicated that the transmission facilities must start commercial operations by 12/02/2019 (or about 48 months counted as of the signing of the concession agreement.

10.4 Calculation of Maximum Permitted Annual Revenue (item 5.5 of the Auction Notice)

For auction notice 011/2013, of December 2013, for the first ±800 kV DC bipole of the Belo Monte transmission system, held on 02/07/2014, the calculated value of the maximum RAP was of R$ 701,043,610.00 (seven hundred and one million, forty-three thousand, six hundred and ten reais), and the winning bid was of R$ 434,647,000.00 (four hundred and thirty-four million, six hundred and forty-seven thousand reais), which represented a discount of 38%.

For auction notice 007/2015, of June 2015, for the second bipole of the ±800 kV DC system, held on 07/17/2015, the maximum value defined for the RAP was of R$ 1,219,791,340.00 (one billion, two hundred and nineteen million, seven hundred and ninety one thousand, three hundred and forty reais) (difference due to the insertion of the 500 kV line, synchronous compensators, and sectioning of two lines at the Rio Terminal, as well as exchange rate variation), and the winning bid was of R$ 988,030,985.00 (nine hundred and eighty eight million, thirty thousand, nine hundred and eighty five reais), which represents a discount of 19%.

10.5 RAP Discount - Variable Portion – PV (item 5.8 of the Notice)

This item indicates that the monthly installments of the RAP will be subject to discounts that reflect the availability conditions of the transmission facilities, according to the methodology presented in the CPST, and according to ANEEL Regulatory Resolution n. 729/2016.

It is important to mention that this variable parcel is not discounted from the agent during the six (6) month grace period for a new Transmission Function, counted as of the date of its entry into commercial operation.

10.6 Auction Schedule (item 17 of the Auction Notice)

Between the Notice Publication event and the Public Session for holding the Auction there is usually a period of one month.

10.7 Project Monitoring and Training (item 15.1 of Attachment 6 of the Auction Notice)

Considering the pioneering 800 kV DC transmission system, the auction notice defines various requirements in terms of monitoring and training that the winning transmission company should sponsor for the technicians from ANEEL and ONS. For example, some of these requirements where relevant to UHV AC, are presented next:

- During the project's basic design phase, the transmission company will allow, the participation of ANEEL and ONS specialists in technical and managerial meetings.

- The transmission company will allow the integration of one (1) collaborator from the ONS in the development of the basic design. The technicians from the ONS will be allowed to monitor the commissioning of the supervision and control systems.

- The transmission company will provide training to the personnel indicated by the ONS

11. Conclusions

For the implementation of the UHV project, there were analyzed the documents presented in this report inherent to the transmission system auctioning process. In this sense, relevant points were indicated that, due to the pioneering nature of this modality of transmission in Brazil, should be analyzed and considered in the auction notice, whenever deemed pertinent. These documents are:

- Reimbursement of Expenses.
- Deadline for the Presentation of the Basic Design.
- Entry into Commercial Operations.
- Calculation of Maximum Permitted Annual Revenue.
- RAP Discount, Variable Portion PV.
- Monitoring of the Basic Design and Training.

12. References

[1] EPE. *Guidelines for the Elaboration of Technical Reports Related to the New Facilities of the Basic Grid.* EPE-DEE-RE-001/2005-R1. May 16, 2005.

[2] AGÊNCIA NACIONAL DE ENERGIA ELÉTRICA. ANEEL Resolution n. 247, of 08/13/1999 – *Alters the general conditions for the rendering of transmission services and contracting of access; comprising the CPST, CUST, and CCT* bound to the signing of the Initial Agreements for the Purchasing and Selling of Electricity.

[3] Law number 9,648 of 05/27/1998 – *Determines that the purchasing and selling* of power between concessionaires or authorized companies must be contracted separately from the access and use of the transmission and distribution systems.

[4] AGÊNCIA NACIONAL DE ENERGIA ELÉTRICA. Notice of Auction n. 007/2015. Second HVDC Link ±800 kV Belo Monte. Bidding process for the contracting of public power transmission service, upon granting of concession, including the construction, operation, and maintenance of transmission facilities of the basic grid of the Brazilian interconnected power system. Brasília, June 2015.

[5] FRONTIN, S. O. *Equipamentos Elétricos – Prospecção e Hierarquização de Inovações Tecnológicas.* Brasília: Editora Goya, 2014.

[6] GOMES, R. A. *Gestão do Sistema de Transmissão do Brasil*. FGV. Rio de Janeiro. 2012.

[7] ABREU, A. M.; SAAVEDRA, A. R.; ARAÚJO, J. A.; MAURÇA, L. B.; FRAGELLI, R. R.; FRONTIN, S. O.; RÊGO, V. B. *Prospecção e Hierarquização de Inovações Tecnológicas Aplicadas a Linhas de Transmissão*. Brasília: Editora Goya, 2010.

[8] AGÊNCIA NACIONAL DE ENERGIA ELÉTRICA. Notice of Auction n. 011/2013. HVDC Link 800 kV Belo Monte. Brasília, December 2013.

[9] CARVALHO, D. S.; ESMERALDO, P. C. V. *O planejamento da transmissão como Indutor de novas tecnologias*. XX SNPTEE. Recife, 2009.

[10] Law n. 9,074 of 07/07/1995 – *Creates the figure of the Independent Power Producer (PIE), and defines the Free Consumer and the free access.*

[11] Law n. 10,848, of March 15, 2004 (Brazil). *Issues provisions on the trade of electricity,* alters law n. *5,655,* and issues other provisions.

[12] AGÊNCIA NACIONAL DE ENERGIA ELÉTRICA. ANEEL Resolution n. 281, of 10/04/1999 – *Defines the general conditions for the contracting of access, comprising the use and connection of the power transmission and distribution systems*.

[13] AGÊNCIA NACIONAL DE ENERGIA ELÉTRICA. ANEEL Resolution n. 67, of 06/08/2004– *Establishes the criteria for the composition of the SIN's Basic Grid*.

[14] AGÊNCIA NACIONAL DE ENERGIA ELÉTRICA. ANEEL Resolution n. 68, of 06/08/2004 – *Establishes the procedures for reinforcements in the DIT, and issues other provisions*; *updated by* ANEEL Resolution n. *312, of October 5, 2008*.

[15] AGÊNCIA NACIONAL DE ENERGIA ELÉTRICA. ANEEL Resolution n. 158, of 05/23/2005– *Establishes the distinction between reinforcements and improvements in the Basic Grid and DIT*.

[16] AGÊNCIA NACIONAL DE ENERGIA ELÉTRICA. ANEEL Resolution n. 191, de 12/12/2005 – *Defines the Transmission Functions and the respective Base Payments, and establishes procedures for determining the operational capacity of the Basic Grid and DIT*.

[17] AGÊNCIA NACIONAL DE ENERGIA ELÉTRICA. ANEEL Resolution n. 729 of 06/28/2016 – *Establishes provisions related to the quality of the public transmission service of the Basic Grid (PV).*

[18] AGÊNCIA NACIONAL DE ENERGIA ELÉTRICA. ANEEL Resolution n. 349 of 01/13/2009 – *Establishes the criteria for locational calculation of the Distribution System Use Rates applicable to certain generating centrals – TUSDg connected at the level of 138 kV or 88 kV, and issues other provisions.*

[19] AGÊNCIA NACIONAL DE ENERGIA ELÉTRICA. ANEEL Resolution n. 399, of 04/13/2010 – Regulated the contracting of the transmission system in *permanent, flexible and temporary character.*

[20] OPERADOR NACIONAL DO SISTEMA. *Network Procedure - Submodule 2.2 – verification of conformity of the new transmission facilities to the minimum requirements.* Rio de Janeiro. 2011.

[21] OPERADOR NACIONAL DO SISTEMA – Network Procedure - *Submodule 2.3* – Minimum requirements for transformers and for substations and their equipment. Rio de Janeiro. 2011.

[22] Law 8,987/1995 of February 13, 1995. Issues provisions on the Service Rendering Concession and Permission Regimen.

CHAPTER 9

Complementary Investigations

José Antonio Jardini
Sergio de Oliveira Frontin
Geraldo Luiz Costa Nicola
John Francis Graham
Liu Guijun
Carlos Alberto Rayol

1. Objective

The objective of this project was to examine the technical and economic feasibility of inserting a 1,000 kV UHVAC system into the Brazilian Interconnected Power System (SIN).

The studies confirmed the feasibility to insert such a system in two stages:

- Initial stage: Milagres – Ourolândia – Igaporã – Pirapora (single circuit).
- Expansion: Addition of another single-circuit: from Ourolândia – Igaporã – Pirapora, and two single circuits (or one double circuit) from Pirapora to Ribeirão das Neves.

The 1,000 kV system, as mentioned, appears as a promising alternative to transmit the excess power from the wind and solar sources located in the North and Northeast regions to the Southeast region.

The studies required in the R1, R2, R3, and R4 planning reports have been presented in the previous chapters and demonstrated the technical and economic feasibility of the project when compared to other transmission alternatives.

The initial stage estimated date for entering into operation might be 2025 and 2026. Considering a 4-year period for the implementation of the system, the project should be auctioned in 2021 or 2022. It is envisioned that a possible deepening of the technical knowledge and conducting a broader study of this transmission alternative should be carried out sometime between 2018 and 2019.

In this context, the main objective of this chapter is to present some complementary investigations related to the present project, which are seen to be necessary because of the changes in the assumptions initially adopted, changes in the scenarios and mainly the effect and consequence of new information received from the manufacturers of UHV equipment. Also, it will be important the experience received from State Grid related to their UHVAC systems.

Thus, the authors hope to contribute to the UHV technology by unveiling its robustness and reliability, safeness and economic competitiveness when inserted into the Brazilian Interconnected Power System.

2. Prospect of the Study

The project herein studied started in November 2014. Then, the Ten-Year Energy Expansion Plan was 2023. In 2015, EPE released the 2024 Expansion Plan, which was effectively used to develop the technical and economic feasibility studies of the 1,000 kV system.

However, in August 2017, EPE published the 2026 Ten-Year Energy Expansion Plan. Thus, the previous studies conducted needed a revision for this new condition analyzing, mainly, the new forecasts for renewable energy in the North and Northeast regions and the amount of excess energy that might be transmitted to the Southeast region. In addition to reviewing the studies for the year 2026, a brief assessment of the wind and solar power generation expansion foreseen in the National Energy Plan (2030) should be included in a future study.

3. Reactive Compensation

The shunt and series reactive compensation in a transmission system (i.e. series capacitors and shunt reactors) determine the load and the voltage level both during transient and steady state conditions. So, the series compensation determined the loading of the 1,000 kV system whereas the shunt compensation determined both the sustained and switched overvoltages.

As an initial assumption, it was considered: series compensation equal to 50% and fixed shunt compensation equal to 85% in all the sections (440 km) of the 1,000 kV line.

New transmission line configurations, new section distances resulting from routing optimization, new line loadings due to the greater expansion of the renewable plants, etc., may, certainly, impact the sizing of such equipment including some of the transmission line parameters. Separately, power flow studies with a higher degree of series compensation were conducted. As expected, an increase on the line loading was observed which leads to receiving a greater amount of the excess energy.

Therefore, it is recommended to carry out an extensive study on the series and shunt compensation, analyzing new concepts and technologies including the possibility to split the capacitor bank in two modules at each line terminal. Also, it should be created new ways to model the load flow of the 1,000 kV line on different generation scenarios.

The use of alternative technologies to replace the series capacitor should also be analyzed. The same effect of the fixed series compensation might be obtained or improved using controllable series compensation to optimize power injection. The use of a UPFC (Unified Power Flow Controller) based on power electronics, and the use of controllable phase shifter transformers in some 1,000/500 kV substations are among these alternatives.

During the initial study, it was concluded that there would be no need of controllable reactive compensation for normal operating conditions and even under emergency conditions of the loading levels studied. A more detailed research should be conducted to confirm this statement considering, for example, switched reactors and static Var compensators (SVC based on thyristors, and/or VSC-based converters such as a Statcom). The alternative of using controllable reactors at various stages (*Multi Stage Controllable Shunt Reactors*) are being analyzed by some international organizations.

The effective application of these new devices will only be possible after a broad review of the studies performed; thus, demonstrating their technical and economic feasibility, in addition to determining the possible impacts on the design of the substations and transmission lines.

We should emphasize that these studies should contemplate new computational models capable of representing the control system actions towards the occurrence of the various electromagnetic transients during the system operation.

4. Arrangement and Type of Substations

The submodule 2.3 of the Grid Procedures [1], which defines the minimum requirements for transformers and substations and their equipment, describes the busbar arrangement for basic grid substations as follows:

> *The busbar arrangements for air insulated substations are defined in the following groups (differentiated according to the voltage class):*
> *a) Busbar with voltage equal to or higher than 345 kV: double busbar with one and a half circuit-breaker scheme.*
> *b) 230 kV busbar: double busbar with single four-switch circuit-breaker.*
> *Alternative busbar arrangements may be used, including those based on SF_6 insulation, provided that they present equal or higher performance than those arrangements described in items a) and b), which should*

be proven by the agent by means of reliability and availability studies (forced and scheduled outage). Additionally, these arrangements should not jeopardize the systemic performance of the basic grid nor limit the operation of existing facilities, or impose restrictions to the basic grid and other facilities connected to it.

The UHV AC systems in Japan, India and China considered the one and a half circuit-breaker scheme based on GIS (Gas Insulated Switchgear). In Brazil, the experience with GIS substations is mainly concentrated on large hydroelectric power plants.

Considering the greater reliability of an SF_6 insulated substation (GIS), a simpler arrangement might be adopted: single circuit breaker - double busbar. This arrangement offers a reliability level similar to the air insulated one and a half circuit-breaker arrangement. For this same reason, the maintenance costs of a GIS-based substation should be lower along the concession period.

Another important aspect for the utility is that the interruptions due to maintenance of GIS substations are less frequent, which gives the utility a high level of availability and lower losses regarding its Permitted Annual Revenue (RAP). All these aspects must be addressed during the cost analysis of the substation life cycle.

On the other hand, for the series and shunt compensation of each terminal in a line section air insulation is necessary, which determines the use of hybrid solutions for these connections.

Another relevant aspect that must be taken into account when studying the definition of the UHV AC substations arrangement is the possibility of using maneuverable spare auto-transformer and reactor units, especially during a contingency in one of the phases. Recall that these components are single-phase units. Although it has been pointed out that this is not a practice in the Chinese UHV AC system, it is considered important in the Brazilian system, since our regulation establishes high penalties due to the unavailability of the transmission system associated to faults in it.

Thus, it is seen the opportunity for complementary investigations of the types and arrangements of UHV AC substations, involving reliability studies to compare the performance expected from air, GIS, and hybrid insulated substations, quantify the costs and possible effects over the maintenance services, and analyze the protection and control systems, determining the possible technical, financial, and environmental impacts. On this respect, the cooperation with the manufacturers becomes important due to the reliability indices and other costs that they might provide.

In conclusion, this study may well constitute in a R&D project for which a database and basic assumptions will have to be defined; in this way qualifying and quantifying the various types and arrangements of the UHV AC substations. The methodologies currently used for this modality of study may need to be altered, so as to include all the above mentioned aspects [2].

5. Technological Innovations Applied to Equipment

This project had the support of Balestro Company, which manufactured and tested both a polymeric surge arrester and the insulator prototypes for the UHV system. This successful experience might be equally replicated by other manufacturers and for other type of equipment to qualify local vendors for the UHV transmission.

On this respect, a greater participation of national manufacturers would be important, so they can present their technological innovations being currently investigated and analyze their feasibility and applicability onto the UHV project. Among the equipment and devices, it can be mentioned:

- Opening resistors of disconnecting switches in gas insulated substations, which help in the reduction of *Very Fast Transient* (VFT) overvoltages.
- Synchronized switching of circuit-breakers for both opening and closing.
- New reactive compensation equipment control devices.
- Standardization of auto-transformers (3x 850 or 3x1000 MVA).
- Transformer analysis (138/1000 kV and 230/1000 kV) to collect power from renewable generation.

6. Technological Innovations Applied to Transmission Lines

In this project, two types of metal structures were analyzed: self-supported and guyed mast tower. A preliminary investigation showed that a trapezoid, chainette type tower might be more advantageous. However, the mechanical and electric designs of the line would have to be reexamined in more detail, focusing on the impact that the cost of the transmission line and its maintenance would impose.

The configuration of the conductor bundle studied was 8 x 795 MCM, Tern, ACSR, spacing equal to 45.7 cm between subconductors. It should also be examined the advantages of other conductors, for example, a conductor based on aluminum alloy and analyze its impact on the weight and height of the towers, foundations and the cost. It should be recalled that greater spacing among subconductors have an impact on the series and shunt compensation. Therefore, the associate studies must be reviewed.

The assessment of the meteorological conditions in the area where the line is to be installed must be updated based on local measurements, so the effective impact regarding the transmission line design can be verified.

A study of the economic location of the towers on the terrain might provide the project more appropriate average span and tower heights. On this regard, a profile of the terrain (central and lateral) must be obtained through, say, satellite images or measurements at representative locations supported by unmanned aerial vehicles (drones).

Another important issue is the possibility to use a double circuit transmission line. Japan has started the implementation of its UHV AC system already applying double circuit towers. China started its pilot 1,000 kV single circuit line in an extension of 640 km, followed by several other sections, most of them in double circuit (currently over 10 thousand kilometers only in double circuit).

In this project, the use of double circuit was not contemplated for the initial stage. However, for the expanded system, there is a possibility of applying this type of tower in the Pirapora – Ribeirão das Neves section.

7. Monitoring Systems

The pioneering nature of the 1,000 kV system in Brazil provides the opportunity for the elaboration of a conceptual monitoring project, both for the equipment and the transmission line. The analysis of the collected data will provide an important input for the improvement of the project and for its future expansion.

Additionally, the current conditions of the Brazilian energy market, regulated by the availability of equipment and penalized through heavy fines (Variable Portion for Unavailability), demand changes in the operation and maintenance philosophy of the transmission lines and substations, a situation in which the monitoring systems may reduce these financial impacts, considering the following benefits:

- The monitoring device allows remote access to the condition of the asset, reducing the frequency of routine inspections. Another benefit of the device is the early detection of incipient faults through statistical analysis of measurements and trends, thus, preventing catastrophic faults, increasing equipment availability, and providing the maintenance teams opportunities of planned interventions, thus, reducing the unplanned ones.
- The decision to postpone equipment replacement should consider the precise evaluation of its current state, based on aspects such as the equipment life history (stress, faults, etc.). The database set up based on the information from the real-time monitoring device is an important tool for this evaluation.
- Operate a transmission network all the way to its limits, or even beyond them, during peak hours or emergencies.

For the proper elaboration of a monitoring project, it is necessary to conduct technical and economic feasibility studies to define the integration architecture for its acquisition, analysis, and availability of data. Mathematical models have been developed to analyze and treat data collected for its diagnostic and prognostics purposes, facilitating and optimizing the scheduling of maintenances for each asset monitored.

Currently, there are several monitoring systems of equipment offering excellent applicative for data collection and storing with more integrated, intelligent and reliable sensors. It would be interesting to analyze the various existing technologies to choose the most adequate one for the 1,000 kV equipment.

As for the transmission lines, it would be interesting to analyze the application of the *Internet of Things* (IoT) technology. This technology consists of a large network of various sensors installed at several points of a given project that extract and transmit information regarding the state of the physical world.

The IoT can be applied along a given transmission line to monitor the status of conductors. In transmission towers, this technology can monitor the state of the tower itself as well as to perform measurements of local environment and meteorological conditions (temperature, humidity, wind speed, rain, etc.).

This set of data sent through telecommunication systems to a local or remote center will be used to simulate the stressed condition of the conductor, vibrations, dynamic loading and to identify possible dangerous situations that might affect the safety and performance of the line.

As for monitoring the 1,000 kV transmission line, It is considered highly relevant the application of sensors that monitor the line loading conditions, local atmospheric conditions (wind and temperature), and the sags at critical spans. By doing so, the line will be able to operate, under specific conditions, at loading levels higher than those designed.

Briefly, the above phenomenon can be explained as follows: the current in the transmission line causes Joule losses, which result in heat on the conductor above the ambient temperature (Ta) produced by the sun (Sol). On the other hand, the wind (V) cools the heat of the conductor. The variables (Ta, V and Sol) are statistic functions that make the conductor operate at a variable temperature along the line. The temperature increase on the conductor causes an increase in the sag. The line design tries to maintain a minimum clearance distance from the ground, which leads to a deterministic design, often called static capacity. On the other hand, by measuring several influential variables during the line operation it is possible to load the line at values higher than the maximum rated voltage defined during the design. This methodology is called *Dynamic Line Rating* (DLR).

The DLR methodology of transmission lines is already consolidated, available and in constant improvement worldwide. This technology proves to be useful during system emergency situations, during the delay of transmission projects and at points where intermittent generation is injected (wind/solar generation).

In addition to the IoT devices, in terms of collection, there are several other types of sensors, such as, temperature measurement sensors, mechanical tension, vibration, and cable position sensors, all available in the market. These sensors will require robust integration with several other existing technologies, such as automation, information, communications, operation, security and safety, meteorology, etc. This technology integration must be done targeting at expressive results for the economic indicators, efficiency, safety, and flexibility indicators during the operation of power systems.

Finally, a conceptual project should be elaborated aiming at implementing a Monitoring Center where all the information from the sensors installed in the equipment and transmission lines would converge. This center would have flexibility and scalability to contemplate its expansion to receive future signals, as well as to allow its integration with other databases and information centers, mainly those existing in the maintenance, supervision, and operation areas. On the integration aspect, emphasis should be given to data security and protection.

It should be emphasized that this center would be a source of data for various other researches to be performed as well as for the development of the Ultra-High Voltage Alternating Current system.

8. Integration of Renewable Sources to the Interconnected System

As mentioned above, the 1,000 kV system was rated to transmit the excess power from the Northeastern region to the Southeast region. This excess power stems mainly from photovoltaic and wind sources.

These renewable sources are taking an important role in the Brazilian energy matrix due to the prolonged periods of drought and the level of reservoirs below the historical limit. This is also a global trend in the search of clean sources of power.

EPE has been carefully monitoring the growing trend of renewable sources in the North and Northeast regions. At the end of 2014, EPE issued the EPE-DE-RE-140/2014-r0 report, called: "Expansion of the Interconnection Capacity for the Excess Power Outflow from the North and Northeast Regions." In this document, EPE proposed a power offer scenario in the North and Northeast regions with an average 45 GW. In these conditions, the excess power from the North and Northeast regions after subtracting the internal demand was about 30 GW. Considering the capacity of the transmission lines from these regions to the Southeast region, there would be a restriction to export the excess power in 2019 of approximately 8,700 MW (average).

Subsequently, EPE conducted complementary studies analyzing the power outflow from the North and Northeast regions mainly on account of the wind power generation projects in the Northeast. Based on these studies, some alternatives were studied for the insertion of a 1,000 kV transmission system to reinforce this outflow [3], [4], [5], [6], [7].

So, the 1,000 kV AC transmission alternative was chosen to connect the south of the state of Ceará to the central region of the state of Minas Gerais, passing through the central region of the state of Bahia. This line will connect the Milagres and Pirapora substations, and will work as a corridor to export the wind and photovoltaic power from the Northeast to the Southeast region. There will be two intermediate substations that can be used as collectors of these sources. The system may be later expanded to connect the Pirapora to the Ribeirão das Neves station.

The growing trend of the renewable energy and its importance can be verified through the analysis of the results from the reserve auctions held in 2014 and 2015. Due to economic and conjunctures factors, the 2016 auction was not carried out but was transferred to December 18, 2017.

These are expressive numbers that if becoming real an even higher amount of excess energy might need to be transferred to the Southeast region. In turn, this would demand the optimization of the transmission alternatives between the Northeast and Southeast regions, including the 1,000 kV transmission line from Milagres to Pirapora.

The continuation of this project will provide highly relevant contributions to the development of new methodologies for planning the expansion of the electric system so as to contemplate the elaboration of scenarios for the insertion of intermittent generation sources, both at the transmission and distribution levels.

The need to set discussions on the electric system expansion planning methodology, considering the uncertainties of the renewable sources, was the subject of a recent work (March 2017) published by Cigré, in partnership with CIRED [8]. Such a work states that the current methodologies must be enhanced because initially they were created considering scenarios with reduced amounts of power from renewable sources. Thus, it should be established new assumptions, new criteria, and new mechanisms to exchange information between the transmission system and the operators of the distribution system.

9. Technological Observatory

For the effective implementation of a UHV AC system in Brazil it is suggested the establishment of an observatory to monitor, at a global level, the initiatives focused on this issue. It should be tracked the projects in China, India and Japan, the technological innovations being studied; the improvements foreseen for the design, construction issues, commissioning, operation and maintenance matters and the enhancement of computational models and tools for studies focused on the design and specification of the transmission lines, substations, and equipment.

We should also follow the initiatives of the manufacturers of equipment and components for transmission lines focused on UHV AC systems, with emphasis on the possibility to manufacture them in Brazil.

Another initiative that should be monitored by this observatory is the work being developed by the Technical Committee of the IEC TC 122, which addresses the standardization aspects related to UHV AC systems. This Committee is currently analyzing issues like: system design, design of substations and transmission lines, construction, commissioning, operation, maintenance, and environment. Brazil has a representative in this TC 122 committee; thus, contributions from the studies developed in this project can broaden the international effort towards this technology.

This knowledge base, when implemented and kept updated, will provide important input for the technicians and companies that come to get involved in this process of modernization of the Brazilian electric grid, with the pioneer insertion of a new level of alternating current.

Also, this knowledge, after being consolidated and internalized, will be made available to the planning and operation agencies, which will permit identifying other possible applications of the 1,000 kV AC system for other areas of Brazil (for example: collecting energy from renewable energy sources close to the coast of the Northeast region).

10. Conclusions

In view of some changes in the assumptions adopted in this project (initiated in 2014), due mainly to the change in some of the scenarios and the recent information received from the equipment manufacturers, it is suggested to perform the following complementary investigations:

- Update the studies considering the 2026 Ten-Year Energy Expansion Plan, analyzing mainly the new renewable energy forecasts for the North and Northeast regions, as well as the amount of excess energy that might be transmitted to the Southeast region.
- Conduct extensive studies to review the series and shunt compensation, considering new concepts and technologies, such as splitting the series compensation bank into more than one module at each line terminal. Also, the possibility to use controllable series compensation and shunt reactors.

- Perform complementary investigations regarding the type and arrangement of the UHV AC substations; performing reliability studies to compare the performance expected from the arrangement of air, GIS, and hybrid insulated substations. This study aims at quantifying the costs and possible effects on the maintenance services, protection and control systems, and the possible environmental impacts.
- Analyze the possibility to maneuver and transfer spare single-phase auto-transformers and reactor units of the UHV line; mainly during contingencies that affect one of the phases.
- Analyze the application of technological innovations in equipment such as opening resistors of disconnecting switches in gas insulated substations. Also, the application of controlled switching on circuit breakers for both opening and closing switching.
- Based on local measurements obtain the meteorological conditions of the area where the UHVAC line is to be installed to thereafter check its impact on the design of the line.
- Study the economic location of the towers using satellite images or measurements in representative sections of the line with the aid of the drone technology.
- Analyze the possibility to use double-circuit UHV lines.
- Analyze the use of non-conventional conductors.
- Identify prospective manufactures of UHV prototype equipment.
- Elaborate a conceptual project for the monitoring of equipment and transmission lines envisioning the creation of a monitoring center for the integration of signals through diagnostic and prognostic applicatives.
- Analyze the application of the dynamic loading methodology on the 1,000 kV transmission system.
- Initiate discussions related to the improvement of the power system expansion planning methodology. This will allow considering the various uncertainties associated to the sources of renewable power.
- Implement a technological observatory to collect and make available information related to the UHV system.

11. References

[1] GRID PROCEDURES. *Submodule 2.3 – Minimum Requirements for Transformers and for Substations and their Equipment.* Operador Nacional do Sistema. Rio de Janeiro, 2011.

[2] FRONTIN, S. O. *Equipamentos de Alta Tensão. Prospecção e Hierarquização de Inovações Tecnológicas*. Goya Editora Ltda: Brasília, 2014.

[3] EPE-DEE-RE-146/2014-rev0 (October 31, 2014), Transmission Expansion Studies – N-SE and NE-SE Interconnection Expansions to Meet the Needs of Extreme Export Scenarios of the North and Northeast Regions – Initial Alternative Conception.

[4] EPE-DEE-NT-049/2015-rev0 (March 16, 2015), Transmission System Expansion Planning Studies – Excess Power Outflow from the North and Northeast Regions – Interconnection capacity increase requirements.

[5] EPE-DEE-RE-147/2014-rev2 (December 08, 2014), Studies for Transmission Expansion Bidding, Technical & Economical Analysis of Alternatives: R1 Report, A Study to Redirect the Wind Power Potential from the East Area of the Northeast Region.

[6] EPE-DEE-RE-148/2014-rev1, (December 08, 2014), Studies for Transmission Expansion Bidding, Technical & Economical Analysis of Alternatives: R1 Report, Northeast-Southeast Interconnection Capacity Increase.

[7] EPE-DEE-DEA-RE-001/2014-ver0, Studies for Transmission Expansion Bidding, Study to Redirect the Wind Power Potential from the Central Region of Bahia.

[8] CIGRE BROCHURE 681. *Planning Criteria for Future Transmission Networks in the Presence of a Greater Variability of Power Exchange with Distribution Systems.* Cigré - Paris, 2017.

Text in *Minion Pro*
an titles in *Rotis SemiSerif 55*

Brasília – Distrito Federal – Brasil
MMXVII

Specialists who contributed with comments and suggestions to the various chapters of the book

Ana Cláudia Balestro
Balestro

Daniel Ferreira Bessa
Balestro

Jader Fernandes de Jesus
Eletrobras Eletronorte

José Galib Tannuri
FDTE

Marcos César de Araújo
Eletrobras Eletronorte

Mario Noboru Takai
Eletrobras Eletronorte

Patrícia de Oliveira Freitas Borin
Eletrobras Eletronorte

Paulo Henrique Barbosa Naves
Eletrobras Eletronorte

Rafael Lewergger Meireles Piccirili
Eletrobras Eletronorte

Silvio Luiz Miranda Brito
Balestro

Vanderlei Guimarães Machado
Eletrobras Eletronorte

Agência Brasileira do ISBN
ISBN 978-85-88041-15-8
9 788588 041158

Agency

ANEEL
Agência Nacional de Energia Elétrica
P&D - Programa de Pesquisa e Desenvolvimento

Proponents

Eletrobras
Eletronorte

STATE GRID
BRAZIL HOLDING S.A.
国家电网巴西控股公司

Executors

ITAEE

FDTE

BALESTRO